MARA -PROJECT

DEVELOPING LONG-TERM DURABILITY
OF MARBLE FACADES

FINAL REPORT

30.4.2001

HKR-Rakennuttaja
National Board of Antiquities
European Commission
Stonecon Oy

0 MARA Project, Final report

1 Appendix 1: Environmental conditions

2 Appendix 2: Test wall

3 Appendix 3: One-sided weather resistance test

4 Appendix 4: Protective agent

5 Appendix 5: Effect of thermal cycling on the physical properties of three marble types

6 Appendix 6: Effect of thermal cycling on the mechanical properties of three marble types

7 Appendix 7: University of Parma, Final report

8 Appendix 8: Cevalor, Final report

9 Appendix 8: Bowing measurements

10 Appendix 10: Financial report

MARA -PROJECT

DEVELOPING LONG-TERM DURABILITY OF MARBLE FACADES

Jouni Maidell, Pekka Mesimäki
Pertti Koskinen, Gianni Royer
Esa Ärmänen, Timo Kirkkomäki
Sonia Pereira, Sandra Lopez, Maria Joao Riabom

ABSTRACT

The need for conserving, restoring and protecting stone buildings and monuments throughout the world is growing continuously. This is particularly actual in the historic cities of Europe where marble and other calcareous stones have been commonly used. The decay of old stone structures is becoming a remarkable technical and economical problem without forgetting the disappearance of our cultural heritage. Deteriorated stone façades may in some cases even present a considerable safety risk.

The badly damaged marble façade of Finlandia Hall in Helsinki, Finland was renewed during the autumn 1998 and spring 1999. In connection with that project the Public Works Department of the City of Helsinki launched with a support from European Commission (Raphael program) a research project "Developing long-term durability of marble façades" known as "MARA –project". This was done, because it was noted that the behaviour of thin stone veneers and stone protection treatments on a long-term basis was not known well enough. Also the deterioration mechanism and the reasons for deterioration were unknown. The connection with the renovation project gave an unique opportunity to reserve a part of the actual façade for scientific purposes. The main goals of the project were to find out the reasons for characteristic behaviour of marble panels in outdoor uses; to find out the means to extend the service life of a marble façade; to find out new information on the material behaviour and to disseminate the results as widely as possible.

The project management has been on the responsibility of Public Works Department of Helsinki City. Other participants of the project have been in Finland the National Board of Antiquities, Stonecon Oy, Technical Research Centre of Finland (VTT) and Helsinki University of Technology (HUT); in Italy Parma University, Internazionale Marmi e Macchine (IMM), Henraux S.p.A and Savema S.p.A; in Portugal Cevalor. A number of other companies producing marble products have also taken part in the project.

The research program was divided in two entities: field tests and laboratory research. In field tests the behaviour of marble structures consisting of thin stone panels was followed in actual circumstances in the façade of Finlandia Hall. Studied matters were the impact of marble panel thickness, stone panel size and initial stone strength on the durability of marble and coating structure. Also the bowing and changes in colour were measured. Different types of marble-coated structures were selected for the research, as well as different qualities of Carrara Bianco. The laboratory tests aimed at determining the reasons for marble weathering and curving. Variables under survey were the qualities of marble, external straining factors and optional structural solutions. Applied research methods were microscope tests, spectrophotometric measurements, weather resistance tests, compression tests, bending and tension stress tests and other tests for physical properties.

According to the studies made the deterioration of marble structure in environmental stresses is caused by granular decohesion of calcite grains marble consists of. This decohesion forms cracks along the grain boundaries and is a consequence of the anisotropic thermal expansion behaviour of calcite crystals. Calcite grains have a tendency of

breaking away from each other when thermal variations affect the material. Freezing and thawing may have an accelerating effect on the process after it has started. Bowing of the panels is caused by gradient of the granular decohesion level through the panel.

According to the studies the damaging of a marble structure takes place very soon after it has been subjected to environmental stresses. The very first cycles seem to be the most damaging, afterwards the deterioration process slows down. The microstructure of marble influences its resistance against environmental stresses; homoblastic structures seem to be degradated very easily, whereas xenoblastic structures are much more resistant.

The effect of the chemical attack from impurities in atmosphere was also studied. In this study samples from the both old and new façades were studied and they both confirmed similar results; traces of chemical attack can be noticed only in the surface of the panels, not inside.

Also the effect of protective agents was studied. Because of the nature of the deterioration it can not be influenced by the use of these products. Still, according to the studies, marble surface can be protected against stains and certain types of chemical effects by the use of protective agents. They are especially effective against stains of organic nature, however the agents themselves seem to be affected by UV –radiation and thermal strains thus limiting their service life.

For studied structural products deterioration seems to be two-folded; on the other hand granular decohesion is weakening the marble as in massive panels, but on the other hand the bond strengths between marble and background is decreasing remarkably.

Environmental conditions by the Finlandia Hall were monitored extensively during the project. Temperature and humidity was measured in several points by the façade by VTT. According to the recorded data the prevailing conditions include several factors that cause strain to the building's marble façades. These factors are annual and daily variation of temperature, freeze-thaw cycling and variation of humidity on different sides of a panel. Annual variation during the monitoring period was from -25°C to +50°C, daily variation was during summertime 15-20°C. The amount of annual freeze-thaw cycles was much bigger than expected; the results showed 60-70 annual cycles. To summarise, the outer surface of panels are suffering from higher environmental stresses (daily variation of temperature, the number of freeze-thaw cycles and relative humidity). These stresses are all affecting to the same direction and thus contributing to the bowing of the panels. The sum of factors was highest on southern walls and lowest on northern walls.

Using the parameters from different studies a theoretical model for interpreting the marble degradation was developed. Microstructural FEM –model, considering an assemblage of calcite grains connected by an interface cementing layer, provided a wealth of evidence that granular decohesion can be produced by thermal variations, even when uniformly distributed.

CONTENTS

1 INTRODUCTION 8

1.1 BACKGROUND 8

1.2 FINLANDIA HALL 9

1.3 CONTENTS OF THE PROJECT 9

1.3.1 Starting point 9

1.3.2 Objectives of the project 10

1.3.3 Limitations, outlines 10

1.3.4 Research areas 10

1.3.4.1 Field tests 10

1.3.4.2 Laboratory tests 11

1.3.4.3 Development of new solutions 11

1.4 ORGANISATION 11

1.4.1 Management, co-ordination 11

1.4.2 Participants 11

1.5 COURSE OF THE PROJECT 12

2 RESEARCH PROGRAM 13

2.1 GENERAL OUTLINE 13

2.1.1 Objectives and tasks 13

2.1.2 Research areas 14

2.1.3 Scope of marble type selection 14

2.2 SAMPLING 15

2.2.1 Sampling procedure 15

2.2.2 Control of cutting direction 15

2.3 FIELD TEST 18

2.3.1 General scope of the research 18

2.3.2 Organisation 18

2.3.3 Research variables 19

2.3.4 Realisation of the field test 21

2.3.5 Research program for field test 25

2.3.5.1 Objective 25

2.3.5.2 Observations at site 26
2.3.5.3 Laboratory tests 27
2.4 OBSERVATION OF WEATHER CONDITIONS 28
2.4.1 Scope of the research 28
2.4.2 Measuring and recording arrangements 28
2.4.3 Other information about weather conditions 29
2.5 LABORATORY RESEARCH ORGANISATION 29
2.6 VTT BUILDING AND TRANSPORT RESEARCH 30
2.6.1 Scope of the research 30
2.6.2 Effect of protective agent 31
2.6.2.1 Objective 31
2.6.2.2 Test wall samples 31
2.6.2.3 Laboratory tests 32
2.6.3 One-side weather resistance test 33
2.6.3.1 Objective 33
2.6.3.2 Weather resistance test 34
2.6.3.3 Properties of marble 35
2.6.4 Evaluation of marble samples from other facade objects 37
2.7 HELSINKI UNIVERSITY OF TECHNOLOGY RESEARCH 38
2.7.1 Scope of the research 38
2.7.2 Test program 38
2.8 PARMA UNIVERSITY RESEARCH 40
2.8.1 Scope of the research 40
2.8.2 Research program 41
2.8.2.1 Direct tensile strength 41
2.8.2.2 Pre-cracked bending test 42
2.8.2.3 Dilatometric tests 44
2.8.2.4 Modelling of granular decohesion 45
2.8.2.5 Microstructural characterisation 45
2.9 CEVALOR RESEARCH 47
2.9.1 Scope of the research 47
2.9.2 Technical testing program 48
2.9.2.1 Workpackages 48
2.9.2.2 Laboratory tests for WP 5 49
2.9.3 Case studies 52
2.10 COLLABORATION WITH IMM 52
2.10.1 Internationale Marmi e Macchine 52

2.10.2 Main objectives and tasks 52
2.11 STRUCTURAL CONSIDERATIONS 53

3 RESULTS AND DISCUSSION 53

3.1 FIELD TEST 53
3.1.1 General 53
3.1.2 Colour measurements 54
3.1.3 Bowing measurements 56
3.1.4 Flexural strength 60
3.1.5 Water absorption, apparent porosity, bulk density 61
3.1.6 Microscopic research 63
3.1.6.1 Mineral composition 63
3.1.6.2 Microstructure 64
3.1.7 Marble coated panels 70
3.1.7.1 Bond strength 70
3.1.7.2 Microstructure 71
3.2 OBSERVATION OF WEATHER CONDITIONS 73
3.2.1 General 73
3.2.2 Daily variation of temperature 73
3.2.3 Temperature gradient over the marble panel 76
3.2.4 Gradient of temperature variation in marble 76
3.2.5 Freeze/thaw -cycling of marble 77
3.2.6 Humidity gradient over the marble panel 78
3.2.7 Acidity of rain water 79
3.2.8 Weather conditions 80
3.2.8.1 Temperature and humidity 80
3.2.8.2 Rainfall and sunshine 82
3.2.9 Discussion 83
3.2.9.1 Temperature gradient 83
3.2.9.2 Daily variation of temperature 84
3.2.9.3 Gradient of temperature variation 84
3.2.9.4 Freeze/thaw -cycling 85
3.2.9.5 Relative humidity 86
3.2.9.6 Acidity of rain water 87
3.2.10 Conclusions 87
3.3 EFFECT OF PROTECTIVE AGENT 88
3.3.1 Laboratory studies 88

3.3.1.1 Resistance to UV-radiation 88
3.3.1.2 Heat resistance 90
3.3.1.3 Chemical resistance 91

3.3.2 Test wall studies 92
3.3.2.1 Flexural strength 92
3.3.2.2 Water absorption, apparent porosity, bulk density 92
3.3.2.3 Microstructure 93
3.3.2.4 Colour measurement 97

3.3.3 Discussion 98
3.3.3.1 Resistance properties 98
3.3.3.2 Strength properties 99
3.3.3.3 Water absorption properties 100
3.3.3.4 Microstructure 100
3.3.3.5 Colour measurements 102

3.3.4 Conclusions 102

3.4 RESEARCH ON ONE-SIDE WEATHER RESISTANCE TEST 104

3.4.1 Flexural strength 104

3.4.2 Water absorption, apparent porosity, bulk density 105

3.4.3 Mineral composition 106
3.4.3.1 X-ray diffraction 106
3.4.3.2 Thermal analysis 107

3.4.4 Microstructure 107
3.4.4.1 Thin section study 107
3.4.4.2 SEM-study 110

3.4.5 Colour measurement, gloss 112

3.4.6 Warping 114

3.4.7 Discussion 115
3.4.7.1 Strength properties 115
3.4.7.2 Water absorption properties 115
3.4.7.3 Composition and microstructure 116
3.4.7.4 Colour measurements, warping 118

3.4.8 Conclusions 119

3.5 EVALUATION OF MARBLE SAMPLES FROM OTHER BUILDINGS 120

3.5.1 Presentation of the objects 120

3.5.2 Mineral composition 120

3.5.3 Thin section study 121

3.5.4 SEM-study 125

3.6 EFFECT OF THERMAL CYCLING ON MARBLE PROPERTIES 130

3.6.1 Thermal microfracturing of marble 130
3.6.2 Marble samples and sample preparation 131
3.6.3 Physical properties 131
3.6.3.1 Density, porosity and water absorption 131
3.6.3.2 Capillary water absorption 135
3.6.3.3 The effect of temperature cycling on the physical properties 137
3.6.4 Microstructural properties 138
3.6.4.1 General aspects 138
3.6.4.2 Mineralogy 139
3.6.4.3 Microcracking 139
3.6.4.4 The effect of temperature cycling on the structural properties 140
3.6.5 Elastic stress-strain behaviour 140
3.6.5.1 Interpretation methods 140
3.6.5.2 Characteristics of uni- and triaxial stress-strain behaviour 141
3.6.5.3 Young´s modulus 144
3.6.5.4 Poisson´s ratio 145
3.6.6 Critical stress states in compression, ... 145
3.6.6.1 Interpretation methods 145
3.6.6.2 Peak strength 149
3.6.6.3 Crack damage strength 150
3.6.6.4 Crack initiation strength 152
3.6.7 Bending test 154
3.6.7.1 Elastic parameters in bending 154
3.6.7.2 Bending strength 155
3.6.7.3 Bending modulus 156
3.6.8 The effect of number of cycles 157
3.6.9 Discussion 159
3.6.9.1 Physical properties 159
3.6.9.2 Mechanical properties 160
3.7 DIRECT TENSILE STRENGTH TEST 161
3.7.1 Test results 161
3.7.2 Discussion 167
3.8 PRE-CRACKED BENDING TEST 168
3.8.1 Test results 168
3.8.2 Discussion 171
3.9 PERMANENT DILATATION TESTS 174
3.9.1 Two-sided treatment 174
3.9.2 One-sided treatment 175
3.9.3 Anisotropic impact 176

3.9.4 Affect of moisture 177
3.9.5 Permanent dilatation by number of cycles 177
3.9.6 Summary 178
3.10 MODELLING OF GRANULAR DECOHESION 179
3.10.1 Microstructurally motivated models 179
3.10.1.1 Theoretical evaluation 179
3.10.1.2 Practical application 183
3.10.1.3 Discussion 186
3.10.2 A phenomenological model in statistical mechanics 187
3.11 MICROSTRUCTURAL CHARACTERIZATION OF MARBLES 189
3.11.1 Skeleton method 189
3.11.2 Marble classification 192
3.12 RESEARCH AT CEVALOR 194
3.12.1 Marble type A 194
3.12.2 Marble type D 197
3.12.3 Marble type E 200
3.12.4 Marble type K 203
3.12.5 Case studies 206
3.12.5.1 The use of marble in facades in the North of Portugal. 206
3.12.5.2 Stone companies 206
3.12.5.3 Architects 207
3.12.5.4 Examples of objects 208
3.12.5.5 Centro tecnológico da piedra 208

4 PRACTICAL APPLICATIONS 210

4.1 INSTRUCTIONS FOR CONSTRUCTING A DURABLE MARBLE FAÇADE 210
4.1.1 General 210
4.1.2 Selection of marble 210
4.2 TECHNICAL SPECIFICATIONS FOR A STONE CLADDING 211
4.2.1 Functional considerations 211
4.2.2 Structural design principals 212
4.2.3 Building physical design principals 213
4.3 MONITORING THE PHYSICAL STATE OF AN EXISTING FAÇADE 214
4.3.1 General 214
4.3.2 Bowing measurements 214

4.3.3 SEM -analyses 215
4.3.4 Flexural strength testing 215
4.3.5 Criteria for façade renovation 215
4.4 RECOMMENDED ACTIONS FOR FAÇADE MAINTENANCE 215

APPENDIXES 216

1 INTRODUCTION

1.1 Background

Marble has been used successfully for centuries in buildings and monuments all over the world. The use of marble and other calcareous stones has been extensive especially in historic cities of Europe, but marble has also been used in modern architecture. Previously, when only massive marble was used, marble was like any other building material with no specific problems. But as marble is in modern architecture most commonly used in thin panels some serious problems have occurred during the last decades.

Special problems of ventilated Carrara White Marble façades are the deterioration of the structural strength of marble and the curving of marble panels. One of the main reasons for the deterioration and fouling of natural stones is the climatical stresses induced to the panels. Also the rising amount of acid compounds and impurities coming mainly from industrial and traffic sources cannot be neglected. Stone structures are today exposed to harsher environmental conditions than ever before. Nowadays commonly used thin stone veneers are even more sensible for weathering than the traditional, massive structures.

The reasons for durability problems in Carrara White Marble façades, and possible means to solve them, have been studied to some degree by estate owners and research institutes in different countries. So far the universal solution for these problems has not been found.

The need for conserving, restoring and protecting stone buildings and monuments in cities throughout the world has been accepted unanimously. The decay of old stone structures is in many areas becoming a remarkable technical and economic problem. Deteriorated stone façades may in some cases even represent a considerable safety risk. The durability problems have led to a strong decrease in the use of marble for outdoor applications.

A famous and well known object with remarkable façade is Finlandia Hall in Helsinki, Finland. Architect Alvar Aalto designed the Finlandia Hall as a part of his Helsinki Centre Master Plan in 1962 to serve as a concert and congress hall. The first construction phase of the Finlandia Hall was completed in 1971 and the additional conference wing in 1975. Since completion the hall has been used for congresses, conferences, meetings, galas and concerts of music from light to classical. During the concert season it is the main venue of the Helsinki Philharmonic Orchestra and the Finnish Radio Symphony Orchestra. Several important international and national meetings and events have been organised in the house, the most important of them are

perhaps the European Security and Co-operation summit in 1975 and the European Council meeting in 1999.

Besides the Finlandia Hall, there are several well-known buildings with deteriorated stone façades, for example Sydsvenska Dagbladet, Malmö, Sweden, Byggnadsförbundet, Stockholm, Sweden, Stadshuset i Nyköping, Sweden, Konstmuseum, Ålborg, Denmark, La Grande Arche de la Défense, Paris, France, Amoco Building, Chicago, USA, Hotel Hesperia, Helsinki, Finland, Enso-Gutzeit Oy, commercial building, Helsinki, Finland, Savings Bank premises in Oulu and Tammisaari, Finland, as well as Tapiola Insurance Company premises in Turku, Finland.

Marble and other calcareous stones have in all times played an essential role in the European architecture. Today there is a significant need for developing new technically and economically suitable methods for marble in order to be able to cope with the huge maintenance task of the existing marble buildings and monuments and to secure the future position of the European marble industry.

1.2 Finlandia Hall

In the Finlandia Hall the marble façades are white for a definite reason. The shapes of the building are separating themselves from their surroundings with sharp-cut features so emphasising the sculptural nature of the building. Whiteness is a feature, which continues through the large entrée hall inside the building adding to the impression of spaciousness. Whiteness is an essential feature to be preserved, and that is why marble coating is considered absolutely necessary. The surface of marble is pervious to light and has a soft gloss. The seams of the stone make the building lighter. These characteristics have been essential in the architect's point of view. Alvar Aalto´s own personal style and artistic ideas are presented in the final results. To him marble was an important link with the Mediterranean culture which he wanted to introduce into Finland.

1.3 Contents of the project

1.3.1 Starting point

The façade of Finlandia Hall showed very soon after completion the tendency for bowing. The condition of the façade was monitored carefully and after certain time it became obvious that the panels should be changed for safety and esthetical reasons. The discussion on the material was alive for several years and finally decision was made to use marble panels also in the renovation. Renovation project was completed in May 1999.

In the preparation of the renovation works it was noted that the behaviour of thin stone veneers and stone protection treatments on a long-term basis was

not known well enough. Also the deterioration mechanism and the reasons for deterioration were unknown. There were many different, partly confrontational theories, but none of which could explain the phenomena comprehensively. MARA –project was established to answer to these questions. The connection with the renovation project gave us an unique opportunity to reserve a part of the actual façade for scientific purposes; by this way we were able to study different products under actual weathering conditions.

1.3.2 Objectives of the project

The main goal of the project is to find out the reasons for the characteristic behaviour of marble panels in outdoor uses. This information can be used in finding better solutions for building a more durable marble façade or in restoring the existing façades and monuments comprising the European cultural heritage.

One of the main goals is to create an active network between European stone companies, experts and research institutes and a model plan for continuous development work between them. The project contributes also to transferring technologies developed outside Europe, dealing with research and use of marble in Europe.

1.3.3 Limitations, outlines

We decided to concentrate only to Italian marbles quarried in Carrara, Massa and Lucca areas. This is because the bowing phenomena is the best known in Italian marbles and also because this project was supposed to explain the behaviour of Carrara Bianco. In those marbles we decided to concentrate in light coloured "white" marbles suitable for use in the façade of Finlandia Hall. Three granite qualities were added for comparison.

The behaviour of marble is strongly defined by its microstructure. In Apunian marbles the range is from pure homoblastic to pure xenoblastic textures, in addition to which there is of course a wide variety of different intermediate textures. Due to the vast amount of different qualities it was necessary to choose some typical qualities to represent the different microstructures; one of homoblastic texture, one xenoblastic and two intermediate. By this way we could cover the whole range of different varieties. The behaviour of other qualities can later be predicted by their microstructure, when behaviour of these representatives is known completely.

1.3.4 Research areas

1.3.4.1 Field tests

The behaviour of marble structures consisting of thin stone panels was followed in actual circumstances in the façade of Finlandia Hall. Studied matters are the impact of marble panel thickness, stone panel size and initial stone strength on the durability of marble and coating structure. Also the

bowing and changes in colour are measured. Different types of marble-coated structures are selected for the research, as well as different qualities of Carrara Bianco.

Each product has about 10 m^2 share of the research wall, the total area of which is about 140 m^2. In addition to this research wall, a certain rack was constructed on the roof of the house in order to carry the specimen for destructive tests. The actual weather conditions i.e. humidity, temperature and the composition of the air by the wall were followed very closely.

The character and degree of damage in a deteriorated marble, which was damaged in real conditions, was studied in laboratory. In the facade research samples were tested and measured in laboratory during the survey in order to determine the change in the stone qualities.

1.3.4.2 Laboratory tests

The laboratory tests aim at determining the reasons for marble weathering and curving. Variables under survey are the qualities of marble, external straining factors and optional structural solutions. Research methods to be used are microscope tests, spectrophotometric measurements, weather resistance test, bending and tension stress test and other tests for physical qualities.

1.3.4.3 Development of new solutions

With the help of information obtained from facade research and laboratory tests, a summary is drawn dealing with the reasons for marble deterioration. Recommended methods for the improvement of marble durability and for prolonging the service life of marble facade coating carried out with the help of modern technology are be developed. Studied factors are the qualities of the original marble, dimensioning of stone construction components, chemical protection treatments on stone panels and constructional solutions of the panels. Also a test method for marble selection in terms of durability is presented.

1.4 Organisation

1.4.1 Management, co-ordination

The project management has been on the responsibility of Public Works Department of Helsinki City. PWD Construction Management Unit has taken the practical actions in the project co-ordination and management. PWD Construction Management Unit has used Stonecon Oy as a consultant both in project management and scientific work.

1.4.2 Participants

Participants of the project are in Finland Stonecon Oy, Technical Research Centre of Finland (VTT) and Helsinki University of Technology (HUT); in

Italy Parma University, Internazionale Marmi e Macchine (IMM), Henraux S.p.A and Savema S.p.A; in Portugal Cevalor. A number of other companies producing marble products have also taken part in the project by providing us material to be studied and a valuable link to stone industry.

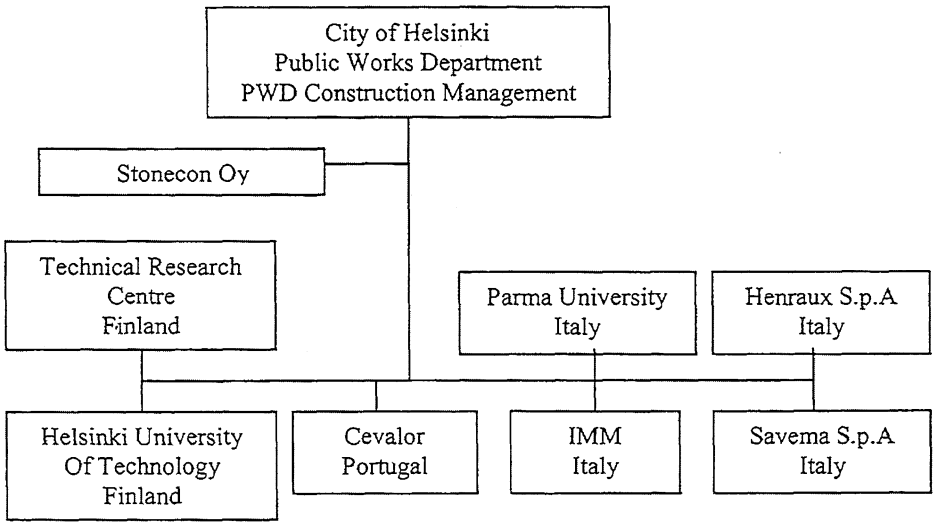

Figure 1. Organisation of MARA Project

1.5 Course of the project

Project started with defining the scope of work in a more detailed way. The entity was divided in smaller subprojects which could then be delivered further to other partners of the project according to their resources. After this we could start the discussions with our collaborators in order to define each subproject more precisely.

Partner agreements were signed in the end of March 1999 after which the actual work could start. First research meeting was held as a project start-up in May 1999 in Finland, in Finlandia Hall to be exact. Since then there has been four other research meetings (in Helsinki, Finland Nov. 1999, Carrara, Italy, May 2000, Helsinki, Finland Nov. 2000, Borba, Portugal, Feb. 2001) and other meetings with laboratories and project management. The laboratories have worked independently between the meetings, having active correspondence through e-mail.

MARA Project has been of wide public interest from the very beginning of the project. Several press conferences have been held following the proceeding of the project, both in Finland and in Italy. The conferences in Italy have been held during the annually organised Carrara Fair. A final seminar where all the results and this report will be published, will be held in May 2001 in Finlandia Hall, Helsinki and in the beginning of June 2001 in Carrara.

Discussions with other projects and experts concentrating on stone research and use have been active during the project. Several meetings have been held for example with MARC 1999 (Course on Modern Architecture Conservation), TEAM (Testing and Assessment of Marble) and CEN –committee.

2 RESEARCH PROGRAM

2.1 General outline

2.1.1 Objectives and tasks

Main objective of Mara research was to develop more durable solutions for a facade cladding of white Carrara marble (Carrara Bianco) in order to achieve a longer service-life. Practical research was focused primarily on the durability properties of marbles.

In order to achieve the main objective Mara project was divided into the following sub-objectives and tasks:

- main causes for marble deterioration in facade claddings
- main influencing factors and the failure mechanism
- method for testing the suitability of a given marble
- technical specifications for a stone cladding
- recommendations for maintenance of a marble facade

Apart from the material research emphasis was given to solving the structural principals to be used for a thin facade cladding in order to ensure a durable solution. In the research Finlandia Hall was used as the main reference object. Previous experiences obtained from Finlandia Hall as well as the ongoing tests at the actual facade gave valuable contribution to the research activities.

The aim was to develop solutions that can be used for new buildings as well as for maintaining and restoring of the existing façades and monuments comprising the European cultural heritage. Results of the project are in many ways useful for design and implementation of natural stone facade claddings. In order to achieve good understanding of the specific problems main emphasis was given to research of Carrara Bianco marble. However, the results can easily be applied for any marble cladding as well as for any stone cladding.

One of the goals was to create an active network between European experts, research institutes and stone producers. The project contributes also to transferring technologies developed outside Europe, dealing with research and use of natural stone in Europe.

2.1.2 Research areas

Main research areas of Mara project were the field test located at Finlandia Hall and the laboratory tests carried out in four European laboratories. In addition structural development and collaboration within an expert network was included. Figure 2 represents the division of main tasks in Mara project.

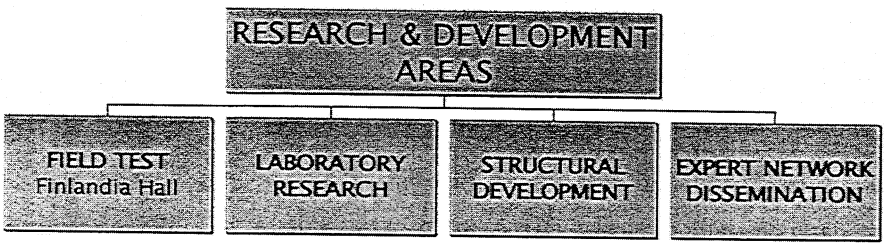

Figure 2. Division of research areas in Mara project

2.1.3 Scope of marble type selection

The aim was to select a range of marbles representing typical types of Carrara Bianco marble. The selection of materials was based mainly on the facts available on the appearance, physical and durability properties as well as the microstructural characterisation of the marbles (see also1.3.3). Previous use and experience of suitability were used as additional criteria when applicable. After several considerations four marble types were selected to be used as samples in the research. In table 1 is given the basic description of the chosen marble types. Marble type A was used as the reference material.

Table 1. Basic properties of Carrara Bianco marbles A, D, E and K used in Mara research project.

	A	D	E	K
microstructural characterisation	homo-/xenoblastic	homoblastic	xenoblastic	homo-/xenoblastic
appearance	white, veined	white, veined, clear contours	white, slightly veined	light grey, slightly veined
strength	medium or high	Low	high	High
porosity	low	Low	low	Low
typical uses	all purposes	mainly interior purposes	all purposes	all purposes
earlier experience about suitability	considered to be one of the best qualities in the region	known to have durability problems when used outdoor	known to be durable	known to be durable
rough geografic location	Carrara	Carrara	Lucca	Massa

Same marble types were used in all tests throughout the project in order to obtain comparable results at the field test and laboratory tests carried out during same time in the participating laboratories.

2.2 Sampling

2.2.1 Sampling procedure

Sampling for all Carrara Bianco marble types was arranged in collaboration with IMM being responsible for the local co-ordination and quality control during the sampling process. Samples were produced by Savema Spa and Henraux Spa as follows:

- all massive marble panels for field test were delivered by Savema Spa
- all samples for laboratory research of marble types A and K were delivered by Savema SPa
- all samples for laboratory research of marble types D and E were delivered by Henraux SPa

Field test panel samples were delivered in connection with the completion of the facade renovation in April 1999. Laboratory samples were then processed of the same raw materials and delivered directly from Italy to each laboratory as explained in Table 2. Carrara Bianco for structural panel coatings were chosen by the suppliers according to the instructions given by the coordinator.

2.2.2 Control of cutting direction

Directions in stone were defined and marked to the blocks at the quarry according to the principal presented in figure 3. Cutting directions chosen for the samples were respectively the following:

- parallel to the rift = along the rift plane (verso; $\gamma = 0$)
- perpendicular to the rift = along the head-grain plane (contro; $\beta = 0$)

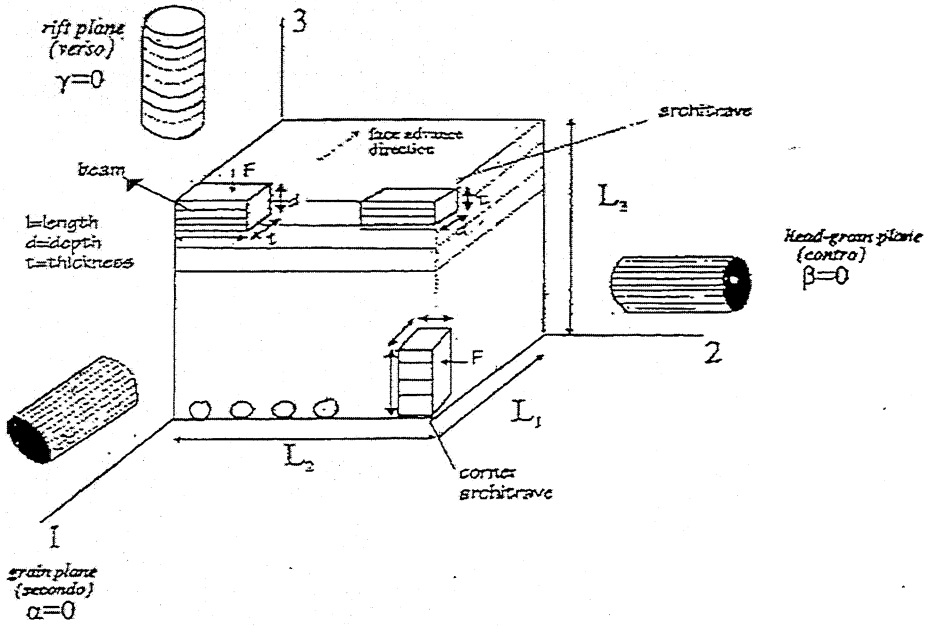

Figure 3. Rift plane, grain plane and head-grain plaine

Table 2. Summary of laboratory samples delivered to each laboratory.

		Research Institute											
		VTT Building and Transport			Helsinki University of Technology			University of Parma			Cevalor		
Marble type	Cutting direction	Size [mm]	Thickness [mm]	Number of samples	Size [mm]	Thickness [mm]	Number of samples	Size [mm]	Thickness [mm]	Number of samples	Size [mm]	Thickness [mm]	Number of samples
A	parallel to rift	800x1200	30	9	800x1200	30	1	800x600	40	1	800x1200	50	1
A	perpendicular to rift	800x1200	30	3	800x1200	30	1	800x600	40	1	800x1200	50	1
D	parallel to rift	800x1200	30	5	800x1200	30	1	800x600	40	1	800x1200	50	1
D	perpendicular to rift	800x1200	30	3				800x600	40	1	800x1200	50	1
E	parallel to rift	800x1200	30	5	800x1200	30	1	800x600	40	1	800x1200	50	1
E	perpendicular to rift	800x1200	30	3				800x600	40	1	800x1200	50	1
K	parallel to rift	800x1200	30	3				800x600	40	1	800x1200	50	1
K	perpendicular to rift	800x1200	30	3				800x600	40	1	800x1200	50	1

Each panel was clearly marked with water resistant colour using the specific code related to the stone type and cutting direction. Marking codes were written both at the edge and at the back of each panel. Rift direction/sawing direction was to be clearly marked on the panel surfaces by using for example dense striping. Test specimens were cut from the panels by respective testing laboratories.

For all Carrara Bianco marble samples IMM stone specialists were responsible for controlling and marking of the cutting directions at quarry and during processing of the test panels. Individual laboratories were responsible for controlling the given directions during preparation of samples and during various testing activities.

2.3 Field test

2.3.1 General scope of the research

Main objective of the field test was to find out the behaviour of different stone types and stone covered structural products in real conditions. The aim of the research was to determine the durability of various marbles in the facades of Finlandia Hall and to study the connection between their real behaviour and that observed in laboratory conditions. In addition, the aim was to examine the behaviour of various structural solutions.

Field test was put into practice using test walls, which were part of the renovated Finlandia Hall facade. In addition to the test walls separate stone samples for destructive laboratory tests were placed on the roof on a supporting structure. By this way the actual test walls remained available for a long-term follow-up research after the Mara project.

Temperature and humidity conditions in the facade cladding as well as the general weather conditions were observed and measured according to a detailed program during the project (see 2.4).

2.3.2 Organisation

Field test was carried out in collaboration with several companies, which took responsibility for delivering the stone samples, structural products and protective agents for the test walls. VTT Building and Transport was responsible for laboratory testing and measurements at site together with HKR Rakennuttaja. Figure 4 shows the organisation structure and the distribution of tasks applied in the field test.

Carrara Bianco samples were delivered by leading Italian stone producing companies Savema Spa and Henraux Spa. Selection of the samples according to the requirements set for the research was controlled by IMM in Carrara. Granite samples were delivered by Erikstone Oy in Finland.

Structural products with stone facing were delivered by:
Joptek Oy, Finland
Aleksin Kivi Oy, Finland
Skanska Prefab AB, Sweden
Stone Panels Inc, USA

Protective chemical agents were delivered by Finnish companies Dyny Clean Kiinteistö Oy and Leni Vesiviljely Oy.

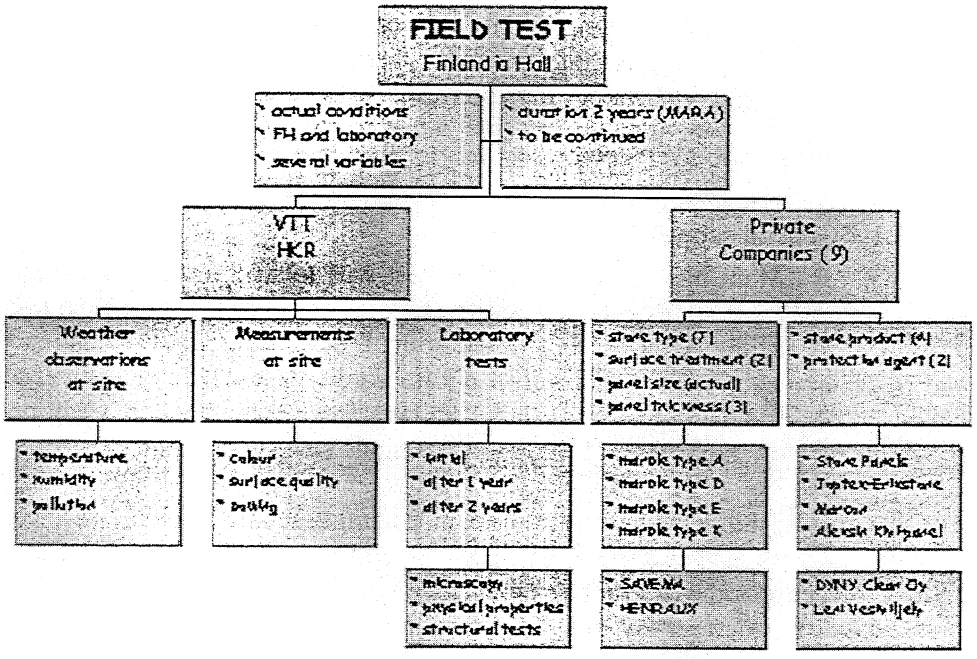

Figure 4. Organisation and task chart of the field test.

2.3.3 Research variables

Parameters included in the field test can be divided in the following groups:

- Carrara Bianco marbles
- granites
- panel size
- panel thickness
- surface finishing
- protective agents
- structural products

Carrara Bianco marbles

Four representative types of white marble from Carrara region were chosen as stone samples. Marble type A was used as reference material. See more detailed at 2.1.3.

Granites
Three types of light coloured granites were included in the research. During the long preparation period for the recent renovation all of these granites have been submitted a permission to be used in the Finlandia Hall façade.
- Tolga White granite from Norway
- Mt Airy granite from USA
- Bethel White granite from USA

Panel size and thickness
Importance of panel size and thickness has often been mentioned as one of the important factors with respect to bowing of the panels. Panel sizes and thicknesses used at the test wall were following:
- sizes according to the architectural design
- panel thicknesses 30, 40, 50 mm

Surface finishing
Honing at 600 was used as the finishing for the actual Finlandia Hall facade cladding panels. It gives Carrara Bianco marble a smoothly shining appearance. Back side of the marble panel is normally with the surface created in the diamond cutting. The surface finishing of the individual panels is for this reason unsymmetric. One of the tested products at the test wall was finished symmetrically at 600 on both sides of the panel.

Surface finishings included in the research were thus:
- unsymmetric finishing
    - front side 600 / back side diamond-sawn
- symmetric finishing
    - front side 600 / back side 600

Protective agents
Chemical impregnating products fill the outer pores of the marble and prevent water and other soluble weathering agents from penetrating in the material. Protection was applied on the outer surface of the tested panels.
Protective surface treatment agents had the following commercial brands:
- Dyny
- Prolapit

Structural products
Basic idea with the structural products is to attach the stone panel into a secondary structural frame. In three of the tested panels marble was glued in the backing material and in one of the panels, marble was fixed mechanically. In the panels where stone is fixed with glue, the thickness of marble coating is only 5-10 mm. Some of the panels are much lighter than massive stone panel due to the low density of the backing material.

Structural products included in the field test were
- Stone Panels
- Joptek-Erikstone
- Marcon
- Aleksin Kivi-panel

2.3.4 Realisation of the field test

Three test walls were placed on the lower roof level of Finlandia Hall as actual parts of the new facade. The walls were built in April and May 1999 during the actual facade renovation of Finlandia Hall. The walls included in the research were view 24, view 23 and view 202. In addition a separate frame was built for the panels intended for destructive laboratory testing during the project.

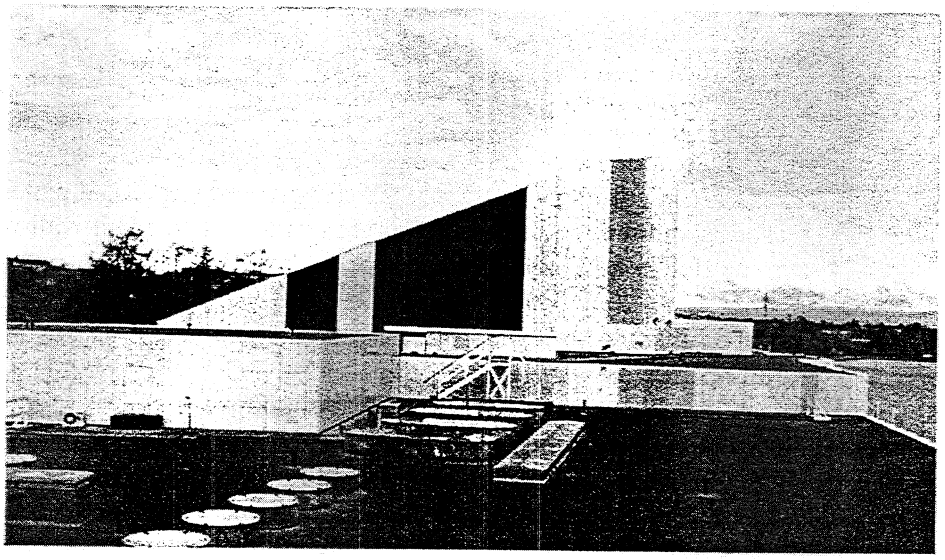

Figure 5. General view of the field test area

Sizes of the panels in the three test walls are according to the architectural plans for the façade. Stone panels were fixed to the load-bearing concrete structure by the same anchors used for the actual façade. Some of the structural products were, however, fixed using special anchors for the product. All test walls are thermally insulated with hard mineral wool with thickness of 150 mm. Panels on the separate frame are supported by the wooden frame structure. Total area of the test wall was 106 m^2 and the total number of full-size test panels was 188 pieces. For each product to be tested the area was between 8 – 13 m^2. Distribution of the test area and the cardinal points are given in table 3.

Table 3. Dimensions of the test walls by views and the separate frame.

	View 24	View 23	View 202	Frame
Cardinal point	south	east	South	South
Height (m)	3,0	3,0	2,0	1
Width (m)	10,5	16,5 + 1,0*1,6	20,8	6
Number of test panels	48	80	60	9

View 24:
This wall is directed towards south, which can in Finnish circumstances, be considered to be a direction with hardest weathering effect due to temperature changes and diagonal rain. Total area used for testing is at this wall about 30m^2. Products tested at this wall are the following:

- Carrara Bianco type A, thicknesses 30, 40 (type B) and 50 (type C) mm
- Carrara Bianco type D, thickness 30 mm
- Carrara Bianco type E, thickness 30 mm
- Structural panel, type F
- Structural panel, type G
- Structural panel, type H

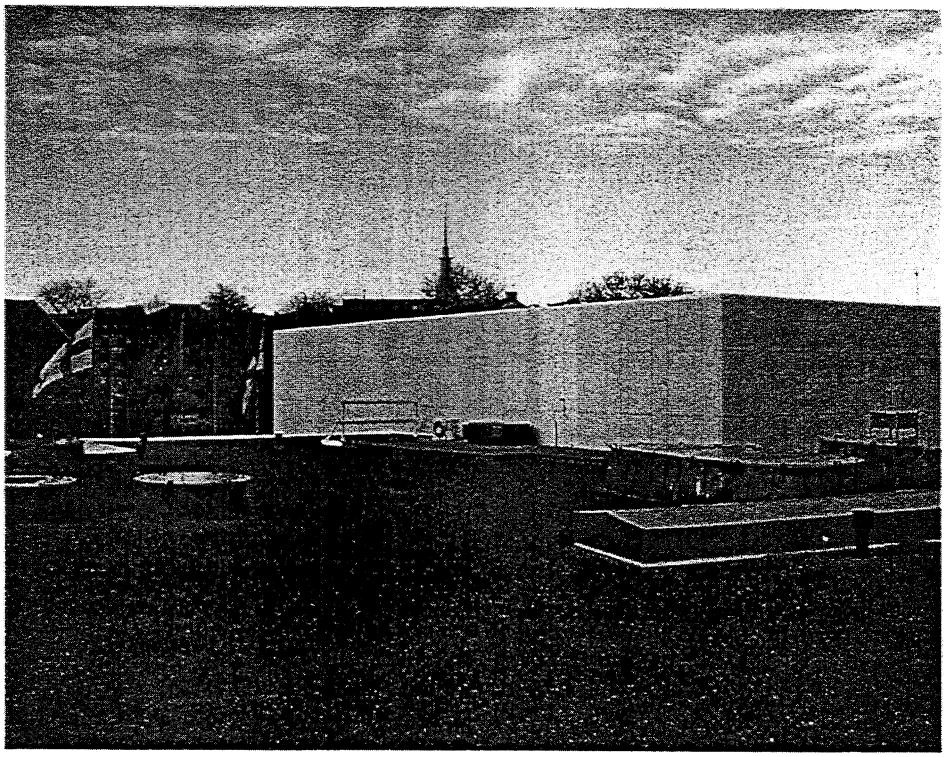

Figure 6. Test wall, view 24

View 23:

This wall is directed towards east with slightly less strenuous weathering conditions than at wall 24. Total area used for testing is at this wall about 51m^2. Products tested at this wall are the following:

- Carrara Bianco type A, thickness 30
- Carrara Bianco type A, thickness 40 (coded as B)
- Carrara Bianco type A, thickness 50 (coded as C)
- Carrara Bianco type D, thickness 30 mm
- Carrara Bianco type E, thickness 30 mm
- Carrara Bianco type K, thickness 30 mm
- Structural panel, type F
- Structural panel, type G
- Structural panel, type H
- Structural panel, type L
- Protective agent type M
- Protective agent type O

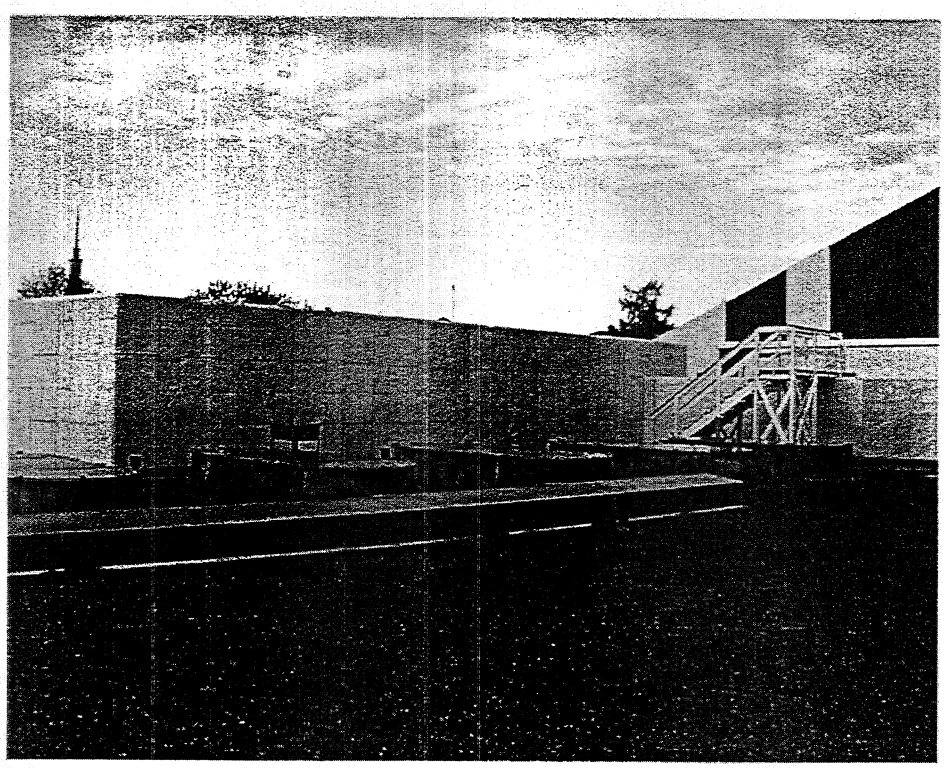

Figure 7. Test wall view 24

View 202:
This wall is directed towards south and is comparable with view 24 with reference to the weather conditions. Total area used for testing is at this wall about 41m^2. Products tested at this wall are the following:

- Carrara Bianco type A, thickness 30
- Carrara Bianco type A, thickness 40 (coded as B)
- Carrara Bianco type A, thickness 50 (coded as C)
- Carrara Bianco type K, thickness 30 mm
- Structural panel, type L
- Protective agent type M
- Protective agent type M
- Protective agent type O
- Granite type P
- Granite type R
- Granite type S
- Surface finishing 600/600

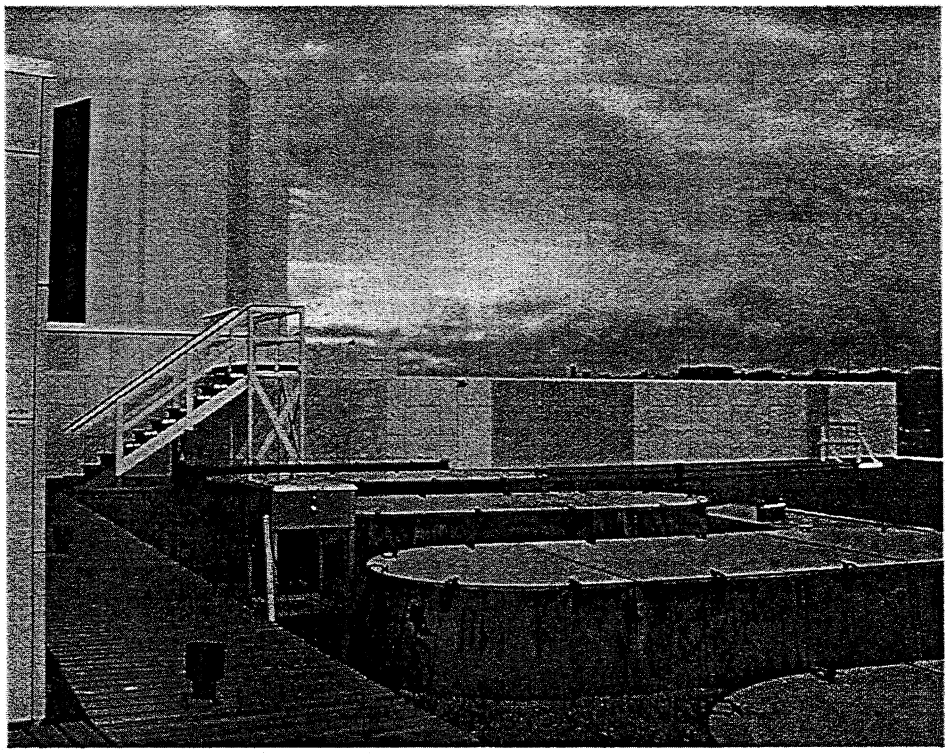

Figure 8. Test wall, view 202

Frame:
Apart from the test walls additional stone samples of some products were placed on the roof on a separate supporting frame. Point of the compass for these panels was south. Idea was to create comparable conditions with the panels in the actual test walls. These samples were used for laboratory tests

in two intervals during Mara project. Total area of the test panels on the frame structure was about $7m^2$. Products on the frame were the following:

- Carrara Bianco type A, thickness 30 mm
- Carrara Bianco type D, thickness 30 mm
- Carrara Bianco type K, thickness 30 mm
- Structural panel, type F
- Structural panel, type G
- Structural panel, type H
- Structural panel, type L
- Protective agent type M
- Protective agent type O

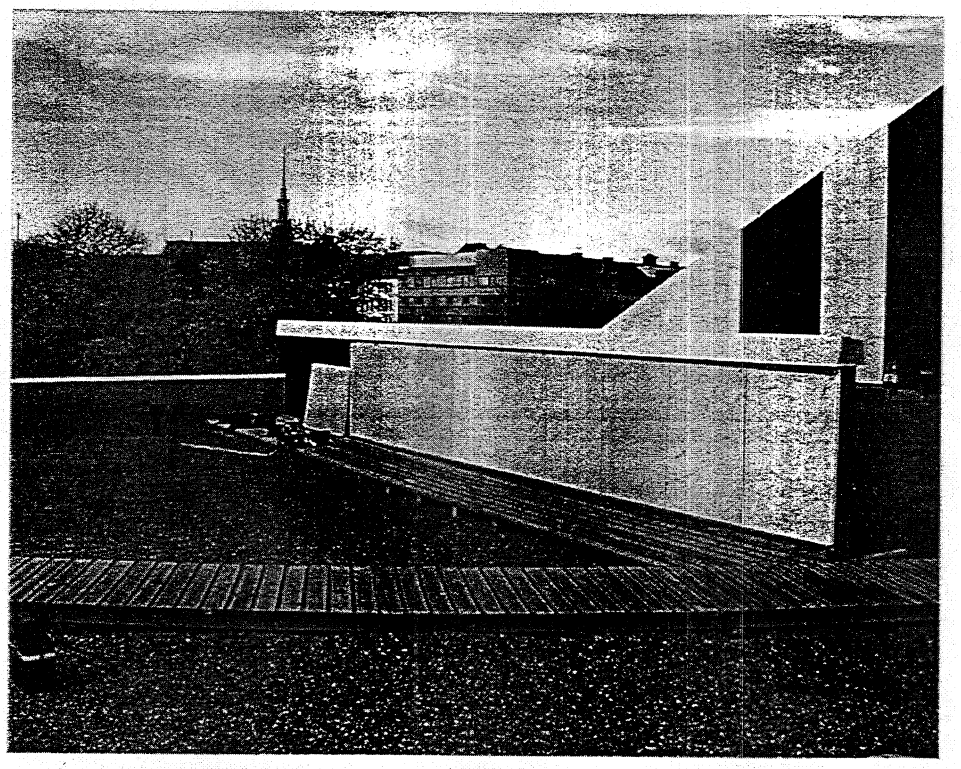

Figure 9. Laboratory test samples on the roof of Finlandia Hall

2.3.5 Research program for field test

2.3.5.1 Objective

The aim of the field test was to identify measurable changes in the functional properties of different marble products during the two-year period of Mara project. It is quite evident that significant changes in stone properties due to weathering normally appear only after several years of service-life. However, using accurate measuring methods, even smaller changes can be registered. On the other hand it is appropriate to continue with the field test

during a longer period of time in order to be able to establish more clearly the changes due to ageing. Main tasks included in the field test were observations and measurements done at site and laboratory tests.

2.3.5.2 Observations at site

Observations and measurements made at site were non-destructive of nature and can be divided in two categories:
- marble surface (colour, roughness)
- bowing of the panels

Changes in the appearance of marble surfaces were measured at site by VTT Building and Transport using a CIELAB system, which is described in detail in *Appendix 1*. Measurements with this device are based on three separate axis: white-black, green-red and blue-yellow. Very small changes in colour of the stone surface could be measured and documented. Based on the measurements the effect of the environmental strain at Finlandia Hall on the colour and the appearance of marbles was determined. In addition visual inspection was performed on more or less continuous basis.

Bowing of stone panels was measured by HKR using special equipment designed for this purpose (see figure 10). This device was used also previously when monitoring the bowing of the old façade of Finlandia Hall. Two panels of each product on each test façade were measured and the changes in straightness were documented. Bowing measurements were repeated five times during the project using each time exactly the same measuring points. Principals applied in bowing measurements are shown in figure 11.

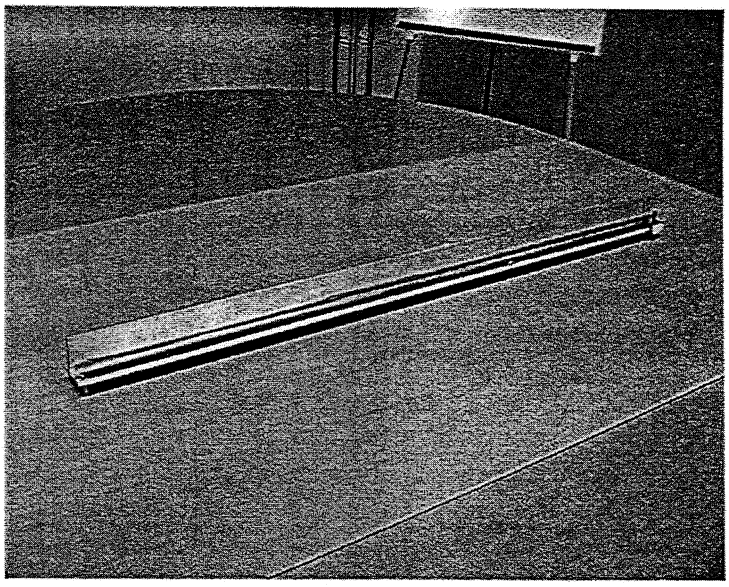

Figure 10. Measuring device for straightness of stone panels.

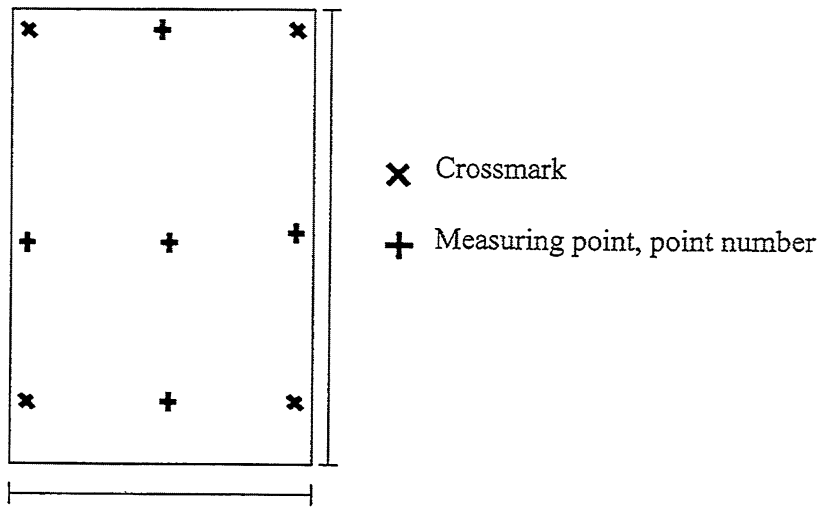

Figure 11. Principals used for the bowing measurements.

2.3.5.3 Laboratory tests

Laboratory tests were destructive of nature and they were repeated three times during the project: in the beginning, after 1 year and after 2 years. For the initial testing unused samples were used. For tests done after 1 and respectively 1,5 years separate stone samples apart from the test walls were used. These samples were placed on a frame structure placed close to the test walls. Half of the samples was cut for tests made after one year and the other half of the samples was put back on the frame to be tested after two years.

Tested properties for massive stone panels were
- flexural strength
- density, water absorption
- microscopic research

Based on the measurements and test results the effect of the environmental strain prevailing at Finlandia Hall on the strength properties as well as on the microstructure and the composition of different marble qualities was determined.

For structural products the following evaluations were made
- adhesion of the glued stones in structural panels
- structural examinations
- microscopic research

Based on the measurements and test results the effect of the environmental strain prevailing at Finlandia Hall on the strength properties of marble clad panels was determined.

2.4 Observation of weather conditions

2.4.1 Scope of the research

The aim was to determine the straining factors that affect the marble and the structures of the facades. This was done by recording the real environmental conditions (temperature, humidity) and their annual variations at Finlandia Hall façade cladding. VTT Building and Transport was responsible for this part of the reseach (Appendix 1).

Four tasks were included in this part of the research:
- designing and installing of the necessary measuring and recording devices
- regular recording of the environmental factors and processing of the data
- acquiring of other necessary information (pH, general weather conditions) and processing of the data
- conclusions and reporting of the results

2.4.2 Measuring and recording arrangements

Prevailing temperatures were recorded from five different marble panels, all of which were placed on roof walls of Finlandia Hall. Four of the panels were chosen in such a way that each one of them was heading to a different cardinal point. The fifth panel was chosen to represent extreme values, and thus it was taken from top of the tower part of the building (point A). The measuring points were as given in table 4.

Table 4. Measuring points for temperature measurements at Finlandia Hall.

Measuring point	Wall number	Cardinal point	Remarks
A	2	South	At the top of the building
B	38	West	
C	13	North	
D	24	South	Field test wall
E	23	East	Field test wall

In each panel specified above there were four thermocouples, which were measuring temperature
- in outdoor air,
- in ventilation gap,
- on outer surface and
- on inner surfaces of the marble panel.

In the measuring point A there was also a fifth thermocouple, which was recording the outer surface temperature of a black granite panel beside the marble panel with the four other thermocouples. Temperature was recorded once an hour in each point, and the values were saved into a data logger.

Recording of temperatures was started in May 1999, and latest measurements were made in the end of February 2001. After Mara project recording of temperatures and humidity is continued for the time being. The data loggers were emptied at regular intervals, and the data collected was downloaded to a transportable computer. Due to power failures or logger malfunction some of the data was, however, lost during the measurement period.

Prevailing relative humidities were recorded from two marble panels, which were panels with the temperature measuring points D and E. In both panels there were three sensors, which were measuring relative humidity in outdoor air, in ventilation slot and in the middle of the marble panel. In order to measure humidity in the middle of the panels, a hole was drilled through the lower edge of the panels before installing them on the roof wall. The sensor was put into the drilled hole, and the hole was sealed. The recording was done as that of temperatures described above. The same data logger as for temperatures was used to save the humidity data.

2.4.3 Other information about weather conditions

The data concerning general weather conditions was acquired from the Finnish Meteorological Institute. Research results from the measurements of acidity of rain water were delivered by the Finnish Environment Institute.

2.5 Laboratory research organisation

Four laboratories from three different countries were involved in the Mara research project. Finnish contribution was given by Building and transport laboratory of Technical research centre of Finland (VTT Building and Transport) and Helsinki University of technology (HUT). Both are located in Espoo.

From Italy University of Parma was chosen because of the previous experience of the key persons available for the research. Cevalor from Portugal was chosen as the leading development and training centre for stone in the country. Figure 12 represents the organisation and task distribution of laboratory research in the Mara project.

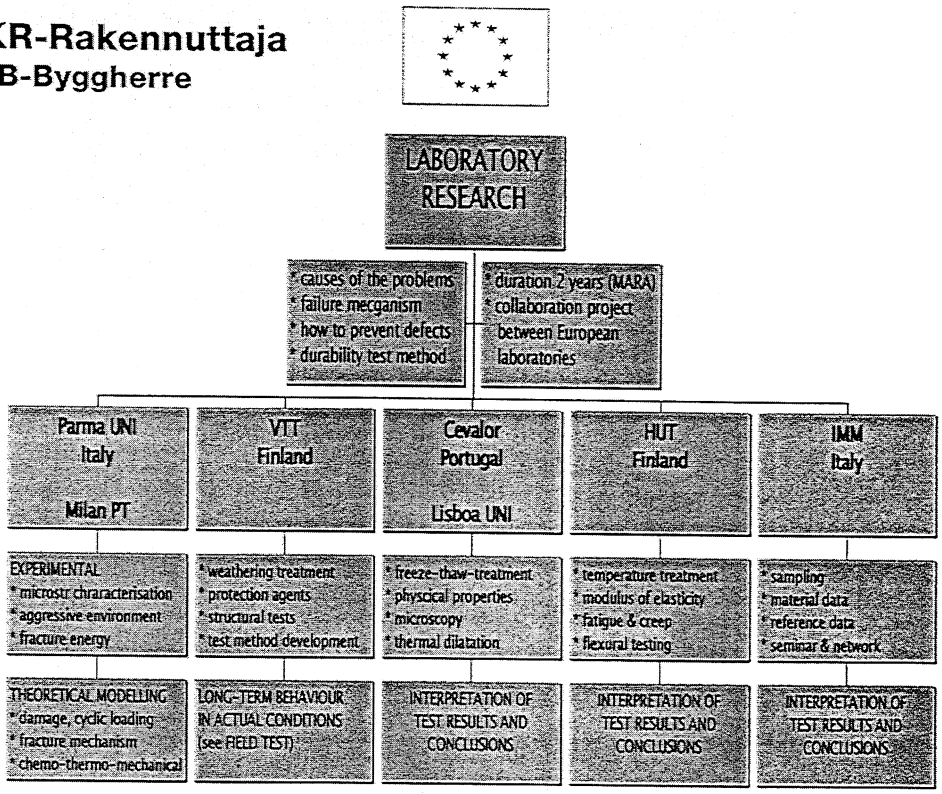

Figure 12. Organisation and task chart of the laboratory research.

Many laboratories involved contributed in the research by bringing a wide range of professional skills and experience to the project. This was very important during the research meetings held during the project. In addition to that the professional contact network behind each laboratory gave a further support to the scientific basis of the research.

On the other hand it was considered as a challenge to manage a multi-laboratory research. This was especially important because of the demanding nature of the objectives in Mara research. Already at the initial stage when the partners where chosen emphasis was given to the consideration of building up a good professional team with ability to collaborate with each other. During the project the effort given to this concern proved to be beneficial.

2.6 VTT Building and Transport research

2.6.1 Scope of the research

Primary goals for the research done at VTT Building and Transport were the following:

- determine the deterioration mechanism of marble,
- set requirements for a durable marble facade structure and
- development of test method for marble suitability.

Research at VTT Building and Transport was also directed to the following studies:

- the environmental conditions at Finlandia Hall (see 2.4)
- the durability of different types of marble,
- the performance of alternative structural solutions and
- the possibilities of using protective treatments.

All parts of the research were done in co-operation with Helsinki University of Technology, University of Parma in Italy and Cevalor in Portugal. VTT Building and Transport was also responsible for all the laboratory tests carried out in connection to the field test (see 2.3).

In addition VTT Building and Transport has also completed a series of tests for Carrara Bianco marble taken from other building objects in Finland. These tests were done in collaboration with the owners of the buildings.

2.6.2 Effect of protective agent

2.6.2.1 Objective

The aim of the subproject was to study the effect of a chemical protective agent on the properties of marble and to determine the quality of the protection mechanism. In addition, the aim of the work was to preliminary evaluate the usefulness of protective agents in marble facades.

In order to achieve the goals set the subproject was divided into three tasks:

- the effect of a protective agent on the durability properties of marble
- the effect of a protective agent on the behaviour of marble exposed to the environmental strains prevailing at Finlandia Hall
- analysis of the results including the evaluation of the usefulness of protective measures

Research was carried out partly at the test wall and partly at the laboratory (Appendix 4).

2.6.2.2 Test wall samples

a) Flexural strength

The flexural strength of the marbles was determined by using the panels taken from Finlandia Hall after 1 and 1.5 years on the test wall. The reference values were measured from the unused panels. The flexural strength of the marbles was determined according to the standard EN 12372:1999.

b) Water absorption, apparent porosity, bulk density

The water absorption, apparent (open) porosity and bulk density of the marbles were determined by using the panels taken from Finlandia Hall after 1

and 1.5 years on the test wall. The reference values were measured from the unused panels.

The water absorption properties of the marbles were determined according to the standard EN 1936:1999.

c) Microstructure

Thin sections of the marble specimens, 0.025x30x50 mm, were prepared at right angles to the surface of the panels. Pieces were cut from the test specimens with a diamond saw, impregnated with epoxy resin and ground first with a grinding machine and then by hand to final thickness (0.025 mm). The thin sections were studied with Leica DM HC LP polarising light microscope and photographed with Leica Q500IW image analysis equipment.

First part of the SEM-study was made by using polished marble sections. Second part of the SEM-study was made by using fracture surface samples of marbles. The samples were broken from the test specimens, any loose material was wiped off and the fractured surfaces were carbon coated.

d) Colour measurement

The behaviour of marble panels on the walls of Finlandia Hall was studied also by measuring the colour of the panel surfaces at regular intervals by CIELAB system. The colour of the panels was measured from eight points, each including three spots. Thus, the colour of the panels was presented as an average of total 24 individual measurement values.

2.6.2.3 Laboratory tests

a) Resistance to UV-radiation

The resistance of the protective agent to UV-radiation was studied according to the standard ISO 4892-2. The effect of radiation was evaluated by using colour measurements using the CIELAB system. The colour co-ordinates of the specimens were measured after the radiation treatment and they were compared with the reference values measured from the treated and untreated panels from which the specimens were prepared.

b) Heat resistance

The heat resistance of the protective agent was studied by treating protected marble specimens in a heat chamber. Three treating temperatures were used: 50°C, 70°C and 110°C. All the specimens were treated in a heat chamber for 100 h. The effect of heat was evaluated by using colour measurements using the CIELAB system. The colour co-ordinates of the specimens were

measured after the heat treatment and they were compared with the reference values measured from the treated and untreated panels from which the specimens were prepared.

c) Chemical resistance

The chemical resistance of the protective agent was studied according to the standard ISO 10545-13:1995. In the test the specimens were immersed vertically to a depth of 25 mm in the vessel containing the test solution maintained there for 12 d. After that the specimens were subjected to running water for 5 d and then boiled for 30 min while completely immersed in water. Finally, the specimens were dried and the effect of chemicals was evaluated visually according to the instructions described in the standard.

d) Resistance to stains

The resistance to stains of the protective agent was studied according to the standard ISO 10545-14:1995. In the test a few drops of staining agents were spread on the surface of the specimens and were left in place for 24 h. After that the specimens were subjected to successively to cleaning procedures described in the standard. After each cleaning procedure the result was evaluated visually and this repeated using more and more effective methods until the stain was removed. The cleanibility class was recorded accordingly as represented in the standard.

2.6.3 One-side weather resistance test

2.6.3.1 Objective

The aim of the research was to study the behaviour of various marbles in one-side weather resistance test and to compare the results with those of the other laboratory weather resistance tests and with the observations made from the marbles that were strained on a test wall in real conditions.

In order to achieve the goals set for the subproject it was divided into four tasks:

- planning of the tests and constructing of the experimental arrangements
- the effect of one-sided weather resistance test on the physical properties
- and on the microstructure of marbles
- analysis of the results and comparisons with other observations
- conclusions concerning especially the practicability of the one-sided test

2.6.3.2 Weather resistance test

a) General arrangements

Two different types of marbles were used in the studies, and they were coded with letters D and E. According to a general assumption formed from practical experiences the marble type E shows a relatively good durability in outdoor applications. Correspondingly, the marble type D was thought to be not durable and thus unsuitable for facades.

One panel of both marbles were chosen for the weather resistance test. The panel of marble D was cut perpendicular to the rift and that of marble E parallel to the rift. The marbles were tested simultaneously.

b) Climate chamber

The tests were basically performed according to the principles presented in the standard DIN 52252/3. A climate chamber that was built to fulfil the requirements set in the standard was used. Except cooling and heating systems the chamber included a fan, water nozzles (4) and lamps (4) producing UV-light (Appendix 3).

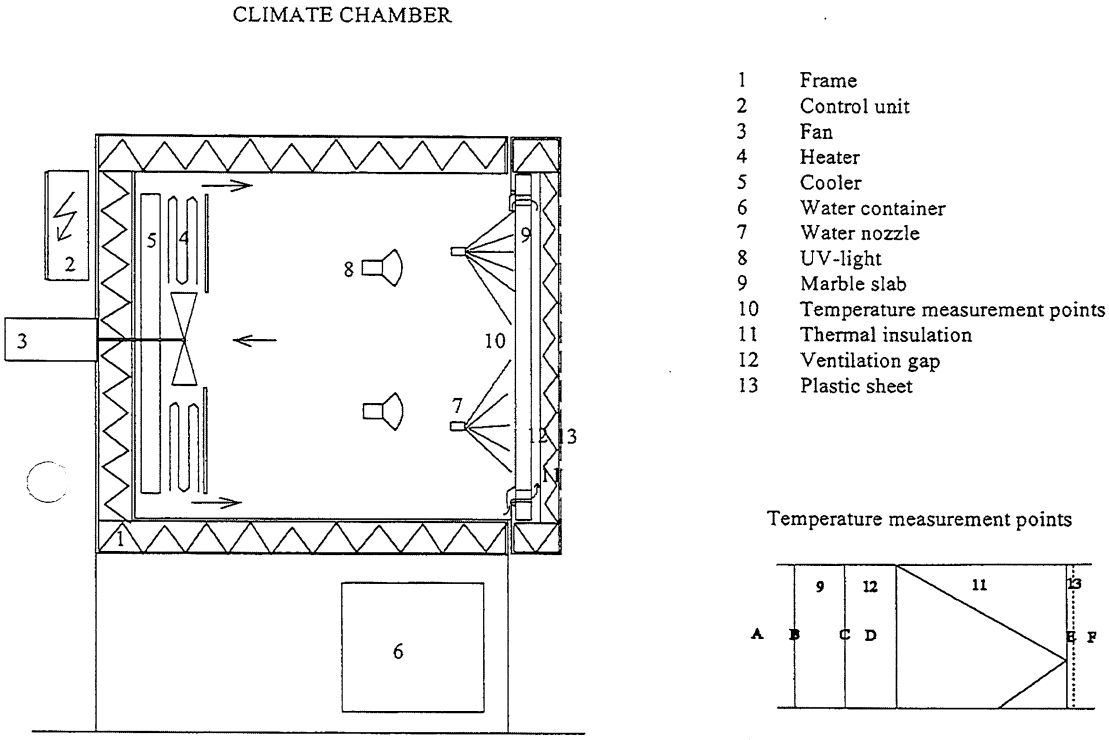

Figure 13. Schematic diagram of the climate chamber and the testing arrangements.

c) Testing program

The cycling procedure was constructed from two separate cycling programs, which were used sequentially. The details of the freeze/thaw cycles of the program 1 are shown in Table 5 and those of the program 2 in Table 5.

Table 5. Freeze/thaw cycle of program 1.

Program phase	Temperature at chamber air	Time (hours:minutes)
Wind	+25 °C	0:10
UV-light, 2400 W/m^2	+25 °C climate chamber air +45...+50 °C marble surface	1:00
Wind	+25 °C	0:10
Water spraying	+25 °C	0:10
Cooling	+25...-25 °C	1:00
Freezing	-25 °C	4:30
Thawing	-25...+25 °C	0:30
Water spraying	+25 °C	0:30
Total time		8:00

Table 6. Freeze/thaw cycle of program 2.

Program phase	Temperature at chamber air	Time (hours:minutes)
Wind	+25 °C	0:10
UV-light, 2400 W/m^2	+25 °C climate chamber air +45...+50 °C marble surface	1:00
Wind	+25 °C	0:20
Cooling	+25...-25 °C	1:00
Freezing	-25 °C	4:30
Thawing	-25...+25 °C	0:30
Wind	+25 °C	0:30
Total time		

2.6.3.3 Properties of marble

a) Flexural strength

The flexural strength of the marbles was determined by using the test specimens taken from the climate chamber after 100 and 200 cycles. The reference values were measured from the pieces of the panels that were left over after sawing the test specimens.

The flexural strength of the marbles was determined according to the standard EN 12372:1999. The samples were sawn from the specimens in such a way that the length of the prisms was either parallel (direction A) or perpendicular (direction B) to the longer side (1200 mm) of the original panels, Figure 14. Six samples were prepared in both directions for each test.

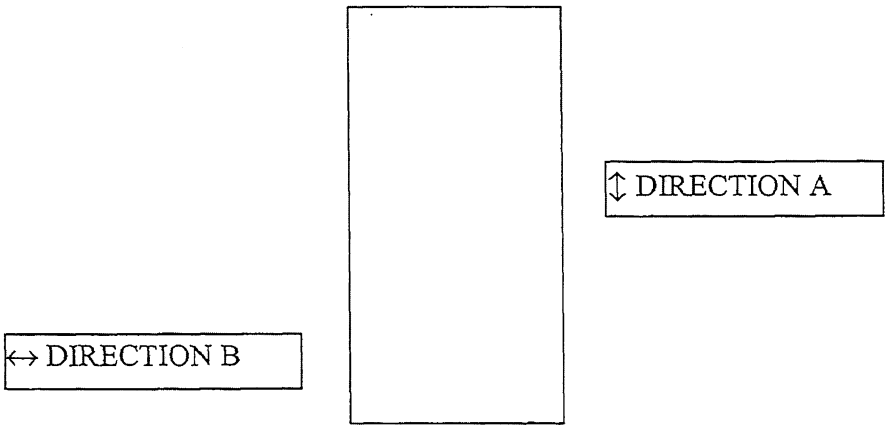

Figure 14. Flexural strength of marbles. Testing directions.

b) Water absorption, apparent porosity, bulk density

The water absorption, apparent (open) porosity and bulk density of the marbles were determined by using the test specimens taken from the climate chamber after 100 and 200 cycles. The reference values were measured from the pieces of the panels that were left over after sawing the test specimens. The water absorption properties of the marbles were determined according to the standard EN 1936:1999.

c) Mineral composition

The mineral composition of the marbles was studied with a Philips PW 1710 X-ray diffractometer. The mineral composition of the marbles was studied also with thermal analysis.

d) Microstructure

Thin sections of the marble specimens, 0.025x30x50 mm, were prepared at right angles to the surface of the panels. Pieces were cut from the test specimens with a diamond saw, impregnated with epoxy resin and ground first with a grinding machine and then by hand to final thickness (0.025 mm). The thin sections were studied with Leica DM HC LP polarising light microscope and photographed with Leica Q500IW image analysis equipment.

First part of the SEM-study was made by using polished marble sections. Second part of the SEM-study was made by using fracture surface samples of marbles. The samples were broken from the test specimens, any loose material was wiped off and the fractured surfaces were carbon coated.

e) Colour measurement, gloss

The behaviour of test specimens during the weather resistance tests was studied also by measuring the colour of the specimen surfaces at regular intervals using the CIELAB system.

The gloss of the surfaces of the marble panels was measured at regular intervals according to the standard ASTM D 523 by using specular angles of 60° and 85°.

f) Warping

Warping of the marble panels was studied by measuring the distance from a measuring rod to the surface of the panel. For the purpose two small metal plates with a hole in the middle were glued on the surface of each marble panel to function as fixed points of the measurements. The distance between the fixed points, L, was 493 mm, and they were installed on the mid-line, parallel to the longer side of the panels. The measuring rod was equipped with supporting feet that could be fitted into holes of the metal plates forming the fixed points. The distance between the lower edge of the measuring rod and the surface of the marble panel was measured in the middle point of the rod by using a dial gauge. The results were compared with the calibration values which were achieved using a straight granite panel. The scale of the dial gauge was adjusted in such a way that a positive value would mean convex bowing of the panel. Correspondingly, a negative value would mean concave bowing of the panel.

2.6.4 Evaluation of marble samples from other facade objects

Marble samples from three different buildings were studied. The buildings were chosen as examples of objects where Carrara Bianco is used as facade material. Common to all buildings were the varying durability problems with the marble facade cladding. The chosen objects were:

- case 1: private owned building situated in Helsinki, built 1965-1966
- case 2: private owned building situated in Helsinki, built 1971, 1985
- case 3: public building situated in Oulu, built in 1979

In addition, the microstructure of a sample taken from the northern tower wall of Finlandia Hall new facade was studied. The cylindrical sample, ∅ 30 mm, was taken in November 2000 by drilling through a 30 mm thick panel. The panels had been installed during summer-autumn 1998.

2.7 Helsinki University of Technology Research

2.7.1 Scope of the research

The objective of this study was to reveal the changes in the particular physical and structural properties of the three Italian marble types exposed to thermal cycling simulating the natural thermal behaviour of the stone façades in Nordic climates. The research was divided in two parts

- material research and
- mechanical research.

Material tests were done at Laboratory of Engineering Geology and Geophysics (Appendix 5). Mechanical studies were carried out by Laboratory of Rock Engineering (Appendix 6).

Material research covers the following marble properties before and after cycling:

- physical properties
- microstructural properties

The physical properties studied were bulk and grain densities, porosity, water absorption, and coefficient of capillary water absorption. The structural properties included mineralogy, and the quantity and quality of resin filled cracks.

Mechanical research can be divided in the following tasks:

- elastic stress-strain behaviour,
- critical stress states in compression,
- bending strength,
- modulus of elasticity in bending and
- measuring of the acoustic emission (AE)

2.7.2 Test program

Three of the marble types were included in the program: A, D and E. For all marble types test samples were cut parallel to the original rift plane. In addition to that another series of samples of type A was prepared cutting perpendicular to the rift.

After sawing all samples were measured and weighed before the cycling and testing phase by Laboratory of Engineering Geology and Geophysics. Before cycling the samples were divided equally into two groups according to the porosity. One group was chosen for thermal cycling and the other for reference samples. In this way the possible deviation caused by the porosity is represented in both groups and the results can be interpreted together.

The temperature and the moisture of the samples were not measured. The samples were always kept at least one day in the same room at the normal room temperature and humidity before the testing.

Half of the samples were thermally cycled. The temperature range in the thermal cycling was -20 to +60 °C degrees. It was chosen to represent the normal average temperature range the marble facade may undergo in actual conditions in Finland. The maximum amount of the cycles were 500 cycles. The tests and treatments in this study refer to dry specimens. Investigation of the effect of freezing or expanding pore water was not included in this study.

The elastic stress-strain behaviour and critical stress states were studied with uniaxial and triaxial compression tests. The modulus of elasticity in bending and bending strength were studied using the three point bending tests. The measuring of the acoustic emission (AE) was used in the uniaxial tests.

Originally it was intended to study the long term strength using creep tests in bending. Due to practical problems in defining the right creep load the creep test was later replaced with a test, where the effect of cycling was studied in bending using 1, 5, 10, 50 and 100 temperature cycles. Only two marble types, APA and LPE were tested. The total number of samples became thus 102 (Table 7, Figure 15).

Table 7. Final test program

Test configuration	*Uncycled tests*	*Cycled tests*
Uniaxial compression test 0.75 MPa/s	12	12
Triaxial compression test, 5 MPa confined	12	12
Bending test	12	12
"Cycling test"		30
Total	36	66
Total of marble samples	**102**	

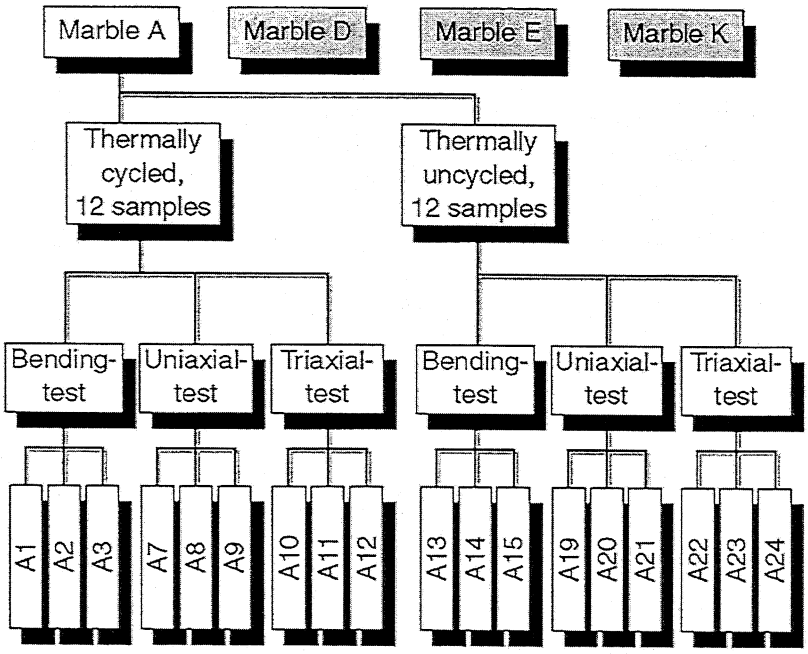

Figure 15. Final test program for one marble type excluding the "cycling" test.

2.8 Parma University research

2.8.1 Scope of the research

Main scope of the experimental activity in University of Parma was to evaluate the leading characteristics of the connection between the constituent calcite grains. Granular decohesion damage occurs when the granular connection is overcome. Standard tests cannot be considered to give quite reliable indications about the durability properties of marble. In order to find a more reliable criteria the experimental procedures were divided in two main categories:

- direct tensile tests with close-loop control of the specimen-head rotations, in order to establishing the strength of the bonding
- bending tests with pre-cracked beam technique, usually employed for ceramic materials, to define the fracture energy.

Apart from these, the University of Parma has given consideration to another series of tests, performed with a high precision dilatometric apparatus. The main goal in these tests, carried out in collaboration with VTT Building and Transport, was to demonstrate that thermally-induced granular decohesion produces, at the macroscopic level, permanent dilatation of marble specimens. This observation is fundamental because it allows to correlate the observed bowing in marble panels, produced by different elongation of material fibres, with damage occurring at the microstructural level.

The aim was to develop, based on the results obtained in the experimental research, reliable theoretical models for explaining the deterioration phenomena at microstructural level such as

- modelling of damage due to cyclic loading,
- modelling of fracture mechanism and microstructure and
- numeric computation and modelling of damage due to chemo-thermo-mechanical actions
- suggestion for a test method to defining the properties and suitability of a given marble for use as a facade caldding material

As a conclusion, the aim was to develop a model for explaining the connection between microstructural behaviour and bowing as a macroscopic consequence of granular decohesion. Finally suggestions of reliable criteria to be applied in the future for restoration activities for Finlandia Hall, was to be given (Appendix 7).

2.8.2 Research program

2.8.2.1 Direct tensile strength

In order to establish the strength of the bonding a direct tensile tests with close-loop control of the specimen-head rotations were carried out. The testing system consisted of a closed-loop electromechnical Instron testing machince with a maximum capacity of 100KN, for which the main characteristics are:

- electromechanical controls with a minimum speed of $2\mu m\ h^{-1}$,
- three control channels, one of which can be external (giving possibility to choose feedback signal that allows a stable tests control),
- closed-loop control with integral and derivative gain (in order to remove the effect of the finite stiffness of the machine).

For the uniaxial tensile test, the specimens were carefully glued to the plates clamped to the testing machine, making the geometrical tolerance between specimens and plates very small. Two cylindrical heads with four micrometers located at right angle one to the other allowed precise positioning of the grips. Attachment of specimens to plates was done directly on the testing machine.

A total number of 23 specimens of the four selected materials, either virgin or conditioned, carved with different orientation with respect to the marble rift plane, were tested under tensile load. The specimen characteristics, with an indication of the reference monograms, are summarised in Table 8.

Table 8. Summary matrix for direct tensile tests.

Direct tensile tests							
N°	Spec. name	Marble-type	test nr.	termal conditioning	Dim (cm)	Angle to rift	comment
1	E1-PA-TT	E	N1	NO	6x12x4	0	-
2	E2-PA-TT	E	N2	NO	6x12x4	0	-
3	E1-PE-TT	E	N1	NO	6x12x4	90	-
4	E2-PE-TT	E	N2	NO	6x12x4	90	-
5	E3-PE-TT/C	E	N3	20 cyc. -20°C to+ 80°C	6x12x4	90	-
6	E4-PE-TT/C	E	N4	20 cyc. -20°C to+ 80°C	6x12x4	90	-
7	K1-PA-TT	K	N1	NO	6x12x4	0	-
8	K2-PA-TT	K	N2	NO	6x12x4	0	-
9	K1-PE-TT	K	N1	NO	6x12x4	90	-
10	K2-PE-TT	K	N2	NO	6x12x4	90	-
11	K3-PE-TT/C	K	N3	20 cyc. -20°C to+ 80°C	6x12x4	90	failed
12	K4-PE-TT/C	K	N4	20 cyc. -20°C to+ 80°C	6x12x4	90	-
13	A1-PA-TT	A	N1	NO	6x12x4	0	-
14	A1-PE-TT	A	N1	NO	6x12x4	90	-
15	A2-PE-TT	A	N2	NO	6x12x4	90	-
16	A3-PE-TT/C	A	N3	20 cyc. -20°C to+ 80°C	6x12x4	90	-
17	A4-PE-TT/C	A	N4	20 cyc. -20°C to+ 80°C	6x12x4	90	-
18	D1-PA-TT	D	N1	NO	6x12x4	0	-
19	D2-PA-TT	D	N2	NO	6x12x4	0	-
20	D1-PE-TT	D	N1	NO	6x12x4	90	-
21	D2-PE-TT	D	N2	NO	4x6x3	90	-
22	D3-PE-TT/C	D	N3	20 cyc. -20°C to+ 80°C	6x12x4	90	-
23	D4-PE-TT/C	D	N4	20 cyc. -20°C to+ 80°C	6x12x4	90	-

2.8.2.2 Pre-cracked bending test

This technique is usually employed for ceramic materials for defining the fracture energy. The fracture toughness, K_c, is considered the main material property qualifying the reliability of brittle materials. The applicability to Carrara marbles of a two-step procedure for fracture toughness determination has been examined.

The testing method used consists of a two-step procedure applied to prismatic bars:

- a starter notch is propagated to a through-thickness configuration using a pre-cracking technique and
- the bar containing a natural crack is fractured under three-point bending loading.

Here special attention is given to the identification of a suitable pre-cracking technique to insert natural flaws in two marbles.

The standard procedure for plane-strain fracture toughness determination requires the introduction of a natural crack of controlled geometry into the specimen. However, the inherent brittleness of marbles, similarly to ceramics, complicates this pre-cracking step. Various experimental techniques have been advanced including diamond saw–through notches or chevron-notches in different specimen geometry, but size effects and actual crack behavior during the test, respectively, complicate the interpretation. Natural cracks of complex shape can be readily inserted in ceramics by Vickers indentation, but it may not apply to rock-like materials.

A conventional linear elastic fracture mechanics (LEFM) interpretation of these methods resorts to the stress intensity factor (SIF) evolution as controlled by the pre-cracking apparatus. SIF evolutions for the two pre-cracking techniques here considered were determined using a combination of the weight function (WF) method (Bueckner, 1970) and the finite element (FE) method. Accordingly, we assume for SIF or K the value

$$K(a) = \int_0^a \sigma(y) h(y,a) dy \qquad (1)$$

where $\sigma(y)$ is the normal stress acting on the perspective crack plane in the uncracked bar and $h(y,a)$ is the weight function for the single-edge-bar geometry (Bueckner, 1970). Three types of specimens were examined:

- specimens artificially indented with a diamond saw,
- natural pre-cracking method B – Bridge method and
- natural pre-cracking method SB – Sandwich Beam method,

Unfortunately, just a few preliminary tests showed that the B-method cannot be directly applied to marbles as micro-cracks are not produced by the indentation method: a starter notch has to be machined instead as shown in the scheme of Figure 16.

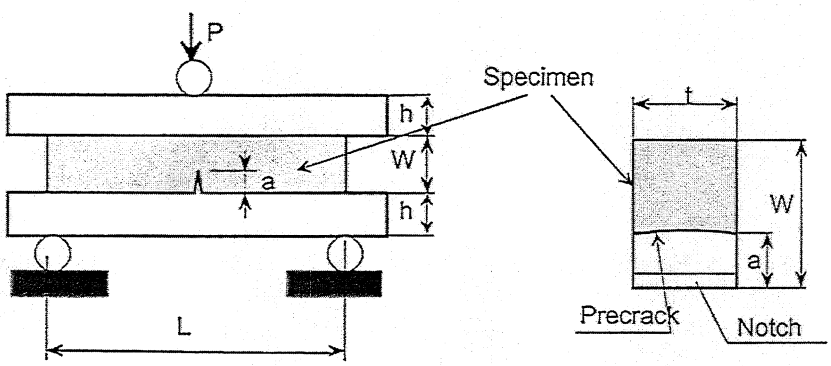

Figure 16. Scheme of the Sandwich-Beam (SB)-method.

The main depth-controlling parameter of the SB-method is the relative bending stiffness of the specimen, $(EI)_s$, and of the sandwich beams, $(EI)_b$, (i.e. $(EI)_b/(EI)_s$ ratio). Two values were examined, namely 1.43 and 4.83. The normal stress distributions in the plane of perspective crack propagation were used in Equation (1) to determine SIF evolution. Subsequent normalization used the bending stress in the specimen defined as $\sigma = 3PL/(2tW^2)$ and the crack length a, as shown in Figure 17.

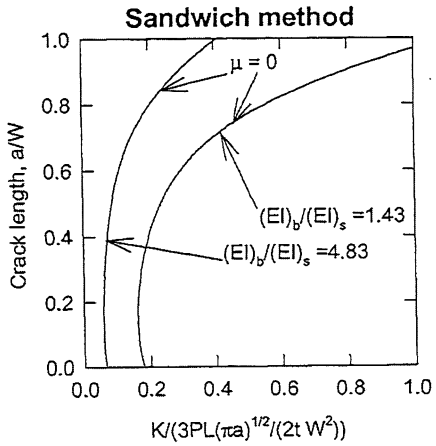

Figure 17. Normalized SIF for the precracking phase of the SB method

In order to investigate the influence of material texture on fracture toughness, approx. thirty prismatic bars (t=10mm, W=20mm, L=100 mm, refer to Figs. 16 and 17) were cut parallel and perpendicular to the material plane of natural schistosity, i.e. the rift plane. The surfaces were polished and a short lateral through notch was inserted using a thin diamond saw. As different marbles reacted differently to the pre-cracking technique, specimens with a sharp 150-μm-wide machined notch were also used to provide a reference value and an alternative experimental route for marbles

The total number of tests performed was thus 50. The natural precracking bridge-method was abandoned after a few preliminary tests. Thus, evaluation of the material fracture toughness was limited to sandwich-beam precracked specimens and to specimens containing natural pre-cracks 150-μm-wide, obtained though a precision diamond saw.

2.8.2.3 Dilatometric tests

In order to assess whether the measured difference in temperature and moisture might be sufficient to provoke bowing, a series of tests was performed using a high-sensitivity dilatometer, able to monitor the expansion of marble while varying its temperature. Since granular decohesion implies volume increase, the permanent dilatation may represent an index of the amount of damage produced. Different qualities of marbles were considered. Dilatometric tests were made in close collaboration with VTT Building and Transport.

Since granular decohesion is always accompanied by opening of intergranular cracks, volume increase and a consequent permanent dilatation should be its counterparts at the macroscopic level. Marble bowing could thus be explained assuming a gradient of the decohesion level through the panel thickness. The reasons why the granular decohesion level should vary through the panel thickness may be numerous and different in type. For ex-

ample, as confirmed by careful measurements, temperature may vary between the inner and outer surface of the façade due to the building internal heating; differences in the humidity level, also confirmed by measurements, might as well play an important role.

2.8.2.4 Modelling of granular decohesion

Experimental observations have provided evidence for that just a few degrees temperature increase, even when uniformly distributed in the specimen, may be sufficient to provoke a progressive detachment of the calcite granules. The characteristic feature of this phenomenon is that the grains remain integral, hardly showing any traces of transgranular cleavage fracture, but rather look as if their cementing material had been gradually destroying.

We recall that possible explanations of the decohesion phenomenon essentially involve three different possible causes:

- the chemical-physical attack of sulfates and chlorides (Winkler 1994);
- the mechanical action of soluble salts which, penetrating in a solution, increase their volume when the solvent evaporates and may expand existing cracks (Franzini, 1995);
- thermal variations, which may cause a self-equilibrated state of stress inside the material (Royer,-Carfagni 1999). Particular hygrometic conditions may, of course, have a synergetic effect with the other causes.

Despite the fact that an universal agreement has not been found yet, our personal experience seems to suggest tentatively that the first two mentioned agents have only a side importance. Examination of the bowing phenomenon in a number of other monuments, show that chemical attack is confined to the superficial crust and hardly any trace of soluble salt can be found inside the slab, despite an evident signs of granular decohesion.

2.8.2.5 Microstructural characterisation

Materials that in nature appear to be composed of aggregates of granules more or less cemented together are usually referred to as natural conglomerates. Despite the generality of our considerations, here we refer to the specific case of Carrara Bianco marble. The various qualities of marble, rather than by appreciable difference in the mineral composition, are distinguished by the dimension, and even more so, by the shape of the constituent grains. These are arranged in microstructural textures which may range between the two extreme cases usually referred to as *homoblastic*, when the grains present gently curved boundaries, and *xenoblastic*, characterized by the close interlacing of weavy contours.

The various qualities of marbles, despite presenting practically the same chemical composition, show considerable differences in their mechanical properties and the experimental evidence suggests relating such differences with the material underlying microstructure. In the present paper we propose

a simple method to describe the microstructural textures, based on the *quantitative* classification of the geometric shape of the grains by means of indicators, likewise the grain area A, the perimeter p or the skeleton s, primarily used in the field of computer vision.

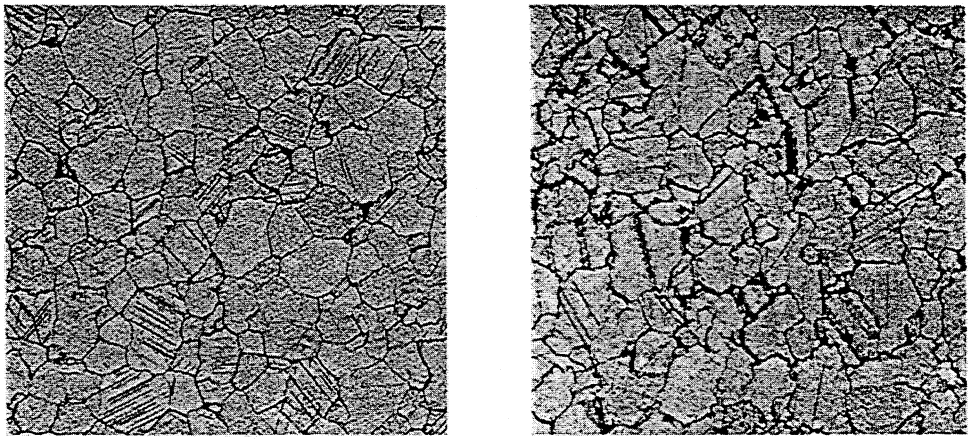

a) b)

Figure 18. Thin sections of typical homoblastic (a) and xenoblastic (b) marbles.

Besides the material classification a possible correlation between the microstructural parameters and mechanical macroscopic properties shall be examined, likewise bending strength or porosity. Recent studies have in fact evidenced that many material properties may be influenced by the underlying microstructure. For example, in (Royer-Carfagni, 1999a) the resulting state of stress in grains subjected to uniform thermal variations has been considered. This stress is originated by the springing apart of contiguous grains due to the anistropic thermal expansion of calcite, since the grains are randomly oriented. In (Royer-Carfagni 1999a) it has been shown that the most dangerous stress at the grain borders, in particular at the texture nodes, where more than two grains converge at one point.

More in particular, the sharper the grain corners are, the less dangerous is the resulting stress, a finding which might suggests that xenoblastic marbles are more resistant than the homoblastic qualities. The experimental investigation (Franzini, 1995) seem to confirm this trend. Another example is given by the fatigue response of marbles subject to cyclic uniaxial (Royer-Carfagni e Salvatore, 1998, 2000). Also in this latter case, tests have confirmed that xenoblastic marbles are, as a rule, more resistant than the homoblastic ones. In conclusion, a quantitative microstructural characterization can allow a prediction of macroscopic mechanical properties and, what is more important as evidenced in (Royer-Carfagni 1999b), an indication of the material natural attitude to granular decohesion thermal damage.

2.9 Cevalor research

2.9.1 Scope of the research

The aim of the work carried out by Cevalor was to give added value to the research of the effect of freezing-thawing treatment on marble properties. Work was completed as a comprehensive series of laboratory tests. In practice the study was divided in six workpackages:

- Workpackage 1 (WP1) - Selection of sites with "old carrara" marble,
- Workpackage 2 (WP2) - Characterisation of the sites.
- Workpackage 3 (WP3) - Collection of samples from sites,
- Workpackage 4 (WP4) - Collection of samples from other stone types,
- Workpackage 5 (WP5) - Testing Campaign,
- Workpackage 6 (WP6) – Comparison of results

Workpackage 5 (WP5) - Testing Campaign, was divided in three tasks:

- initial characterisation,
- testing campaign each 25 cycles of the freeze/thaw;
- Interpretation of results

The chemical characterisation included in the research was done by IGM, Geologic Institute and the microscopic observation by FCT/UNL, Lisbon Univers. All the above referred tests were done for five types of marbles, four Italian and one Portuguese. The testing procedure is given in figure 19 (Appendix 8).

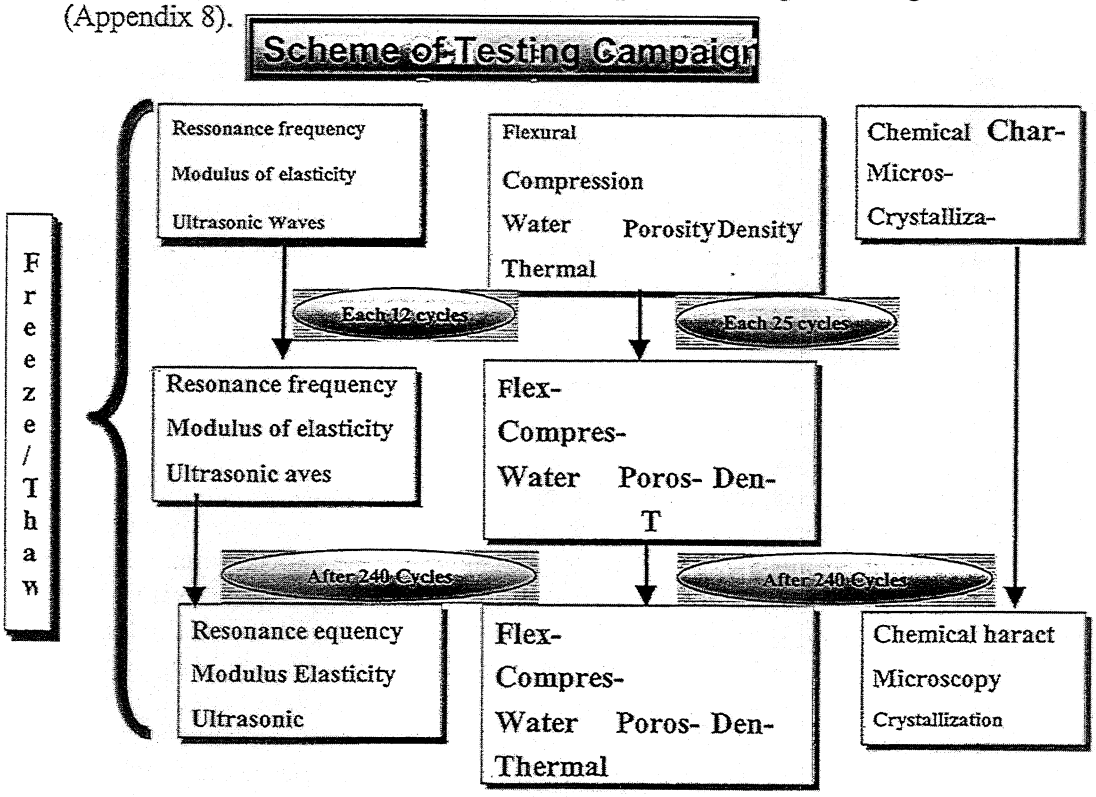

Figure 19. Testing procedure of Cevalor studies

2.9.2 Technical testing program

2.9.2.1 Workpackages

Workpackage 1 - Selection of Sites With "Old Carrara" Marble
Samples of old Carrara Bianco were taken from the Finlandia Hall original façade. In this case the stone has been submitted to several climates variations prevailing in Finland. It's aspect is already characterised by the appearance of decay phenomenas.

Workpackage 2 - Characterisation of The Sites
The Northern countries are characterised by cold winters, with temperatures usually below zero (the annual temperature variations in Finland is from – 30°C to 30°C, leading to situations where stone facade temperatures vary from – 30°C to + 50°C). In southern countries with a more mild climate and hot summers (average temperature around 22°C-35°C) white stone facades can reach up to 60°C.

Workpackage 3 - Collection of Old Carrara Sample From Sites
The Old Carrara sample was provided by the project management.

Workpackage 4 - Collection of Samples From Other Stone Varieties
Several Carrara marble varieties were selected, for testing. In addition a variety of Portuguese marbles was selected by Cevalor initiative, in order to compare obtained values. Portuguese marble with code V was chosen because of its physical/mechanical similarity with the Italian marbles.

Workpackage 5 - Testing Campaign
In order to study the behaviour of the chosen materials, when subjected to climate variations, several tests were done. The following tests were agreed (done according to European Standards defined by CEN/TC 246):

- Freeze/Thaw (prEN 12371),
- Resonance Frequency and Dynamic Modulus of Elasticity (prEN WI00246035),
- Ultrasonic propagation Speed (prEN WI00246012),
- Resistance to Flexural Strength Under Concentrated Load (EN 12372),
- Resistance to Compression (EN 1926),
- Water Absorption at P.t.N, Open and Total Porosity, Volumetric Mass (prEN WI036 and EN 1936),
- Thermal Shock (prEN WI00246016),
- Chemical Characterisation,
- Microscopic Observation,
- Crystallisation Test (prEN 12370).

2.9.2.2 Laboratory tests for WP 5

Freeze/Thaw (prEN 12371)

This European standard specifies a method to assess the effect of freeze/thaw cycles on natural stones. According to the climatic variation and the oscillation between high and low temperatures, were made for each sample about 240 cycles, each cycle consists of a 6 hour freezing period in air until –20°C, followed by 6 hour thawing period until + 20°C during which the specimens are immersed in water.

In order to control the behaviour of the stones, three criteria were used to assess the action of freezing and thawing cycles on the specimens:

visual inspection
measurement of the apparent volume
measurement of the dynamic elastic modulus
measurement of ultrasonic speed
measurement of resonance frequency

For each stone 7 specimens with (300x50x50) mm were used. One specimen was used to monitor the core temperature. In the beginning of the test all samples were dried at 70°C in the oven until constant mass, after dried the specimens were immersed to constant mass was attained.

Resonance Frequency and Dynamic Modulus of Elasticity (prEN WI00246035)

This standard defines methods to determine the fundamental resonance frequency and the calculation of the dynamic modulus of elasticity. The used method was based on continuos longitudinal excitation, with a frequency generator range of 2,8 kHZ.

The calculation of the longitudinal dynamic modulus of elasticity was calculated by the longitudinal resonance frequency and the real density of the stone.

Ultrasonic propagation Speed (prEN WI00246012)

The European standard specifies a method for the determination of the velocity of propagation of pulses of ultrasonic longitudinal waves in natural stone.

A pulse of longitudinal vibrations is produced by an electro-acoustical transducer held in contact with one surface of the stone under test. After traversing a known path length in the stone, the pulse of vibrations is con-

verted into an electrical signal by a second transducer and electronic timing circuits enable the transit time of the pulse to be measured.

Resistance to Flexural Strength Under Concentrated Load (EN 12372)

This European standard specifies a method for the determination of flexural strength under a concentrated load. The load on the specimens was increased uniformly at a rate of 0,25 Mpa/s.

For each stone 6 specimens with (300x50x50) mm were used for initial characterisation, and 2 specimens each 25 cycles during the freeze/thaw campaign. In the beginning all of the test samples were dried at 70°C in the oven until constant mass was attained.

Resistance to Compression (EN 1926).

This European standard specifies a method for determining the compressive strength of natural stones. The load on the specimens was applied at a constant stress rate of 1 Mpa/s.

For each stone 6 specimens with (50x50x50) mm were used for initial characterisation, and 2 specimens each 25 cycles during the freeze/thaw campaign. In the beginning all of the test samples were dried at 70°C in the oven until constant mass was attained.

Water Absorption at P.t.N, Open and Total Porosity, Volumetric Mass (prEN WI036 and EN 1936)

These European standards specifies methods for determining the water absorption, the real density, the apparent density, and the open and total porosity of natural stones.

After drying the specimens at 70 °C in oven until constant mass, the apparent density and the open porosity were determined by vacuum assisted water absorption and submerged weighing of specimens.

Definitions:
Apparent density = the ratio between the mass of the dry specimen and its apparent volume
Apparent volume = the volume limited by the external surface of the specimen, including any voids
Open porosity = the ratio (as percentage) between the volume of the open pores and the apparent volume of the specimen

For each stone 6 specimens with (50x50x50) mm were used for initial characterisation, and 2 specimens each 25 cycles during the freeze/thaw campaign.

Thermal Shock (prEN WI00246016)

This European standard specifies a method to assess possible modifications, of natural stones under the effect of sudden changes in temperature (thermal shocks)

After drying at 70° C until constant mass was attained, the specimens were submited to successive cycles, each formed by drying at 70° C followed by immediate immersion in water at 20±5°C

For each stone 6 specimens with (200x200x2) mm were used for initial characterisation, and 2 specimens each 25 cycles during the freeze/thaw campaign.

Chemical Characterisation

The chemical analyse consist in determination of major elements by ray X florescence. This test was made in the beginning and after the end of the freeze/thaw.

Microscopic Observation

The microscopic observation consisted in two types of observation, the petrography and the SEM, Scanning Electron Microscope. The tested samples were observed, at different stages of freeze/thaw.

Crystallisation Test (prEN 12370).

This European standard specifies a test method to assess the relative resistance of natural stones with an open porosity greater than 5%, the objective is to evaluate the damage caused by the crystallisation of salts.

For each stone 6 specimens with (40x40x40) mm were used for the initial characterisation and 2 specimens after the end of freeze/thaw campaign. In the beginning of the test all samples were dried at 70°C in the oven to constant mass. The Crystallisation tests were made

2.9.3 Case studies

In addition to the technical testing program a study was made to collect data about experiences on use of marble in Portugal. The aim of this work was to find objects in Portugal with facades of Carrara Bianco or Portuguese marbles. This was done in the first place by contacting the following groups:
- Stone Companies
- Architects Offices
- Building Companies

Information was then collected by interviews of parties involved in the specific object and other technical experts available. Main objects were documented by photographing.

2.10 Collaboration with IMM

2.10.1 Internationale Marmi e Macchine

Internationale Marmi e macchine (IMM) is an organisation representing the Italian stone industry in Carrara region. General purpose of IMM activities is to promote the use of building stone for building purposes and monuments. For this purpose IMM provides versatile development, expert and marketing services. One of IMM activities is to participate in the European standardisation and international development work. Main even organised by IMM is the annual international stone fair in Carrara, which has been organised since late 1970's. Carrara stone fair is directed in the first place to stone material production and stone processing equipment. In addition a professional seminar is organised each year for real estate owners, designers and other professionals in the stone field.

2.10.2 Main objectives and tasks

In Mara project IMM had several roles. Main objective was to provide the project with information and better understanding of Carrara Bianco, its production and use in the buildings worldwide. On the other hand IMM gave support to collaboration with the local marble producers and played an active role as an organiser of the dissemination seminars in connection to the stone fairs in Carrara in 1999, 2000 and in 2001 for the presentation of the final results of the project.

In the beginning of the project IMM gave professional assistance to choice of the stone types and took responsibility for the local quality control during the sampling process. This is very important in a multi-laboratory project like Mara in order to guarantee equal quality of stone material used in individual laboratories. For comparability of the research results it is essential to be able to provide all laboratories with similar samples.

2.11 Structural considerations

Aim of the study is to find recommendable structural solutions for a natural stone cladding. Special attention is paid to the conditions in the northern climate and especially the specific requirements in the case of Finlandia Hall. Approach is based on techno-economical functionality requirements combined with the structural stability and safety considerations.
The work was divided in the following areas:
- cladding panels
- fixing technology
- physical design principals
- other design considerations

Alternative solutions for the cladding panel were evaluated. Structurally we can divide the alternative panel products into the following types:
- massive stone panel
- thin stone on a light honeycomb backing
- thin stone on a concrete backing
- reinforced stone panel

Alternative solutions were studied both in the field test and in laboratory. main emphasis was given to the durability and technical reliability aspects.

Different technical solutions available today were evaluated based on the new knowledge gained from Mara research. Additional methods were a literature review and a theoretical approach combined with numerous practical experiences obtained in actual conditions. Development and testing of new fixing and installation methods was not included in the research. Collected data was summarised in the form of recommended design principals and examples of acceptable solutions.

3 RESULTS AND DISCUSSION

3.1 Field test

3.1.1 General

The field test was established in order to gain information about the changes appearing in the products included in the test. Being carried out in the natural conditions without any accelerating factors included, it was expected that significant signs of alteration could not be recorded during the two-year period of Mara project. However, evident changes could be measured in some of the samples already during the first year. Clear correlation could be noted between real behaviour of marble samples and that observed in laboratory conditions. This was especially the case with marble type D, which showed the most significant decay of quality during the test.

From the research point of view it is clearly appropriate to continue with the field test during a longer period of time in order to be able to establish more

clearly the behaviour of the tested marbles in controlled conditions (Appendix 2).

3.1.2 Colour measurements

The colour of the marble panels chosen for this part of the study was measured 5 times between 23.6.1999 and 8.3.2001 with 5-6 months intervals.

All the marbles were initially white, the L value of the unused panels varying between 80 and 90. Marbles D and E had the highest value and marble K the lowest. The values of the coordinates a and b were close to zero, although all marbles had a slight greenish-blueish hue. The colour coordinate L of marble panels placed on the eastern wall (23) in initial stage (measurement 1) is shown in Figure 20 and the development of the L-value for marble A samples can be seen in Figure 21.

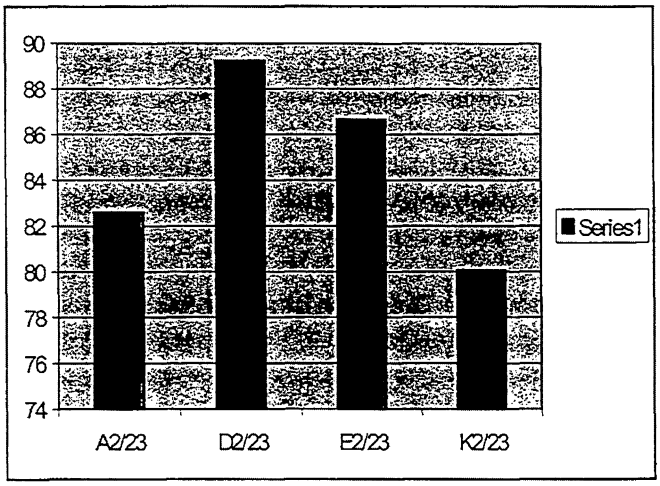

Figure 20. CIELAB colour coordinate L of the marbles. Eastern wall, first measurement 23.6.1999 (1).

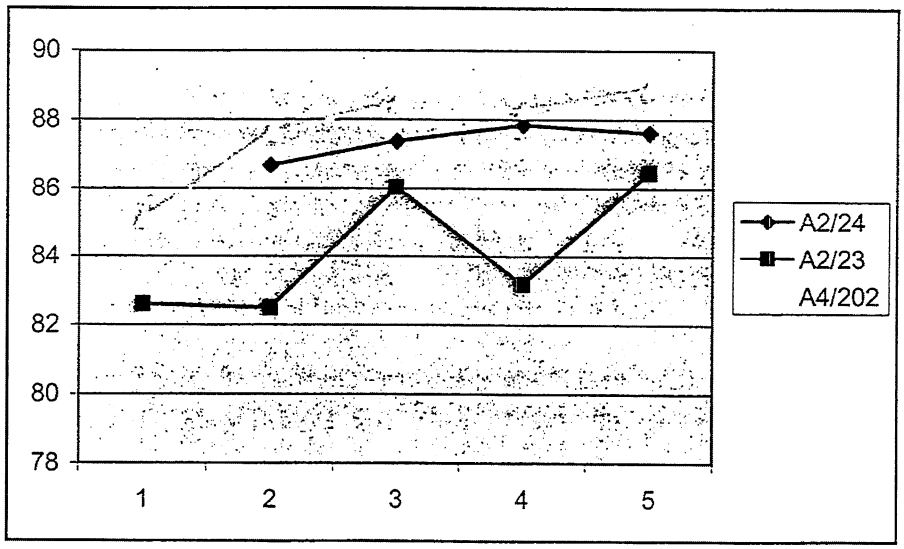

Figure 21. CIELAB colour coordinate L of marble A.

According to the colour measurements the whiteness of the marbles increased. This was evident especially during the first year. After that the changes seem to have been slow, if not negligible. In addition, there has been a slight tendency for the coordinates a and b to move towards more positive values. This means that the marbles are getting more yellow and more red, which could refer to fouling of the marble surfaces. Until now the changes have, however, been small. Results of the measurements of colour coordinates a and b for marble A are shown in Figures 22-23. Detailed results are presented in Appendix 1.

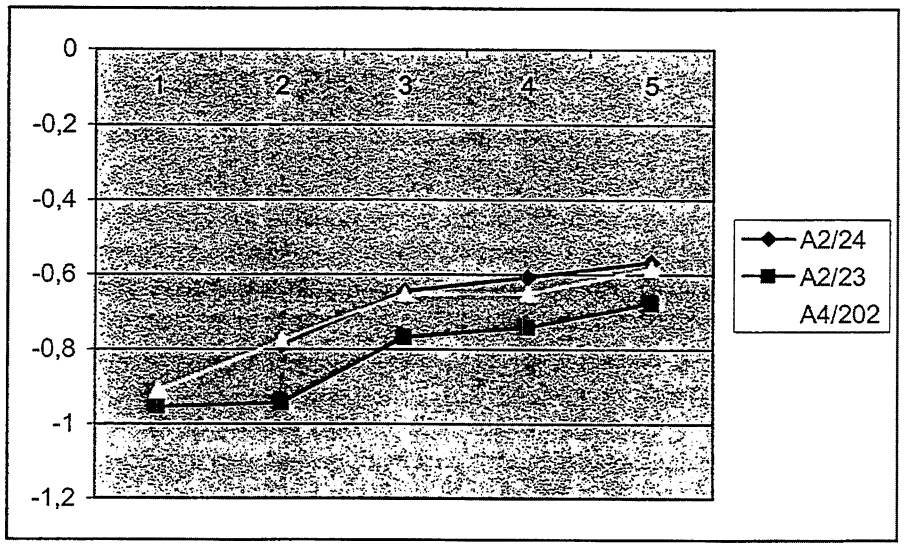

Figure 22. CIELAB colour coordinate a of marble A.

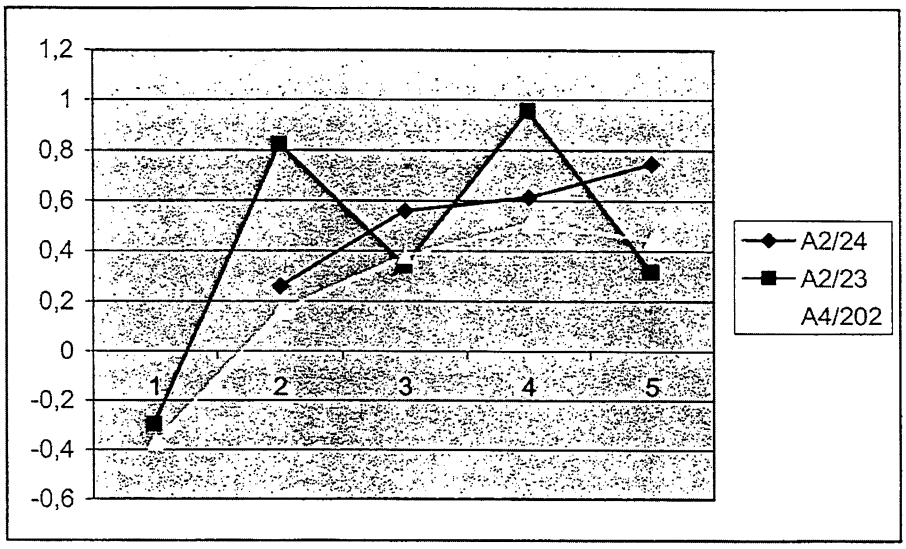

Figure 23. CIELAB colour co-ordinate b of marble A.

3.1.3 Bowing measurements

Straightness of the marble panels was measured five times during the project. The first measurement documented the initial stage of the panels and it was done a few months after completion of the field test façades to ensure that the panels have properly settled to their positions. The panels were measured between 22nd September 1999 and 8th March 2001. Continuation of bowing measurements after this project has not been decided yet, but some kind of monitoring will most certainly continue.

In the beginning it seemed that two years is too short time to notice any differences between the products. The measurements showed this first conjecture to be wrong, very clear differences can be seen in the results (presented more in detail in appendix 9). For example on the wall 24 facing south, massive marble panels have showed very clear bowing (see figure 24).

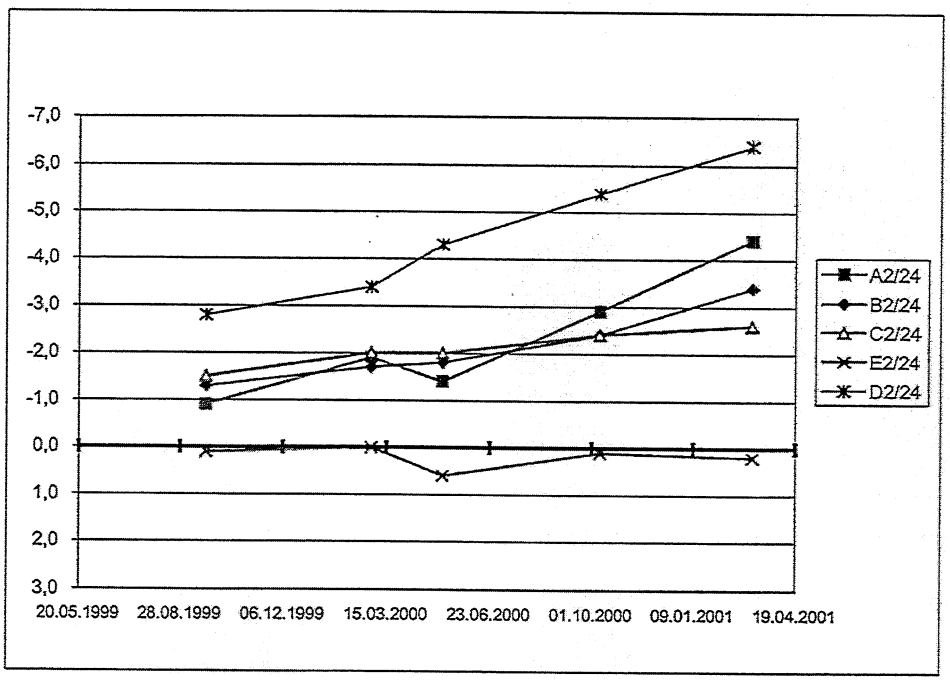

Figure 24. Measured bowings on wall 24. Massive marble panels.

The magnitude of bowing seems to be following the degree of homoblasticity, the most bowed is product D, which is presenting pure homoblastic marbles, and the less bowed –or practically straight- is product E presenting pure xenoblastic marbles. Same phenomena can also be seen on walls 23 and 202, the former facing east and the latter facing south (see figures 25 and 26).

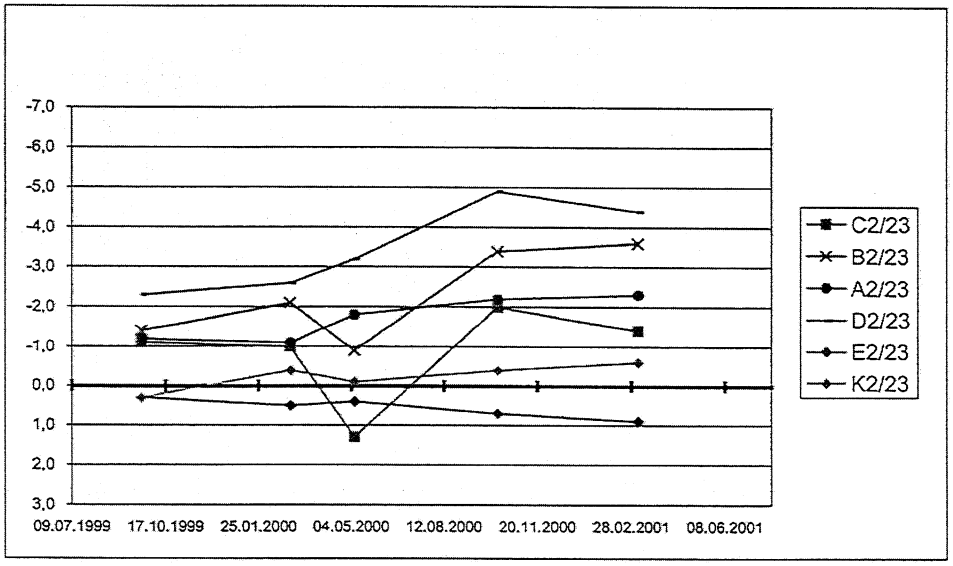

Figure 25. Measured bowings on wall 23. Massive marble panels.

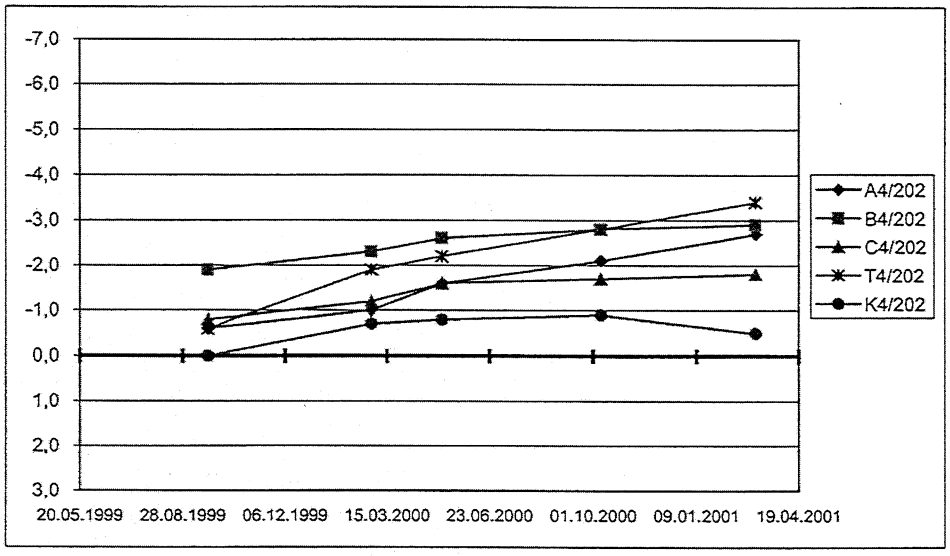

Figure 26. Measured bowings on wall 202. Massive marble panels.

Bowing measurements show also quite clearly the function of two different protective agents. In figure 27 are presented the bowing measurements from the wall 202. Product A is also added in the figure for comparison since products M and O are derived from it by adding protective agent. These measurements confirm, although they can be considered as indicative due to the relatively short observation time, the results introduced later in this report. Protective agent seems not to be able to prevent marble from bowing.

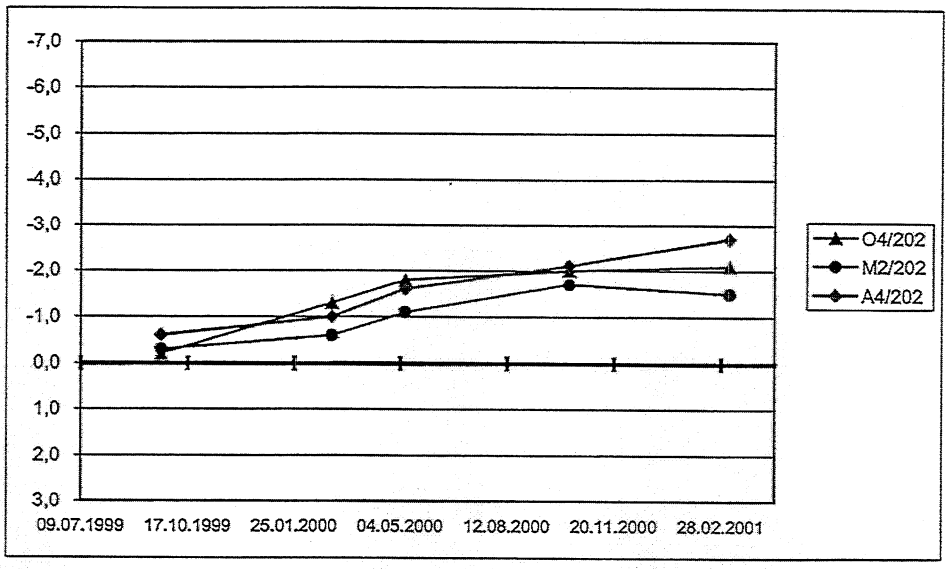

Figure 27. Measured bowings on wall 202. Protective agents.

Also several types of different structural products were included in the field tests. Products present very different structural ideas and also significant differences in their performance can be seen. Also for these products the observation time has been too short to make final conclusions, but some very clear conjuctions can be made already now. Figures 28 and 29 present the results. Also in these figures product A has been added for comparison, although it is not used in the structural products.

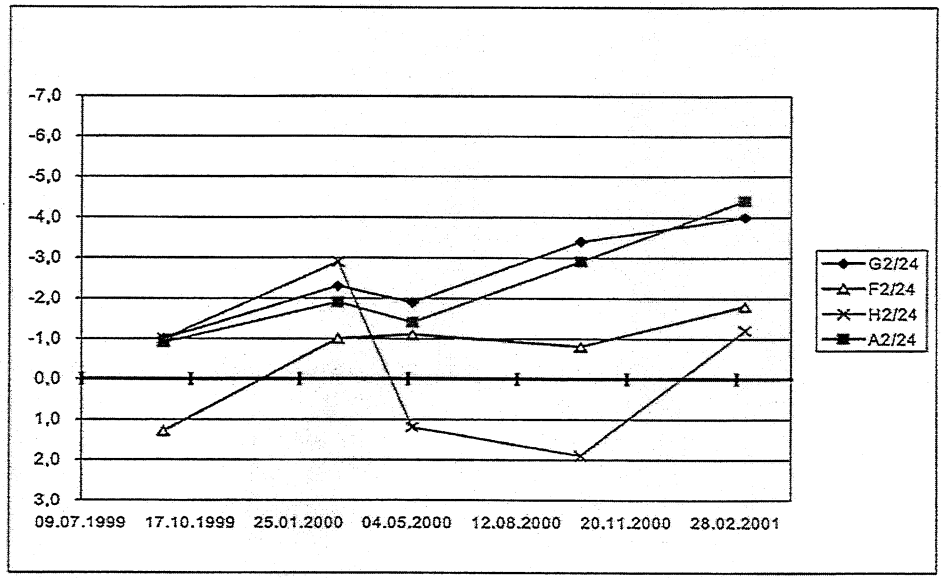

Figure 28. Measured bowings on wall 202. Structural products.

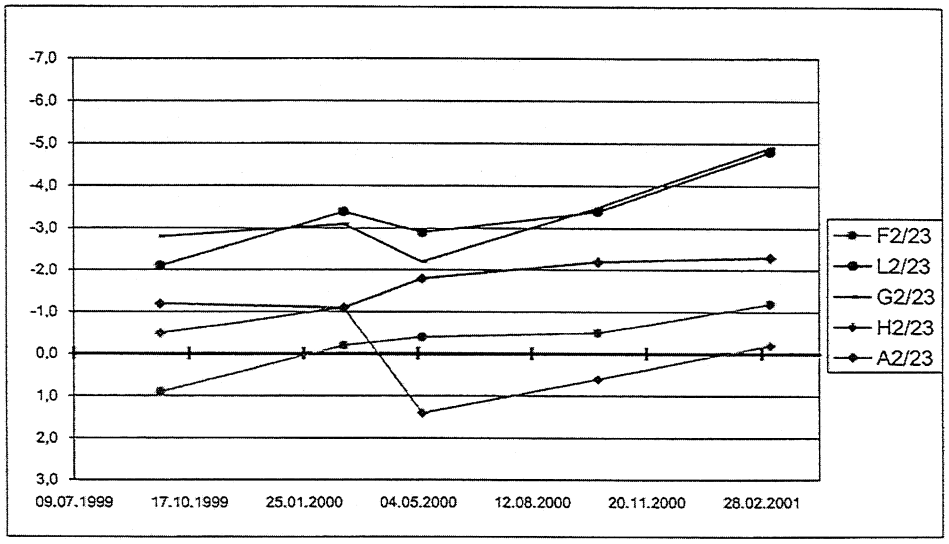

Figure 29. Measured bowings on wall 23. Structural products.

Also three different granites were included in the field tests. Measured bowings are presented in figure 30. Bowing as a word is very much of exaggeration in this context, practically no changes in the straightness of these products can be seen.

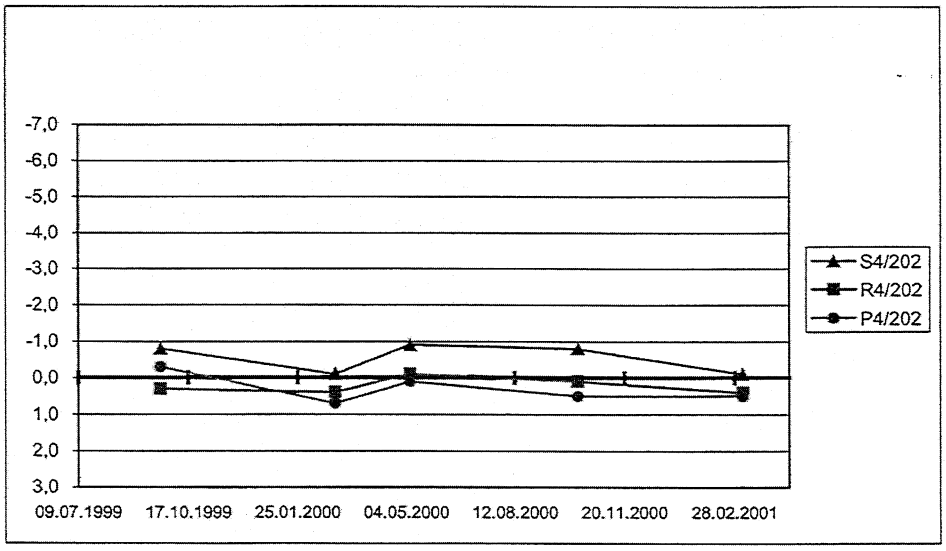

Figure 30. Measured bowings on wall 202. Granites.

3.1.4 Flexural strength

Initial values of flexural strength of marbles A, D, E and K are presented in figure 31. The relative changes of the flexural strengths, ΔR_{tf}, of the marbles that have taken place on the test wall are presented in Table 9. The basis of

the comparison is in all cases the flexural strength of the unused marble. Detailed measurement results are shown in Appendix 1.

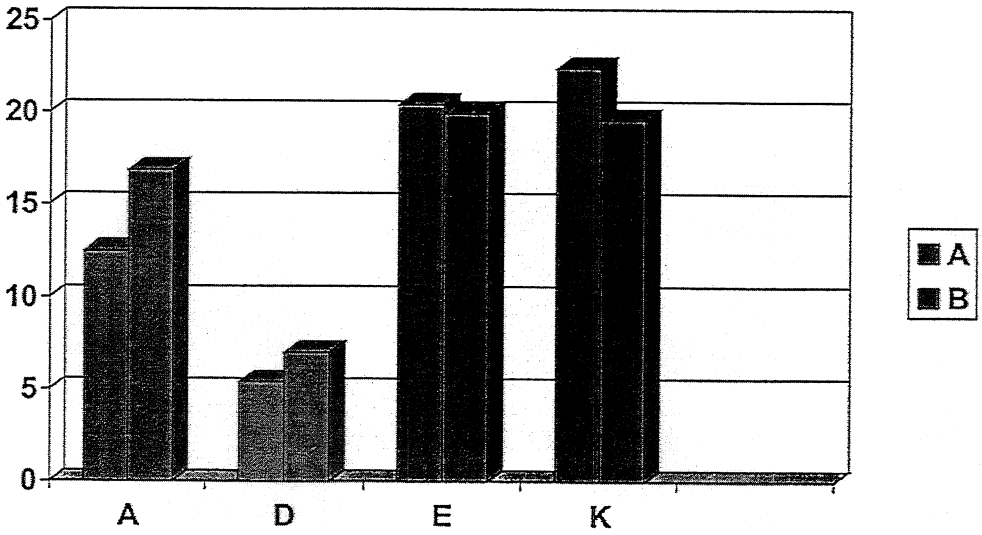

Figure 31. The initial flexural strengths of the marbles (MPa).

Table 9. The relative changes of the flexural strengths of the marbles on the test wall.

Marble type	Δ W	
	1 year (%)	1,5 years (%)
A		
direction A	-16	-20
direction B	-17	-17
D		
direction A	-35	-34
direction B	-48	-42
E		
direction A	-17	+11
direction B	+20	+21
K		
direction A	-3	-2
direction B	-2	+4

3.1.5 Water absorption, apparent porosity, bulk density

The water absorption, apparent porosity and bulk density of marble A in initial stage and after 1 and 1.5 years on the test wall at the Finlandia Hall are presented in Table 10. The corresponding values of marbles D, E and K

are presented in Appendix 1. The presented results are average values (av.) and standard deviations (s.d.) calculated from the testing data of individual samples.

Table 10. Water absorption, apparent porosity and bulk density, marble A.

	water absorption w-%	**apparent porosit** vol-%	**bulk density** kg/m^3
unused			
av.	0.113	0.307	2713
s.d.	0.003	0.009	0
s.d. (%)	2.7	2.9	0
test wall / 1 year			
av.	0.202	0.546	2710
s.d.	0.010	0.027	2
s.d. (%)	5.0	5.0	0.07
test wall / 1.5 years			
av.	0.200	0.540	2706
s.d.	0.018	0.049	1
s.d. (%)	9.0	9.1	0.04

Water absorptions of the marbles are shown in Figure 32.

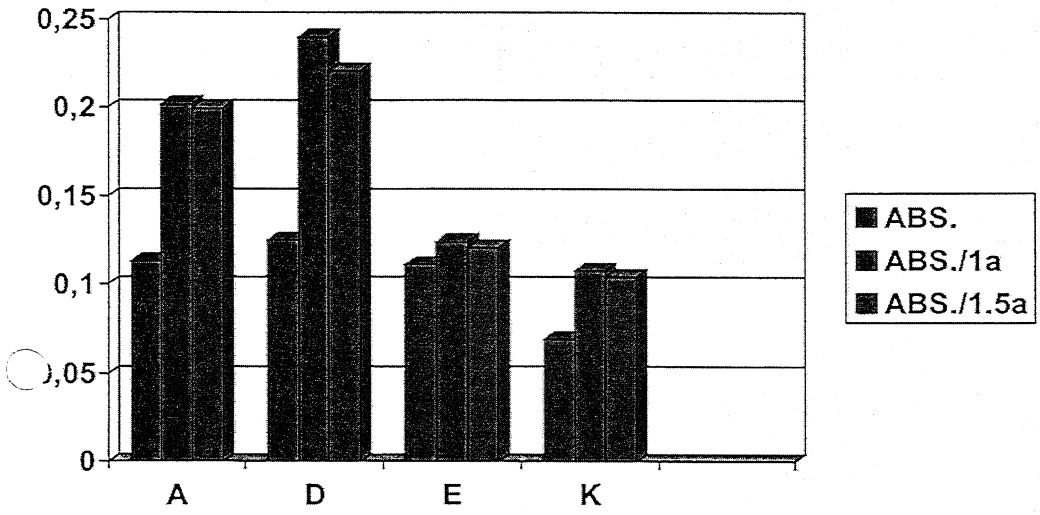

Figure 32. Water absorption of the marbles (w-%).

The relative changes of the water absorption, ΔW, and apparent porosity, Δp_o, of the marbles that have taken place on the test wall are presented in Table 11. The basis of the comparison is in all cases the value of the unused marble.

Table 11. The relative changes of the water absorption and apparent porosity of the marbles on the test wall.

Marble type	Δ W	
	1 year (%)	1,5 years (%)
A	+79	+77
D	+92	+77
E	+12	+9
K	+57	+51

3.1.6 Microscopic research

3.1.6.1 Mineral composition

According to the X-ray diffraction diagram marble A consisted almost entirely of calcite, i.e. calcium carbonate, $CaCO_3$. Quartz, α-SiO_2, and feldspar, Na-K-Ca-aluminium silicate, were also observed. The contents of these accessory minerals were, however, low, at most only a couple of weight percents. Structural products

According to the X-ray diffraction diagram marble D consisted almost entirely of calcite, i.e. calcium carbonate, $CaCO_3$. Quartz, α-SiO_2, and dolomite, $CaMg(CO_3)_2$, were also observed. The contents of these accessory minerals were, however, low, at most only a couple of weight percents.

According to the X-ray diffraction diagram marble E consisted almost entirely of calcite, i.e. calcium carbonate, $CaCO_3$. Marble contained also a substantial amount, probably 5-10 w-%, of dolomite, $CaMg(CO_3)_2$. Quartz, α-SiO_2, was also observed, but its content was low.

According to the X-ray diffraction diagram marble K consisted almost entirely of calcite, i.e. calcium carbonate, $CaCO_3$. Quartz, α-SiO_2, and dolomite, $CaMg(CO_3)_2$, were also observed. The contents of these accessory minerals were, however, low, at most only a couple of weight percents.

The thermal behaviour of all the marbles was practically identical. The thermal curves contained only one phenomenon, the disintegration reaction of calcite in the temperature region of 700°C-950°C. In the curves of the marble E there was, however, a small effect, "a shoulder", at about 750°C. This probably refers to dolomite in which the disintegration reaction includes two separate steps, first of which is comprised of the dissociation of magnesite and the second of the dissociation of calcite. Weight losses of the marbles at 1000°C, Δm_T, and temperatures of the maximum rate of the weight change, T_{max}, taken as the temperatures of the peaks of the DTG-curves as well as the thermal curves of marbles are shown in Appendix 1.

3.1.6.2 Microstructure

Photographs of the microstructure of marble A, unused and after 1 year on the test wall, are shown in Figs. 33-34. Following observations were made:

- groundmass fine-grained, fairly even grained, not oriented, massive
- average grain size 200-300 µm
- slightly porphyroblastic, some larger porphyroblasts (max ∅ 6 mm) in the groundmass
- nearly pure carbonate rock, contains only very little opaque minerals
- alteration of the grains insignificant
- no changes observable after 1 year on the test wall

Figure 33. Microstructure of marble A. Unused. Plane-polarized light.

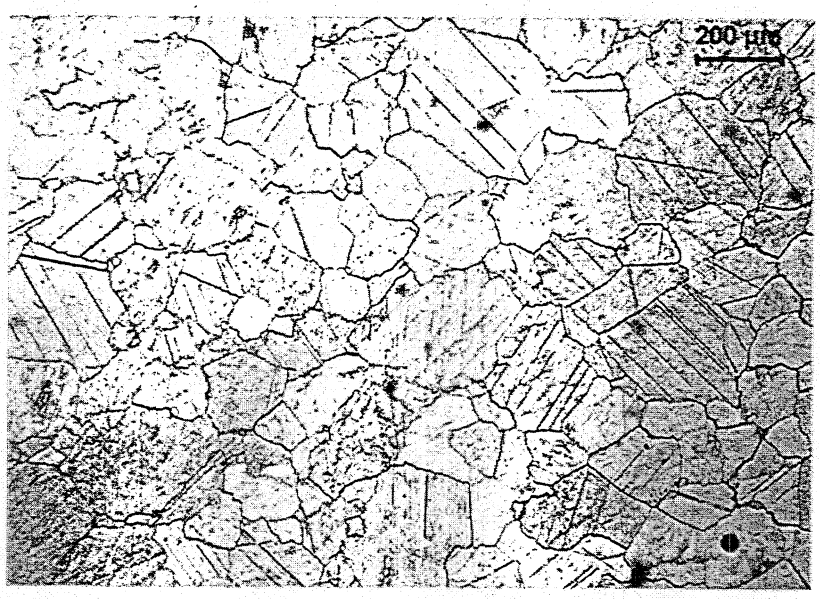

Figure 34. Microstructure of marble A. 1 year on the test wall. Plane-polarized light.

Photographs of the microstructure of marble D, unused and after 1 year on the test wall, are shown in Figs. 35-36. Following observations were made:

- fine-grained, fairly even grained, nor oriented, massive
- average grain size 200-300 µm
- nearly pure carbonate rock, contains very little mica type minerals
- some alteration of the grains
- no changes observable after 1 year on the test wall

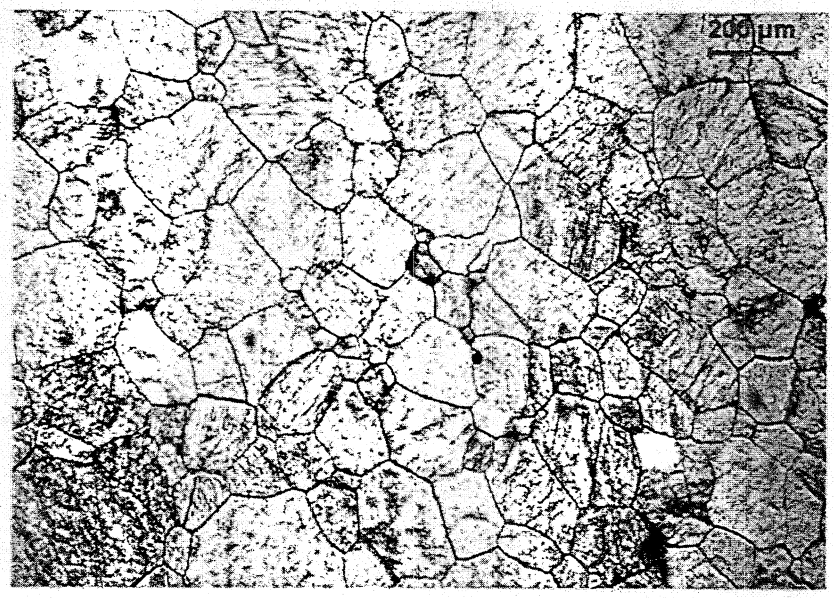

Figure 35. Microstructure of marble D. Unused. Plane-polarized light.

Figure 36. Microstructure of marble D. 1 year on the test wall. Plane-polarized light.

Photographs of the microstructure of marble E, unused and after 1 year on the test wall, are shown in Figs. 37-38. Following observations were made:

- fine-grained, not oriented
- grain size varies from microcrystalline up to 0.8 mm
- very fine-grained (cryptocrystalline) lenses among the groundmass, the lenses pass gradually into groundmass
- nearly pure carbonate, contains some opaque and mica type minerals
- some alteration of the grains
- no changes observable after 1 year on the test wall

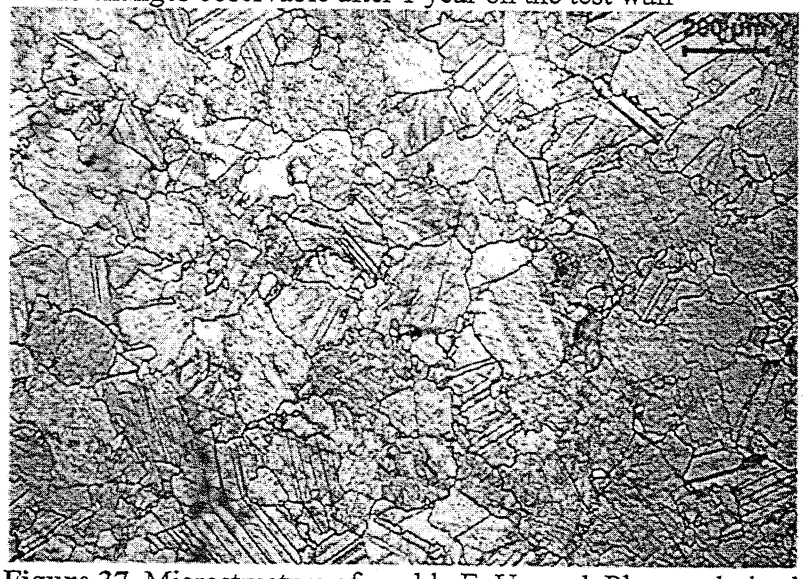

Figure 37. Microstructure of marble E. Unused. Plane-polarized light.

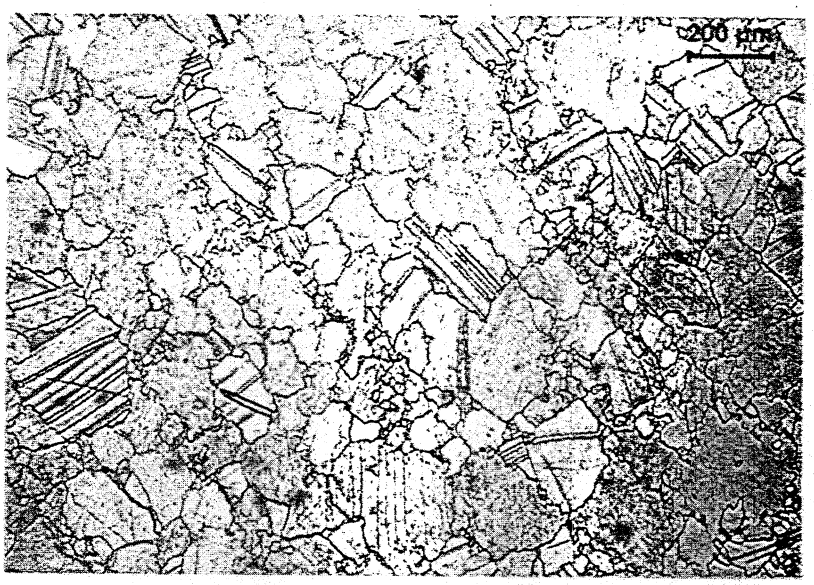

Figure 38. Microstructure of marble E. 1 year on the test wall. Plane-polarized light.

Photographs of the microstructure of marble K, unused and after 1 year on the test wall, are shown in Figs. 39-40. Following observations were made:

- fine-grained, not oriented
- average grain size about 200 µm
- very fine-grained (cryptocrystalline) lenses and veins among the groundmass, lense boundaries are distinguished from the groundmass
- nearly pure carbonate rock, contains some opaque minerals
- little alteration of the grains
- no changes observable after 1 year on the test wall

Figure 39. Microstructure of marble K. Unused. Plane-polarized light.

Figure 40. Microstructure of marble K. 1 year on the test wall. Plane-polarized light.

SEM-pictures of fractured surfaces of marble D, both unused and after 1 and 1.5 years on the test wall, are shown in Figs. 41-43. The individual grains can easily be distinguished from each other. Clear cracks can also be noticed between all the grains. These cracks become wider when the marble is exposed to the environmental strains on the test wall. The maximum crack width after 1.5 years on the test wall is around 1 µm. Respective pictures of marbles A, E and K can be found in Appendix 1.

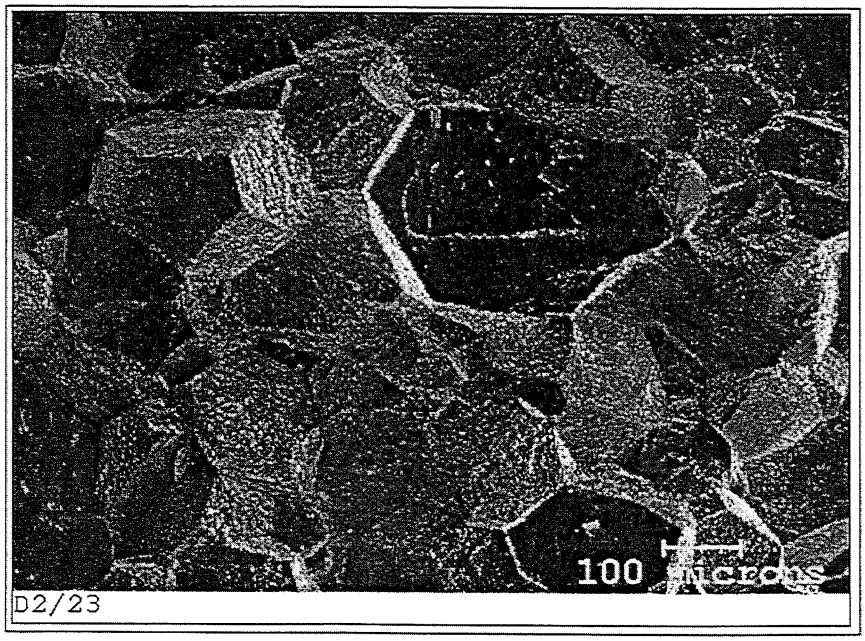

Figure 41. Marble D, unused. SE-image of fractured surface, 100x.

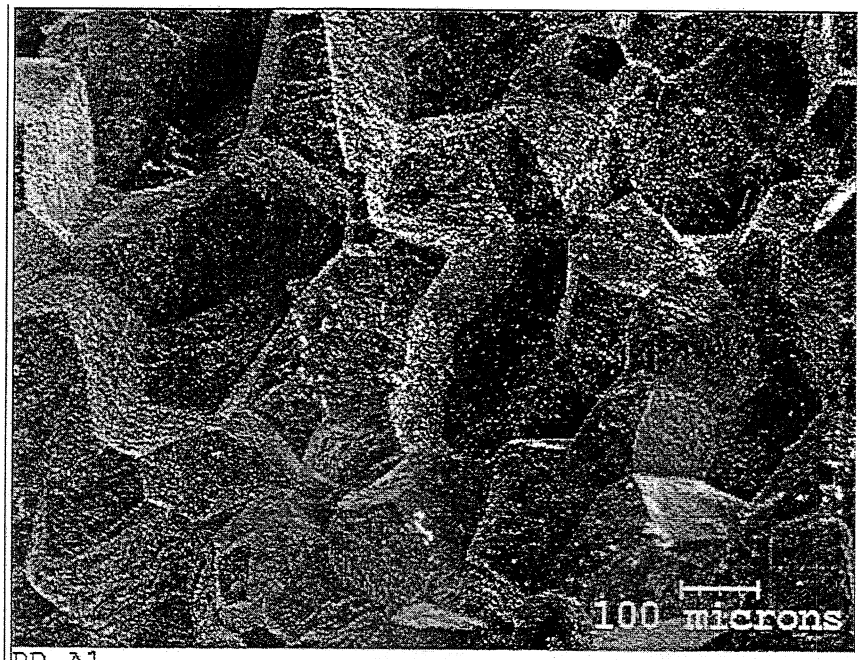

DR A1

igure 42. Marble D,1 year on field test. SE-image of fractured surfa
00x.

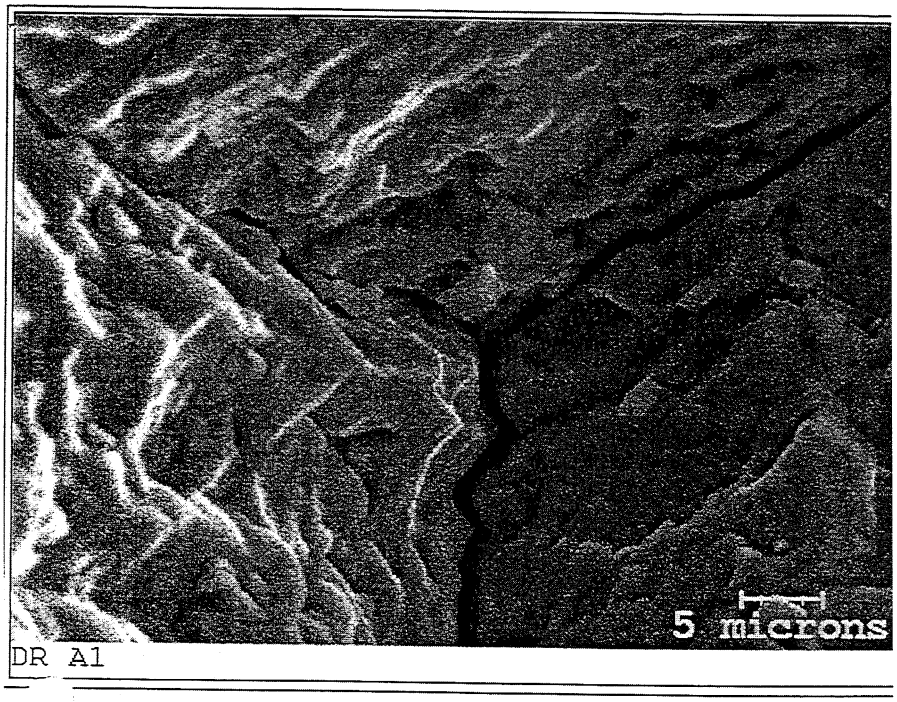

igure 43. Marble D, 1 year on the test wall. SE-image of fractured surfa
500x.

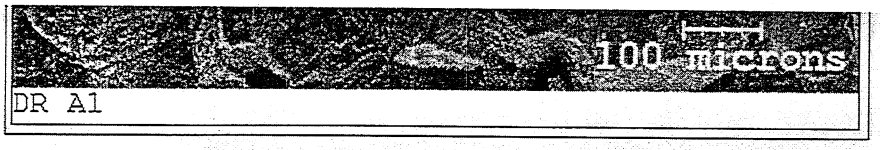

Figure 42. Marble D,1 year on field test. SE-image of fractured surface, 100x.

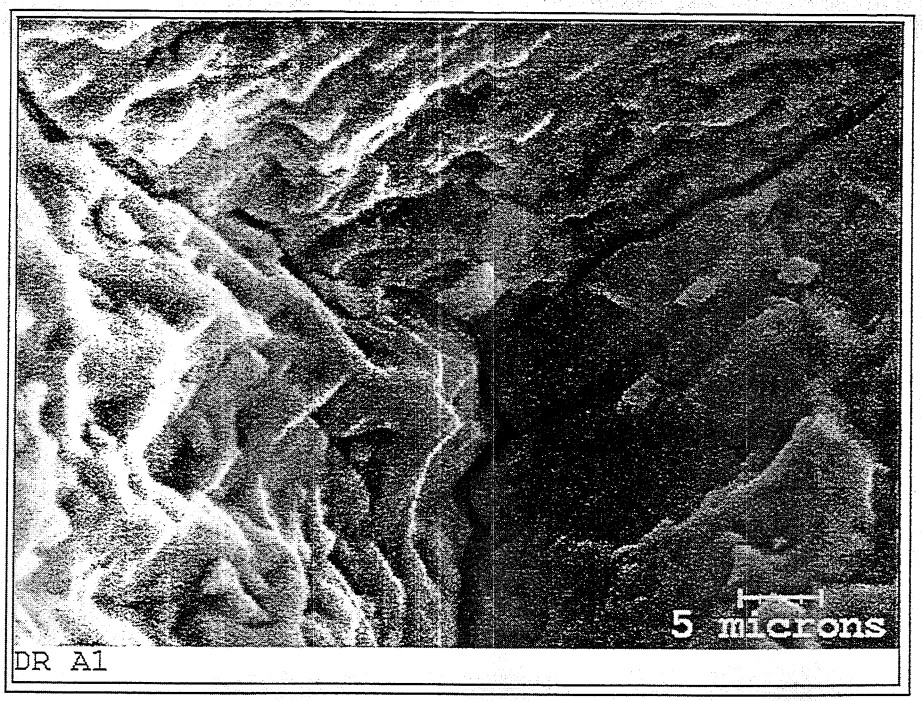

Figure 43. Marble D, 1 year on the test wall. SE-image of fractured surface, 2500x.

3.1.7 Marble coated panels

3.1.7.1 Bond strength

Bond strengths of marbles of the marble clad elements in initial stage and after 1 and 1.5 years on the test wall at Finlandia Hall are presented in Figure 44. Complete measurement results are shown in Appendix 1.

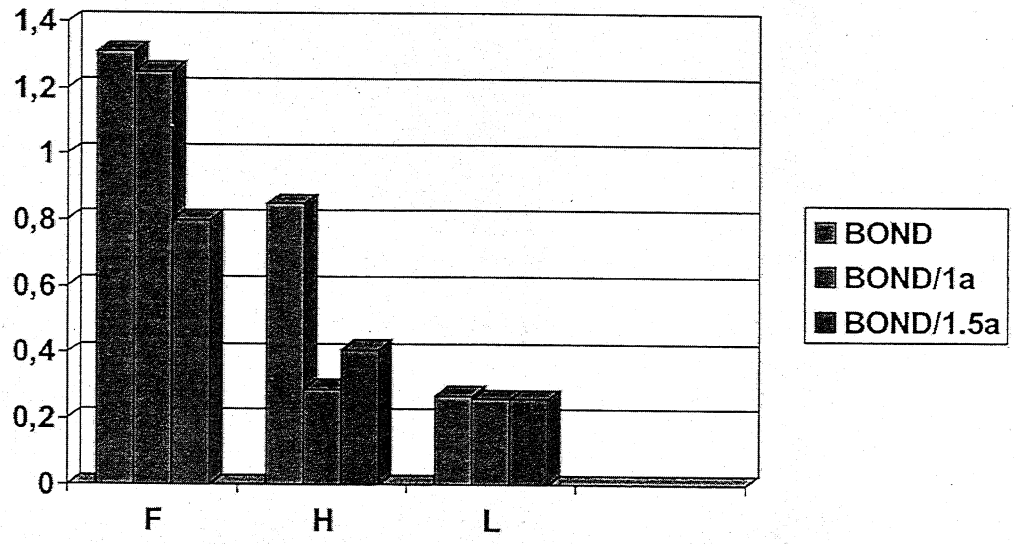

Figure 44. Bond strength of marble in marble clad elements (MPa).

The relative changes of the bond strength that have taken place on the test wall are presented in Table 12. The basis of the comparison is in all cases the bond strength in the unused elements.

Table 12. The relative changes of the bond strengths of marble in the marble clad elements on the test wall.

element type	change of bond strength 1 year %	1.5 years %
F	-5	-39
H	-66	-52
L	-4	-4

In the element type F the breaking point was usually the interface between marble and concrete. Only in a couple of cases the loosening took place, at least partly, deeper inside concrete.

In the unused element of type H the breaking point was either the interface between marble and the rest of the structure (1/3) or the interface between the glass fiber sheet and the aluminium honey comb structure (2/3). In the elements of type H that had been on the test wall the breaking point was, however, always the interface between marble and the rest of the structure.

In the element type L the breaking point was always the interface between marble and the rest of the structure. Thus, the loosening of marble took place from the top of the glue layer.

3.1.7.2 Microstructure

Photographs of the microstructure of marble clad element F, unused and after 1.5 years on the test wall, are shown in Figs. 45. Following observations were made:

- contact between marble and concrete tight and cohesive
- a narrow layer of third material, probably primer, between marble and concrete
- material (primer) layer rather continuous, though pores are common; thickness of the layer generally 20-30µm, in places even 60 µm
- in the unused element only a few very tiny cracks along the marble/concrete contact zone
- in the element strained for 1.5 years on the test wall some slight and narrow cracking at the marble/concrete contact zone

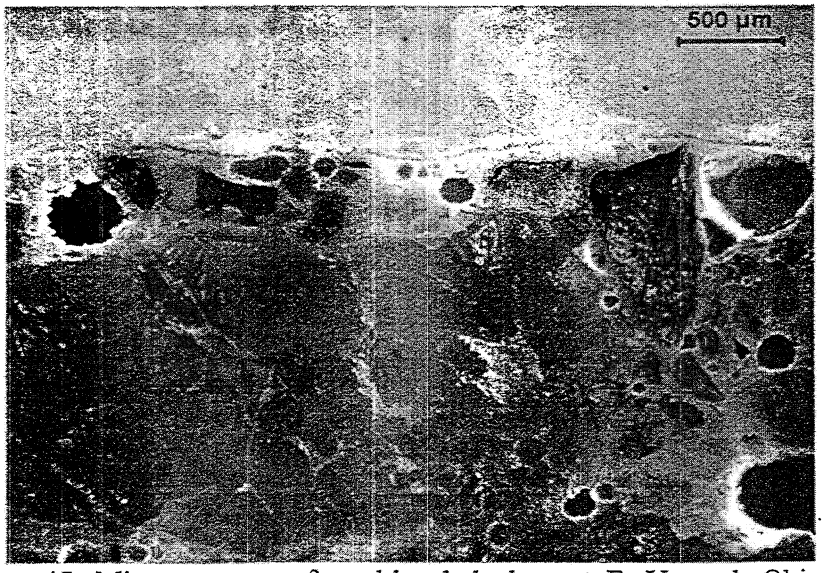

Figure 45. Microstructure of marble clad element F. Unused. Objective 2.5x, oblique illumination.

Photographs of the microstructure of marble clad element H, unused and after 1.5 years on the test wall. Following observations were made:

- a layer of glue between marble and metal structure, thickness of the layer approximately 1 mm
- structure of the unused element partly cracked along the contact zone marble/glue
- in the unused element the upper half of the glue layer tinted yellowish
- in the element strained for 1.5 years on the test wall the upper half of the glue layer tinted brownish
- open crack on about 60 % of the contact zone marble/glue

Photographs of the microstructure of marble clad element L unused on the test wall, is shown in Figure 46. Following observations were made:

- a layer of glue between marble and metal structure, thickness of the layer approximately 0.5 mm
- the glue contains a lot of porosity
- in the unused element the glue layer partly detached from marble
- in the element strained for 1.5 years on the test wall the glue layer rather tightly attached to marble, only minor cracking in some parts of the contact zone

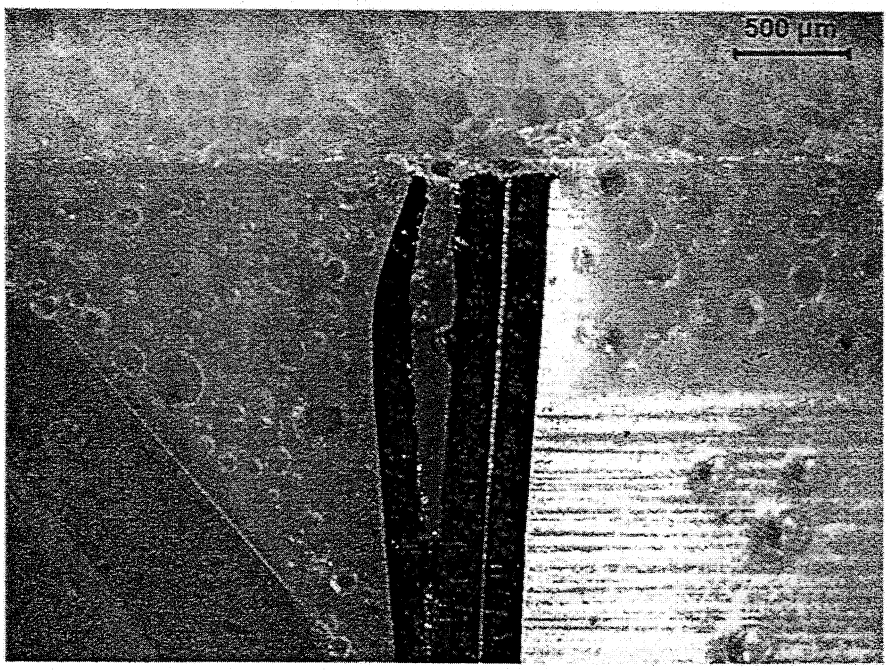

Figure 46. Microstructure of marble clad element L. Unused. Objective 2.5x, oblique illumination.

3.2 Observation of weather conditions

3.2.1 General

Environmental conditions cause various effects on a facade cladding. Temperature changes, gradients over marble panels and the number of freezing and thawing are the most important strains caused by weather. In addition impurities and aggressive compounds found in typical industrial city air are can be mentioned as catalytic factors for the deterioration.

The features of the results which were considered most important considering especially the strains caused by the environmental factors to the marble facade are described more closely in this chapter. In most cases the daily maximum and minimum temperatures are used when examining the results. Complete file of temperature nd humidity measurement data from Finlandia Hall facade is can be found in Appendix 1.

3.2.2 Daily variation of temperature

Daily variation of temperature was studied by using the maximum and minimum temperatures observed daily on outer and inner surfaces of marble panels. Results from measuring point A located on the top of the southern wall, are presented is Figures 47-50. Pictures are grouped in the series of four, each representing the same measurement period. The four pictures in the same series are coded with letters a-d, and they have the following meaning:

a) daily max and min temperatures on outer surface of marble (°C)
b) daily max and min temperatures on inner surface of marble (°C)
c) difference between daily max and min temperatures on outer surface of marble (°C)
d) difference between daily max and min temperatures on inner surface of marble (°C)

Complete data for all measuring points (A, B, C, D and E) about the daily variations of temperature between the period 26.5.1999 - 28.2.2001.
are presented in Appendix 1.

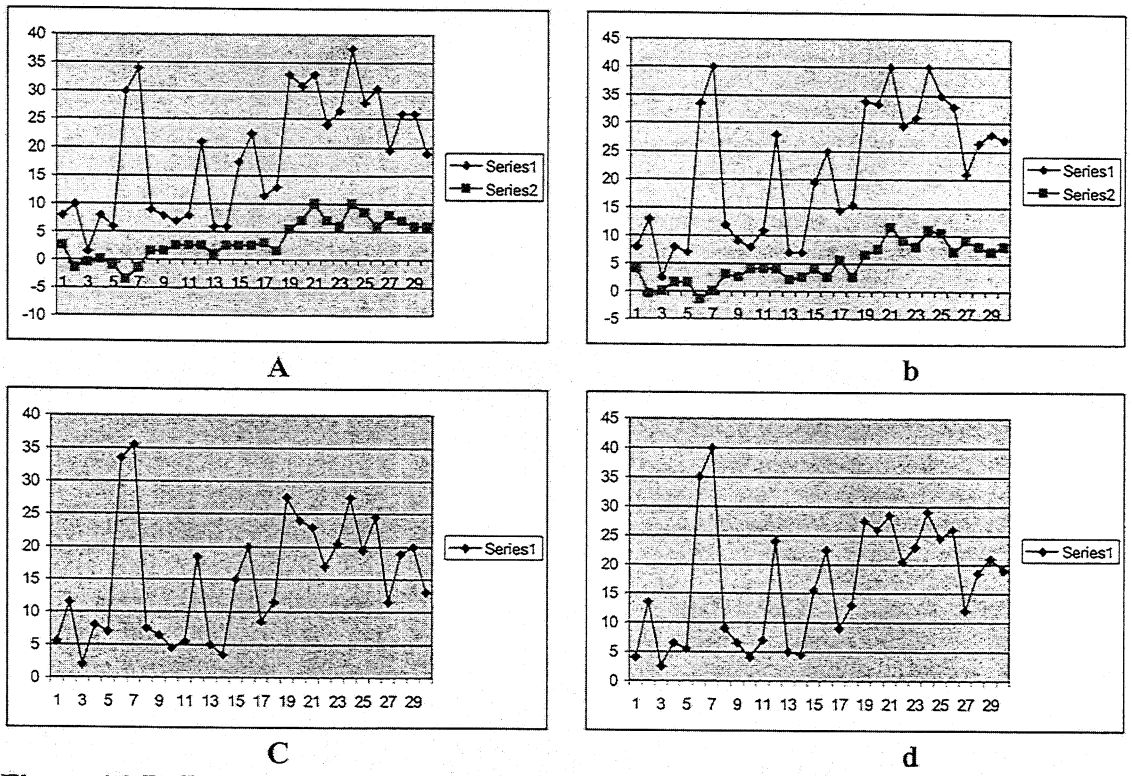

Figure 47. Daily temperature variation during measurement period 1.4.-30.4.2000

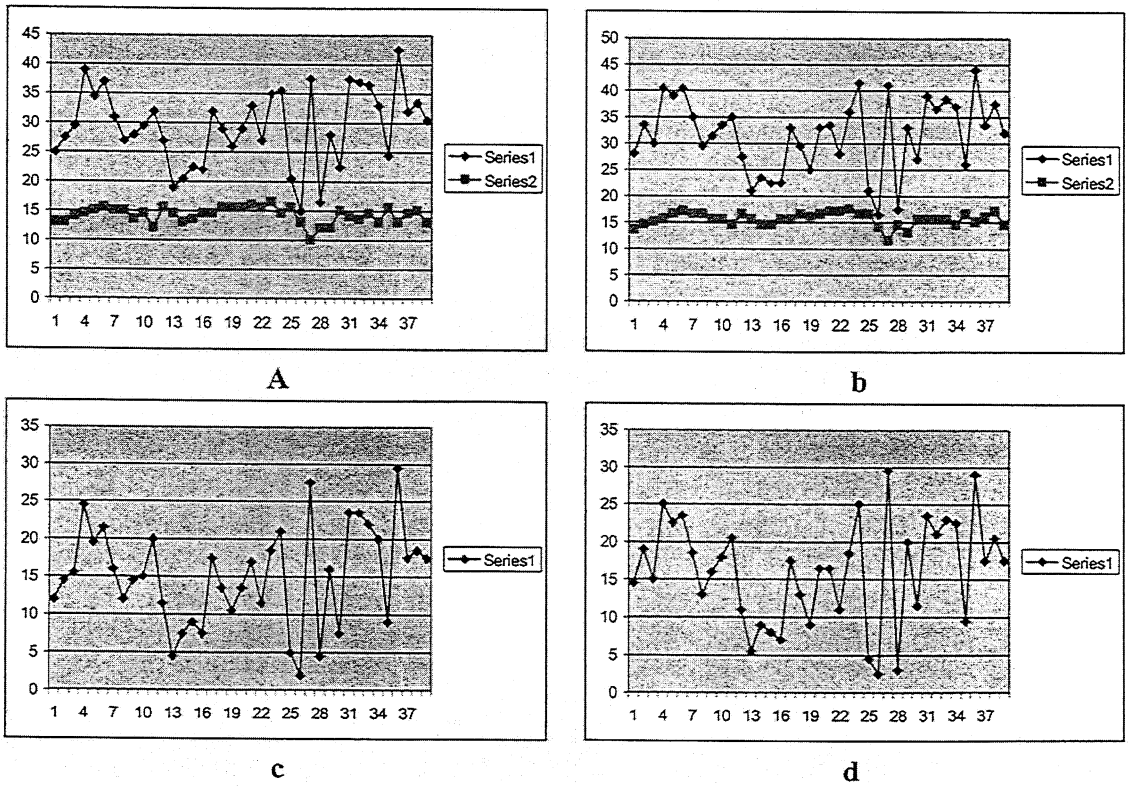

Figure 48. Daily temperature variation during measurement period 1.7.-8.8.2000.

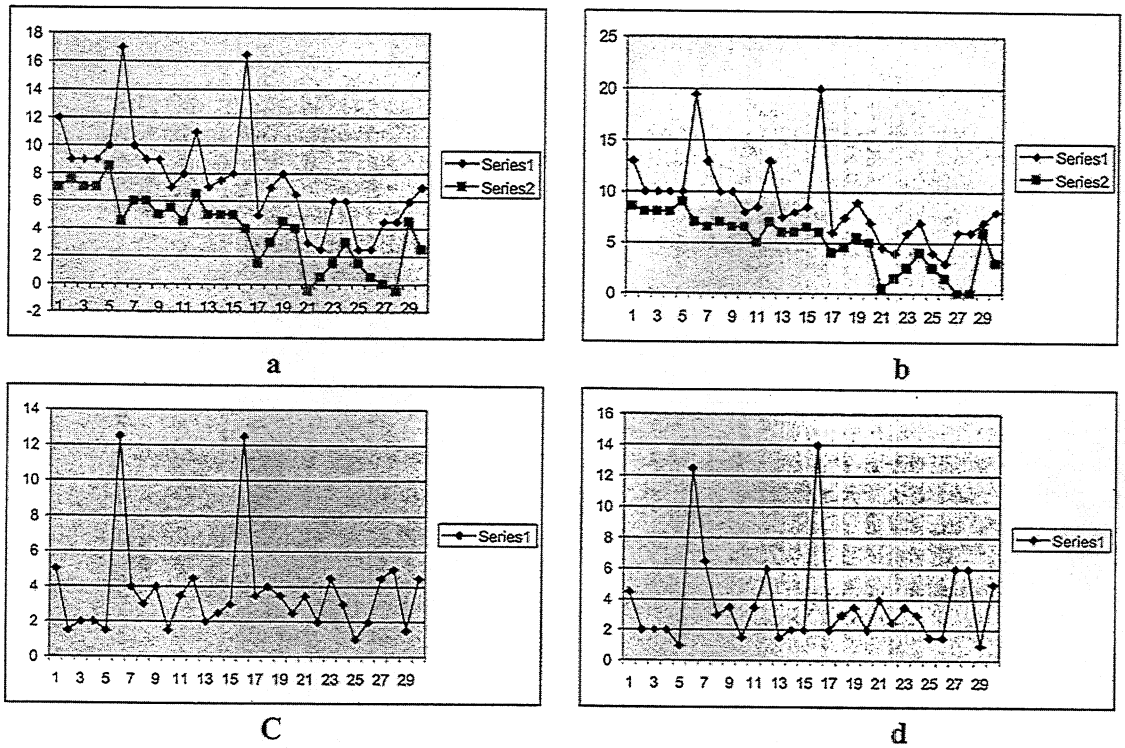

Figure 49. Daily temperature variation during measurement period 1.11.-30.11.2000.

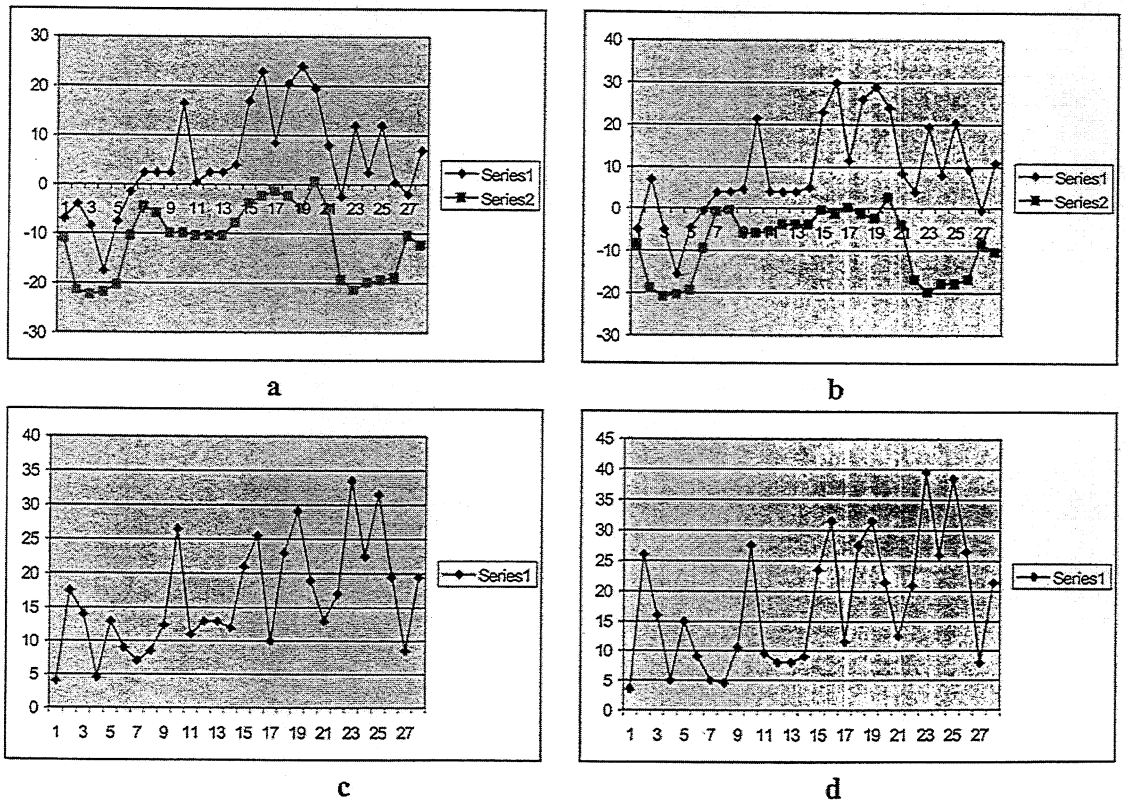

Figure 50. Daily temperature variation during measurement period 1.2.-28.2.2001.

3.2.3 Temperature gradient over the marble panel

Temperature gradient prevailing in the panes was revealed by examining temperatures on the outer and inner surfaces of marble. The results for measuring point A are presented in Figure 51 giving four examples of the daily behaviour of surface temperatures of the measurement panels. The days chosen for the examples represent various seasons. Complete data for all measuring points (A, B, C, D and E) are presented in Appendix 1.

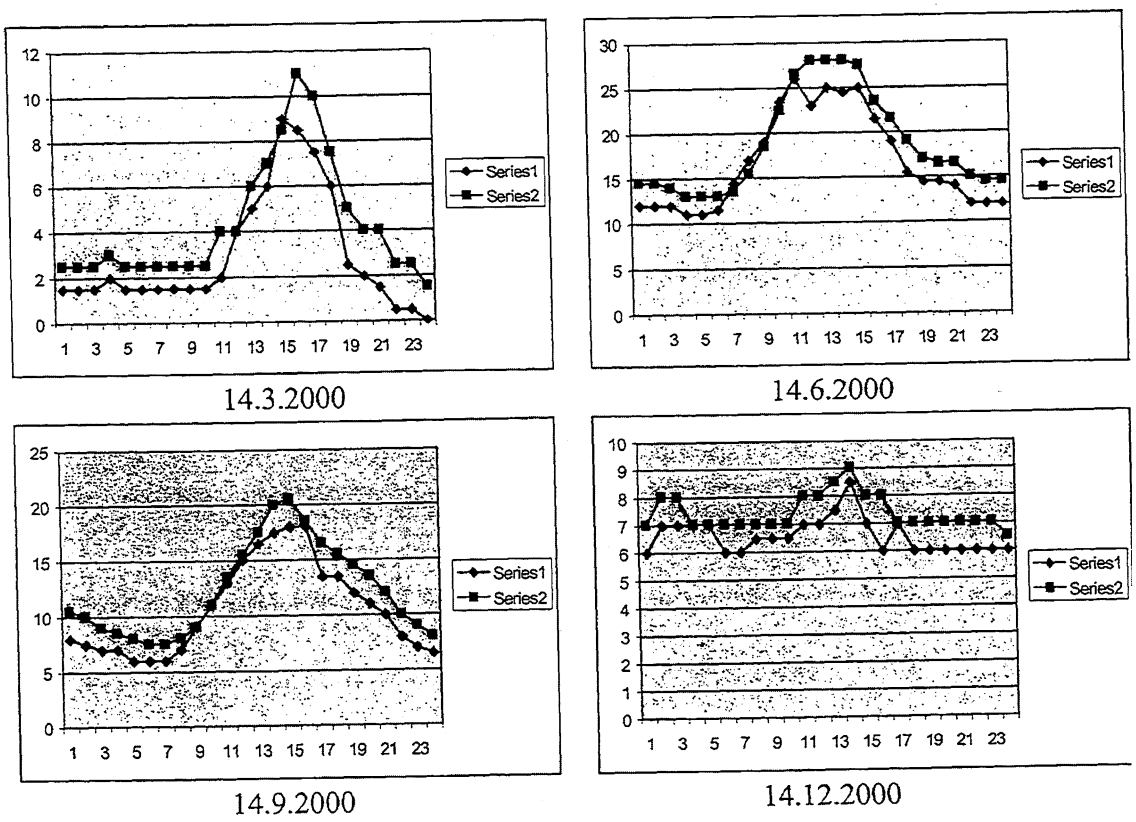

Figure 51. Temperature of outer (Ser 1) and inner (Ser 2) marble surface (°C) at measuring point A.

3.2.4 Gradient of temperature variation in marble

The gradient of temperature variation over the marble panels was examined as the difference between the range of temperature variation on outer and inner surfaces. The difference is calculated in such a way that the variation on inner surface is diminished from the variation on outer surface. Thus, a positive difference means that the variation has been greater on outer surface and a negative difference that the variation has been greater on inner surface. The results are shown in Figs. 52-55.

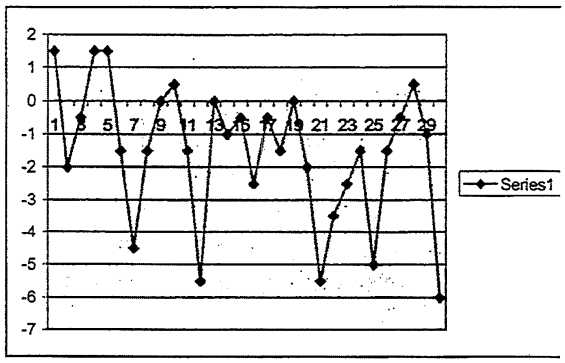

Figure 52. Gradient of temperature variation during measurement period 1.4.-30.4.2000.

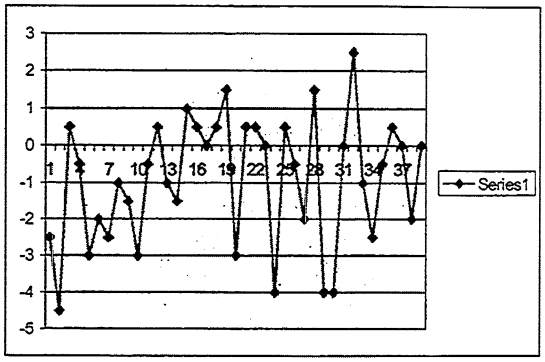

Figure 53. Gradient of temperature variation during measurement period 1.7.-8.8.2000.

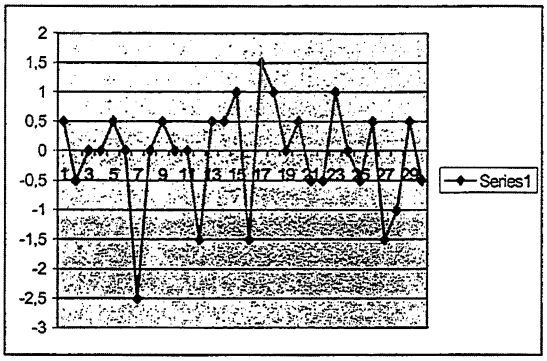

Figure 54. Gradient of temperature variation during measurement period 1.11.-30.11.2000.

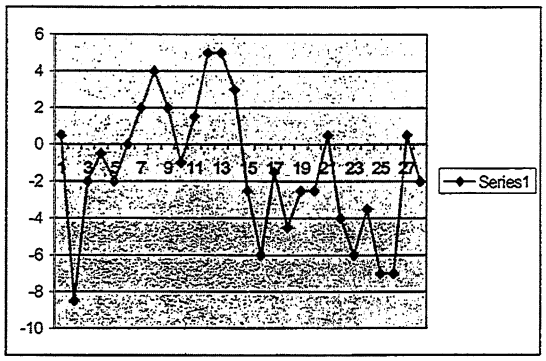

Figure 55. Gradient of temperature variation during measurement period 1.2.-28.2.2001.

3.2.5 Freeze/thaw -cycling of marble

The number of freeze/thaw -cycles occurred on marble surfaces was calculated from the data dealing with the daily variation of temperature. Freeze/thaw-cycle was defined as a day during which the maximum temperature was higher than +0.3°C and the minimum temperature lower than -0.3°C. The number of such days in every month, i.e. the number of freeze/thaw -cycles, on outer (OUT) and inner (IN) surfaces of each measuring panel is presented in Table 13.

Table 13. The number of freeze/thaw -cycles on marble surfaces.

month/year	panel A		panel B		panel C		panel D		panel E	
	OUT	IN	OUT	IN	OUT	IN	OUT	IN	OUT	IN
5/1999	x	x	x	x	x	x	1 [7]	1 [7]	4 [7]	2 [7]
6/1999	0	0	0	0	0	0	0	0	0	0
7/1999	0	0	x	x	0	0	0	0	0	0
8/1999	0	0	x	x	0	0	0	0	0	0
9/1999	0	0	x	x	0	0	0	0	0	0
10/1999	1	0	x	x	4 [4]	3 [4]	1	1	1 [8]	1 [8]
11/1999	7	5	x	x	x	x	10	9	7	5
12/1999	14	13	x	x	x	x	23	21	15	13
1/2000	4 [1]	4 [1]	x	x	x	x	16	15	13	14
2/2000	x	x	x	x	x	x	8	3	12	11
3/2000	16 [2]	14 [2]	x	x	x	x	1	0	25	23
4/2000	5	2	14 [3]	8 [3]	10 [5]	8 [5]	0	0	5	4
5/2000	0	0	4	3	0 [6]	0 [6]	1	1	1	0
6/2000	0	0	0	0	0	0	0	0	0	0
7/2000	0	0	0	0	0	0	0	0	0	0
8/2000	0	0	0	0	0	0	0	0	0	0
9/2000	0	0	1	0	1	0	0	0	0	0
10/2000	2	1	4	3	4	3	2	2	3	2
11/2000	2	0	7	5	6	4	1	1	3	3
12/2000	7	6	1	2	2	2	11	11	5	5
1/2001	21	20	0	0	5	7	9	8	10	11
2/2001	19	20	2	2	1	7	9	10	12	13

x = no results available
[1] → 11.1.2000 [2] 7.3.2000 → [3] 29.3.2000 → [4] → 20.10.1999 [5] 29.3.-12.4.2000
[6] 17.5.2000 → [7] 11.5.1999 → [8] 20.10.1999 →

3.2.6 Humidity gradient over the marble panel

The gradient of relative humidity over the marble panels was studied by using the maximum and minimum relative humidities observed daily in outdoor air above the panel and inside the ventilation slot behind the panel. The results from measuring points D and E are shown as pictures presented below. There are four curves in every picture. They are coded with numbers 1-4, and they have the following meaning:

Series 1	maximum relative humidity in outdoor air
Series 2	minimum relative humidity in outdoor air
Series 3	maximum relative humidity in ventilation slot
Series 4	minimum relative humidity in ventilation slot

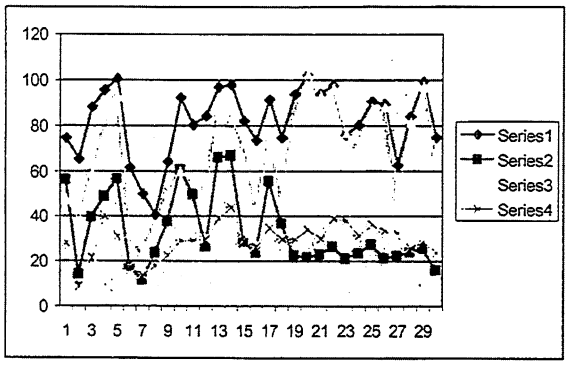

Figure 56. Daily variation of relative humidity during period 1.4.-30.4.2000. Measuring point D.

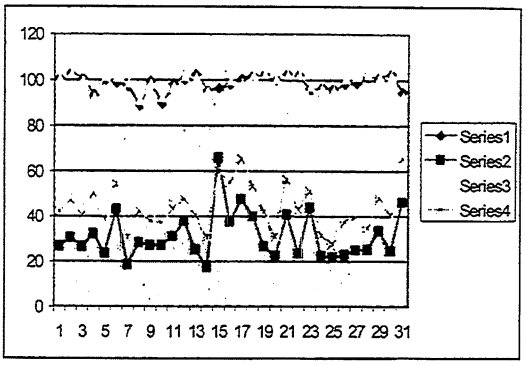

Figure 57. Daily variation of relative humidity during period 1.8.-31.8.2000. Measuring point D.

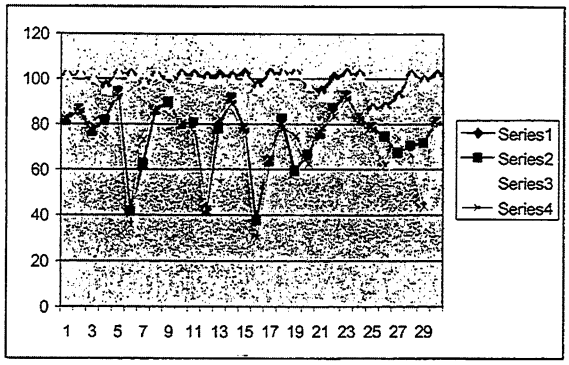

Figure 58. Daily variation of relative humidity during period 1.11.-30.11.2000. Measuring point D.

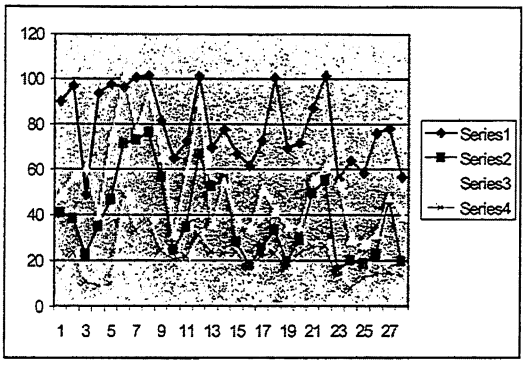

Figure 59. Daily variation of relative humidity during period 1.2.-28.2.2001. Measuring point D.

3.2.7 Acidity of rain water

Finnish Environment Institute has a measurement station at Nupuri, Espoo, about 20 km northwest from Finlandia Hall, where pH of rain water is continuously monitored. Monthly averages from the year 1999 are presented in Table 14.

Table 14. Acidity of rain water at Nupuri measurement station in 1999.

month	pH
January	4.30
February	4.80
March	4.89
April	5.32
May	*
June	*
July	5.34
August	*
September	4.93
October	5.06
November	4.98
December	4.63

* result abandoned due to contamination

The weighted pH-average of the year 1999 was 4.80. It was calculated from the monthly averages by weighing the values presented in Table 15 with the monthly depths of rainfall. The results from the year 2000 were not available by the time of reporting.

3.2.8 Weather conditions

3.2.8.1 Temperature and humidity

Daily maximum and minimum temperatures and corresponding relative humidities in Helsinki area are presented according to the data of Finnish Meteorological Institute in Figs. 60-67. Series 1 represents the maximum values and Series 2 the minimum values.

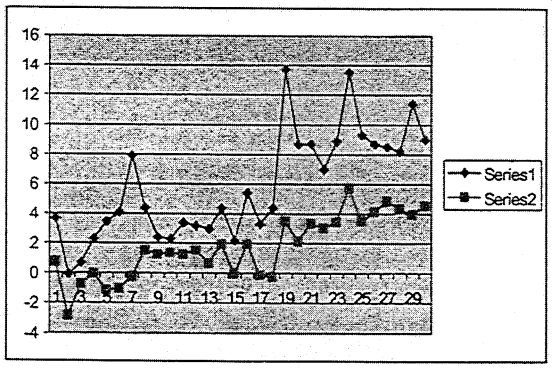

Figure 60. Daily variation of temperature (°C) in Helsinki during period 1.4.-30.4.2000.

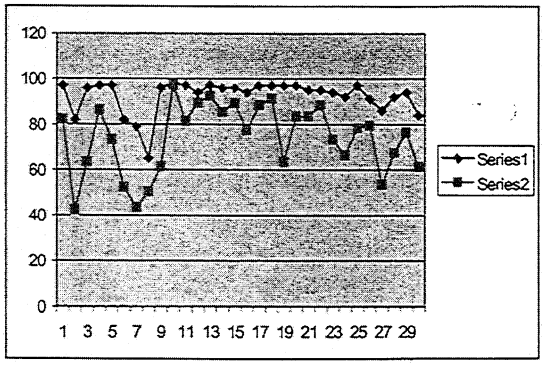

Figure 61. Daily variation of relative humidity (%) in Helsinki during period 1.4.-30.4.2000.

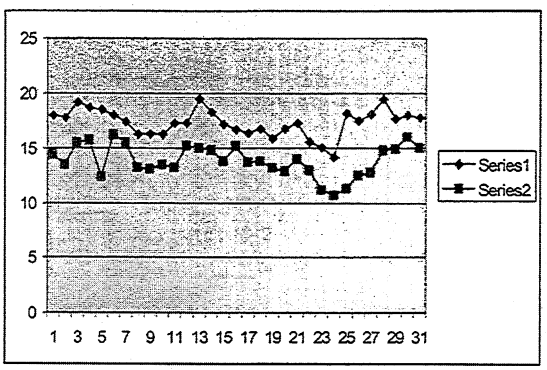

Figure 62. Daily variation of temperature (°C) in Helsinki during period 1.8.-31.8.2000.

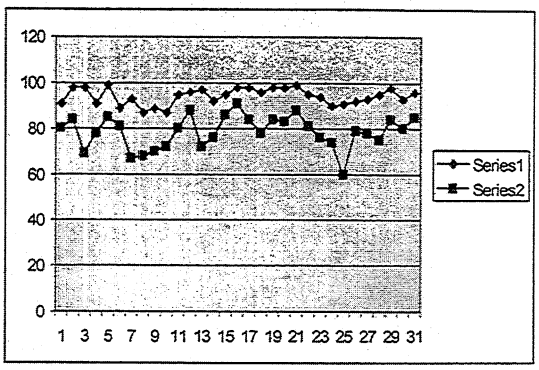

Figure 63. Daily variation of relative humidity (%) in Helsinki during period 1.8.-31.8.2000.

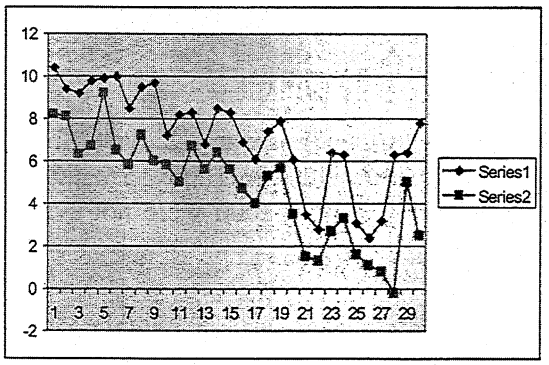

Figure 64. Daily variation of temperature (°C) in Helsinki during period 1.11.-30.11.2000.

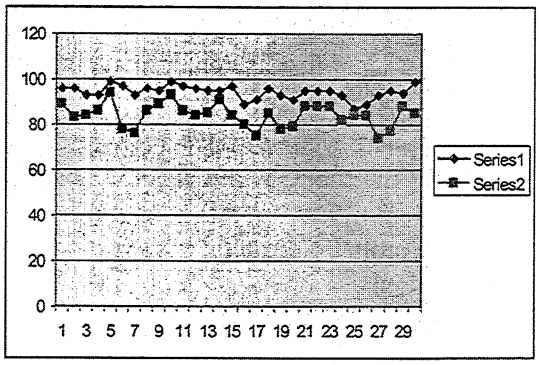

Figure 65. Daily variation of relative humidity (%) in Helsinki during period 1.11.-30.11.2000.

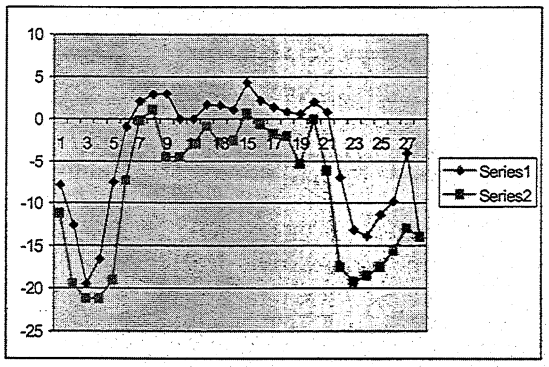

Figure 66. Daily variation of temperature (°C) in Helsinki during period 1.2.-28.2.2001.

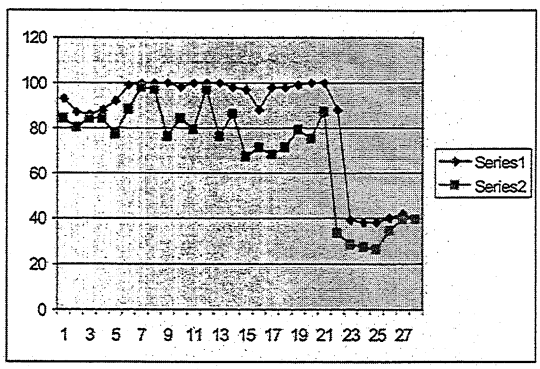

Figure 67. Daily variation of relative humidity (%) in Helsinki during period 1.2.-28.2.2001.

3.2.8.2 Rainfall and sunshine

Daily rainfall and the amount of sunshine in Helsinki area are presented according to the data of Finnish Meteorological Institute in Figs. 68-75.

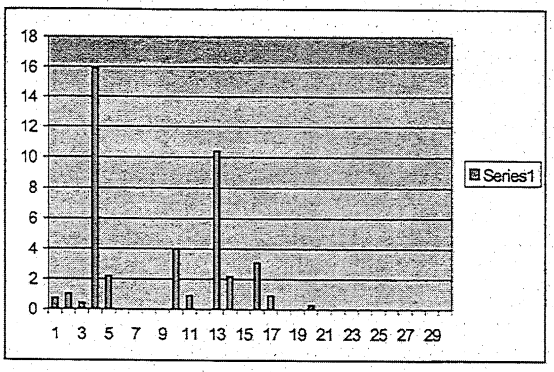

Figure 68. Daily rainfall (mm) in Helsinki during measuring period 1.4.-30.4.2000.

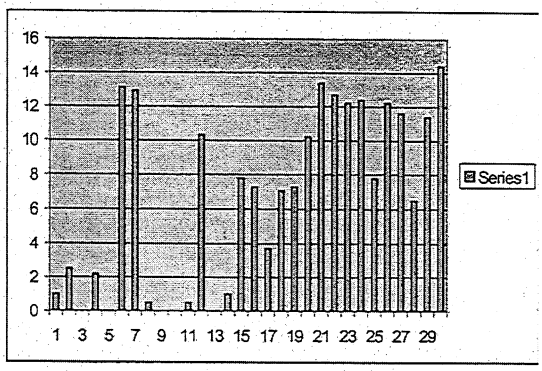

Figure 69. Daily amount of sunshine (h) in Helsinki during period 1.4.-30.4.2000.

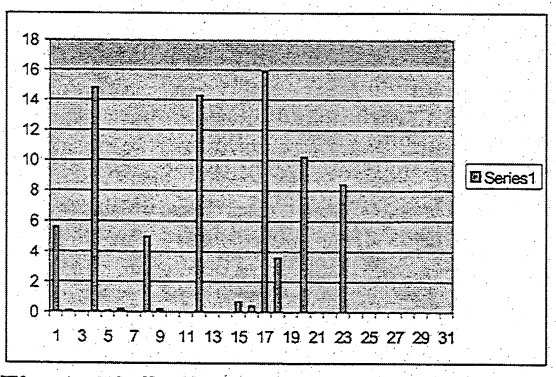

Figure 70. Daily rainfall (mm) in Helsinki during measuring period 1.8.-31.8.2000.

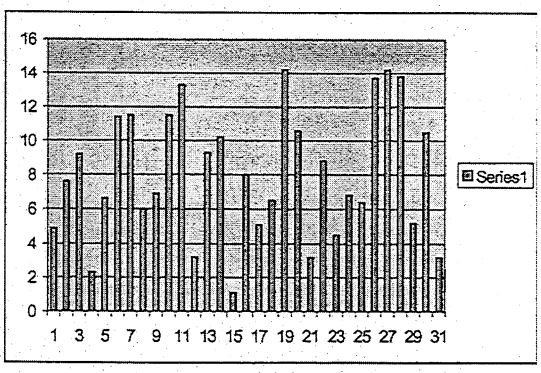

Figure 71. Daily amount of sunshine (h) in Helsinki during measuring period 1.8.-31.8.2000.

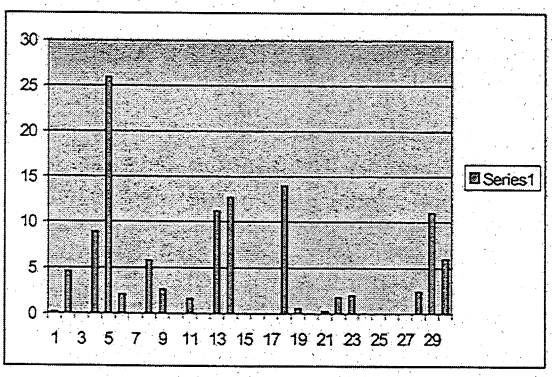

Figure 72. Daily rainfall (mm) in Helsinki during measuring period 1.11.-30.11.2000.

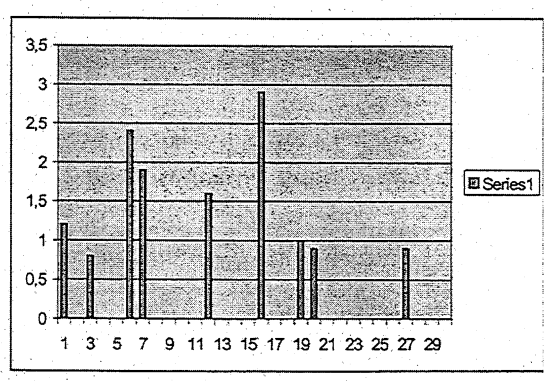

Figure 73. Daily amount of sunshine (h) in Helsinki during period1.11.-30.11.2000.

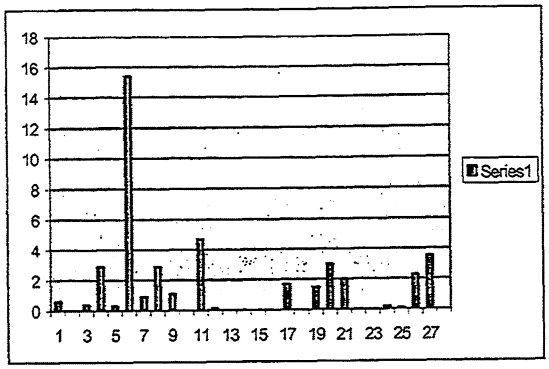

Figure 74. Daily rainfall (mm) in Helsinki during measuring period 1.2.-28.2.2001.

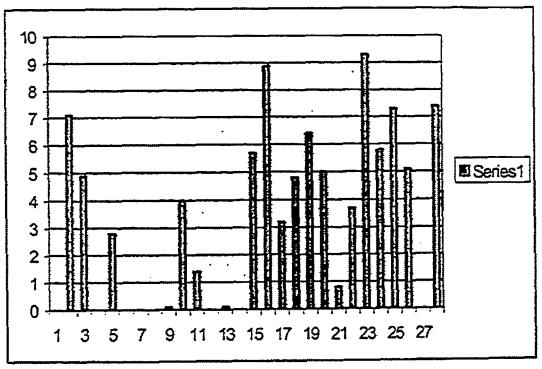

Figure 75. Daily amount of sunshine (h) in Helsinki during period 1.2.-28.2.2001.

3.2.9 Discussion

3.2.9.1 Temperature gradient

According to the temperature data recorded it seems that in general temperature on the inner surface of marble slabs was higher than that on the outer surface. Especially this was the case on western and northern walls, where the inner surface temperature was 1-2°C higher than the corresponding outer surface temperature. Only during the warmest season of the year, June-August, the temperatures were almost the same on both sides of the slab. Occasionally the outer surface temperature was even higher.

On eastern wall the outer surface temperature was usually higher than the inner surface temperature during summer time. The temperature difference varied between 1-4°C. A similar trend was observed in the warmest days of autumn, but then the temperature difference was only about 1°C in favour of the outer surface. For the rest of the year the inner surface was a little warmer than the outer surface.

Measurements from southern wall resembled those from eastern wall. During summer time and the warmest days of autumn the outer surface was warmer, but otherwise the temperature was higher on the inner surface. The temperature differences during summer and autumn were approximately as high as on eastern wall, but during winter the inner surface was about 1°C and during spring even 1-5°C warmer than the outer surface. However, the results from the measuring point A, which was also on southern wall, were different from those presented above. At that point the inner surface temperature was always 1-2°C, during summer time even 2-4°C, higher the outer surface temperature. Because the measuring point A located on top of the wall of the tower part of the building, this could be due to "chimney effect". In that case high inner surface temperatures would be a consequence of the effect of warm air rising up from the roof through the ventilation slot.

3.2.9.2 Daily variation of temperature

The daily variation of temperature of the marble slabs was substantial. It was most prominent during the warm seasons reflecting the natural weather conditions. Except the season the variation depended also on the location of the slab with respect to the cardinal points.

On northern wall the average daily variation of temperature during summer (June-August) was 10-15°C, during spring (February-April) 5-10°C and during winter (November-January) only 2-3°C. In April and in September it was around 10°C and in October around 5°C. The maximum temperature recorded varied accordingly from 30-35°C in summer to around zero in winter. The minimum temperature varied between 5-10°C in summer, but could be as low as -25°C in winter.

On western wall the average daily variation of temperature varied between 15-20°C during the time period from March to September. In winter, from November to January, the variation was only 1-5°C. Between these two periods, i.e. during February and October, the variation was 5-10°C. The maximum temperature varied from 35-40°C in summer to around zero in mid-winter. The minimum temperature was around 10°C in summer but as low as -25°C in winter.

On eastern wall the average daily variation of temperature varied between 15-20°C in summer (June-August), between 5-10°C in spring (March-April) and between 2-5°C in winter (November-January). During May and September it was 10-15°C and during February and October around 5°C. The maximum temperature varied from 35-40°C in summer to about 5°C in winter. The corresponding minimum temperatures were 10°C and -25°C.

On southern wall the average daily variation of temperature varied between 15-20°C in summer (May-September), between 10-15°C in spring (March-April) and between 5-10°C in winter (October-February). The maximum temperature varied from 35-40°C in summer to about 15°C in winter. The minimum temperature was about 10°C in summer and about -25°C in winter. On top of the tower wall (measuring point A) the daily variation during summer and spring times was roughly 5°C higher. Correspondingly, the maximum temperatures were there even 10°C higher than on lower parts of the roof walls. Highest temperatures were measured on the outer surface of black granite slab beside the measuring point A. They were in general 5-10°C higher than the temperatures on the outer surface of the marble slab.

3.2.9.3 Gradient of temperature variation

The daily variation of temperature did not occur evenly in the marble slabs. This can be considered to be significant, because uneven straining of marble could be one of the factors leading to bowing of the slabs.

On northern wall the differencies in the temperature variation between the surfaces were small, and the direction of the gradient changed frequently from one side to another. Most of the time, however, the variation was wider on the outer surface of the slab. Compared to the variation on the inner surface the difference was only 0-1°C.

On western wall the temperature variation was wider on the outer surface of the slab. The difference was noteworthy, 2-4°C, during warm season (April-September), but almost insignificant, 0-1°C, for the rest of the time. In mid-winter the difference between the surfaces in this respect was practically zero.

Also on eastern wall the temperature variation was wider on the outer surface of the slab. The difference was remarkable, 3-4°C, in summer (May-September). During spring (February-April) and late autumn (October) the difference was smaller but clear, 0-2°C. In winter (November-January) the variation was practically the same on both sides of the slab.

On southern wall the temperature variation was wider on the outer surface of the slab except during winter time when the situation was the other way around. In winter (November-February) the difference was 1-2°C, in January even 3-4°C, in favour of the inner surface, but during the rest of the year the difference was 2-3°C, in May-June even 3-4°C, higher on the outer surface. The turning points occurred in October-November on one hand and in March on the other, so that the direction of the difference during these months can be either way.

Again the results from the measuring point A deviated from the trend presented for the southern wall in general. Excluding the mid-winter the variation in that point was wider on the inner surface of the slab. The difference was 2-3°C during February-September and 0-2°C during October-December. In March it was 3-4°C and in September even 5°C. In January the variation was 2-3°C wider on the outer surface. The observed behaviour could be a consequence of the "chimney effect" as discussed in chapter 5.2.

3.2.9.4 Freeze/thaw -cycling

The number of freeze/thaw -cycles during the whole monitoring period of 22 months was amazingly high. The most reliable results were those from the measuring points D and E as their data covered the time period almost completely. The number of freeze/thaw -cycles defined as presented in chapter 4.5 was around 90 in the former and even 110 in the latter. In addition, it must be noted that data from two important months, March and April, were missing from two whole years. These could have meant 20-30 cycles more, which means that the total amount for two years would have

been 120-140. Thus the annual amount of freeze/thaw -cycles seems to something like 60-70, while the earlier estimate has been about 20.

The definition of a freeze/thaw -cycle used in this study can be criticised for not being strict enough as the temperature limits were set to -0.3°C for freezing and +0.3°C for thawing. Water in marble probably requires lower temperatures in order to freeze, correspondingly higher temperatures in order to melt. Setting the temperature limits further from zero to both directions would diminish the amount of freeze/thaw -cycles, even considerably if the limits are set far enough. As long as the threshold values for temperatures are not known, the estimates presented here can be used bearing in mind the limitations due to deficiencies in the definition. On the other hand only one cycle per day was calculated in this study as maximum and minimum daily temperatures were used. In reality more than one cycle can occur even in the same day.

The worst directions from the frost resistance point of view seem to be south and east. Considerable amount of data was lacking from north and west walls. The results would indicate that the amount of cycles would have been lower in these directions, although considerable especially on western wall.

The amount of freeze/thaw -cycles seemed to a little lower on the inner surface of the marble slab than on the outer surface. The difference was about 10%. As this causes a higher strain on the outer surface than on the inner this could be one of the factors contributing to bowing of the slabs.

Only during the three summer months, June-August, no freeze/thaw -cycles were observed. The worst period of time in this respect was naturally that from November to March. It seemed that the southern wall was especially strained during November-January while the others suffered most in February-March. During October some cycles were detected in all directions. Excluding the southern wall the situation was the same during April. During May and September some occasional freeze/thaw -cycles were observed on other walls except the southern one.

3.2.9.5 Relative humidity

In general the values of relative humidity were fairly high. During autumn and winter times the average relative humidity values were even higher than during spring and summer. This was due to the fact that the daily minimum rose from the value of about 20%, which was typical of summer time, to 60-80%, or even higher.

On the southern wall there seemed to be a difference between the relative humidity of outdoor air and that of the ventilation slot for the most of the time meaning a humidity gradient over the marble slab. The direction of the gradient was not same all of the time, however. During summer time (May-August) the average relative humidity was higher inside the ventilation slot,

though the difference was rather small. It was due to the fact that the minimum value was higher than that of oudoor air and thus the variation of relative humidity was smaller inside.

The situation was exactly the other way around during November-December, when the minimum relative humidity inside the ventilation slot was smaller than that of outdoor air meaning wider variation of humidity inside. However, the the most remarkable difference was observed during January-April. During that time period both the maximum and the minimum relative humidities were higher in outdoor air than in the ventilation slot. Thus, the conditions were considerably more humid on the outer surface of the marble than on the inner surface. Only during September-October the humidity conditions were similar on both sides of the marble slab.

On the eastern wall the humidity conditions were much more even than on the southern wall. There were no great differencies between the relative humidities of outdoor air and that of the ventilation slot. Only during winter time, from January to March, both the maximum and the minimum relative humidities were higher in outdoor air than in the ventilation slot. Thus, the conditions were considerably more humid on the outer surface of the marble than on the inner surface.

The differencies in relative humidity between outdoor air and the ventilation slot causes a higher strain on the outer surface of marble slab than on the inner. Thus, this could be one of the factors contributing to bowing of the slabs.

3.2.9.6 Acidity of rain water

The pH-value of rain water varied between 4.3 and 5.3 during 1999 the weighed average being 4.8. The values of the year 2000 were not available, but most probably the situation was very similar to that in 1999. Although the acidity of rain water has diminished, i.e. the pH-value increased, during the last decade it still acts like a weak acid. Thus, it forms a straining factor to all materials subjected to rain water. Its effect must especially be taken into account when materials like marble which are very reactive in acidic surroundings are considered.

3.2.10 Conclusions

According to the temperature and humidity data recorded the prevailing environmental conditions include several factors that cause strain to the marble facades of Finlandia Hall. The intensity of these factors was not the same everywhere but depended on the cardinal point towards which the walls were directed. It seemed that in general the sum of the straining factors was highest on southern walls and lowest on northern walls.

The annual variation of temperature is one of the straining factors. The minimum temperature recorded during the time period in question was

about -25°C on all walls. The corresponding maximum temperature varied from about 35°C on the northern side to about 50°C on top of the southern side of the tower part of the building.

The daily variation of temperature was also considerable. The average variation was highest on southern walls, 15-20°C during summer and 5-10°C during winter time. On northern walls the average variation was lowest varying between 10-15°C during summer and 2-3°C during winter. Occasionally the daily variation could be even twice the average.

Freeze/thaw -cycling caused also strains to marble and facade structures. According to the results the annual amount of cycles can be as high as 60-70. The freeze/thaw -effect was prominent at least on southern and eastern walls, probably also on western walls.

At least two other straining factors were observed: variation of humidity and acidity of rain water. During summer and spring time the relative humidities, especially the daily minimum values, were varying sharply depending whether it was raining or not. During colder seasons the humidity conditions were much more even. The pH-value of rain water varied between 4 and 5 creating acidic conditions that can affect the highly reactive marble.

In addition, three factors causing a higher strain on the outer surface of marble slab than on the inner were observed: the average daily variation of temperature, the number of freeze/thaw -cycles and the relative humidity were higher on the outer surface. The differences were small, but all of them affected in the same direction. Thus, these could be at least some of the factors contributing to bowing of the slabs.

3.3 Effect of protective agent

3.3.1 Laboratory studies

3.3.1.1 Resistance to UV-radiation

According to the colour measurements the whiteness (colour co-ordinate L) increased in the UV-chamber. However, the increase was higher in untreated marble than in protected marble. There was also a clear tendency for the colour co-ordinate a to move towards more positive and for the colour co-ordinate b to move towards more negative values. This means that marble became more red and more blue. The change of the co-ordinate a was small and about the same both in reference and protected marble, but the change of the co-ordinate b was somewhat higher in the protected specimens than in the reference specimens. The detailed results are presented in Appendix 1.

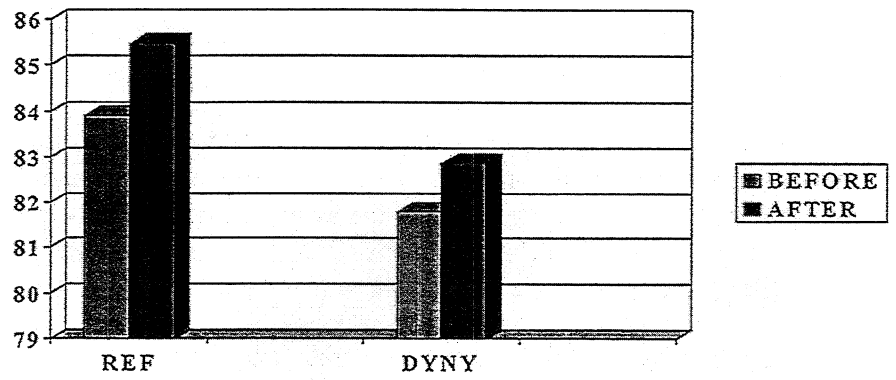

Figure 76. CIELAB colour co-ordinate L of marble A before and after UV-treatment. REF = unprotected, DYNY = protected.

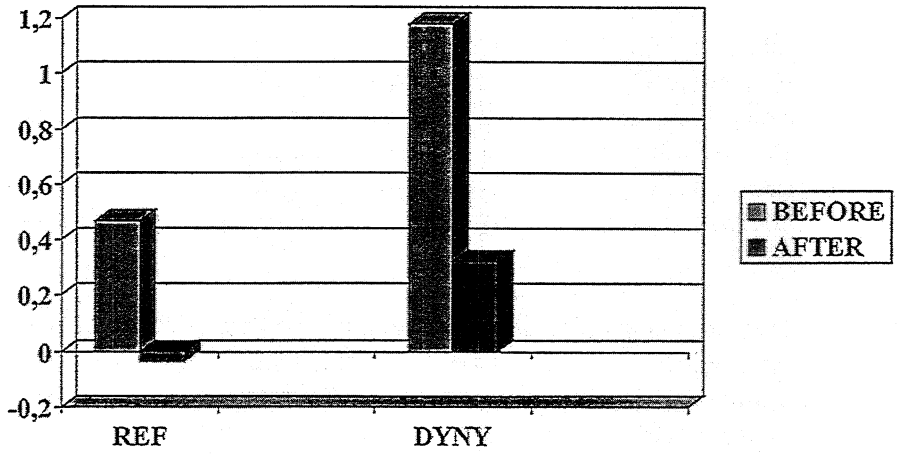

Figure 77. CIELAB colour co-ordinate b of marble A before and after UV-treatment. REF = unprotected, DYNY = protected.

The colour differences, ΔE, of the specimens calculated from the measurements are shown in Table 15. According to the results some colour change takes place by the effect of UV-light. It is notable, however, that the change in the unprotected marble specimens was higher than that in the protected specimens. Also, it must be noticed that the use of the protective agent in itself changes the colour of marble (ΔE = 2.31). Especially, the protective agent seemed to have a decreasing effect on the whiteness of marble. In addition, the colour difference between the unprotected and protected marble increased in the UV-treatment (ΔE = 2.62).

Table 15. Colour change of unprotected and protected (Dyny) marble A in UV-treatment.

	ΔE
unprotected	1.66
protected	1.39

3.3.1.2 Heat resistance

According to the colour measurements the whiteness (colour co-ordinate L) increased in the heat treatments as a function of temperature, i.e. the higher the temperature the higher the value of the co-ordinate L. However, the increase was as high in untreated marble as in protected marble. Instead, no clear tendency for the colour co-ordinates a or b could be observed. Thus, in this respect no change of colour took place in the marble. Detailed results are presented in Appendix 1.

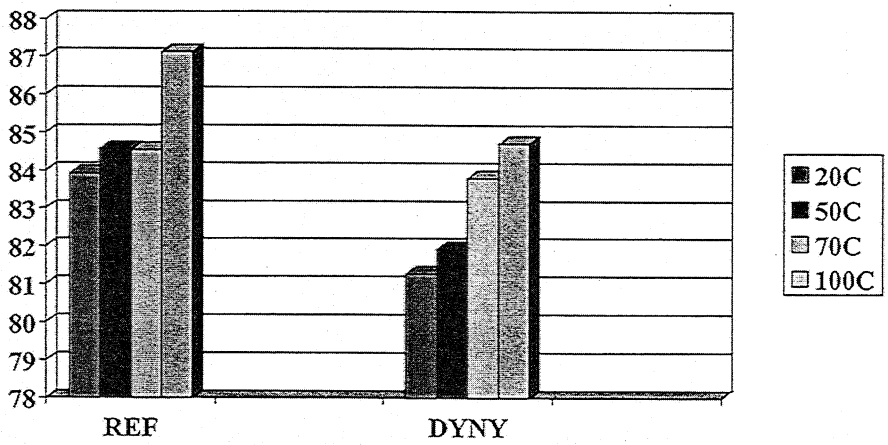

Figure 78. CIELAB colour co-ordinate L of marble A before and after various heat treatments. REF = unprotected, DYNY = protected.

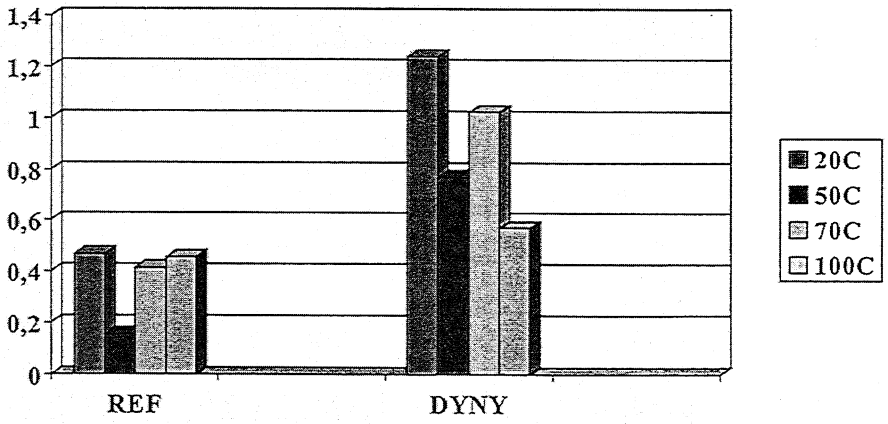

Figure 79. CIELAB colour co-ordinate b of marble A before and after heat treatment. REF = unprotected, DYNY = protected.

The colour differences, ΔE, between the treated and untreated specimens calculated from the measurements are shown in Table 16. According to the results a clear colour change takes place by the effect of heat. It is notable that in the unprotected marble specimens this change was significant only at 100°C. In the protected specimens the change was evident already at 70°C. Also, it must be noticed that the use of the protective agent in itself changes the colour of marble. Especially, the protective agent seemed to have a decreasing effect on the whiteness of marble. However, this colour difference between the unprotected and protected marble did not change in the heat treatments.

Table 16. Colour change of unprotected and protected (Dyny) marble A in heat treatments.

heat treatment	ΔE
unprotected	
50°C	0.73
70°C	0.64
100°C	3.22
protected	
50°C	0.79
70°C	2.53
100°C	3.49

3.3.1.3 Chemical resistance

According to ISO 10545-13:1995 both unprotected and protected (Dyny) samples were treated with the following chemicals:
- hydrochloric acid
- citric acid
- potassium hydroxide

Observations made of the test specimens after the test showed that the protective treatment (Dyny) did not improve the chemical resistance of marble, at least not with respect to the chemicals applied. The resistance classes of marble as specified in the standard are also shown for each chemical. Complete test data is available at Appendix 1.

D. Resistance to stains

Test results were classified according to the ease of removing the particular stain from the surface as well as to the irreversible damage caused to the surface. Following chemicals were applied to both the unprotected and protected (Dyny) samples:

- iodine
- olive oil
- red staining agent

According to the results the protective agent used (Dyny) clearly improved the cleanibility of marble. Especially this seemed to be the case when the stain contained organic compounds. Complete test data is available at Appendix 1.

3.3.2 Test wall studies

3.3.2.1 Flexural strength

A clear decrease of flexural strength could be measured during the test period for the protected samples. Depending on the protective agent used and the testing direction applied the strength values of the protected samples compared with the untreated sample decreased during 1,5 years with 26-32 %. In Figure 80 test result with protective agent Dyny are presented. The measurement results are shown in detail in Appendix 1.

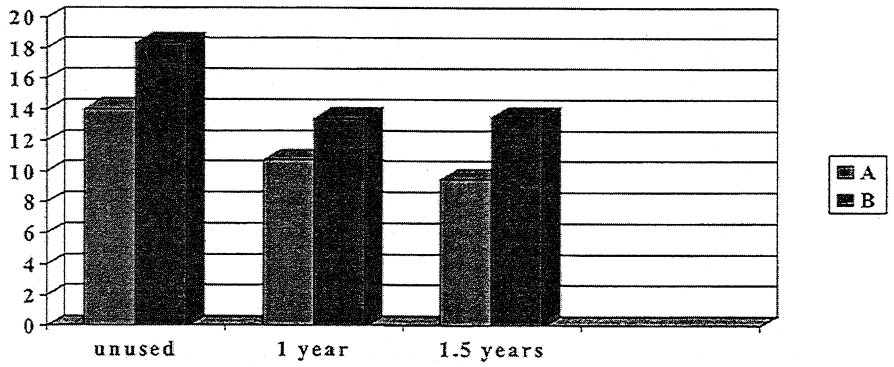

Figure 80. Flexural strength of marble A protected with Dyny (MPa).

3.3.2.2 Water absorption, apparent porosity, bulk density

The water absorption and apparent porosity of marble type A protected with the tested agents at initial stage and after 1 and 1.5 years on the test wall at Finlandia Hall are presented in Figures 81 and 82. A significant increase of the values could be measured during the test period for the protected samples. Depending on the protective agent used and the testing direction applied the strength values of the protected samples compared with the untreated sample increased during 1,5 years by 65-74 %. The measurement results are shown in detail in Appendix 1.

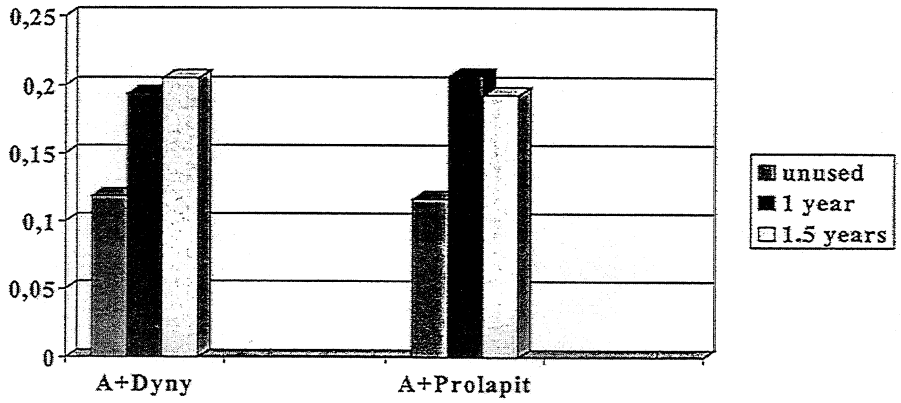

Figure 81. Water absorption of the protected marbles (w-%).

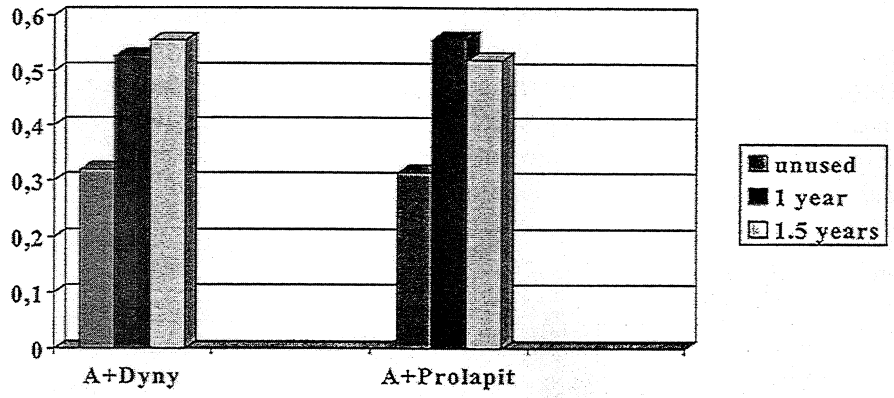

Figure 82. Apparent porosity of the protected marbles (vol-%).

3.3.2.3 Microstructure

A. Thin section study

Microstructure photograph of marble A protected with "Prolapit" after 1 year on the test wall is shown in Figure 83. The following observations were made:

- groundmass fine-grained, even-grained, not oriented
- average grain size 200-300 µm
- nearly pure carbonate rock, some quartz and little opaque minerals were detected
- no signs of deterioration observable

Figure 83. Microstructure of marble A protected with Prolapit. 1 year on the test wall. Plane-polarized light.

B. SEM-study

BSE- and SE-images of marble A protected with the agents "Dyny" and "Prolapit" after 1 year on the test wall show that grain boundaries can partly be distinguished. No signs of deterioration could be seen in the structure of marbles. Protective agents formed a layer on the surface of the marble panels. The layers seemed unaltered after 1 year on the test wall. The layer thickness was 15-30 µm with the agent "Dyny" and 10-15 µm with the agent "Prolapit". Detailed results are presented in Appendix 1.

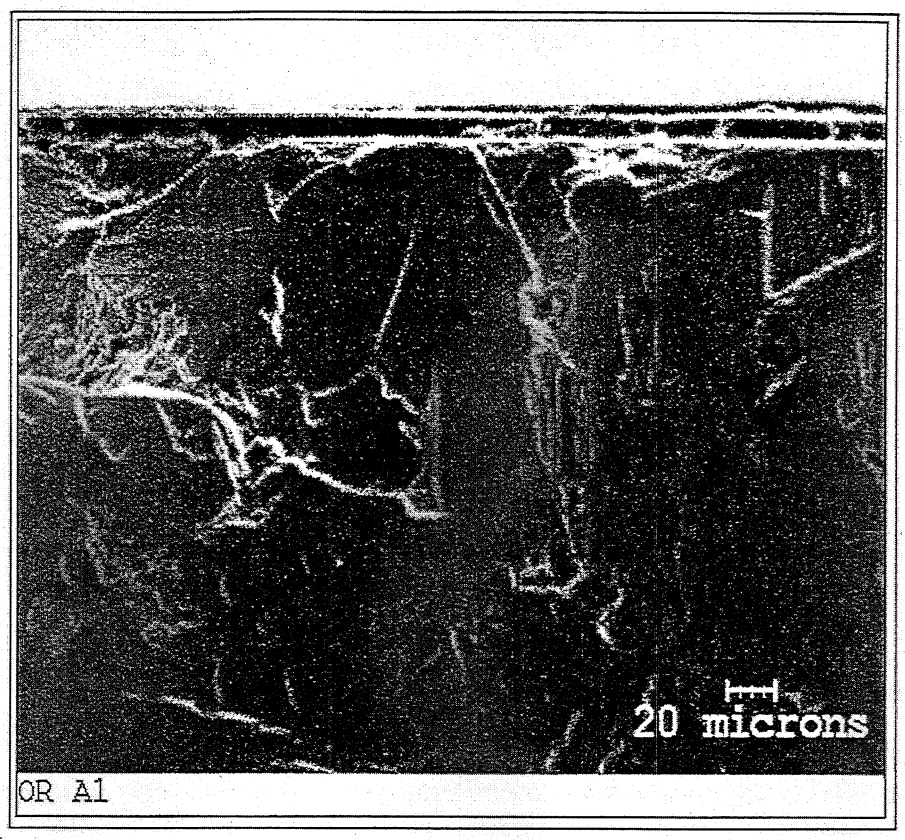

Figure 84. Marble A + Dyny. A layer of protective agent on the surface of the panel having a thickness 15-30µm. 1 year on the test wall. SE-image, 300x.

SEM-pictures of fractured surfaces of marble A protected with agents "Dyny" and "Prolapit" after 1 and 1.5 years on the test wall are shown in Figs. 85-86. The individual grains can, at least for the most part, be distinguished from each other. Cracks can be noticed between some of the grains. The maximum crack width observed in the specimens was around 0.6-0.7 µm.

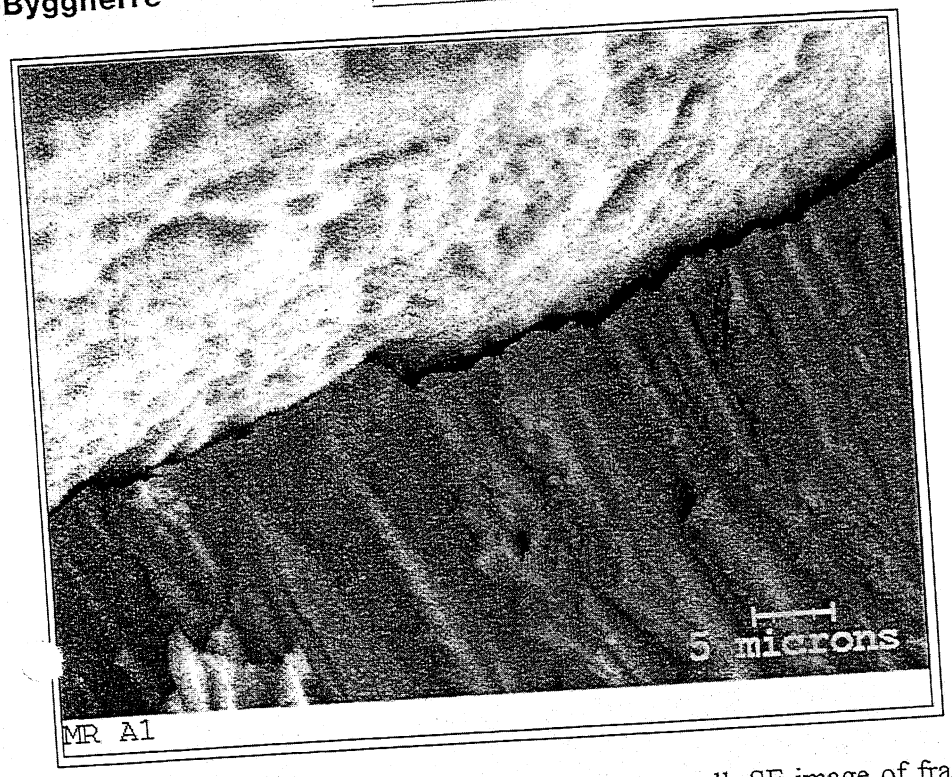

Figure 85. Marble A + Dyny. 1 year on the test wall. SE-image of fractured surface, 2500x.

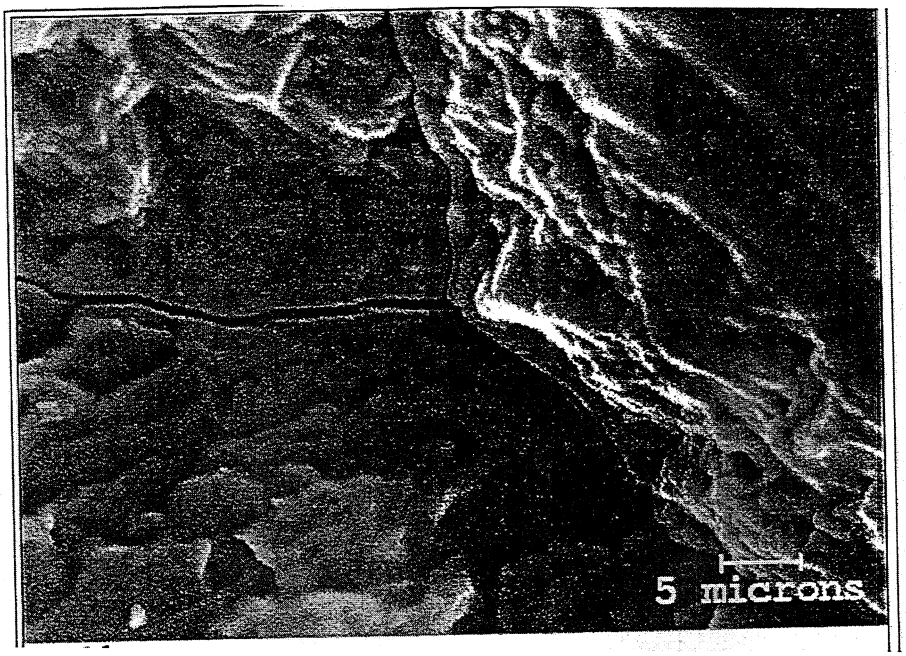
5 microns

3.3.2.4 Colour measurement

The colour of the protected marble panels chosen for this part of the study was measured 5 times during the project between 23.6.1999 – 8.3.2001. Marbles with both of the protective agents were white, the L value of the unused panels varying between 81 and 83. The values of the co-ordinates a and b were near zero, even though the marbles had a slight greenish hue. Compared to unprotected marble A, the value of the co-ordinate L was a little lower and that of the co-ordinate b a little higher.

According to the colour measurements the whiteness of the marbles increased. The increase was fairly even. Also, there was a clear even if slight tendency for the co-ordinates a and b to move towards more positive values. This means that the marbles are getting more yellow and more red, which could refer to fouling of the marble surfaces. So far the changes have, however, been small. As a whole, the behaviour of the protected marble panels was similar to that of the unprotected panels. The results from the colour measurements for all the marbles are shown in Appendix 1.

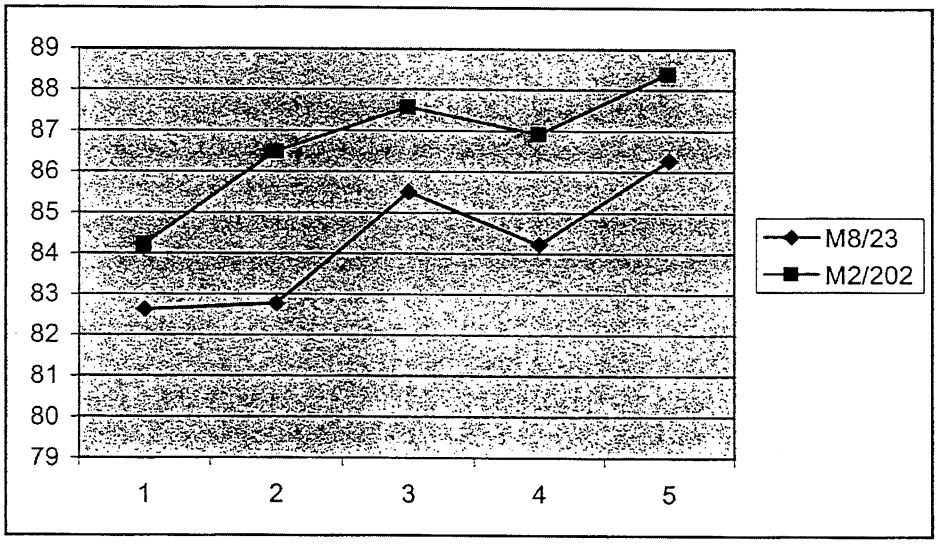

Figure 87. CIELAB colour co-ordinate L of marble A + Dyny.

The colour differences, ΔE, of the protected marbles calculated from the values of the first (1) and the last (5) measurements are shown in Table 17. According to the results the colour change of protected marbles is evident. However, the change is of the same order of magnitude as the change observed with unprotected marble A.

Table 17. Colour change of the protected marbles in time period 6/99-3/01 (CIELAB).

marble	wall	ΔE
A+Dyny	23	3.66
	202	4.18
A + Prolapit	23	3.92
	202	4.17

3.3.3 Discussion

3.3.3.1 Resistance properties

According to the colour measurements the protective agent used in the laboratory studies (Dyny) altered the colour of marble. It decreased the whiteness of marble, in marble A the L value of CIELAB co-ordinates dropped from about 84 to 81-82, and increased the yellowish hue, in marble A the value of co-ordinate b rose from about 0.5 to about 1.2. The colour difference caused by these changes was fairly obvious.

Treatment in the UV-chamber increased the whiteness of protected marble. Because it increased the whiteness of unprotected marble as well, the change was most probably not due to chemical degradation of the protective agent but a consequence of the deterioration of marble itself. As discussed in the report of the subproject "Test wall" thermal treatment is used to increase the whiteness of marble, and the process is presumably based on the microstructural cracking accomplished by thermal variations. Thus, the increased whiteness in the UV-chamber is not directly caused by radiation but elevated temperature it generates at least on the surface of marble.

On the other hand, UV-radiation dropped the value of co-ordinate b of protected marble almost to the same level as that of unprotected marble. This indicates that the protective agent is, at least to a certain extent, sensitive to UV-radiation and may show some degradation when subjected to it.

Heat treatments had the same effect on the whiteness of protected and unprotected marble as UV-radiation. Most probably also the reason for the increase was the same, i.e. microstructural cracking of marble caused by thermal variation. However, a decrease in the value of co-ordinate b was also observed in protected marble. As above this refers to some sort of degradation of the protective agent due to heat. The colour change taking place for this reason was almost insignificant, though.

The protective agent used in the studies was resistant against alkalies, but it could not protect marble from the etching effect of acidic compounds. It

must be noted, however, that the test used to evaluate the behaviour of the agent was not very suitable for the purpose, because in this test specimens were immersed as whole in the chemical. Thus, the potential protective effect of the agent got covered by the very vigorous reaction of marble itself. In any case, there were some signs that the protective agent didn't take part in the reaction. Its resistance against acidic compounds should be studied again by using a method in which only the surface with the protective agent is subjected to acids.

The protective agent used in the studies improved considerably the resistance of marble to stains of organic nature. The mechanism of protection seemed simply to be that it prevented the organic compounds from intruding into marble, which made marble surface relatively easy to be cleaned. However, most probably there are some organic compounds that can react with the protective agent and can in that way cause a stain which is much more difficult to remove. This kind of signs was to be observed when the only inorganic chemical of the test, iodine, was applied on the protected surface, even if it could be cleaned as easily as from unprotected marble.

3.3.3.2 Strength properties

The initial flexural strength of protected marble (type A) varied between 14 and 19 MPa.The lowest values were measure in testing direction A and the highest in testing direction B, the strength ratio A/B varying between 0.7-0.8. This refers to some kind of schistosity in stone structure. The results of unprotected marble A in the subproject "Test wall" were similar to those determined here.

The strength of protected marble decreased considerably on the test wall, which most probably is a sign of the effect of some sort of a deterioration process. The loss of strength was 25-30%, and it was about the same in both directions and with both protective agents. The results in the subproject "Test wall" were precisely parallel to those discussed here. Thus, the loss of strength can be considered to be a real phenomenon, and it can't be explained to be due to sampling or random variation of strength. In fact, the strength losses detected in protected marble were somewhat higher than those determined for unprotected marble. If the difference is real, there must a factor in the deterioration mechanism that is affected by the changes in marble properties due to protective agents in an accelerating way. At least, the difference can't be explained with difference in the strain level accomplished by environmental conditions, as both protected and unprotected marble slabs were placed on the same test wall for the same period of time.

The fact that the strengths were of the same order of magnitude after 1 and 1.5 years on the test wallwas also a very noteworthy feature in the results. This would indicate that the loss of strength on the test wall happened very soon after the slabs were installed, and after that the deterioration process

proceeded only slowly. Also in this respect the results were parallel to those of unprotected marble.

According to the results of the strength measurements the protective agents used in the study can't prevent the loss of strength taking place in marble when subjected to environmental strains. Thus, the deterioration mechanism in question is not dependend on at least any straigth reaction of e.g. water and/or acidic compounds or other impurities with marble surface.

3.3.3.3 Water absorption properties

Protected marble was very dense. The water absorption was about 0.12 w-%, apparent porosity 0.31-0.32 vol-% and bulk density 2712-2715 kg/m^3. The results were similar to those of unprotected marble. This is explained by the nature of the test which was used in the measurements, because in the test the specimens are totally immersed in water instead of subjecting water only to the surface treated with the protective agent. Thus, the test is not able to evaluate the protective capability of the agent.

The water absorption and apparent porosity of protected marble increased considerably, around 65-75%, on the test wall. The increase observed in unprotected marble was practically the same. No further increase in the values of the water absorption properties could be observed between 1 and 1.5 years on the test wall. Thus, the results in this respect were in line with those from the strength determinations.

The fact that porosity of marble increases when subjected to environmental strains refers to a deterioration mechanism that causes cracks to marble structure. These cracks can go either straight through the individual grains or, more probably, along the grain boundaries.Emergence of cracks to marble structure would also explain the loss of strength observed. It seems, however, that at least a certain amount of cracks appears almost immediately when marble is subjected to strains but then the process slows down and the degree of cracking stays more or less at same level. Also, it seems likely that the mechanism causing the cracks is not affecting through reactions occurring on the outer surface of marble, as already discussed above.

3.3.3.4 Microstructure

According to the definition by prof. Royer-Carfagni from University of Parma marble structures can be classified along the axis of xenoblastic-homoblastic. Xenoblastic marble structure is characterized by interlacing of irregular grains that are closely fitted to each other along their wavy contours. On the other hand, homoblastic marble structure is characterized by regular-shaped grains with straight or gently curving boundaries. Thin section study of the protected marbles revealed that the structure was intermediate, i.e. it was between the two extremes showing both xenoblastic and homoblastic features. Marble was fairly even-grained, and the average grain

size was around 0.2 mm. The results were similar to those observed for unprotected marble in the subproject "Test wall".

No changes could be observed in the microstructure of protected marbles taken from the test wall with SEM-study of polished marble sections. As thin sections polished sections can be used to reveal the structure type of marbles, but the method is not sensitive enough to monitor the changes taking place in the microstructure due to environmental strains. Also, polished marble fractions can be used to determine the condition of the layer of the protective agent on marble surface. According to the observations made the protective layer of both of the agents seemed unaltered after 1 year on the test wall. The layer thickness of the agent "Dyny" was 15-30 µm and that of the agent "Prolapit" 10-15 µm.

The structural type of marble could be identified also in the SEM-study of fractured surface specimens of protected marbles. As already stated above, the structure of marble was intermediate: in part the individual grains could be easily seen, in part no grain boundaries could be distinguished in the structure.

SEM-study of fractured specimens revealed also cracks in the specimens of marbles that had been on the test wall. The maximum crack width observed was about 0.6-0.7 µm, though in general the cracks were narrower. The behaviour of the protected slabs was exactly the same as that of the unprotected marble. Thus, protective agents can't prevent marble from cracking.

Crack formation is a clear sign of deterioration occurring in marble. The fact that the cracks go along the grain boundaries, not straight through the grains, indicates to a mechanism that tends to separate the grains from each other. Thus, cracking can be a consequence of thermal variations taking place in marble slabs as the thermal expansion behaviour of calcite crystals of which the grains of marbles are composed is anisotropic, i.e. the expansion coefficient is higher in the direction of one crystallographic axis than in the other perpendicular to the first one. This kind of a deterioration mechanism would also explain the inefficiency of protective agents to prevent marble from damaging when subjected to thermal variations.

Another possible explanation can be the freeze/thaw effect which tends to widen the cracks already existing in marble structure and also in this way to create new. Naturally, both of the mentioned mechanisms can act simultaneously. It seems, though, that freezing and thawing is of minor importance as it could be expected that protective agents could at least retard the effect of that type of a deterioration mechanism. As stated, nothing of the kind could be observed.

3.3.3.5 Colour measurements

According to the colour measurements the protective agents didn't alter the colour of the marble to a considerable extent. The initial value of CIELAB co-ordinate L (whiteness) of the protected slabs was around 83, which was only slightly lower than that of the unprotected marble. In the laboratory tests discussed in chapter 5.1 the darkening effect of the protective agent was much more obvious. Also, the agents didn't change the slight greenish hue of marble with the value of co-ordinate a of about -1, but they had a small effect in the axis of blue-yellow, as they altered the original blueish hue to neutral or even to a little bit of yellow with the value of the co-ordinate b varying between 0 and 0.1.

The whiteness of the protected marbles increased when the slabs were subjected to environmental strains on the walls of Finlandia Hall. Presumably this is a sign of the deterioration process taking place in marble. It is common knowledge in the manufacturing of marble products that their whiteness can be increased by thermal treatment. As it is obvious that variation of temperature causes granular decohesion in marble, it seems plausible to suppose that it is just this deterioration that is reflected also in the colour of marble as increased whiteness. This theory of the reason for increasing whiteness on the walls is supported by the observation that the colour change was evident especially during the first year, but after that the rate of change seem to have slown down. A similar time-dependent behaviour was observed in the strength and water absorption properties, which without any doubt are directly connected to deterioration.

A minor but clear tendency for the co-ordinates a and b to move towards more positive values was observed in the protected marble slabs. This means that they are turning more red and more yellow, which could refer to fouling of marble surfaces.

It is noteworthy that the behaviour of the protected marble slabs also in this respect was similar to that of the unprotected marble. Thus, the protective agents haven't had any effect on the colour change of marble. So far this changes has, however, been small, and in addition most of it is due to increased whiteness, not to change of the other co-ordinates. The time period of monitoring the colour changes, about 20 months, has been so short that no definite conclusions can yet be made. For good reason it can be expected that the effect of the protective agents, if any, will be seen only during longer periods of time, as the outer surface of unprotected marble starts to lose its gloss and gets more apt to fouling.

3.3.4 Conclusions

According to the studies made the deterioration of marble structure taking place when subjected to environmental strains is caused by granular decohesion, which forms cracks along the grain boundaries. Granular decohesion seems to be a consequence of the anisotropic thermal expansion behaviour

of calcite crystals. For this reason marble grains that are composed of calcite crystals break away from each other when thermal variations occurring naturally affect the material, e.g. in facades. The strain caused by freezing and thawing may have an accelerating effect on the deterioration process after it has started and enough cracks have been formed.

The results achieved show that the damaging of marble structure takes place very soon after it has been subjected to environmental strains, probably already during the very first cycles of thermal variation. After that the deterioration process slows down, and the properties of marble will stay more or less stable. Thus, in order to predict the behaviour of marble for any longer periods of time a longer period of time for monitoring the marble properties would also be required. A reliable view e.g. of the rate of strength decrease as an indication of the progress of the deterioration process can be acquired only in that way.

Because of the nature of the deterioration mechanism described above it can't be influenced by the use of protective agents. If other factors, e.g. freeze/thaw effect and chemical degradation, have a significant contribution to the deterioration process during later stages, these might be retarded with the use of some sort of a protection on the outer surface of marble. More long-term studies dealing with thsi issue would, however, be needed.

Measurements of marble colour can be used to monitor the fouling of marble surfaces. So far protected marble has shown similar behaviour as unprotected marble. However, in order to get a reliable picture of the effect of possible protective treatments on the fouling behaviour the period of time used for monitoring the colour should be much longer than that used in this project, probably at least 5 years.

According to the laboratory studies marble surface can be protected against stains and certain types of chemical effects by the use of protective agents. They are especially effective against stains of organic nature. The agents themselves, however, seem to be affected by UV-radiation and thermal strains. Thus, their service life is limited. Long-term monitoring of the resistance of the protective layer on marble surface would be needed in order to determine the proper period for renewal of the protection procedure

According to the measurements the walls of Finlandia Hall have already deteriorated. The strength decrease of marble about two years after installing the slabs is 20-30%. Continuous monitoring of the microstructure and the strength properties as well as the colour of the wall marble is recommended.

3.4 Research on one-side weather resistance test

3.4.1 Flexural strength

The flexural strength of marble D cut perpendicular (PE) to the rift in initial stage and after 100 and 200 cycles in the climate chamber is presented in Figure 88. A and B presented in the figure are testing directions along the surface plane. Corresponding values for marble E cut parallel to the rift (PA) are presented in Figure 89. After 200 cycles the flexural strength of marble D has decreased 34-65 % depending on the testing direction. Respectively the values for marble type E have diminished
6-12%. The measurement results are shown in detail in Appendix 1.

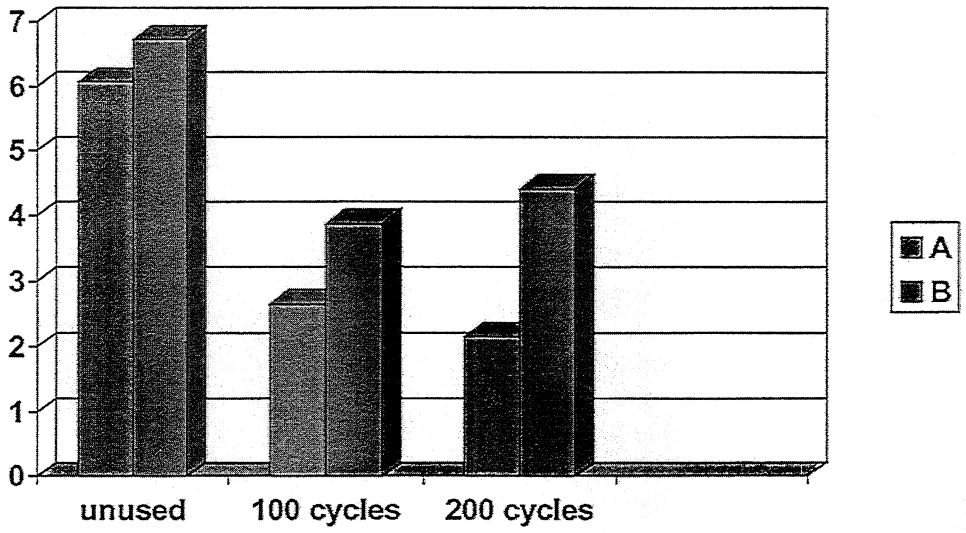

Figure 88. Flexural strength of marble D (PE) (MPa).

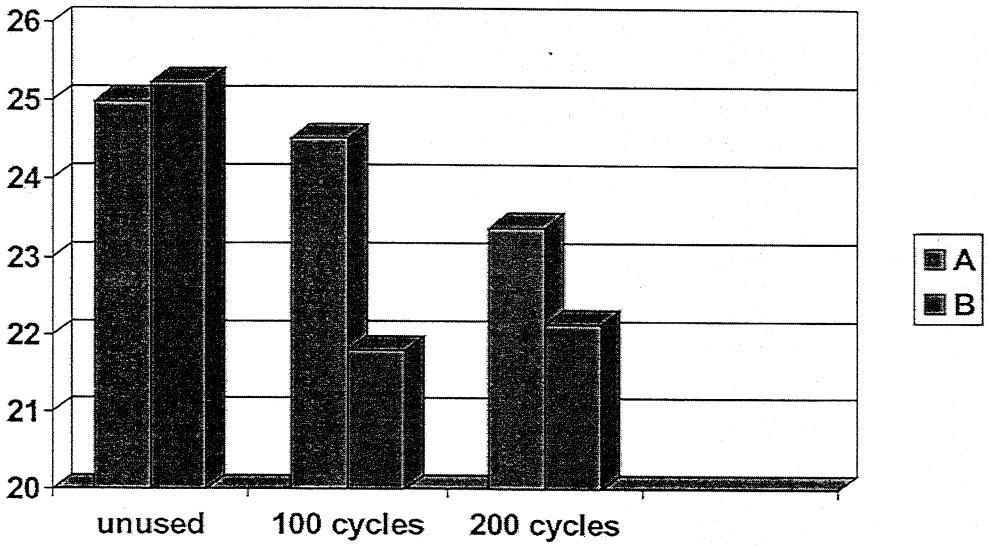

Figure 89. Flexural strength of marble E (PA) (MPa).

3.4.2 Water absorption, apparent porosity, bulk density

The water absorption and apparent porosity of marble type D (PE) at initial stage and after 100 and 200 cycles in the climate chamber is presented in Figures 90 and 91. A notable increase of the values could be measured after 100 cycles, but during the additional 100 cycles the values remained practically unchanged. The measurement results are shown in detail in Appendix 1.

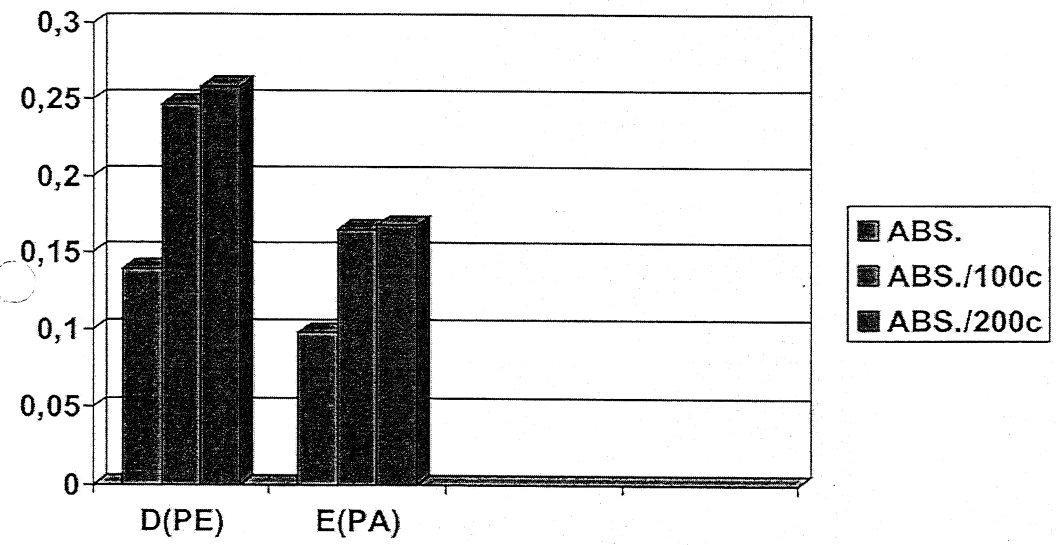

Figure 90. Water absorption of the marbles D and E (w-%).

3.4 Research on one-side weather resistance test

3.4.1 Flexural strength

The flexural strength of marble D cut perpendicular (PE) to the rift in initial stage and after 100 and 200 cycles in the climate chamber is presented in Figure 88. A and B presented in the figure are testing directions along the surface plane. Corresponding values for marble E cut parallel to the rift (PA) are presented in Figure 89. After 200 cycles the flexural strength of marble D has decreased 34-65 % depending on the testing direction. Respectively the values for marble type E have diminished 6-12%. The measurement results are shown in detail in Appendix 1.

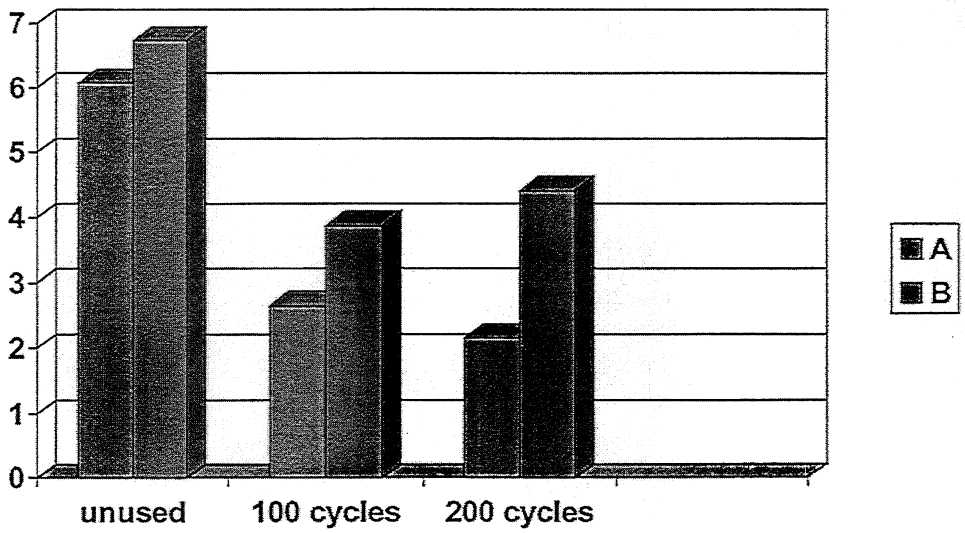

Figure 88. Flexural strength of marble D (PE) (MPa).

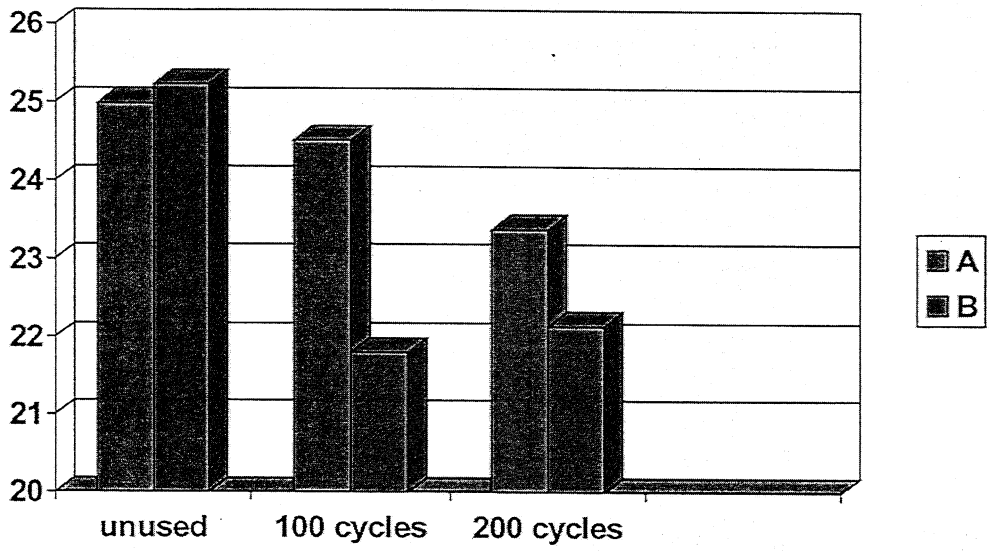

Figure 89. Flexural strength of marble E (PA) (MPa).

3.4.2 Water absorption, apparent porosity, bulk density

The water absorption and apparent porosity of marble type D (PE) at initial stage and after 100 and 200 cycles in the climate chamber is presented in Figures 90 and 91. A notable increase of the values could be measured after 100 cycles, but during the additional 100 cycles the values remained practically unchanged. The measurement results are shown in detail in Appendix 1.

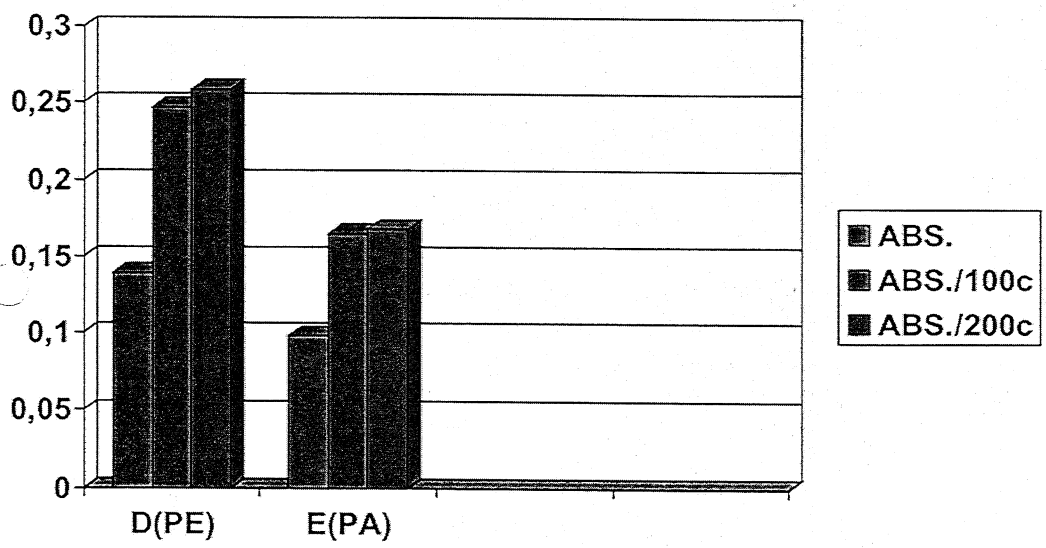

Figure 90. Water absorption of the marbles D and E (w-%).

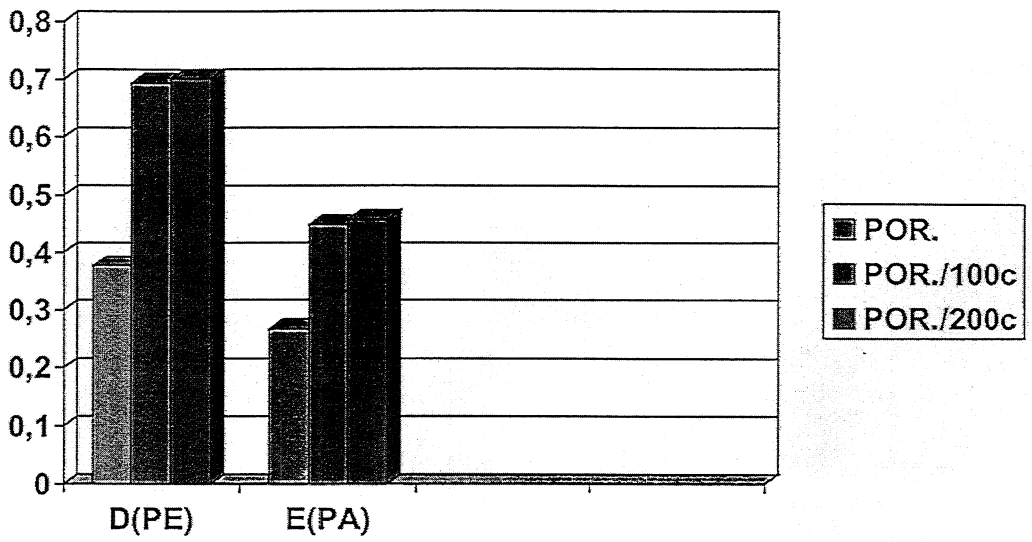

Figure 91. Apparent porosity of the marbles D and E (vol-%).

The relative changes of the water absorption, ΔW, and apparent porosity, Δp_o, of the marbles that have taken place during the weather resistance tests are presented in Table 18. The basis of the comparison is in all cases the value of the unused marble.

Table 18. The relative changes of water absorption and apparent porosity of marbles D and E in the weather resistance test.

marble type	ΔW 100 cycles %	ΔW 200 cycles %	Δp_o 100 cycles %	Δp_o 200 cycles %
D(PE)	+78	+86	+84	+86
E(PA)	+68	+71	+68	+71

3.4.3 Mineral composition

3.4.3.1 X-ray diffraction

According to the X-ray diffraction diagram marble D (PE) consisted almost entirely of calcite, i.e. calcium carbonate, $CaCO_3$. Quartz, α-SiO_2, and dolomite, $CaMg(CO_3)_2$, were also observed. The contents of these accessory minerals were, however, low, at most only a couple of weight percents. The diffraction diagram of marble D(PE) is shown in Appendix 1.

According to the X-ray diffraction diagram marble E(PA) consisted almost entirely of calcite, i.e. calcium carbonate, $CaCO_3$. Marble contained also a substantial amount, probably about 5 w-%, of dolomite, $CaMg(CO_3)_2$. Quartz, α-SiO_2, was also observed, but its content was low. The diffraction diagram of marble E(PA) is shown in Appendix 1.

3.4.3.2 Thermal analysis

The thermal behaviour of the marbles was practically identical. The thermal curves contained only one phenomenon, the disintegration reaction of calcite in the temperature region of 700°C-950°C. In the curves of the marble E(PA) there was, however, a small effect, "a shoulder", at about 750°C. This probably refers to dolomite whose disintegration reaction includes two separate steps, first of which is comprised of the dissociation of magnesite and the second of the dissociation of calcite.

The weight losses of the marbles at 1000°C, Δm_T, and the temperatures of the maximum rate of the weight change, T_{max}, taken as the temperatures of the peaks of the DTG-curves are shown in Table 19. The thermal curves of the marbles are shown in Appendix 1.

Table 19. The weight loss and the temperature of the DTG-peak of the marbles in thermal analysis.

marble	Δm_T w-%	T_{max} °C
D(PE)	44.2	922
E(PA)	45.1	917

3.4.4 Microstructure

3.4.4.1 Thin section study

Photographs of the microstructure of marble D(PE), unused and after 100 cycles in the climate chamber, are shown in Figures 92 and 93. Following observations were made:

- fine-grained, fairly even grained, nor oriented, massive
- average grain size 200-300 µm
- nearly pure carbonate rock, contains very little quartz
- some alteration of the grains
- signs of granular decohesion after 100 cycles in the climate chamber

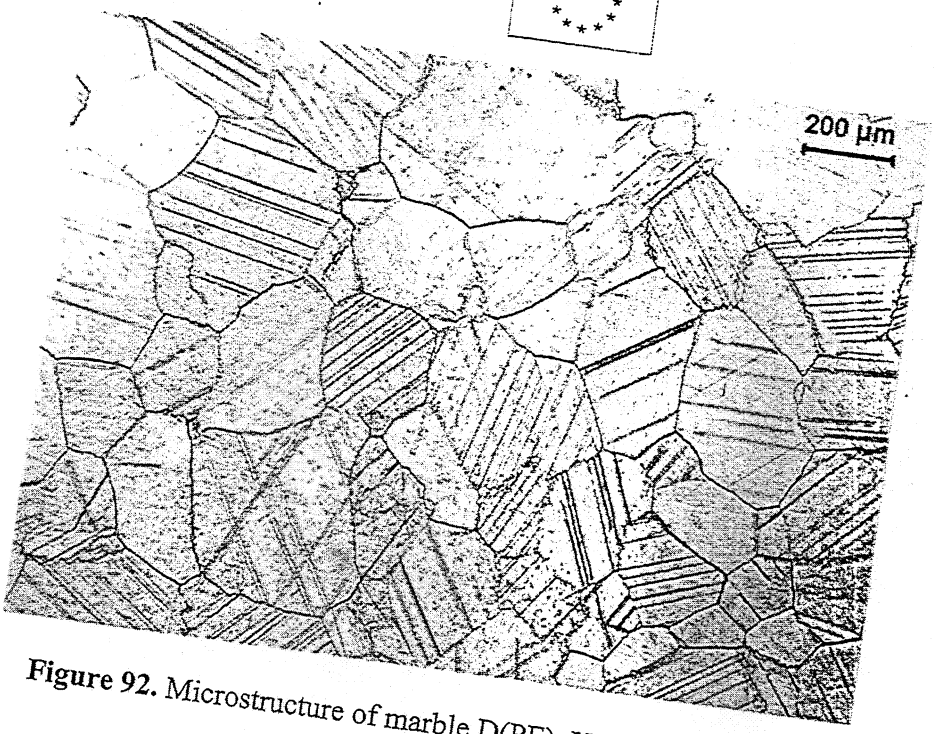

Figure 92. Microstructure of marble D(PE). Unused. Plane-polarized light.

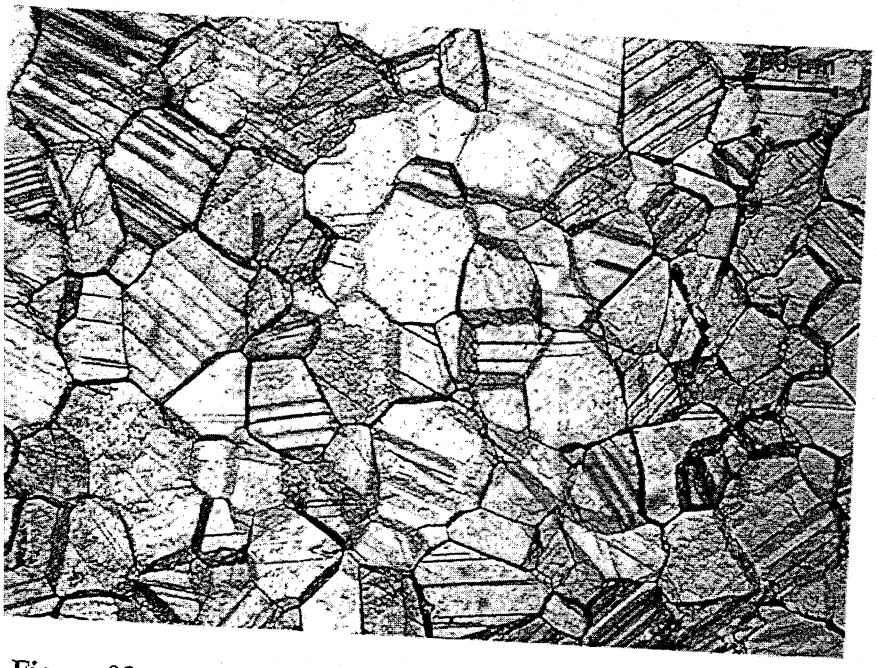

Figure 93. Microstructure of marble D(PE) 100 cycles in the

Photographs of the microstructure of marble E(PA), unused and after 100 cycles in the climate chamber, are shown in Figures 94 and 95. Following observations were made:

- fine-grained, not oriented
- grain size varies from microcrystalline up to 0.5 mm
- nearly pure carbonate rock, contains some quartz and opaque minerals
- some alteration of the grains
- no changes observable after 100 cycles in the climate chamber

Figure 94. Microstructure of marble E(PA). Unused. Plane-polarised light.

Figure 95. Microstructure of marble E(PA). 100 cycles in the climate chamber. Plane-polarised light.

3.4.4.2 SEM-study

BSE- and SE-images of marble D (PE) both unused and after 100 cycles in the climate chamber show that grain boundaries can clearly be distinguished. Strains caused by 100 cycles in the climate chamber seemed to effect the structure of the marble in such a way that the grain boundaries could be distinguished even more easily.

BSE- and SE-images of marble E(PA)Show that grain boundaries can only partly and even then very vaguely be distinguished. No changes could be seen in the structure of the marble after 100 cycles in the climate chamber.

SEM-pictures of fractured surfaces of marble D(PE) after 100 cycles in the climate chamber, are shown in Figures 96-97. The individual grains can easily be distinguished from each other. Clear cracks can also be noticed between the grains. These cracks become considerably wider when the marble is exposed to the freeze/thaw strains in the climate chamber. The maximum crack width after cycling in the climate chamber can be around 6-7 µm. The homoblastic structure of the marble can be clearly seen.

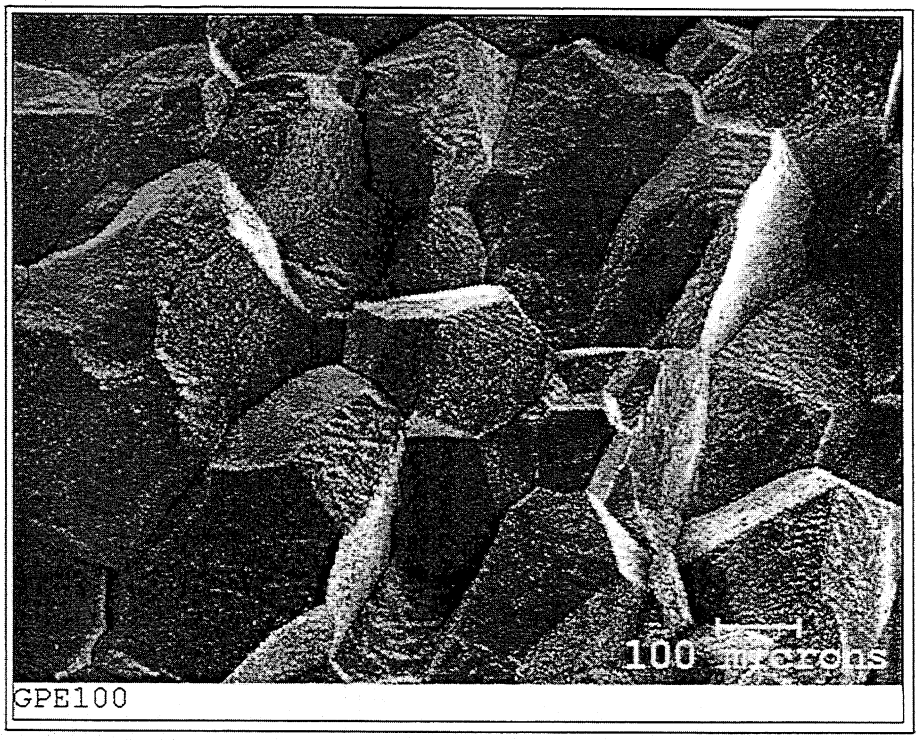

Figure 96. Marble D(PE), 100 cycles in the climate chamber. SE-image of fractured surface, 100x.

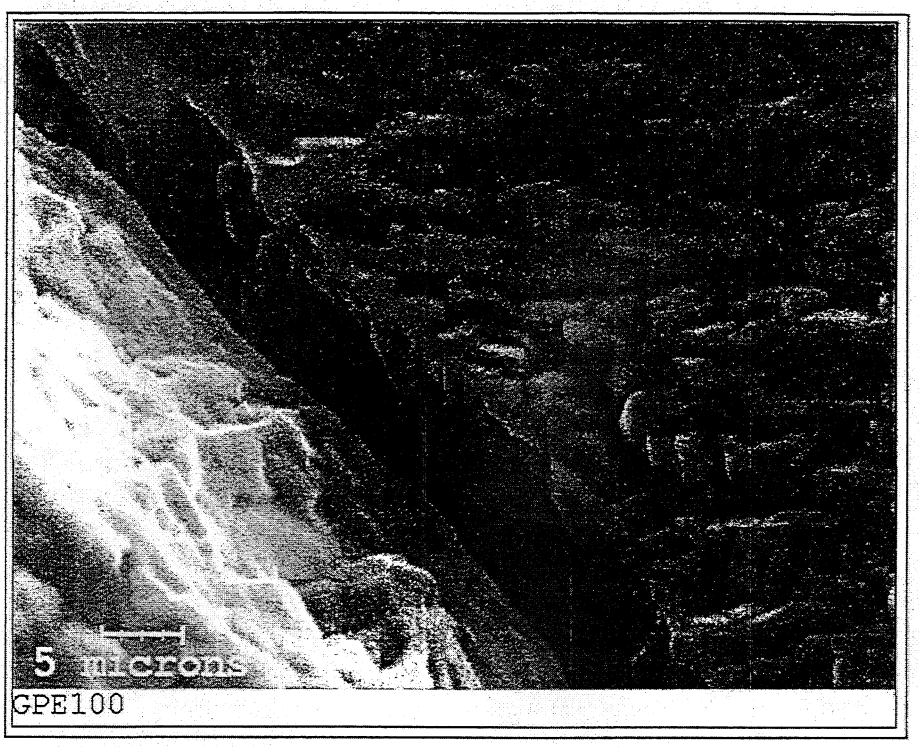

Figure 97. Marble D(PE), 100 cycles in the climate chamber. SE-image of fractured surface, 2500x.

SEM-picture of fractured surface of marble E (PA) after 200 cycles in the climate chamber, is shown in Figure 98. The grain boundaries can be seen only in some places. Thus, it is impossible to distinguish the grains from each other. Some very narrow cracks can be noticed between some of the grains. Some more of these cracks exist and they become a little wider when the marble is exposed to the freeze/thaw strains in the climate chamber. The maximum crack width after cycling in the climate chamber is 0.2-0.3 µm. The xenoblastic structure of the marble can clearly be seen.

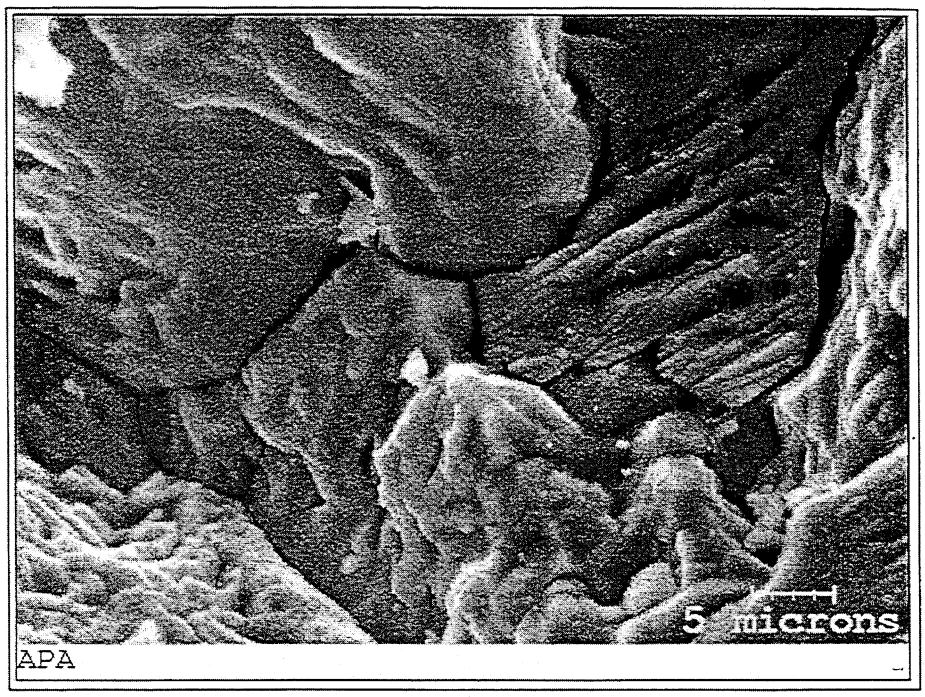

Figure 98. Marble E(PA), unused. SE-image of fractured surface, 2500x.

3.4.5 Colour measurement, gloss

During the weather resistance tests the colour of the marble panels was measured 4 (100 cycles) or 5 times (200 cycles). The number of cycles of the measurements were as follows:

code	100 cycles number of cycle	200 cycles number of cycle
1	0	0
2	26	53
3	53	93
4	103	150
5		200

According to the colour measurements the whiteness of the marbles seemed to increase, though the changes were not very notable or even unambiguous at all points. Instead, there was a clear tendency for the co-ordinate a to move towards more negative and for the co-ordinate b to move towards more positive values. This means that the marbles became more yellow and more green. This could refer to fouling of the marble surfaces, possibly due to impurities from the water spraying system of the climate chamber. The results from the colour measurements of the marbles are shown in Figures 99-101. The detailed results are presented in Appendix 3.

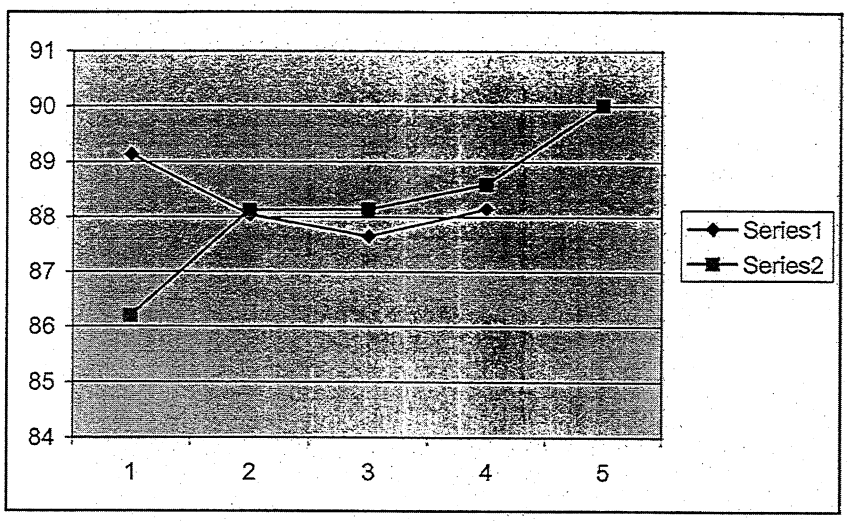

Figure 99. CIELAB colour co-ordinate L of marble E(PA). Series 1 = weather resistance test with 100 cycles, series 2 = weather resistance with 200 cycles.

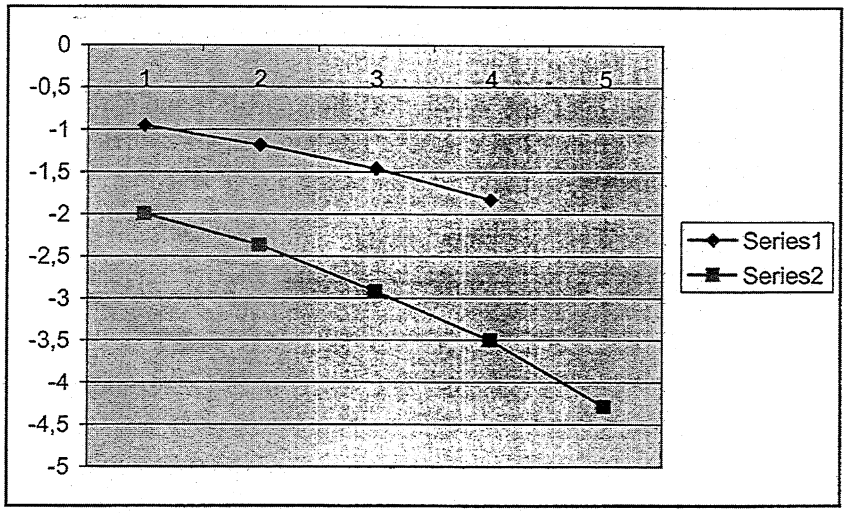

Figure 100. CIELAB colour co-ordinate a of marble E(PA). Series 1 = weather resistance test with 100 cycles, series 2 = weather resistance with 200 cycles.

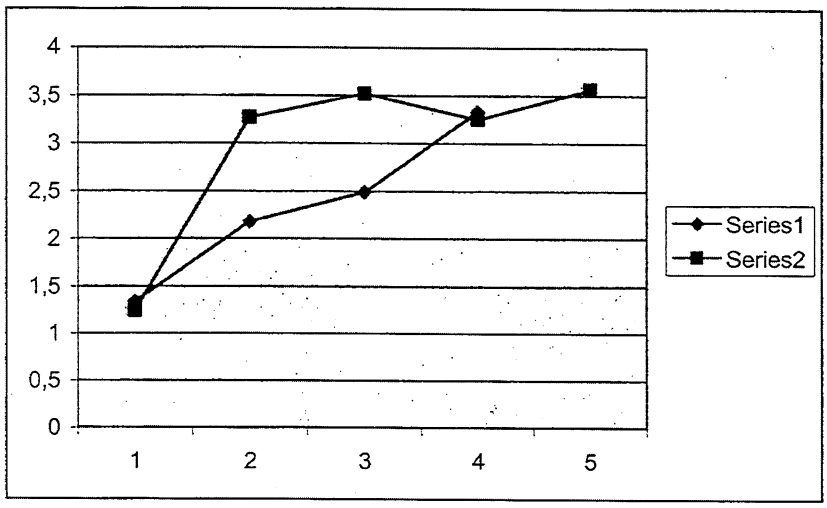

Figure 101. CIELAB colour co-ordinate b of marble E(PA). Series 1 = weather resistance test with 100 cycles, series 2 = weather resistance with 200 cycles.

No change in the values of gloss could be observed in any of the marble specimens. The surfaces of the marble panels used in the weather resistance test were not polished.

3.4.6 Warping

In the weather resistance tests all the panels showed convex bowing, i.e. they bowed towards the inside of the climate chamber. The degree of bowing was, however, hardly noticeable. The measured displacements, δ, and the corresponding radii of curvature, r, are presented in Table 20.

Table 20. Bowing of the marble panels in the weather resistance tests presented as displacements (δ) and radii of curvature (r).

marble	test mm	δ m	r
D(PE)	100	0.12	250
200	0.07	430	
E(PA)	100	0.08	380
200	0.12	250	

3.4.7 Discussion

3.4.7.1 Strength properties

The flexural strengths of the marble types chosen for the study differed considerably from each other. Marble E was very strong with an initial flexural strength of around 25 MPa. On the other hand marble D was weak with an initial flexural strength of 6-7 MPa. Marble D seemed to be somewhat (10%) weaker in testing direction A than in direction B, which could refer to some kind of schistosity in stone structure. In this respect, the strength results of marble E were more even.

The strength of marble D decreased noticeably on the test wall, which most probably is a sign of the effect of some sort of a deterioration mechanism. The loss of strength in testing direction B was 35-40%, but it was even more pronounced, 55-65%, in direction B, where the marble already originally was weaker. On the other hand, marble E showed far better durability. The loss of strength observed in marble E was about 5% in testing direction A and a bit over 10% in testing direction B.

The results in the subproject "Test wall" were parallel to those discussed here. Thus, the loss of strength can be considered to be a real phenomenon, and it can't be explained to be due to sampling or random variation of strength. The strength losses detected in the weather chamber seemed, however, to be a little higher than those observed in the test wall after 1 or 1.5 years. According to the results of the subproject "Environmental condition" this is most probably a consequence of the fact that the strain level due to thermal variations and freeze/thaw cycles has been somewhat higher in the weather chamber than on the test wall. In the measurements made at Finlandia Hall around 80 freeze/thaw cycles were observed during the period of 1.5 years of the test wall study. In this respect only the test with 100 cycles would correspond roughly to 2 years and the test with 200 cycles to 4 years on the test wall. It must be noted, however, that the 1.5 years period of the test wall specimens included only one winter. On the other hand, the daily thermal variation of temperature in marble was clearly greater in the weather resistance tests than in reality.

The fact that the strengths were of the same order of magnitude after 100 and 200 cycles in the weather chamber was also a very noteworthy feature in the results. This would indicate that the loss of strength in the weather chamber happened already during the very first cycles, and after that the deterioration process proceeded slowly. Also in this respect the results were parallel to those of the test wall specimens.

3.4.7.2 Water absorption properties

Both marble types were very dense. The water absorption of marble D was 0.14 w-% (apparent porosity 0.38 vol-%) and that of marble E only 0.10 w-

% (apparent porosity 0.27 vol-%). The bulk density of both types was between 2713-2715 kg/m^3.

The water absorption and apparent porosity of both marble types increased considerably in the weather chamber. The relative increase in marble D was around 85%. The increase observed in the specimens taken from the test wall was practically the same. The relative increase in marble E was about 70%, which was considerably more than observed in the test wall specimens (9-13%). This can be due to the higher level of strains subjected to marbles in the weather chamber compared to the 18-month period on the test wall as discussed above in chapter 5.1. It is interesting, however, that the high increase in water absorption properties of marble E, which refers to crack formation in the structure, is not very extensively reflected in its strength properties. This could refer to the existence of other features in the microstructure of marble E that can compensate the weakening effect of cracking. It can be considered, however, that heavy cracking of marble forms a risk factor for durability properties in the long run.

The increase in the values of the water absorption properties between specimens subjected to 100 and 200 cycles in the weather chamber was small. Thus, the results in this respect are in line with those from the strength determinations.

The fact that porosity of marbles increases when subjected to thermal strains refers to a deterioration mechanism that causes cracks to marble structure. These cracks can either go straight through the individual grains or, more probably, along the grain boundaries. Emergence of cracks to marble structure would also explain the loss of strength observed. It seems, however, that at least a certain amount of cracks appears almost immediately when marble is subjected to strains but then the process slows down and the degree of cracking stays more or less at the same level. Also, it is obvious that the various marble types show very different tendencies for cracking. Likewise, the effect of cracking on mechanical properties seems to be different in different types of marbles..

3.4.7.3 Composition and microstructure

According to X-ray diffraction and thermal analysis both marble types chosen for the study composed almost completely of calcite. In addition, both of them contained small amounts of quartz and some dolomite. In marble E the content of dolomite was substantial, probably about 5%.

According to the definition by prof. Royer-Carfagni from University of Parma marble structures can be classified along the axis of xenoblastic-homoblastic. Xenoblastic marble structure is characterized by interlacing of irregular grains that are closely fitted to each other along their wavy contours. On the other hand, homoblastic marble structure is characterized by regular-shaped grains with straight or gently curving boundaries.

Thin section study of the marble types revealed that the structure of marble D was clearly homoblastic and that of marble E clearly xenoblastic.

The average grain size of the marble types was around 0.2 mm. Marble D was fairly even-grained, but in marble E the variation of grain sizes was more pronounced, probably because of its xenoblastic nature. Especially this was shown as very fine-grained (cryptocrystalline) lenses among the groundmass.

The composition and the microstructure of the marbles were similar to those of the corresponding marbles used in the subproject "Test wall". This confirms that the marble slabs used in the various projects were of the same quality, thus, probably also of the same origin.

No changes could be observed in the microstucture of marbles after the weather resistance tests with thin section study. It is presumable, however, that this only indicates that the method is not suitable for monitoring the deterioration process taking place in marble. Instead, thin sections can be used for characterizing the type of microstructure of various marbles.

SEM-study of polished marble sections didn't give any new information on the structure or on the change of structure of marbles. As thin sections polished sections can be used to reveal the structure type of marbles, but the method is not sensitive enough to monitor the changes taking place in the microstructure due to environmental or thermal strains.

The various structural types of marbles could be identified also in the SEM-study of fractured surface specimens of marbles. The individual grains could be distinguished very easily in marble D (homoblastic). On the other hand the structure of marble E was massive with only a few individual grains or parts of grains to be distinguished from the even-grey background (xenoblastic).

SEM-study of fractured specimens revealed cracks already in the unused marbles. These were especially prominent in marble D, but some, although narrow, cracks could be found in the specimen of unused marble E, too. All the cracks found were located between the grains, i.e. they went along the grain boundaries. The presence of cracks along with the interlocking tendency of grains in marble structure seem to explain at least part of the differencies observed in the strength properties of unused marbles.

Cracking was remarkably more serious in the specimens of marbles that had been in the weather chamber. The amount of cracks was considerably higher and the cracks were wider than in the unused specimens. Especially marble D was badly deteriorated; according to the mere microstructural features marble E was in relatively good condition. The maximum crack width ob-

served was even 6-7 µm in marble D, 0.2-0.3 µm in marble E. However, in general the cracks were narrower in both marble types.

Crack formation on the test wall is a clear sign of deterioration occurring in marble. The fact that the cracks go along the grain boundaries, not straight through the grains, indicates to a mechanism that tends to separate the grains from each other. Thus, cracking can be a consequence of thermal variations taking place in marble slabs as the thermal expansion behaviour of calcite crystals of which the grains of marbles are composed is anisotropic, i.e. the expansion coefficient is higher in the direction of one crystallographic axis than in the other perpendicular to the first one. Another possible explanation can be the freeze/thaw effect which tends to widen the cracks already existing in marble structure and also in this way to create new. Naturally, both of the mentioned mechanisms can act simultaneously.

3.4.7.4 Colour measurements, warping

According to the colour measurements both marble types were very white with the L value of CIELAB co-ordinates varying between 86 and 89. Both marbles had a slight greenish hue with the value of co-ordinate a varying between -1 and -2.5. They had also a slight yellowish hue with the value of the co-ordinate b varying between +1 and +2.

The whiteness of the marbles increased when the slabs were subjected to thermal strains in the weather chamber. Presumably this is a sign of the deterioration process taking place in marble. It is common knowledge in the manufacturing of marble products that their whiteness can be increased by thermal treatment. As it is obvious that variation of temperature causes granular decohesion in marble, it seems plausible to suppose that it is just this deterioration that is reflected also in the colour of marble as increased whiteness. Also in this respect the behaviour of the marble slabs was similar to that of the slabs on the test wall.

A minor but clear tendency for the co-ordinate a to move towards more negative and for the co-ordinate b to move towards more positive values was observed in all the marble types. This means that they are turning more green and more yellow. This could refer to fouling of marble surfaces, possibly by the effect of impurities from the pipelines. Mostly for this reason the colour change of the marbles after the tests was clear.

Bowing of the marble slabs in the weather resistance tests was hardly noticeable. In real conditions at Finlandia Hall bowing of the marbles used in the tests was much more prominent. Thus, even if it is possible to achieve similar changes of marble properties in one-sided weather resistance test as in real conditions, the test, at least in the form used in the project, fails to produce the factor/factors that cause the slab to bow.

3.4.8 Conclusions

According to the studies made the deterioration of marble structure taking place when subjected to thermal strains is caused by granular decohesion, which forms cracks along the grain boundaries. Granular decohesion seems to be a consequence of the anisotropic thermal expansion behaviour of calcite crystals. For this reason marble grains that are composed of calcite crystals break away from each other when thermal variations affect the material.. The strain caused by freezing and thawing may have an accelerating effect on the deterioration process after it has started and enough cracks have been formed.

The marble structure, however, influences its resistance against environmental strains. Homoblastic marble structure seems to be very apt to granular decohesion, which means that its durability e.g. in facades is poor. On the other hand, xenoblastic marble structure is much more resistant. However, it seems that thermal variations can generate heavy cracking also to xenoblastic marbles, although their strength properties are not affected to the same extent. Thus, no final conclusions about the durability of xenoblastic marbles in the long run can be made according to the results of this project.

The results achieved show that the damaging of marble structure takes place very soon after it has been subjected to thermal strains, probably already during the very first cycles of thermal variation. After that the deterioration process slows down, and the properties of marble will stay more or less stable. Thus, in order to predict the behaviour of marble for any longer periods of time a longer period of time for monitoring the marble properties would also be required. A reliable view e.g. of the rate of strength decrease as an indication of the progress of the deterioration process can be acquired only in that way.

According to the results it is possible to simulate the changes in the marble properties caused by real environmental conditions with the one-sided weather resistance test. E.g. the loss of strength, the increase in porosity and the microstructural alterations occurring in marble when tested in the weather chamber were very similar to those observed to take place in marble on the test wall. Thus, the test can be used to predict the behaviour of marbles as facade material and to classify various types of marbles according to their suitability for the purpose. However, the test is slow and expensive to perform. Also, the inability to produce bowing in the test slabs is a serious disadvantage.

3.5 Evaluation of marble samples from other buildings

3.5.1 Presentation of the objects

Marble samples from three different buildings were studied. Some background information dealing with these cases are presented as follows:

case 1
- private owned building situated in Helsinki
- part of the facades coated with marble, supporting structure from concrete elements, ventilation slot between marble and concrete, metal fixings
- built in 1965-1966
- severe deterioration: very notable warping and considerable loss of strength
- marble panels taken off in 1999
- white marble from Carrara, exact type or origin unknown

case 2
- private owned building situated in Helsinki
- facades coated with marble, supporting structure from concrete elements, ventilation slot between marble and concrete, metal fixings
- built in two parts: older part is approximately 25 years and younger part approximately 15 years old
- severe deterioration: some warping and considerable loss of strength
- older part in much better condition
- white marble from Carrara, exact type or origin unknown

case 3
- public building situated in Oulu
- facades coated with marble, supporting structure from concrete elements, ventilation slot between marble and concrete, metal fixings
- built in 1979
- no warping, no loss of strength, breaking around the fixings
- panels taken off in 2000
- white, heavily structured marble from finnish Lapland

In addition, the microstructure of a sample taken from the northern tower wall of Finlandia Hall was studied. The cylindrical sample, ∅ 30 mm, was taken in November 2000 by drilling through a 30 mm thick panel. The panels on that wall had been installed during summer-autumn 1998.

3.5.2 Mineral composition

The marble from the building representing case 1 was practically pure calcite, i.e. calcium carbonate. It contained only a few percents of quartz, feldspar and possibly mica as impurities. The weight loss of the marble in thermal analysis was 44.0 w-%.

The marbles from the building representing case 2 were practically pure calcite, i.e. calcium carbonate. The marble from the older part contained only a few percents of quartz, the marble from the younger part a few percents of quartz and feldspar as impurities. The weight loss of the older marble in thermal analysis was 44.3 w-% and that of the younger 44.2 w-%.

The main component of marble from the building representing case 3 was dolomite, i.e. calcium magnesium carbonate. Thus, it was not question about marble. It contained also a notable amount of quartz and feldspar plus some mica and calcite as impurities. The weight loss of the dolomite in thermal analysis was 43.3 w-%.

3.5.3 Thin section study

A photograph of the microstructure of the marble from case 1 is shown in Figure 102. Following observations were made:

- fine-grained ground mass, slightly oriented, average grain size 0.1-0.2 mm
- in places more coarse-grained veinlets with a thickness of about 1 mm, veinlets show the same orientation as the ground mass
- grain boundaries clear, often straight, grains easily distinguished
- nearly pure carbonate rock, only a little quartz and opaque minerals, possibly feldspar

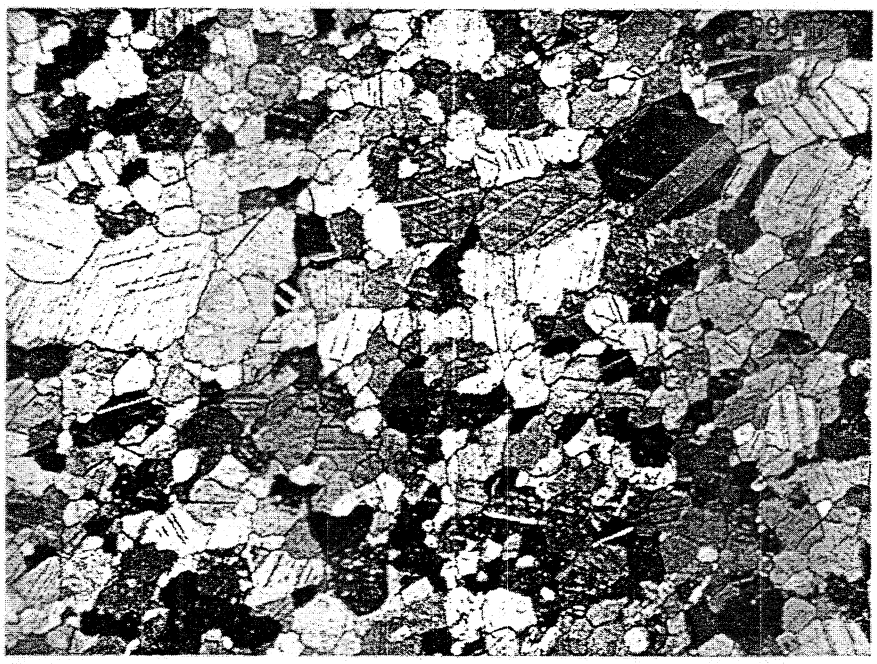

Figure 102. Microstructure of marble from case 1. Cross-polarized light.

Photographs of the microstructure of the older marble from case 2 is shown in Figure 103. Following observations were made:

- ground mass fine-grained, even-grained, not oriented
- grain boundaries easily distinguished
- a few very fine-grained cryptocrystalline lenses, max. length about 10 mm, inside the ground mass
- no heavy cracking
- outer surface dirty and uneven

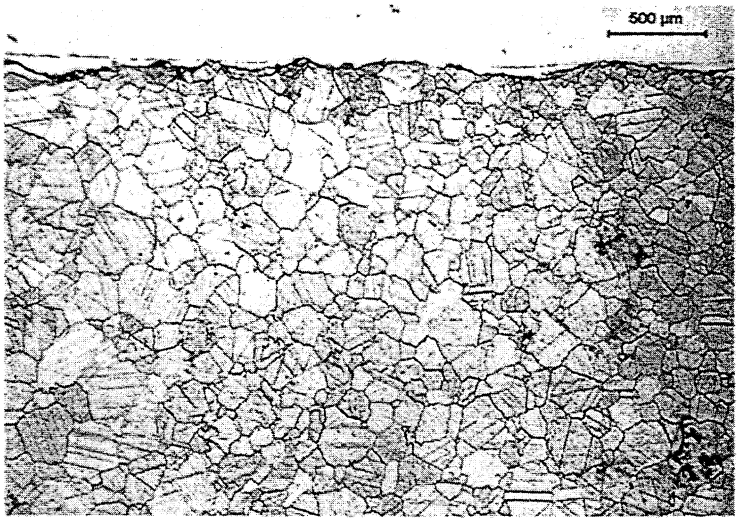

Figure 103. Microstructure of older marble from case 2. Plane-polarized light.

Photographs of the microstructure of the younger marble from case 2 are shown in Figure 104. Following observations were made:

- ground mass fine-grained, fairly even-grained, not oriented
- grain boundaries easily distinguished
- a few very fine-grained cryptocrystalline lenses, max. length about 2-3 mm, inside the ground mass
- cracks between the grains extending to a depth of about 2-3 mm from the outer surface and to a depth of about 1-2 mm from the inner surface, some cracks cut the surface
- outer surface dirty

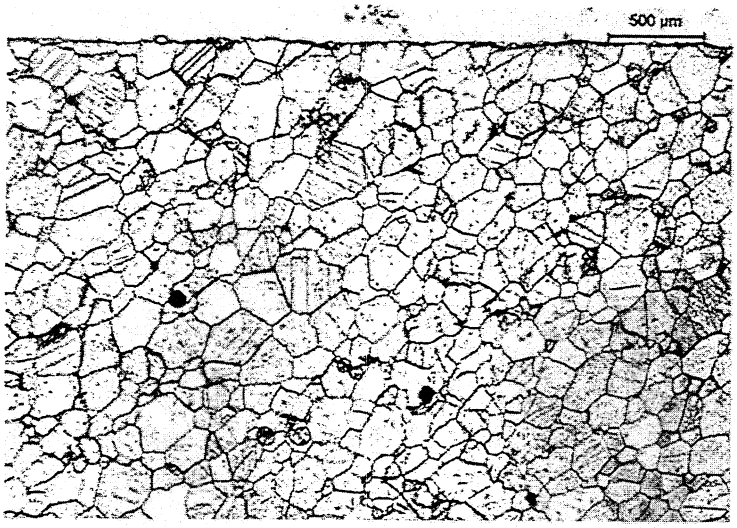

Figure 104. Microstructure of younger marble from case 2. Plane-polarized light.

A photograph of the microstructure of the dolomite from case 3 is shown in 8re 94. Following observations were made:

- ground mass very fine-grained, microcrystalline, dense
- clearly oriented, layered
- in places more coarse-grained veinlets with a thickness of about 1 mm, mostly oriented parallel to layering, a few also cross the layering
- some separate fine- to medium-grained quartz grains in rows, parallel to layering
- mainly carbonate rock, moderate content of quartz, other minerals include feldspar (probably plagioclase), mica (probably muscovite) and opaque minerals
- in places mica forms veinlets, partly with opaque minerals

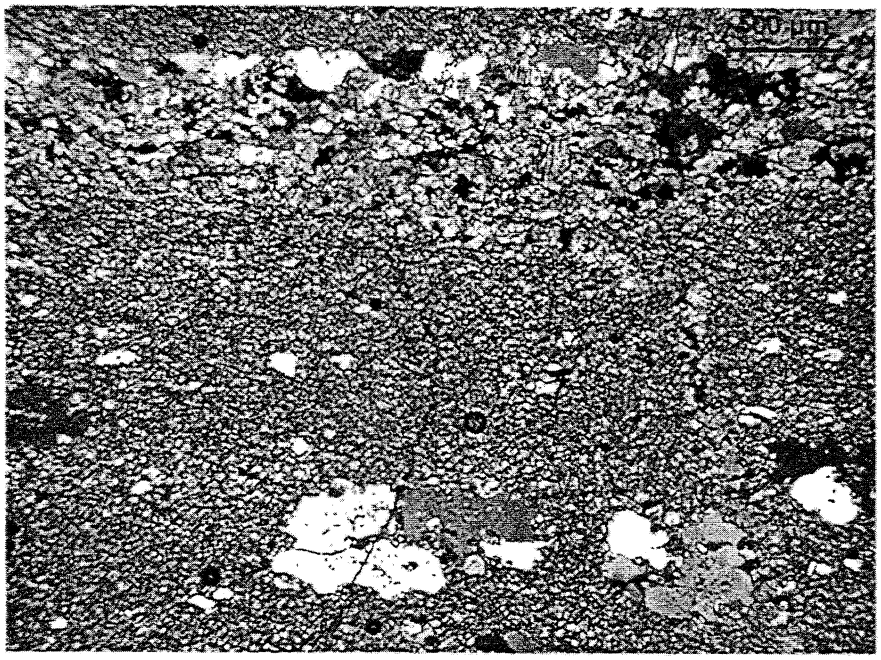

Figure 105. Microstructure of dolomite from case 3. Cross-polarized light.

A photograph of the microstructure of the marble from Finlandia Hall is shown in Figure 106. Following observations were made:

- fine-grained, fairly even-grained, slightly oriented
- average grain size 0.2-0.3 mm
- grain boundaries clear, straight, grains easily distinguished
- nearly pure carbonate rock, a little quartz and opaque minerals

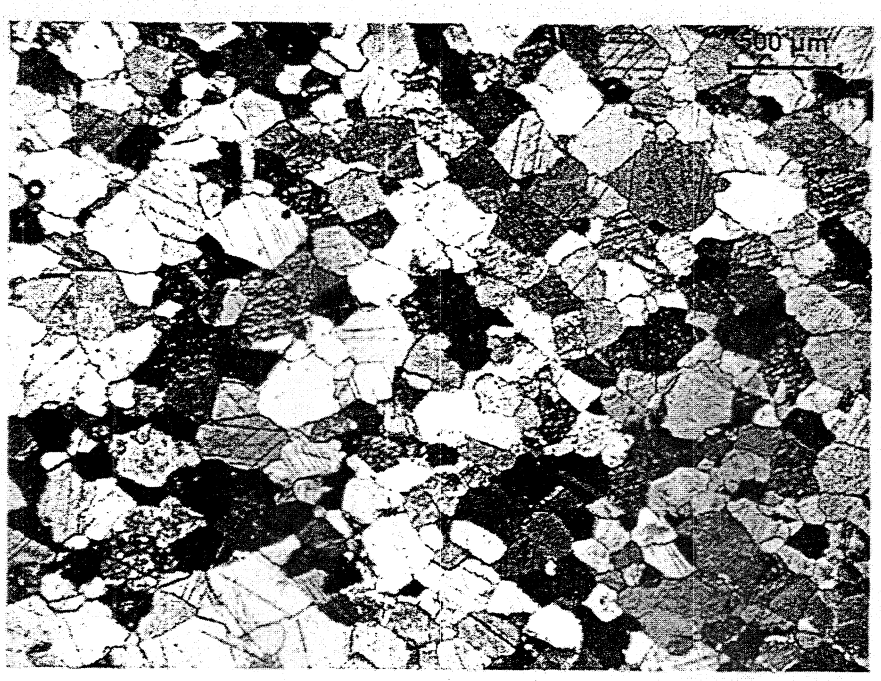

Figure 106. Microstructure of marble from Finlandia Hall. Cross-polarized light.

3.5.4 SEM-study

SEM-pictures of fractured surfaces of marble from case 1 is shown in Figure 107. The individual grains can at least for the most part be distinguished from each other. Cracks can be noticed practically between all the grains. The maximum crack width is around 2 µm. The average grain size of the marble is about 200 µm.

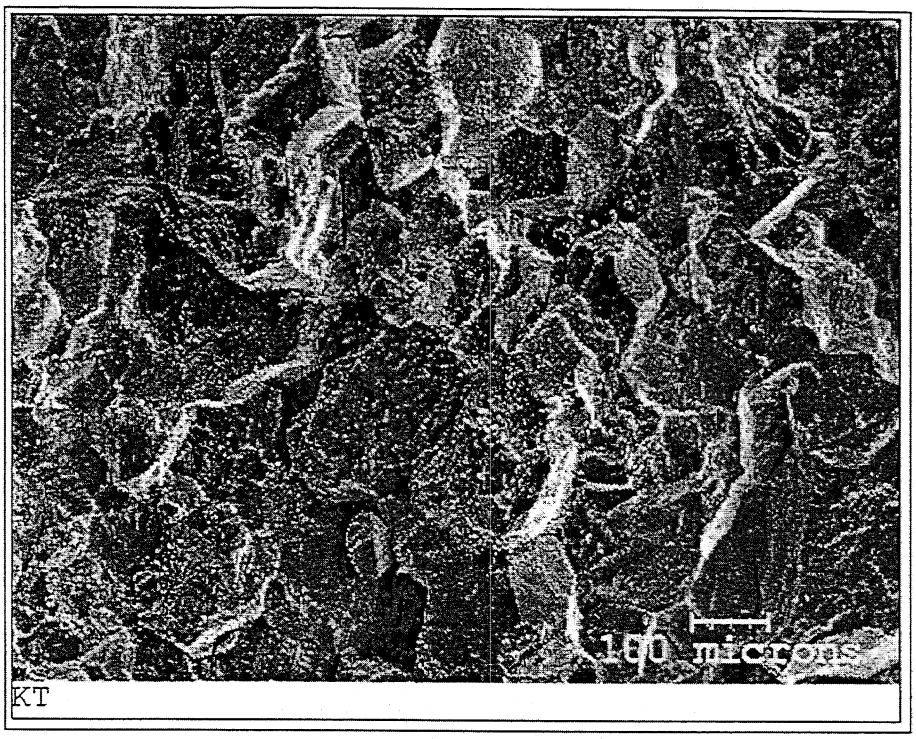

Figure 107. Marble from case 1. SE-image of fractured surface, 100x.

SEM-pictures of fractured surfaces of marble from case 2 are shown in Figures 108 and 109. The individual grains can at least for the most part be distinguished from each other in the marble of the older part. In the marble of the younger part the grains are almost detached from each other. Wide cracks can be noticed between all the grains. The average grain size of the older marble is about 200 µm, that of the younger marble around 200-300 µm.

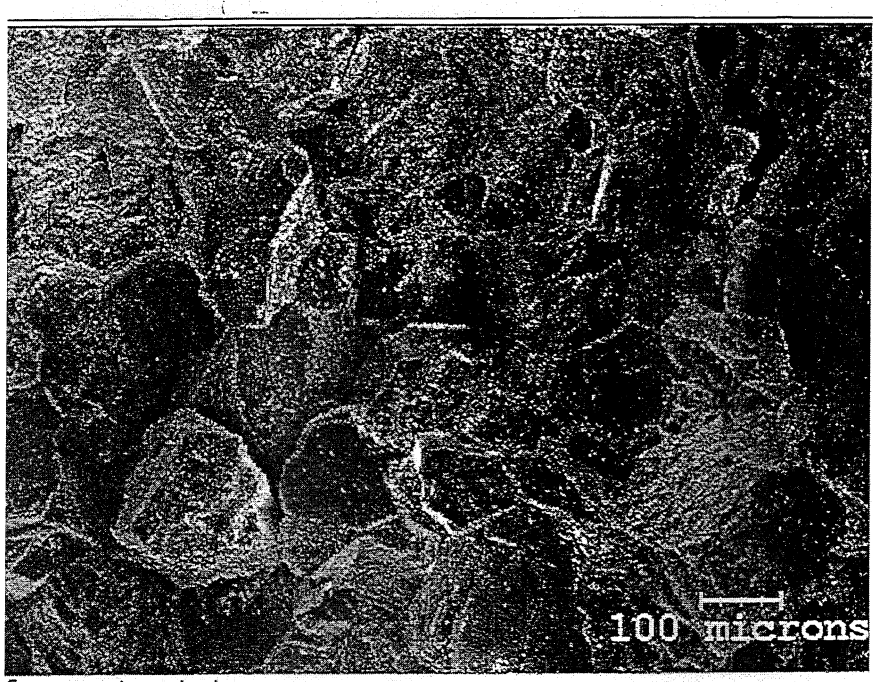

6, murtopinta

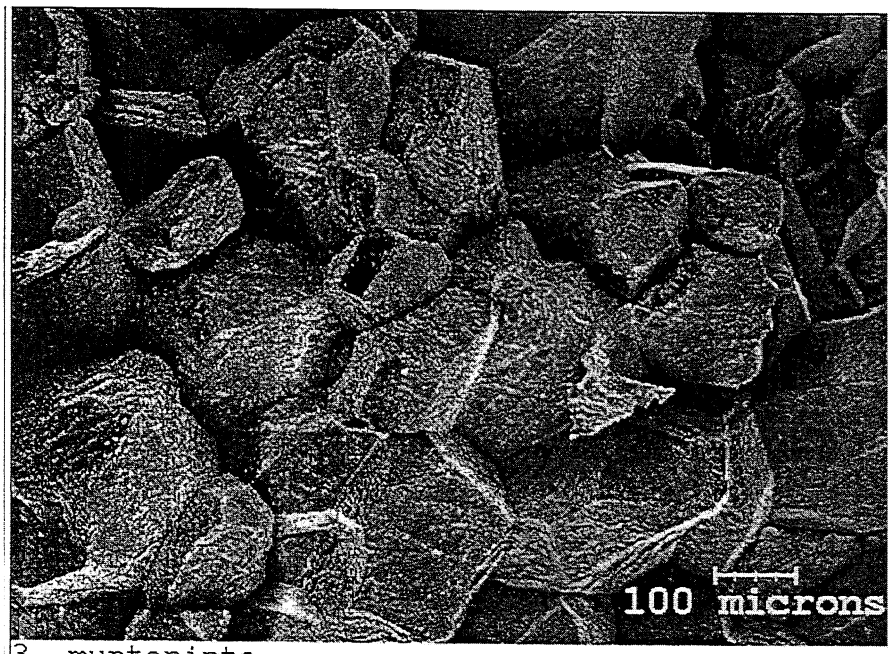

3, murtopinta

igure 109. Marble from case 2, younger part. SE-image of fractured s
ce 00x.

SEM-pictures of fractured surfaces of dolomite from case 3 is shown in Figure 110. The individual grains can easily be distinguished from each other. The microstructure is intact; only a few very narrow cracks can be noticed between some of the grains. The average grain size of the dolomite is about 20-30 µm.

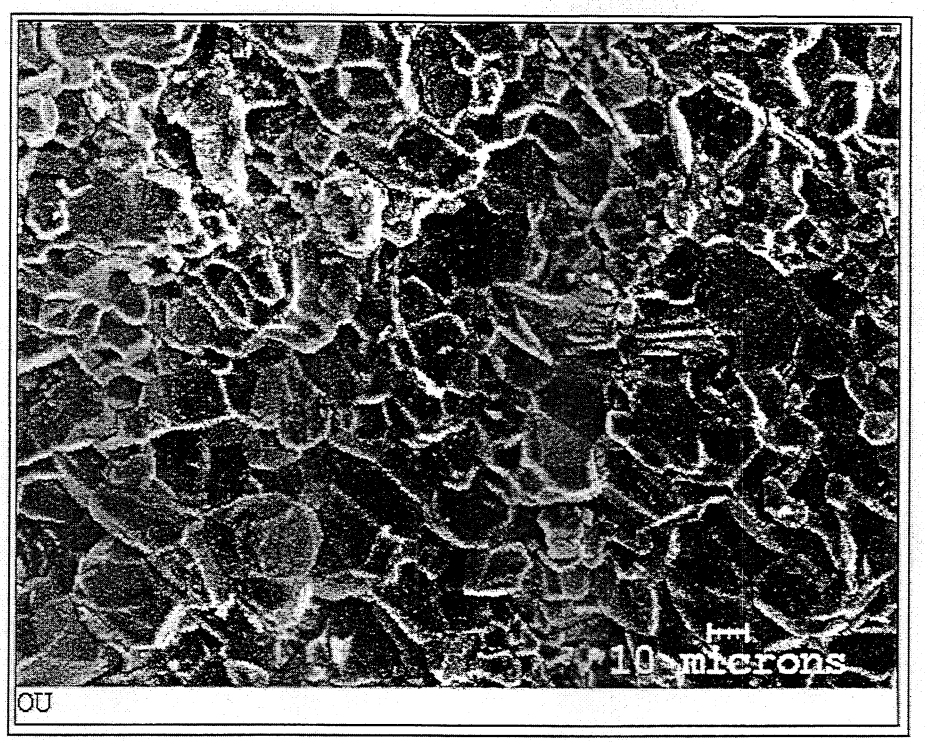

Figure 110. Dolomite from case 3. SE-image of fractured surface, 500x.

SEM-pictures of fractured surfaces of marble from Finlandia Hall is shown in Figure 111. The individual grains can at least partly be distinguished from each other. Cracks can be noticed between some of the grains. The maximum crack width is around 0.8-0.9 µm. The average grain size of the marble is about 200 µm.

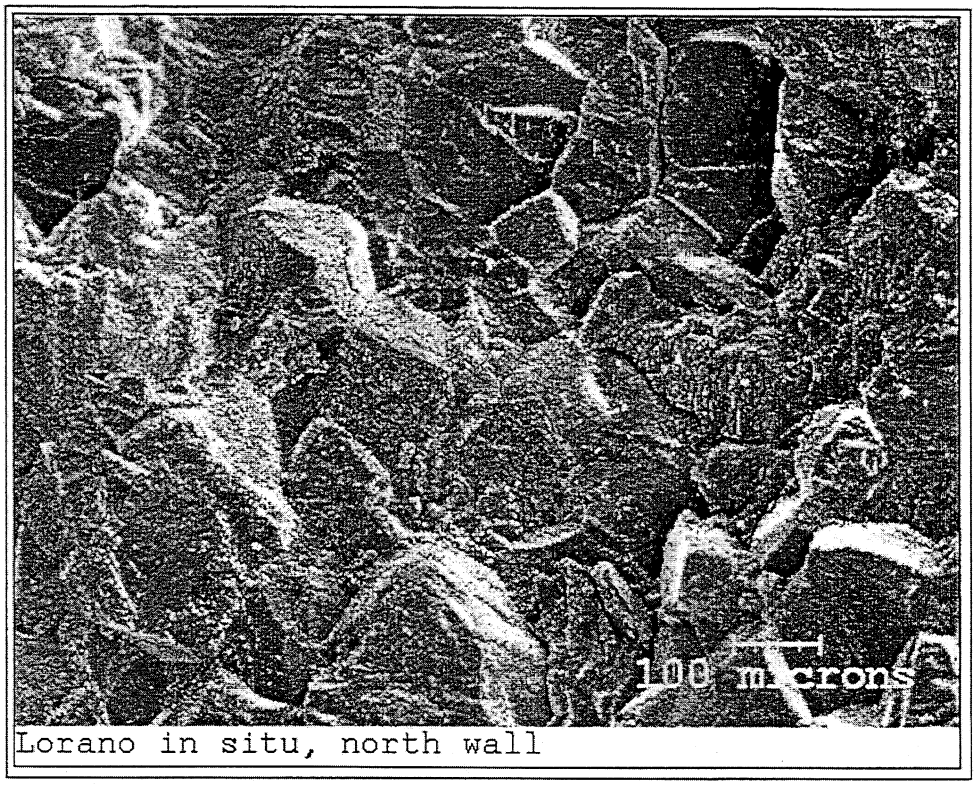

Figure 111. Marble from Finlandia Hall, north wall. SE-image of fractured surface, 100x.

In connection with the SEM-study also the chemical composition of the marble from the northern wall of Finlandia Hall was surveyed by using an energy dispersive PGT Imix spectrometer (EDS). The analysis was made from the fractured surface very close to the outer surface of the panel. The composition observed was practically that of the unused marble, only a little chlorine was detected.

3.6 EFFECT OF THERMAL CYCLING ON MARBLE PROPERTIES

3.6.1 Thermal microfracturing of marble

Stone facades are exposed to thermal loads created by periodic temperature changes. Diurnal temperature changes can be remarkable in Nordic climates like for example in Finland. Temperature increase creates thermal expansion of marble. Because marble is composed of thermally anisotropic minerals as calcite, temperature changes result in the development of thermal stresses within the material. Thermal stresses often combine to produce tensile strains, which can exceed the strength of the material leading to fracturing, which serves to relieve the internal stresses. Fractures due to thermal stresses extend over relatively small areas and are therefore referred to as microfractures (Sage 1988, Winkler 1997).

In addition to the extent of temperature changes, the development of thermal microfractures in marble is related to the presence of structural discontinuities within the material, to the physical properties, thermal properties and spatial orientation of minerals present. Structural discontinuities exist as intra-, inter-, and/or transgranular fractures (Krantz 1983). These are sites of weakness and serve as stress concentrators and potential locations for thermal microfracture initiation and propagation.

Physical properties of minerals and their contacts determine the strength, which thermal stress has to exceed before the initiation of microfracturing. Thermal stresses depend on thermal and physical properties like thermal expansitivity and modulus of elasticity. Also high thermal gradients created by rapid temperature changes and low thermal diffusivity induce thermal stresses. Spatial orientation of calcite crystals in marble affects the developing thermal stresses. When heated to 100°C calcite contracts 0.042% perpendicular to its crystallographic c-axis and expands 0.189% parallel to its c-axis. Unfavorable crystallographic orientations of contiguous grains can lead to high stress concentrations and fracturing of grain boundaries. According to Royer-Carfagni (1999) thermal fracturing tends to favor decohesion of grain boundaries rather than cleavage fractures of single crystals.

Thermal microfracturing may increase the porosity and result in strength reduction of marble. Sage (1988) has reported a 70-170 % increase in water absorption and 49-64 % reduction in flexural strength of medium grained marbles subjected to heating from 24 to 66°C. Microfractures generated at the surface of marble structures provide an additional pore network of flow channels, which permit the migration of aggressive solutions beneath the surface. The result is the accelerated deterioration of marble.

Diurnal atmospheric heating-cooling cycles of rock are believed to be sufficient to dilate marble in a matter of a few years (Winkler 1997). According

to Sage (1988) the first heating cycle causes the largest thermal strain and porosity increase in a medium-grained crystalline marble. Repeated heating cycles to the same temperature cause only minor changes in thermal strain. Widhalm et al. (1996) reported the increasing water absorption capacity with growing number of heating-cooling cycles in Carrara-marble.

3.6.2 Marble samples and sample preparation

The materials of this study consist of three different types of Carrara Bianco -marble with the codes A, D and E. Sample A was tested in two directions:

- parallel to the rift (APA)
- perpendicular to the rift (APE)

The sample preparation included sawing of the specimens with diamond saw, coding of the samples, temperature cycling of the one part of the specimens, and the preparation of thin sections of the fluorescence resin impregnated specimens. At the Laboratory of Engineering Geology and Geophysics the specimens were washed and dried in room temperature before the measurements of the physical properties.

To be able to study structural and mineralogical properties of the marble types and structural changes caused by temperature cycling, six thin sections of every marble sample were prepared, representing untreated, temperature cycled, and mechanically tested specimens.

A half of each sample (12 specimens) was temperature cycled in dry conditions. One temperature cycle lasting about 8 hours consisted of altering the temperature from -20°C to +60°C. In the study specimens were decided to be exposed to about 500 cycles. Detailed report of the thermal cycling and the mechanical tests is given in Appendixes 5 and 6.

3.6.3 Physical properties

3.6.3.1 Density, porosity and water absorption

Grain density gives the average density of the solid rock material and the closed pores. The value of grain density is mainly dependent on the mineralogy. Because of this it was used to indicate the mineralogical homogeneity of the samples and the possible mineralogical changes caused by temperature cycling.

Bulk density gives the average density of the solid rock material and the open and closed pores. Bulk density is the normal index property measured from building stones. The mineralogy and porosity affect the value of the bulk density.

Porosity i.e. effective porosity, gives the pore volume percentage in which water can be absorbed from the specimen surface. The value of porosity depends on the amount of the open interconnected pores. Porosity was used to indicate the volume of initial cracking and possible thermal cracking caused by temperature cycling.

Water absorption gives the weight percentage of rock material in which water can be absorbed. The value of the water absorption is affected with the porosity and the grain density of rock material.

Coefficient of capillary water absorption gives the speed of water absorption into capillary pores of rock material from the horizontal surface upwards. The amount, aperture, and interconnectivity of the open pores affect the coefficient. The coefficient was used to characterize the initial crack network and the possible thermal cracking caused by temperature cycling. The physical index properties determined in this study are summarized in Table 21.

Table 21. The physical properties, their symbols and units used in the study.

Physical Property	Symbol	Unit
Grain density	ρ_g	kgm^{-3}
Bulk density	ρ_b	kgm^{-3}
Porosity	n_e	vol-%
Water absorption	W_m	w-%
Coefficient of capillary water absorption	C	$gm^{-2}s^{-0.5}$

The physical properties were determined using the water immersion procedure, which was modified particularly for this study and deviated from the standard test procedures for building stones. Normal tap water was used in the study. The used procedure based on the measurement of dry mass weighted in air (m_d), water saturated mass weighted in air (m_s), and water saturated mass weighted in water (m_{sub}). In addition the temperature of water was measured to determine water density (ρ_w). In the measurement of the coefficient of capillary water absorption also the partially saturated mass (m_i) after immersion time t_i was measured seven times during the 72 hours immersion. The physical properties were calculated using the following formulas:

$$\rho_g = \frac{m_d \rho_w}{m_d - m_{sub}} \qquad (2)$$

$$\rho_b = \frac{m_d \rho_w}{m_s - m_{sub}} \qquad (3)$$

$$n_e = \frac{(m_s - m_d)}{(m_s - m_{sub})} \times 100\ \% \qquad (4)$$

$$W_m = \frac{(m_s - m_d)}{m_d} \times 100\ \% \qquad (5)$$

$$C = \frac{m_i - m_d}{A\sqrt{t_i}} \qquad (6)$$

ρ_g = Grain density (kgm^{-3}),
ρ_b = Bulk density (kgm^{-3}),
n_e = The effective porosity (%),
W_m = Water absorption (w-%),
C = Capillary water absorption coefficient ($gm^2s^{-0.5}$),
m_d = The mass of the dried specimen weighted in air (kg),
m_s = The mass of the saturated specimen weighted in air (kg),
m_{sub} = The mass of the saturated specimen weighted in water (kg),
m_i = The mass of the specimen after immersion time t_i weighted in air (kg),
t_i = The immersion time corresponding to the capillary absorption time phase (s),
A = The area of the specimen base (m^2), and
ρ_w = Density of water (kgm^{-3}).

The average values with standard deviation of the physical properties of the untreated and temperature cycled marble samples are presented in the Tables 22 and 23. Untreated E deviates from other marble samples by much smaller porosity and coefficient of capillary water absorption. The same phenomenon is evident in temperature cycled samples, but the differences between the marble types are diminished by temperature cycling.

Table 22. Average values and standard deviations of the physical properties of the untreated marble samples (N=24).

Marble Type / Standard Deviation (Sd)	Grain Density (kgm^{-3})	Bulk Density (kgm^{-3})	Porosity (vol-%)	Water Absorption (w-%)	Capillary water absorption coefficient ($gm^{-2}s^{-0.5}$)
E	2721	2717	0.16	0.06	0.12
Sd	1.49	1.37	0.01	0.00	0.02
D	2720	2710	0.37	0.14	1.28
Sd	1.79	2.07	0.02	0.01	0.15
APA	2717	2708	0.34	0.13	0.87
Sd	1.18	1.24	0.01	0.00	0.05
APE	2718	2708	0.36	0.13	0.94
Sd	0.39	0.60	0.01	0.01	0.14

Table 23. Average values and standard deviations of the physical properties of the temperature cycled marble samples (N=12).

Marble Type / Standard Deviation (Sd)	Grain Density (kgm^{-3})	Bulk Density (kgm^{-3})	Porosity (vol-%)	Water Absorption (w-%)	Capillary water absorption coefficient ($gm^{-2}s^{-0.5}$)
E	2721	2709	0.43	0.16	1.11
Sd	1.32	1.36	0.02	0.01	0.10
D	2721	2704	0.61	0.23	2.96
Sd	1.73	1.36	0.05	0.02	0.50
APA	2717	2702	0.55	0.20	2.28
Sd	1.24	1.31	0.01	0.00	0.17
APE	2717	2702	0.57	0.21	2.43
Sd	0.46	0.98	0.04	0.01	0.35

Scatter diagrams were used to indicate the relation between two physical properties. Porosity-capillary water absorption coefficient -chart in Figure 112 shows a clear logarithmic positive correlation between the open pore volume and the speed of capillary water absorption of the untreated samples. Increasing porosity seems to accelerate the capillary water absorption in other marble types than E, which seems to have very modest pore network.

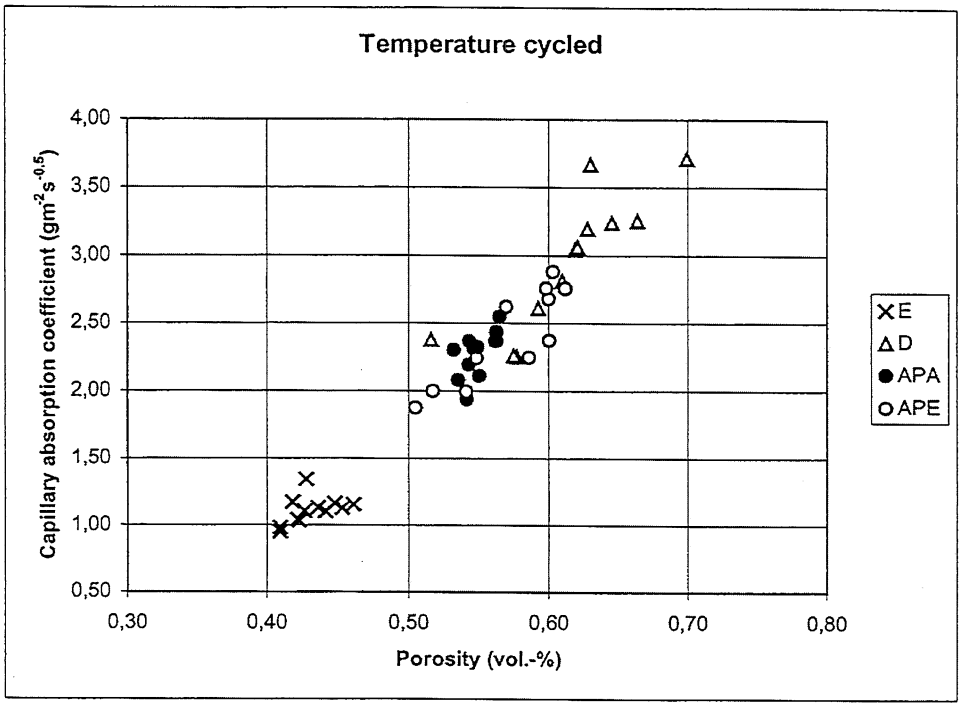

Figure 112. The porosity-capillary water absorption coefficient-relationship of the Temperature cycled marble samples E, D, PA and APE (N=12)..

3.6.3.2 Capillary water absorption

Figure 113 shows the average capillary water absorption curves of the untreated marble samples. Marble D has the highest speed and amount of capillary water absorption. Both Eand APE samples have very similar behaviour despite of the different orientation of the specimens. Also the capillary absorption phase (the first linear part) and the diffusion phase (the latter linear part) are clearly distinguishable (see Hammecker et al. 1993). On the other hand E shows much slower capillary absorption and the two absorption phases are not easily distinguishable.

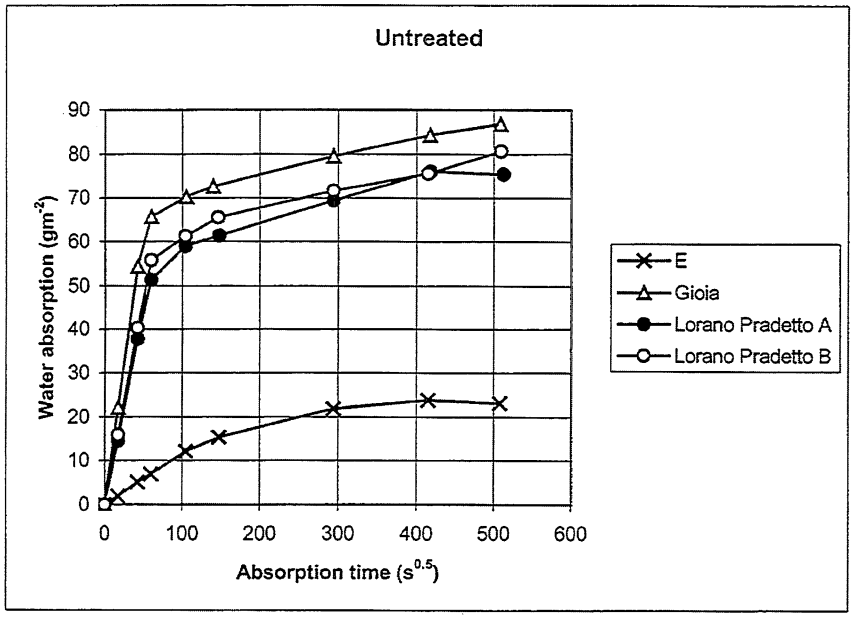

Figure 113. The average capillary water absorption curves of the untreated marble samples of E,D, Eand APE (N=24).

Figure 114 shows the average capillary water absorption curves of the temperature cycled marble samples. Marble D has the highest speed and amount of capillary water absorption. After temperature cycling both E and APE samples have very similar behaviour despite of the different orientation of the specimens. Also the capillary absorption phase and the diffusion phase are clearly distinguishable. Marble E shows slower capillary absorption but now the two absorption phases are readily distinguishable. All marble types have similar diffusion properties (slope of the latter linear part) after cycling.

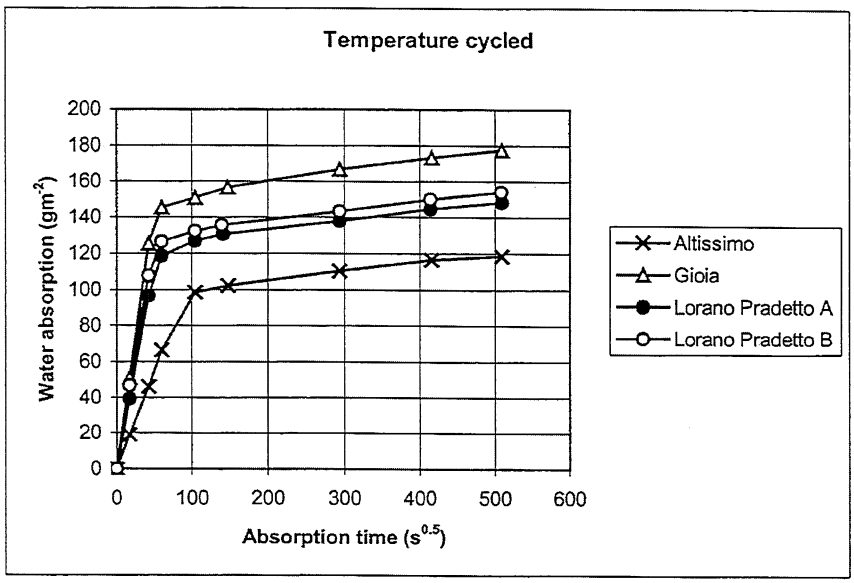

Figure 114. The average capillary water absorption curves of the temperature cycled marble samples of E,D, E and APE (N=12).

3.6.3.3 The effect of temperature cycling on the physical properties

The summary of the changes of the physical properties of the marble samples due to temperature cycling is presented in Table 24. Temperature cycling causes no measurable changes in grain densities of the samples, but a slight reduction (from 0.2 to 0.3 %) in bulk density is noticeable due to porosity increase.

Temperature cycling has a strong effect both on porosity and capillary water absorption coefficient. Marble D and both A samples have been subjected to very similar porosity increase (from 58 to 65 %), but in E an increase of 169 % has occurred. Similar behaviour can be seen in water absorption values. D and both A-samples have been subjected to an increase of 54 to 64 %, but in E the remarkable increase of 167 % has occurred. Sage (1988) reported 70 to 170 % increase in water absorption in heating of marble to + 66°C, which gives a very good reliability to the results obtained in this study.

Of all the determined physical properties, the temperature cycling has the most remarkable effect on the coefficient of capillary water absorption. In D E and APE the increase of this coefficient varies between 131 and 162 %, while E is subjected to an increase of 825 % due to temperature cycling. The behaviour of E and APE samples with different structural orientation is very similar in temperature cycling.

Table 24. The changes (untreated -> cycled) of the physical properties of the marble samples due to temperature cycling.

Marble Type / Change %	Grain Density (kgm^{-3})	Bulk Density (kgm^{-3})	Porosity (vol-%)	Water Absorption (w-%)	Capillary water absorption coefficient ($gm^{-2}s^{-0.5}$)
E (change %)	2721 -> 2721 (0 %)	2717 ->2709 (-0.3 %)	0.16->0.43 (+169 %)	0.06->0.16 (+167 %)	0.12->1.11 (+825 %)
D (change %)	2720 -> 2721 (0 %)	2710->2704 (-0.2 %)	0.37->0.61 (+65 %)	0.14->0.23 (+64 %)	1.28->2.96 (+131 %)
E (change %)	2717 -> 2717 (0 %)	2708->2702 (-0.2 %)	0.34->0.55 (+62 %)	0.13->0.20 (+54 %)	0.87->2.28 (+162 %)
APE (change %)	2718 -> 2717 (0 %)	2708->2702 (-0.2 %)	0.36->0.57 (+58 %)	0.13->0.21 (+62 %)	0.94->2.43 (+159 %)

Detailed data with curves of the changes in the determined physical properties caused by temperature cycling in all marble samples is presented in Appendix 5.

3.6.4 Microstructural properties

3.6.4.1 General aspects

Structural index properties determined from the marble samples included
- mineralogical composition,
- structure of rock and
- average grain size.

These properties were determined from thin sections TS-1 and TS-2 with a polarizing microscope. Resin filled fractures were determined from all types of thin sections. Fracture quality was determined by calculating the amount of resin filled fractures across the reference line belonging to following fracture categories: intragranular, intergranular, and transgranular.

Thin sections TS-1 and TS-2 were compared to reveal the structural changes caused by temperature cycling only. Thin sections TS-3 and TS-4 were compared to reveal the differences in structure of rupture created by bending strength test of the untreated and temperature cycled specimens. Thin sections TS-5 and TS-6 were compared to indicate the differences in the structure of rupture created by uniaxial compressive strength test of the untreated and temperature cycled specimens.

3.6.4.2 Mineralogy

Marble structures are classified from xenoblastic to homoblastic varieties. Xenoblastic structure is characterized by interlacing of irregular crystals closely fitted along their wavy contours. Homoblastic structure in marble is characterized by regular-shaped grains with straight or gently curving boundaries (Royer-Carfagni 1999).

All marble types show similar average grain size from 0.17 to 0.21 mm and standard deviation from 0.03 to 0.05 mm. D is the most coarse-grained type. E represent the xenoblastic end-member and D the homoblastic end-member, while A samples show intermediate structure. Xenoblastic structure causes uneven grain-size in E. Increased porosity and the coefficient of capillary water absorption coefficient seem to be related more to homoblastic than xenoblastic structure. All the marble types are composed of carbonate minerals with a small fraction of opaque minerals. Table 25 shows the mineralogy, grain size, and structure of the marble types.

Table 25. Mineralogy, grain size, and structure of the marble types (stdev = standard deviation, N= number of calculated grains).

Marble type	Grain size, average (mm)	Grain size stdev (mm)	N	Structure	Main minerals	Accessory minerals
E	0.18	0.05	222	Xenoblastic	Carbonates	Opaques
D	0.21	0.03	176	Homoblastic	Carbonates	Opaques
APA	0.17	0.03	215	Homoblastic/ Xenoblastic	Carbonates	Opaques
APE	0.19	0.04	199	Homoblastic/ Xenoblastic	Carbonates	Opaques

3.6.4.3 Microcracking

A. Temperature cycling

The crack densities were measured in three thin sections. Absent or very localized resin filling made reliable and comparable measurements of crack densities impossible in five thin sections. Microcrack densities of the untreated (TS-1) and temperature cycled (TS-2) thin sections based on the observation of resin filled cracks are presented in Appendix 5.

B. Bending strength test

The rupture in bending occurs frequently along the grain boundaries both in untreated and temperature cycled specimens. Cracks parallel to rupture are present especially in some temperature cycled specimens. E and D also show a decohesion zone near the rupture in untreated specimens. Cleavage

cracks are seldom associated with the rupture in bending. The quality of the rupture in the marble specimens after bending strength test based on the observation of resin filled cracks is presented in Appendix 5.

C. Compressive strength test
The cracking created by compression is located frequently along the grain boundaries both in untreated and temperature cycled specimens. Transgranular cracks exist mainly in temperature cycled specimens and intragranular cracks in untreated but also in temperature cycled specimens, especially in E. The quality of microcracks in the marble specimens after uniaxial compressive strength test based on the observation of resin filled cracks is presented in Appendix 5.

3.6.4.4 The effect of temperature cycling on the structural properties

Mineralogical changes are not expected to be caused by temperature cycling from -20°C to + 60°C. Mineralogical studies show no changes and this result is also supported by grain density measurements. The changes caused by temperature cycling are related to pore structure of marble i.e. thermal microfracturing. Increase of crack density of especially intergranular but also intragranular cracks was directly observed in the thin sections of D - marble, but this is evident also in the other marble types. This is also indicated by the clear increase of the values of porosity and coefficient of capillary water absorption. Thermal microfracturing mainly results in the decohesion of grain boundaries, but also in the opening of the cleavage cracks in some cases.

According to thin section studies, temperature cycling affects the location, where the bending rupture occurs in marble. Rupture occurs basically along grain boundaries in untreated and temperature cycled specimens, but transgranular cracks parallel to bending rupture may be created easier in temperature cycled than untreated specimens.

According to thin section studies, temperature cycling does not affect the cracking created by uniaxial compression. The only effect that can be claimed is that the transgranular cracking may be more frequent in temperature cycled than in untreated specimens.

3.6.5 Elastic stress-strain behaviour

3.6.5.1 Interpretation methods

For all compression test samples the elastic parameters, Young's modulus *(E)* and Poisson's ratio *(ν)*, are defined. The definition is basically done as secant value from the range of -0.01% radial strain *(ε_r)* to half of peak strength *(σ_p)* (Figure 115). The range is changed only if axial or radial

stress-strain behaviour is clearly non-linear within this range. The definition of the determination limits is presented in Hakala (1996). (Appendix 6.)

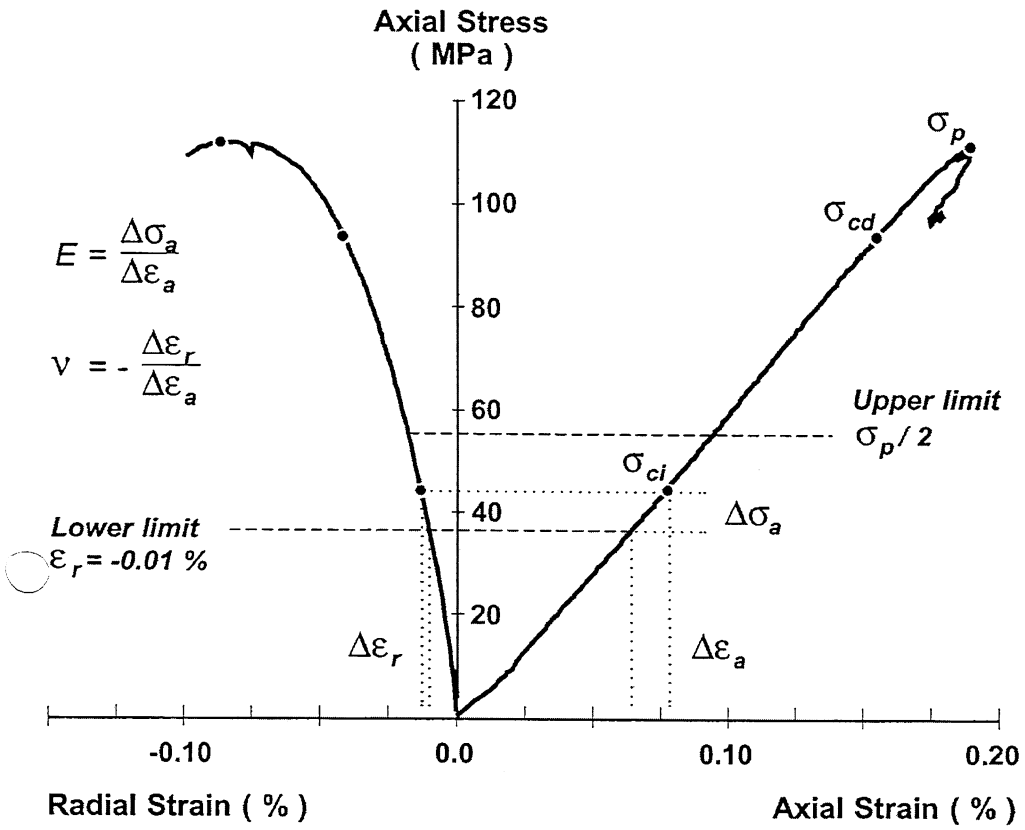

Figure 115. Determination of elastic parameters in compression.

3.6.5.2 Characteristics of uni- and triaxial stress-strain behaviour

On the test sample scale all the marbles are very homogenous and non orientated massive rock. The deviation of observed stress-strain and strength bahaviour is therefore relatively small (Figures 116-118).

Based on the test result marble E is the strongest of the studied marble types. Peak strength, crack damage and crack initiation values are noticeably higher than the rest of the marble types have. On the other hand, there doesn´t seem to be big differences in the critical strain values between the E marble and the rest of the marble types. Therefore, it can be said that the E is more brittle compared to the other marbles.

Between the cycled and reference samples, there is clear difference in critical strain values, especially in uniaxial tests. The axial stress-strain behaviour of cycled samples is nonlinear at the beginning of the test. This is due to the micro cracks (damage) developed during the thermal cycling process.

In triaxial test the differences between reference and cycled samples are smaller than in uniaxial tests.

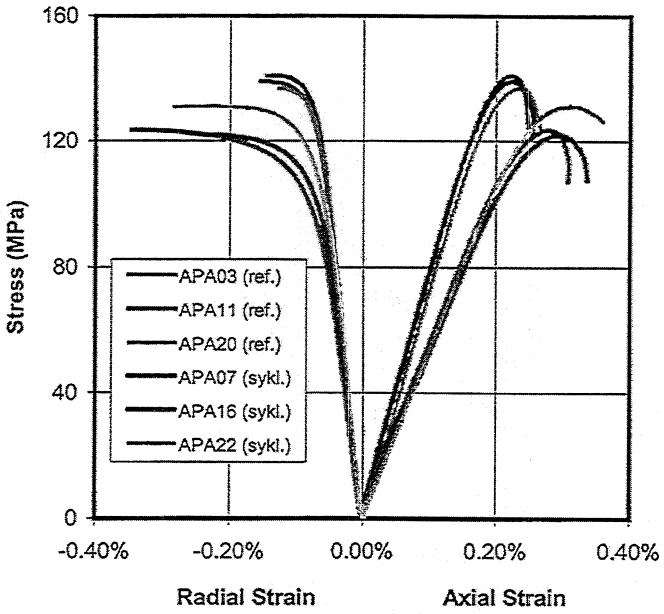

Figure 116. Uniaxial stress-strain behaviour of marble E.

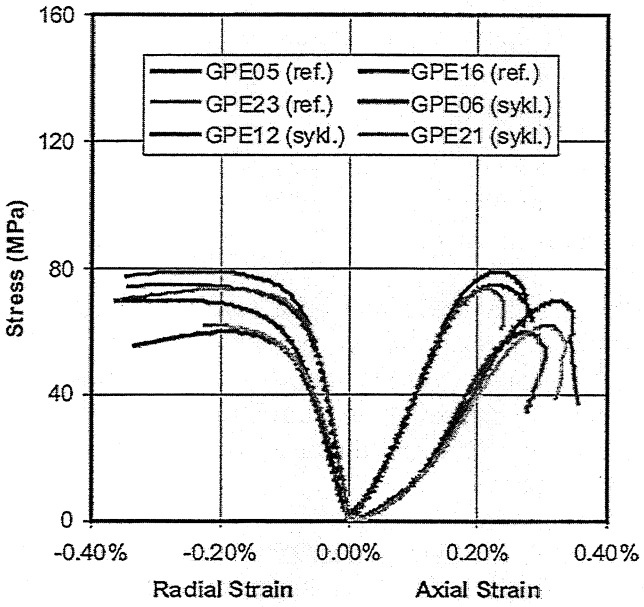

Figure 117. Uniaxial stress-strain behaviour of marble D.

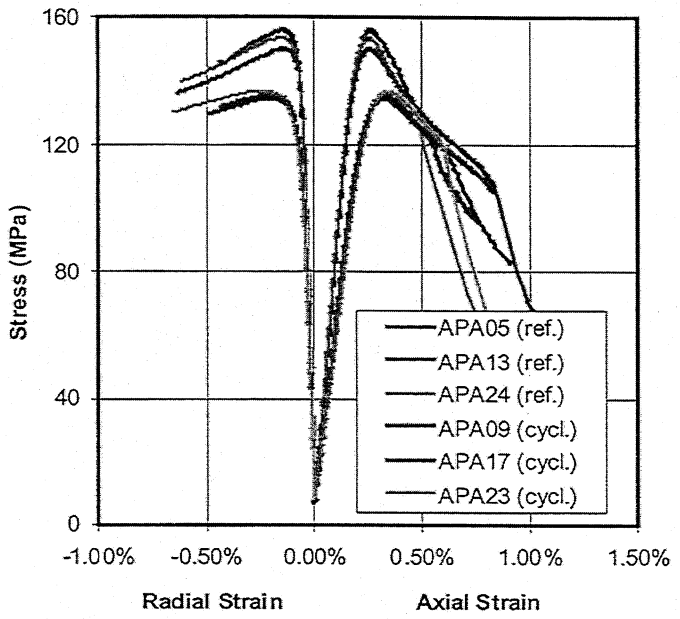

Figure 118. Triaxial stress-strain behaviour of marble E.

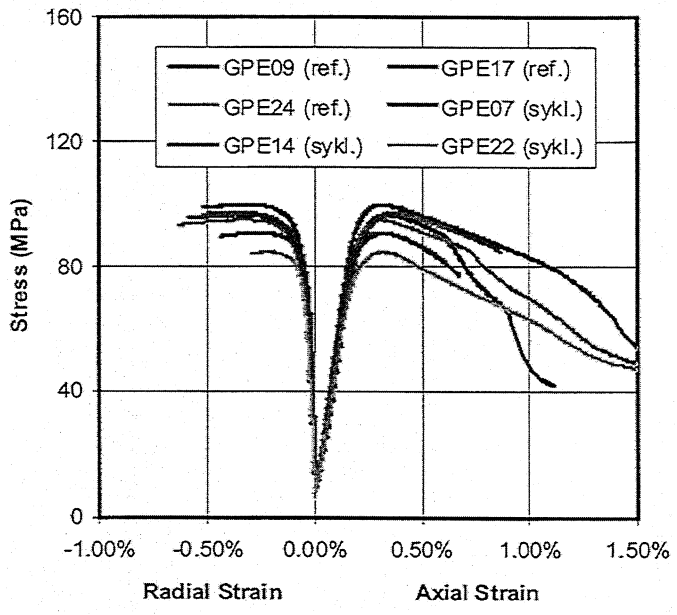

Figure 119. Triaxial stress-strain behaviour of marble D.

3.6.5.3 Young´s modulus

The uniaxial Young´s modulus of the studied marble samples were between 73 GPa and 26 GPa. The corresponding triaxial values were between 81 GPa and 34 GPa. Marble E was clearly most rigid of the tested marble types. The Young´s modulus of reference E samples were about 70 - 80 GPa. The corresponding value for APA, APE and D marble types were about 45 - 55 GPa. The maximum standard deviation of one uniaxial test group were 3.1 GPa, which was about 13% of the average value. The maximum standard deviation of one triaxial test group was 4.2 GPa being 11% of the average value.

The thermal cycling has clear influence to the Young´s modulus of the tested marble types. In every case the cycled Young´s modulus were lower than the corresponding reference values. The biggest difference was in the results of APE samples. The average Young´s modulus of cycled samples were only about 45% of the reference values. The corresponding numbers of samples were about 70%. The uniaxial Young´s modulus of APA and D samples were about 65% - 75% of the reference values. In the triaxial test the corresponding rations are the same in the case of Eand APE marbles, but for APA and D it was about 90%. (Appendix 6.)

In triaxial tests the confinement of 5 MPa increases the Young´s modulus. The Young´s modulus in triaxial tests were between 107% and 154% of the corresponding uniaxial value. In most cases it was about 110% of the uni-axial value.

Table 26. Summary of the average values of the results and the differences between uniaxial and triaxial values.

Sample group		Uniaxial Young´s modulus (GPa)	Triaxial Young´s Modulus (GPa)	Difference tria./unia. (%)
E	**reference**	71.9	81.1	113%
	cycled	51.1	56.3	110%
	difference	71%	69%	
APA	**reference**	46.2	50.6	110%
	cycled	34.8	47.4	136%
	difference	75%	94%	
APE	**reference**	47.8	53.1	111%
	cycled	21.5	22.9	107%
	difference	45%	43%	
D	**reference**	45.7	50.1	110%
	cycled	29.8	45.9	154%
	difference	65%	92%	

3.6.5.4 Poisson´s ratio

The uniaxial Poisson´s ratio of the studied marble samples were between 0.15 and 0.45. The corresponding triaxial values were between 0.20 and 0.40. The difference between marble types were big, but the maximum standard deviation of one test group in both tests were only about 7% of the average value (Appendix 6).

According to the test results the thermal cycling has influence at least to the Poissons ratio of the APA and APE marbles (Table 27). The cycled uniaxial Poisson´s ratio were about 55% - 65% and trixial about 80% - 90% of the reference value. The triaxial cycled Poisson´s ratio of E samples were 78% of the reference value, but the differences between uniaxial values were insignificant. Both average Poisson´s ratios of cycled D samples were nearly the same as the reference values.

The confinement of 5 MPa in triaxial tests lower slightly the Poisson´s ratio. Exept for cycled APA and APE samples, the difference were in most cases about 10% - 20% (Table 27).

Table 27. Summary of Poisson´s ratio.

Sample group		Uniaxial Poisson´s ratio	Triaxial Poisson´s ratio	Difference tria./unia. (%)
E	**reference**	0.37	0.34	91%
	cycled	0.36	0.26	74%
	difference	96%	78%	
APA	**reference**	0.41	0.39	94%
	cycled	0.26	0.31	116%
	difference	64%	79%	
APE	**reference**	0.32	0.29	93%
	cycled	0.17	0.26	148%
	difference	55%	88%	
D	**reference**	0.39	0.35	89%
	cycled	0.42	0.32	78%
	difference	106%	92%	

3.6.6 Critical stress states in compression,

3.6.6.1 Interpretation methods

A. Critical Stress States from Stress-Strain data

The critical stress states here refer to crack initiation stress (σ_{ci}), crack damage stress (σ_{cd}) and peak strength (σ_p) (Figure 120).

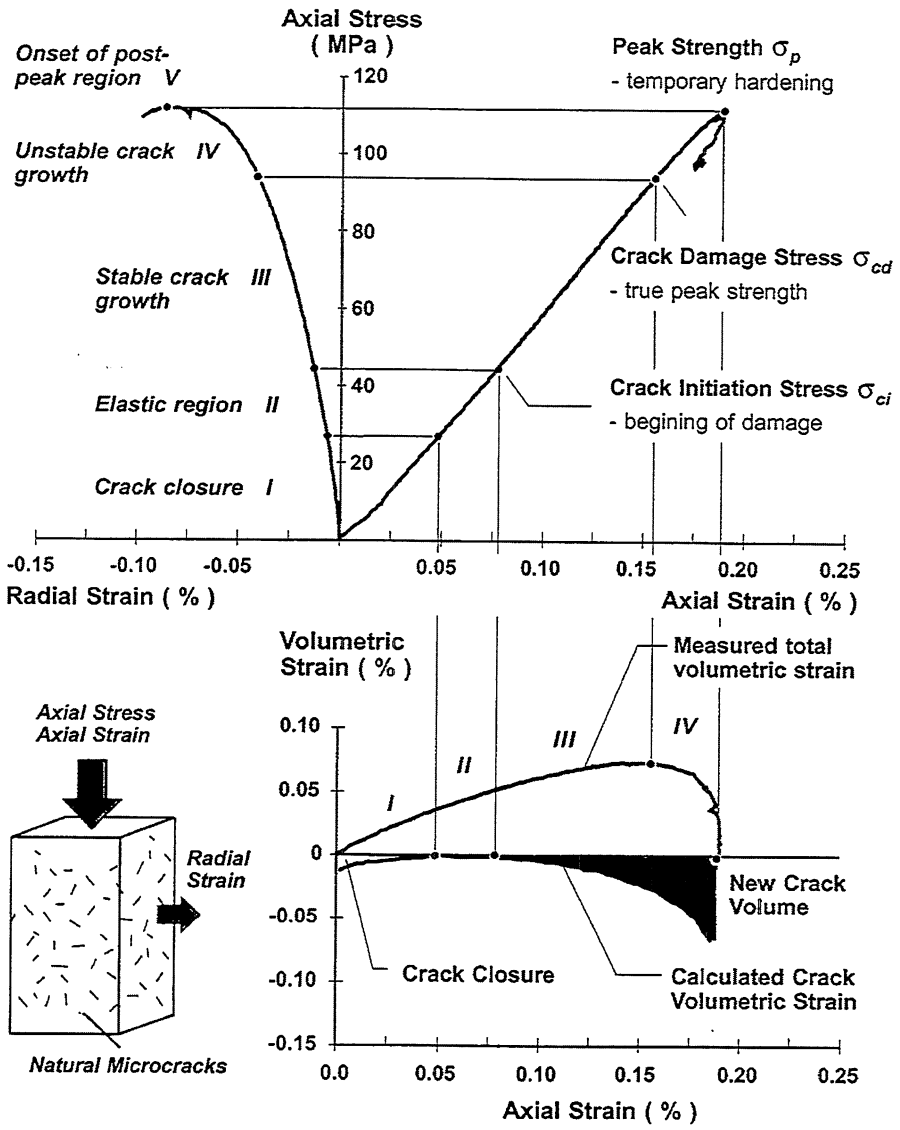

Figure 120. Determination of critical stress states σ_{ci}, σ_{cd} and σ_p (modified from Martin 1994).

The crack damage stress (σ_{cd}) is defined as the reversal of the volumetric strain (ε_v) curve. At this point the total volume of the specimen turns from compaction to dilation. The total volumetric strain (ε_v) is approximated from axial (ε_a) and radial strains (ε_r).

$$\varepsilon_v = \varepsilon_a + 2\varepsilon_r \tag{7}$$

The crack initiation stress is defined as a stress level where the crack volumetric strain ($\varepsilon_{v,cr}$) deviates from zero (Figure 120). The crack volumetric

strain ($\varepsilon_{v,cr}$) is calculated by subtracting the elastic deformations ($\varepsilon_{v,e}$) of the rock matrix from the total volumetric strain (ε_v). The elastic volumetric strain ($\varepsilon_{v,e}$) is defined by Young's modulus (E) and Poisson's ratio (ν) and current major (σ_1) and minor principal stresses (σ_3).

$$\varepsilon_{v,e} = \frac{1-2\nu}{E}(\sigma_1 - \sigma_3) \tag{8}$$

After subtracting the elastic volumetric strain ($\varepsilon_{v,e}$) from the total volumetric strain (ε_v), the crack volumetric strain curve is shifted so that the maximum value is zero (Figure 120).

The peak strength (σ_p) is defined as the highest observed axial stress.

B. Critical Stress States from Acoustic Emission data

Based on the knowledge of the former observations in the Laboratory of Rock Engineering (Hakala 1996) the use of acoustic emission measurements supports the analyse of the crack initiation (σ_{ci}) and crack damage (σ_{cd}) stresses. It seems to correspond well with the states of brittle failure, which are normally defined indirectly from stress-strain behaviour (Figure 121). The AE may give even more accurate results than the volumetric strain curves, because the measured fracturing is a direct observation of damage.

In this study the AE was measured during the compression and bending tests. For each event time, duration, sum of counts, energy, amplitude and rise time was recorded. The axial force from MTS was recorded as an external channel to syncronize the AE data with the stress-strain data.

The AE results are presented in the form of a cumulative number of counts as a function of axial stress. The results are divided to six different sub-groups according to the energy level. The dividing process have done so that the number of events is about the same in all six sub-groups.

The idea of defining the crack initiation (σ_{ci}) and crack damage (σ_{cd}) stresses from the cumulative amount of AE events - stress graph is shown in the Figure 122.

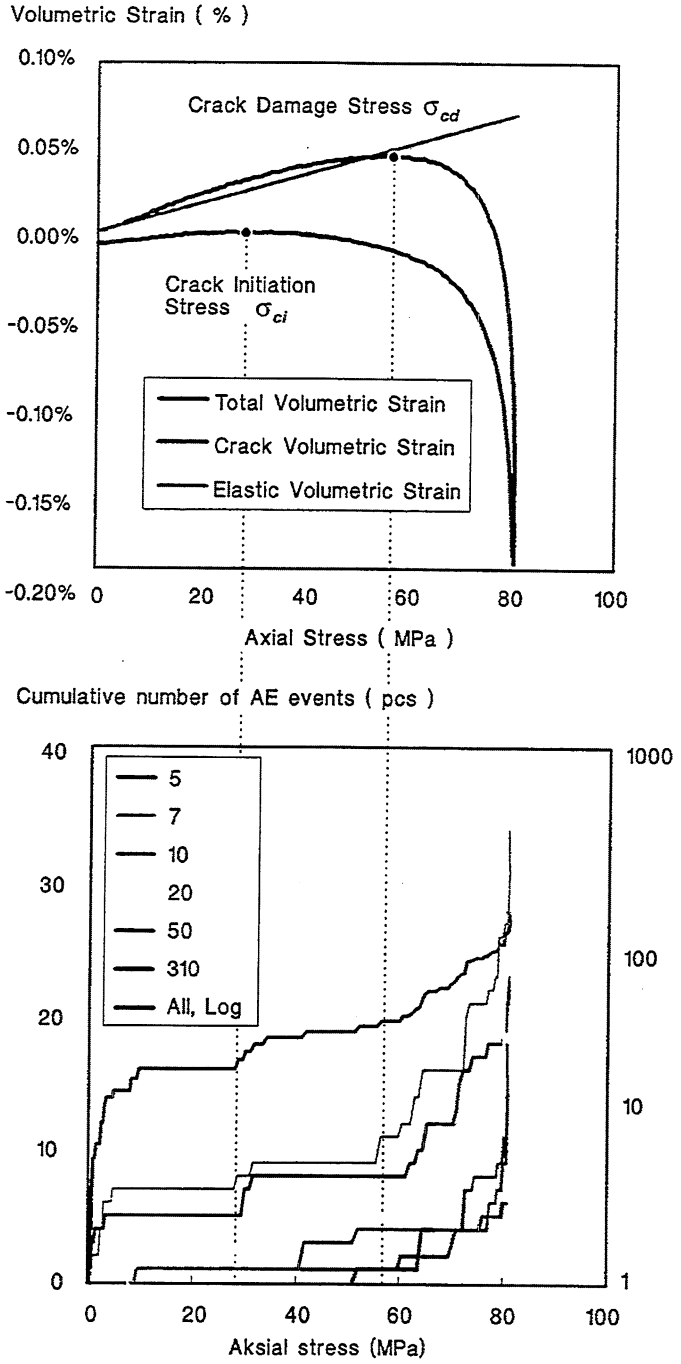

Figure 121. Comparison of typical strain and AE.

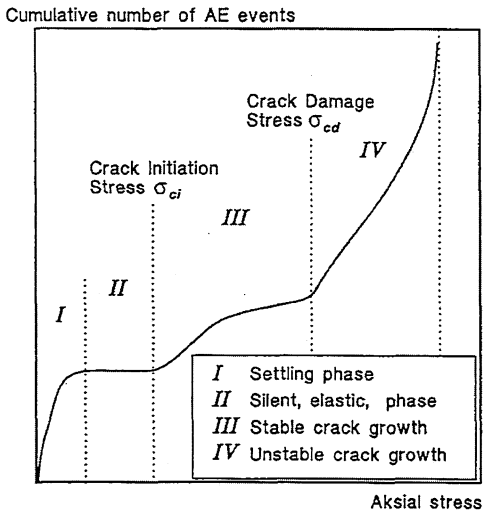

Figure 122. Definition of crack initiation stress and crack damage stress from typical design of AE data.

3.6.6.2 Peak strength

The measured uniaxial peak strength values varied from 141 MPa to 60 MPa. The corresponding triaxial values varied from 154 MPa to 84 MPa. From tested marble types E was clearly the strongest. The uniaxial peak strength was about 139 MPa ± 1.6 %. The average peak strength of the other marble types were between 73 MPa and 84 MPa. The maximum standard deviation was 3.7% of the corresponding average value (Appendix 6).

The triaxial peak strength of E marbles was about 152 MPa ± 0.9%. The average triaxial peak strength of the other marble types was between 86 MPa and 94 MPa and the standard deviations between 1.8% (1.5 MPa) and 5.6% (5.1 MPa).

According to the test results the thermal cycling has clear influence to the peak strengths of the tested marble types. The average peak strength of cycled samples were significantly lower than the corresponding reference values in every case (Table 28). The uniaxial peak strength of the cycled samples were between 84 - 96% of the reference values and the corresponding triaxial values were between 90% - 94%.

The confinement of 5 MPa in triaxial tests increases the measured peak strength of tested marble types. The triaxial values were 108% - 142% of the corresponding uniaxial values. If only deviatoric stress is considered the triaxial values were 104% - 134% of the uniaxial values.

Table 28. Summary of peak strength test results. The values in the

parentheses in the difference column are calculated reducing the confinement of 5 MPa from the triaxial value.

Sample		Uniaxial Peak strength (MPa)	Triaxial Peak strength (MPa)	Difference tria. / unia. (%)
E	**reference**	138.9	151.7	109% (106%)
	cycled	125.4	135.9	108% (104%)
	difference	90%	90%	
APA	**reference**	72.8	93.0	128% (121%)
	cycled	69.7	85.6	123% (116%)
	difference	96%	92%	
APE	**reference**	84.1	103.0	123% (117%)
	cycled	75.3	94.1	125% (118%)
	difference	90%	91%	
D	**reference**	75.7	97.0	128% (121%)
	cycled	63.7	90.7	142% (134%)
	difference	84%	94%	

3.6.6.3 Crack damage strength

The crack damage strength was definded in two different method. One method was based on the volumetric strain data by MTS and the other Acoustic Emission (AE) data.

The uniaxial crack damage values of tested four marble types according to the volumetric strain data varied from 121 MPa to 39 MPa. According to the AE data the uniaxial crack damage values were between 112 MPa and 21 MPa. The triaxial values varied from135 MPa to 53 MPa (Appendix 6).

The standard deviation of one test group in uniaxial test were between 1.6% (0.7 MPa) and 21.1% (13.2 MPa). In triaxial test the standard deviations varied from 1.6% (1.7 MPa) to 6.8% (4.7 MPa).

The tested E marble had clearly higher crack damage strength than the other marble types. In uniaxial tests the value was about 118 MPa ± 2.8 % and the triaxial value was about 133 MPa ± 1,6 %. The average uniaxial crack damage strength of the other marble types were between 43 MPa and 57 MPa and the triaxial values were between 54 MPa and 77 MPa (Table 29).

According to the test results the thermal cycling had clear influence only to the E and APE marble types. The cycled uniaxial crack damage value of D marble indicates also some reducing of the crack damage value during the

cycling, but the triaxial cycled value was even slightly higher than the reference value. The differences between reference and cycled values of triaxial APA and D and uniaxial APA values were all with in the standard deviations.

The confinement of 5 MPa in triaxial tests clearly increases the crack damage strength of tested marble types. The triaxial values were 112% - 239% of the corresponding uniaxial values. Without the confinement of 5 MPa in the triaxial values, the triaxial crack damage strength were still 106% - 222% of the uniaxial values. Generally in most of the cases the triaxial value were about 25% bigger.

The differences between the average values defined from MTS data to the values defined from AE data varied so, that the AE based values were between 79% to 106% of the MTS data based values. In general the AE based crack damage values were slightly lower, about 10%, than the MTS based values.

Table 29. Summary of the average crack damage values and the differences.

Sample group		Uniaxial			Triaxial	
		σ_{cd} (MPa)	σ_{cd} (AE) (MPa)	σ_{cd} (AE) / σ_{cd} (%)	σ_{cd} (MPa)	tri-x / uni-x (%)
E	**reference**	118.1	106.2	*90%*	132.7	112% (108%)
	cycled	93.6	87.4	*93%*	114.5	122% (117%)
	cycl./ref. (%)	*79%*	*82%*		*86%*	
APA	**reference**	45.0	44.8	*96%*	52.8	117% (106%)
	cycled	42.3	33.4	*79%*	58.2	137% (126%)
	cycl./ref. (%)	*94%*	*75%*		*110%*	
APE	**reference**	56.8	54.7	*96%*	77.3	136% (127%)
	cycled	50.7	40.0	*82%*	70.7	146% (135%)
	cycl./ref. (%)	*89%*	*73%*		*92%*	
D	**reference**	42.5	45.1	*106%*	68.5	161% (150%)
	cycled	29.0	29.2	*101%*	69.3	239% (222%)
	cycl./ref. (%)	*68%*	*65%*		*101%*	

The crack damage values of E samples were 69% - 87% of the corresponding peak strength valueas (Table 30). The other marble types had a little lower ratio, from 45% - 75%.

Table 30. Summary of crack damage values (σ_{cd}) as a function of peak strength (σ_p).

Sample group		$avg.\sigma_{cd}/\ avg.\sigma_p$		
		Uniaxial (%)	Uniaxial (AE) (%)	Triaxial (%)
E	reference	85%	76%	87%
	cycled	75%	69%	84%
APA	reference	62%	59%	58%
	cycled	61%	48%	68%
APE	reference	68%	65%	75%
	cycled	65%	53%	75%
D	reference	56%	60%	71%
	cycled	45%	47%	77%

3.6.6.4 Crack initiation strength

The defined uniaxial crack initiation values of four studied marble types varied according to MTS based volumetric strain data from 94 MPa to 10 MPa. The Acoustic Emission (AE) data based values varied between 86 MPa and 10 MPa. The triaxial crack initiation values varied from 123 MPa to 33 MPa (Appendix 6).

The standard deviations of one test group in uniaxial test were between 2.5% (0.6 MPa) and 35.5% (8.0 MPa). In triaxial test the standard deviations varied from 1.7% (0.6 MPa) to 21% (12 MPa).

The average crack initiation values of E samples were clearly higher than the other tested marble types had. The uniaxial values was about 87 ± 6 MPa and the triaxial value was about 106 ± 12 MPa. The average uniaxial crack initiation strength of the other marble types were between 35 MPa and 13 MPa. The triaxial values were between 54 MPa and 77 MPa.

According to the test results the thermal cycling had clear influence only to the E marble. The average crack initiation values of cycled E samples were 43% and 80% of the corresponding reference values. In triaxial tests the values and differerences of the other marble types were within the standard deviations. In uniaxial tests the average cycled crack initiation values of APA and APE were 54% - 85% of the reference values. The cycled values of D samples were even slightly higher or about the same as the reference values.

The confinement of 5 MPa in triaxial tests increases the crack initiation strength in most of the cases. Only the triaxial value of cycled E marble were clearly lower than the uniaxial value. Otherwise the triaxial values were 107% - 254% of the corresponding uniaxial values.

Without the confinement of 5 MPa the triaxial crack initiation values of APA reference samples and cycled E samples were lower than the uniaxial values. Otherwise the triaxial values without the confinement of 5 MPa were 14% - 122% higher than the corresponding uniaxial values.

The crack initiation values defined from AE data were in most cases lower than the values defined from MTS data based volumetric strain curves. Only the cycled APE samples had lower MTS based value. Otherwise the the AE data based values were between 49% to 95% of the MTS value.

Table 31. Summary of average crack Initiation values and the differences.

Sample group		Uniaxial			Triaxial	
		σ_{ci} (MPa)	σ_{ci} (AE) (MPa)	σ_{ci} (AE)/ σ_{cd} (%)	σ_{ci} (MPa)	tri-x / uni-x (%)
E	reference	88.5	84.2	95%	105.9	120% (114%)
	cycled	69.6	67.7	97%	46.0	66% (59%)
	cycl./ref.(%)	79%	80%		43%	
APA	reference	34.6	18.8	57%	37.0	107% (92%)
	cycled	19.1	13.1	69%	33.8	177% (151%)
	cycl./ref.(%)	55%	66%		91%	
APE	reference	28.8	22.5	78%	44.4	154% (137%)
	cycled	15.6	19.1	122%	39.7	254% (222%)
	cycl./ref.(%)	54%	85%		89%	
D	reference	23.5	13.4	57%	38.3	163% (142%)
	cycled	24.2	11.9	49%	45.4	187% (167%)
	cycl./ref.(%)	103%	89%		119%	

Table 32. Summary of crack initiation strengths (σ_{ci}) as a funktion of compresson strengths (σ_p).

Sample groups		avg.σ_{ci}/ avg.σ_p		
		Uniaxial (%)	**Uniaxial (AE)** (%)	**Triaxial** (%)
E	**reference**	*63.7*	*60.6*	*69.8*
	cycled	*55.5*	*53.8*	*33.8*
APA	**reference**	*47.5*	*27.2*	*39.6*
	cycled	*27.4*	*18.8*	*39.5*
APE	**reference**	*34.2*	*26.8*	*43.1*
	cycled	*20.5*	*25.5*	*42.5*
D	**reference**	*31.0*	*17.7*	*39.4*
	cycled	*37.7*	*18.8*	*50.1*

3.6.7 Bending test

3.6.7.1 Elastic parameters in bending

For all bending test samples the elastic parameter, Young's modulus *(E)* was defined. The loading method in the bending tests were three point loading (Figure 123). The Young's modulus *(E)* was defined by dividing the bending force *(F)* with the deflection at the center line *(y)* (Lama & Vutukuri 1978). The length of the beam *(L)* was needed, as well as the moment of inertia of the section *(I_z)* too.

$$E = \frac{F L^3}{48 y I_z} \tag{9}$$

The moment of inertia for rectangular samples is calculated from the width *(b)* and thickness *(h)* of the sample.

$$I_z = \frac{b h^3}{12} \tag{10}$$

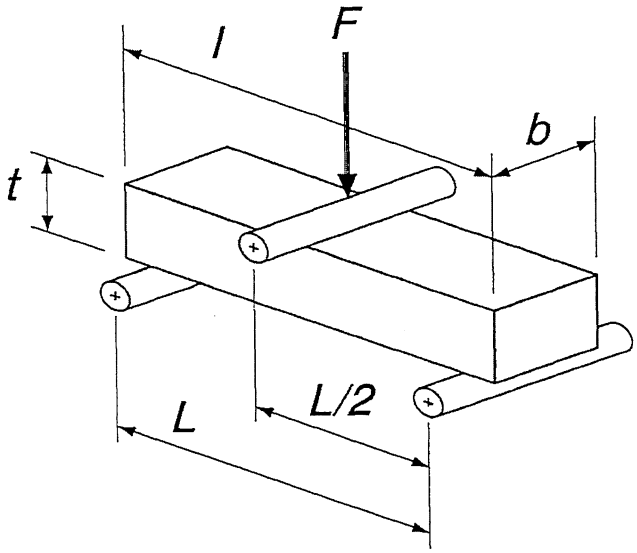

Figure 123. Three point loading of the bending test sample.

3.6.7.2 Bending strength

The measured bending strength values of four tested marble types varied from 25 MN/m^2 to 1.9 MN/m^2. The standard deviations of one test group were between 1% (0.1 MN/m^2) and 26% (2.2 MN/m^2) (Appendix 6).

From tested marble types E was clearly strongest. The average bending strength were about 24.3 MN/m^2± 2.2%. The bending strength of APA and APE marbles were about 15.2 MN/m^2± 15%.

The D marble were clearly the weekest of the tested marble types, 8.4 MN/m^2, and the standard deviation of the resutls (26%) were noticeably higher than the deviation of the other sample groups. One reason for that might be, that the samples looked visually different. The D18 sample looks quite a homogenous. There are only some gray spots. The D10 sample is not so homogenous and the D03 sample have a lot of gray spots. The gray material in the D samples may have an affect to the deviation of the measured bending strength of D marble.

According to the test results the thermal cycling has clear influence to the bending strength of the tested marble types (Table 33). The average bending strength of cycled samples were clearly lower than the corresponding bending strength of reference samples. The E marble had the smallest influence by the thermal cycling. The cycled bending strength were about 81% of the reference value. APE and APA marbles had the cycled value about 58% of the reference value. The D marble had biggest influence by the thermal cycling. The average cycled bending strength were only 23% of the reference value.

Table 33. Summary of the average bending strength values.

Sample group		Bending strength (MN/m^2)
E	**reference**	24.3
	cycled	19.8
	cycl./ref. (%)	*81%*
APA	**reference**	16.9
	cycled	10.1
	cycl./ref. (%)	*60%*
APE	**reference**	13.5
	cycled	7.6
	cycl./ref. (%)	57%
D	**reference**	8.4
	cycled	1.9
	cycl./ref. (%)	*23%*

3.6.7.3 Bending modulus

The defined bending modulus of four tested marble types varied from 46 GPa to 1.5 GPa. The standard deviations of test groups were between 17% (5.1 GPa) and 4% (0.1 GPa). From tested marble types E had clearly highest bending modulus, about 43.4 GPa ± 4.1%. The average bending modulus of APA and APE marbles were about 29.1 GPa ± 13%. The D marble had the lowest bending modulus, only 8.1 GPa ± 17% (Appendix 6).

Thermal cycling had clear influence to the bending modulus of the tested marble types. The average bending modulus of cycled samples were clearly lower than the corresponding modulus of reference samples.

The differences between the average bending modulus values of the reference samples to the cycled samples were between 20% and 68% (Table 34). The average values of the cycled samples were in every case significantly lower than the average values of reference samples. The cycled bending modulus of E samples were about 68% of the reference value. APE and APA marbles had the cycled value about 28% of the reference value. The D marble had the biggest influence by the thermal cycling. The average cycled bending modulus were about 20% of the reference value.

Table 34. Summary of the bending modulus.

Sample group		Bending Modulus (GPa)
E	**reference**	*43.4*
	cycled	*29.6*
	cycl./ref. (%)	68%
APA	**reference**	*30.4*
	cycled	*8.1*
	cycl./ref. (%)	27%
APE	**reference**	*26.4*
	cycled	*7.8*
	cycl./ref. (%)	29%
D	**reference**	*8.1*
	cycled	*1.6*
	cycl./ref. (%)	20%

3.6.8 The effect of number of cycles

The effect number of cycles were tested with APE and E samples and with the bending test configuration. The samples in this tests were cycled 1, 5, 10, 50 and 100 times. The measured bending strength values of APE samples varied from 12 MN/m^2 to 6.4 MN/m^2. The standard deviations of test groups were between 1.8 MN/m^2 and 0.1 MN/m^2. The maximum and minimum standard deviations of the average values were between 20% and 1.4% (Appendix 6).

The measured bending strength values of E samples varied from 24 MN/m^2 to 17 MN/m^2. The standard deviations of one test groups were between 2.3 MN/m^2 and 0.2 MN/m^2. The maximum and minimum standard deviations of the average values were between 10% and 0.9%.

The bending strength values of the reference and cycled samples measured in the bending tests were enclosed to the results of the this tests. They represent a non-cycled and 500 times cycled samples. All the average values and standard deviations for marble APE and E are presented in Appendix 6.

According to the test results presented in the chapter 3.7.7.2 (Bending strength) the thermal cycling at 500 times has clear influence to the bending strength. From the results of the APE samples in Table 35 it can be seen that the biggest difference in the bending strength is between the non-cycled and the one time cycled samples. That means that the major decrease in the bending strength of APE marble happens during the first cycle.

Taking into consideration the standard deviations it is clear that the differences between the different sample groups after five cycles are insignificant. The differences between the bending strength of 50, 100 and 500 times cycled samples are well within the deviation. So, most of the total decrease of the bending strength of APE marble seems to happen during the very first five cycles.

Table 35. The summary of the average bending strength values and the differences between the test groups for marble type APE.

Cycles (pcs)	Average Bending strength (MN/m2)	Difference (MN/m2)	Difference (%)
0	16.9		
1	11.2	-5.7	67%
5	10.1	-1.1	90%
10	9.8	-0.2	98%
50	8.9	-0.9	90%
100	10.5	1.6	118%
500	10.1	-0.4	96%

The results of the E marble are presented in Table 36. According to these test results the biggest difference in the bending strengths is between one time and five times cycled samples. The differences between the bending strength of sample groups after five cycles are insignificant. So, the biggest and main decrease of the bending strength of E marble happens during the very first five cycles too.

Table 36. The summary of the average bending strength values and the differences between the test groups for marble type E.

Cycles (pcs)	Average Bending strength (MN/m2)	Difference (MN/m^2)	Difference (%)
0	24.3		
1	22.7	-1.7	93%
5	18.6	-4.1	82%
10	19.6	1.0	105%
50	20.2	0.6	103%
100	19.1	-1.1	95%
500	19.8	0.7	104%

3.6.9 Discussion

3.6.9.1 Physical properties

This study reveals the clear effect of thermal cycling on the physical properties related to pore structure of marble at the temperature range simulating the Nordic climate. Pore structure is modified by introduction of thermal microfracturing, which results in the decohesion of the grain boundaries and cleavage fractures. Thermal cycling seems not to change mineralogy or density of marble types tested in this study.

Loosening of the grain structure leads to the increase of porosity and it speeds up the capillary water absorption remarkably. This means also a decay in the strength properties and may expose more pore surface to weathering and accelerated intrusion of external weathering agents. This may be also a partial reason for the bending of marble claddings.

Materials used in this study consisted of three marble types, which were expected to have different quality properties already before thermal cycling. Marble E with xenoblastic microstructure represents the good marble quality with low porosity and small coefficient of capillary water absorption. Type D, on the contrary, represents poor quality with higher porosity and big coefficient of capillary water absorption, whereas type A with intermediate microstructure represents also intermediate porosity and capillary water absorption characteristics.

This study indicates that the greatest reduction of the marble quality due to thermal cycling is directed to marble type E with the best original quality, so the thermal cycling seems to equalize the differences in pore characteristics between the marble types. The amount of quality reduction is in accordance with the results of earlier studies found in literature. Different structural orientation seems not to affect the behaviour of marble type A in thermal cycling.

The realized study with 500 cycles of treatment only, did not shed light on the changes of the physical properties of the marble types as a function of thermal cycles. According to the literature the greatest changes in the pore structure of marble are expected to be introduced during the first thermal cycles and only minor changes during repeated cycles. Obviously the majority of the changes in the physical properties revealed in this study occur already long before 500 cycles of treatment. Probably even the first drying of the untreated specimens to the temperature of +60°C modifies the pore structure of certain marbles so much, that "untreated" may not be a proper term in this study.

3.6.9.2 Mechanical properties

The testing program was very good and made clear the effect of thermal cycling. Taking into consideration that all the marble types were very homogenous and non-orientated massive rock, the amount of samples in same test group were enough. The deviations were very small .

Normally in uniaxial and triaxial tests the radial deformation is measured with roller chain extensometer. The roller chain couldn't be used because of the square cross-section of the samples. Instead of the chain extensometer the radial deformation was measured with two separately readen 30 mm long strain gages.

The test results presented in this report are fully comparable. There are no differences in handling of the samples and all the tests are made in the same manner. But, the method used in this study does not agree with the standards of ISRM. The cross-section of the samples were square instead of being circular. So, that may affect to the observed results and it is should be taken in to consideration if comparing to other test results.

The E marble is the strongest of all the studied four marble types. Both uniaxial (139 MPa) and triaxial (152 MPa) peak strengths and bending strength (24 MN/m^2) were significantly higher than the rest of the marble types had. The values were still high after the thermal cycling, which lowered the peak strengths only about 10% and bending strength about 20%. The Young's modulus (72 GPa) and bending modulus (43 GPa) of APA samples are considerably higer compared to the other marble types too. After the thermal cycling they were about 70% of the un-cycled reference values.

Type APA and APE have very same kind of strength parameters. The uniaxial (84 MPa) and <riaxial (103 MPa) peak strengths of APE seems to be a little higher than the uniaxial (73 MPa) and triaxial (93 MPa) values of APA. But, on the other hand, APA have a little higher bending strength (17 MN/m^2) than APE (14 MN/m^2). The Young's modulus (APA 46 GPa and APE 48 GPa) and the bending modulus (APA 30 GPa and APE 26 GPa) were at the same level. The effects of the thermal cycling were very equal too.

The cycled peak strengths were about 90% - 96% of the reference values. The bending strengths were about 60% after the cycling of the values they used to be before cycling. The bending modulus are correspondingly only about 30% after the cycling. The only exception seems to be the cycled Young's modulus. Both, uniaxial and triaxial, tests proves that the cycled Young's modulus of APE is only about 45% of the reference value. The difference between uncycled and cycled values of APA samples are clearly smaller. The cycled value was 75% of the reference value.

The D marble is the weakest of the studied marble types. The uniaxial (76 MPa) and the triaxial (97 MPa) peak strengths and the Young´s mudulus (46 GPa) were at the same level with the values of APE and APA samples. But, the bending strength (8 MN/m^2) and modulus (8 GPa) were considerably lower. Thermal cycling seems to have enormous effect to the bending values of D marble. It is after the cycling process only about 20% of the already very low reference values.

The crack damage and crack initiation values were defined from uniaxial and triaxial tests. The uniaxial values were defined with two different method, using the volumetric strain data by MTS and the Acoustic Emission (AE) data. In general the uniaxial crack damage values were little over 60% and triaxial about 75% of the peak strength. Correspondingly the uniaxial crack initiation values were about 35% and triaxial about 45% of the peak strength. Thermal cycling didn´t have any clear effect to the crack damage and initiation values. In most cases the values were lower after cycling, but in some cases they were even slightly higher after the cycling.

The determination of the crack initiation values of cycled samples may not be as straightforward. It is questionable if it is correct to define the crack initiation value for broken material from the volumetric strain data. There is not necessarily any more the elastic phase in the strain data, which is needed in the determination. The cycled samples were not possible unbroken, but it is not clear if they were too broken for the determination of crack initiation value.

The cycling test of APE and E samples proves that even the very first cycles can have the most significant influence. The numbers of the cycles does not have any major influence after the first five cycles. The differences after that in bending strengths are within the deviation.

3.7 DIRECT TENSILE STRENGTH TEST

3.7.1 Test results

Test results for each marble type before and after conditioning of the samples are presented in Figures 124-127. The diagrams represent the axial load as a function of the relative displacement measured across the specimen notch (50 mm gauge length). Each one of the pictures refers to the same material qualities. A softening branch appears for all type of materials, and the steepest slopes, as well as the highest peak loads, are showed, as a rule, by xenoblastic marbles (E and K types). We observe, in passing, that without a careful closed loop control, the post-critical branches would have not appeared. Complete results ar presented in Appendix 7.

From the test measurements it is also evident that the orientation of the rift plane may influence the material response. In general, we might expect that specimens loaded at right angle to rift plane show less resistance than when

the rift plane is parallel to the specimen axes. Possible differences are not very clear for E and even more so for K-type marbles (both are xenoblastic textures), but they become extremely clear for the other qualities. For D-marbles, in particular, the peak load for "pe-" type specimens (rift perpendicular to the specimen axis) may be less than half of "pa-" type specimens (rift parallel to the specimen axis) (Appendix 7).

We observe in passing that such order is in accord with a material classification based upon the granular texture, since E is the most xenoblastic marble, D the most homoblastic, while K and A are intermediate cases but K is more xenoblastic than A.

E-type:comparison between conditioned and non conditioned specimens

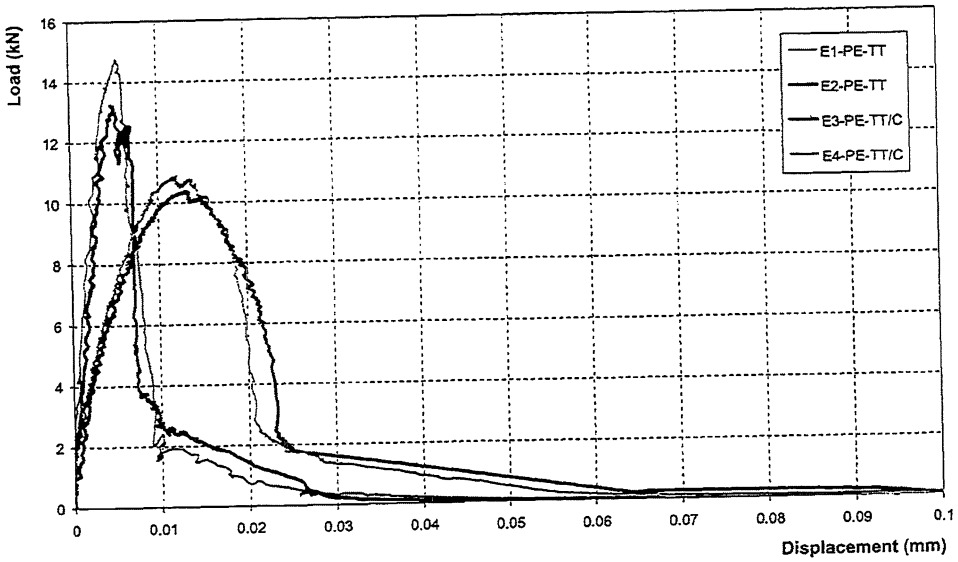

Figure 124. Comparison among non-conditioned and conditioned samples E-type marble. Specimens carved perpendicularly to rift plane.

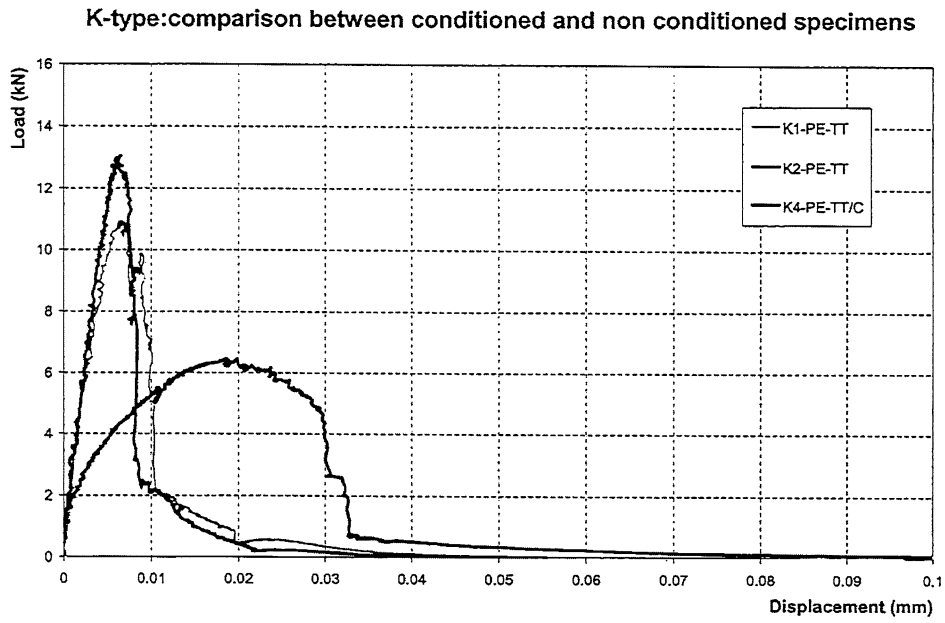

Figure 125. Comparison among non-conditioned and conditioned samples. K-type marble. Specimens carved perpendicularly to rift plane.

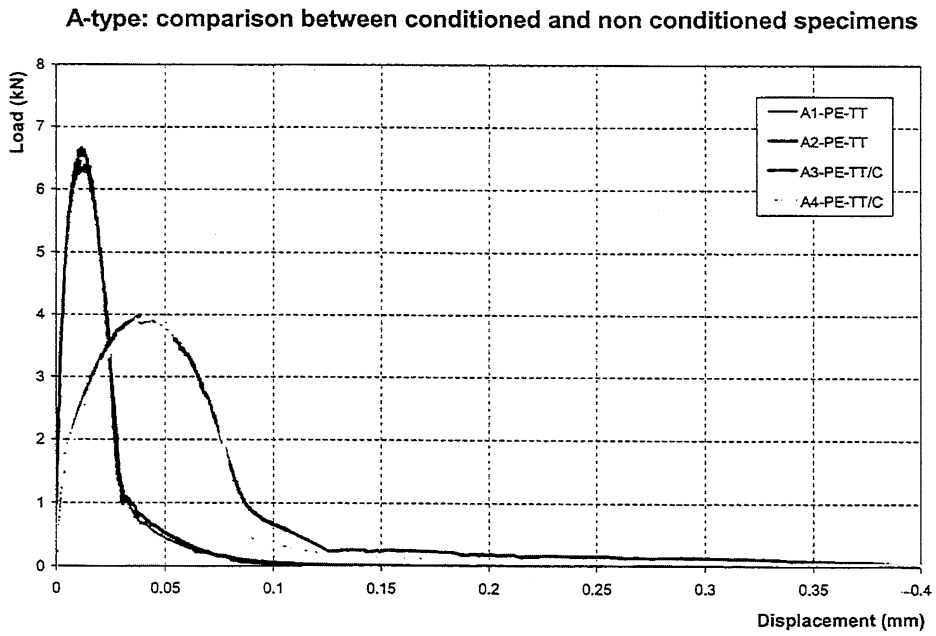

Figure 126. Comparison among non-conditioned and conditioned samples. A-type marble. Specimens carved perpendicularly to rift plane.

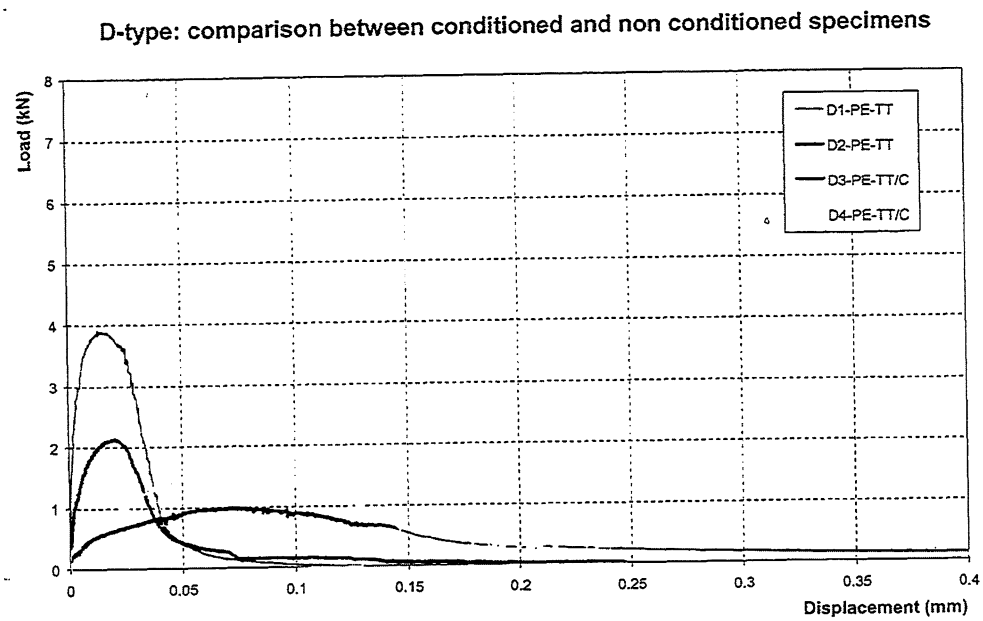

Figure 127. Comparison among non-conditioned and conditioned samples. D-type marble. Specimens carved perpendicularly to rift plane.

Different marble qualities show different attitudes towards thermal conditioning. The damaging effects for each marble type can be evaluated by examining the graphs represented in Figures 128-131, where for each material quality the responses of conditioned and unconditioned specimens are juxtaposed. In all cases, thermal treatments produce a generalized loosening of the rock: the peak load diminishes and the softening branches result less steep, while the area contained under the graph increases.

E type marble is the one for which the responses between conditioned and unconditioned sample differ the less. On the other hand, D type marbles show the greatest changes. Again, the microstructural texture seems to play a fundamental role. This is not surprising, since the greater inter-connection of xenoblastic granules with respect to the homoblastic ones, surely produces a greater resistance to the desegregation produced by thermal variations.

During the tests, the symmetric opening of the crack, controlled through the rotation of the specimens' heads, has been checked using laser Electronic Speckle Pattern Intorfermetry (ESPI). It has thus been possible to determine the exact instant of the crack nucleation, as well as the crack progression at the peak loads. Figure 128 refers to E-type unconditioned specimen with the rift plane parallel to the axes (ref. E1-PA-TT). Comprehensive measurement data is presented in Appendix 7.

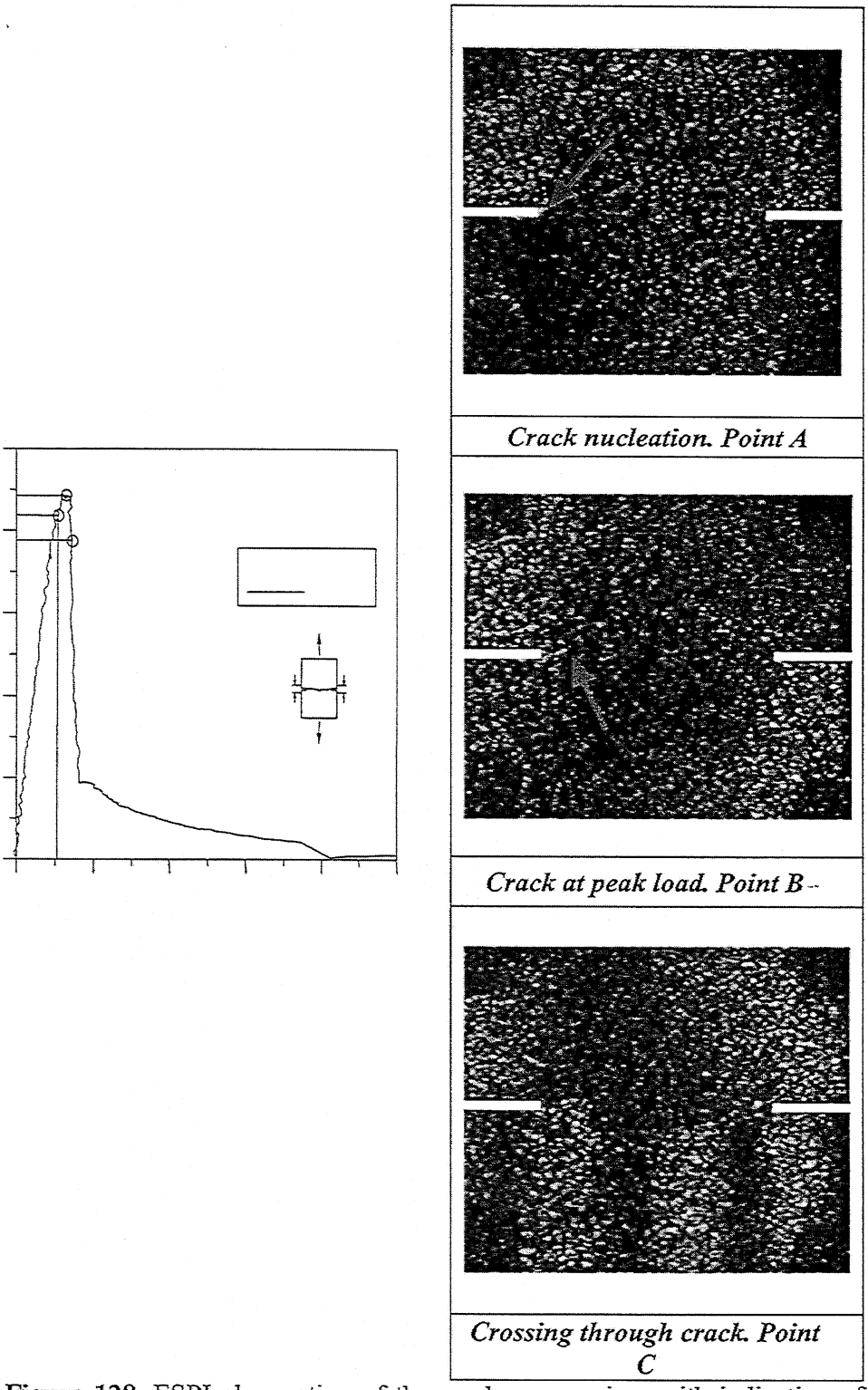

Figure 128. ESPI observation of the crack progression, with indication of crack nucleation (Point A in the graph), crack extension at peak load (point B) and crossing through crack (point C). Test # E1-PA-TT.

Processing the images obtained through the ESPI apparatus, it has also been possible to calculate the local strains in the specimen. Table 37 collects the data for six representative tests corresponding to the instant in which the crack nucleation occurs (points A in the previous graphs). The points where local strain has been calculated are in material portions in neighbourhoods of the borders and of the centre of the main initiating crack.

Comparing these data with the average strain also reported in the table, calculated by dividing the relative displacement recorder by transducers by the transducer length (50 mm), we notice that such values are of the same order of magnitude of the local measurements at the borders of the initiating crack. This is a confirmation that the crack has not opened yet, otherwise the relative displacement of the crack surfaces would have affected the average strain. In other words, if a main crack had opened, the average strain would have resulted greater than the local strain (Figure 129).

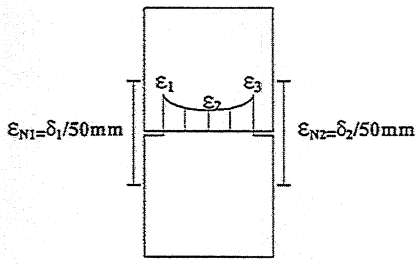

Figure 129. The three different location at which local strain has been calculated from ESPI data.

Table 37. Local strain (at 3 different location, Figure129) obtain from ESPI measurements and corresponding average strain obtain from transducers (50 mm gauge length). Crack initiation (points A in the graphs).

	Strain				
	From ESPI			from transducers	
Test	ε_1	ε_2	ε_3	ε_{N1}	ε_{N2}
E1-PE-TT	0.000107	0.0000628	0.0000877	0.0000852	0.0000828
E3-PE-TT/C	0.0000747	0.0000482	0.0000715	0.0000798	0.0000772
K1-PE-TT/C	0.0000612	0.0000531	0.0000935	0.0000802	0.000143
K4-PE-TT/C	0.000116	0.0000506	0.000104	0.000124	0.000123
D1-PE-TT	0.0000925	0.0000547	0.0000826	0.0000912	0.0000788
D3-PE-TT/C	0.000305	0.000158	0.000253	0.000342	0.000369

The values of the peak stress, peak strain, tangent elastic modulus both in the hardening and in the softening branches (calculated at 50% of peak load) are summarized for the all the 23 tests in Table 38. An indication of the material fracture energy can also be obtained, albeit roughly, by calculated the area under the load vs. displacement graphs.

Table 38. Summary matrix for direct tensile tests.

Specimen	Peak stress	Ultimate strain	Young's Modulus (50% peak load)	Young's Modulus in softening (50% peak load)	Material fracture energy
	(MPa)	(με)	(GPa)	(GPa)	(Joule/m^2)
E1-PA-TT	8.89	745.10	65.97	-83.01	65.48
E2-PA-TT	8.80	1966.40	58.93	-80.27	63.75
E1-PE-TT	8.95	2483.70	90.83	-107.15	70.76
E2-PE-TT	8.06	1807.95	56.41	-102.80	65.70
E3-PE-TT/C	6.12	38757.20	29.88	-39.92	157.73
E4-PE-TT/C	6.41	32556.70	31.34	-89.30	141.85
K1-PA-TT	6.13	514.70	37.46	-91.97	72.51
K2-PA-TT	8.21	18799.15	61.13	-167.38	65.15
K1-PE-TT	7.07	1928.70	37.65	-56.99	64.25
K2-PE-TT	8.30	3001.80	64.23	-55.26	55.55
K3-PE-TT/C	Failed	-	-	-	-
K4-PE-TT/C	3.86	21586.30	11.09	-46.09	110.29
A1-PA-TT	5.76	20906.45	41.11	-15.67	156.35
A1-PE-TT	4.18	3324.65	30.20	-15.13	107.06
A2-PE-TT	4.62	36115.95	33.09	-14.64	118.40
A[illegible] TT/C	2.32	12131.95	3.56	-2.98	185.42
A[illegible] T/C	2.33	15478.85	3.08	-3.97	167.01
D1-PA-TT	3.21	4016.10	26.07	-3.29	152.84
D2-PA-TT	2.73	8234.45	14.07	-2.07	202.17
D1-PE-TT	2.21	2576.30	14.84	-5.04	74.88
D2-PE-TT	1.38	4942.50	4.94	-2.97	93.95
D3-PE-TT/C	0.54	11830.20	0.49	-0.22	94.35
D4-PE-TT/C	0.56	11681.75	0.55	-0.46	79.37

3.7.2 Discussion

It is interesting to notice that the local strain measured in unconditioned sample (no thermal treatment) is of the same order of magnitude for the all materials. This means that in the pre-critical regime, before a main crack is developed, the tensile response is the same for all material types, independently of the microstructure. This is not surprising, since in the pre-critical stage no possibly grain sliding occurs.

Thermal treatments do not influence considerably the response of material E in the pre-critical stage. However, the conditioning increasing the strain level in material K and even more son in material D. For the latter, the strain becomes three times that calculated in the unconditioned samples. This is a clear effect of the microstructural loosening produced by thermal changes, which is of course more effective in the homoblastic than in the xenoblastic materials.

An interesting finding from the exam of this table is that, apparently, the fracture energy of xenoblastic marbles is less than that of homoblastic marbles. This is an immediate consequence of the greater apparent ductility of the homoblastic with respect to the xenoblastic qualities. In fact, the peak load decreases is somewhat compensated by the increased ductility, so that the underlying area increases as a whole.

Analogously, we notice that for the same material the fracture energy may be enhanced by thermal treatments. This is again to be attributed to a ductility increase, caused this time by a generalized loosening of the granular microstructure, which accompanies the thermal treatment. Also in this case, the energy increase is percentile more evident in homoblastic than in xenoblastic marbles. In other words, we find that thermal treatment apparently increases the material toughness. We anticipate that tests with the pre-cracked beam technique show, on the contrary, the opposite trend: thermal treatment diminishes the marble toughness.

A possible explanation for this somehow paradoxical result may be the following. In a direct tensile tests a "cloud" of microcracks is usually produced around a dominant crack. Such irregularity is usually referred to a s the process zone. The value of the fracture energy calculated by evaluating the area under the graphs represents an indication not only of the fracture energy spent when opening a dominant crack, but also of the energy dissipated in the process zone.

Evaluating the local strains be means of laser interferometry, it has been possible to estimate the extension of the process zone. The conclusion is that the process zone is much larger in the homoblastic than in the xenoblastic marbles. This is essentially due to the geometry of the grains: homoblastic textures may allow consistent grain sliding before failure.

Consequently, the energy necessary to produce the specimen rupture, which is equal to the product between the specific fracture energy and the total area of all the fractures produces, may results greater in the homoblastic than in the xenoblastic marbles. In fact, despite the specific fracture energy since in the former the number of fractures produced is much larger than in the latter.

The same argument can also explain the apparent energy increase due to thermal treatments. We anticipate that when a dominant crack is introduced *a priori*, likewise in the case of pre-cracked beams (Section 3.9), the nucleation of a dominant crack is driven by the introduced discontinuity. In other words, the formation of a process zone is restricted by the presence of a sharp notch. This is way the results obtainable with pre-cracked bending may be qualitatively opposite.

3.8 PRE-CRACKED BENDING TEST

3.8.1 Test results

For the two-step procedure previously outlined, i.e. *i*) insertion of a natural crack *ii*) fracture toughness tests under 3-Point-Bending, a high-capacity servo-hydraulic MTS testing machine and an electro-mechanical MTS testing machine were used, respectively. To determine crack length, a visuali-

zation technique using a mix of magic blue and acetone was adopted (Appendix 7).

Normalized pre-crack lengths could be obtained in the different marbles with the two techniques. The load at which propagation from the notch occurred could not be determined accurately, as, differently from ceramics (Nicoletto & Esposito, 1991-1996), a distinct "click" sound could not be heard. This appears to be a peculiarity of marbles, confirmed by the unsuccessful use of acoustic emission techniques on this material. It can be noted that the two marbles responded differently to the pre-cracking techniques.

The B method did not generally give acceptable performance due to the highly localized stresses that develop in the specimen at the bridge corner. This stress concentration generally caused the marble to crush (especially D-type) before the stress intensity for cracking initiation was attained at the machined notch. On the other hand, both marbles could be confidently pre-cracked with the SB method. Suitable values of the $(EI)_b/(EI)_s$ ratio where 4.83 for E-marbles and 1.82 for D-marbles, respectively.

The total number of tests performed has been collected in Table 35. The natural precracking bridge-method was abandoned after a few preliminary tests. Thus, evaluation of the material fracture toughness was limited to sandwich-beam pre-cracked specimens and to specimens containing natural pre-cracks 150-μm-wide, obtained though a precision diamond saw.

Each test is referred to with simple initials. The first two letters indicate the material (E, K, A, D) and the test number; the second two letters give the position of the marble rift plane with respect to the specimen axis (-pe=perpendicular; -pa=parallel); the letters –BE stand for Bending-Test. For what the precracking method is concerned, the initials B or SB indicate natural pre-cracking obtained through either the bridge method (B) or the sandwich beam method (SB), whereas N is used in the case of notched specimens (the notch obtained with a diamond saw).

Finally, possible thermal treatments are mentioned through C1 and C2. Each initial refers to a different conditioning: C1 indicates 60 thermal cycles from –10°C to +30°C, whereas C2 indicates 60 thermal cycles from 5°C to +45 °C (notice that the thermal interval is the same, but in C2 the 0°C point is not comprised). Thus, for example, E3-PE-BE-N/C1, indicates the third bending test on E-type marble, with rift plane perpendicular to specimen axis, pre-cracked with a notch and subjected to C1-type thermal conditioning (–10°C to +30°C).

Table 39. Test summary for pre-cracked beam bending tests

Bending tests								
N°	Spec. name	Marble-type	test nr.	termal conditioning	Dim (cm)	Angle to rift	Technique	Fracture toughness ($MPam^{0.5}$)
1	E1-PE-BE-N	E	N1	NO	1x2x10	90	notch	1.08
2	E1-PA-BE-N/C1	E	N1	60 cyc.-10°C to+30°C	1x2x10	0	notch	1.05
3	E2-PA-BE-N/C2	E	N2	60 cyc.+5°C to+45°C	1x2x10	0	notch	1.03
4	E1-PE-BE-N/C1	E	N1	60 cyc.-10°C to+30°C	1x2x10	90	notch	1.04
5	E2-PE-BE-N/C1	E	N2	60 cyc.-10°C to+30°C	1x2x10	90	notch	1.06
6	E3-PE-BE-N/C1	E	N3	60 cyc.-10°C to+30°C	1x2x10	90	notch	1.05
7	E4-PE-BE-N/C2	E	N4	60 cyc.+5°C to+45°C	1x2x10	90	notch	1.19
8	E5-PE-BE-N/C2	E	N5	60 cyc.+5°C to+45°C	1x2x10	90	notch	1.19
9	E6-PE-BE-N/C2	E	N6	60 cyc.+5°C to+45°C	1x2x10	90	notch	1.04
10	K1-PA-BE-SB	K	N1	NO	1x2x10	0	sand.beam	1.34
11	K2-PA-BE-N	K	N2	NO	1x2x10	0	notch	0.93
12	K1-PE-BE-SB	K	N1	NO	1x2x10	90	sand.beam	1.25
13	K2-PE-BE-N	K	N2	NO	1x2x10	90	notch	0.78
14	K3-PE-BE-N	K	N3	NO	1x2x10	90	notch	0.79
15	K4-PE-BE-N	K	N4	NO	1x2x10	90	notch	0.72
16	K1-PA-BE-N/C1	K	N1	60 cyc.-10°C to+30°C	1x2x10	0	notch	0.78
17	K2-PA-BE-N/C2	K	N2	60 cyc.+5°C to+45°C	1x2x10	0	notch	0.86
18	K1-PE-BE-N/C1	K	N1	60 cyc.-10°C to+30°C	1x2x10	90	notch	0.74
19	K2-PE-BE-N/C1	K	N2	60 cyc.-10°C to+30°C	1x2x10	90	notch	0.72
20	K3-PE-BE-N/C1	K	N3	60 cyc.-10°C to+30°C	1x2x10	90	notch	0.73
21	K4-PE-BE-N/C2	K	N4	60 cyc.+5°C to+45°C	1x2x10	90	notch	0.74
22	K5-PE-BE-N/C2	K	N5	60 cyc.+5°C to+45°C	1x2x10	90	notch	0.71
23	K6-PE-BE-N/C2	K	N6	60 cyc.+5°C to+45°C	1x2x10	90	notch	0.62
24	A1-PA-BE-SB	A	N1	NO	1x2x10	0	sand.beam	1.14
25	A2-PA-BE-N	A	N2	NO	1x2x10	0	notch	0.69
26	A1-PE-BE-SB	A	N1	NO	1x2x10	90	sand.beam	0.9
27	A2-PE-BE-N	A	N2	NO	1x2x10	90	notch	0.6
28	A3-PE-BE-N	A	N3	NO	1x2x10	90	notch	0.89
29	A4-PE-BE-N	A	N4	NO	1x2x10	90	notch	0.86
30	A1-PA-BE-N/C1	A	N1	60 cyc.-10°C to+30°C	1x2x10	0	notch	0.69
31	A2-PA-BE-N/C2	A	N2	60 cyc.+5°C to+45°C	1x2x10	0	notch	0.55
32	A1-PE-BE-N/C1	A	N1	60 cyc.-10°C to+30°C	1x2x10	90	notch	0.51
33	A2-PE-BE-N/C1	A	N2	60 cyc.-10°C to+30°C	1x2x10	90	notch	0.77
34	A3-PE-BE-N/C1	A	N3	60 cyc.-10°C to+30°C	1x2x10	90	notch	0.77
35	A4-PE-BE-N/C2	A	N4	60 cyc.+5°C to+45°C	1x2x10	90	notch	0.48
36	A5-PE-BE-N/C2	A	N5	60 cyc+5°C to+45°C	1x2x10	90	notch	0.63
37	A6-PE-BE-N/C2	A	N6	60 cyc.+5°C to+45°C	1x2x10	90	notch	0.62
38	D1-PA-BE-SB	D	N1	NO	1x2x10	0	sand.beam	-
39	D2-PA-BE-N	D	N2	NO	1x2x10	0	notch	-
40	D1-PE-BE-SB	D	N1	NO	1x2x10	90	sand.beam	-
41	D2-PE-BE-N	D	N2	NO	1x2x10	90	notch	-
42	D3-PE-BE-N	D	N3	NO	1x2x10	90	notch	0.34
43	D4-PE-BE-N	D	N4	NO	1x2x10	90	notch	0.3
44	D1-PA-BE-N/C1	D	N1	60 cyc.-10°C to+30°C	1x2x10	0	notch	0.19
45	D2-PA-BE-N/C2	D	N2	60 cyc.+5°C to+45°C	1x2x10	0	notch	0.18
46	D1-PE-BE-N/C1	D	N1	60 cyc.-10°C to+30°C	1x2x10	90	notch	0.17
47	D2-PE-BE-N/C1	D	N2	60 cyc.-10°C to+30°C	1x2x10	90	notch	0.2
48	D3-PE-BE-N/C1	D	N3	60 cyc.-10°C to+30°C	1x2x10	90	notch	0.24
49	D4-PE-BE-N/C2	D	N4	60 cyc.+5°C to+45°C	1x2x10	90	notch	0.08
50	D5-PE-BE-N/C2	D	N5	60 cyc.+5°C to+45°C	1x2x10	90	notch	0.1

E/K/A/D= Marble type
PA/PE= Parallel or perpendicular to plane rift
BE=3 point Bending test
N= Notch Technique
P= Sandwich beam precracking technique
C1=termal cycle 1 (from -10 °C to +30°, 4 cycles a day for 15 days)
C2=termal cycle 2 (from +5 °C to +45°, 4 cycles a day for 15 days)

3.8.2 Discussion

Examining the data in Table 39, it is evident that E-type marble (xenoblastic texture) is much tougher than the D-type marble (homoblastic texture). Intermediate cases are represented by K and A type, the former being tougher than the latter. As a general conclusions, the xenoblastic marbles are tougher than the homoblastic varieties. This finding can be explained from the different microstructural texture arrangements.

Another noteworthy remark is that the notch values are always lower than the natural crack data, essentially for two reasons:

- elimination of a toughening effect in the crack wake,
- reduced mixed mode effect at the crack tip.

On the other hand, the notch width, when lower than the average grain size, is expected to act as a wake-free natural crack. The fracture toughness data of the E-type marble are in line with the data of (Sglavo, 1999).

Passing to discuss the thermally treated marbles, we notice again that the conditioning, as a rule, lowers the fracture toughness. The most remarkable differences are, again, in the homoblastic texture marbles, in the A type and even more so in the D type, for which the fracture toughness may become even less than one half of the original value. No sensible differences can be noticed between the two types of thermal conditioning, which give similar results.

The bending response of E-type marbles is represented in Figure 130. From this picture, it is evident that the orientation of rift plane and the thermal conditioning can only have a limited influence on the response. E-type marbles result tougher and rather resistant to thermal damage.

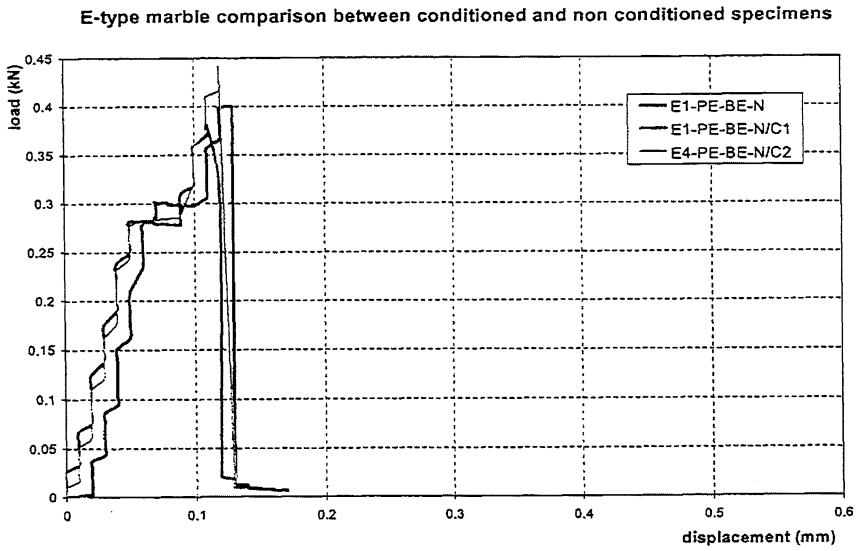

Figure 130. Comparison between condition and unconditioned E-type marbles. Rift plane perpendicular to specimen axis.

Completely different is the behavior of D-type marbles, reported in detail in Appendix 7. For such a material, both the orientations of the rift plane, as well as the thermal conditioning, play a decisive role in the response. Among the thermal treatments, the one referred to as C2, as results clear from Figure 131, seems to produce the most remarkable degradation.

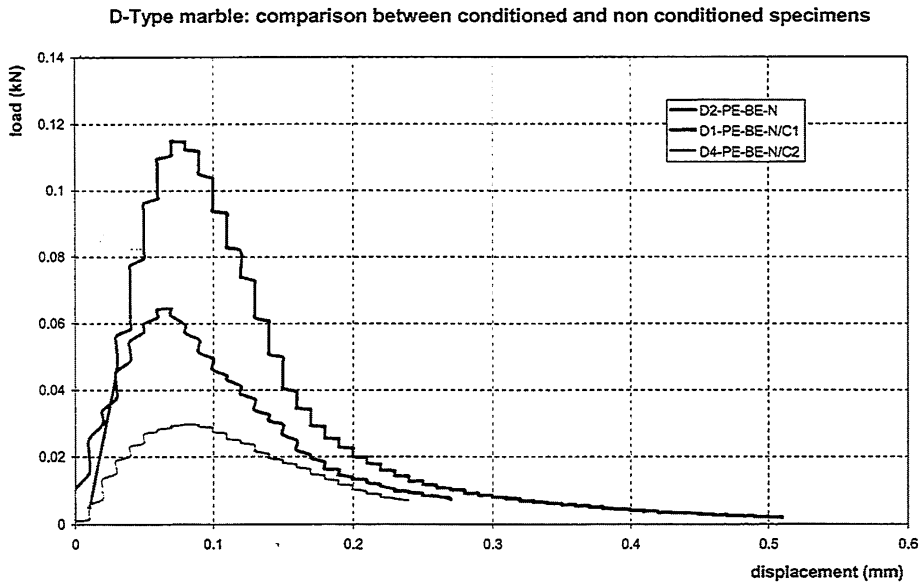

Figure 131. Comparison among the bending response of unconditioned (D2-PE-BE-N) and two differently conditioned (D1-PE-BE-N/C1 and D4-PE-BE-N/C2) D-type marbles (Table 39).

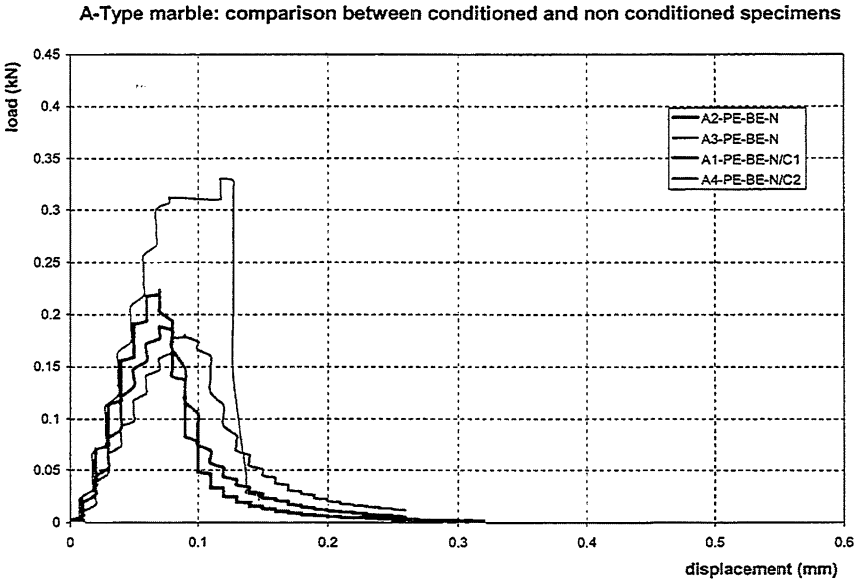

Figure 132. Comparison among the bending response of A-type marbles for unconditioned and two differently-conditioned specimens.

The behavior of A-type marbles is represented in Figure 133. The difference in the material response between naturally pre-cracked (with sandwich beam tecnique) and notched specimens as well as the difference in the rift plane orientation is evidenced according to the test data. We have already noticed that naturally precracked beams are more resistant than notched specimens, and of course, -pe samples are weaker than –pa samples. The thermal conditioning, as reported before, has a remarkable effect on toughness.

Similar graph is reported in Figure 133 for K-type marble. This case can be considered intermediate between E and A marbles. The effects of thermal conditioning are in any case very limited.

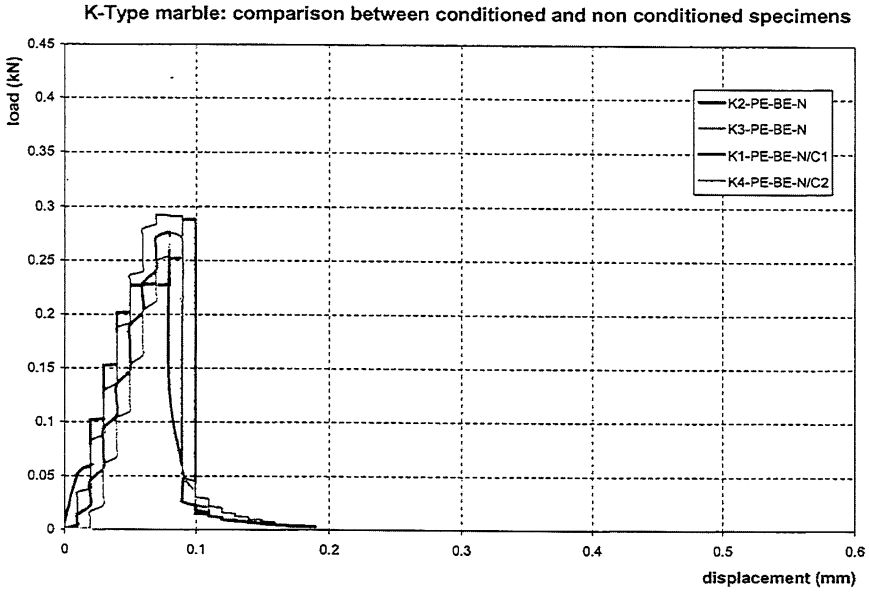

Figure 133. Comparison among the bending response of unconditioned and two differently-conditioned K-type marbles. Rift plane orthogonal to specimen axes.

What should be noticed, apart the aforementioned considerations, is that the apparent ductility of the four materials is comparable, whereas the main difference are in the peak load. We recall, in passing, that in linear elastic fracture mechanics the peak load is the parameter that determine the material toughness. The fact the final sag is comparable for the various materials is another indication that, due to the high discontinuity produced by the precracking, the extension of the process zone results very limited. To this respect, this kind of tests seems to be more accurate in directly describing fracture toughness than tensile tests.

3.9 PERMANENT DILATATION TESTS

3.9.1 Two-sided treatment

Specimens were subjected to quasi-static thermal cycles varying from approximately $-50°C$ to $+55°C$ (such values are not too far from the temperature excursion measured at the top of the roof of Finland all, during seasonal changes) and their dilatation continuously recorded by the experimental apparatus. Figure 134 shows the results for an A-type marble.

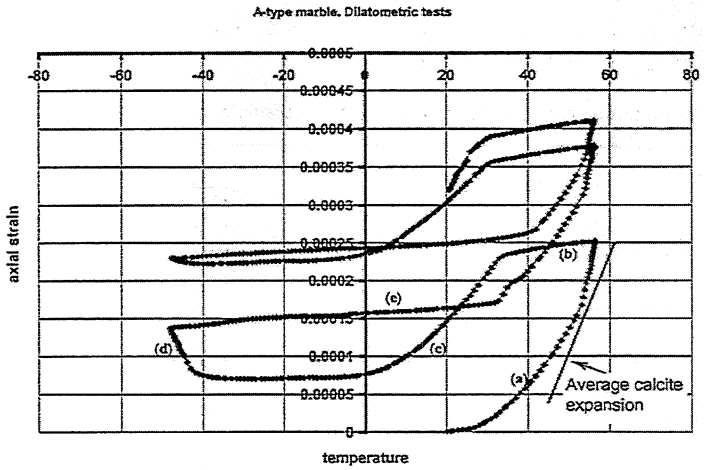

Figure 134. Average strain as a function of temperature for A-type Marble. First and second cycle.

Five different phases can be recognised in the material response. The first one, referred to as (a), corresponds to the first temperature increment, from t=+20°C (room temperature) to t=+55°C. What should be noticed is the superlinear growth of thermal strain, which should be compared with the slope of the straight line also drawn in Figure 134, corresponding to the theoretical average dilation of pure calcite ($\alpha=12\cdot10^{-6}$ °C^{-1}). The greater expansion of the composite with respect to the component can be attributed to the development of cracks. SEM investigations show that these are transgranular in type. Moreover, the analysis of the simple model discussed in (Giacomini *et al.*, 2001), shows that the transgranular cracking is very likely to be accompanied by the relative sliding of the grain borders, in order to accommodates the incongruent deformation of the grains themselves.

The cooling stage can be conveniently distinguished into three branches: phase (b), from t=+55°C to t=+30°C; phase (c), from t=+30°C to t=–40°C; phase (d), from t=–40°C to t=–50°C. The main difference between (b) and (c) is that the graph in (b) is pseudo-horizontal, whereas the beginning of (c) is indicated by a sudden change in the slope. This can be explained assuming that the frictional contact among the grains prevents an instantaneous recovery of the strain. Reverse sliding starts only at the beginning of phase (c)

and then gradually slows down, as logically expected, when the temperature is further decreased. This may be a confirmation that the dilatation accumulated during phase (a) should be, at least partially, attributed to sliding of the grains. The distinguishing character of phase (d) consists in the fact that, lowering the temperature beyond a certain limit, the material expands rather than further contracting.

This phase can be correlated with the breaking of intergranular bonds subsequent to the incongruent granular contraction at low temperatures. We observe in passing that the aforementioned model (Giacomini *et al.*, 2001) suggests that *tensile* stresses at the grain borders are greater for negative (temperature decrease) rather than for positive temperature variations, for the same temperature interval. This may explain why marble deterioration is more pronounced in cold rather than warm climates.

Finally, if at this point temperature is increased again, the material starts to expand once more, entering phase (e). The distinguishing character of (e) is that the slope of the corresponding graph is almost parallel to that of phase (b), an evident sign, in our interpretation, of the significant role played by friction. Phase (e) ends at $t \cong +30°C$. It is important to notice that if the cycle had stopped t room temperature ($t=+20°C$), marble would have shown a significant permanent dilatation.

In further cycles the strain follows a similar characteristic trend, where all the five aforementioned phases can again be recognized. A few comments are however necessary. First of all, the slope of the graphs referring to phases (b) and (e) goes slowly increasing, an indication that the friction coefficient diminishes with ongoing cycles, probably do to the smoothening out of the contact surfaces. Secondly, the beginning of phases (a), characterized by superlinear growth of strain with temperature, is shifted rightwards with ongoing cycles. For example, it was around 33°*C* in the 2nd cycle; it becomes around 42°*C* at the 9th cycle.

What is even more important is that, the volume increase occurring in phases (d) diminishes with cycling. This is a characteristic of ongoing damage. The higher is the number of thermal cycles the specimen has undergone, the lower is the number of bonds that can be broken if a new cycle is performed. In fact, roughly speaking, if the weakest bonds have already been broken in the previous history, the strongest bonds are the ones that remain active.

3.9.2 One-sided treatment

One-sided thermal variations may as well produce a permanent dilatation. Figure 135 represents, for example, the response of the same A-type marble when its temperature is varied from +20°*C* to –35°*C* (the two pictures refer to cycles 1-2 and 4-5 respectively). Again, similarly to phase (d) in Figure 135, we notice a characteristic expansion when the temperature is decreased

beyond a certain limit. However, such contribution decreases very quickly at each cycle, as Figure 135b confirms. These experiments show that, in general, two-sided thermal conditioning may be more dangerous than one-sided variations.

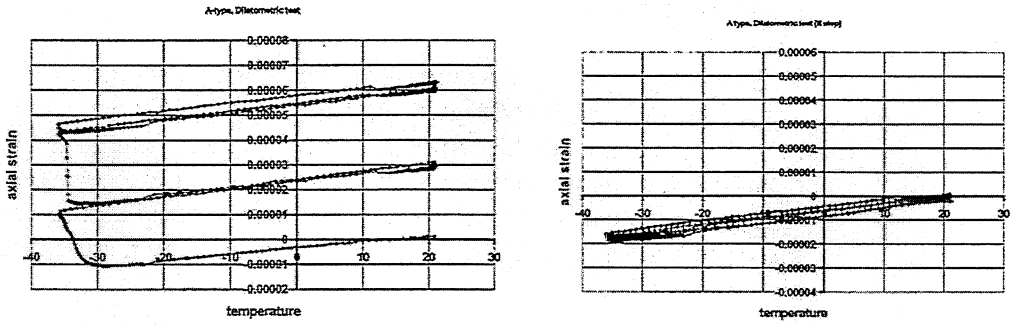

a b

Figure 135. Average strain as a function of temperature for marble A. Thermal cycles between t=+20°C and t=–35°C. Cycles **a**)1-3 and **b**) 4-6.

3.9.3 Anisotropic impact

It is also important to mention that the marble response may show remarkable anisotropy. Figure 136 shows, for example, the behavior of the same quality of marble when the average strain is measured in a direction at right angle with respect to the one considered before. Despite there are similarities with Fig 134, now the distinction among the aforementioned five phases (a)-(e) is less clear than before. Such a noteworthy difference is due to the fact that, in general, there are directions where the orientation of the grains is statistically more pronounced so that also the marble response is influenced at the macroscopic level

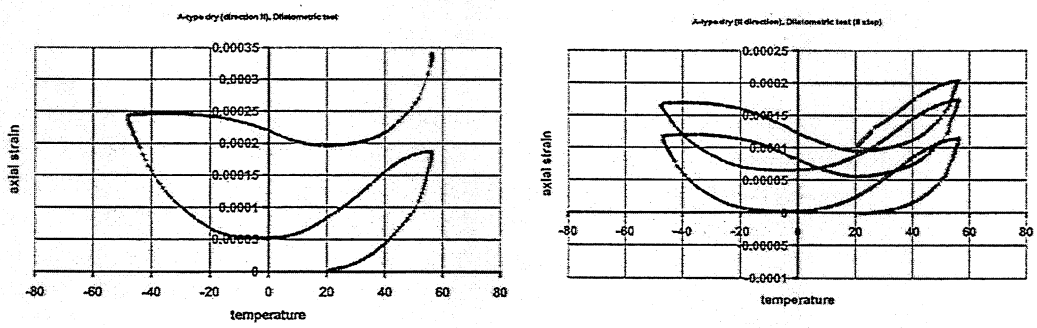

a b

Figure 136. Average strain vs. temperature for A-type Marble. Same material as in Figure 135, but specimens rotated 90°. Thermal cycles between t=+55°C and t=–50°C. Cycles n. 1-2 **a** and n. 4-5 **b**.

3.9.4 Affect of moisture

In order to investigate the influence of moisture, wet sample were also tested. The diagrams for the same A-type marble, with specimens cut in the very same direction as in Figure 134 and 135, are reported in Figure 137. What should be noticed here is the first phase, again referred to as phase (a), which produces a much larger dilatation than for the dry sample in Figure 134. Correspondingly, also the dilatation at very low temperatures, called again phase (d), is much less than in Figure 134. This is an evidence that the effect of humidity is that of facilitating the relative sliding of the grains. In rough words, we may say that humidity acts as a lubricant.

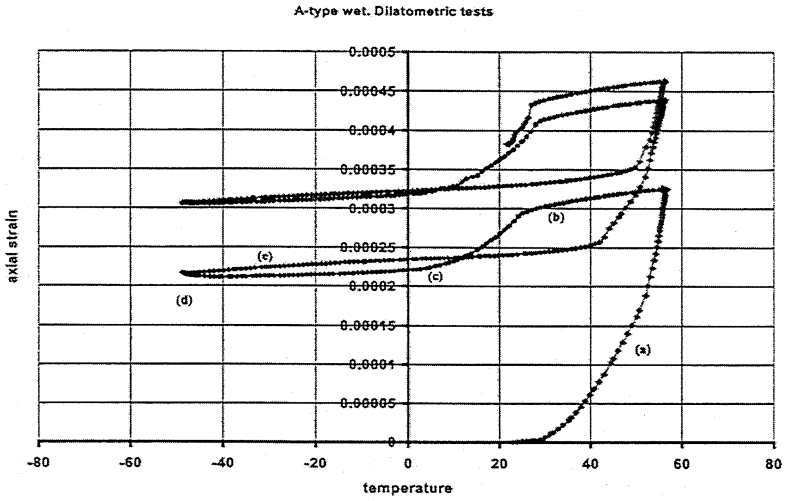

Figure 137. Average strain vs. temperature. A-type Marble in wet conditions. First and second cycle.

These considerations, especially those concerning humidity, may only be considered conjectural at this time. It is however expected that at least some of the questions mentioned will be clarified by further studies.

3.[illegible] Permanent dilatation by number of cycles

Measuring the permanent dilatation produced by thermal cycling may also be a an appropriate test to assess the vulnerability of different marble qualities. Figure 138 represents, in semi logarithmic scale, the measured permanent dilatation as a function of the number of thermal cycles from $-50°C$ to $+55°C$ performed on three different marble types. It is noteworthy that such graphs are, approximately, represented by straight lines. The slope of each graph may thus be an index of the material attitude to damage: smaller slopes correspond to more durable materials.

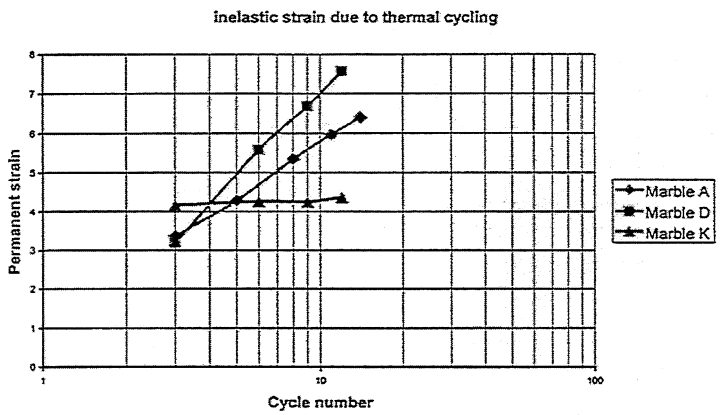

Figure 138. Permanent dilatation vs. number of cycles (log-log scale) for three marble qualities. Cycles performed between –50°*C* and +55°*C*.

Figure 138 represents, in semi logarithmic scale, the measured permanent dilatation as a function of the number of thermal cycles from –50°*C* to +55°*C* performed on three different marble types. It is noteworthy that such graphs are, approximately, represented by straight lines. The slope of each graph may thus be an index of the material attitude to damage: smaller slopes correspond to more durable materials. Measuring the permanent dilatation produced by thermal cycling may also be a an appropriate test to assess the vulnerability of different marble qualities.

3.9.6 Summary

In summary, we can affirm that thermal variations can produce granular decohesion similar to that observed in Finland Hall façade and produce, at the macroscopic level, the permanent dilatation of marble. In this study, we have evidenced the anisotropy of marble response and we have discovered the effects of humidity, which acts as a lubricant and may accelerate the accumulation of permanent strain. It is very probable that differences in the thermo-hygrometric conditions between the inner and the outer surface of the façade may be responsible of a different dilatation of the inner and outer material fibers. This would explain the bowing of the facade panels.

The reason why marble qualities behave differently is to be found, once again, in the microscopic arrangement of the crystals. Any marble is composed for more than 99% of pure calcite, whereas the other accessory components have practical no influence on the mechanical properties even if they are responsible for chromatic effects, likewise the veining. Due to the higher imbrications, granular decohesion is certainly more favored in homoblastic than in xenoblastic marbles. Indeed, the curve with lowest slope in Figure 135 corresponds to xenoblastic marbles. Therefore, this study suggests that the grain texture may be a major qualifying characteristic for selecting marbles able to endure over the years.

3.10 MODELLING OF GRANULAR DECOHESION

3.10.1 Microstructurally motivated models

3.10.1.1 Theoretical evaluation

We will now focus our attention on the effects of thermal variations and propose a simple micro-mechanically motivated model, which can provide an explanation of the degradation process in marbles subjected to thermal changes (Appendix 7).

In our interpretation, the causes of decohesion are attributed to the anisotropy of the thermal expansion of calcite. Calcite crystallizes in the rhombohedric form and, as a result of this asymmetry, its coefficient of thermal expansion is greater in the direction of the optic axes than at right angle to that. Consequently, since the grains of marble are usually randomly oriented, any temperature increase, even if uniform, may produce the springing apart of continuous grains, resulting in a self-equilibrated state of stress.

In order to present a qualitative model, which without redundant hypotheses reproduces all but the basic features of the phenomenon, we consider a marble portion composed of a certain number of identical calcite grains in plane stress or plane strain. Rigorously speaking, 21 elastic constants are necessary to represent the elasticity of calcite, but here we will assume, at least as a first order approximation, that the material is elastically homogeneous and orthotropic. Analogously, we will assume thermal orthotropy with respect to the same directions of elastic symmetry. Therefore, referring to a particular orthogonal system of axes (x_1,x_2), the constitutive relations for the material here considered can be written in the form

$$\begin{pmatrix} \varepsilon_{11} \\ \varepsilon_{22} \\ \varepsilon_{12} \end{pmatrix} = \begin{bmatrix} \frac{1}{E_1} & -\frac{\nu_1}{E_1} & 0 \\ -\frac{\nu_2}{E_2} & \frac{1}{E_2} & 0 \\ 0 & 0 & \frac{1}{2G} \end{bmatrix} \begin{pmatrix} \sigma_{11} \\ \sigma_{22} \\ \sigma_{12} \end{pmatrix} + \begin{pmatrix} \alpha_{11} \\ \alpha_{22} \\ \alpha_{12} \end{pmatrix} \Delta t, \qquad (11)$$

where σ_{ij} and ε_{ij} (i,j=1-2) represent the components of stress and strain respectively, whereas Δt denotes the temperature increase. For what the elastic moduli and coefficients of thermal expansion is concerned, if x_2 is oriented in the direction of the optic axis of calcite, we assume from the Literature (Winkler 1994) the values reported in Table 40.

Table 40. Values of the elastic parameters and coefficients of thermal expansions for modelling the calcite response

Elastic moduli	*GPa*	Coefficient of expansion	$°C^{-1}$
E_1	94.5	α_{11}	$-4.3 \cdot 10^{-6}$
E_2	140	α_{22}	$2.6 \cdot 10^{-5}$
$E_1/\nu_1 = E_2/\nu_2$	1400	α_{12}	0
G	42.9		

The simplest assemblage of crystal granules that can conveniently represent the phenomenon is presented in Figure 139. Here, the constituent square-shaped grains are identical, but are differently oriented. In particular, the local x_1 axis of those grains labelled with an A letter is horizontal, whereas the B grains are rotated of 90 degrees.

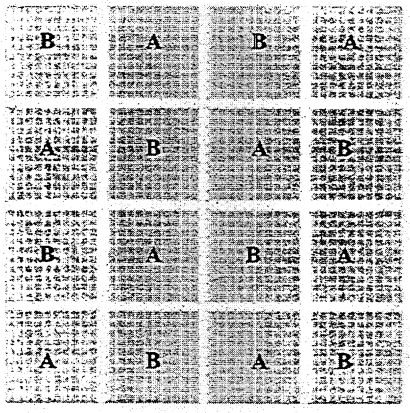

Figure 139. The assemblage of calcite grains in the FEM model.

The deformation of the assemblage consequent to a temperature variation, in particular for a temperature decrease, is qualitatively of the type represented in Figure 140. The resulting grain shapes are the consequence of the anisotropic thermal expansion of calcite which, because of the particular orientation of the orthotropy axes, produces the springing apart of contiguous grains and the nucleation of an internal stress state.

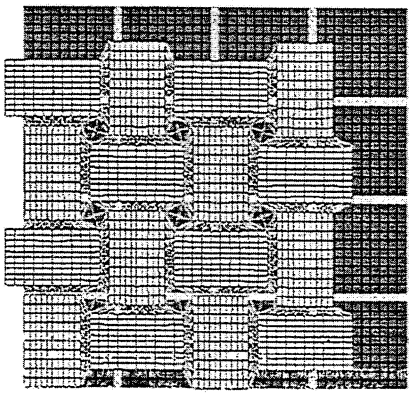

Figure 140. Thermal strains in chessboard-oriented calcite grains.

For quantitative prediction, it is fundamental to model the interface cohesive forces between any two contiguous grains. The interface contact forces are simulated by truss elements, much shorter than the grain diameter, obeying to an elastic, non-linear, softening constitute relation. The bars are of two different types and, for convenience, will be referred to using the labels *s* and *n*. Elements *n* are placed at right angle to the grain boundaries, whereas the *s* elements are at 45° with respect to them, forming the diagonal of an ideal truss. It is clear that, to the first order, the *s*-elements model the contact layer response to shear actions.

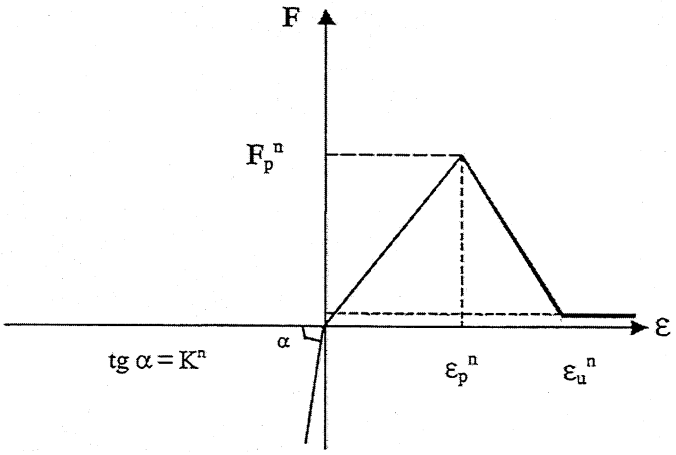

Figure 141. Constitutive relationship for the *n*-type elements.

The constitutive relationship for the *n*-type bars is represented in Figure 141. The slope of the compression branch, indicated with K^n has been calculated to be comparable to the elasticity of calcite itself, in order to reproduce the contact forces when grains are pressed together. Representative parameters for what the tensile response is concerned are represented by the peak load and peak strain F_p^n and ε_p^n and by the ultimate strain ε_u^n. These

parameters have been calculated from the direct tensile tests described in Section 3.8.

The constitutive relationship for the *s*-type elements is instead represented in Figure 142. This is an odd function in the strain and the corresponding parameters ε_p^s and ε_u^s have been taken, as a first order approximation, equal to ε_p^n and ε_u^n. Besides, we have taken $F_p^s = F_p^n$.

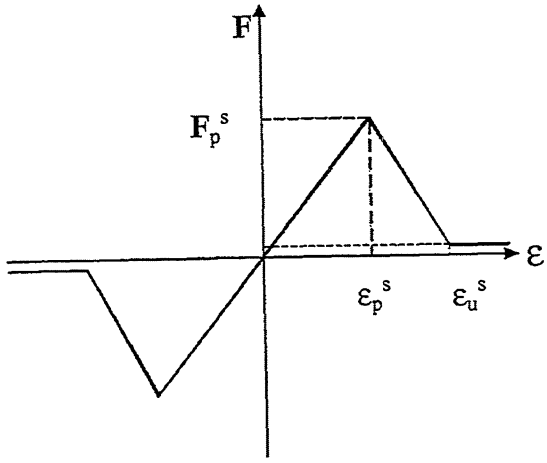

Figure 142. Constitutive relationship for the *s*-type elements.

The grains themselves have been modelled using standard isoparametric linear elastic elements in plane stress or plain strain, both thermally and elastically orthotropic according to the constitute law. The numerical solution of the proposed model has been obtained using the ABAQUS FEM code. Each grain has been set, for convenience, 1*cm* wide and 0.1*cm* thick and it is composed of 100 orthotropic linear elastic finite elements in plane stress, with mechanical properties as in Table 40.

The parameters representative of the constitutive laws (Figures 141 and 142) for the truss elements composing the interface layer are summarized in Table 41. These numbers refer to a particular material type, but experiments on different qualities of Carrara white marbles, apparently very similar, have provided values that differ from these even of an order of magnitude. It is likely that these parameters, which characterize the cohesive properties of the interface layer between any two grains, give an indication the marble attitude towards granular decohesion.

Table 41. Considered values of the representative parameters for the constitutive relationships in Figures 141 and 142.

F_p^n	3.52 N	F_p^s	3.52 N
ε_p^n	815 με	ε_p^s	815 με
ε_u^n	$1.6 \cdot 10^4$ με	ε_u^s	$1.6 \cdot 10^4$ με
K^n	$0.5 \cdot 10^{-10}$ N/με		

3.10.1.2 Practical application

For this assembly, we are interested in calculating the state of stress in the elements when subjected to a (negative) temperature variation Δt=–60°C. Such a value has been suggested by the measured temperature on the façade of the Finland Hall in Helsinki. The resulting deformed shape is represented in Figure 143 where, for convenience, the undistorted mesh is also drawn in the back. Observing the elongation of the bars composing the interface layer, we have an indication of the interface forces exchanged between the grains.

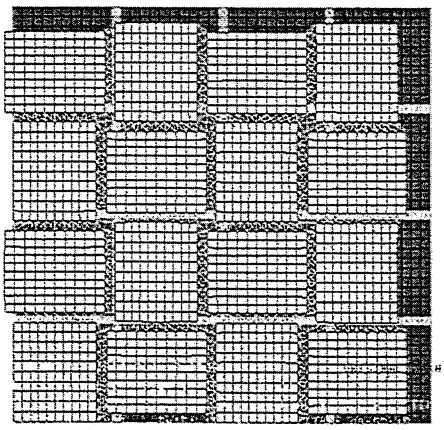

Figure 143. Deformation of the grain assemblage for Δt=–60°C. Displacements 100 x magnified.

It is interesting to notice that the most dangerous states of stress are usually located at the grain interfaces. This result is in agreement with the conclusions obtained in closed form in (Royer-Carfagni 1999), through an approximate model.

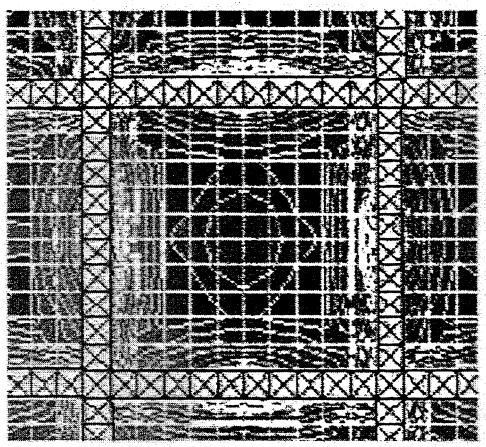

Figure 144. Von-Mises stress state in a neighborhood of a representative grain.

For the same grain, Figures 145a and 145b represent the normal and tangential components of the contact stress. Such values have been calculated assuming that the axial load in the truss elements is uniformly distributed upon an appropriate portion of the grain boundary. In general, since we assume that both strains and local rotations are small, the *s*-type members are responsible of the shear stress, whereas both *s* and *n*-type members contribute to the normal component. However, at the grain corners, where five bars converge, we have conventionally calculated the stress acting on each one of the two sides of the corner in the following way.

Commenting first Figure 145a, we notice that the resultant of the normal stress acting on each one of the sides of the grain is practically zeroed. We also observe that, in general, the central portions on each side is compressed whereas tensile stresses act in proximity of the grain corners, particularly in the direction where the material shrinks the most.

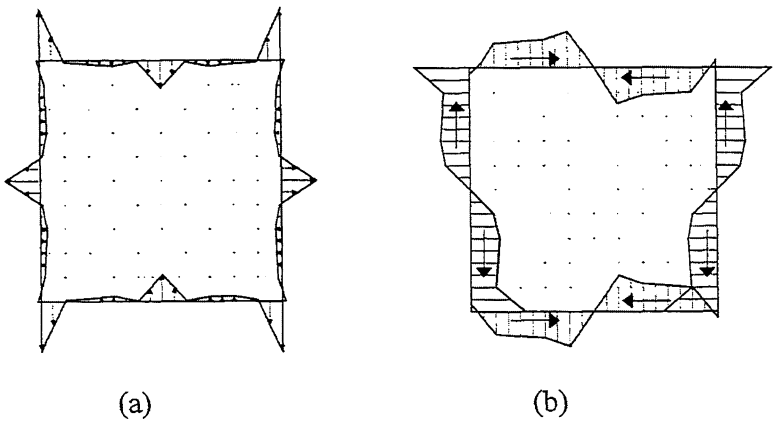

Figure 145. Normal (a) and shear (b) components of stress corresponding to Δt=–60°C.

The shear stress diagram, reported in Figure 145b, is, by symmetry, represented by odd functions. It is interesting to notice that, apart from a small central portion, important shear stresses are present on the whole grain boundary. This is not surprising since it is clear, observing also Figure 143, that the anisotropic thermal expansion induces the relative "sliding" of continuous grains, which is opposed by the shear resistance of the interface layer. The decay of the shear stress on the horizontal sides of the grain, in proximity of the grain corners, is due to the yielding of some of the *s*-elements there located, which enter the softening branch (Figure 142). In particular, yielding is in general achieved in the diagonal truss members connecting the corners of the grains at a texture node. Such point, as results clear also from Figure 143, is usually the "critical" point of the assembly.

Evidently, in our model, yielding of the truss members indicates granular decohesion damage. In order to further discuss such an effect, it may be interesting to compare these results with those obtained from a slightly different model. In particular, we consider the case in which the truss interface members remain indefinitely elastic, i.e. the linear branches departing from the origin in the constitute laws of Figures 141 and 142 are indefinitely extended beyond the peak load, so that softening is eliminated. The diagrams of the normal and shear stresses, previously reported in Figure 145, now become as represented in Figure 146.

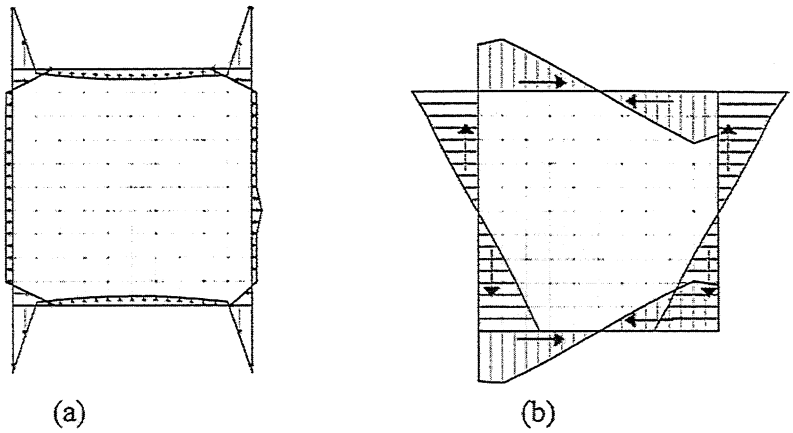

Figure 146. Normal (a) and shear (b) components of stress corresponding to Δt=–60°C for indefinitely elastic truss members.

3.10.1.3 Discussion

What is clear from the comparisons of Figures 145 and 146 is that now the normal stress presents very high peaks in correspondence of the grain boundaries, whereas the diagram of the shear stress is almost triangular in shape. The analysis of the stress state in each grain confirms that the most dangerous state of stress are exactly at the grain corners, in complete agreement with the results of the approximate analysis contained in (Royer-Carfagni 1999). Yielding of the truss members, when they present a softening regime, smoothens out these peak loads, as indicated by Figure 145.

In conclusion, despite all the approximations introduced, which render any consideration valid only at the qualitative level, the model appears capable of reproducing the basic features of the granular decohesion damage due to thermal actions. The numerical simulation shows that, in agreement with an approximate analytical solution discussed elsewhere (Royer-Carfagni, 1999), the stress state is the most critical at the grain borders, thus justifying the intergranular, rather than transgranular, nature of fractures.

Moreover, stress concentrations appear at the grain corners, in proximity of the texture nodes. Such concentrations produce the yielding of the neighbouring truss elements (modelling the interface layer), an indication of ongoing damage in the cohesive bonding between the grains. In particular, we can infer that the collapse mechanics is due to shear stresses, which similarly to mode II fracture, produce the relative sliding of the grain boundaries.

As a final remark, the model indicates that, as a consequence of plausible constitutive laws for the cohesive interface layer, negative temperature variations are more dangerous than positive variations. This finding provides a possible explanation of why, as confirmed by experience, marble

deterioration is more pronounced in monuments exposed to cold rather than warm climates.

3.10.2 A phenomenological model in statistical mechanics.

Measuring the permanent dilatation produced by thermal cycling may also be a an appropriate test to assess the vulnerability of different marble qualities. The experiments referred to in Section 3.10 have in fact shown a correlation between the microstructural damage (granular decohesion) and the macrostructural permanent expansion of marbles.

Figure 147 has been already in Section 3.10. and represents, in semilogarithmic scale, the measured permanent dilatation as a function of the number of thermal cycles from $-50°C$ to $+55°C$ performed on three different marble types. It is noteworthy that such graphs are, approximately, represented by straight lines. This observation, if confirmed by the experience, could allow to represent the marble behavior at very high cycle number just performing a limited series of experiments. In fact, the long-term behavior could be obtained just extrapolating the data from the interpolation line.

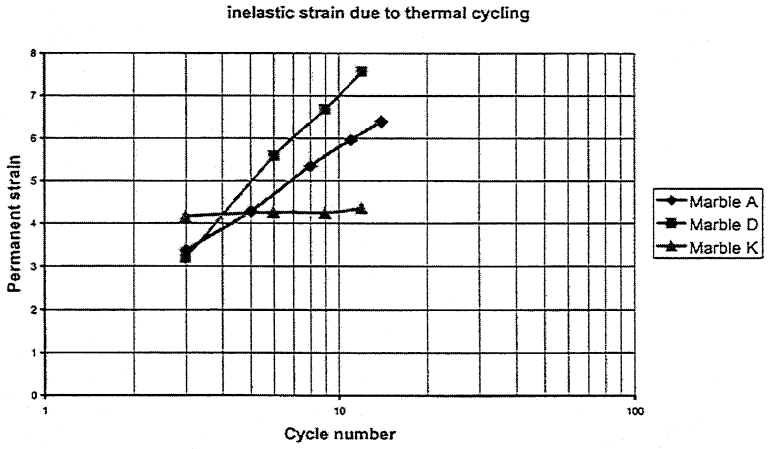

Figure 147. Permanent dilatation vs. number of cycles (semilogaritmic scale) for three different qualities of marble. Cycles performed between $-50°C$ and $+55°C$.

The aim of this Section is to present a simple, phenomenological model, able to interpret this intriguing behavior, in particular the pseudo-linear dependence of permanent strain on the logarithm of the number of thermal cycles n, as shown in Figure 147.

One of the principal hypotheses consists in assuming that the increment in inelastic deformation is produced by a series of events that are *independent* one from the other. In other words, the occurrence of a process in a certain

particle does not influence the behavior of the neighboring constituent elements. One argument, in particular, uphold such a hypothesis. At the microscopic level, SEM observations have shown that the degradation mechanism is essentially due to decohesion of the constituent grains. Hardly any transgranular cracking at all can be found, so the process can be considered to occur at a length scale of the same order of magnitude as the diameter of a unit grain.

Therefore, by our way of thinking, the basic process producing inelastic deformation consists in the braking of the granular bonding at some place. In particular, we may suppose that breaking occurs when the average stress in the considered point, say τ, equals a certain activation stress τ_a. We further assume that braking of one bonding produces a relative displacement of the specimen's ends by a certain quantity v_p so that, if h denotes the height of the sample,

$$\varepsilon_p = \frac{v_p}{h} \tag{12}$$

represents the plastic contribution to the specimen's overall axial strain due to the yielding of *one* bond. Of course, each bond can yield only once. We may model this that by saying that its activation stress becomes very large (practically infinite) after it has flowed.

Now, taking into account all these assumptions, we want to characterize the material response when the specimen is cyclically thermally loaded. The key-point in the analysis is recognizing that in real materials, especially rocks, various circumstances, such as micro-inhomogeneous, micro-cracks, micro-inclusions, produce a system of self-balanced micro-stresses when the specimen is uniformly heated.

As a result of the theoretical conclusion (Appendix 7) the following equation (13) has been formed for anticipated logarithmic dependence:

$$\varepsilon(n) = \varepsilon_p \frac{\Theta\ \Pi_0}{\gamma^{[T_u]}} \ln(n) + A\ , \tag{13}$$

Formula (4.2.18) expresses the macroscopic material's behavior when subjected to cyclic thermal loading. The quantities ε_p and Π_0 appearing therein are clearly material parameters, unlinked to the testing conditions. On the other hand, constant A is representative of the strain increase consequent to the initial settling of the specimen, occurring as a rule in the very first cycle. This parameter may depend upon the most disparate causes (i.e. bedding errors, micro-inhomogeneities, etc.) and should consequently be considered a random variable. The results of the tests performed do in fact exhibit wide

scattering as far as this parameter is concerned, confirming a non-continuous dependence on the macroscopic testing conditions.

Consequently, increasingly heterogeneous materials (but this parameter may depend also on the microstructure, i.e. xenoblastic vs. homoblastic textures) are characterized by increasingly large values of the function $P^{[T_L]}(\tau')$, corresponding to great Θs and small γs. Moreover, it is clear that

$$T_1 < T_2 \quad \Rightarrow \quad \gamma^{[T_1]} > \gamma^{[T_2]} \ . \tag{14}$$

In fact, the higher the applied temperature variation is, the greater the probability that granular bonds be subjected to high stresses.

As a final remark, it is worth stressing once again that the central assumption underlying all the above considerations is that of the *statistical independence* of the events causing the effect as observed at the macroscopic level.

3.11 MICROSTRUCTURAL CHARACTERIZATION OF MARBLES.

3.11.1 Skeleton method

Observation of material thin sections has suggested the following empirical observations. Homoblastic textures contain convex grains of various dimensions closely packed together, whereas grains of almost the same dimensions, mainly concave shaped, form xenoblastic textures. Therefore, it is natural to consider as representative parameters, able to describe the shape of the grains, the area A and the perimeter P. In fact, for the same value of P, the area is smaller for concave than for convex grains. Therefore, A/P^2 has been the first parameter to be considered (Appendix 7).

We have also addressed the question whether, in order to differentiate the two texture types, another parameter connected to the waves of the contour could be useful. We have thus referred to shape indexes usually employed in Computer Vision (CV) (Gonzalez & Woods, 1991), developed in particular for the automatic recognition of text characters. Among the various indices used in this field, we indeed find A/P^2, now referred to as compactness, and the convexity, defined as the ration between A and the figure convex hull. A third parameter able to define the contour roughness is the skeleton S (Jain, *et al.*, 1995, Parker, 1997).

The numerical algorithm used in this research finds the skeleton in the following manner: for each point internal to the figure, the distance from points of the border is calculated. If the resulting function has more than one absolute minimum, in other words if at least two points of the border presents

the same minimal distance, then the points belongs to S. For figures defined by polylines, S is composed (Figure 148) by three different kinds of lines:

i) bisectors of acute angles,
ii) segments which are equidistant from two non-adjacent sides and
iii) parabola sectors (equidistant from one vertex and one side, when a concave angle is present).

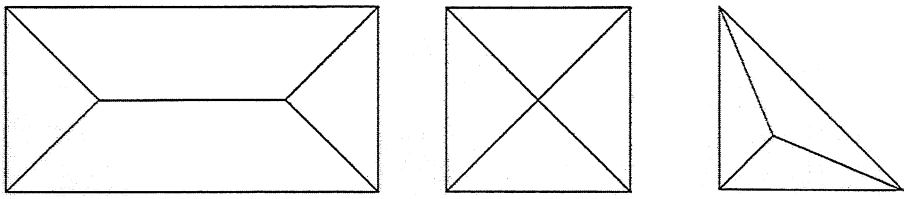

Figure 148. Polygons and corresponding skeleton.

The skeleton is usually used in CV for *thinning* the object contours. However here it is used to characterize the grain shape. In fact the number and length of the various branches composing the skeleton are influenced by the contour protuberances. To illustrate, we consider in Figure 149 the skeletons of the represented polygon. Perturbing with a little asperity one of the sides of the polygon, significantly modifies the skeleton, suggesting that wiggly contours have are characterized by high values of S.

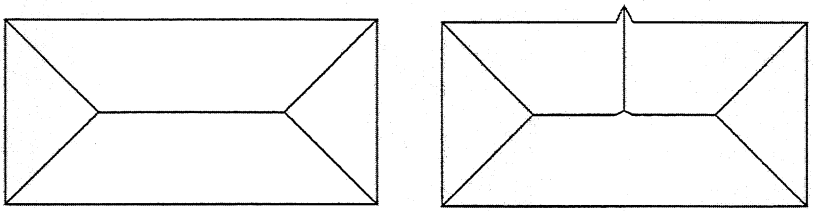

Figure 149. Influence of the contour roughness on the skeleton S.

Four distinct parameters have been considered for shape characterization: A/P^2, A/S^2, $A/(P*S)$) and P/S. The first should be indicative of the figure compactness, the second is influenced by the contour roughness, while the third is intermediate between the two. The last parameter (P/S) is perhaps the less discriminating, since for the same value of P, very similar figures may present very different S.

We have first tested the method with simple geometrical figures and, successively, we have passes to the analysis of the grain shapes microscopically observed through thin material sections. The shape indexes have been calculated using the Image Processing function available in MATLAB. In order to obtain digital images, we proceeded as follows. For polygons, it is

sufficient to draw them with a standard graphic software, which indeed use the matrix binary representation. Digitalizing the grain shapes is more complicated.

Testing the image processing procedure with simple polygons, we have noticed that the skeleton shape appears different from what expect on the base of the definition. Most likely, this is due to the algorithm from which S is defined: the software extract the skeleton using a modified thinning, using an iterative procedure. Computing time is reduced, but the skeleton is only approximated. In particular, very little protuberances are neglected by the algorithm.

Once the procedure has been set, we have applied our method to 20 different qualities of marble. Of course, the procedure is not completely automatic, since it is the operator who defines, using the computer mouse, the grain contours. In order to evaluate how the selection of the vertexes in the approximating polyline and their location influences the shape parameters, we made different tests. For example, for the xenoblastic grain represented in Figure 150, we have repeated the data acquisition procedures 10 times, maintaining fixed the number of vertexes of the approximating polyline and, more or less, their position. In this way, our intention was to evaluate the influence of the operator. The results are reported in Table 42.

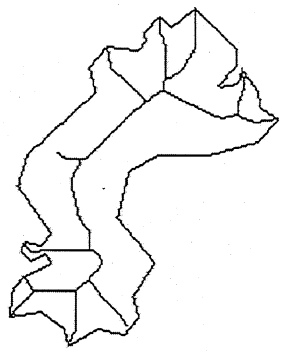

Figure 150. The xenoblastic grain considered in the repeatability tests for the contour acquisition.

Table 42. Tolerances in the shape parameters in the repeatability tests.

Variation	ΔA)	ΔP)	ΔS)	$\Delta A/P^2$)	$\Delta A/S^2$)	ΔA/(P*S))
Absolute	586	22,6	154,1	0,001486	0,018185	0,008421
% of the average	5,5 %	3,47 %	8,27 %	6 %	18,57 %	10,23 %

It is clear that the parameter which shows the highest deviation is S. However the approximation is, in general, acceptable. As a second repeatability

test, we have considered possible changes when the number of vertexes in the approximating polyline is gradually varied. This has caused a progressive smoothening out of the grain contours because possible irregularities are neglected. In other words, the grain gradually becomes homoblastic.

3.11.2 Marble classification

In order to evaluate the efficiency of the classification obtained through the parameters A/P^2, A/S^2, $A/(P*S)$ e P/S, we have considered 20 marble qualities, differing not only for their mechanical properties, but also for the microstructural layout. In particular, we have selected 7 xenoblastic, 6 intermediate and 7 homoblastic marbles, referred to in Table 43. The corresponding properties have been derived from (Gattiglio et al., 1980) and the number in parentheses refer to the reference number therein reported.

Table 43. The 20 considered marble qualities, with indication of the originating quarry.

Xenoblastic texture	Intermediate texture	Homoblastic texture
Bianco Fondone (1)	Statuario Fossa del Donato (6)	Arabescato Boccanaglia (3)
Arabescato Cervaiole (2)	Nuvolato Fantiscritti (11)	Calacatta Boccanaglia (4)
Bianco Ravaccione (8)	Arabescato Gioia (13)	Venato Crestola (5)
Statuario Ravaccione (9)	Bianco Costa (15)	Bianco Lorano (7)
Bardiglio Costa (16)	Venato Carpano (17)	Zebrino Ponti di Vara (10)
Venato Madielle (19)	Bianco Valsora (18)	Venato Cima di Gioia (12)
Bianco Trambiserra (20)		Venato La Piana (14)

For each marble, the data in (Gattiglio et al., 1980) furnish the main mechanical properties and micrographs of three thin sections, cut parallelly to rift, head grain or grain plane. Despite grains are, as a matter of fact, 3D objects, we surmise that their shapes can be conveniently characterized through a 2D analysis, by means of three thin sections at right angle one another. For each marble type, we have considered 15 different grains, 5 for each thin sections. For each of the 15 images, the area (A), the perimeter (P) and the skeleton (S) have been calculated.

The classification obtained by considering the average values of the shape parameters are reported in table 40, where each material is identified by the same number reported in Table 44. It should be noticed that the classification derived from A/P^2, A/S^2 e $A/(P*S)$ are comparable, and are in agreement with the empirical classifications reported in the Literature: xenoblastic (homoblastic) textures are characterized by the lower (higher) values of

the cofficients A/P^2, A/S^2 e $A/(P*S)$, whereas the qualities classified as intermediate occupy the central positions.

Table 44. Classification obtained through parameters A/P^2, A/S^2, $A/(P*S)$ e P/S.

Marble n.	A/P^2*10^{-2}	Marble n.	A/S^2*10^{-2}	Marble n.	$A/(PS)*10^{-2}$	Marble n.	P/S
2 (X)	1,480	2 (X)	1,949	2 (X)	1,694	2 (X)	1,135
20 (X)	1,530	20 (X)	2,077	20 (X)	1,776	1 (X)	1,140
9 (X)	1,753	1 (X)	2,776	9 (X)	2,203	20 (X)	1,154
19 (X)	1,954	9 (X)	2,806	19 (X)	2,333	16 (X)	1,185
1 (X)	2,098	19 (X)	2,807	1 (X)	2,402	19 (X)	1,199
8 (X)	2,229	8 (X)	3,650	8 (X)	2,835	15 (I)	1,210
16 (X)	2,721	16 (X)	3,849	16 (X)	3,204	6 (I)	1,231
15 (I)	3,085	15 (I)	4,586	15 (I)	3,715	9 (X)	1,238
17 (I)	3,267	17 (I)	5,510	17 (I)	4,194	17 (I)	1,273
13 (I)	3,726	6 (I)	5,848	6 (I)	4,657	8 (X)	1,278
6 (I)	3,761	13 (I)	6,318	13 (I)	4,822	5 (H)	1,283
11 (I)	3,857	11 (I)	6,597	11 (I)	5,034	4 (H)	1,290
18 (I)	3,940	18 (I)	6,964	18 (I)	5,203	3 (H)	1,292
7 (H)	5,113	5 (H)	8,836	5 (H)	6,769	13 (I)	1,295
5 (H)	5,263	7 (H)	9,358	7 (H)	6,865	12 (H)	1,298
4 (H)	5,369	4 (H)	9,363	4 (H)	7,004	11 (I)	1,300
10 (H)	5,490	12 (H)	9,642	12 (H)	7,332	18 (I)	1,314
12 (H)	5,633	3 (H)	9,871	3 (H)	7,395	7 (H)	1,327
14 (H)	5,670	14 (H)	11,253	14 (H)	7,896	14 (H)	1,393
3 (H)	5,684	10 (H)	13,590	10 (H)	8,573	10 (H)	1,548

On the other hand, the classification obtained through P/S is not in agreement with our expectation. This result is not surprising because of the reasons mentioned above. The coefficient P/S does not represent a reliable parameter for the texture classification. It is then possible to provide a first quantitative classification of the marble textures based on the shape parameters. Such classification is reported in Table 45.

Table 45. Shape-parameter range for xenoblastic, intermediate and homoblastic textures.

Xenoblastic	$A/P^2<0,03$	$A/S^2<0,04$	$A/(P*S)<0,035$
Intermediate	$0,03<A/P^2<0,045$	$0,04<A/S^2<0,08$	$0,035<A/(P*S)<0,06$
Homoblastic	$A/P^2>0,045$	$A/S^2>0,08$	$A/(P*S)>0,06$

From an intuitive point of view, it is logical that the greater interlocking of xenoblastic textures with respect to the homoblastic textures may influence the mechanical material properties. We have thus tried to examine a possible correlation between the shape parameters and the the mechanical characteristics of marbles. The corresponding values have been also found in the literature (Gattiglio, et al., 1980).

In general, based on the available test data, xenoblastic marbles present greater flexural strength, smaller water absorption, smaller coefficient of thermal dilatation, higher elastic modulus, than the homoblastic qualities. Other mechanical properties, likewise the compression strength (even after freezing and thawing cycles) or the impact-test resistance, which mainly depend on the development of transgranular microfractures, are not correlated with the shape parameters. However, a very good correlation has been noticed for the coefficient of water absorption, which increases almost linearly with the values of any of the shape-parameters A/P^2, A/S^2 and $A/(P*S)$. This finding is justified by the referring to a microstructural motivated model, highlighting in particular some inconsistency in the standards according to which the water absorbtion is calculated. More detailed presentation of the subject is available in Appendix 7.

3.12 RESEARCH AT CEVALOR

3.12.1 Marble type A

Table 46. Initial characterisation of sample A (cut against)

Initial Characterisation	Sample A (Cut against)	
	Average	Standard deviation
Resist. to Compression (Mpa)	83,0	5,0
Water Absorption at PtN (%)	0,12	0,01
Open Porosity (%)	0,4	0,1
Volumetric Mass (Kg/m^3)	2707	1,2
Microscopic Observation	See report in annex	
Resistance to Flexural Strength under conc. Load (Mpa)	13,0	1,0

Table 47. Initial characterisation of sample A (cut in favour)

Initial Characterisation	Sample A (Cut in favour)	
	Average	Standard deviation
Resist. to Compression (Mpa)	95,5	12,9
Water Absorption at PtN (%)	0,12	0,01
Open Porosity (%)	0,4	0,0
Volumetric Mass (Kg/m^3)	2693	18
Resonance Frequency (HZ)	2188	-
Ultrasonic Propagation Speed (m/s)	6,4x10^{-2}	-
Thermal Shock	No visual remark	-
Crystallisation Test	being done	-
Dynamic Modulus of Elasticity (x10^9 N/mm^2)	4,6x10^9	-
Microscopic Observation	See report in annex	-
Resistance to Flexural Strength under conc. Load (Mpa)	16,3	0,7

Table 48. Characterisation of the sample A marble resistance, each 25 cycles of freeze/thaw

Resistance characterisation	Each 25 cycles of the freeze/thaw								
	26	53	81	101	143	167	191	216	232
Resist. to Compression (Mpa)	89,0	83,6	84,8	85,1	90,9	86,0	89,6	78,9	84,7
Water Absorption at PtN (%)	0,17	0,18	0,19	0,17	0,18	0,20	0,20	0,19	0,26
Open Porosity (%)	0,5	0,6	0,5	0,6	0,6	0,6	0,6	0,5	0,7
Volumetric Mass (Kg/m^3)	2711	2698	2699	2698	2697	2699	2695	2701	2699
Resonance Frequency (HZ)	2243	2243	2313	2282	2352	2452	2138	2020	1980
Ultrasonic Propagation Speed (x10^{-2} m/s)	6,1	6,0	6,0	6,1	6,1	6,1	6,0	6,4	6,4
Thermal Shock	No visual remark								
Dynamic Modulus of Elasticity (x10^9 N/mm^2)	4,9	4,9	5,2	5,1	5,4	5,8	4,4	4,0	3,8
Microscopic Observation	See report in annex								
Resistance to Flexural Strength under conc. Load (Mpa)	12,7	11,3	11,8	10,1	10,0	11,6	8,8	8,4	8,1

The crystallisation tests were made in the beginning and at the end of 232 cycles of freeze/thaw. The results were generally; loss mass and tarnished appearance. The loss of material, during the initial characterisation test was of 1,5% and after the 232 cycles, was of 3,18%, this may be a consequence of the increase on the porosity and consequently of the water absorption.
It's possible to conclude that marble, when submitted to thermal variations, and in presence of salt mist, shows alterations.

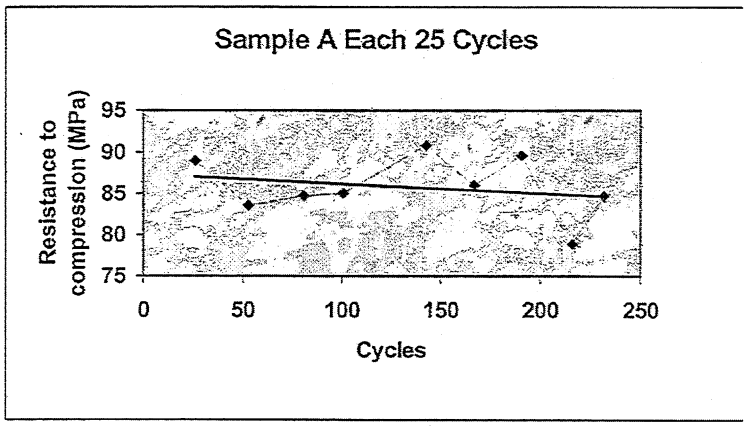

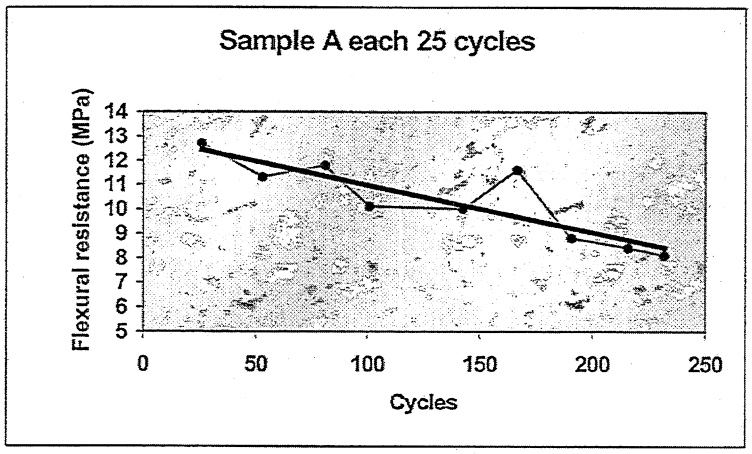

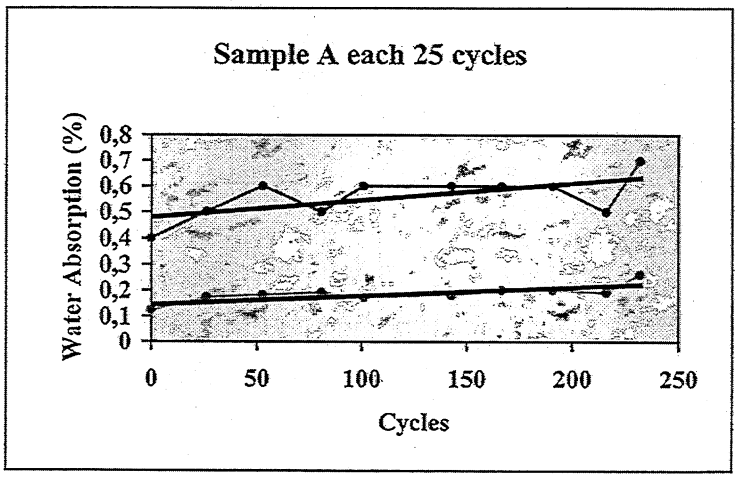

Figure 151. Interpretation of marble A test results.

It's a marble who appears to have a lower mechanical resistance specially when submitted to flexural tests. It can easily occur modifications in the structure, with the appearance of elastic proprieties, which leads to reductions on the resistance to flexural strength. After 232 cycles of freeze/thaw, a high increase in the porosity was noted, and consequently the water absorption became higher, specially when compared with the initial characterisation (porosity 0,4% and water absorption 0,12%).

3.12.2 Marble type D

Table 49. Initial characterisation of sample D (cut in favour)

Initial Characterisation	Sample D (Cut in favour)	
	Average	Standard deviation
Resist. to Compression (Mpa)	73,6	8,2
Water Absorption at PtN (%)	0,16	0,03
Open Porosity (%)	0,4	0,0
Volumetric Mass (Kg/m^3)	2703	10,8
Microscopic Observation	See report in annex	
Resistance to Flexural Strength under conc. Load (Mpa)	4,6	0,6

Table 50. Initial characterisation of sample D (cut against)

Initial Characterisation	Sample D (Cut against)	
	Average	Standard deviation
Resist. to Compression (Mpa)	92,5	7,6
Water Absorption at PtN (%)	0,15	0,01
Open Porosity (%)	0,5	0,1
Volumetric Mass (Kg/m^3)	2702	1
Resonance Frequency (HZ)	1993	-
Ultrasonic Propagation Speed (m/s)	$4,4x10^{-2}$	-
Thermal Shock	No remark	
Crystallisation Test	Loss mass (92,43 %)	
Dynamic Modulus of Elasticity (N/mm^2)	$3,9x10^9$	-
Microscopic Observation	See report in annex	
Resistance to Flexural Strength under conc. Load (Mpa)	4,2	0,3

Table 51 Characterisation of the sample D marble resistance, each 25 cycles of freeze/thaw

Resistance characterisation	Each 25 cycles of the freeze/thaw							
	28	62	86	116	142	170	198	245
Resist. to Compression (Mpa)	71.3	86.9	72.4	87.6	86.6	86.7	86.0	82.0
Water Absorption at PtN (%)	0.18	0.18	0.18	0.21	0.19	0.18	0.18	0.19
Open Porosity (%)	0.42	0.39	0.50	0.53	0.48	0.49	0.50	0.47
Volumetric Mass (Kg/m^3)	2629	2654	2681	2645	2685	2641	2669	2682
Resonance Frequency (HZ)	1808	2168	1872	2150	1493	1580	1538	2133
Ultrasonic Propagation Speed ($x10^{-2}$ m/s)	4.2	4.3	4.1	4.1	4.0	4.1	3.9	4.0
Thermal Shock	No visual remark							
Dynamic Modulus of Elasticity ($x10^9$ N/mm^2)	3.1	4.5	3.4	4.4	2.2	2.4	2.5	4.4
Microscopic Observation	See report in annex							
Resistance to Flexural Strength under conc. Load (Mpa)	4.3	3.5	2.9	2.7	3.8	3.3	3.5	3.3

The crystallisation tests were made in the beginning and at the end of 245 cycles of freeze/thaw. The results were the degradation of the specimens The loss of material, during the initial characterisation test was of 49,36 % and after the 245 cycles, was of 92,43%, this may be a consequence of the increase on the porosity and consequently of the water absorption.
It's possible to conclude that marble, when submitted to thermal variations, and in presence of salt mist, show alterations.

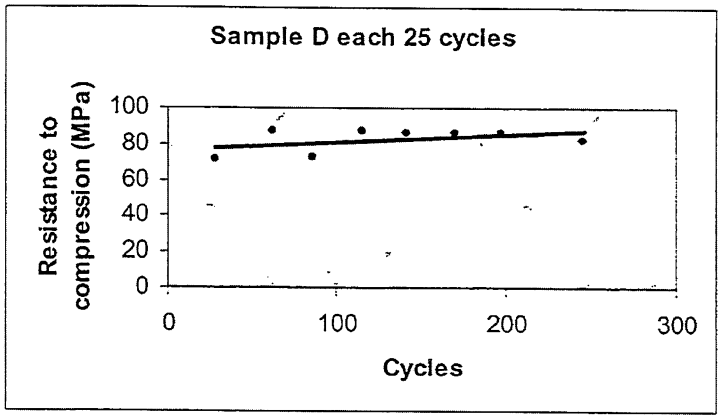

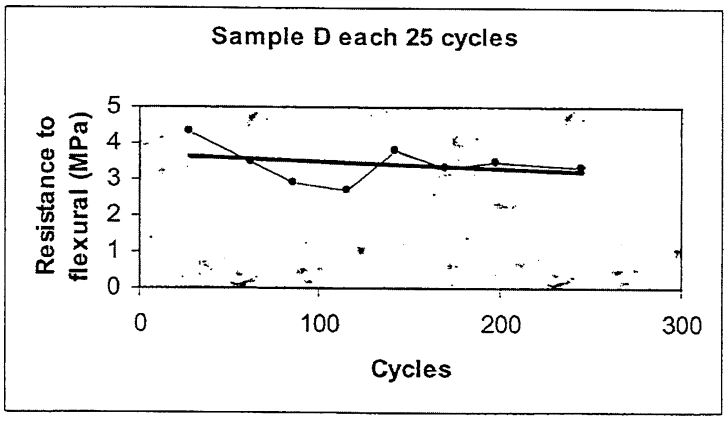

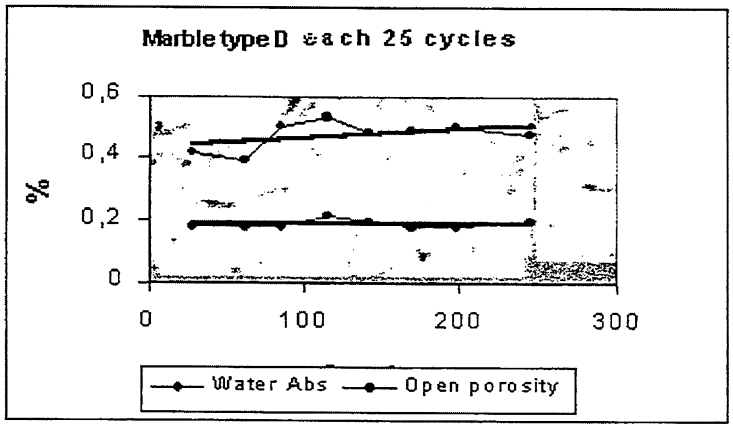

Figure 152. Interpretation of marble D test results.

It's a marble who appears to have a lower mechanical resistance specially when submitted to flexural tests. It can easily occur modifications in the structure, with the appearance of elastic proprieties, which leads to reductions on the resistance to flexural strength.

After 116 cycles of freeze/thaw, a high increase in the porosity was noted, and consequently the water absorption became higher, specially when compared with the initial characterisation (porosity 0,4% and water absorption 0,15%). After that become constant, maybe because the degradation of the grains were given fine material to fulfil the porous. That can be confirm with the microscopy report (see in annex).

3.12.3 Marble type E

Table 52 - Initial characterisation of Sample E (cut against)

Initial Characterisation	Sample E (Cut against)	
	Average	Standard deviation
Resist. to Compression (Mpa)	102,8	7,5
Water Absorption at PtN (%)	0,11	0,01
Open Porosity (%)	0,4	0,0
Volumetric Mass (Kg/m^3)	2705	2
Microscopic Observation	See report in annex	
Resistance to Flexural Strength under conc. Load (Mpa)	21,8	1,7

Table 53. Initial characterisation of sample E (cut in favour)

Initial Characterisation	Sample E (Cut in favour)	
	Average	Standard deviation
Resist. to Compression (Mpa)	103,5	10,7
Water Absorption at PtN (%)	0,11	0,01
Open Porosity (%)	0,3	0,03
Volumetric Mass (Kg/m^3)	2714	3
Microscopic Observation	See report in annex	
Resistance to Flexural Strength under conc. Load (Mpa)	18,1	2,4

Table 54. Characterisation of the sample E marble resistance, each 25 cycles of freeze/thaw

Resistance characterisation	Each 25 cycles of the freeze/thaw							
	28	**46**	**74**	**102**	**150**	**174**	**202**	**216**
Resist. to Compression (Mpa)	104.7	112.5	116.9	106.9	112.5	118.6	120.2	120.3
Water Absorption at PtN (%)	0.13	0.16	0.16	0.16	0.17	0.17	0.16	0.17
Open Porosity (%)	0.30	0.40	0.29	0.29	0.37	0.43	0.44	0.40
Volumetric Mass (Kg/m^3)	2656	2601	2656	2648	2650	2682	2676	2675
Resonance Frequency (HZ)	2127	1887	1717	1848	1980	2225	2283	2647
Ultrasonic Propagation Speed (x10^{-2} m/s)	6.1	6.1	6.0	6.0	6.0	6.0	6.1	5.9
Thermal Shock	No visual remark							
Dynamic Modulus of Elasticity (x10^9 N/mm^2)	4.3	3.3	2.8	3.3	3.7	4.8	5.0	6.7
Microscopic Observation	See report in annex							
Resistance to Flexural Strength under conc. Load (Mpa)	14.8	16.4	13.2	13.4	11.7	13.9	13.0	12.3

The Crystallisation tests were made in the beginning and after 216 cycles of freeze/thaw. The results obtained were the same, just tarnished appearance. But no colour or structural changes on the samples were noticed (see photo 1 and 2)

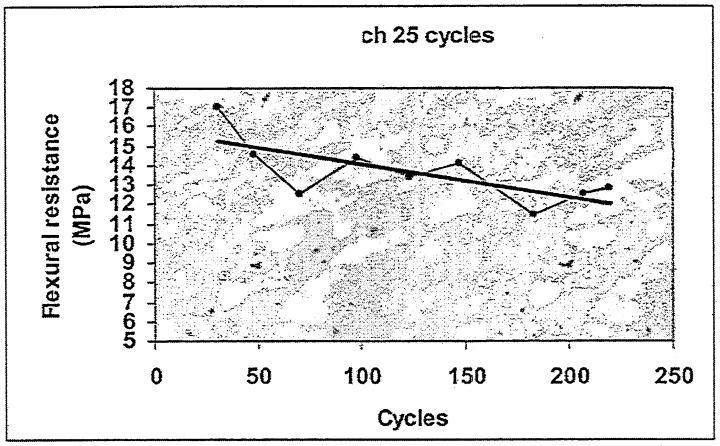

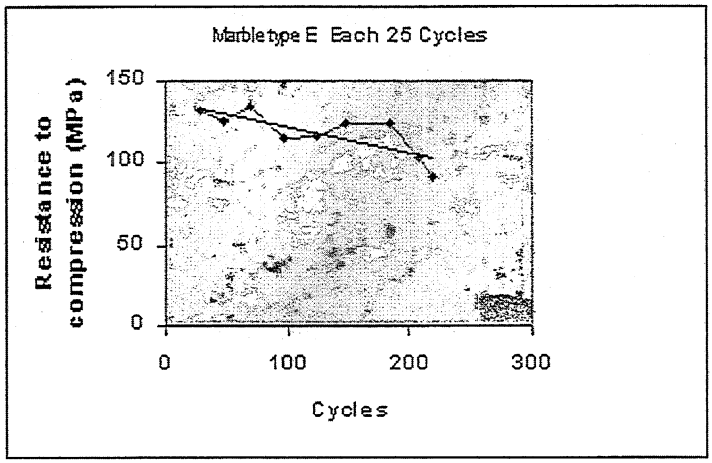

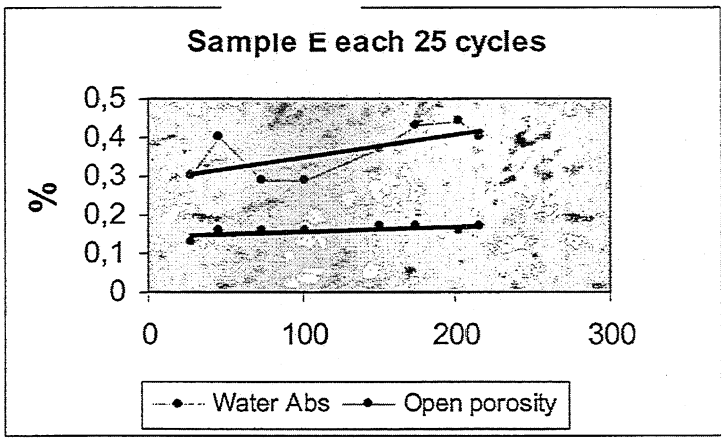

Figure 153. Interpretation of marble E test results.

It's a marble with highest mechanical resistance, to flexural and compression, and to freeze/thaw environments.

After 240 cycles of freeze/thaw, no visual alteration appeared, nor loss mass. The physical tests have given basically constant results, so it is possible to conclude that no alteration in the structure occurred, this is supported by the results obtained by microscopy (see report in annex).

3.12.4 Marble type K

Table 55. Initial characterisation of sample K (cut against)

Initial Characterisation	Sample K (cut against)	
	Average	Standard deviation
Resist. to Compression (Mpa)	79,6	7
Water Absorption at PtN (%)	0,05	0,01
Open Porosity (%)	0,15	0,00
Volumetric Mass (Kg/m^3)	2715	2
Resonance Frequency (HZ)	1748	-
Ultrasonic Propagation Speed (m/s)	6,5x10^{-2}	-
Thermal Shock	No visual remark	-
Crystallisation Test	No alteration	
Dynamic Modulus of Elasticity (x10^9 N/mm^2)	3,0x10^9	-
Microscopic Observation	See report in annex	
Resistance to Flexural Strength under conc. Load (Mpa)	23,1	2,1

Table 56. Initial characterisation of sample K (cut in favour)

Initial Characterisation	Sample K (cut in favour)	
	Average	Standard deviation
Resist. to Compression (Mpa)	111,5	3,4
Water Absorption at PtN (%)	0,05	0,01
Open Porosity (%)	0,15	0,00
Volumetric Mass (Kg/m^3)	2715	2
Microscopic Observation	See report in annex	
Resistance to Flexural Strength under conc. Load (Mpa)	21,4	0,6

Table 57. Characterisation of the sample K marble resistance, each 25 cycles of freeze/thaw

Resistance characterisation	Each 25 cycles of the freeze/thaw								
	30	48	70	98	124	148	184	208	220
Resist. to Compression (Mpa)	132,2	125,1	134,6	114,3	115,6	123,0	123,9	102,6	92,0
Water Absorption at PtN (%)	0,10	0,11	0,13	0,12	0,13	0,13	0,13	0,15	0,13
Open Porosity (%)	0,25	0,30	0,35	0,26	0,33	0,31	0,28	0,25	0,31
Volumetric Mass (Kg/m^3)	2737	2716	2717	2709	2693	2711	2689	2689	2684
Resonance Frequency (HZ)	1920	2000	1974	1607	1712	1917	1942	1582	1712
Ultrasonic Propagation Speed (x10^{-2} m/s)	6,2	6,3	6,2	6,2	6,2	6,2	6,2	6,2	6,1
Thermal Shock	No visual remark								
Dynamic Modulus of Elasticity (x10^9 N/mm^2)	3,6	3,9	3,8	2,5	2,8	3,6	3,7	2,4	2,8
Microscopic Observation	See report in annex								
Resistance to Flexural Strength under conc. Load (Mpa)	17,0	14,6	12,5	14,4	13,4	14,1	11,5	12,5	12.8

The crystallisation tests were made in the beginning and at the end of 220 cycles of freeze/thaw. The results were generally, tarnished appearance and no loss mass.

The loss of material, during the initial characterisation test was of 0,25% and after the 220 cycles, was of 0%, this may be a consequence of no significant increase on the porosity and consequently of the water absorption.

It's possible to conclude that marble, when submitted to thermal variations, and in presence of salt mist, wasn't shown alterations.

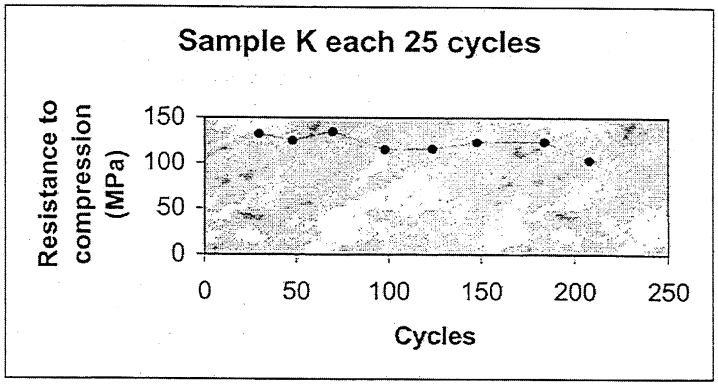

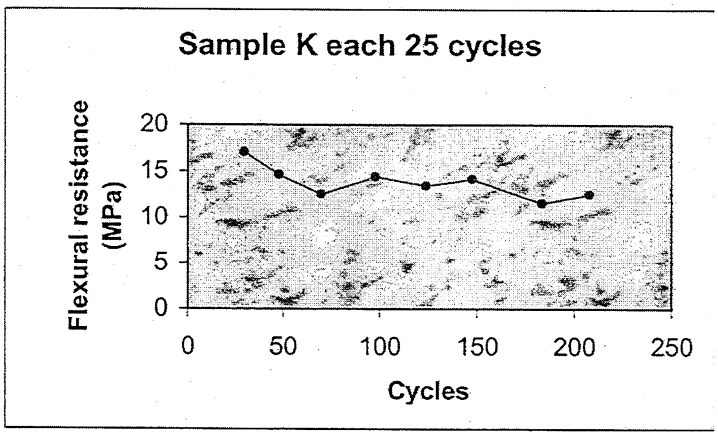

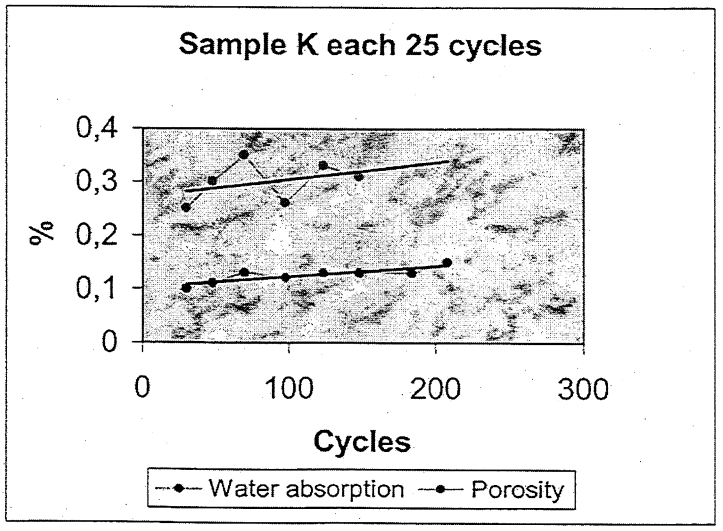

Figure 154. Interpretation of marble K test results.

According to the graphics, it's possible to conclude that the Italian marble sample K, is the most resistant sample of all the tested proposed samples for this project.

Thus, it can be said that in terms of physical and mechanical characterisation this marble presents a good behaviour when submitted to the temperature of freeze/thaw cycles, used in this project.

The interpretation of the compression and flexural resistance results, show that this marble doesn't present relevant alterations showing a slight decrease of resistance, although no conclusive.

Relatively to the absorption of water and open porosity the results also showed a certain tendency for the increase of the porosity, although not significant.

3.12.5 Case studies

3.12.5.1 The use of marble in facades in the North of Portugal.

Buildings
Being the north of Portugal, a region rich in granite, it is normal that the buildings are mainly built in this material. However during the 60's it was very common to have concrete buildings with the facade of the lower floor in marble.

Today these buildings are not in very good conditions, many slabs have fallen down and they need urgent renovation. In the modern buildings the architects are using more and more Portuguese limestone.

Gravestones
During the times stone has always been used for the building of graves. In Portugal marble, granite and limestone are very much applied in the tombs and mausoleums. In this field we can find some applications of Carrara Marble. The use of this material was always a sign of richness. It was used not only in graves on the ground and mausoleums but also in graves on the walls.

3.12.5.2 Stone companies

Company A
This is an importer of Carrara marble but never applied in outside facades.

The types that are usually imported are Gioia, Didora, CD, Semap and Statuario. In interior walls, the only problem are yellow stains that can appear. To avoid this problem they use a special kind of glue.

This company once applied a Green greek marble with white veins that also started to bow. This material had to be substituted by other material.
For exterior they always use Portuguese marble.

Company B
This company uses Carrara Marble but never applies it in outside facades
In the inside works they never had problems. Is not a direct importer, buys the marble from other Portuguese importers.

Company C
Never applied **Carrara Marble** in outside facades, but 20 years ago this company was responsible for the building of a **Carrara Marble** grave in a graveyard near Porto. Our days this grave is completely bowed.

Company D
Being located in the south of Portugal, this company is used to build facades in marble and limestones. Never had any problems with the facades built until now. Uses **Carrara Marble** in interiors

Compagny E
Is a company specialist in gravestones (graves and mausoleums).
These graves are built either in granite or marble. Never used Carrara Marble. The mausoleums are general built by one single wall, with 8 cm of thickness and 280 cm length and 60 cm.

3.12.5.3 Architects

The architects contacted never used **Carrara Marble** for outside facades. The reason it is the high price and not the problems related with the application of this material. In most of the cases they never had heard about the problems related with bowing, and some knew the Finland Hall case.
In this moment, most of the architects are using for outside facades of important buildings Portuguese limestones.

In the 19th century, in the graveyards Portuguese marble was not applied for the graves. The most common marble was **Carrara Marble.**
The restoring that she usually does to grave stones is gluing small pieces and cleaning but in Braga graveyard there are some graves on the walls that show bowing as we can see in the pictures (Figure 155).

3.12.5.4 Examples of objects

ATRIUM SALDANHA

- **Location** - Lisbon
- **Outside Facade** – Estremoz Marble
- Ventilated facade with mechanic fixation
- Bushammered
- 3 cm
- 80 cm/ 120 cm
- 12 000 m2
- Protected with Grafitix
- The outside facade was meant to be built in Giallo Dorato.
- **Inside** – Greek marble

The only problem with façade is the dirty, and never appear bowing problems. This building company never applied Carrara in outside facades

OPORTO BUILDING

- **Location** – Porto
- **Outside Facade** –Estremoz Marble
- Bush hammered
- Halfen fixings
- Stone thickness 3 cm
- Granite Yellow Boticas Polished

No problems with this façade (Figure 156).

3.12.5.5 Centro tecnológico da piedra

To complete our research we contacted other Technological Centres in other countries. We contacted a Technological Centre in Spain (Macael) region . In this spanish area there are many buildings with outside facades in Macael marble, and even the Technological Centre building is in Macael marble. Never bowing problems in this buildings, only problems with some braked? stones in facades with mechanical fixation. In this centre there is an investigation going on to try to find the reason of the breaking stones on floors built with rectangular tiles (2m x 1 m). These tiles appear broken in the middle 2m x 1m. When they are square that doesn't happen. Until now they think that this phenomena is due the calcite orientation .

Figure 155. A gravestone in Braga (North Portugal) showing clear warping.

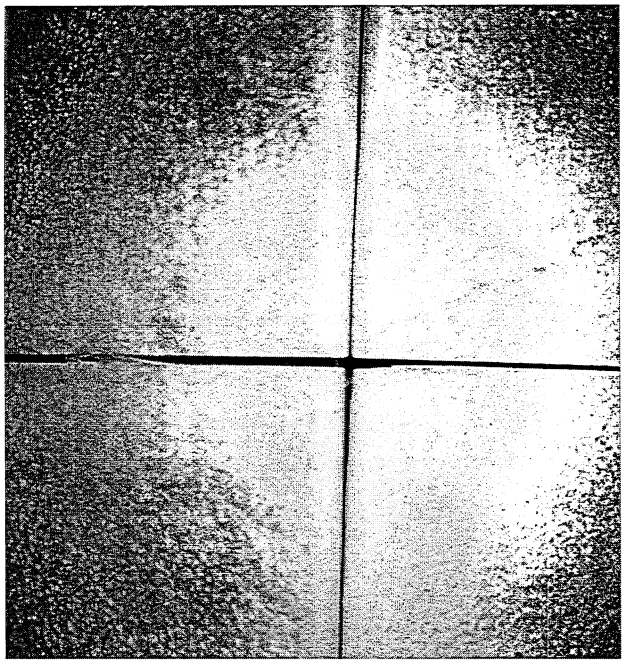

4 PRACTICAL APPLICATIONS

4.1 Instructions for constructing a durable marble façade

4.1.1 General

This research has indicated quite clearly that deterioration of marble panels is due to the granular decohesion of calcite grains. According to Royer (see annex 7) thermal variations are causing granular decohesion even when uniformly distributed throughout the specimen. Very low temperatures (-20°..-30°C) seem to be more damaging, even without frost effect. But also temperatures from +30°C to +50°C are causing permanent changes in the microstructure of some marbles. This kind of surface temperatures can be quite easily measured also in Nordic climates as Koskinen has showed. Weathering agents i.e. humidity and acid rain, are accelerating, rather than starting the degradation process.

Deterioration can be divided in two main categories; physical and esthetical. The latter can be very easily seen as bowing and changes in colour. This phenomena changes the appearance of the façade to somewhat different from architect's original idea. The former is more difficult to see and also more dangerous. The material is, as discussed in previous chapters, gradually losing it's strength, which may cause a considerable safety risk if not recognised early enough.

4.1.2 Selection of marble

Marble is nowadays used in the façades for esthetical reasons. Therefore, the selection of material should start from selecting a few (5..10) possible qualities for further studies according to the desired appearance; colour, veining etc.

These selected marbles shall then be examined more carefully under microscope. Recent studies have shown clearly that many material properties are influenced by the microstructure. Therefor the texture of each marble should be defined comprehensively and only those of xenoblastic or intermediate microstructures are qualified for further studies. Texture of each marble is defined by indicators A/P^2 and A/S^2 (see Royer, annex 3).

In this stage also the flexural strength for virgin specimen is tested and those below 12 MPa are rejected. Bending should be done according to EN12372 with the modification of drying temperature, which should not exceed +40 degrees centigrade. This modification is essential since higher temperatures may cause serious damage for the studied material and thus distort the results.

Those qualities passed these preliminary tests shall proceed to further examinations which include testing certain physical properties for virgin, un-

conditioned samples and thermally treated samples. Thermal treatment is done for dry samples as thermal cycles from -25°C to +50°C. Control of the weathering chamber should be done by measuring the actual temperature inside a few samples being located in the chamber so that they give representative picture of the temperature of all of the samples. This is a very easy and reliable way to ensure that samples are actually induced to the desired thermal stress.

Dry samples can be used because driving force for deterioration seems to be thermal changes and humidity is "only" accelerating the process. Using dry samples gives us more certainty that all different qualities are in exactly the same conditions, which is vitally important when comparing materials. Marble classification form can be summarised as below (modified from Royer, annex 3):

Marble type:		
Texture: (xenoblastic or homoblastic) A/P^2=...., A/S^2=.....		
Test	Unconditioned samples	After 20 cycles from –25°C / +50°C
Bending strength	*12 MPa*	*10 MPa*
Water absorption	*0,12*	*0,2*

Values filled in the form represent the requirements for material to be used in the case of Finlandia Hall. For other cases these threshold values must be reconsidered according to the conditions the façade must tolerate.

4.2 Technical specifications for a stone cladding

4.2.1 Functional considerations

Apart from the right choice of stone material it is essential for the desired function of a natural stone cladding to use the correct solutions for structural implementation of the object. A modern stone facade is many ways quite different from the historical buildings. Throughout the history of architecture stone has been used as a massive, load-bearing structure. In the modern facade construction, however, stone has typically the role of giving the building its final appearance and a shelter against weathering agents. Stone is in the modern applications cut in thin panels and fixed in the building with mechanical anchors.

Change from massive structures to thin veneers has brought along many new technical and functional requirements. With respect to the stone itself it is evident that used as a thin veneer the importance of weather resistance properties is emphasized because of the slenderness of the stone panels. This is in fact one of the reasons giving rise to the severe nature of the

problems with marble facades. On the other hand technical solutions for fixing the stone to the building must be designed taking into account both the requirements coming from the modern building technology as well as the aspects related to the stone cladding itself. In modern construction stone cladding is normally built with thin stone panels of 30-50 mm thickness.

Important design consideration is the physical functionality of the stone veneer. This is especially important in northern climate areas where the temperature gradient between inside and outside of the building is greater than in the southern areas. Main aspects to be taken into account in the physical design of the facade cladding are the thermal and humidity conditions and the expected deformations in materials and structures.

In order to secure the desired quality of the stone material and the installation work a specific quality control system for the building project is needed. Quality control measures are to be taken
- at the quarry
- at the processing plant
- at building site

Controlling laboratory testing of the material properties shall be carried out according to the quality assurance plan of the project.

4.2.2 Structural design principals

The approach was divided into design and dimensioning aspects in the following four areas:
- connection between panel and fixing
- fixing anchor / secondary frame structure
- connection between fixing anchor and a secondary frame structure
- connections into the concrete/steel frame of the building

As a conclusion following structural principals are recommended to be applied for a natural stone cladding:
- panels are fixed independently to the frame of the building using load bearing and restraint anchors of stainless steel or aluminium (figure T1)
- anchors are placed in the joints between stone panels and fixed to the edges of the stone panel with stainless steel pins (figure T2)
- load bearing anchors, placed in the lower part of each panel, carry the weight of the stone panels and part of the wind forces;
- restraint anchors, placed in the upper part of each panel, take only wind forces

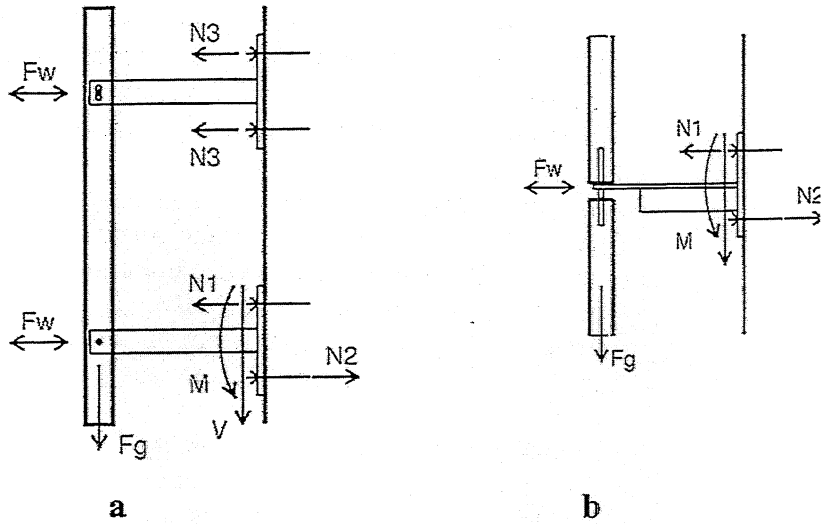

Figure T1. Static principals of a natural stone cladding. Vertical fixing (a), horizontal fixing (b).

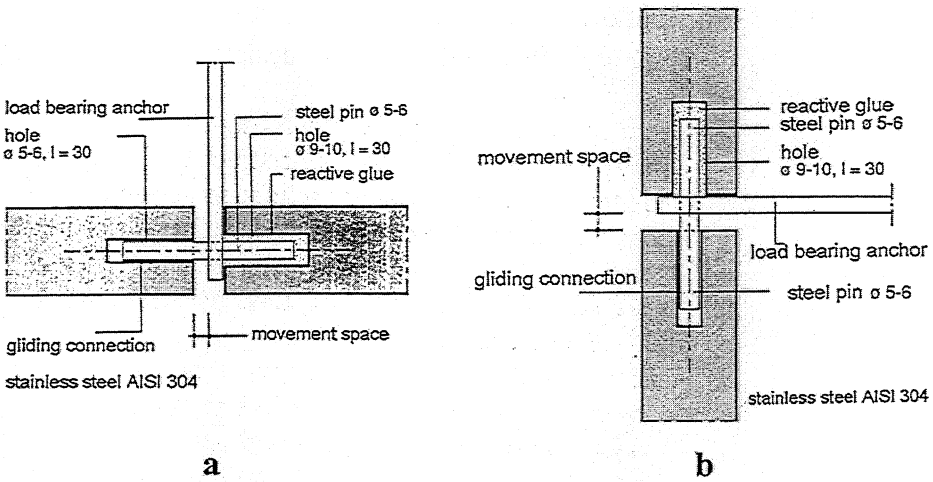

Figure T2. Connection between stone panel and the fixing anchor. Vertical fixing (a), horizontal fixing (b).

4.2.3 Building physical design principals

The approach was divided into design and dimensioning aspects in the following four areas:
- water permeability/tightness
- jointing method
- ventilation of the facade structure

- deformations due to temperature, humidity and movements
- protective impregnating treatments

As a conclusion following physical design principals shall be applied for a natural stone cladding:

- stone cladding shall be jointed by elastic mass to prevent rain penetration and to allow small deformations of structural elements without a risk for internal strains
- humidity in the wall structure shall be led out using a ventilation gap placed behind the stone cladding; proper function of the ventilation gap is arranged by using sufficient openings for both air going in and coming out
- connections between panels are designed elastic to allow deformations due to thermal expansion
- internal stresses, due to fixings and deformations between structural elements, are eliminated by proper design of the fixings
- protective agents shall be considered if there is a need to protect the cladding against environmental impurities

4.3 Monitoring the physical state of an existing façade

4.3.1 General

Monitoring of the physical state of façades should be included in every real estate's maintenance program. Considering marble façades, designing of the monitoring program starts from recognising the most critical part of the façade where the climatical stresses are the most severe. Typically the highest temperatures can be measured in the façades facing south, south-west and west. In Nordic climates these are also the compass directions where temperature changes are the strongest. The focus of monitoring should be on these parts of a façade, but of course also other parts of façade must be monitored, possibly less intensively.

The first and easiest inspection should be visual inspections. Changes in colour and appearance should be followed carefully.

4.3.2 Bowing measurements

A practical way of monitoring the process of granular decohesion is to measure the bowing of panels. As Royer explains in his report (annex 3), bowing is caused by differences in the level of granular decohesion through the thickness of a marble panel. By measuring the bowing we can thus notice the starting decohesion and later follow the progress of deterioration.

Measuring can be done with different types of "rulers", but essential is that bowing in both directions, concave and convex, can be measured with the same apparatus. According to our experiences from measurements, an accuracy of 0,1 mm is enough for following the development of bowing and also

practically reasonable. Bowing measurements are recommended to be done in the first stage in every six months; time period can later be adjusted if needed.

4.3.3 SEM -analyses

In addition to bowing measurements also more accurate methods are needed. These methods include SEM –analyses and testing the flexural strength of the panels on the façade continuously during the lifetime of the façade. Samples for the former should be taken from the previously defined most critical part of the façade. These samples can be very small and so the traces of sampling are easily hidden from spoiling the view. The amount of the samples must be considered regarding the façade in question, but for Finlandia Hall –case two samples every second year should be enough. The idea of these samples is to actually peek inside the panels and to verify the condition of them. Also the openings between the calcite grains can be measured and their importance can be interpreted.

4.3.4 Flexural strength testing

Sampling for the flexural testing is more difficult, but this testing is considered to be essential. The only possible way of sampling- due to the amount needed for statistically reliable results- is to release complete panels from the façade. This requires a bit of arrangements since estate owner should stock spare panels for the ones decided to be tested and also since the initial strength of the panels tested must be known in order to define the decrease of the strength. Practical solutions for the latter are numerous, but one recommendation is to select one block for the monitoring, test the strength of it and then install the rest of the panels made of it. These panels should be marked clearly for later identification. Samples are then taken (and tested) from these panels once every five years.

4.3.5 Criteria for façade renovation

From the above described method can be derived very easily otherwise very difficult decision to be made: when to renovate the façade. One must set, when designing the façade, certain threshold values allowed for bowing and loss of strength. When monitoring is giving values close to these values, planning of the renovation should be started and when those values are exceeded, renovation works should be started.

4.4 Recommended actions for façade maintenance

Because of the nature of the deterioration process, even the most careful maintenance cannot prevent the panels from bowing and loosing their strength. Therefore, the effort should be put on upholding the outlook of the façade as long as possible. This is done by cleaning the panels with suitable method according to the amount of dirt accumulating on them. When cleaning the panels also the state of the joint sealings can be easily checked and fixed if needed. This is essential to prevent the frost damage the water leaks into the façade could otherwise produce.

The physical state of fixings should be checked every once and a while. Even stainless steel can be subjected to corrosion in some conditions, which may lead to serious accidents if not recognised early enough.

APPENDIXES

1. VTT Building and Transport, Environmental conditions
2. VTT Building and Transport, Test wall
3. VTT Building and Transport, One-sided weather resistance test
4. VTT Building and Transport, Protective agent
5. Helsinki University of Technology, Laboratory of Engineering Geology and Geophysics
6. Helsinki University of Technology, Laboratory of Rock Engineering
7. University of Parma
8. Cevalor
9. Bowing measurements
10. Financial report

APPENDIX 1

VTT BUILDING AND TRANSPORT

RESEARCH REPORT

Developing long term durability of marble facades

Subproject "Environmental conditions"

Espoo, April 20, 2001

Juho Saarimaa
Research Director

Pertti Koskinen
Senior Research Scientist

Encl.: Final report (96 pages)

VTT

CONTENTS

	page
CONTENTS	2
1 BACKGROUND	3
2 OBJECTIVE	4
3 EXPERIMENTAL	4
3.1 Measuring and recording arrangements	4
3.2 Other information	5
4 RESULTS	5
4.1 General remarks	5
4.2 Temperature gradient over the marble slab	5
4.3 Daily variation of temperature	8
4.3.1 Measuring point A	9
4.3.2 Measuring point B	18
4.3.3 Measuring point C	23
4.3.4 Measuring point D	31
4.3.5 Measuring point E	42
4.4 Gradient of temperature variation in marble	52
4.4.1 Measuring point A	52
4.4.2 Measuring point B	55
4.4.3 Measuring point C	57
4.4.4 Measuring point D	60
4.4.5 Measuring point E	64
4.5 Freeze/thaw -cycling of marble	67
4.6 Humidity gradient over the marble slab	68
4.6.1 Measuring point D	69
4.6.2 Measuring point E	72
4.7 Acidity of rain water	76
4.8 Weather conditions	77
4.8.1 Temperature and humidity	77
4.8.2 Rainfall and sunshine	84
5 DISCUSSION	91
5.1 Temperature gradient	91
5.2 Daily variation of temperature	92
5.3 Gradient of temperature variation	93
5.4 Freeze/thaw -cycling	94
5.5 Relative humidity	94
5.6 Acidity of rain water	95
6 CONCLUSIONS	95

1 BACKGROUND

The need for conserving, restoring and protecting stone buildings and monuments throughout the world is growing continuously. This is particularly actual in the historic cities of Europe where marble and other calcareous stones have been commonly used. The decay of old stone structures is becoming a remarkable technical and economic problem. Deteriorated stone facades may in some cases even represent a considerable safety risk. The durability problems have led to a strong decrease in the use of marble for outdoor applications.

One of the most important reasons for the deterioration and fouling of natural stones is the rising amount of acid compounds and other impurities coming mainly from industrial and traffic sources. Today stone structures are exposed to harsher environmental conditions than ever before. Thin stone veneers that are commonly used nowadays are even more sensitive for weathering than traditional massive stone structures.

Carrara marble was used as the original facade material for Finlandia Hall. In the early 1980's the marble plates began to warp. Warping was especially noticeable in larger plates because of lapping. It also became apparent that the plates' inner strength was rapidly weakening. Extensive studies were undertaken to determine the cause of the deterioration. The conclusion was that the phenomenon was mainly due to climatic factors and especially to acid rain, which gradually converts marble to gypsum.

The badly damaged marble facade of Finlandia Hall was renewed during the autumn of 1998 and the spring of 1999. In connection with the refurbishment, the City of Helsinki launched the research project "Developing long-term durability of marble facades" known as "MARA-project". The main aims of the project were to extend the service life of the new facade, to formulate an appropriate maintenance strategy and to create reliable technical criteria and methods to assess the suitability of marble for facade applications.

As already stated above the degradation of marble is a universal problem, which has been especially highlighted by recent cases of damage to old buildings and historic monuments. However, in Europe there are also a number of other architecturally significant new buildings that have fallen victim to the same kind of deterioration as Finlandia Hall. Because research results can therefore be widely exploited, the MARA-project received financial support from the EU's Raphael cultural heritage programme.

VTT Building and Transport was responsible for four subprojects of the main study. The primary goals of these subprojects were to determine the deterioration mechanism of marble, to set requirements for a durable marble facade structure and to develop a reliable method for testing marble quality. The subprojects also included studies of the environmental conditions at Finlandia Hall and of the stresses these cause to marble, of the durability of different types of marble, of the performance of alternative structural solutions and of the possibilities of using protective treatments. The studies were made in co-operation with Helsinki University of Technology, Parma University in Italy and Cevalor in Portugal.

2 OBJECTIVE

The aim of the subproject was to record the real environmental conditions (temperature, humidity) and their annual variations prevailing at Finlandia Hall and in this way to determine the stressing factors that affect marble and the structures of the facades.

In order to achieve the goals set for the subproject it was divided into four tasks:

- designing and installing of the necessary measuring and recording devices
- regular recording of the environmental factors and processing of the data
- acquiring of other necessary information (pH, general weather conditions) and processing of the data
- conclusions and reporting of the results

3 EXPERIMENTAL

3.1 Measuring and recording arrangements

Prevailing temperatures were recorded from five different marble slabs, all of which were placed on the roof walls of Finlandia Hall. Four of the slabs were chosen in such a way that each one of them was directed towards a different cardinal point. The fifth slab was chosen to represent extreme values, and thus it was taken from the top of the tower part of the building (point A). The measuring points were as follows:

measuring point	wall	cardinal point
A	2	south
B	38	west
C	13	north
D	24	south
E	23	east

Temperatures were measured with copper-constantan thermocouples. In each slab specified above there were four thermocouples, which were measuring temperatures in outdoor air, in ventilation slot and on outer and inner surfaces of the marble slab. In the measuring point A there was also a fifth thermocouple, which was recording the outer surface temperature of a black granite slab beside the marble slab with the four other thermocouples. Temperatures were recorded once an hour in each point, and the values were saved into a data logger. Each of the measuring points A, B and C had their own small data logger, type Squirrel SQ 8. Measuring points D and E had a common data logger, type Squirrel 1000.

The recording of temperatures was started in May 1999, and it was continued until the end of February 2001. The data loggers were emptied at regular intervals, and the data collected was downloaded to a transportable computer. Due to power failures or logger malfunction some of the data was, however, lost during the measurement period.

Prevailing relative humidities were recorded from two marble slabs, which were the slabs of the temperature measuring points D and E. Humidities were measured with Vaisala sensors, type HMP 44. In both slabs there were three sensors, which were measuring relative humidities in outdoor air, in ventilation slot and in the middle of the marble slab. In order to measure humidity in the middle of the slabs, a hole (∅ 10 mm, length 150 mm) was drilled through the lower edge of the slabs before installing them on the roof wall. The sensor was put into the drilled hole, and the hole was sealed.

The recording was done as that of temperatures described above. The same data logger as for temperatures was used to save the humidity data.

3.2 Other information

The data concerning general weather conditions was acquired from the Finnish Meteorological Institute. Research results from the measurements of acidity of rain water were delivered by the Finnish Environment Institute.

4 RESULTS

4.1 General remarks

The complete file of measurement data from Finlandia Hall is appended to this report as a CD-disc. The features of the results which were considered most important especially in regard of the stresses caused by the environmental factors to the marble facade are described more closely in chapters to follow. In most cases the daily maximum and minimum temperatures are used when examining the results.

4.2 Temperature gradient over the marble slab

Temperature gradient prevailing in the slabs was revealed by examining temperatures on outer and inner surfaces of marble. The results are presented in Figs. 1-5, each of which show four examples of the daily behaviour of surface temperatures of the measurement slabs. The days chosen for the examples represent various seasons.

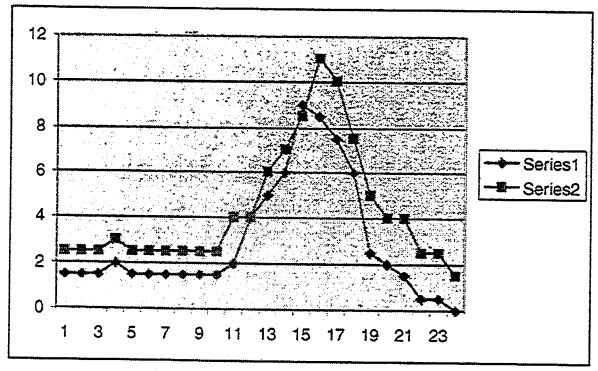

14.3.2000

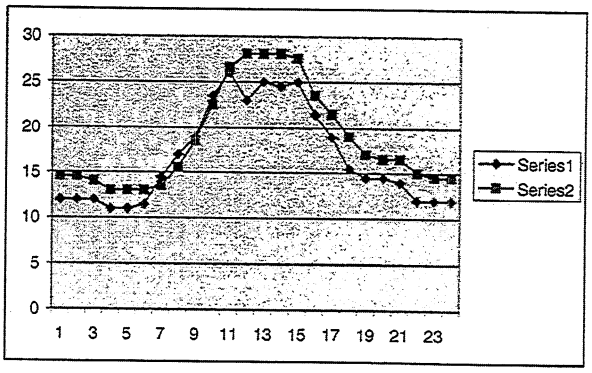

14.6.2000

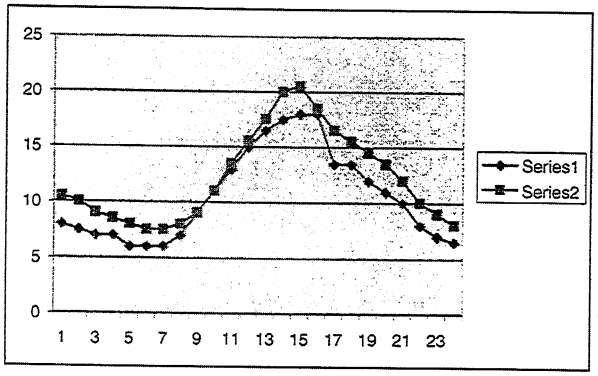

14.9.2000

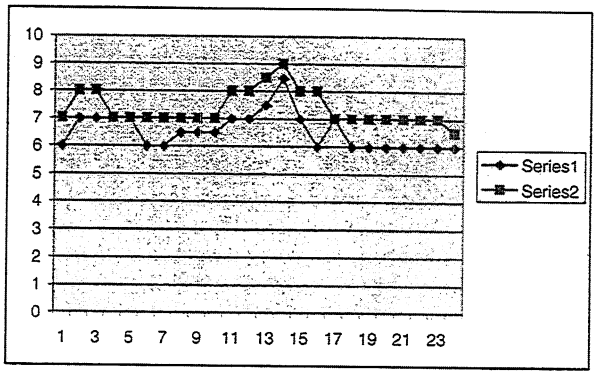

14.12.2000

Figure 1. Measuring point A. Temperature of outer (Ser 1) and inner (Ser 2) marble surface (°C).

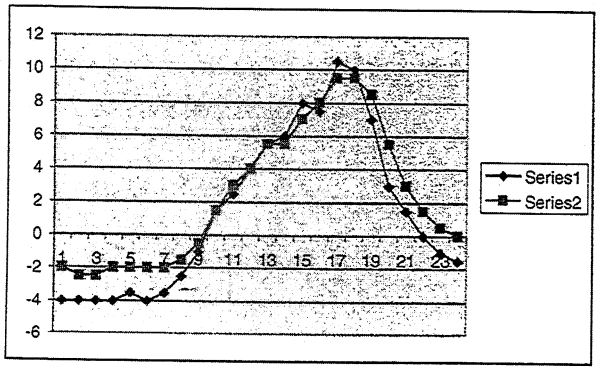

30.3.2000

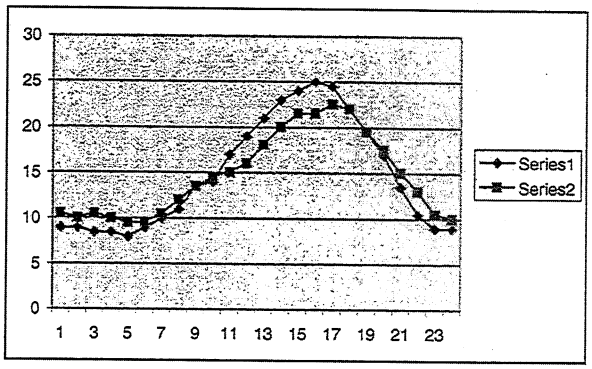

14.6.2000

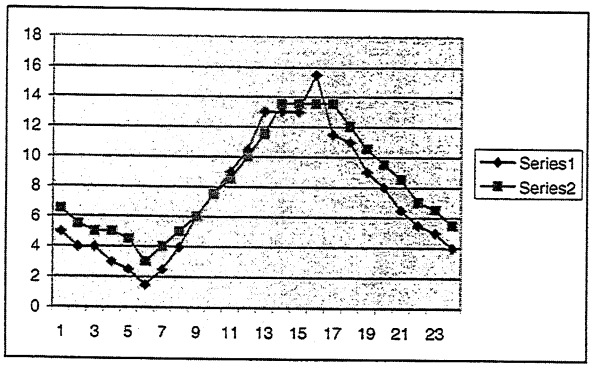

14.9.2000

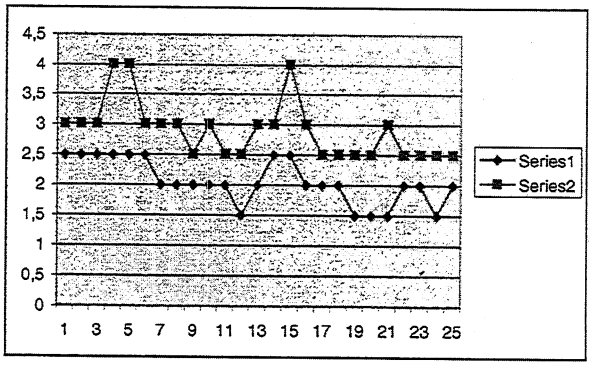

14.12.2000

Figure 2. Measuring point B. Temperature of outer (Ser 1) and inner (Ser 2) marble surface (°C).

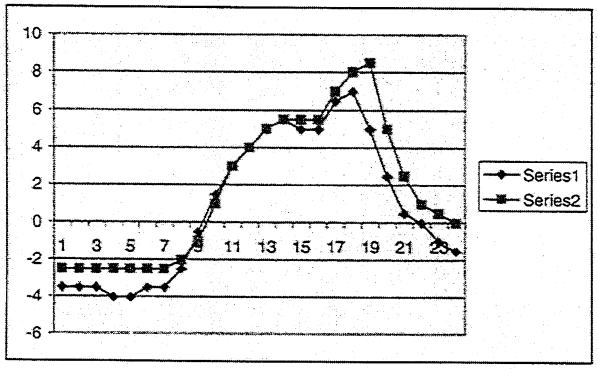

30.3.2000

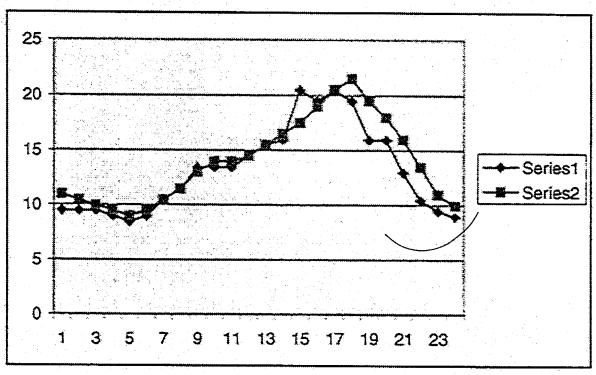

14.6.2000

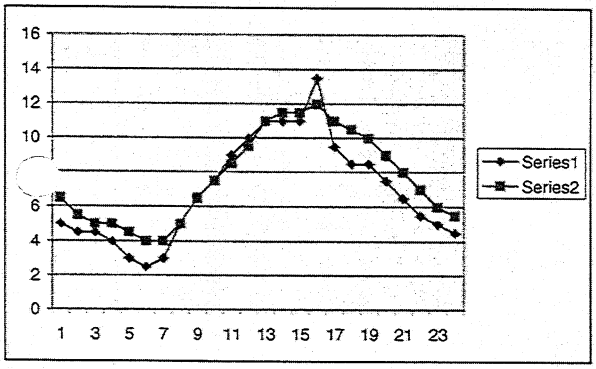

14.9.2000

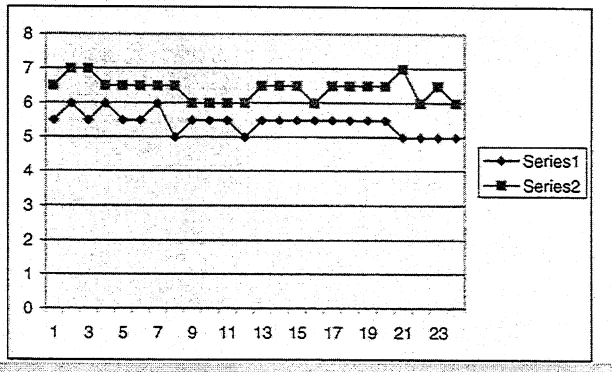

14.12.2000

Figure 3. Measuring point C. Temperature of outer (Ser 1) and inner (Ser 2) marble surface (°C).

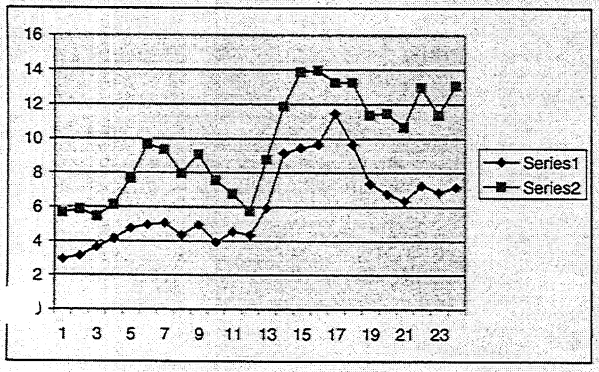

14.3.2000

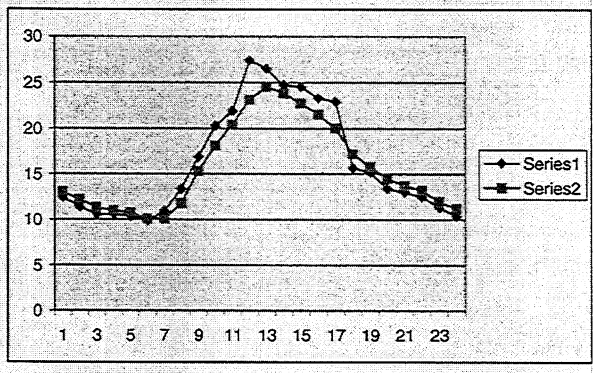

14.6.2000

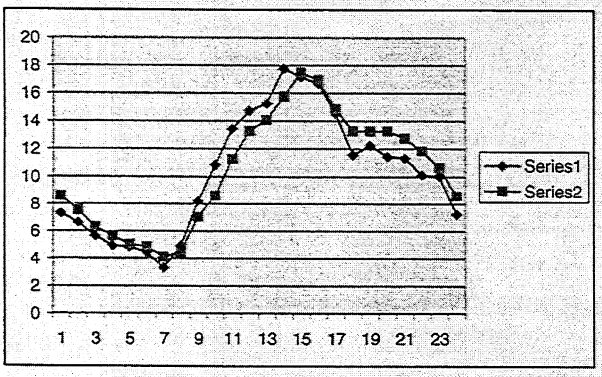

14.9.2000

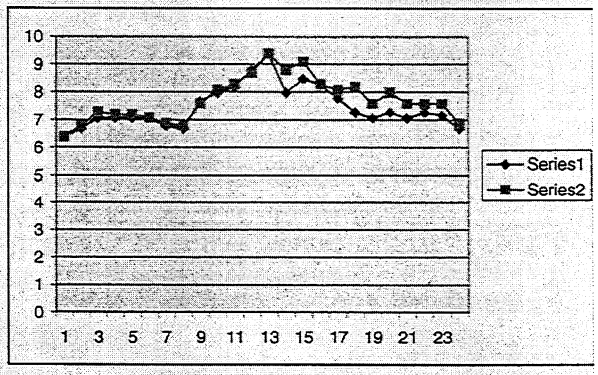

14.12.2000

Figure 4. Measuring point D. Temperature of outer (Ser 1) and inner (Ser 2) marble surface (°C).

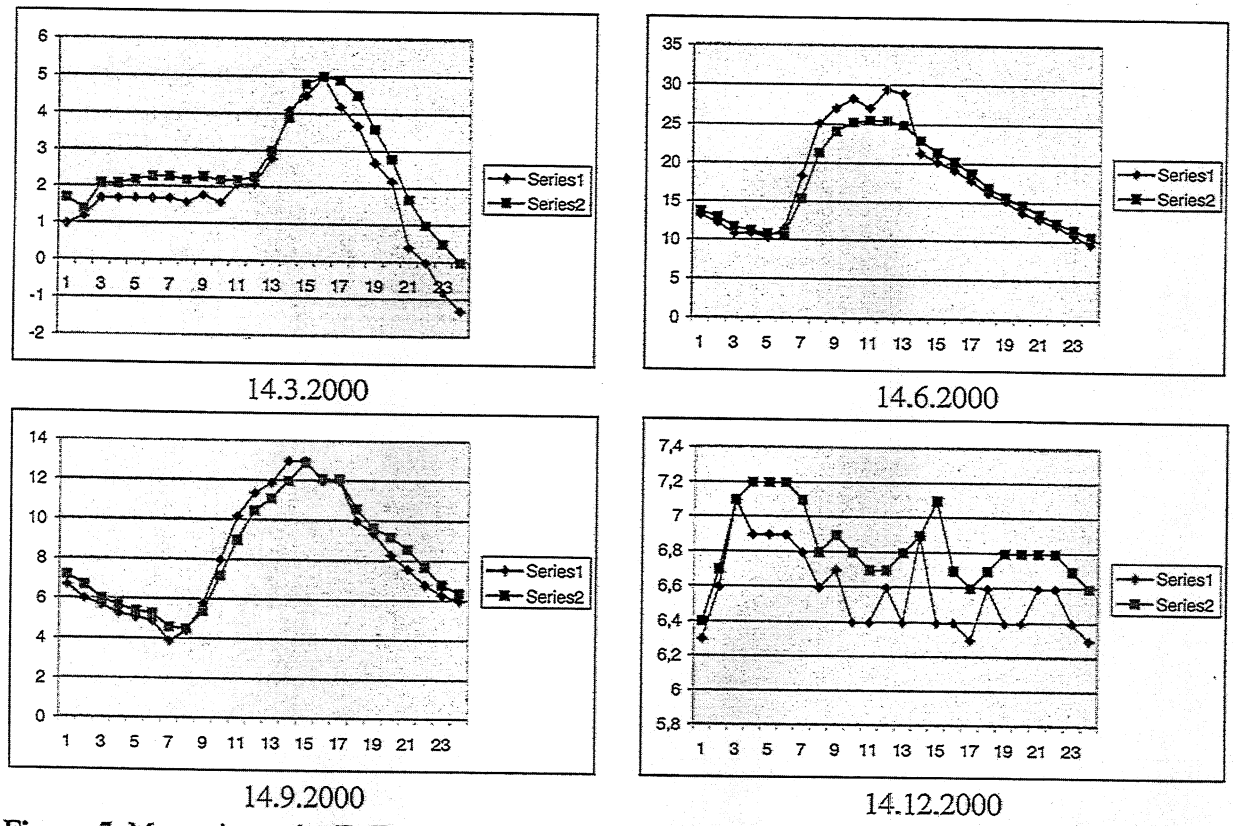

Figure 5. Measuring point E. Temperature of outer (Ser 1) and inner (Ser 2) marble surface (°C).

4.3 Daily variation of temperature

Daily variation of temperature was studied by using the maximum and minimum temperatures observed daily on outer and inner surfaces of marble slabs. The results from every measuring point are shown as pictures presented in this chapter, Figs. 6-92. The pictures are grouped into the series of four, each representing the same measurement period. The four pictures in the same series are coded with letters a-d, and they have the following meaning:

a) daily maximum (Series 1) and minimum (Series 2) temperatures on outer surface of marble (°C)
b) daily maximum (Series 1) and minimum (Series 2) temperatures on inner surface of marble (°C)
c) difference between daily maximum and minimum temperatures on outer surface of mable (°C)
d) difference between daily maximum and minimum temperatures on inner surface of marble (°C)

4.3.1 Measuring point A

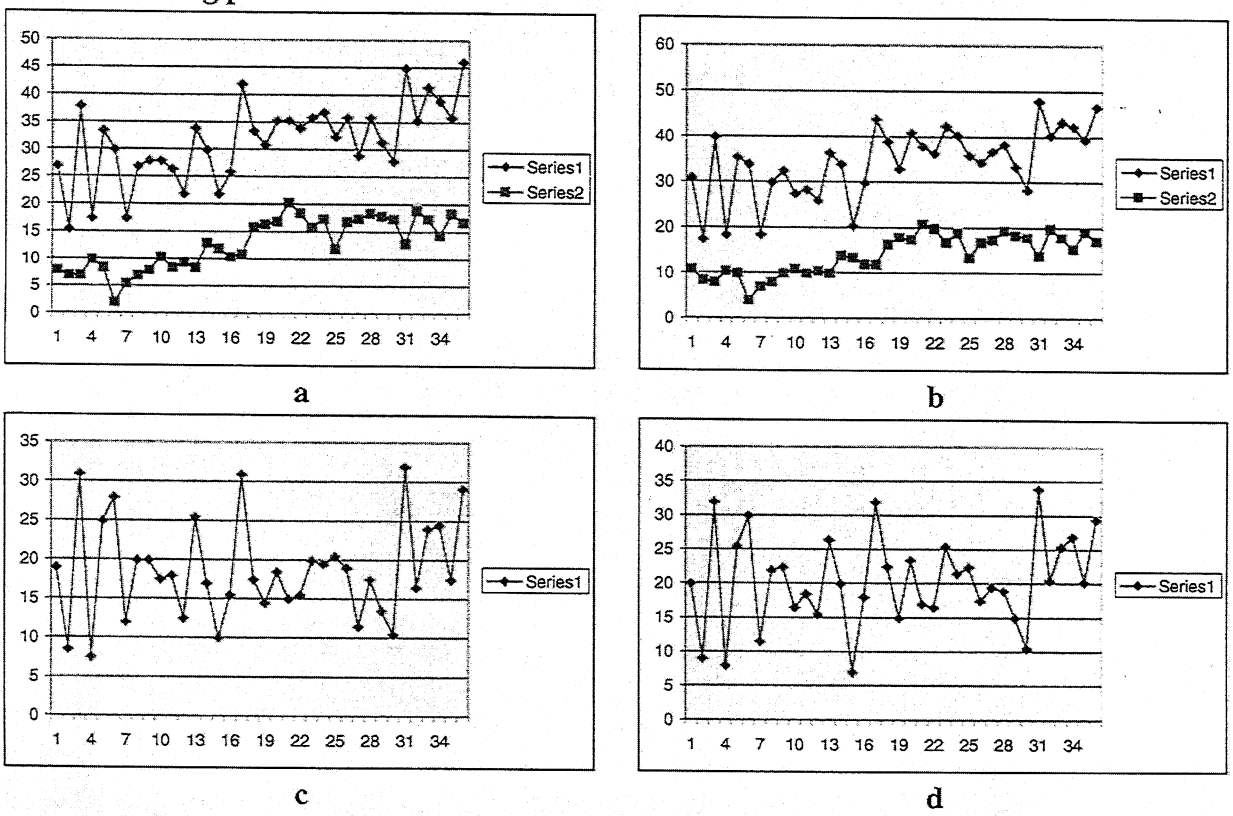

Figure 6. Daily temperature variation during measurement period 26.5.-30.6.1999.

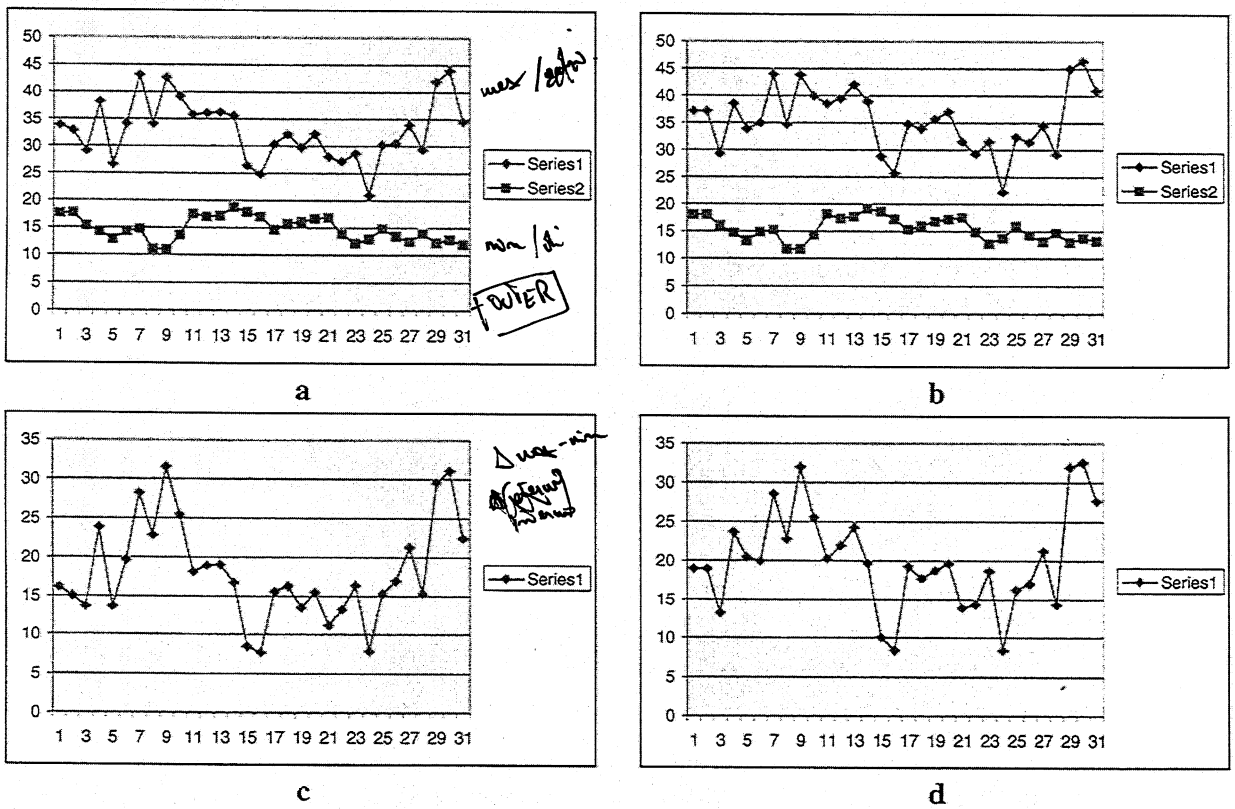

Figure 7. Daily temperature variation during measurement period 1.7.-31.7.1999.

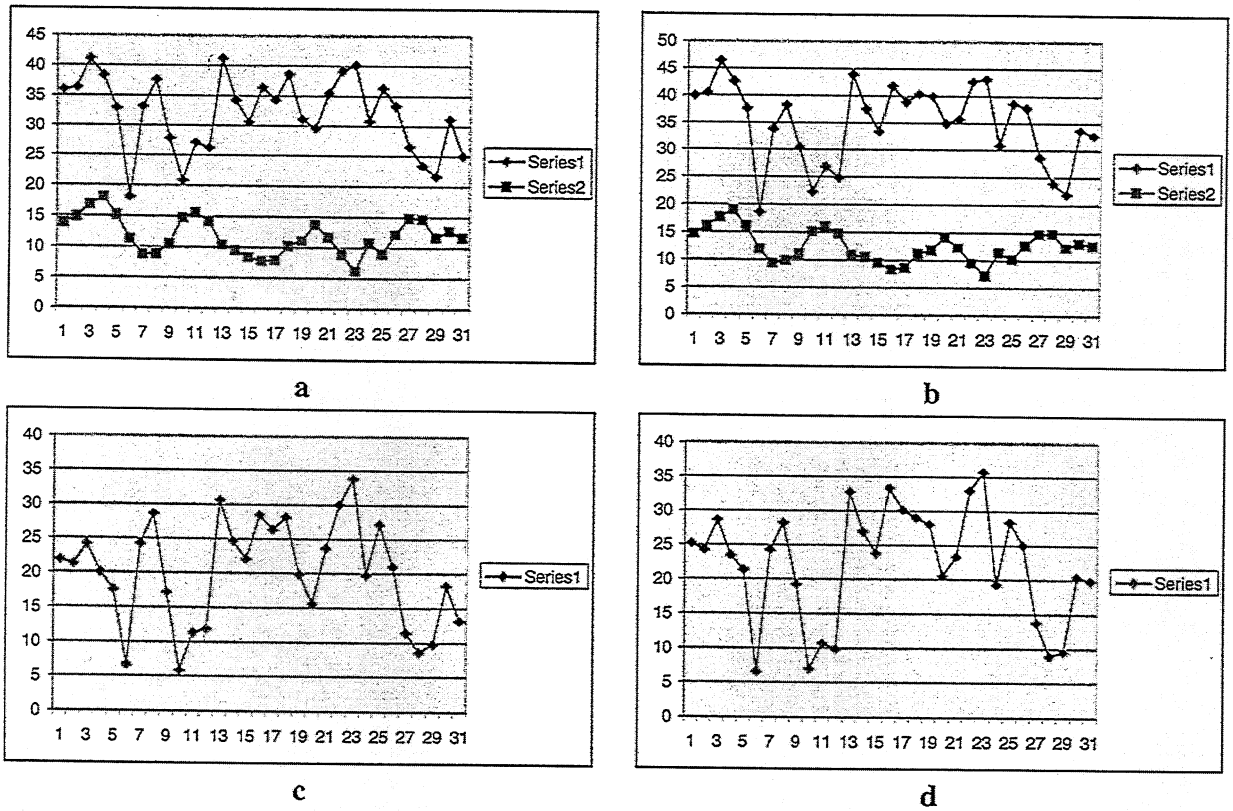

Figure 8. Daily temperature variation during measurement period 1.8.-31.8.1999.

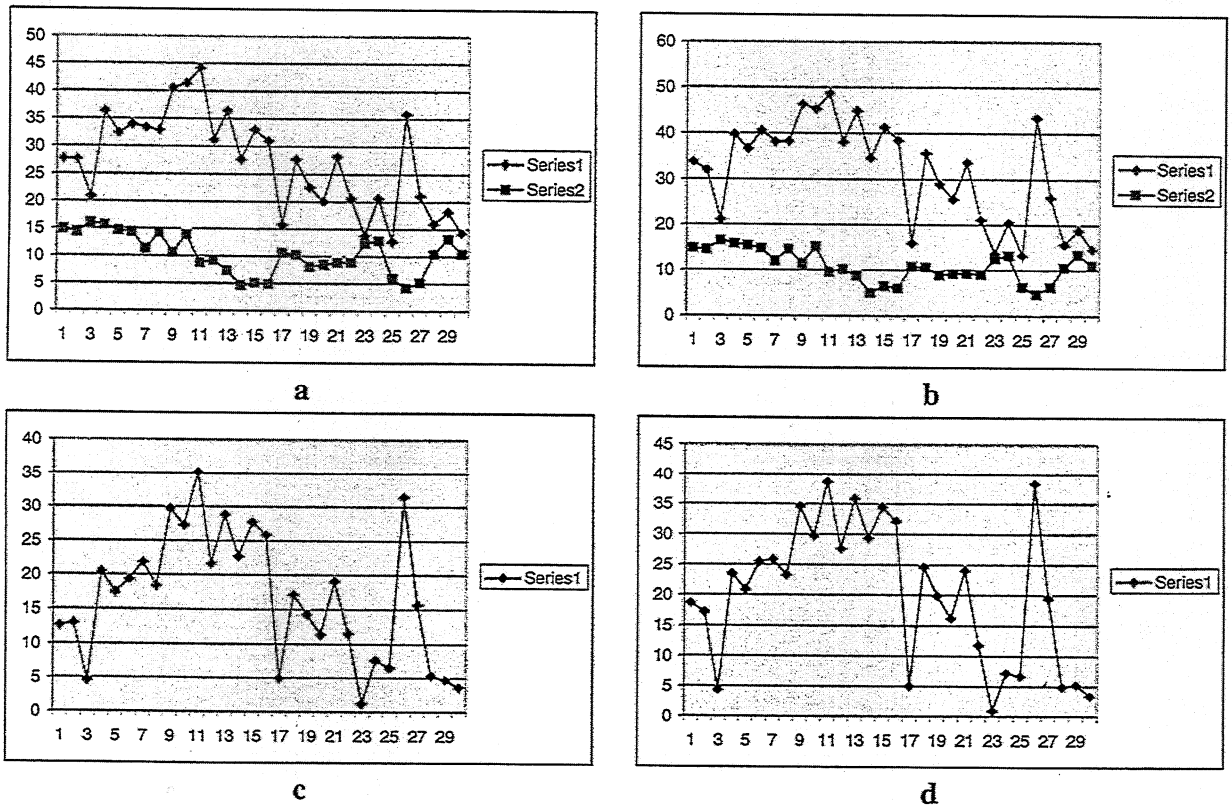

Figure 9. Daily temperature variation during measurement period 1.9.-30.9.1999.

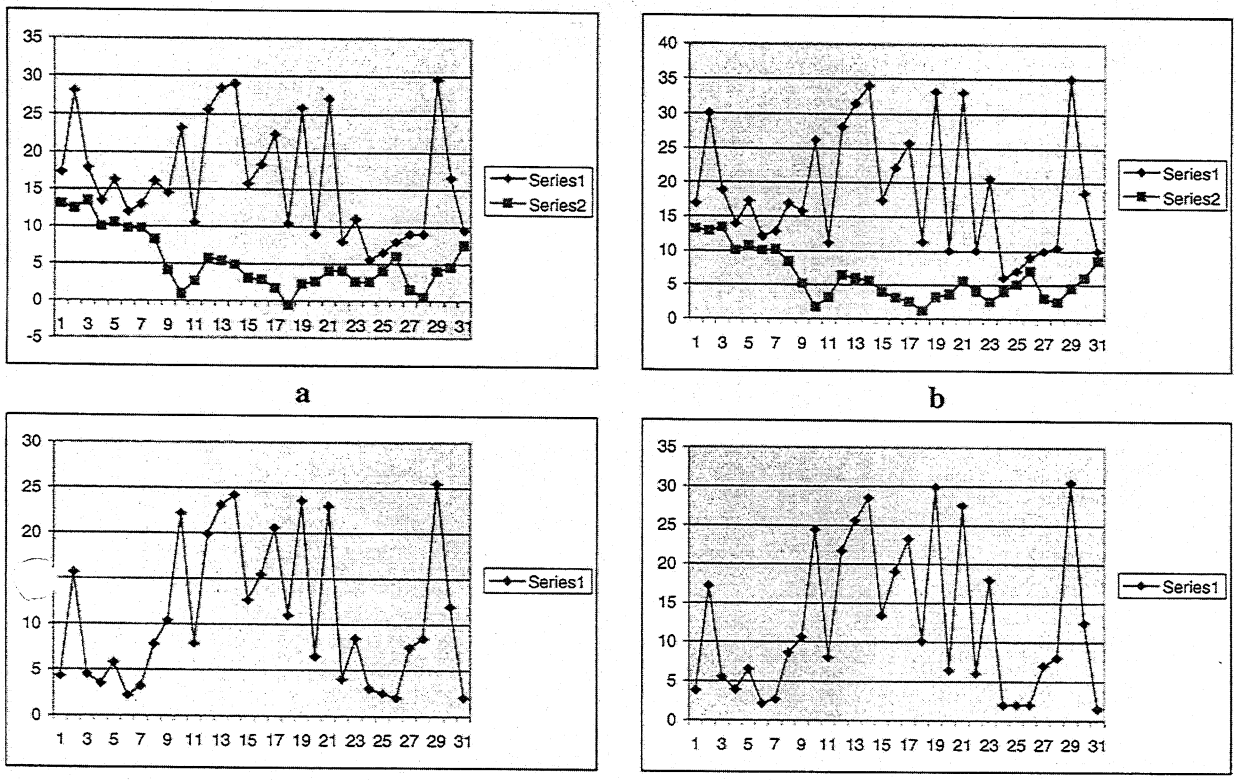

Figure 10. Daily temperature variation during measurement period 1.10.-31.10.1999.

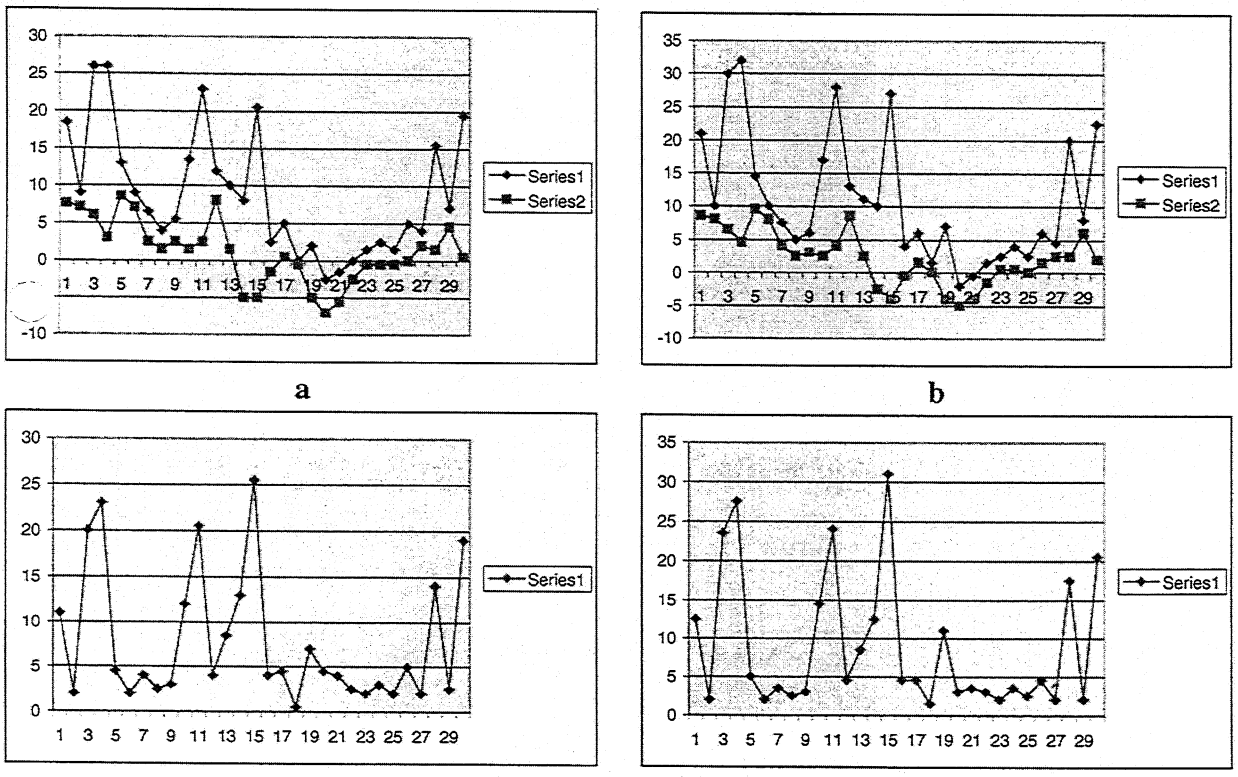

Figure 11. Daily temperature variation during measurement period 1.11.-30.11.1999.

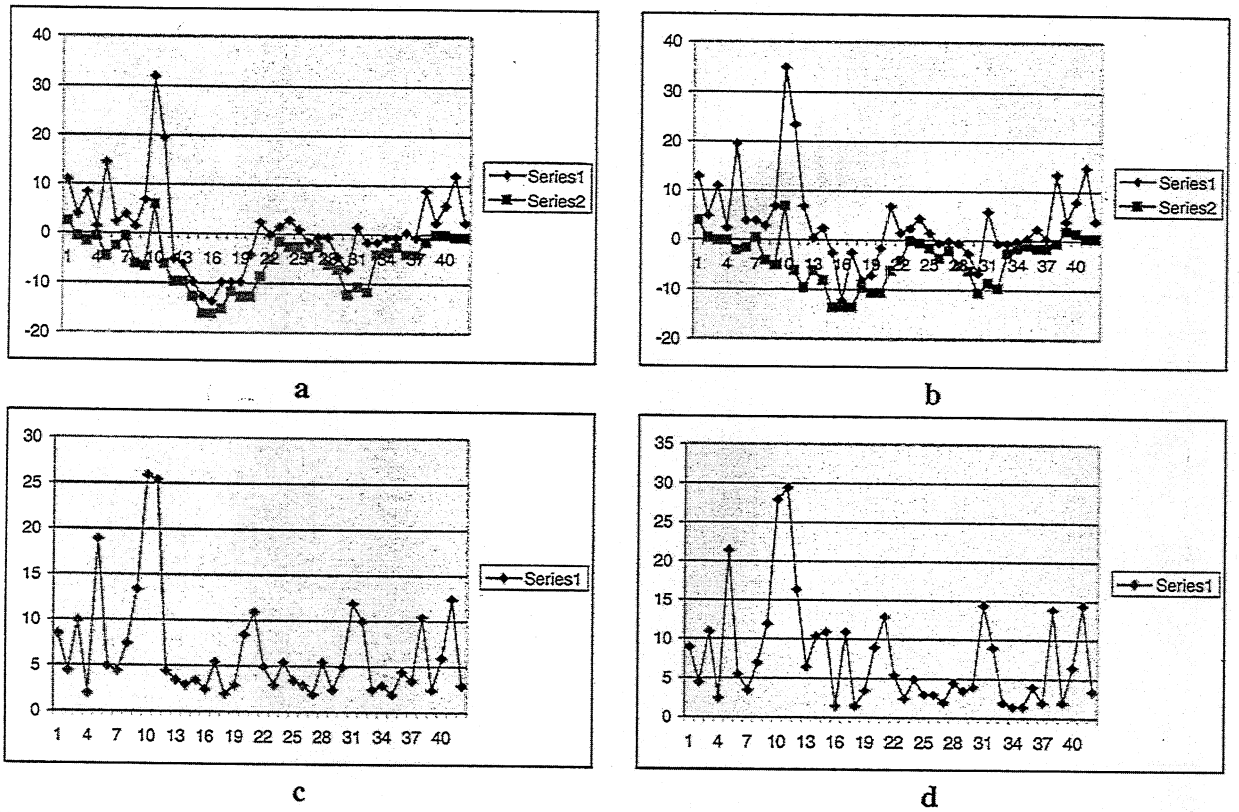

Figure 12. Daily temperature variation during measurement period 1.12.1999-11.1.2000.

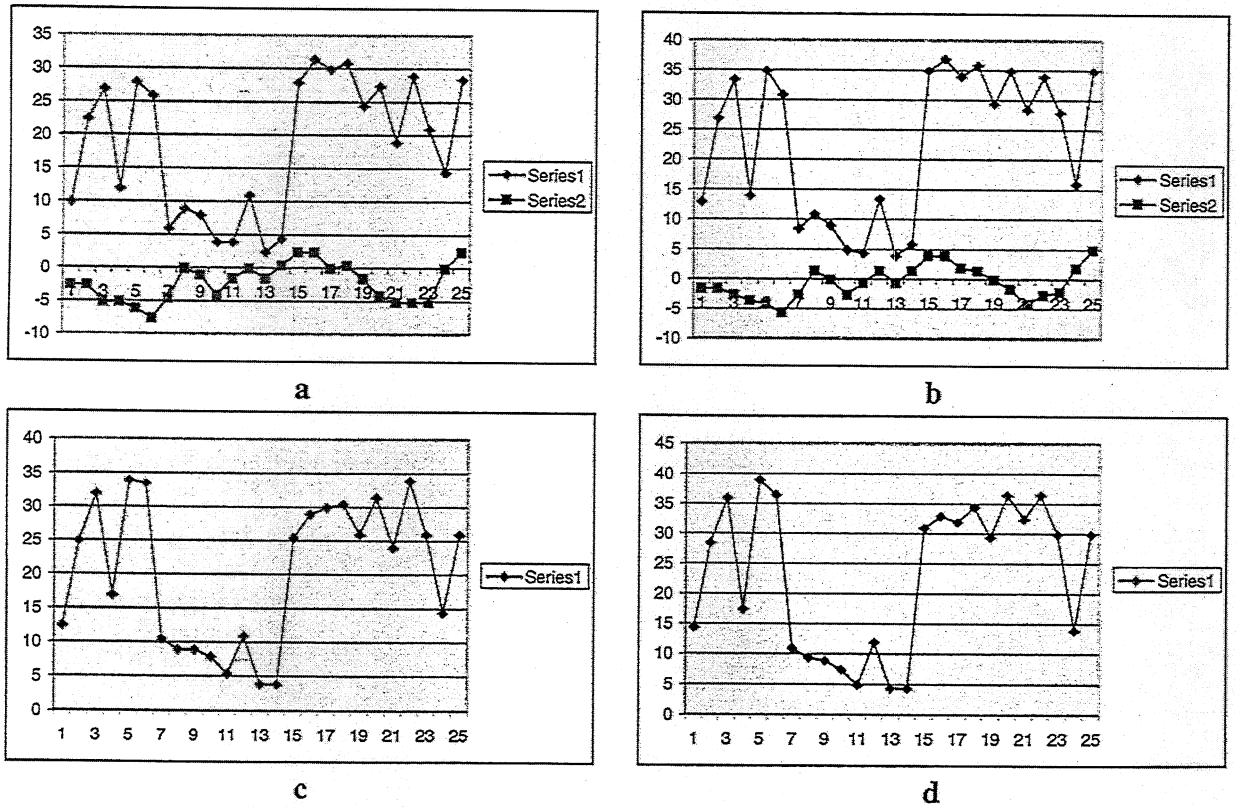

Figure 13. Daily temperature variation during measurement period 7.3.-31.3.2000.

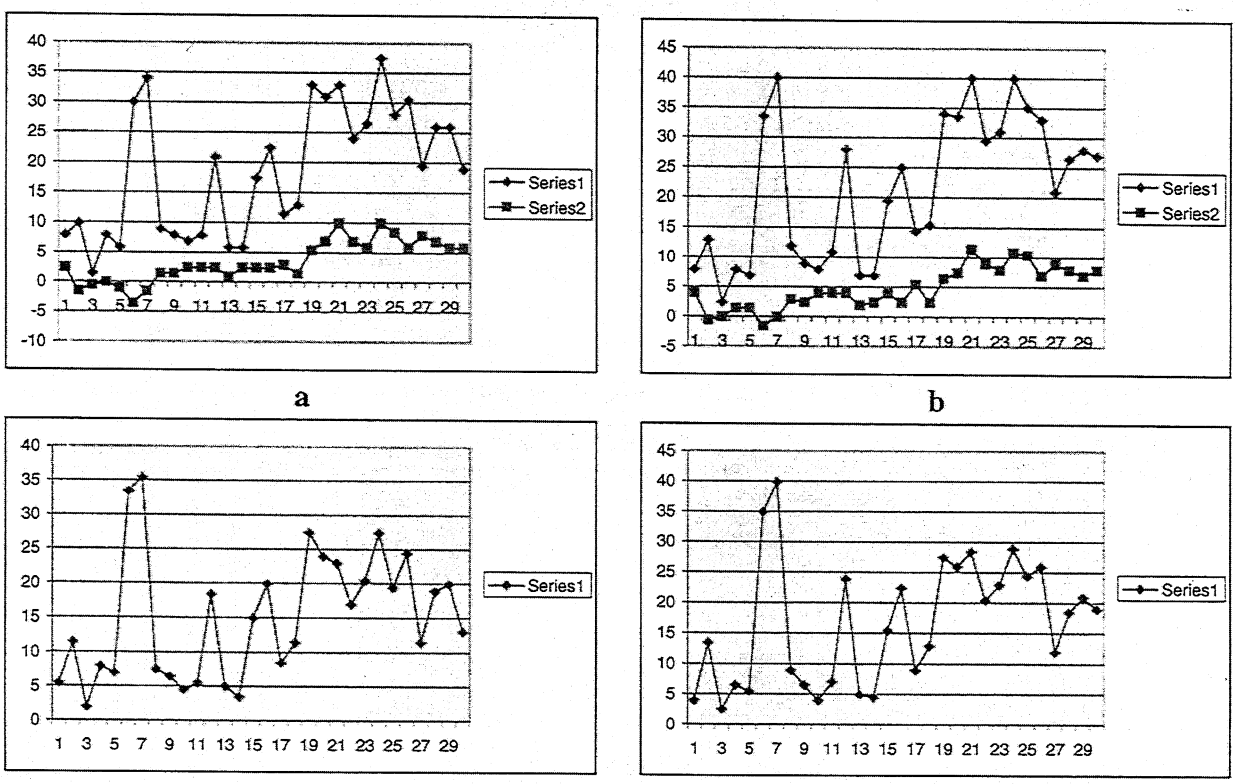

Figure 14. Daily temperature variation during measurement period 1.4.-30.4.2000.

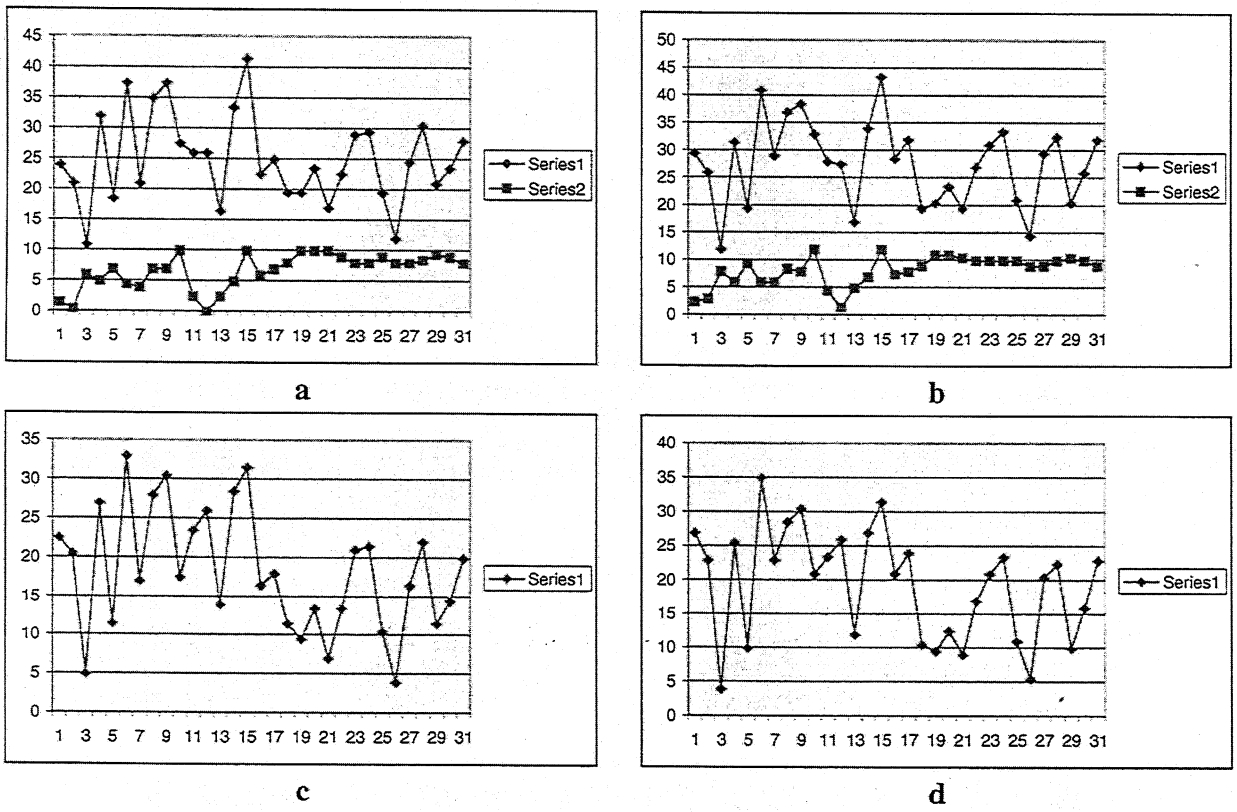

Figure 15. Daily temperature variation during measurement period 1.5.-31.5.2000.

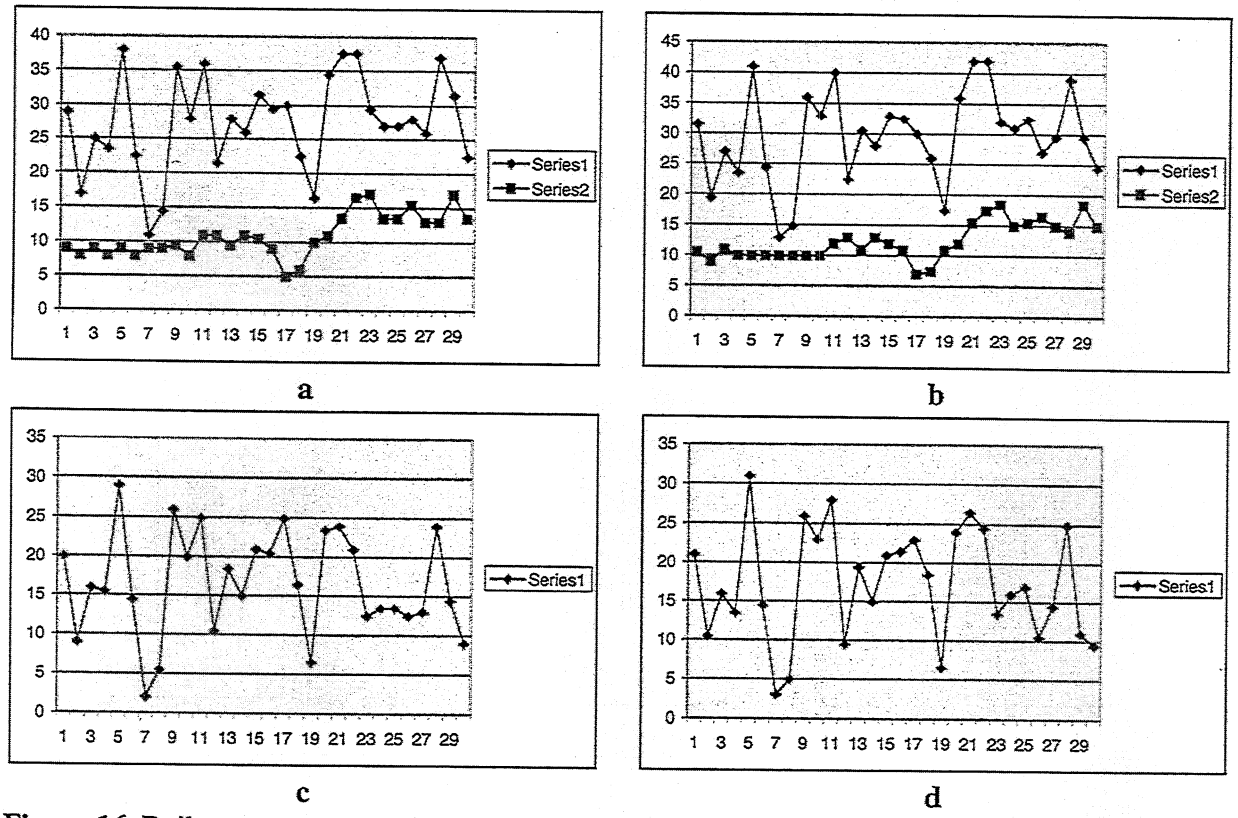

Figure 16. Daily temperature variation during measurement period 1.6.-30.6.2000.

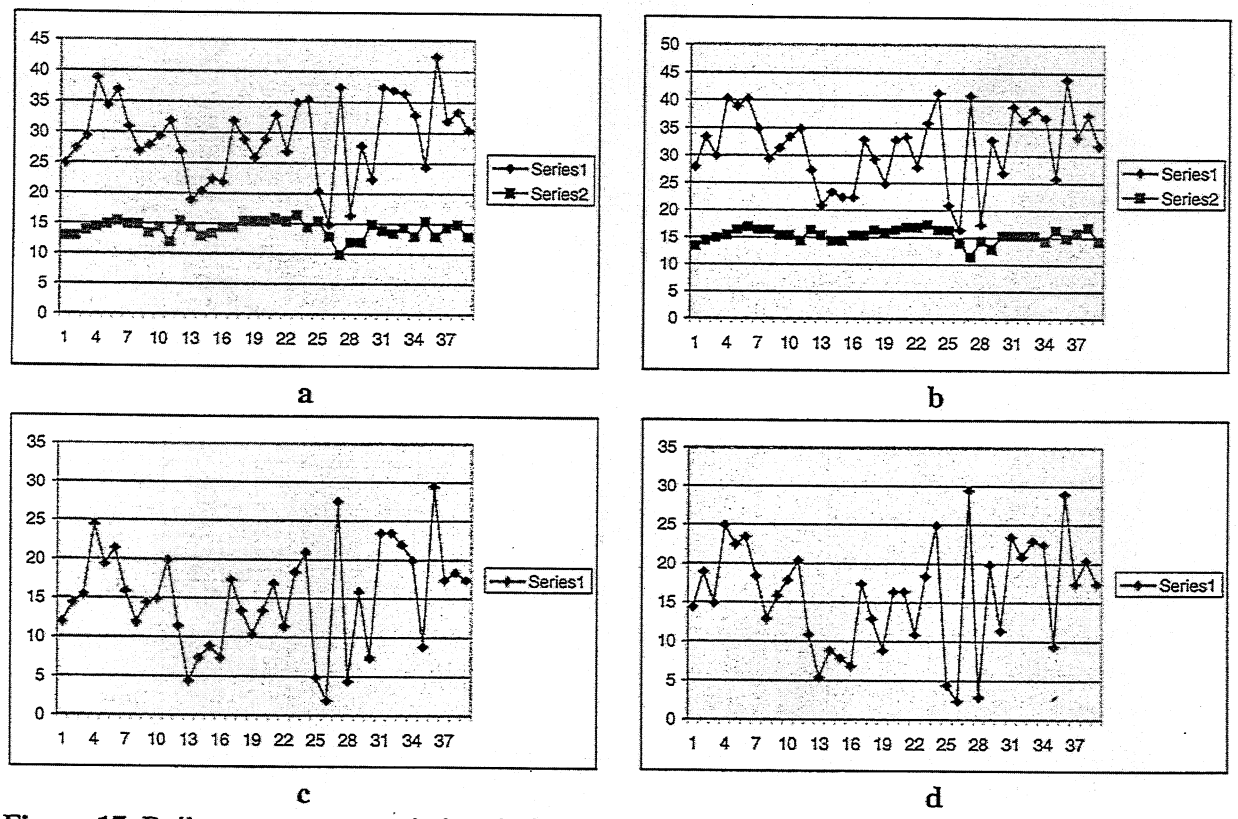

Figure 17. Daily temperature variation during measurement period 1.7.-8.8.2000.

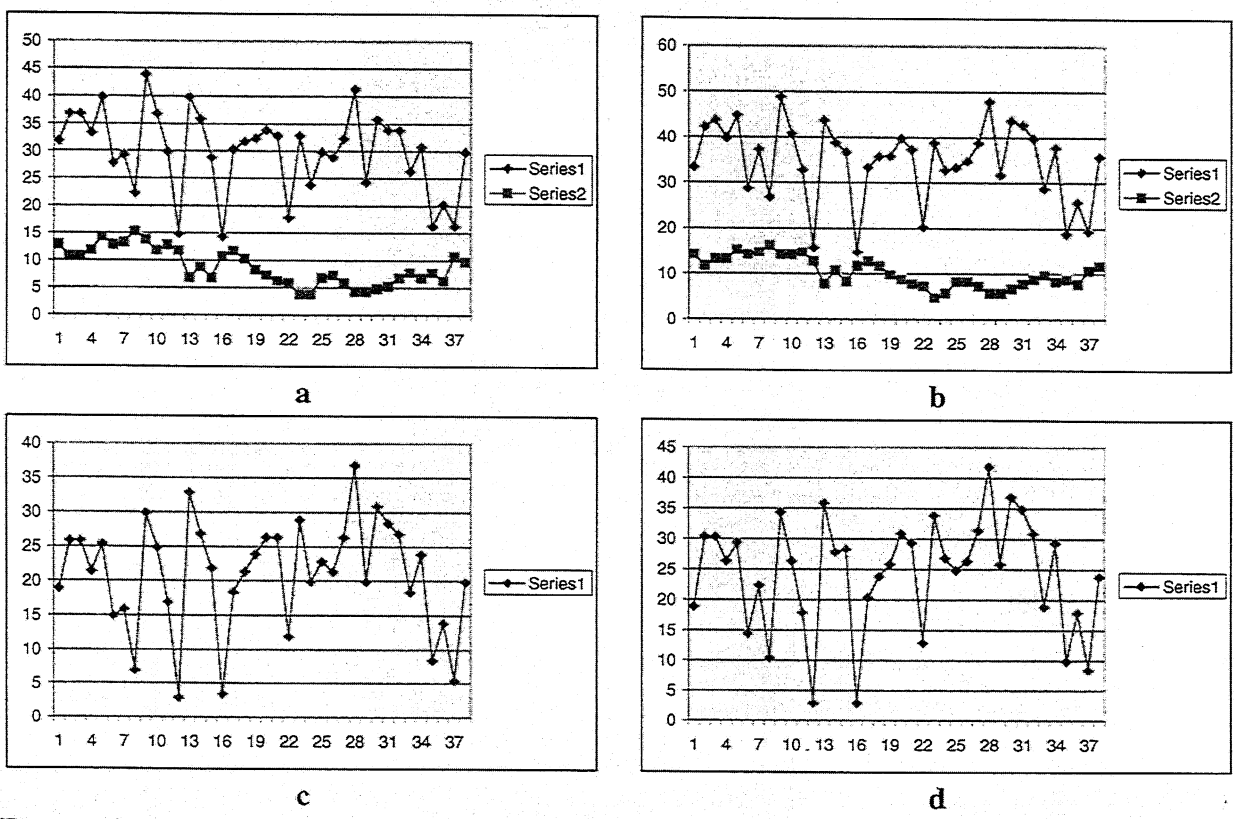

Figure 18. Daily temperature variation during measurement period 24.8.-30.9.2000.

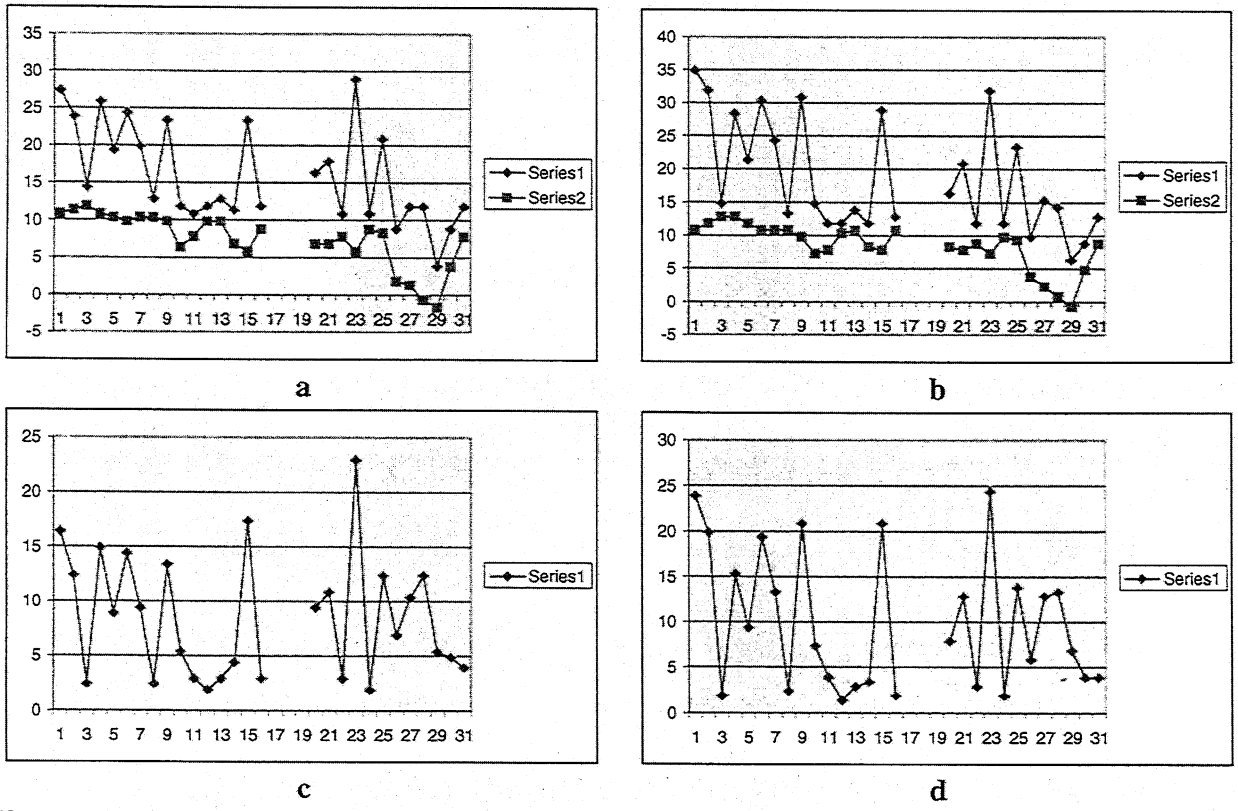

Figure 19. Daily temperature variation during measurement period 1.10.-31.10.2000.

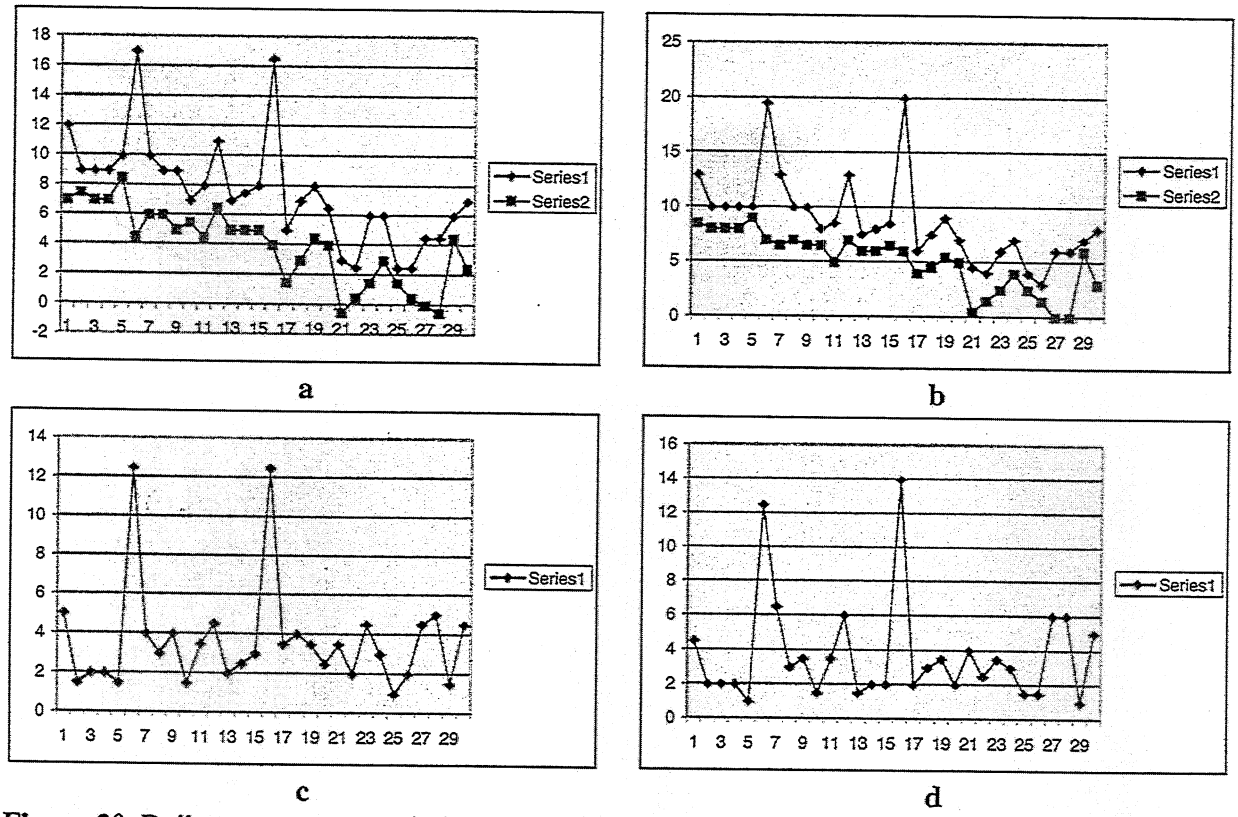

Figure 20. Daily temperature variation during measurement period 1.11.-30.11.2000.

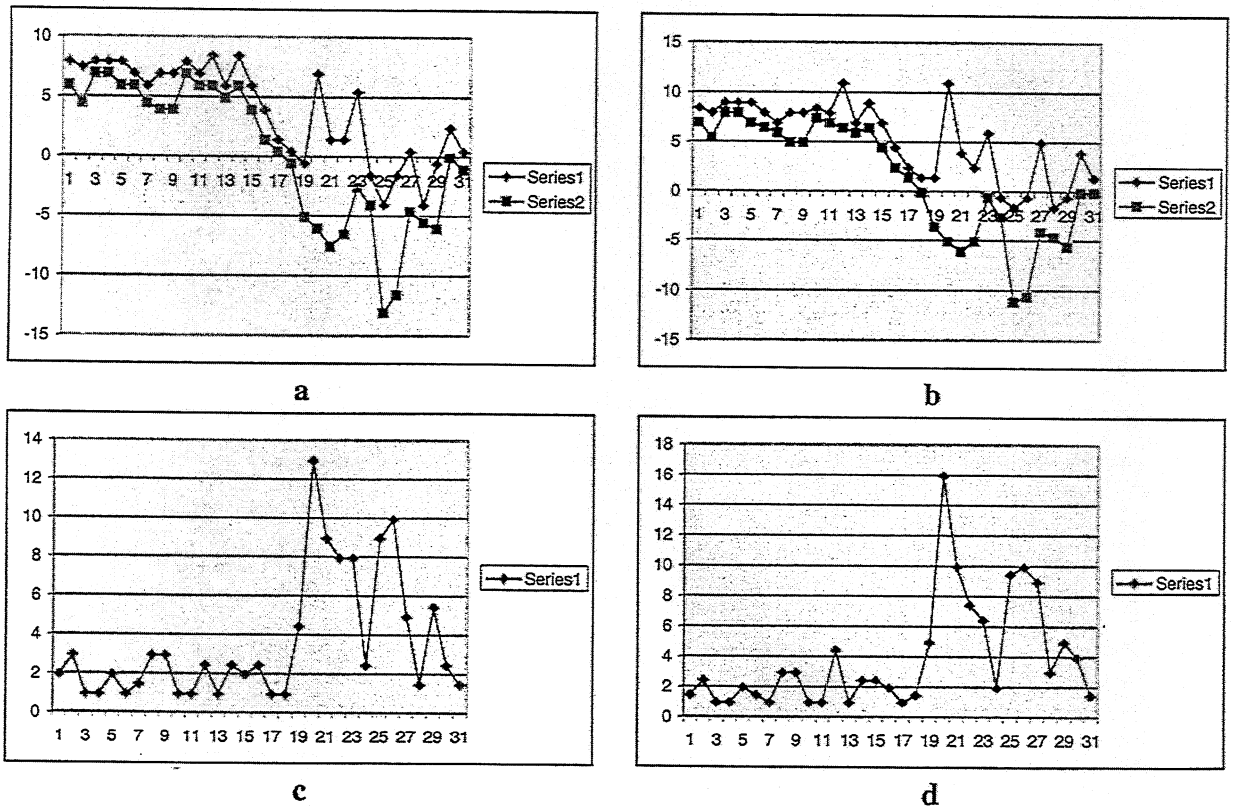

Figure 21. Daily temperature variation during measurement period 1.12.-31.12.2000.

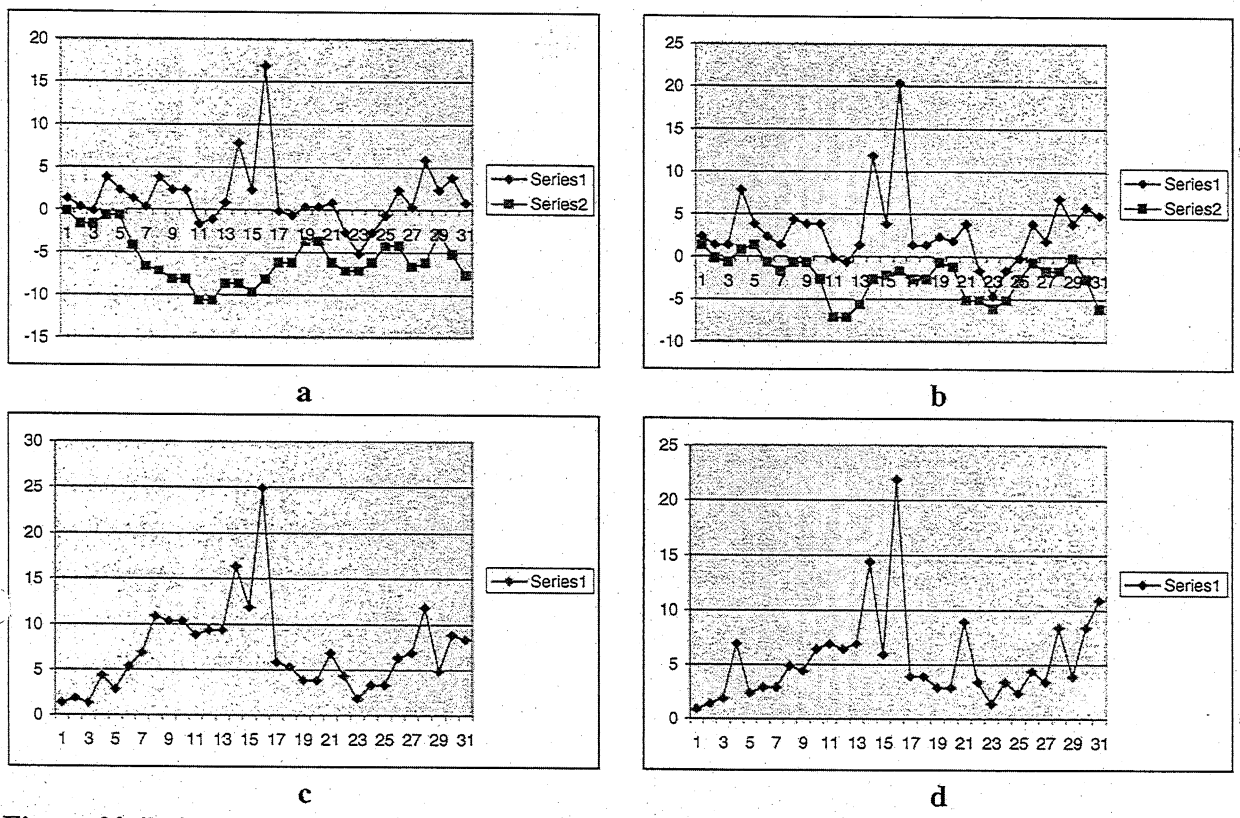

Figure 22. Daily temperature variation during measurement period 1.1.-31.1.2001.

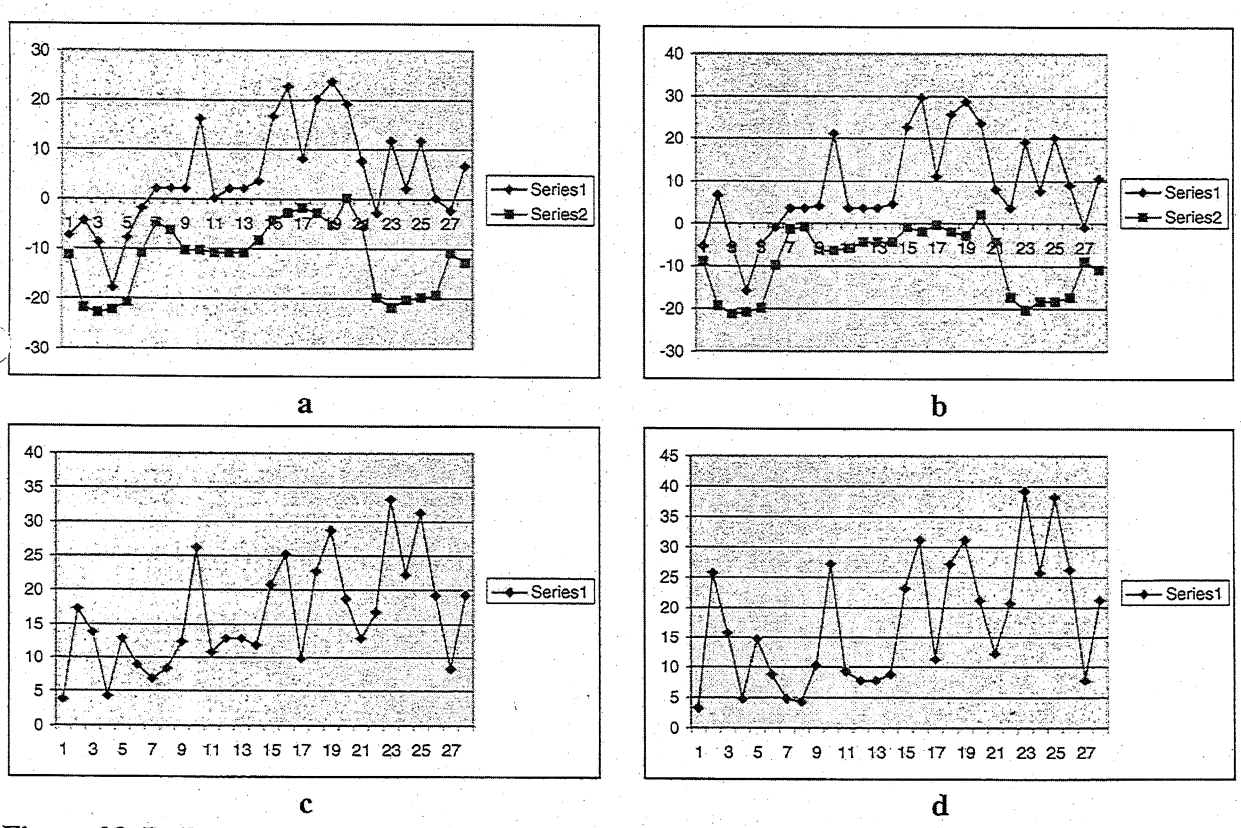

Figure 23. Daily temperature variation during measurement period 1.2.-28.2.2001.

4.3.2 Measuring point B

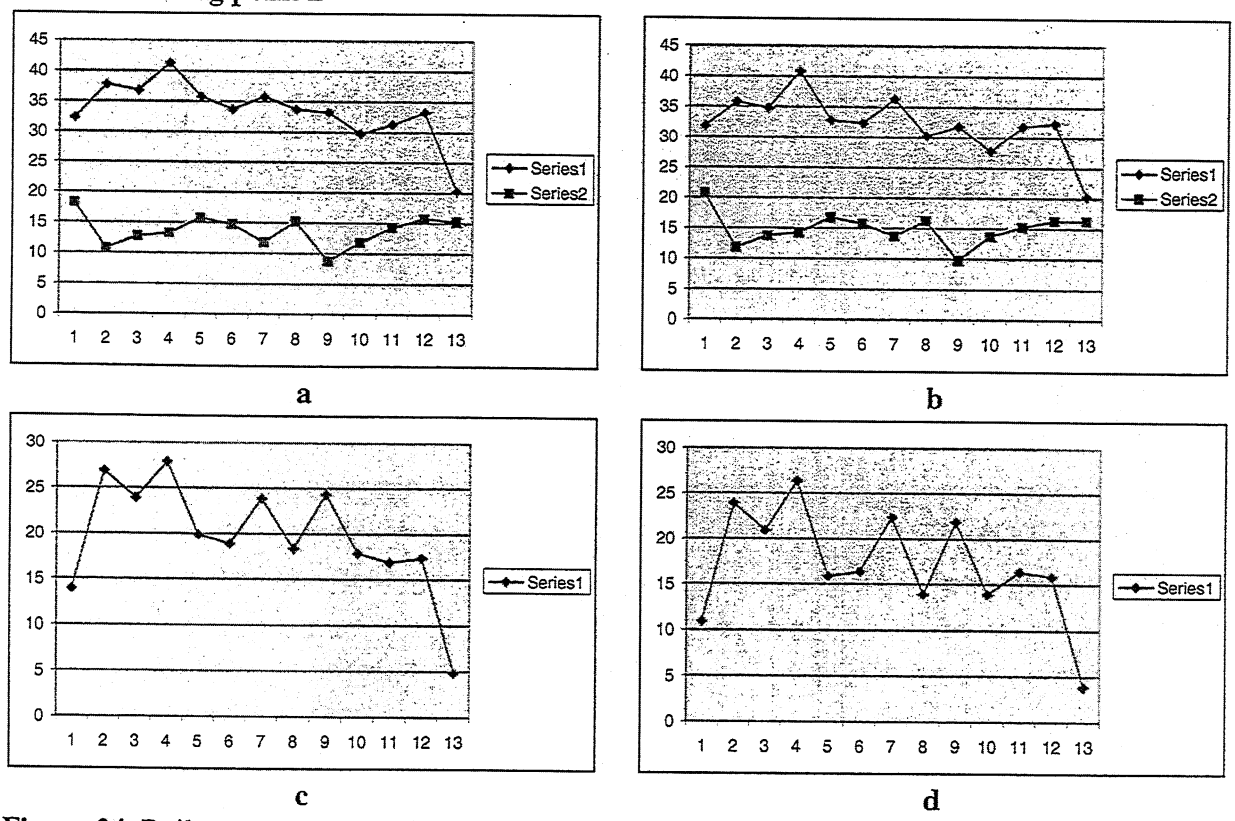

Figure 24. Daily temperature variation during measurement period 11.6.-23.6.1999.

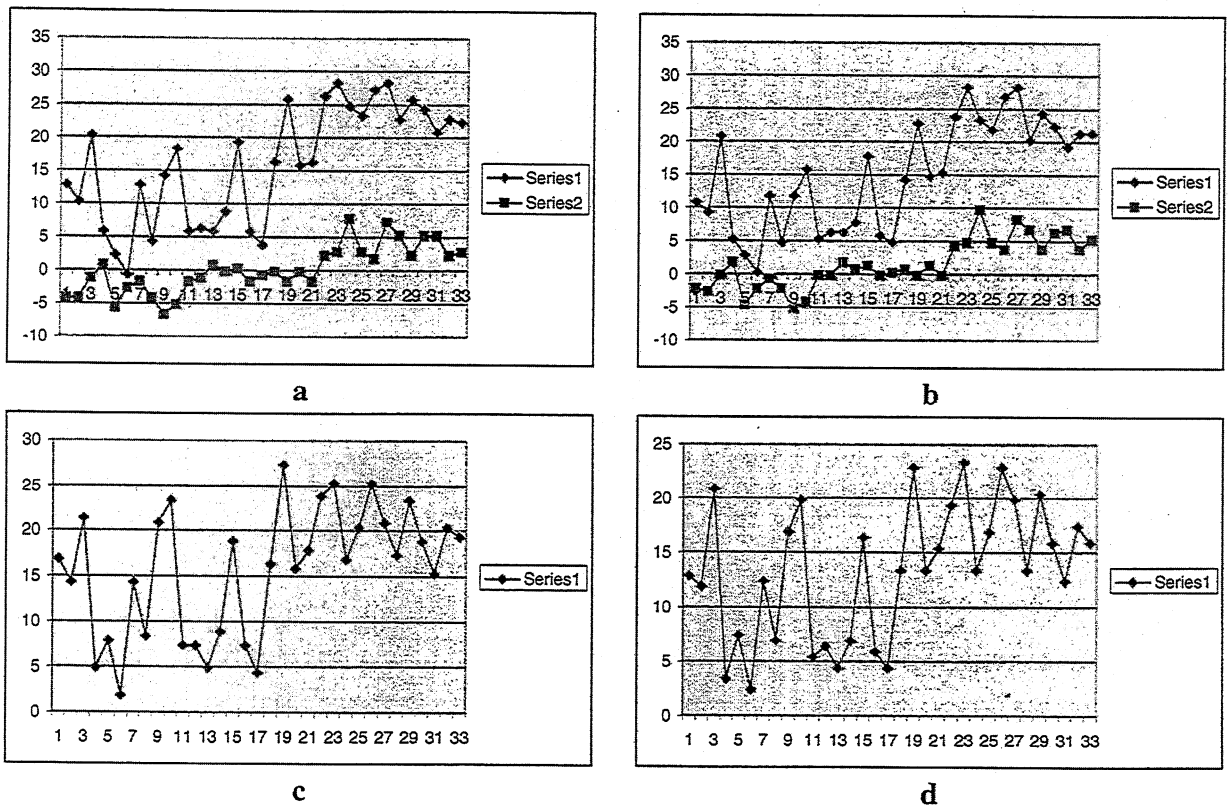

Figure 25. Daily temperature variation during measurement period 29.3.-30.4.2000.

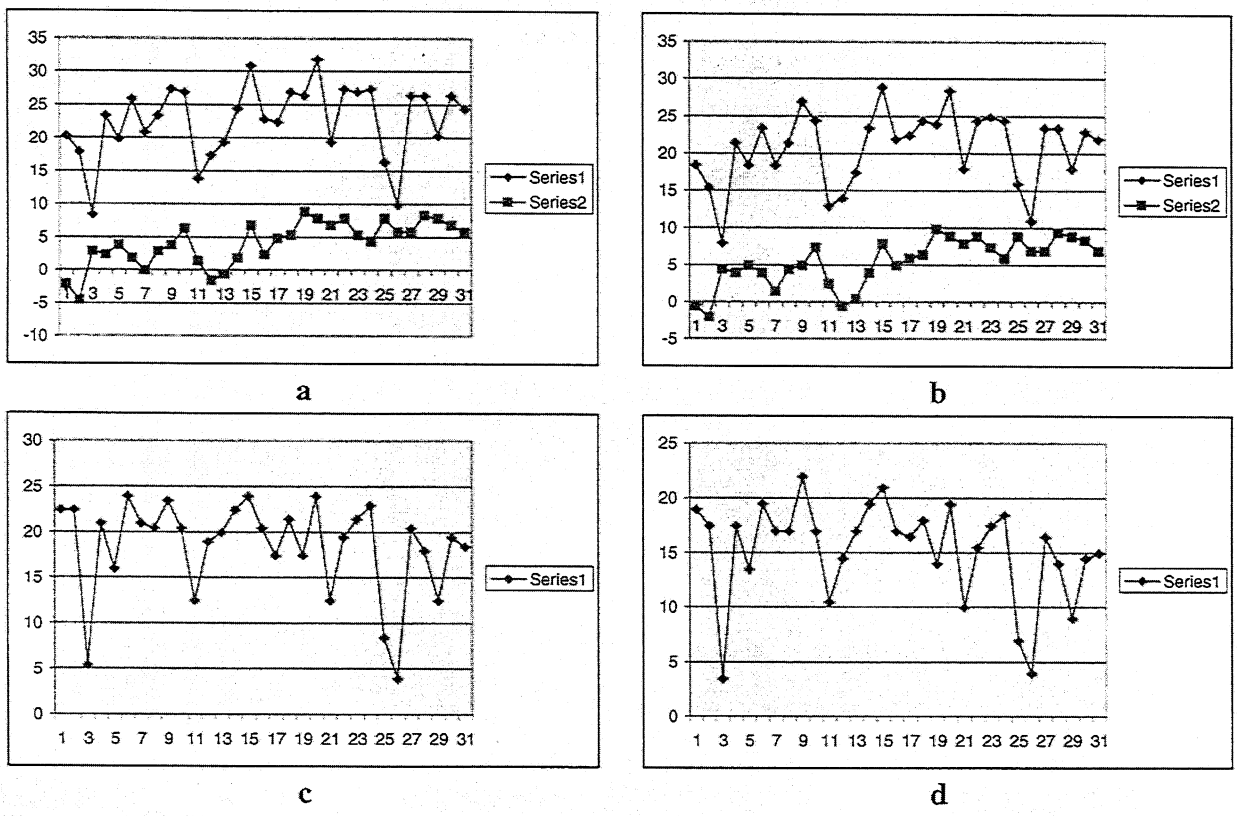

Figure 26. Daily temperature variation during measurement period 1.5.-31.5.2000.

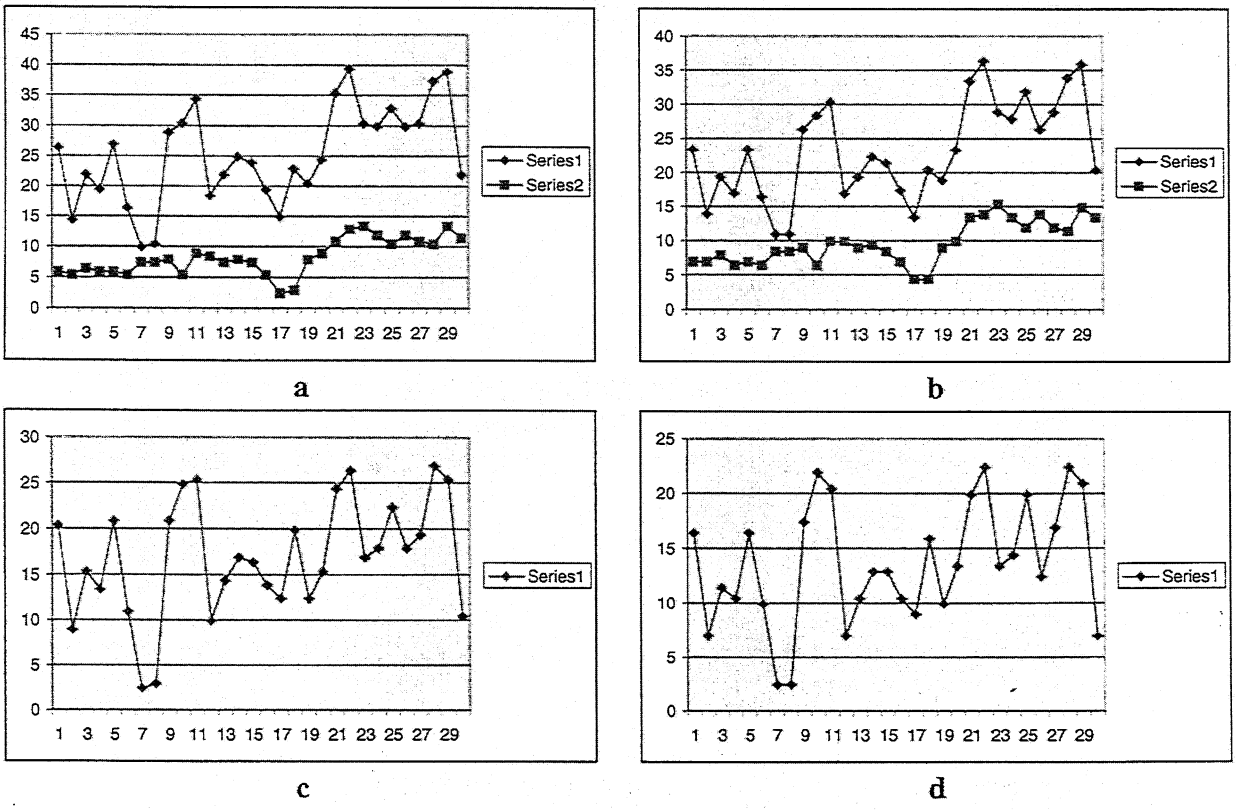

Figure 27. Daily temperature variation during measurement period 1.6.-30.6.2000.

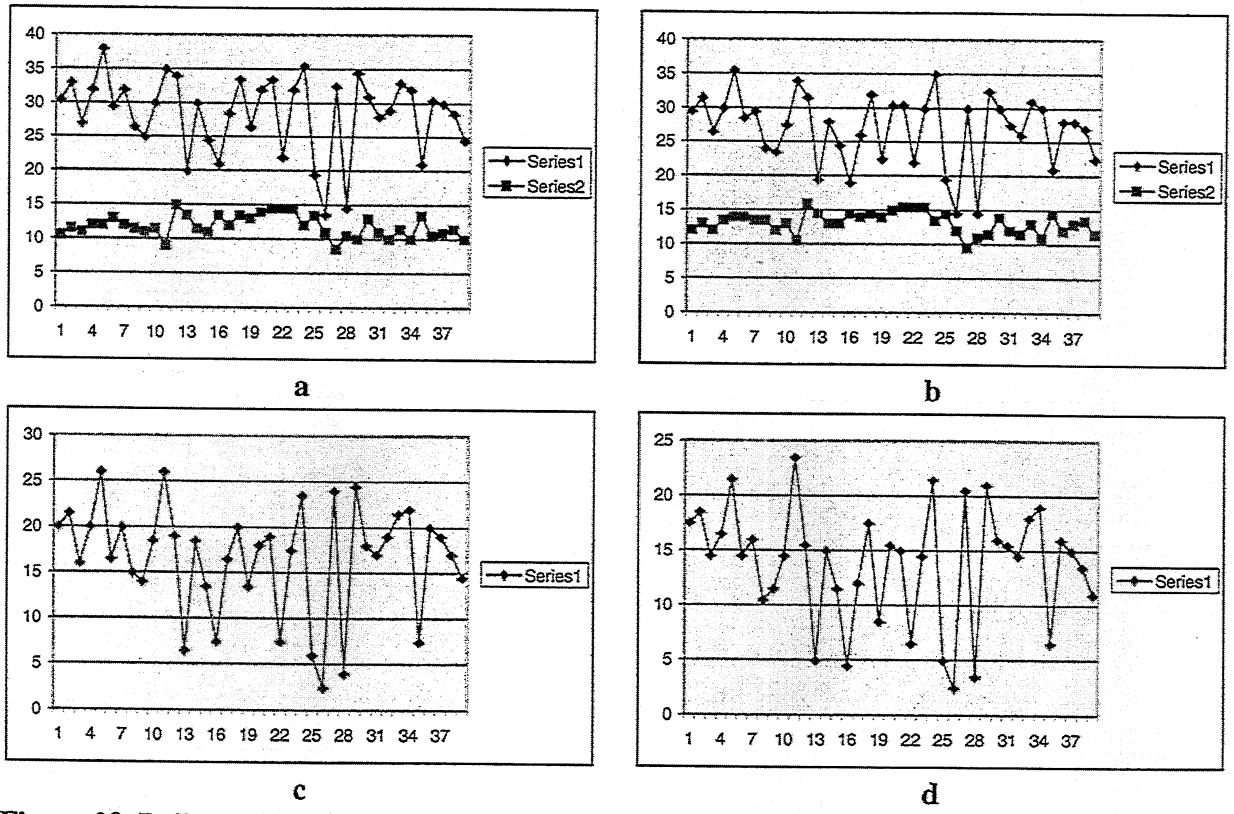

Figure 28. Daily temperature variation during measurement period 1.7.-8.8.2000.

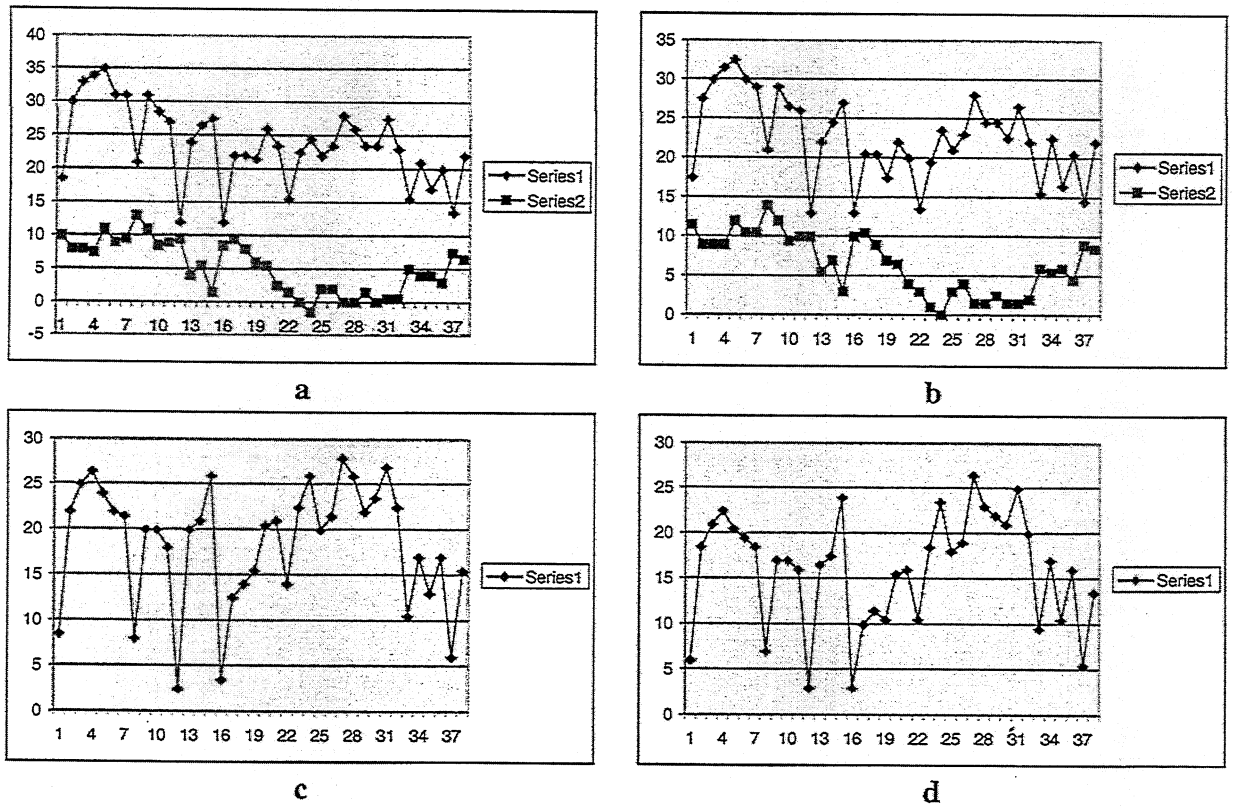

Figure 29. Daily temperature variation during measurement period 24.8.-30.9.2000.

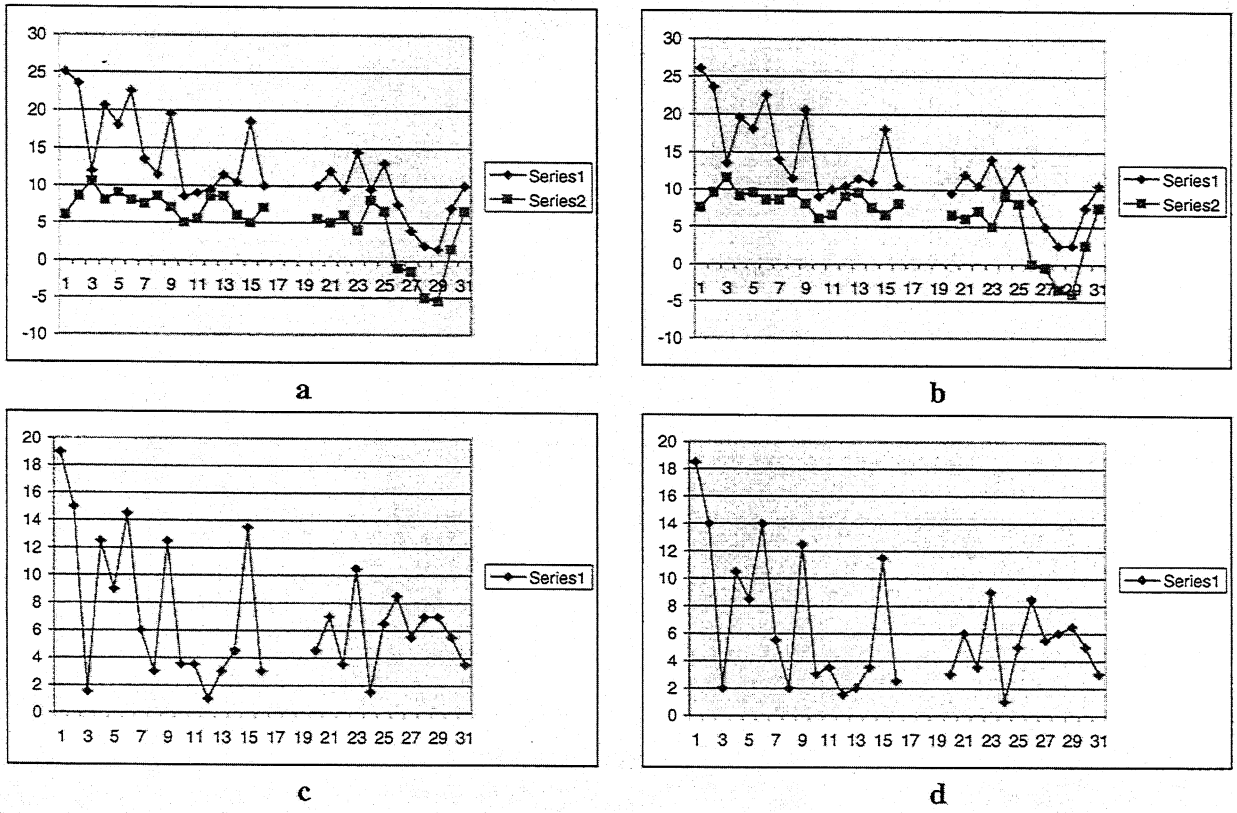

Figure 30. Daily temperature variation during measurement period 1.10.-31.10.2000.

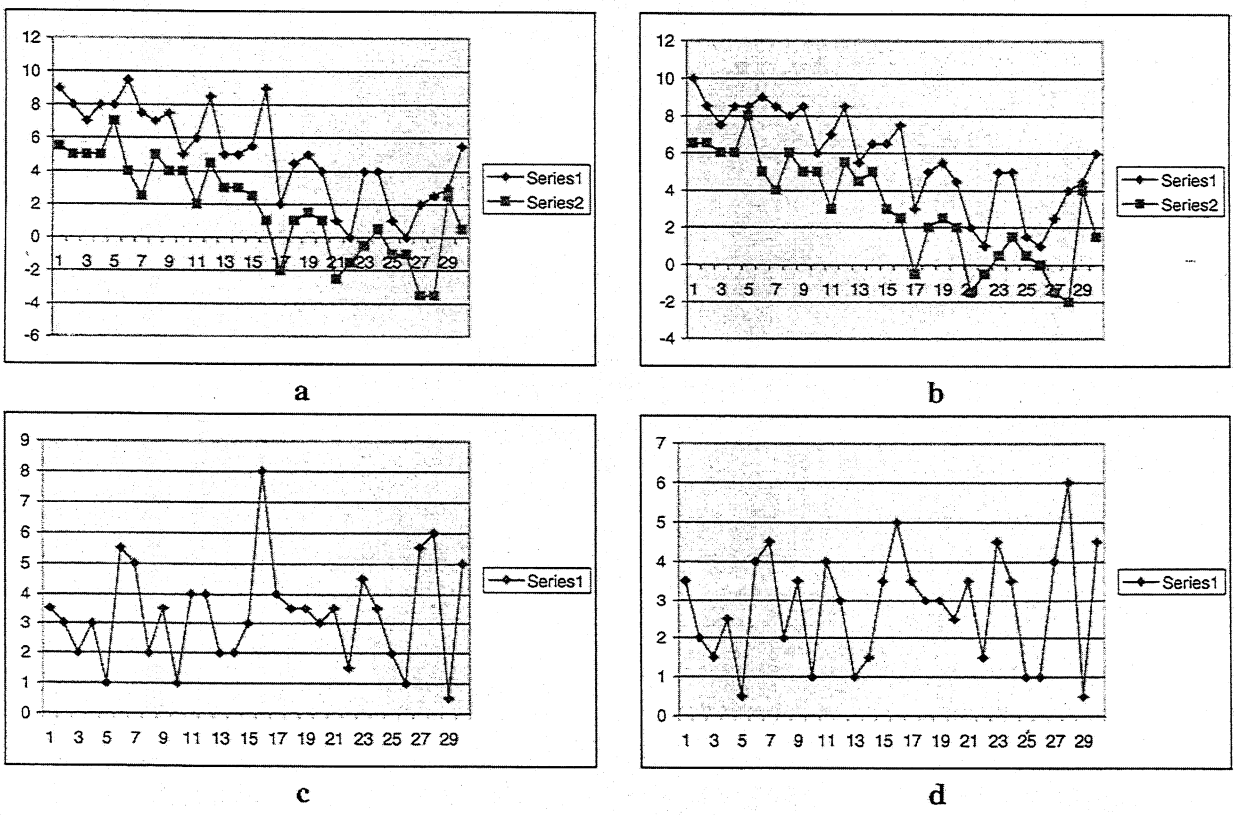

Figure 31. Daily temperature variation during measurement period 1.11.-30.11.2000.

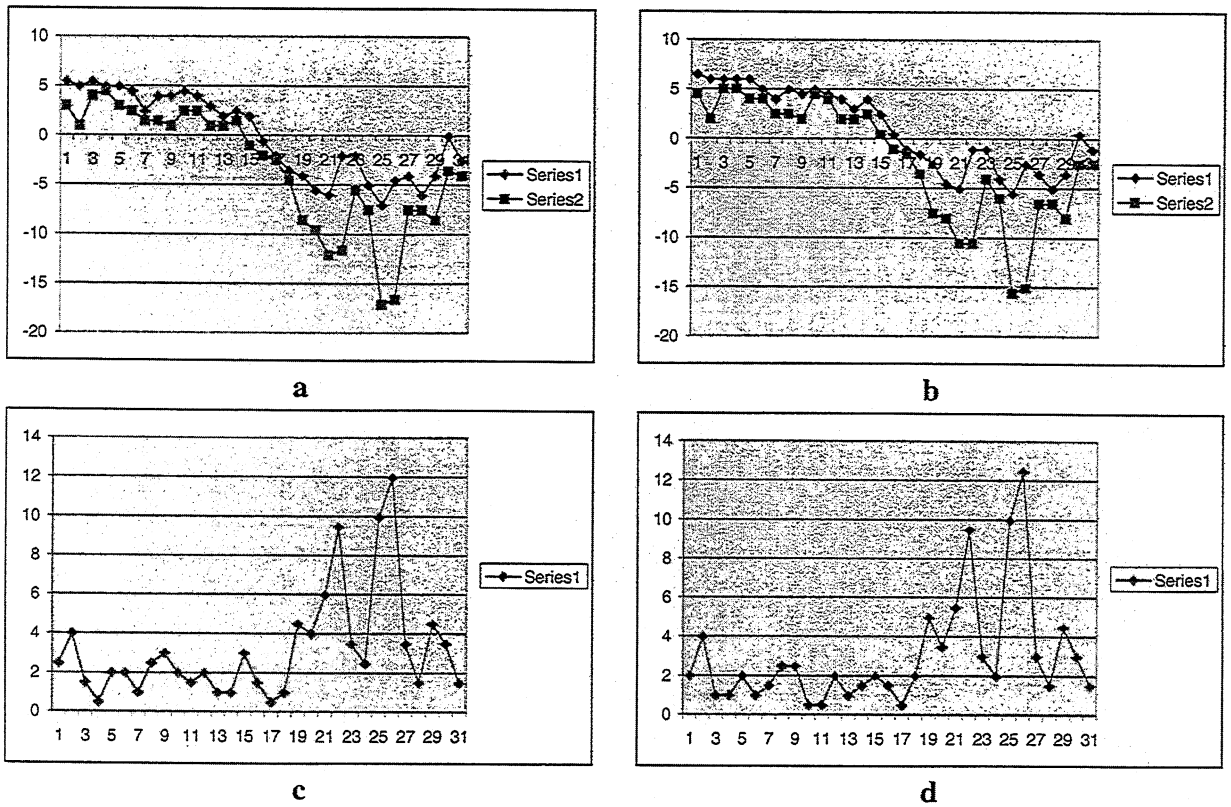

Figure 32. Daily temperature variation during measurement period 1.12.-31.12.2000.

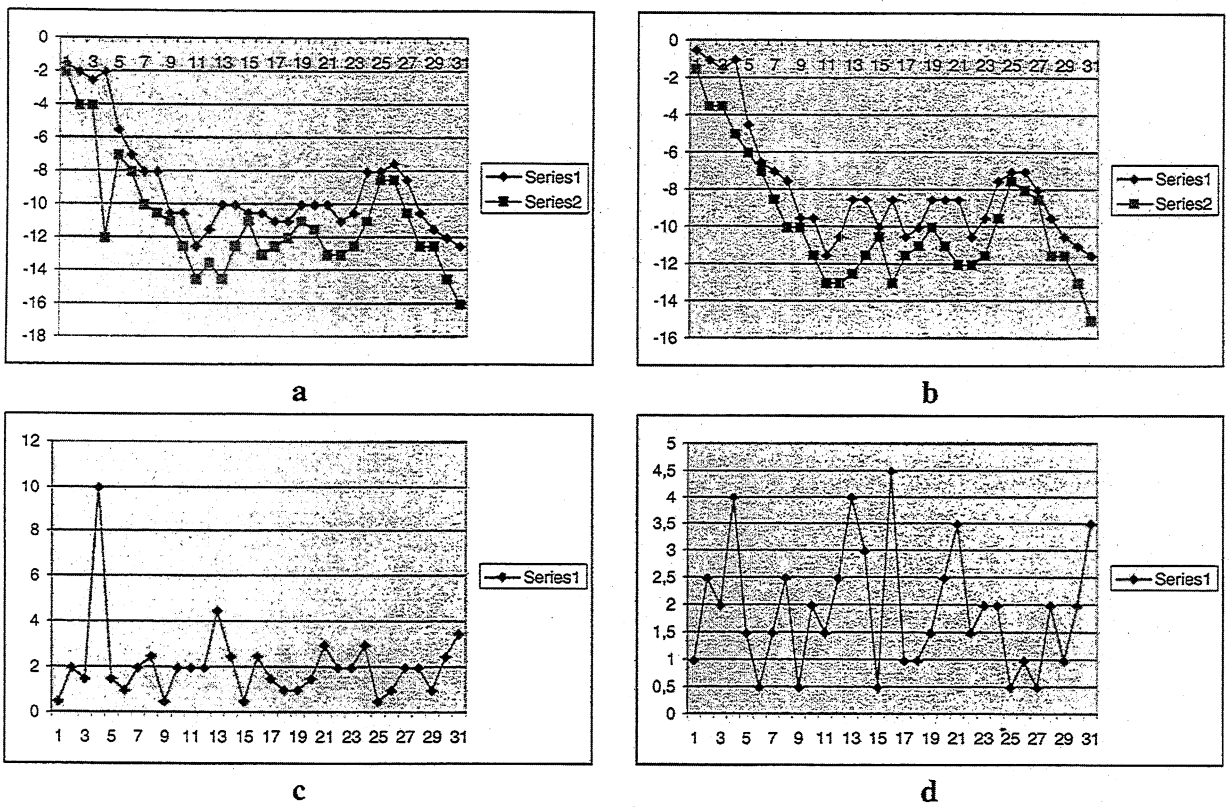

Figure 33. Daily temperature variation during measurement period 1.1.-31.1.2001.

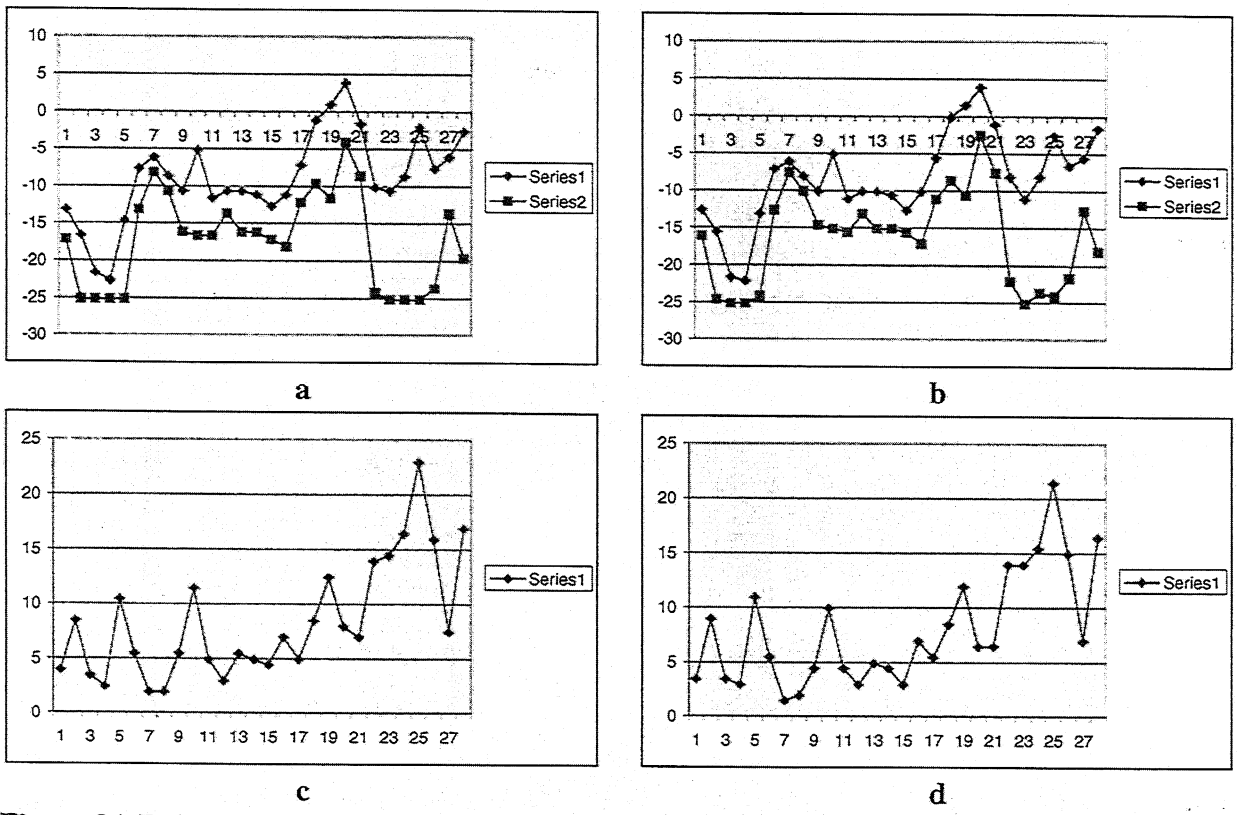

Figure 34. Daily temperature variation during measurement period 1.2.-28.2.2001.

4.3.3 Measuring point C

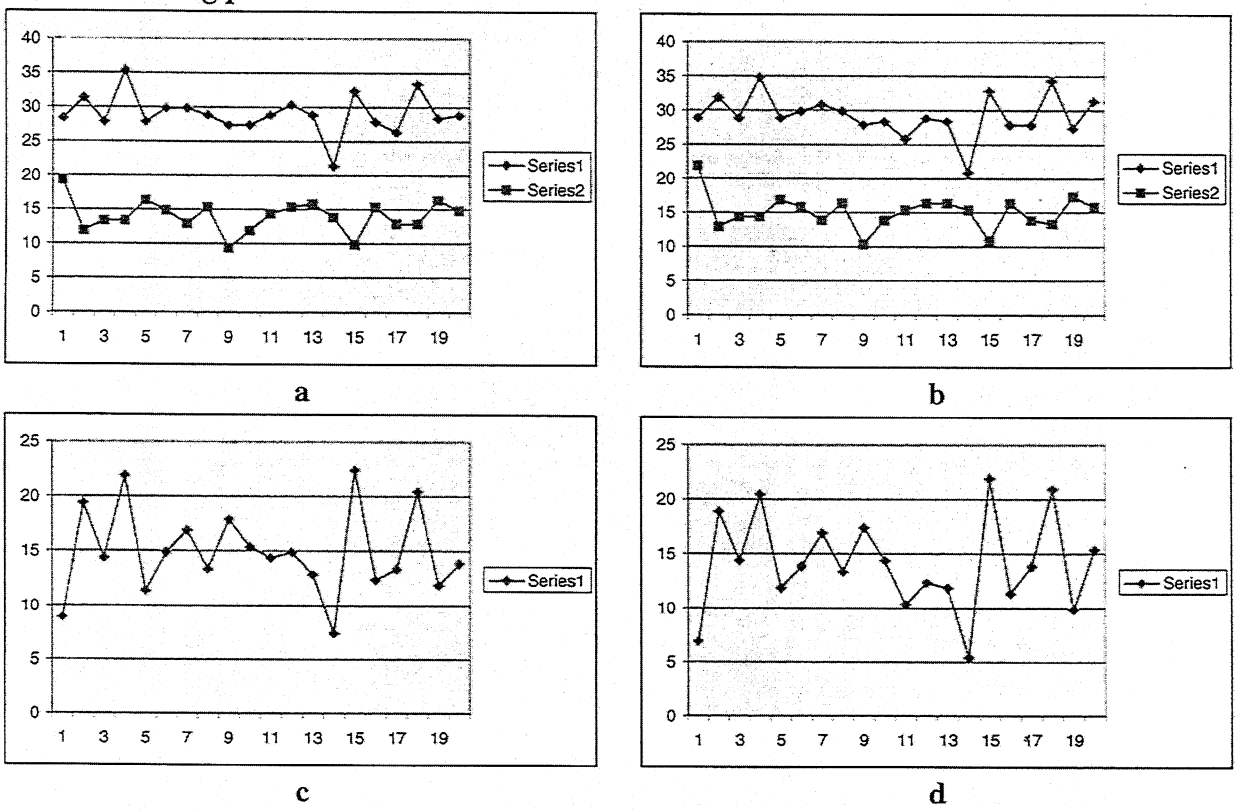

Figure 35. Daily temperature variation during measurement period 11.6.-30.6.1999.

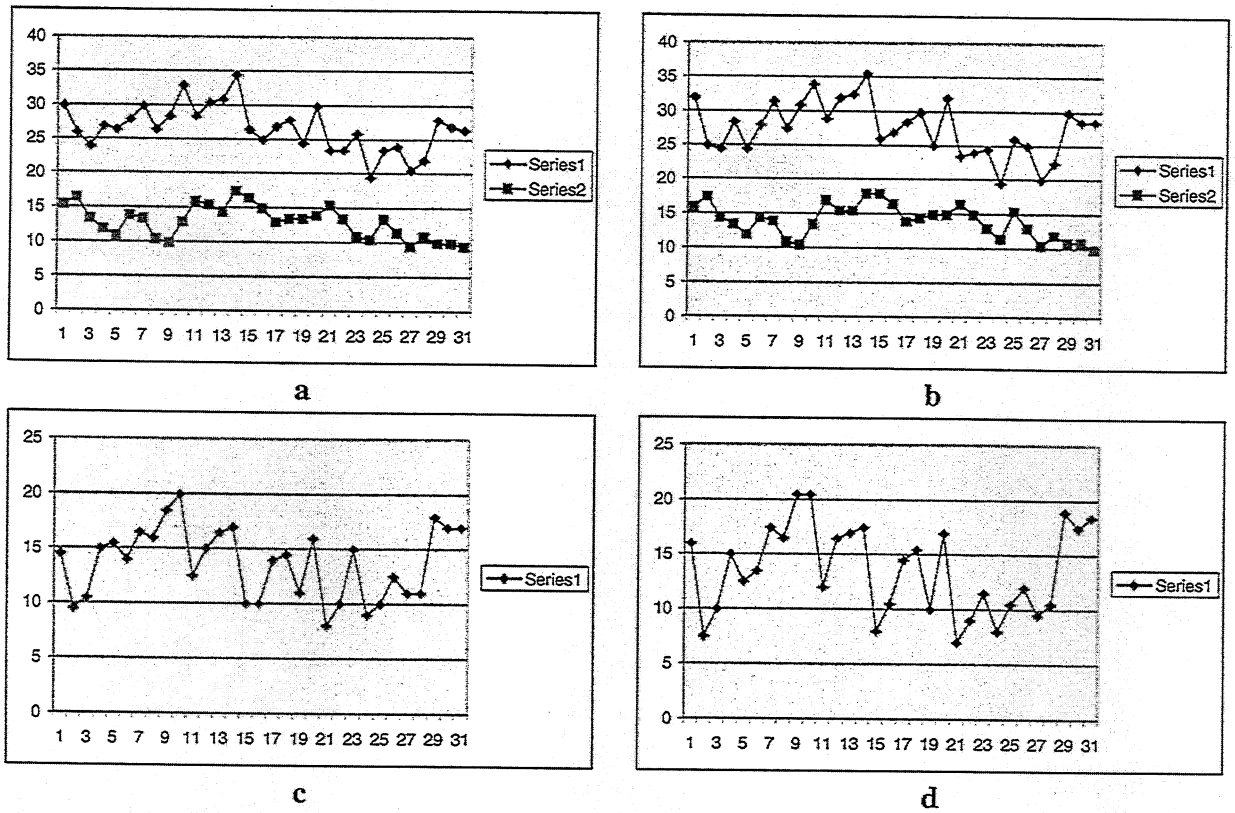

Figure 36. Daily temperature variation during measurement period 1.7.-31.7.1999.

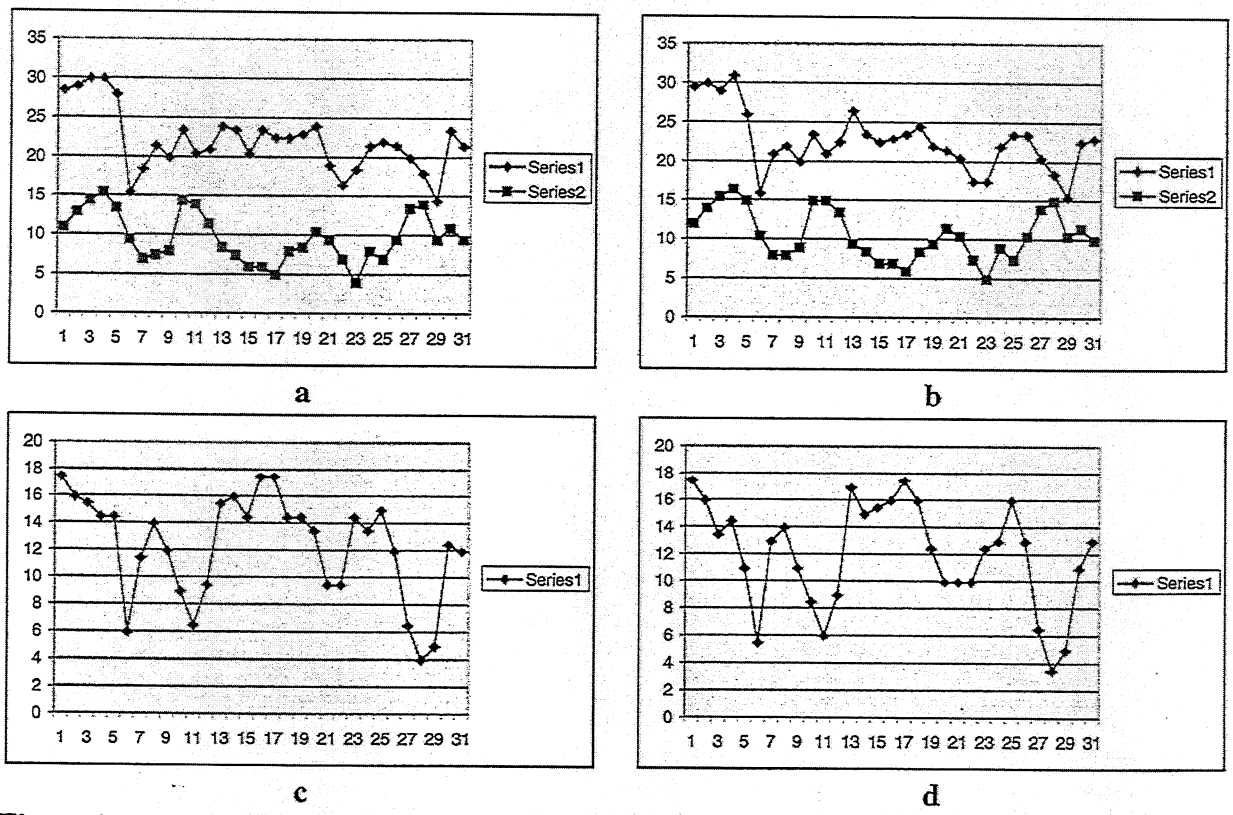

Figure 37. Daily temperature variation during measurement period 1.8.-31.8.1999.

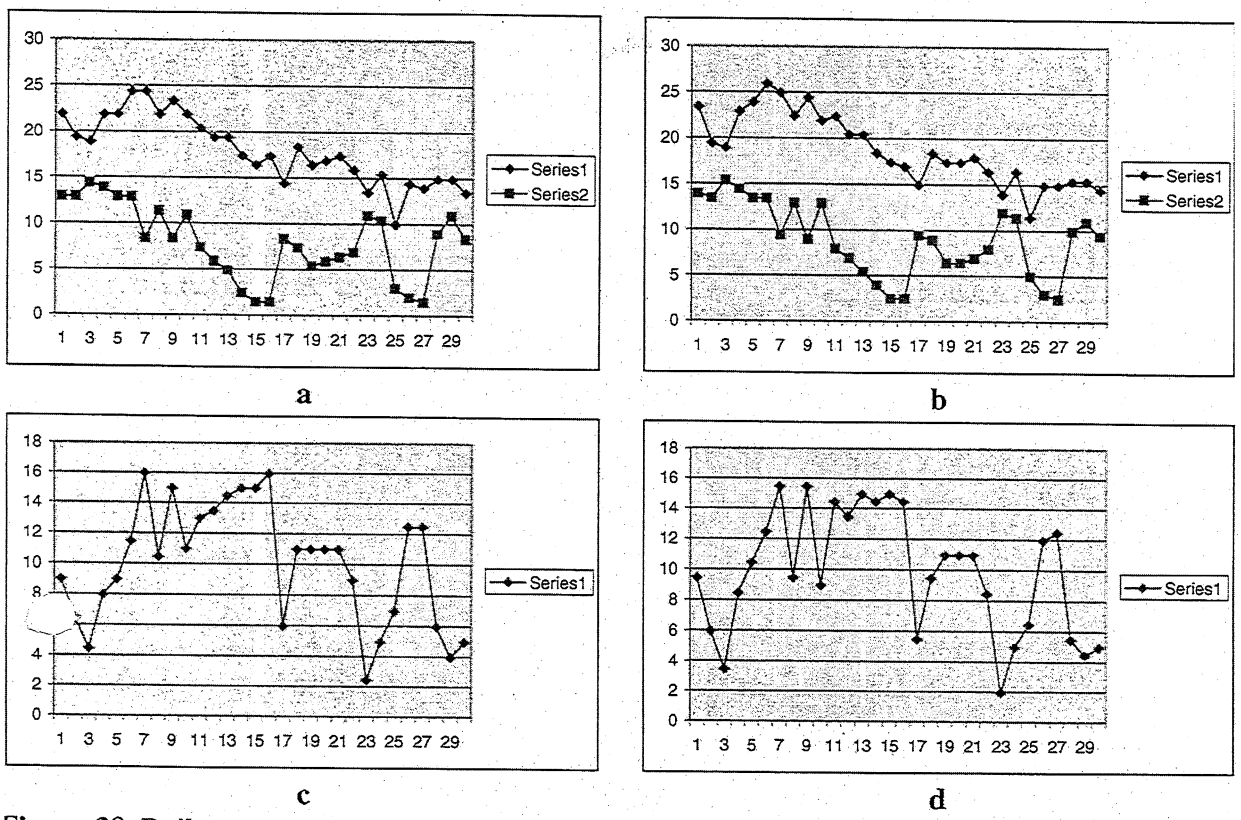

Figure 38. Daily temperature variation during measurement period 1.9.-30.9.1999.

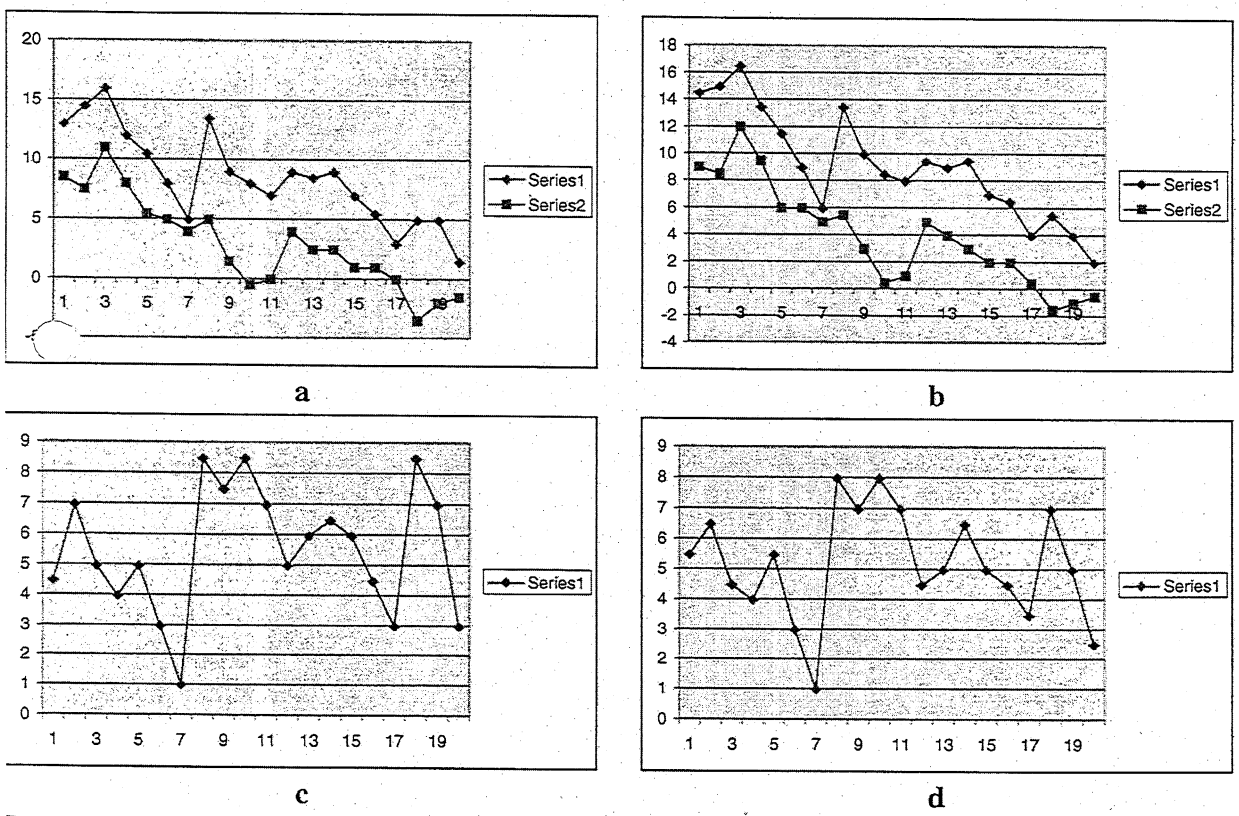

Figure 39. Daily temperature variation during measurement period 1.10.-20.10.1999.

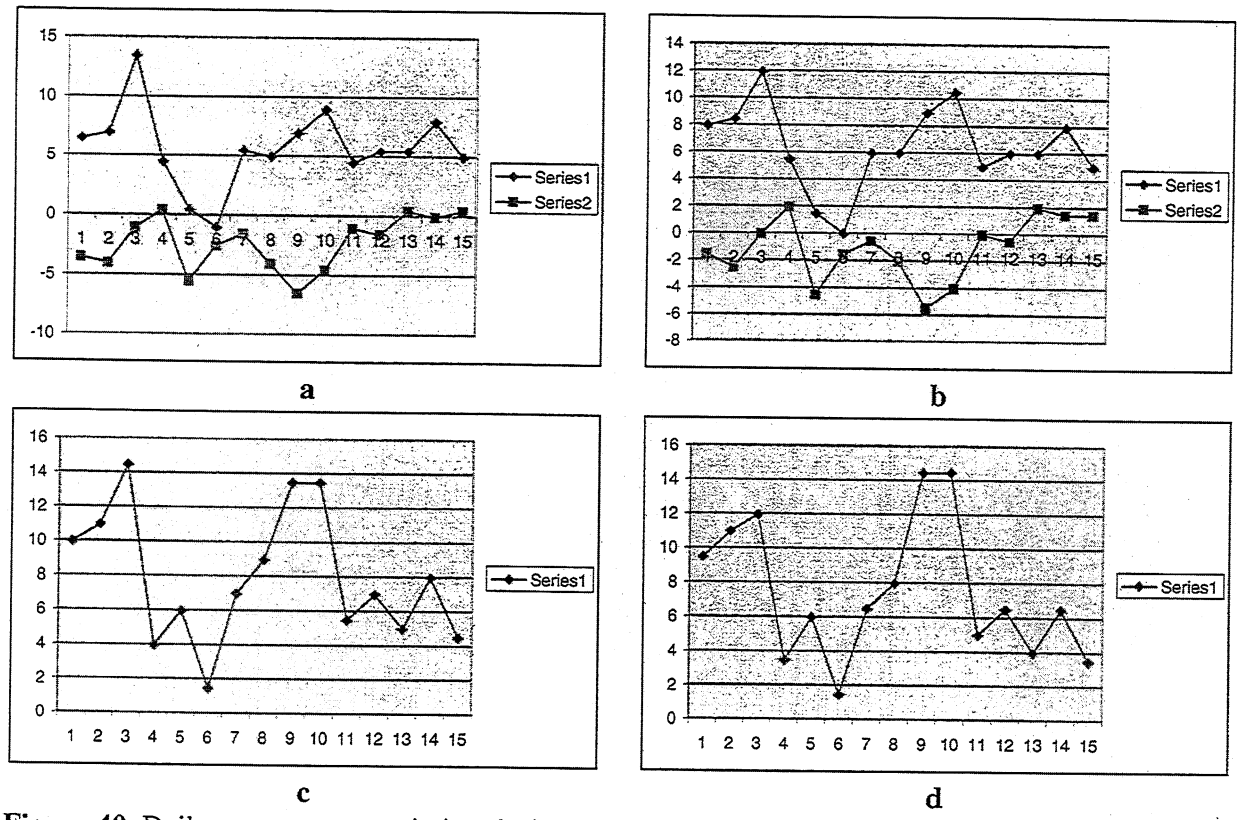

Figure 40. Daily temperature variation during measurement period 29.3.-12.4.2000.

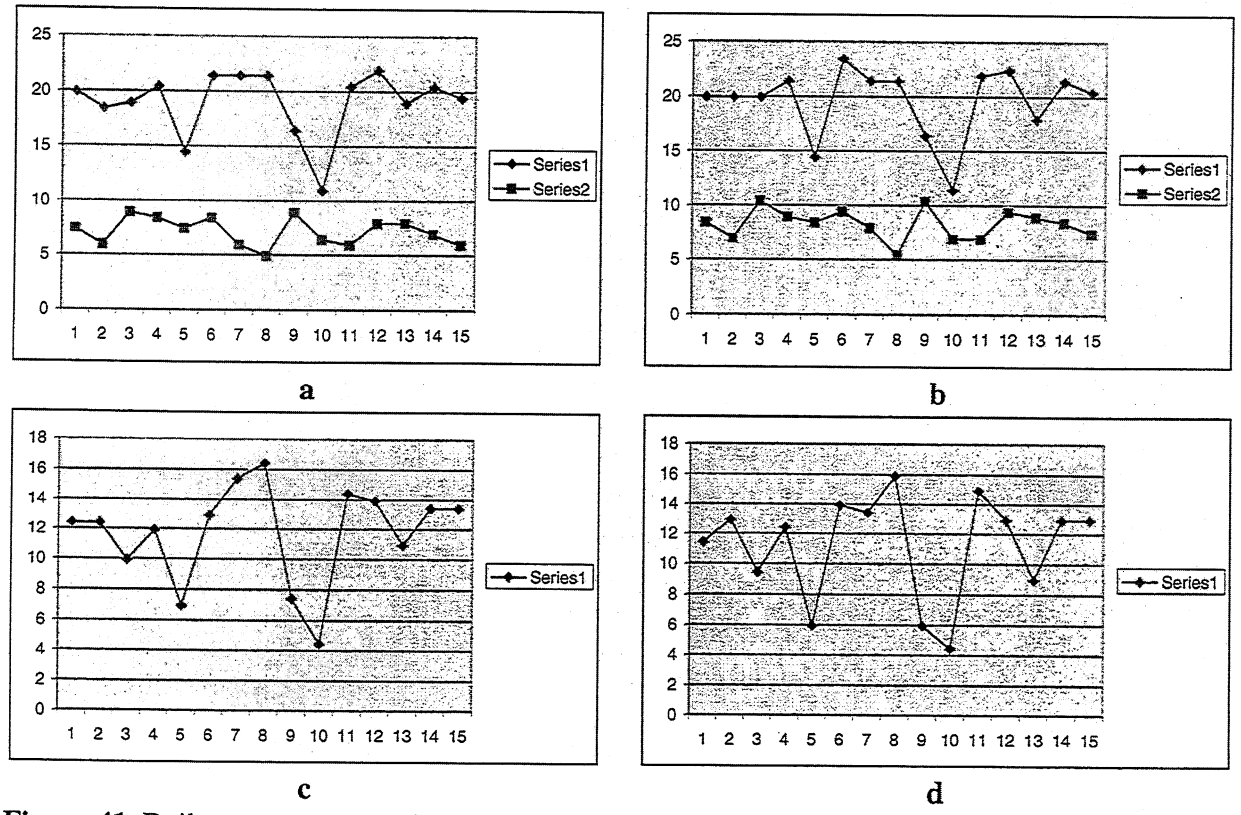

Figure 41. Daily temperature variation during measurement period 17.5.-31.5.2000.

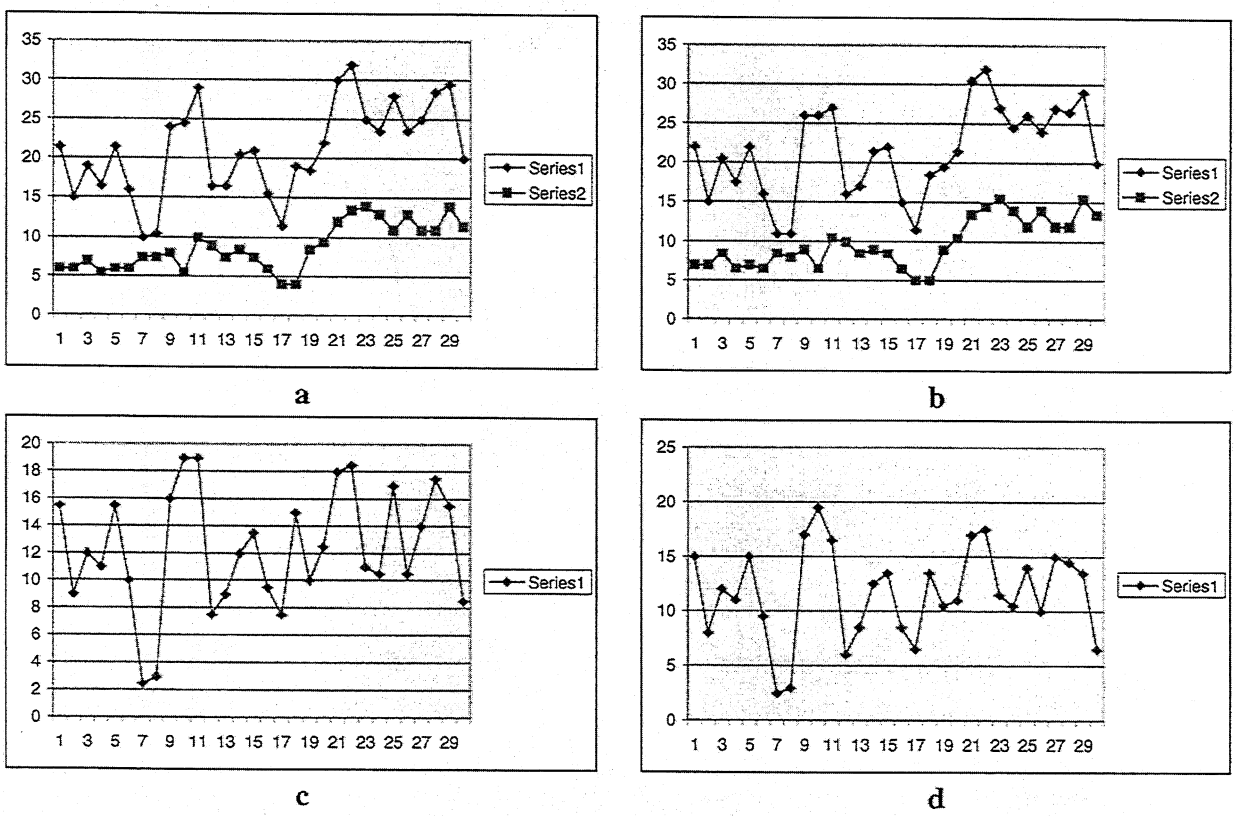

Figure 42. Daily temperature variation during measurement period 1.6.-30.6.2000.

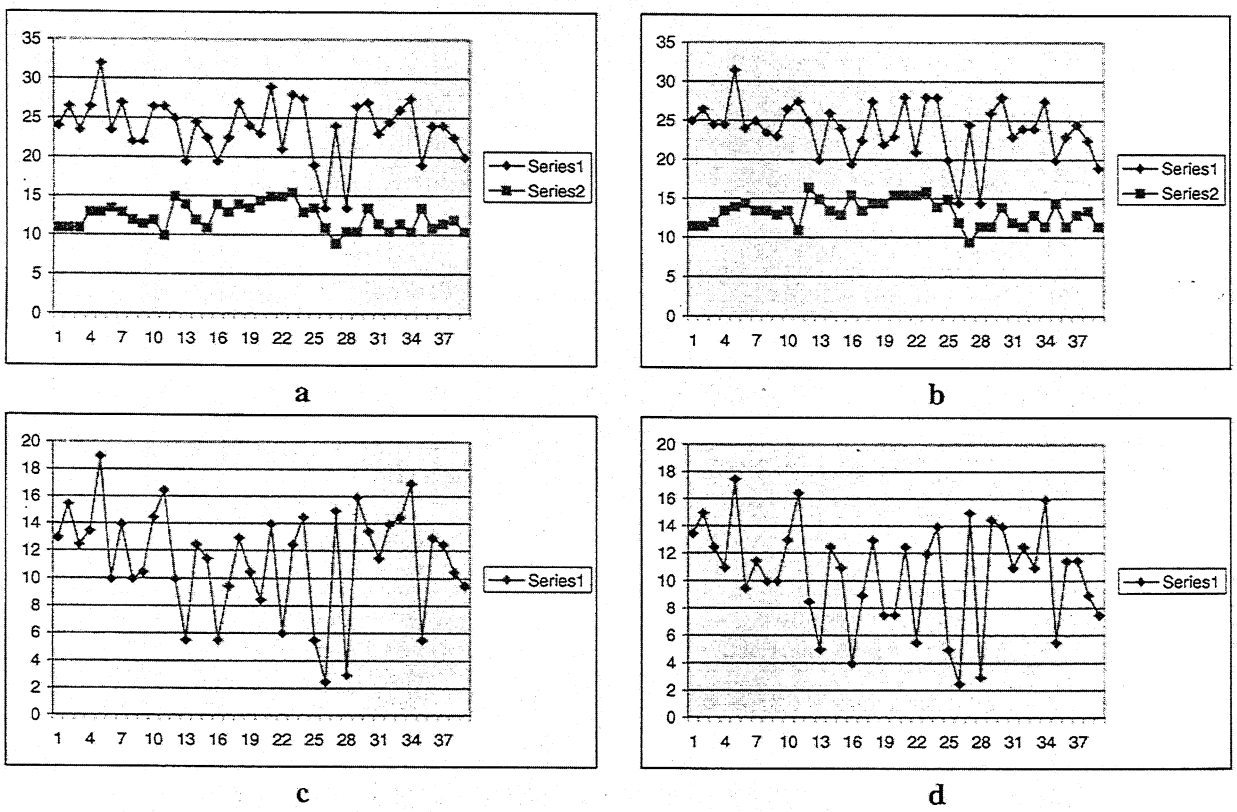

Figure 43. Daily temperature variation during measurement period 1.7.-8.8.2000.

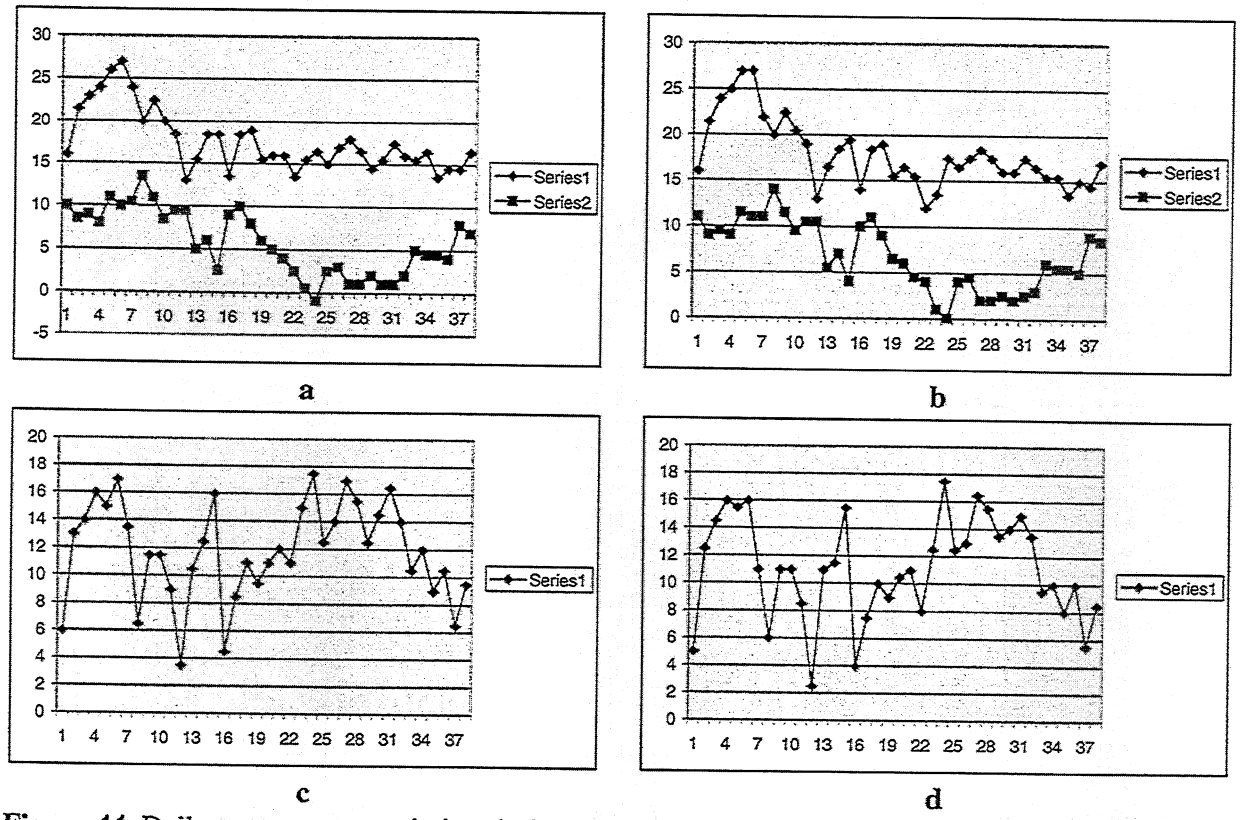

Figure 44. Daily temperature variation during measurement period 24.8.-30.9.2000.

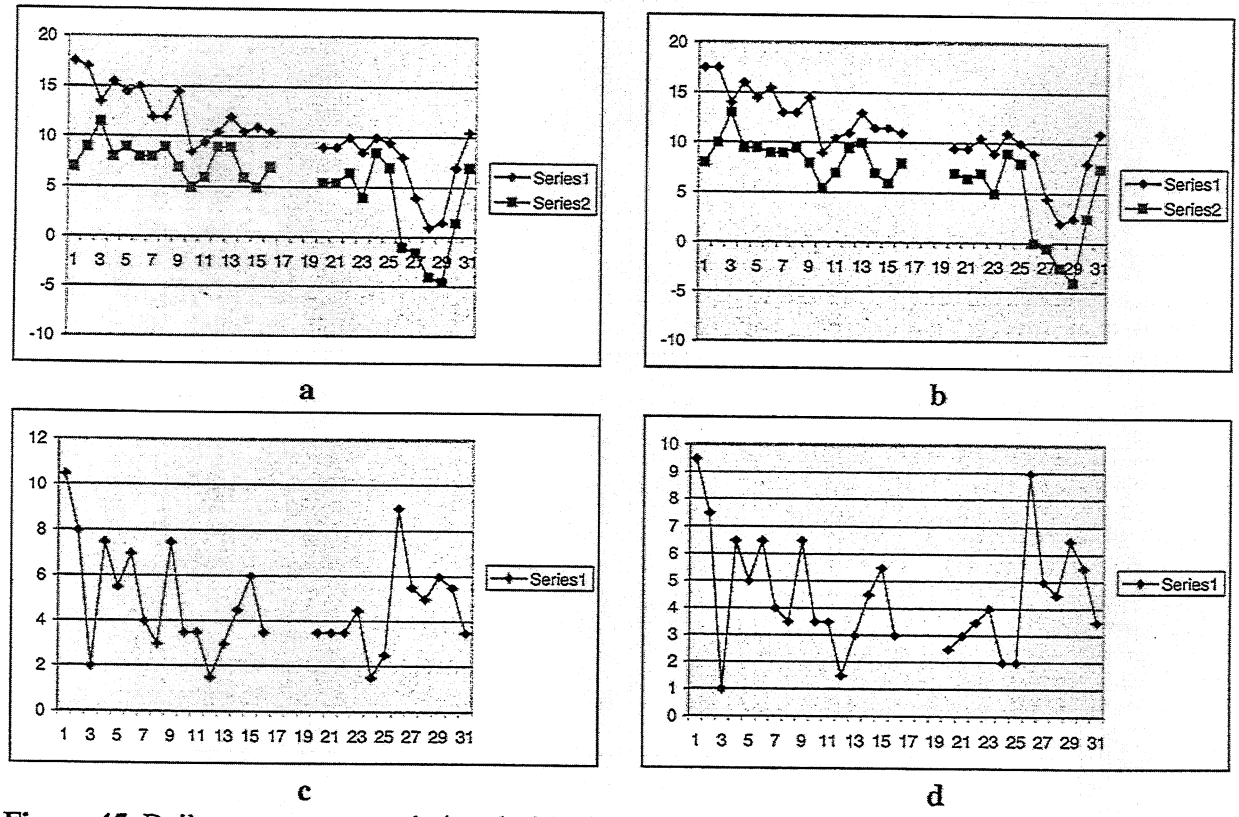

Figure 45. Daily temperature variation during measurement period 1.10.-31.10.2000.

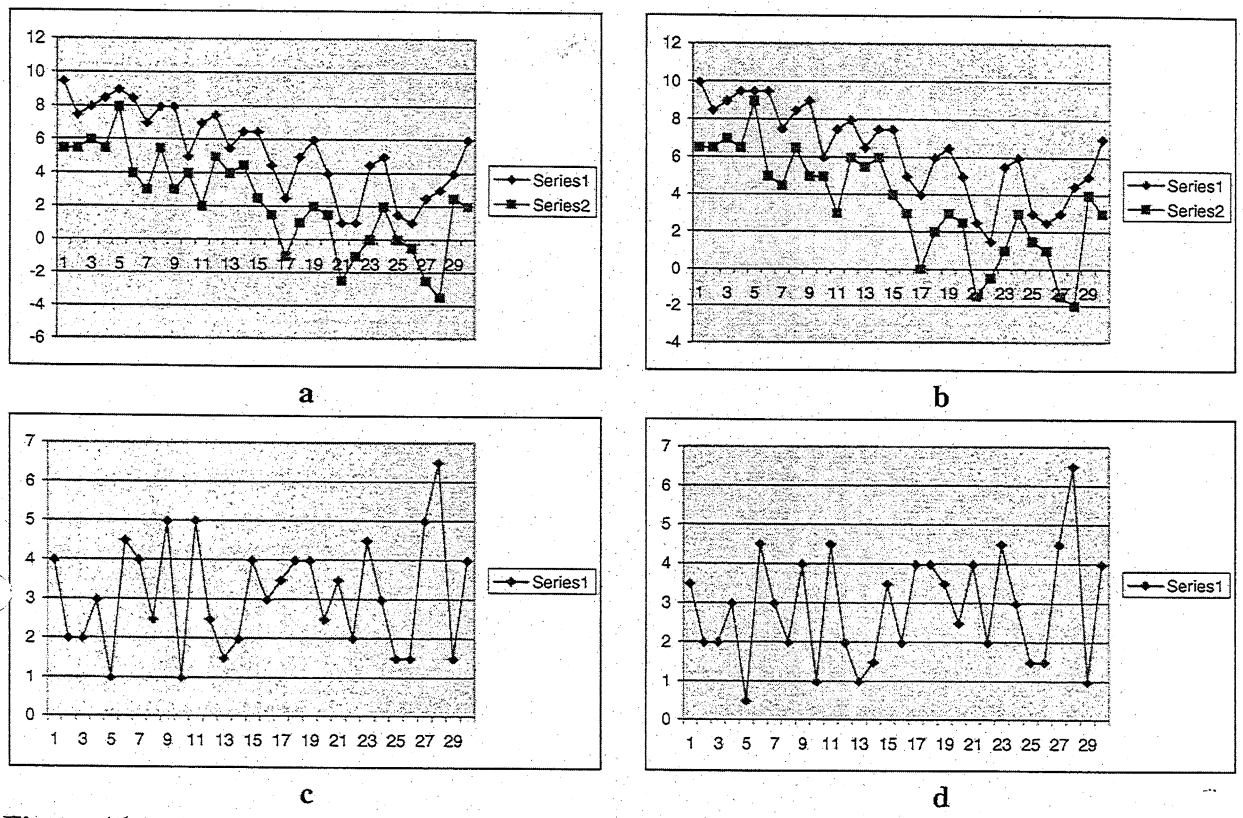

Figure 46. Daily temperature variation during measurement period 1.11.-30.11.2000.

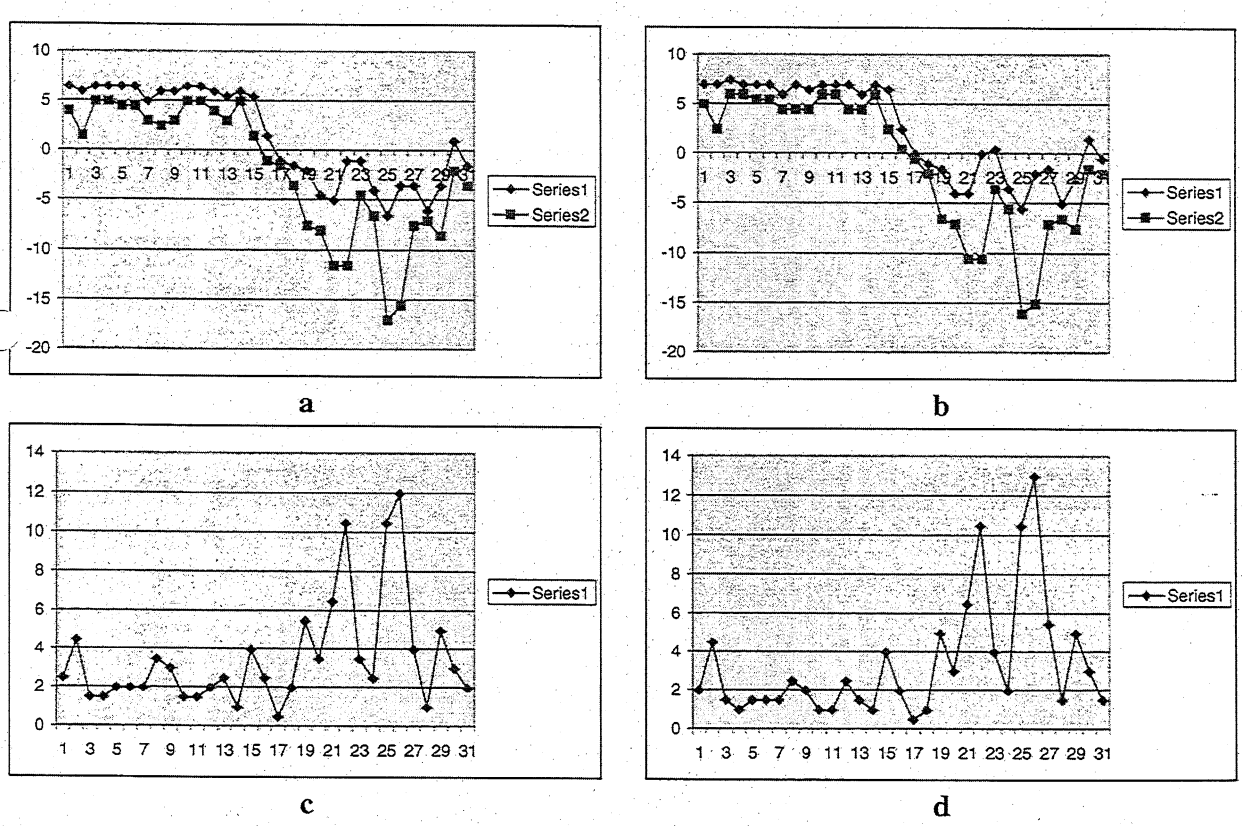

Figure 47. Daily temperature variation during measurement period 1.12.-31.12.2000.

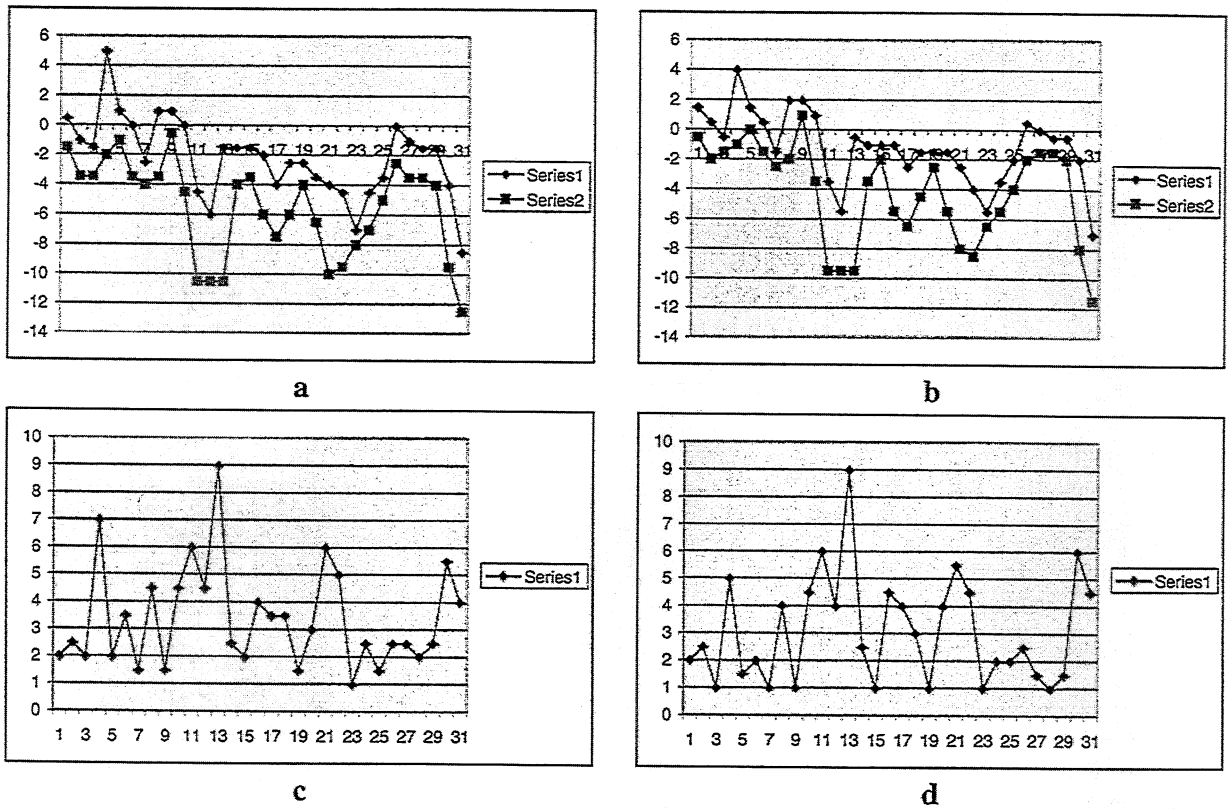

Figure 48. Daily temperature variation during measurement period 1.1.-31.1.2001.

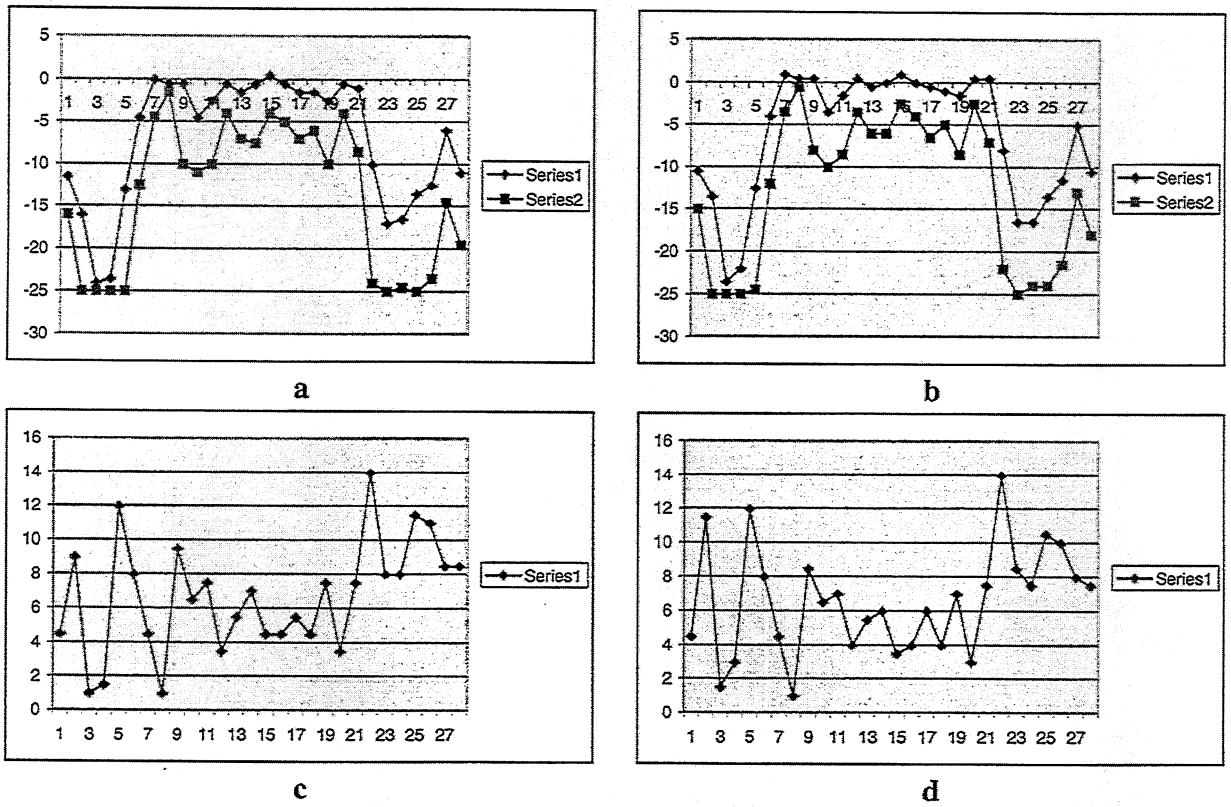

Figure 49. Daily temperature variation during measurement period 1.2.-28.2.2001.

4.3.4 Measuring point D

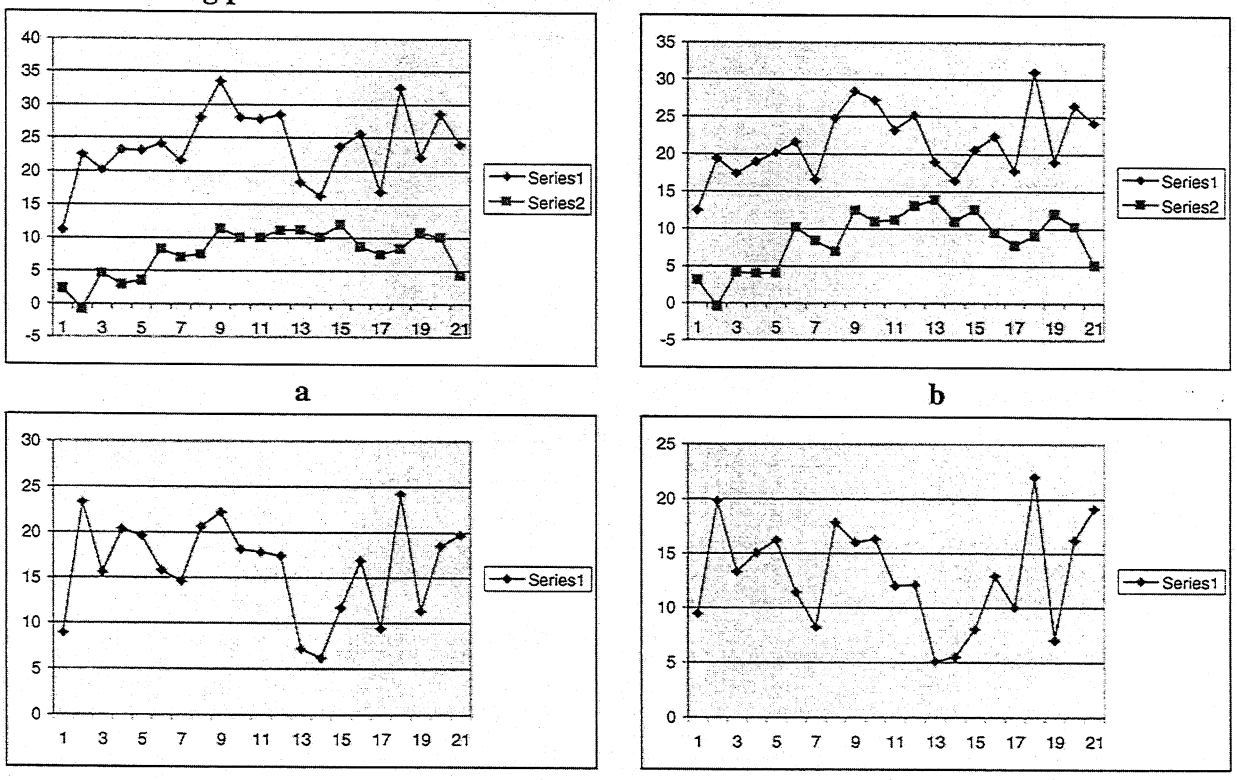

Figure 50. Daily temperature variation during measurement period 11.5.-31.5.1999.

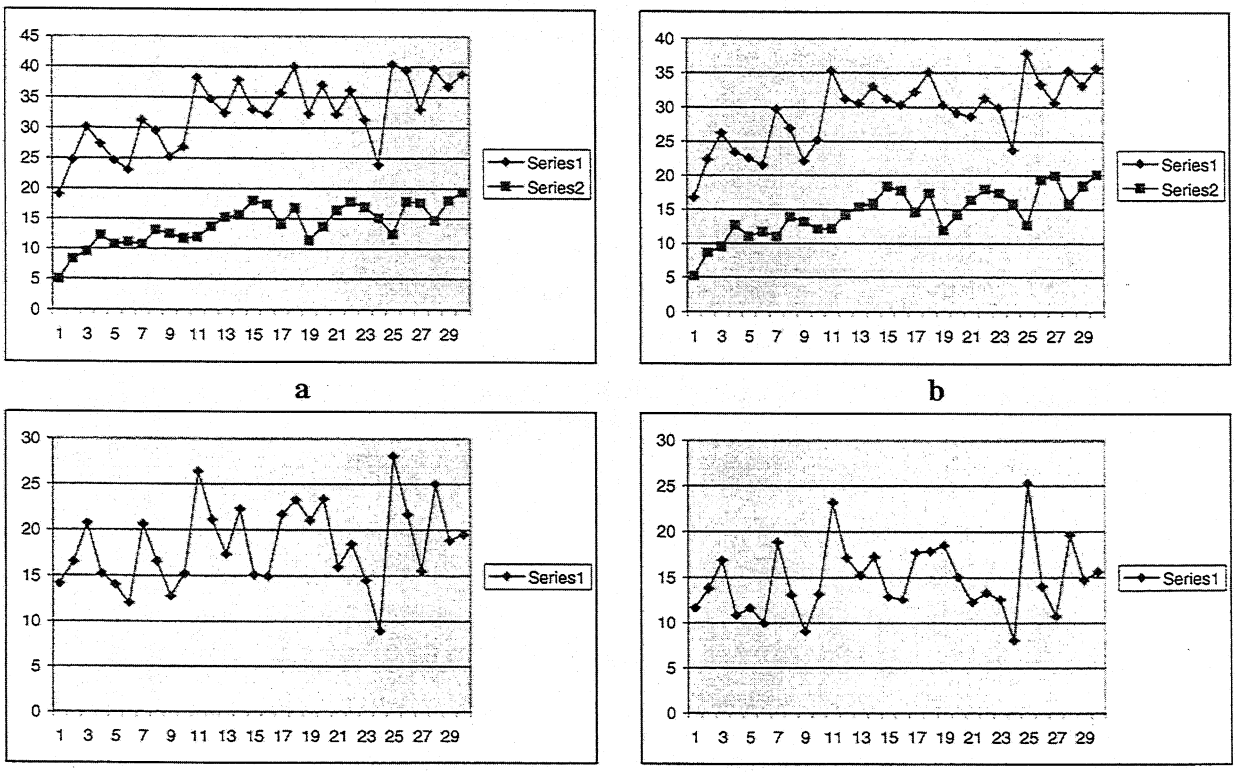

Figure 51. Daily temperature variation during measurement period 1.6.-30.6.1999.

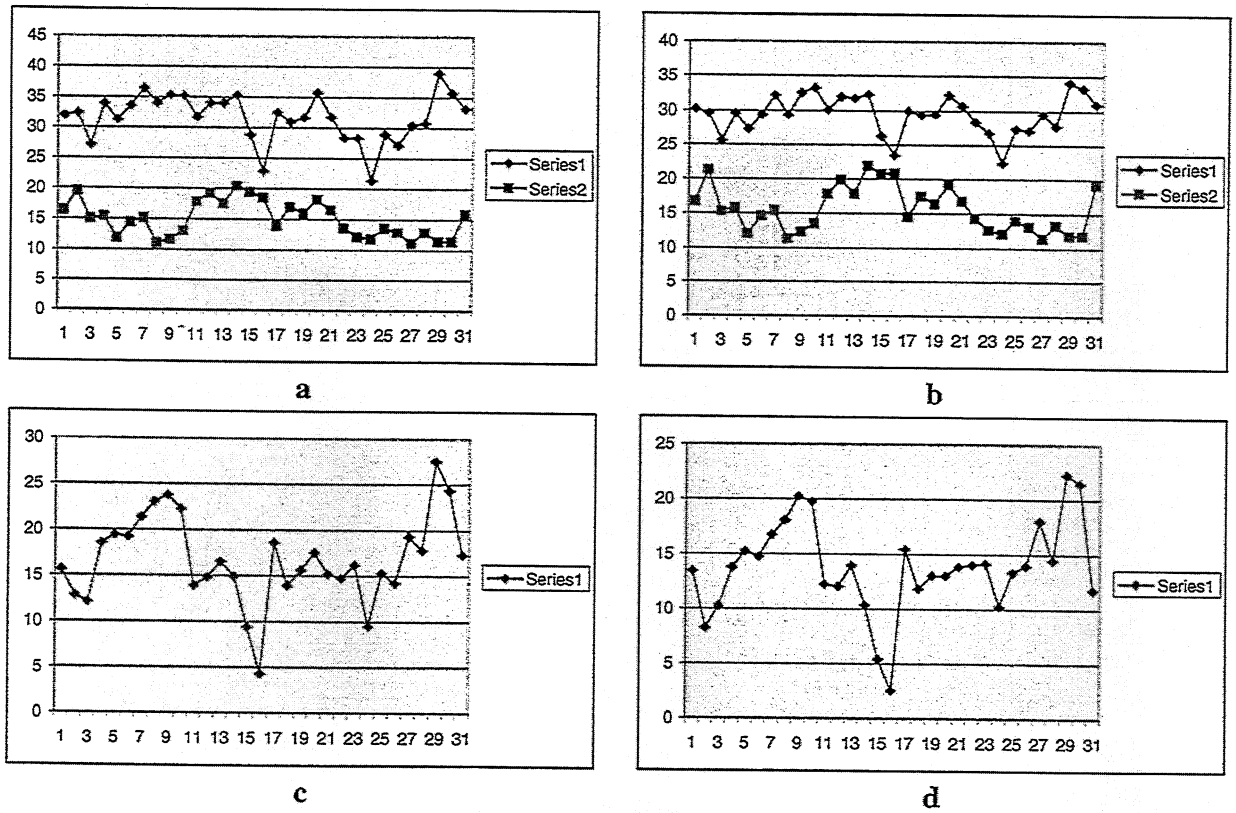

Figure 52. Daily temperature variation during measurement period 1.7.-31.7.1999.

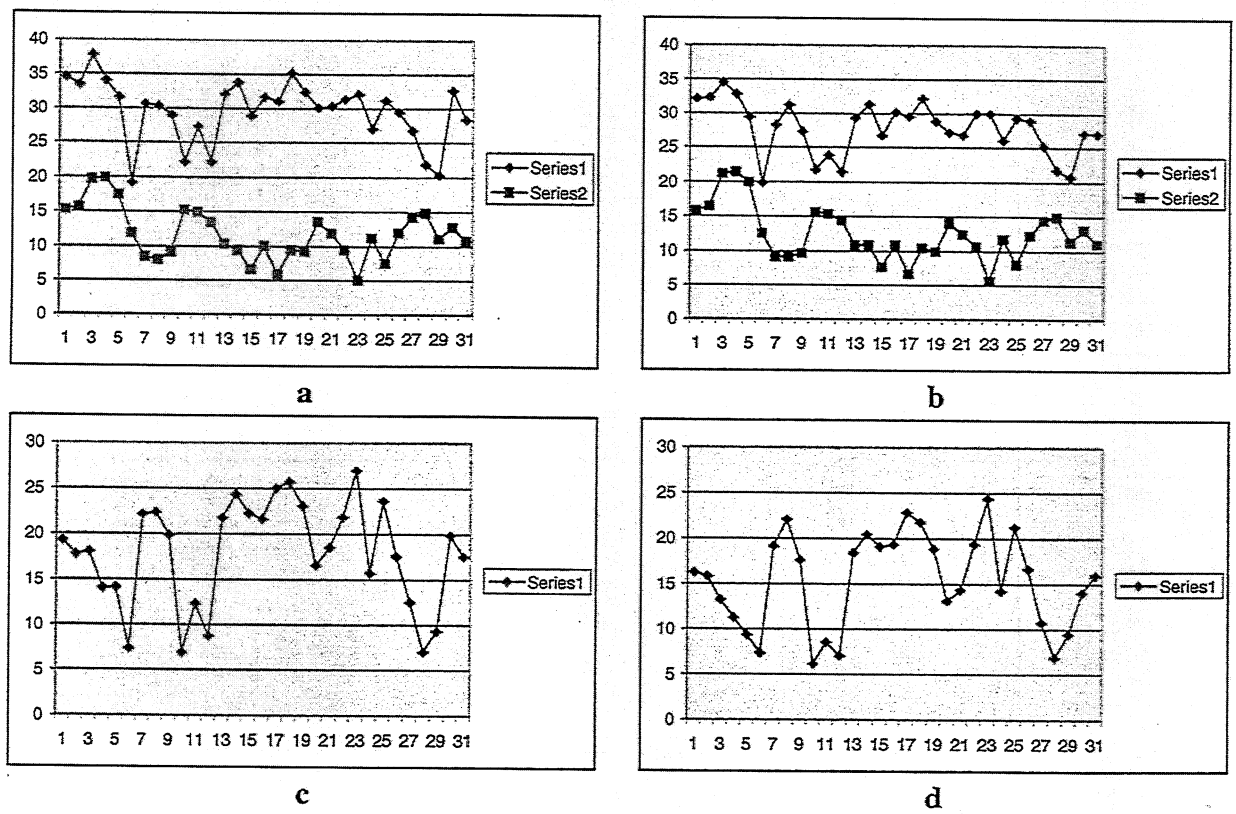

Figure 53. Daily temperature variation during measurement period 1.8.-31.8.1999.

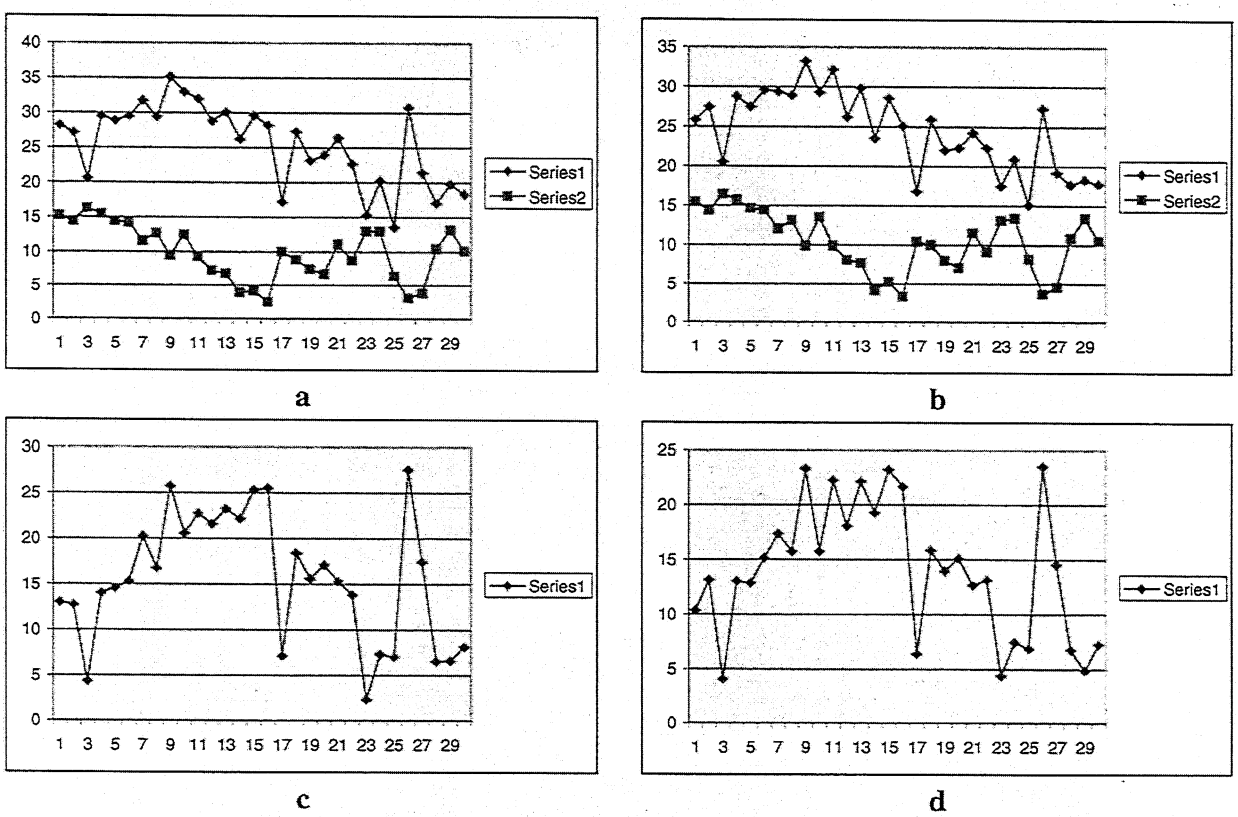

Figure 54. Daily temperature variation during measurement period 1.9.-30.9.1999.

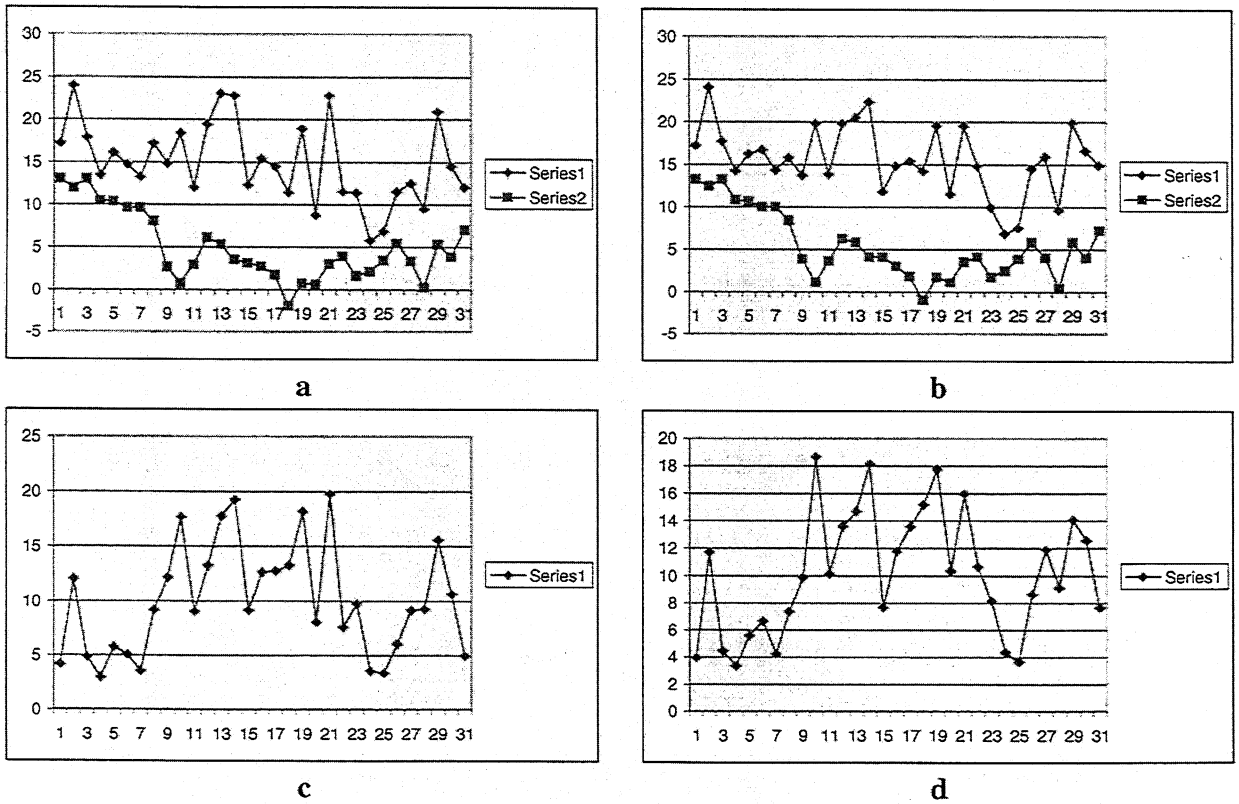

Figure 55. Daily temperature variation during measurement period 1.10.-31.10.1999.

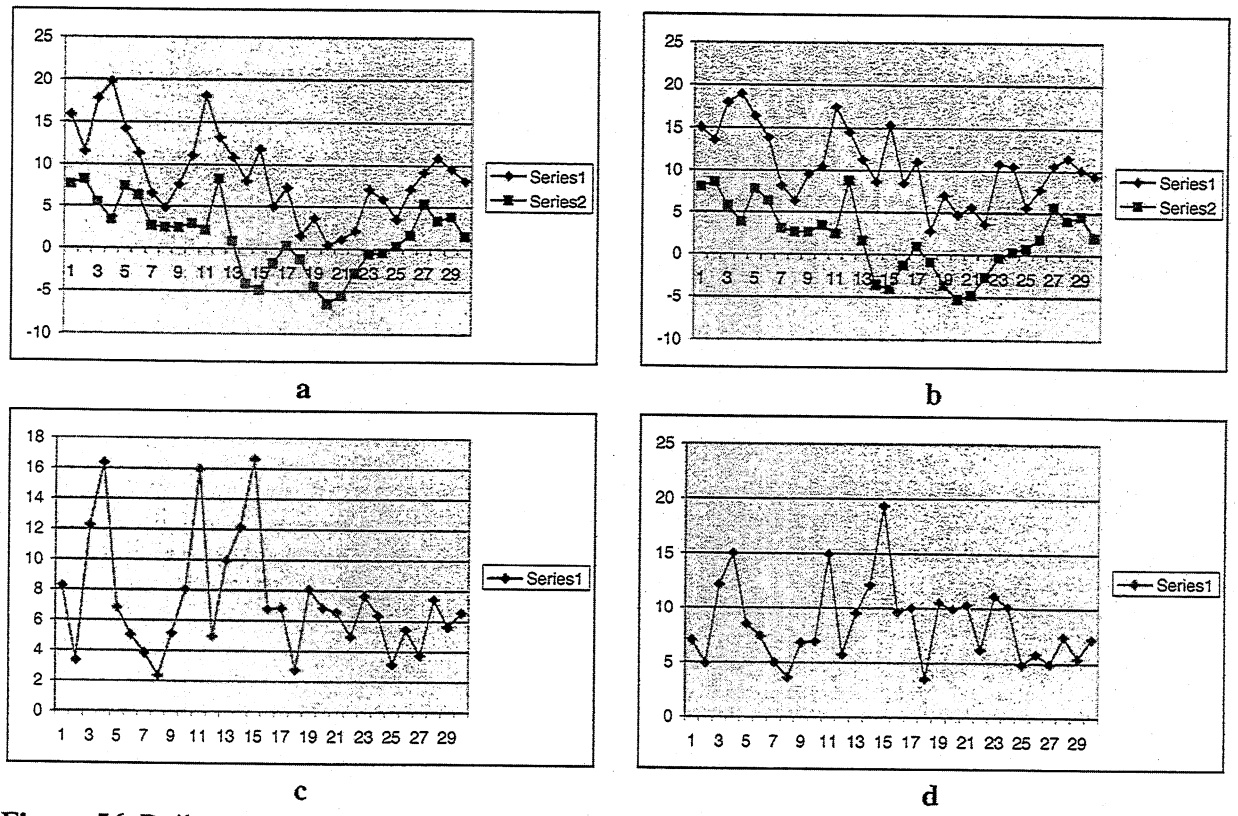

Figure 56. Daily temperature variation during measurement period 1.11.-30.11.1999.

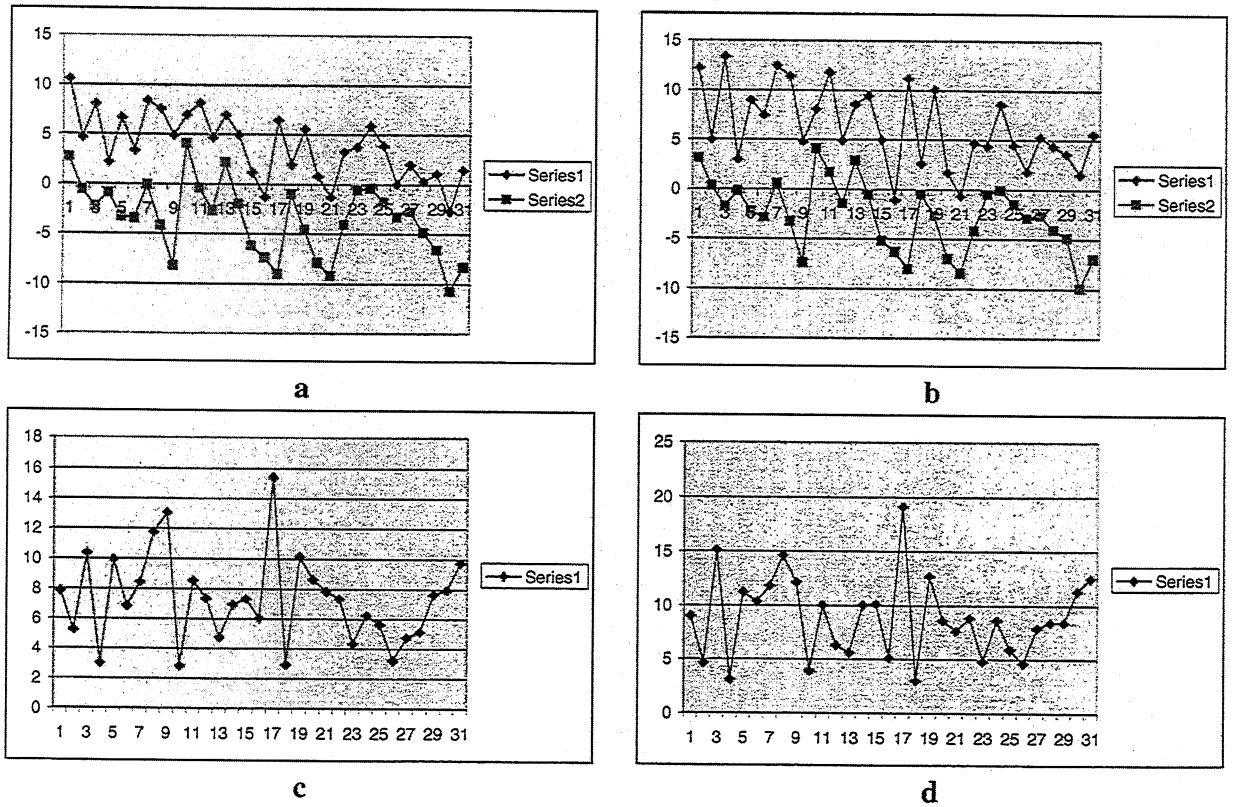

Figure 57. Daily temperature variation during measurement period 1.12.-31.12.1999.

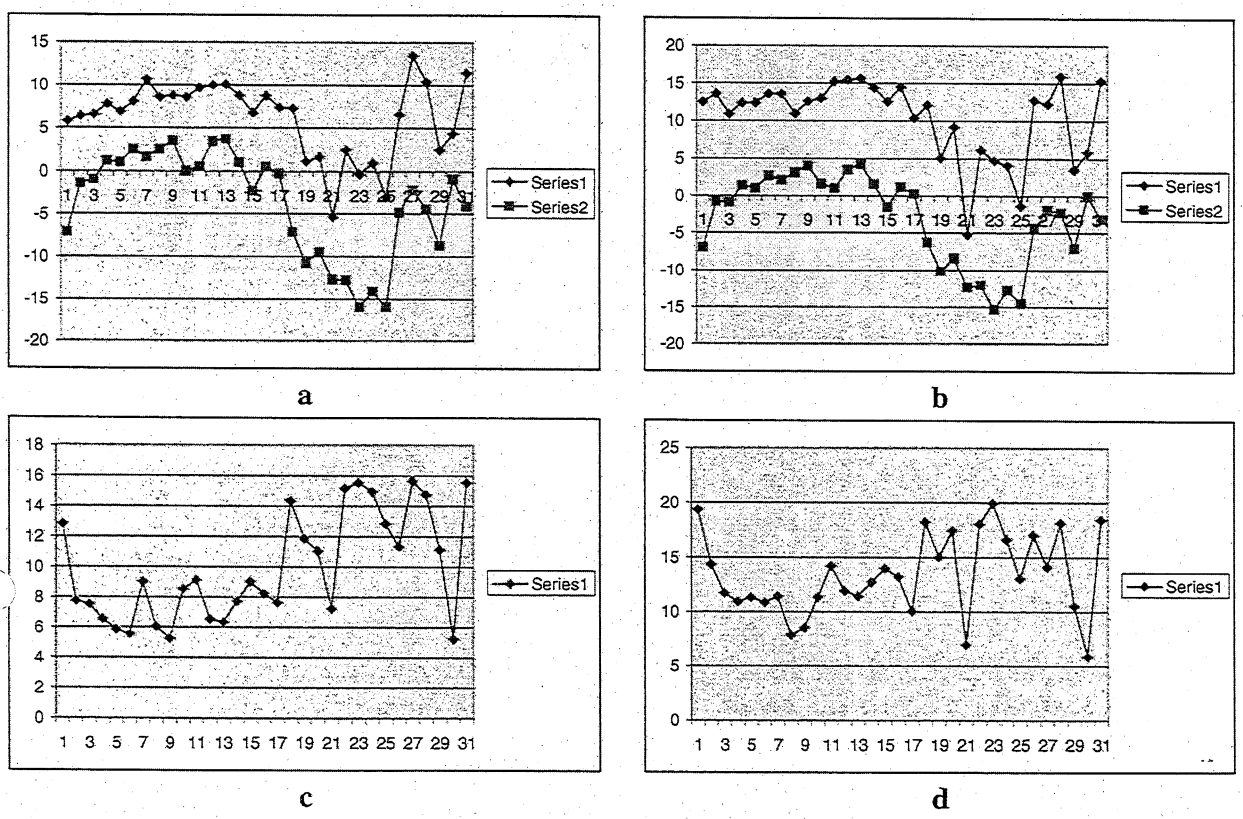

Figure 58. Daily temperature variation during measurement period 1.1.-31.1.2000.

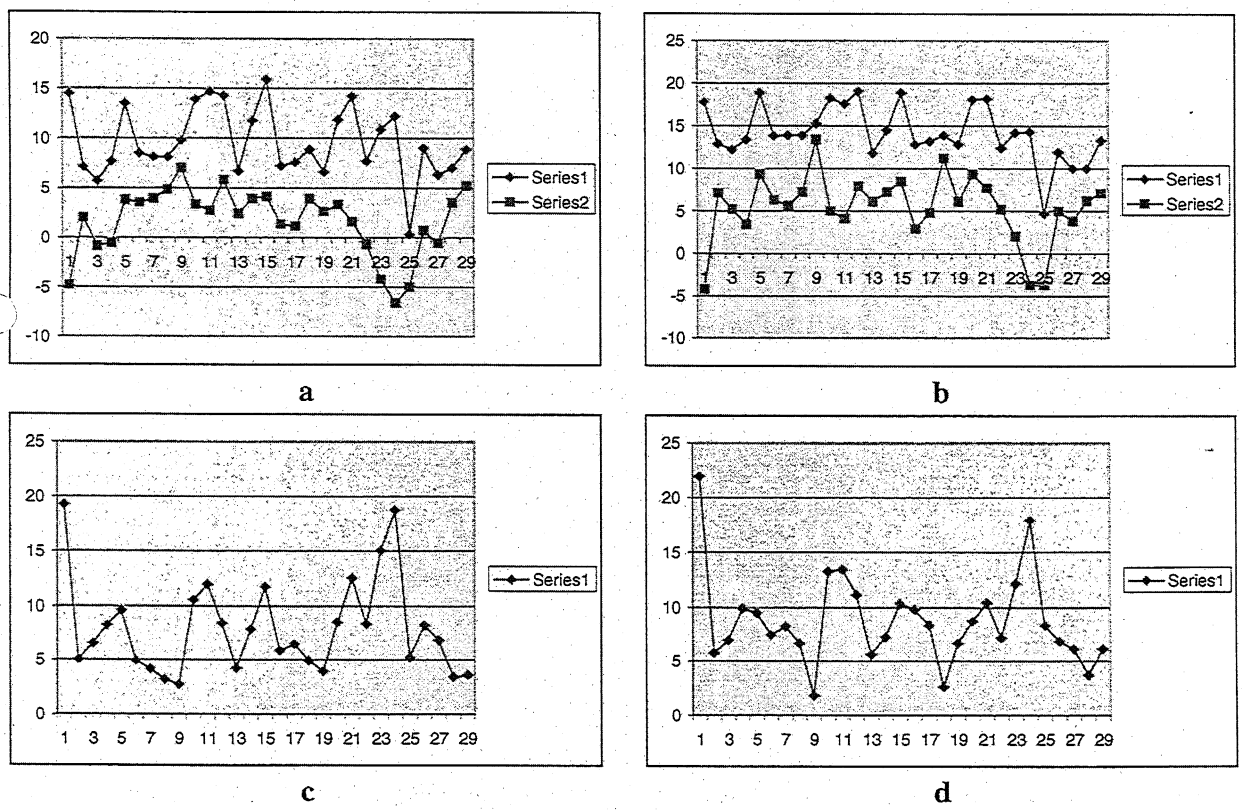

Figure 59. Daily temperature variation during measurement period 1.2.-29.2.2000.

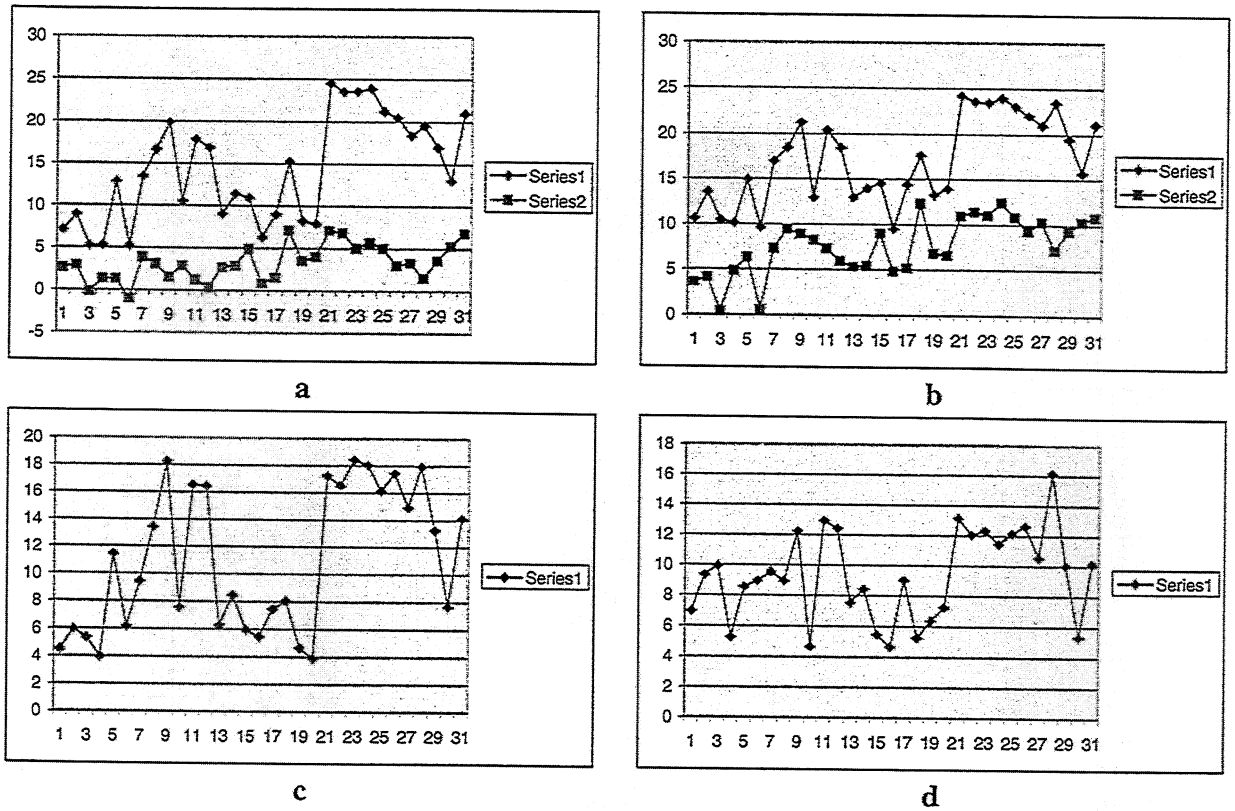

Figure 60. Daily temperature variation during measurement period 1.3.-31.3.2000.

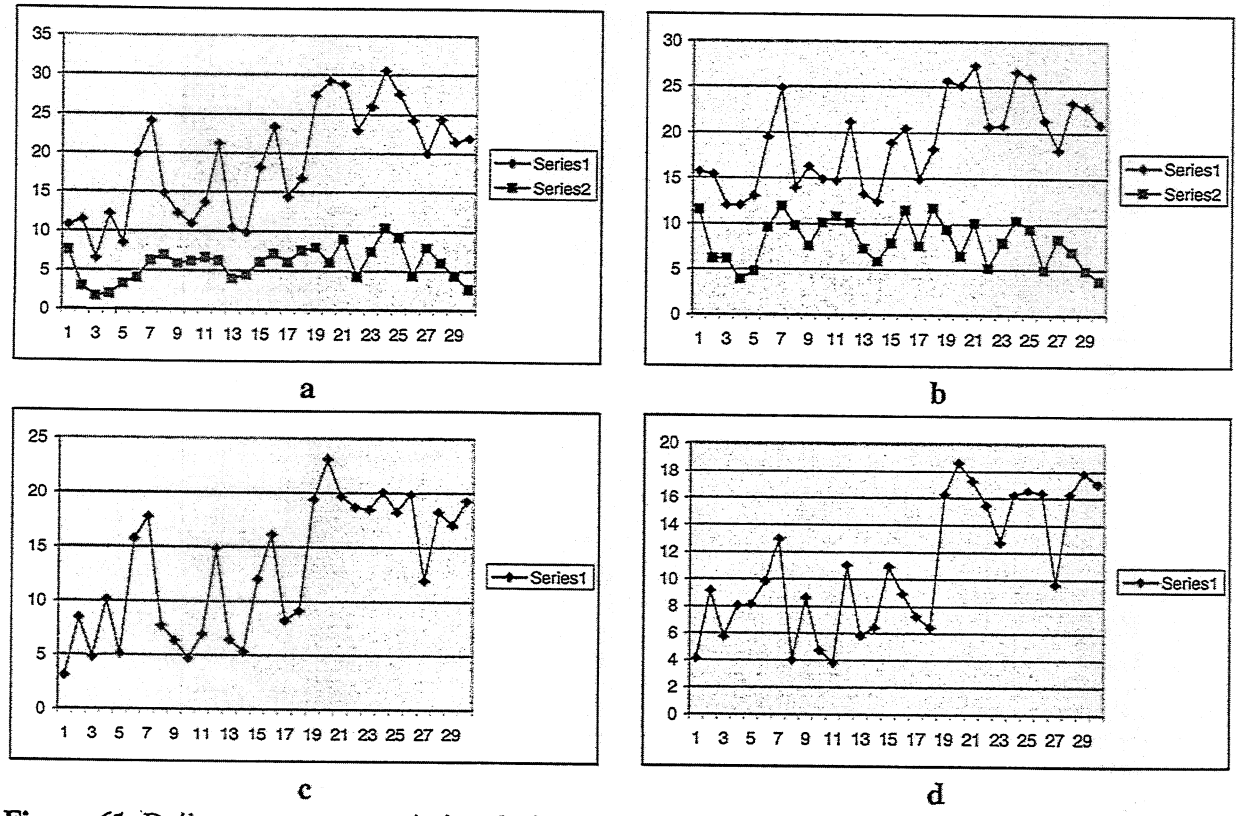

Figure 61. Daily temperature variation during measurement period 1.4.-30.4.2000.

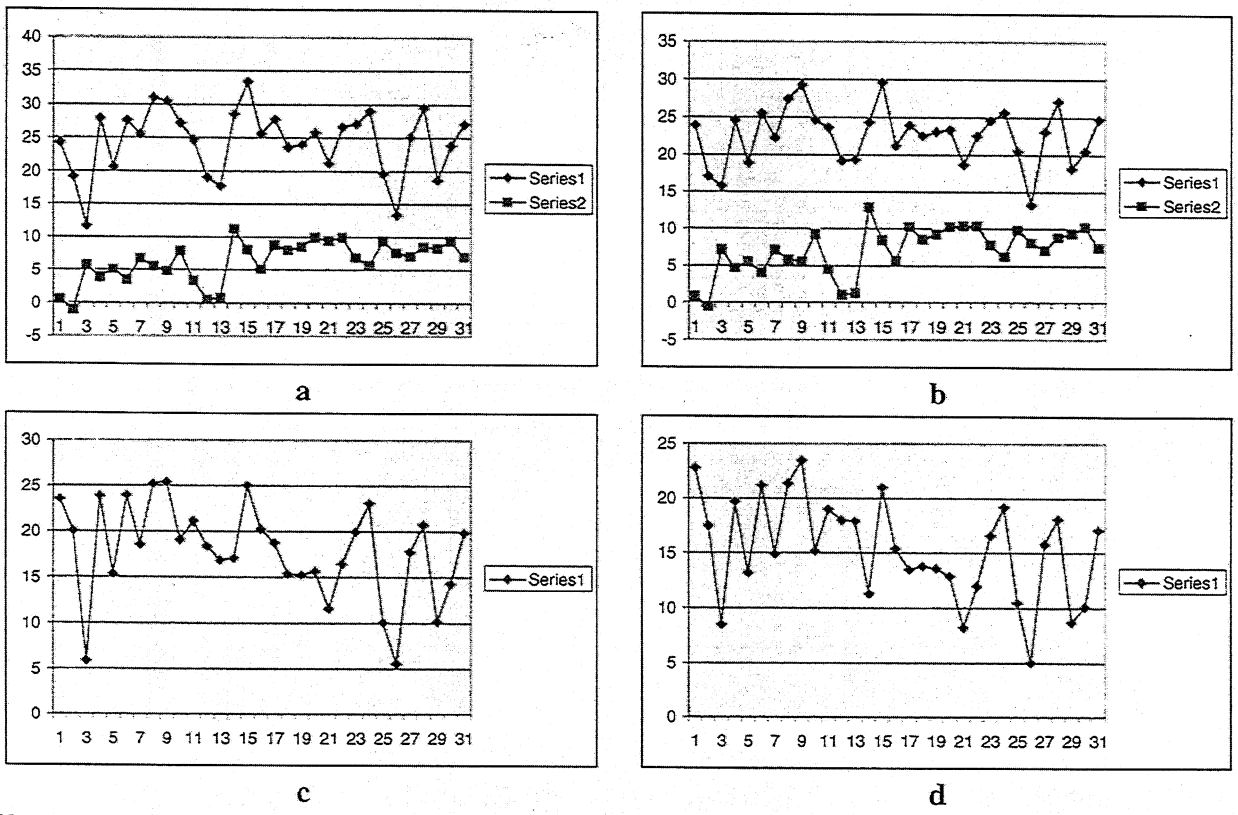

Figure 62. Daily temperature variation during measurement period 1.5.-31.5.2000.

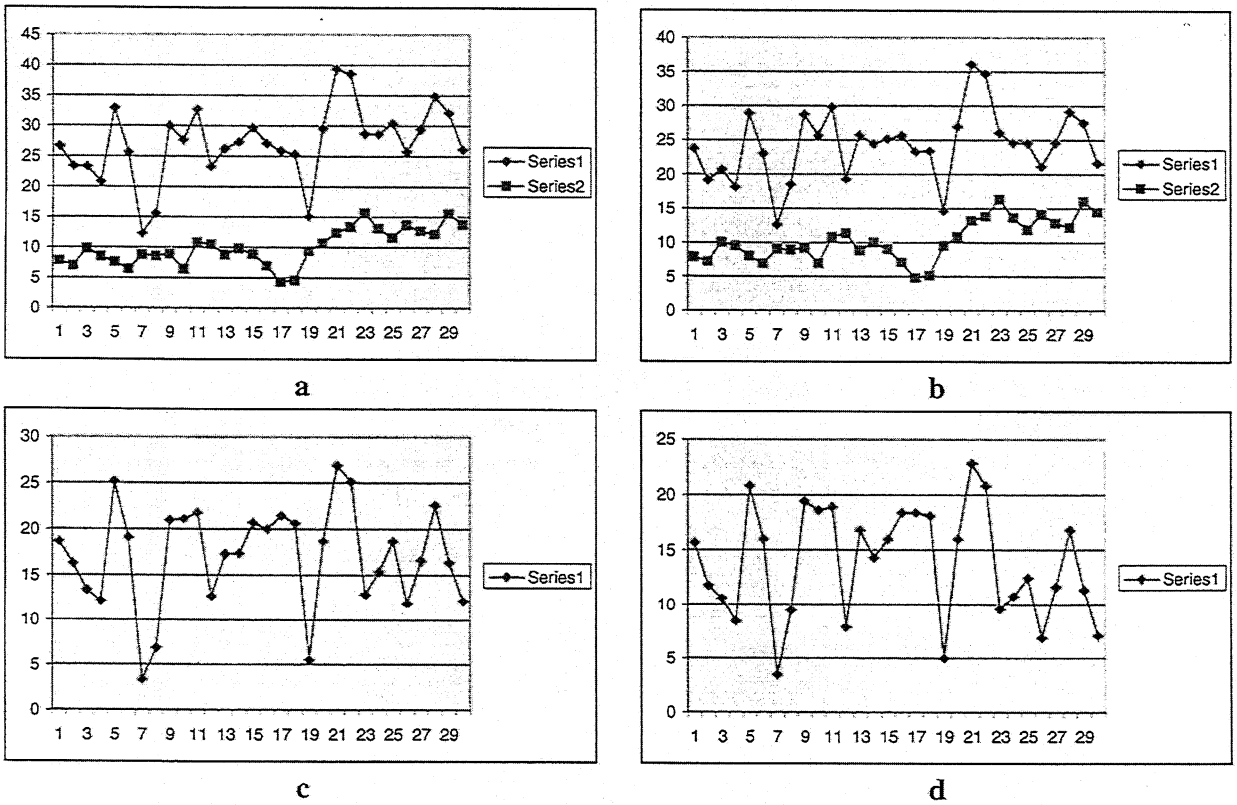

Figure 63. Daily temperature variation during measurement period 1.6.-30.6.2000.

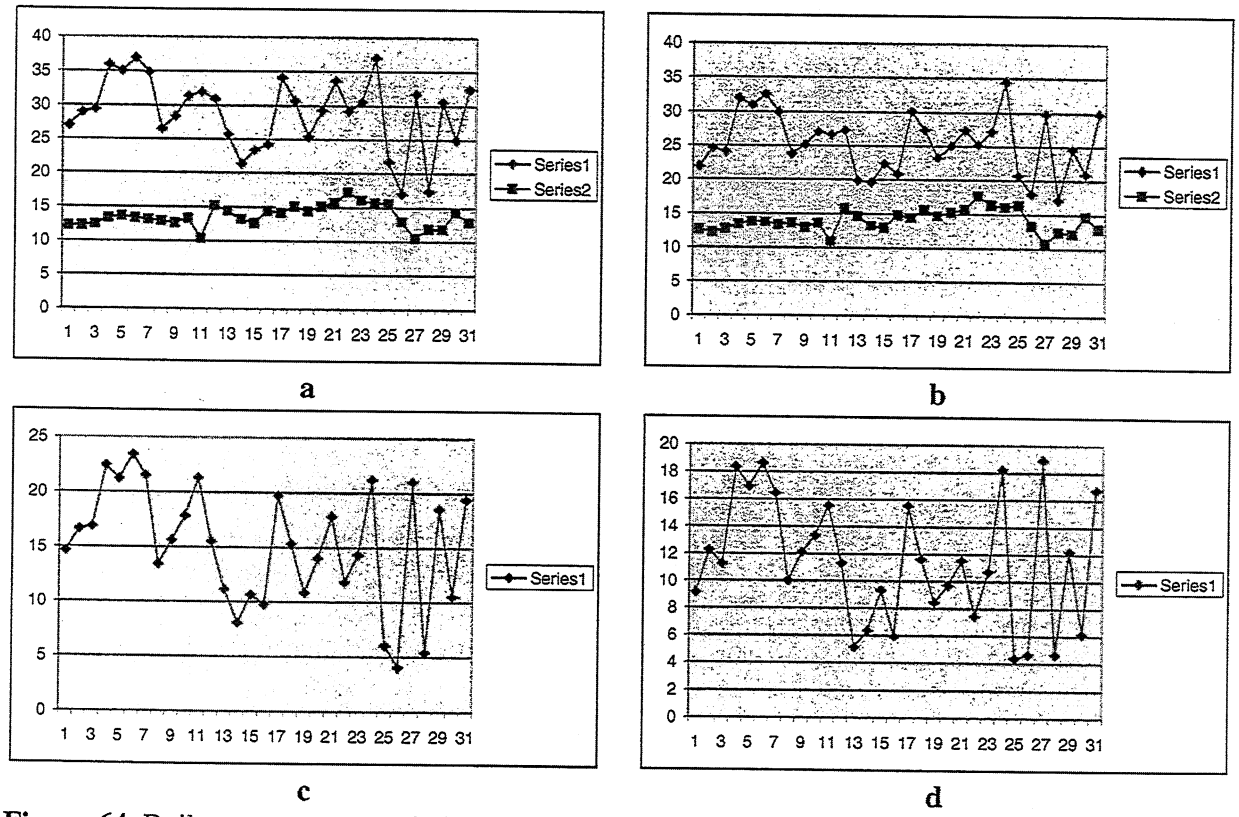

Figure 64. Daily temperature variation during measurement period 1.7.-31.7.2000.

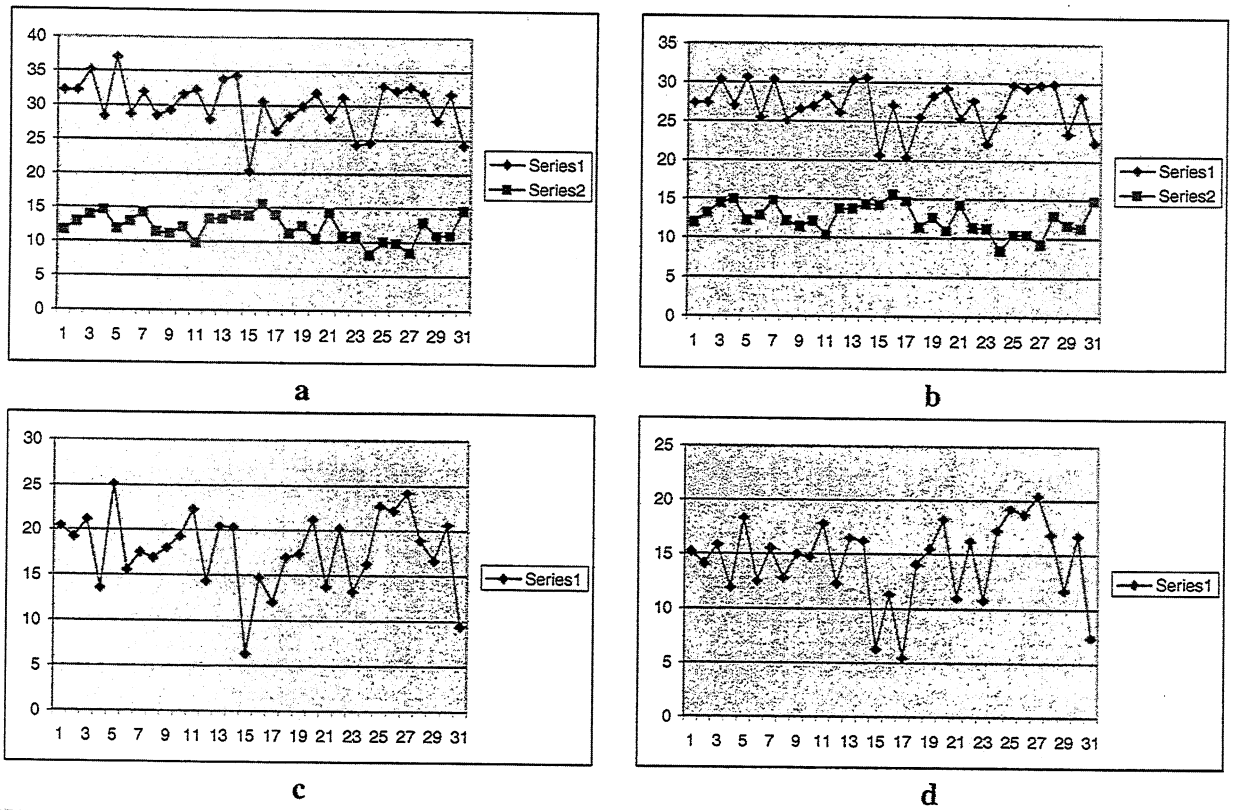

Figure 65. Daily temperature variation during measurement period 1.8.-31.8.2000.

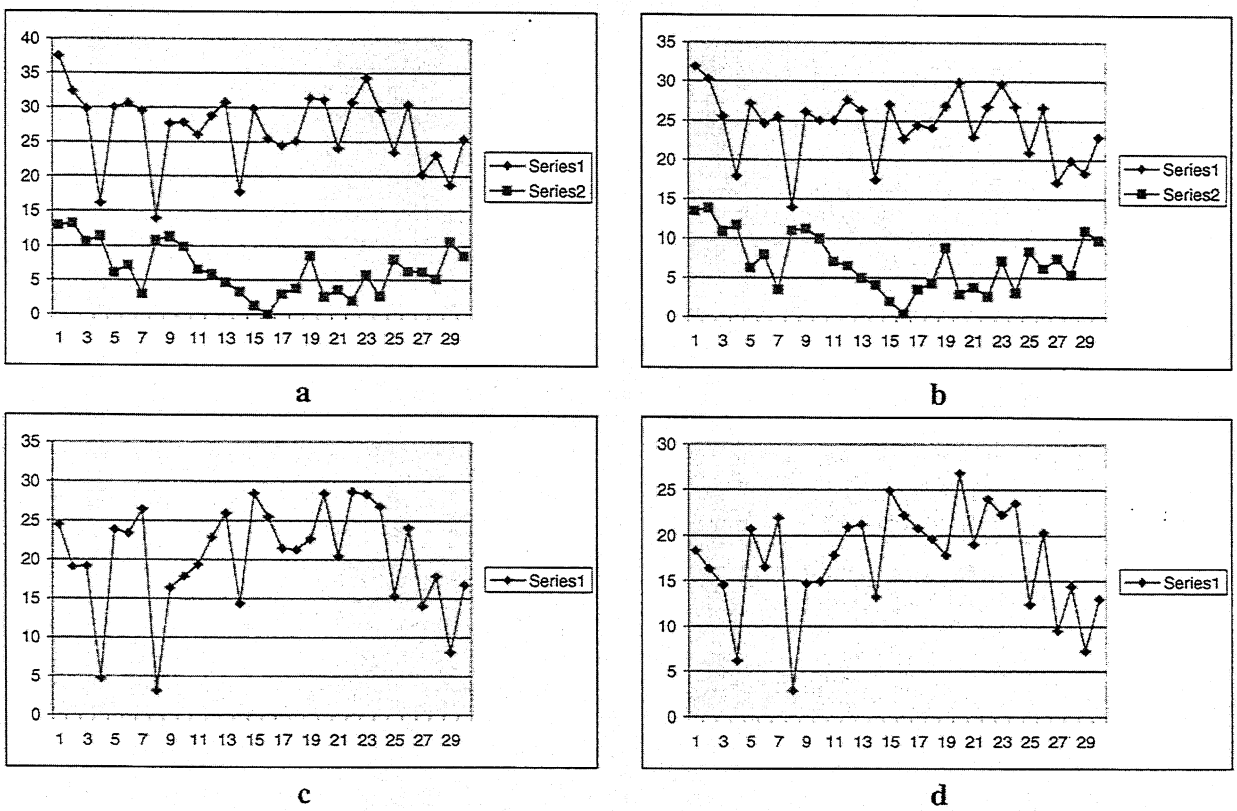

Figure 66. Daily temperature variation during measurement period 1.9.-30.9.2000.

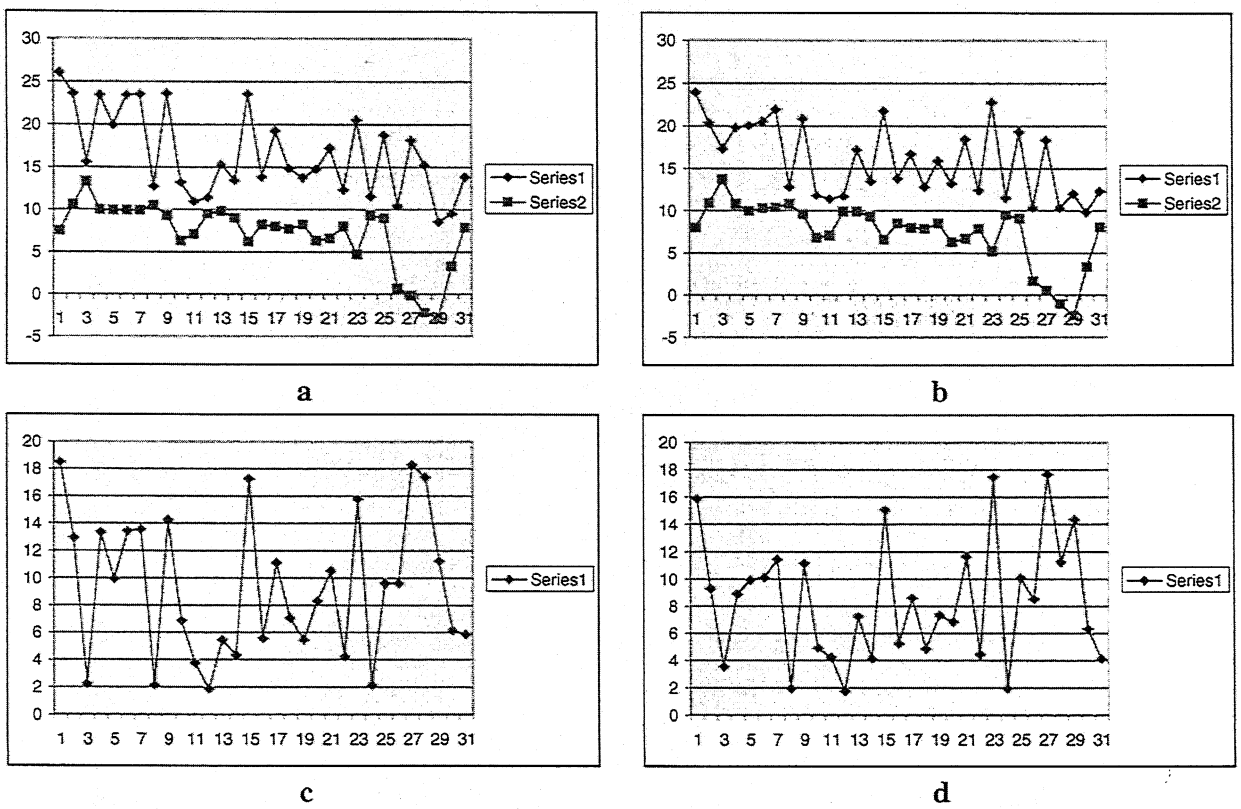

Figure 67. Daily temperature variation during measurement period 1.10.-31.10.2000.

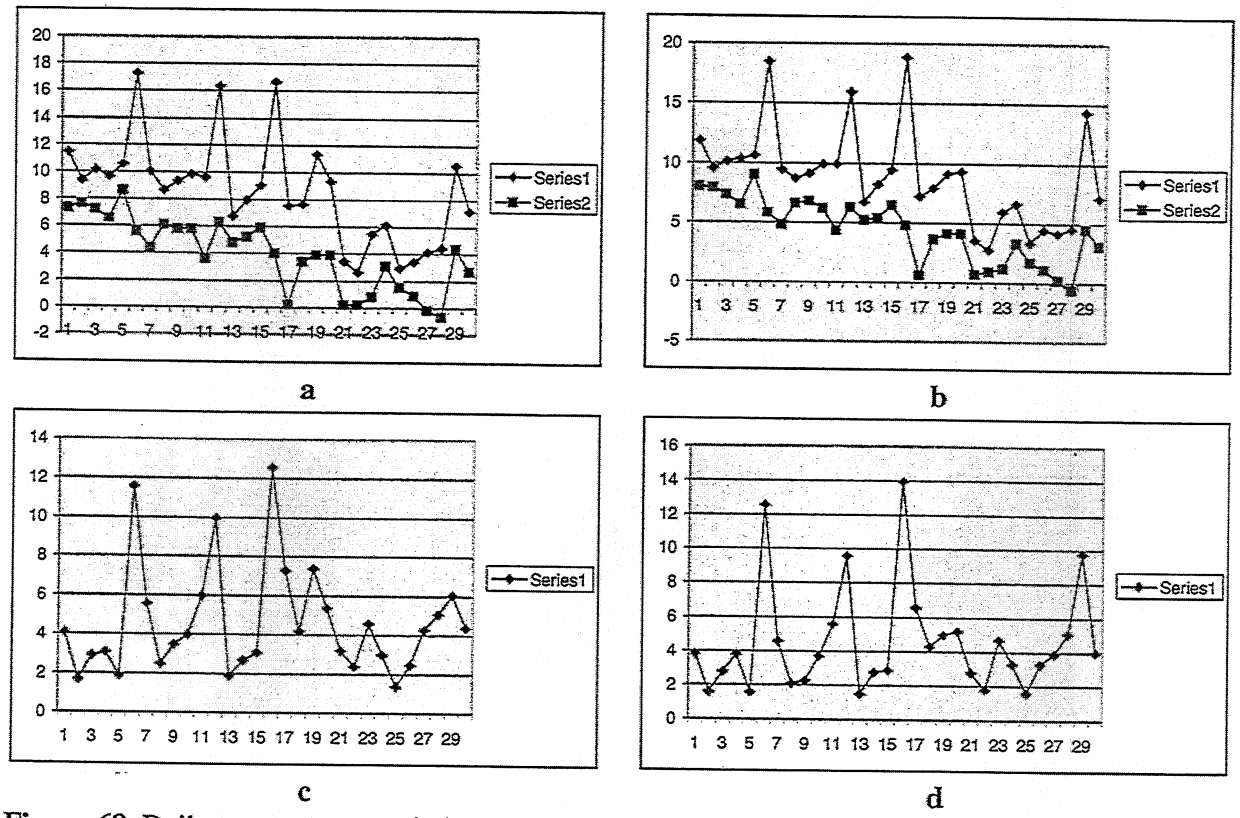

Figure 68. Daily temperature variation during measurement period 1.11.-30.11.2000.

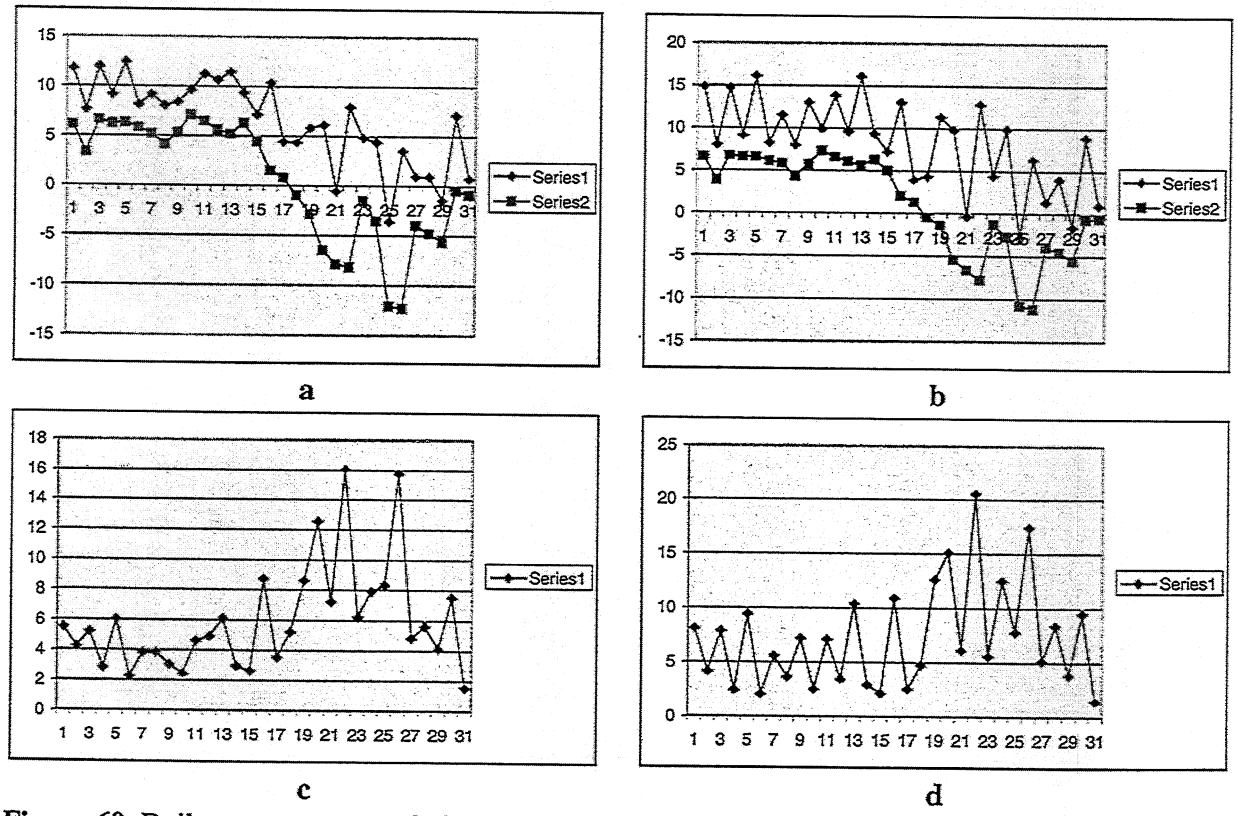

Figure 69. Daily temperature variation during measurement period 1.12.-31.12.2000.

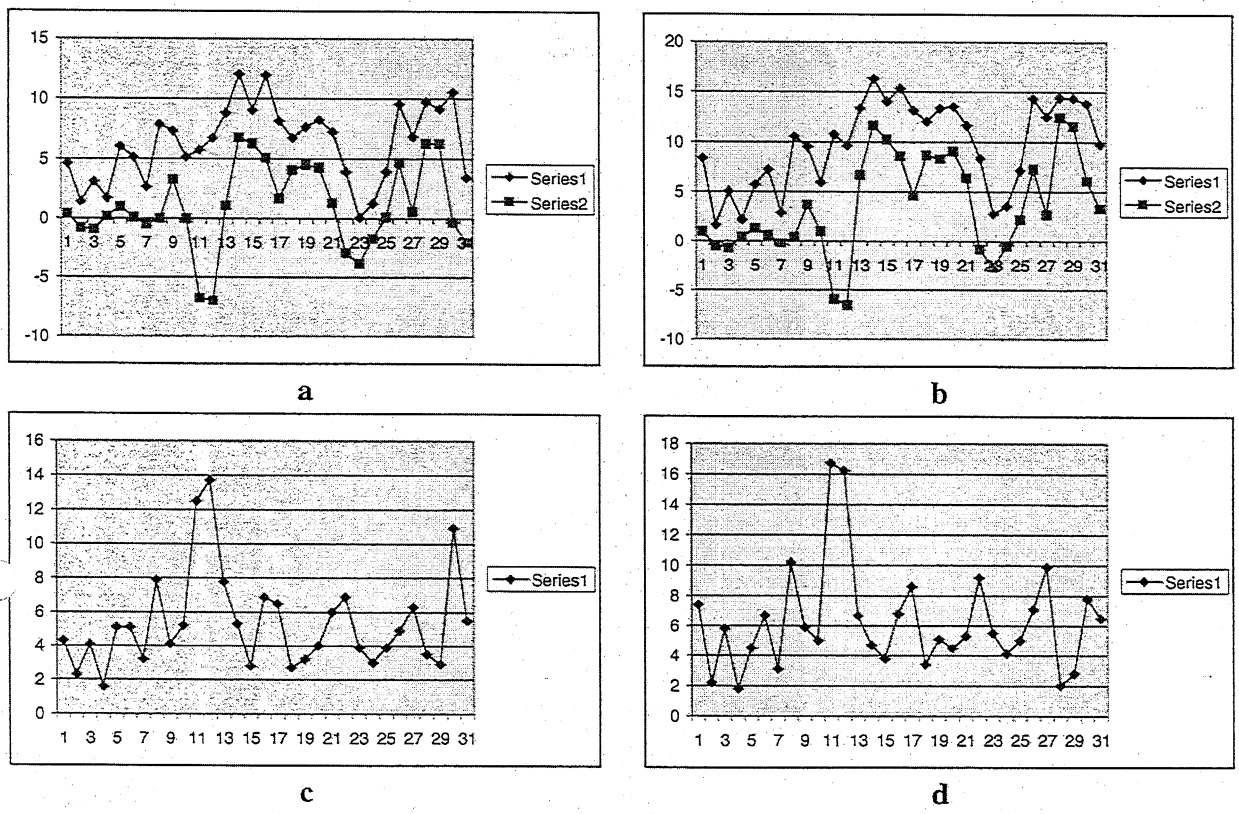

Figure 70. Daily temperature variation during measurement period 1.1.-31.1.2001.

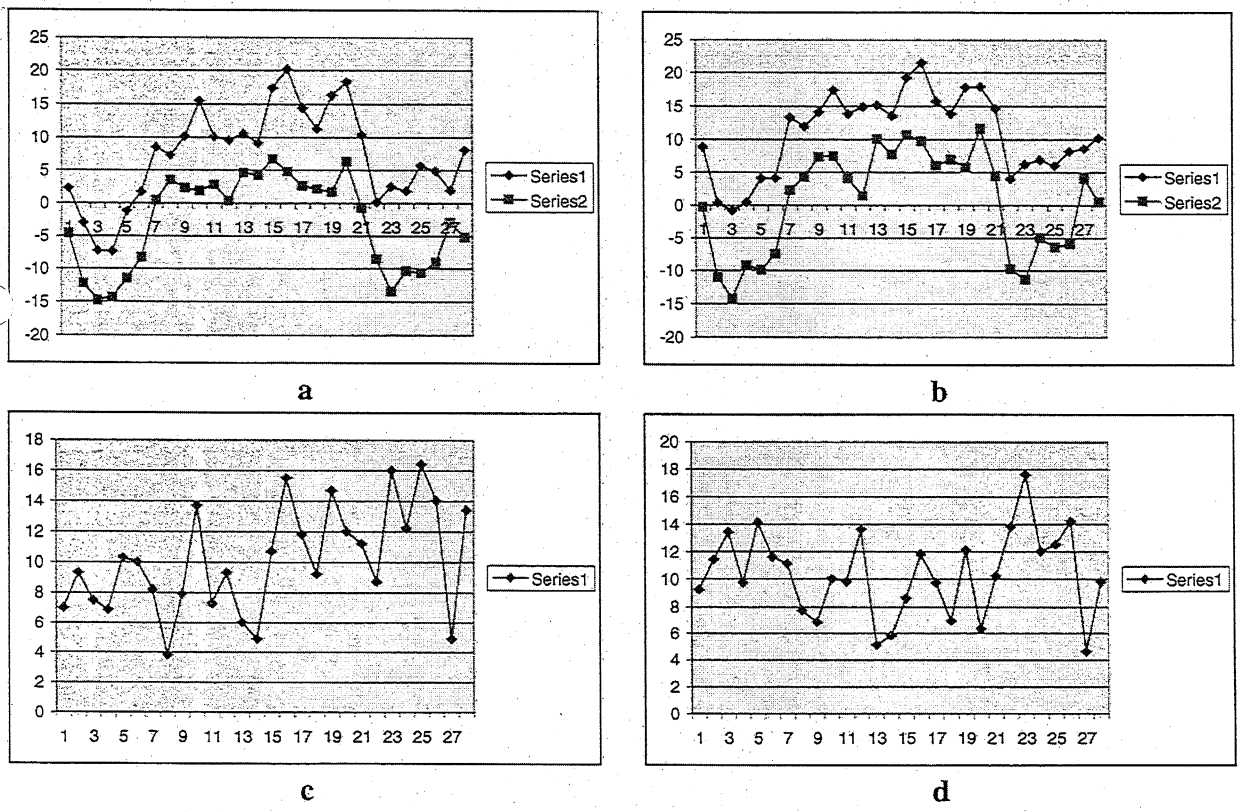

Figure 71. Daily temperature variation during measurement period 1.2.-28.2.2001.

4.3.5 Measuring point E

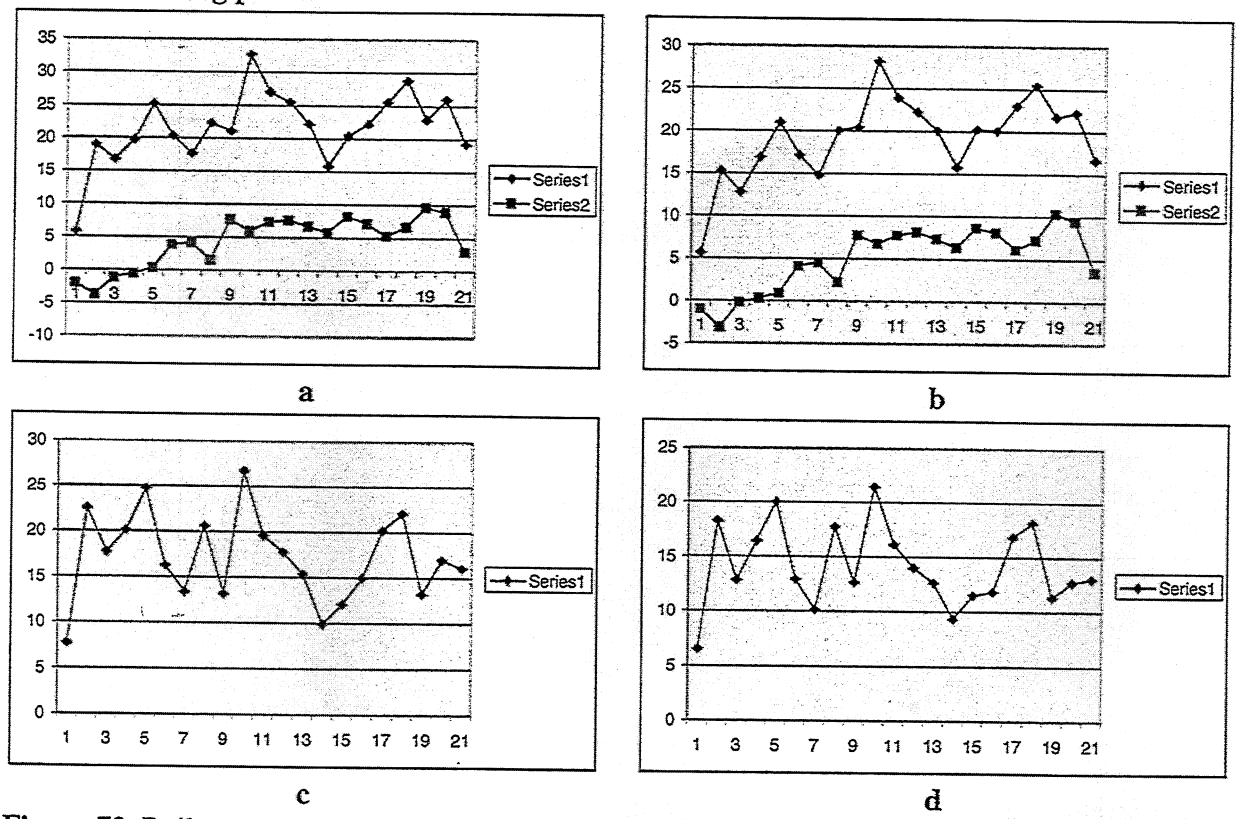

Figure 72. Daily temperature variation during measurement period 11.5.-31.5.1999.

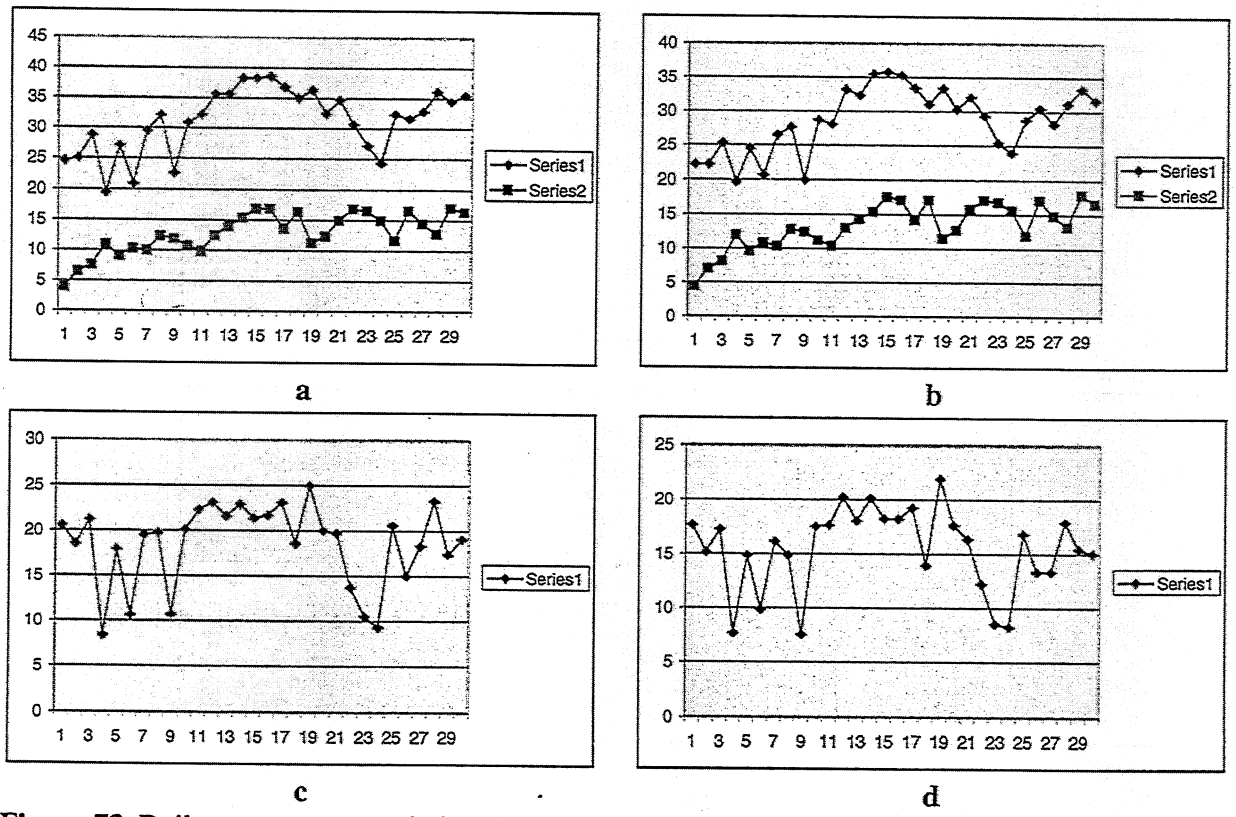

Figure 73. Daily temperature variation during measurement period 1.6.-30.6.1999.

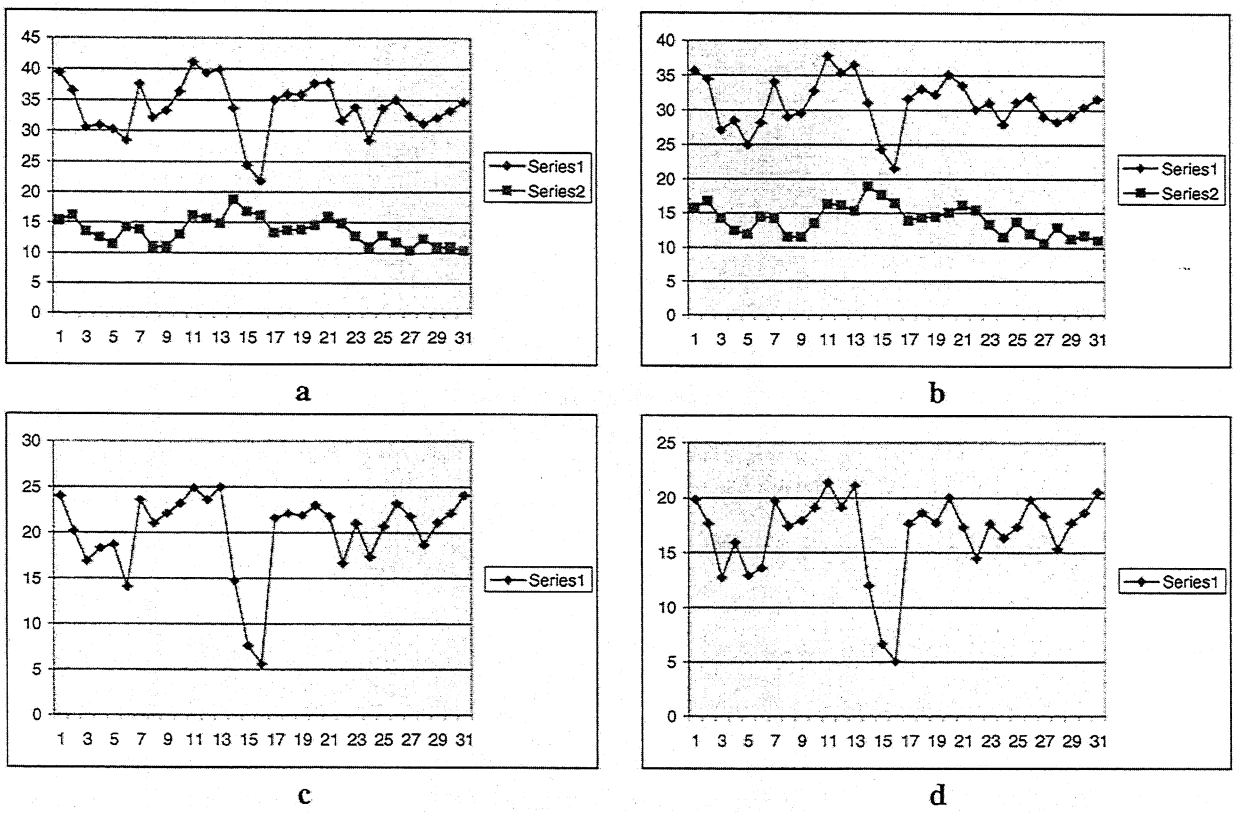

Figure 74. Daily temperature variation during measurement period 1.7.-31.7.1999.

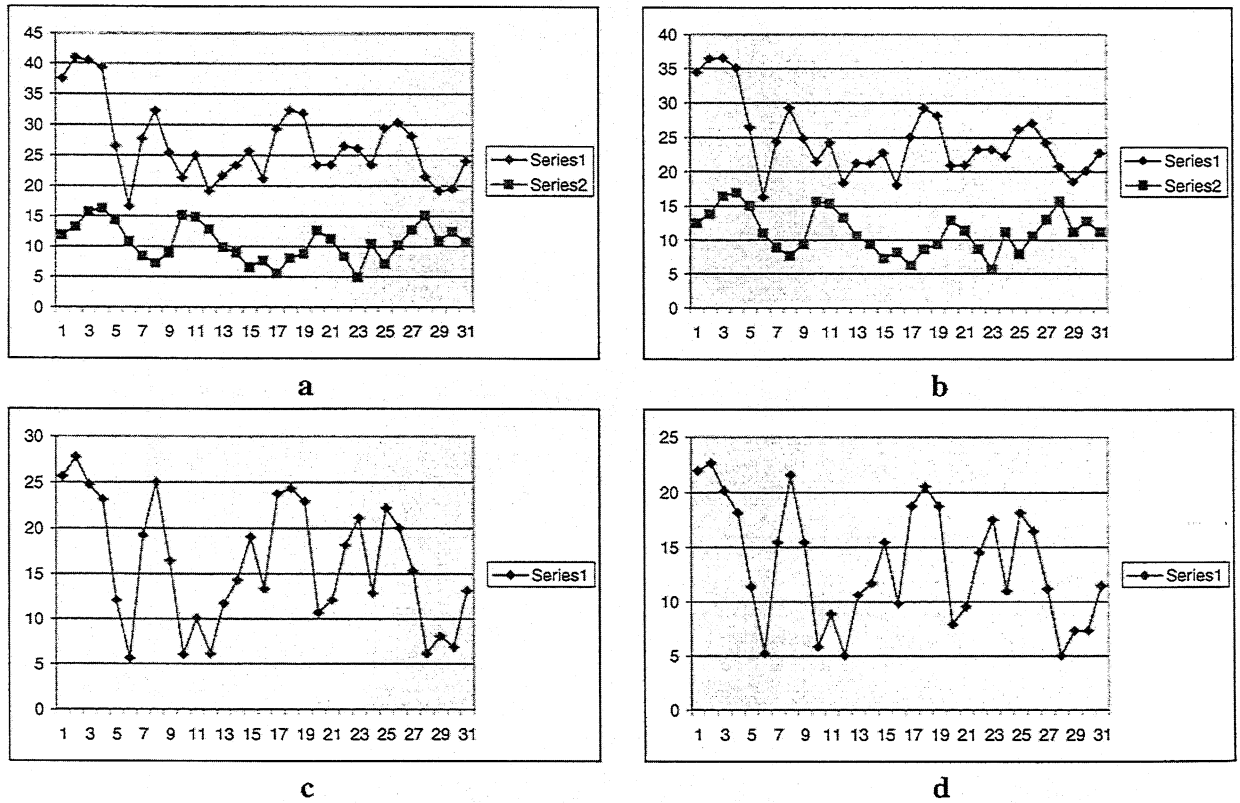

Figure 75. Daily temperature variation during measurement period 1.8.-31.8.1999.

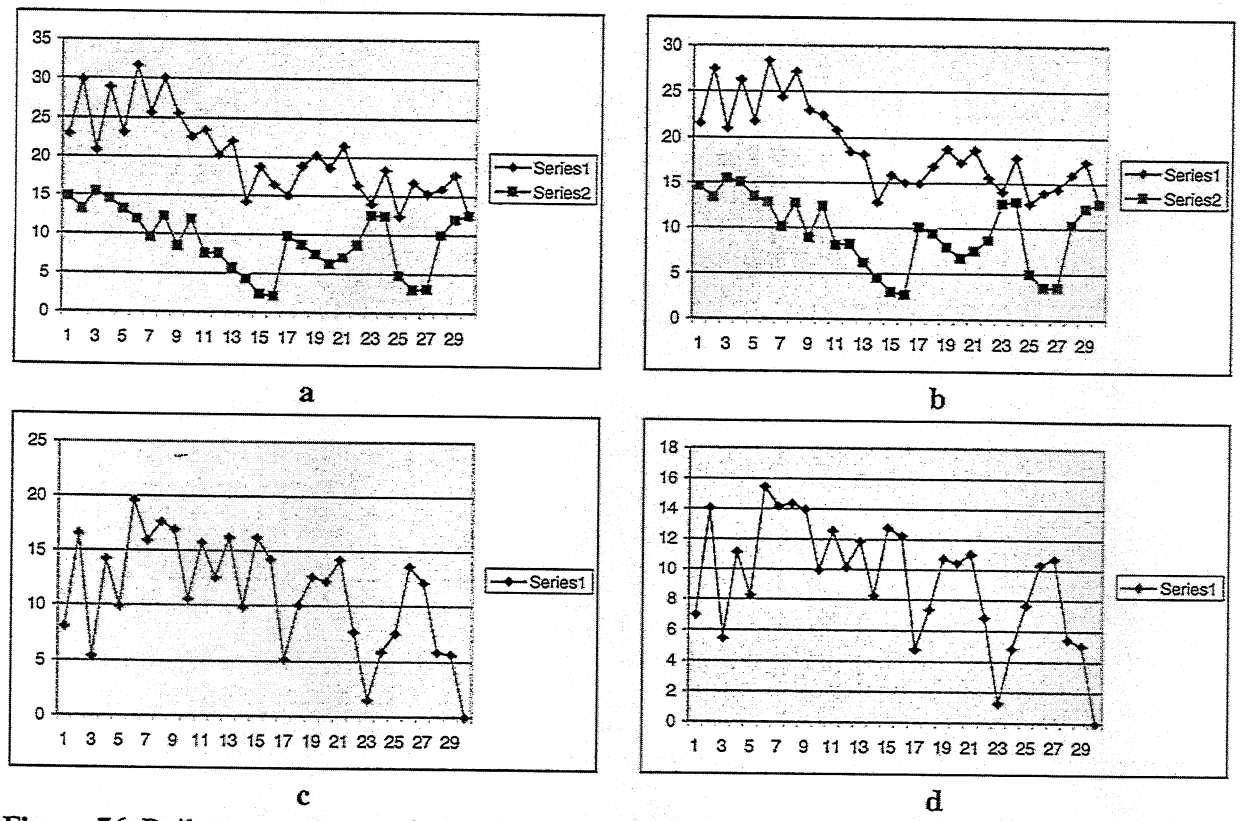

Figure 76. Daily temperature variation during measurement period 1.9.-30.9.1999.

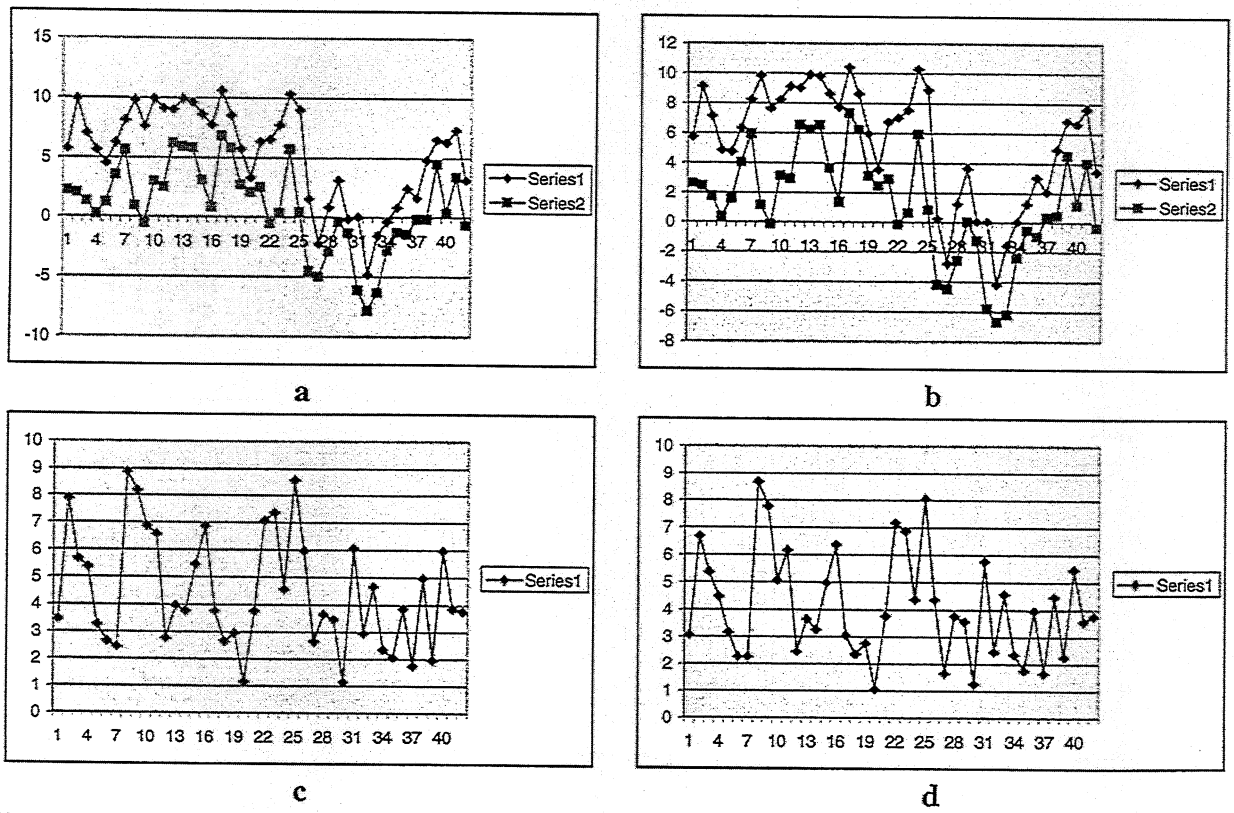

Figure 77. Daily temperature variation during measurement period 20.10.-30.11.1999.

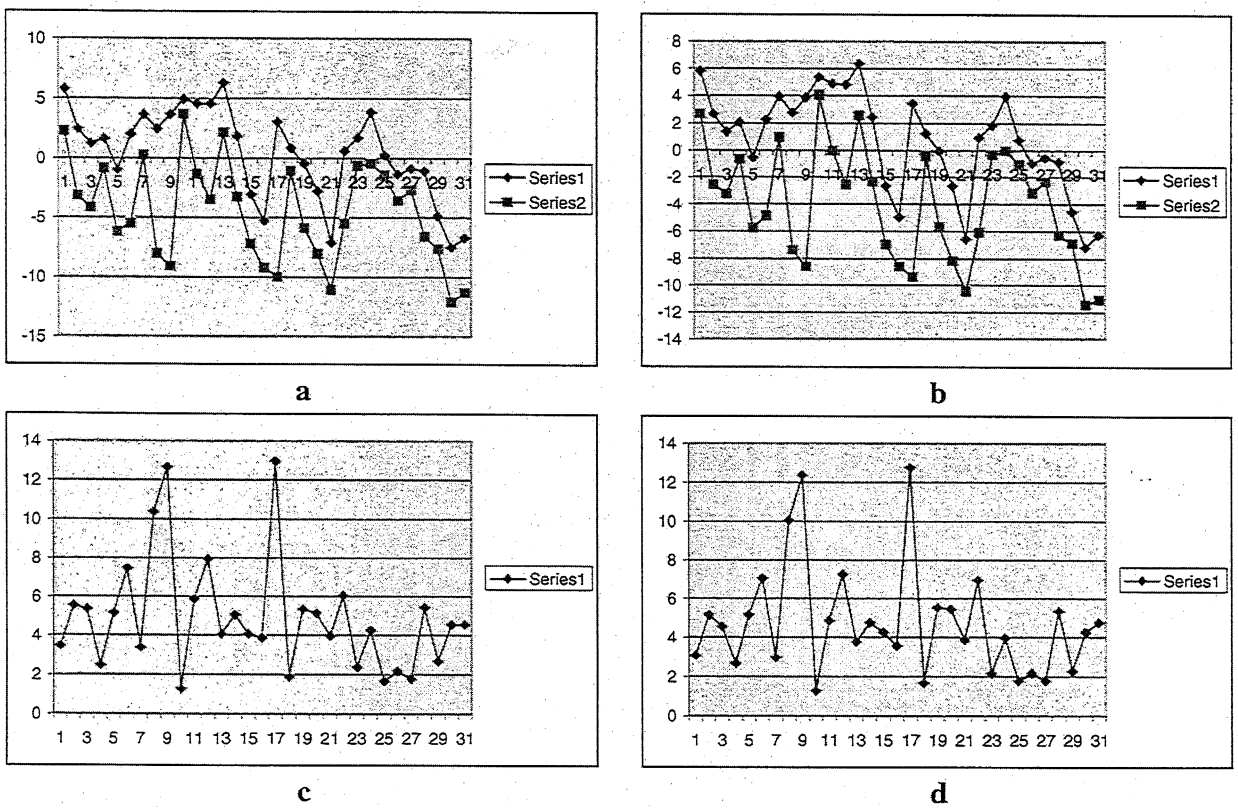

Figure 78. Daily temperature variation during measurement period 1.12.-31.12.1999.

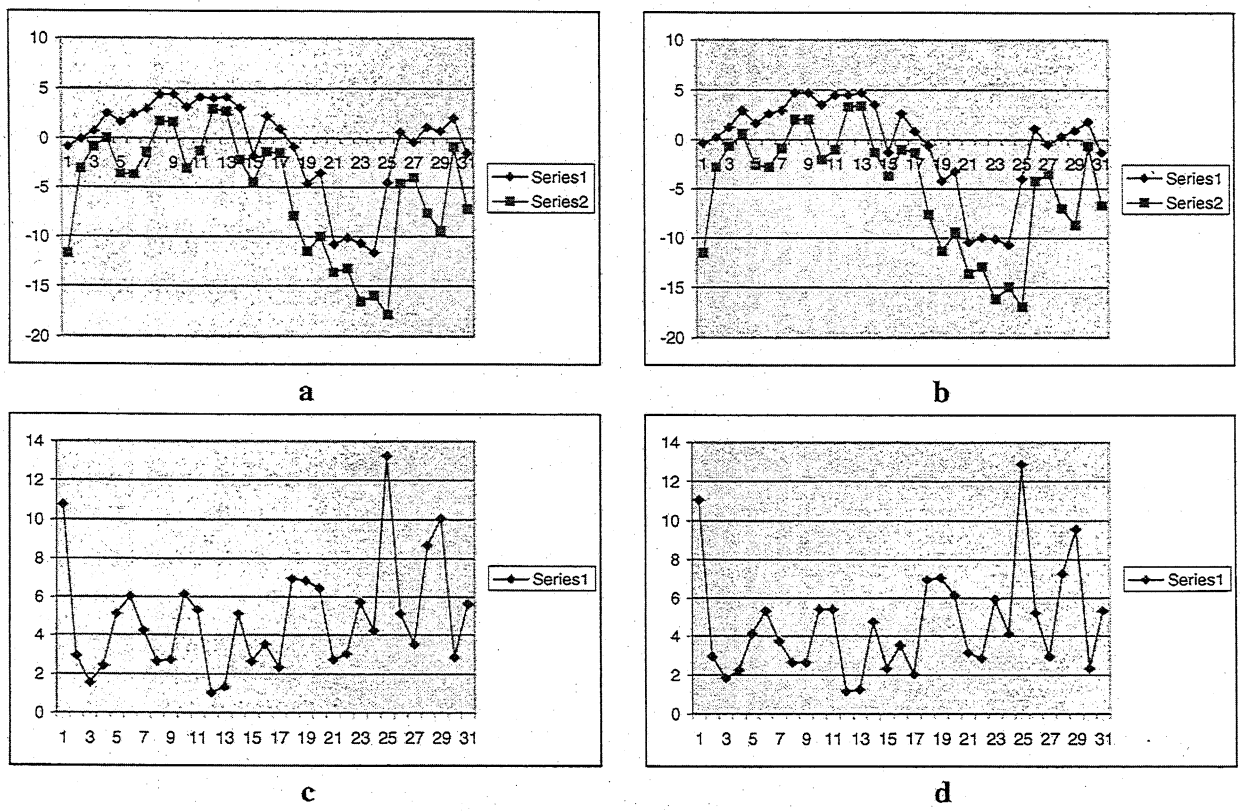

Figure 79. Daily temperature variation during measurement period 1.1.-31.1.2000.

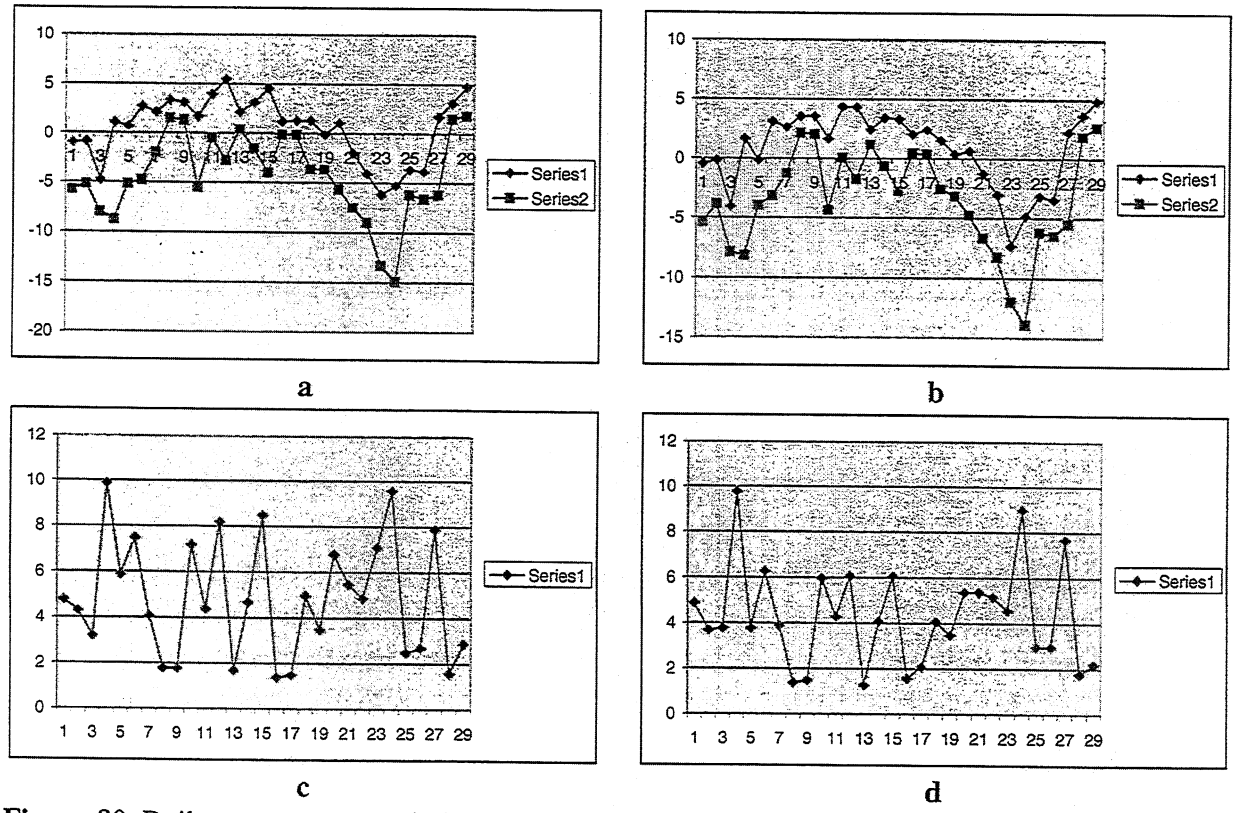

Figure 80. Daily temperature variation during measurement period 1.2.-29.2.2000.

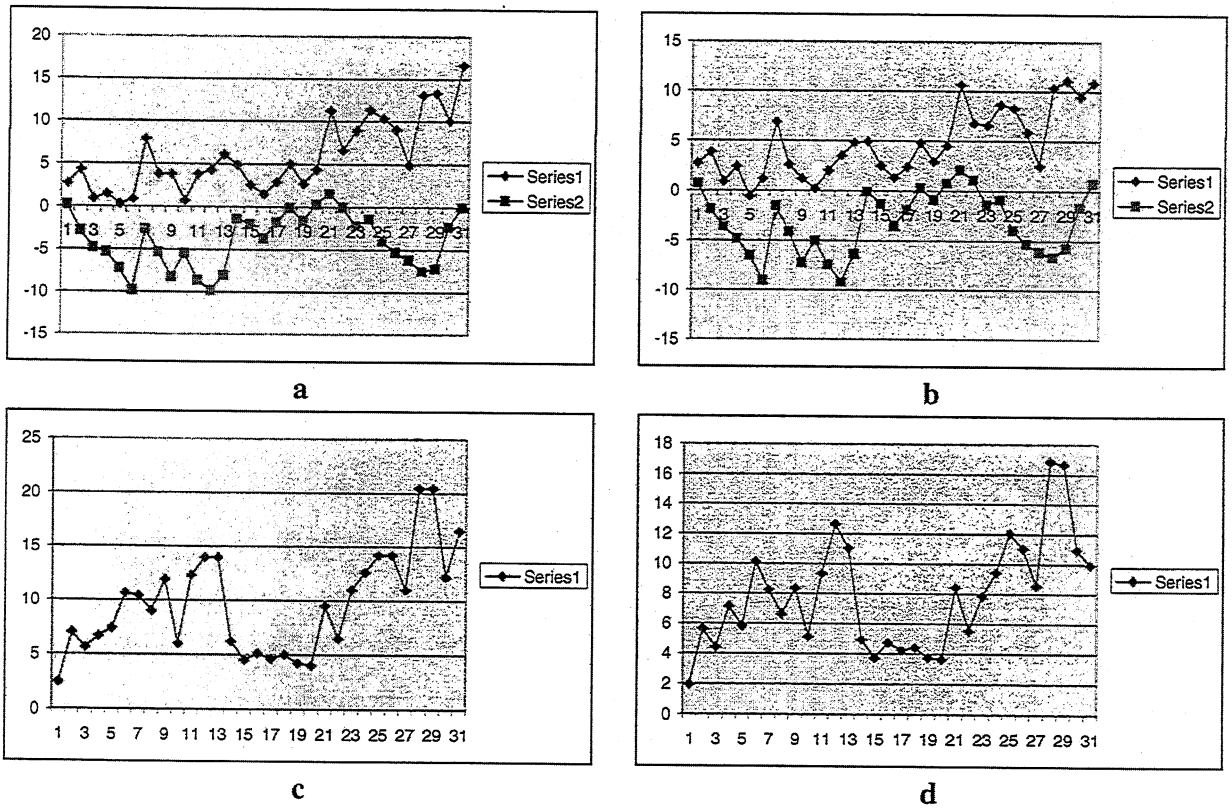

Figure 81. Daily temperature variation during measurement period 1.3.-31.3.2000.

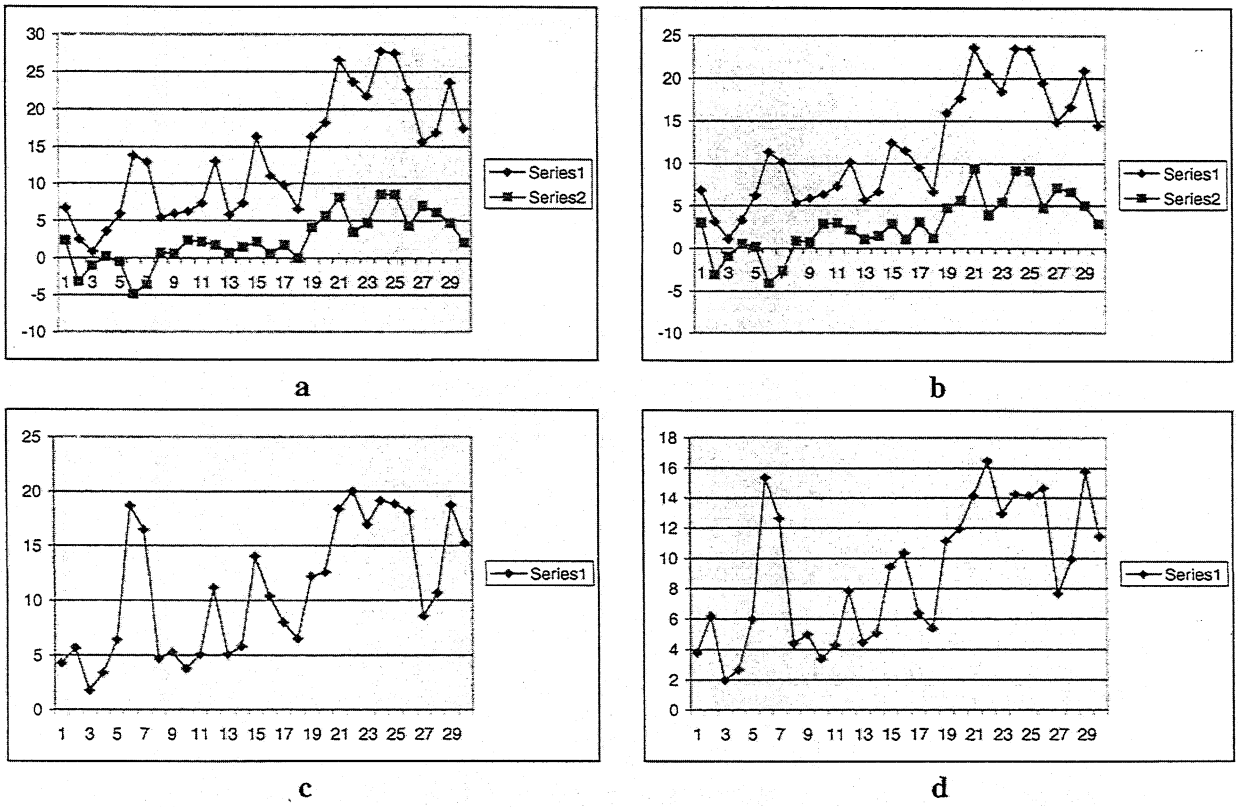

Figure 82. Daily temperature variation during measurement period 1.4.-30.4.2000.

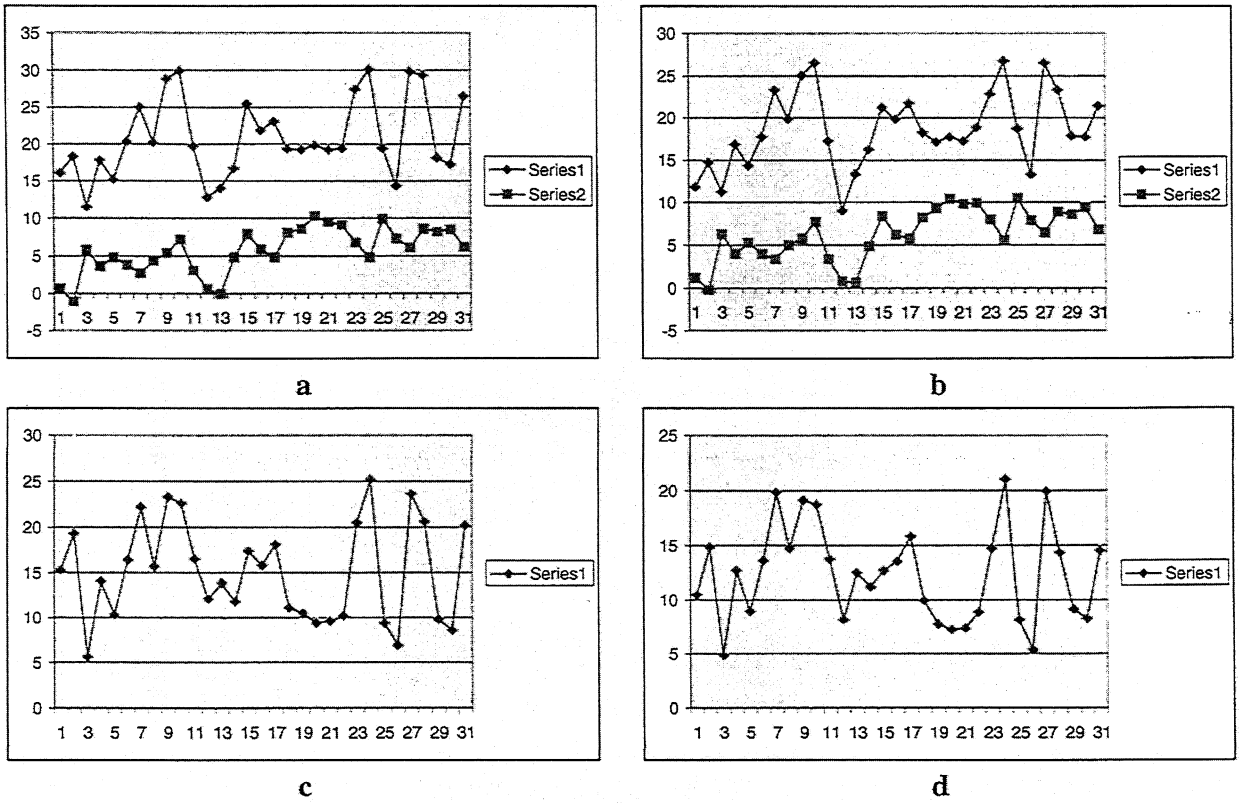

Figure 83. Daily temperature variation during measurement period 1.5.-31.5.2000.

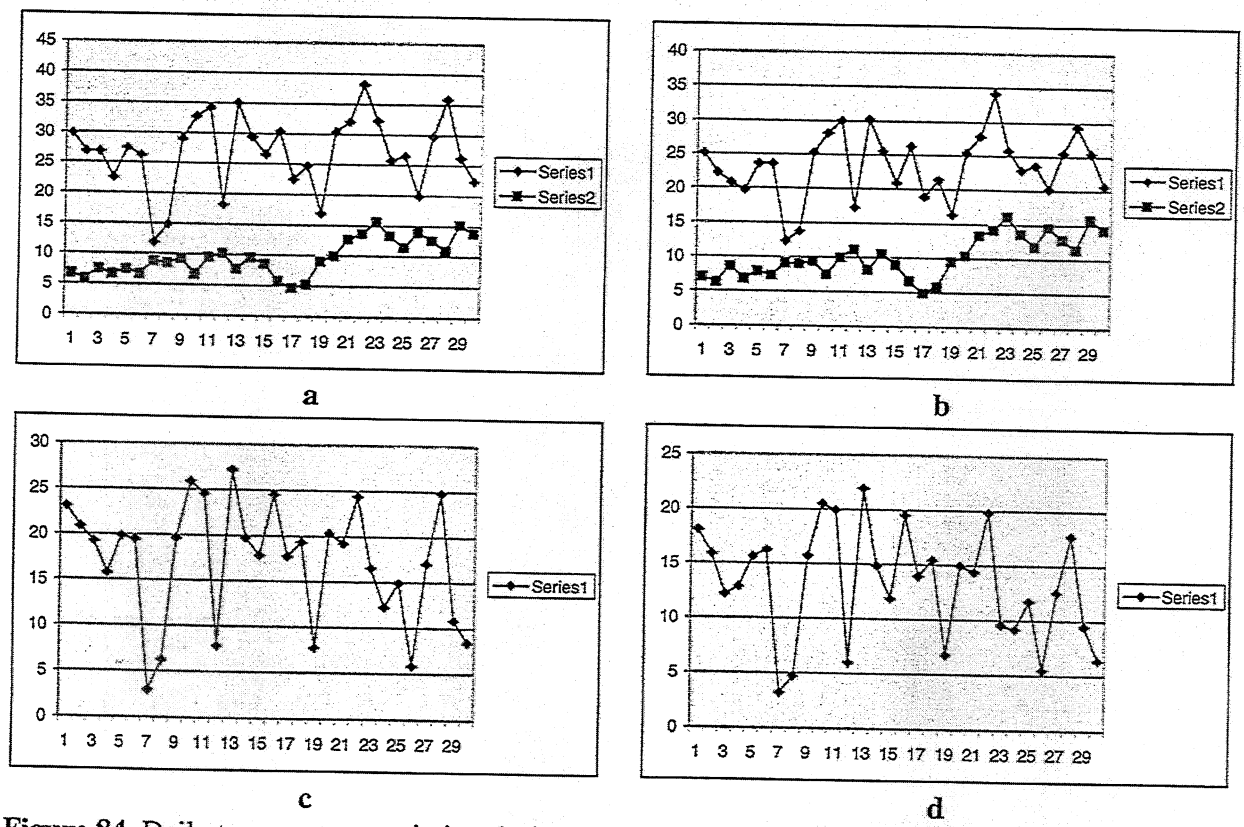

Figure 84. Daily temperature variation during measurement period 1.6.-30.6.2000.

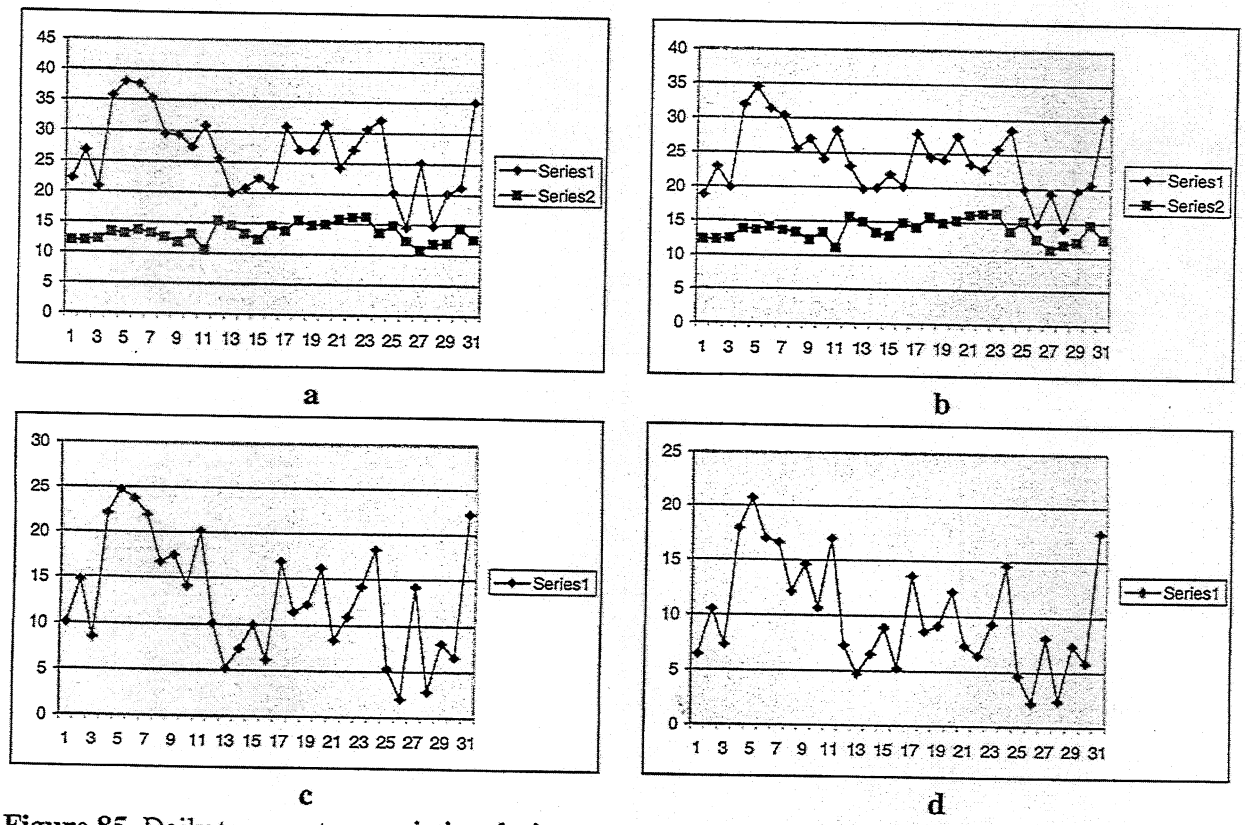

Figure 85. Daily temperature variation during measurement period 1.7.-31.7.2000.

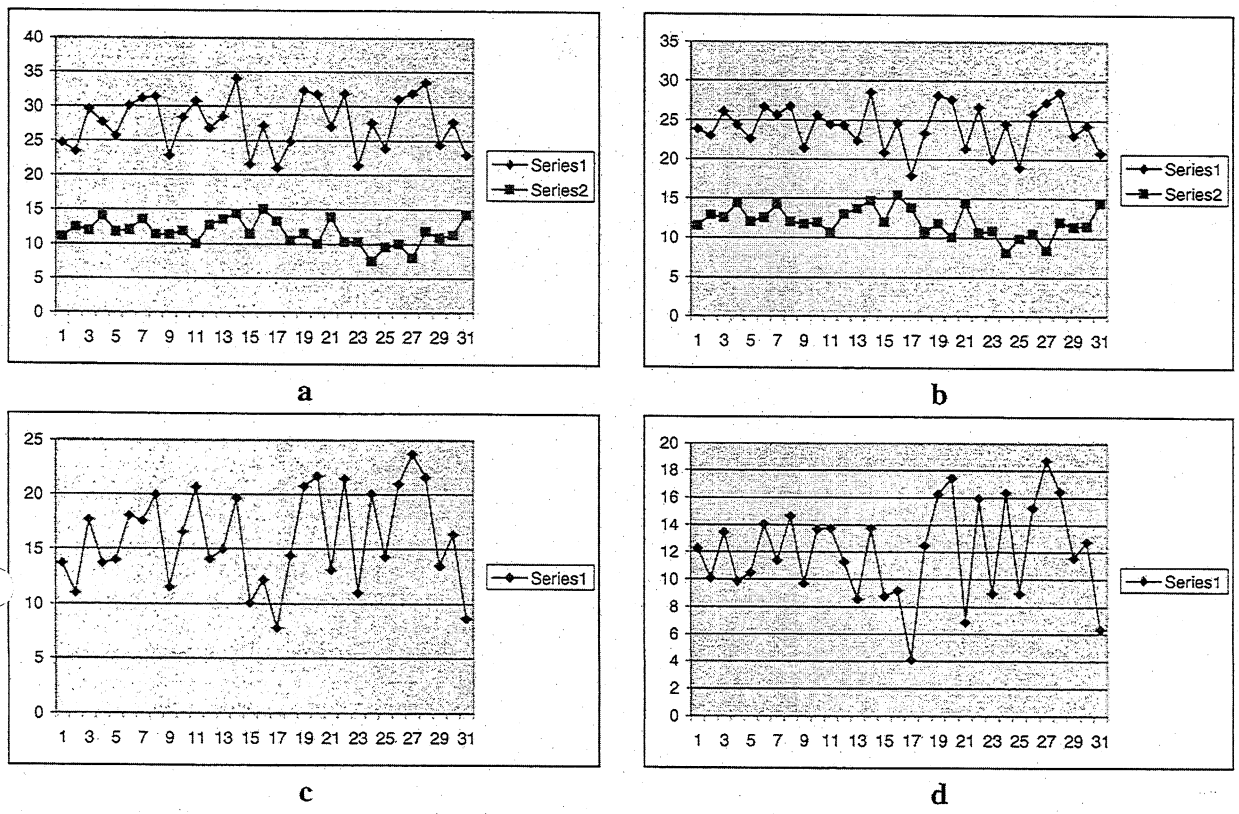

Figure 86. Daily temperature variation during measurement period 1.8.-31.8.2000.

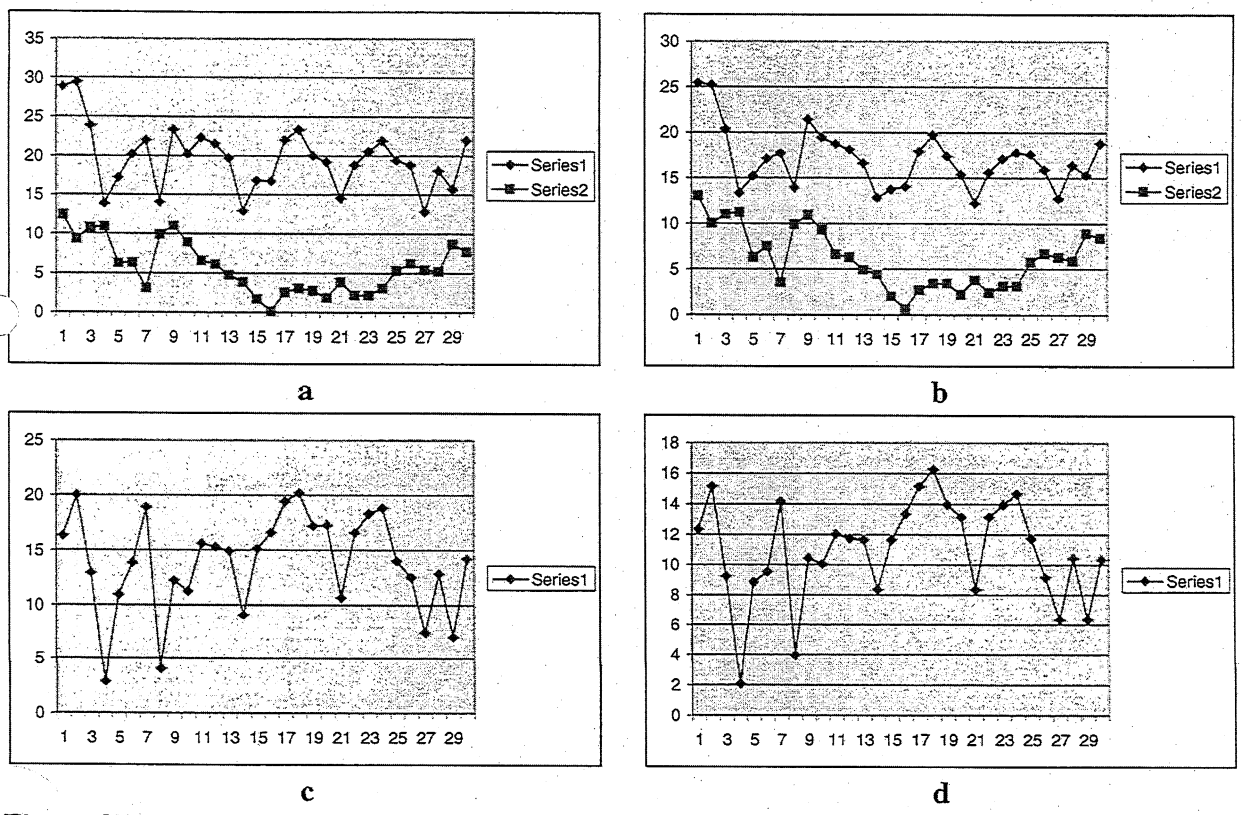

Figure 87. Daily temperature variation during measurement period 1.9.-30.9.2000.

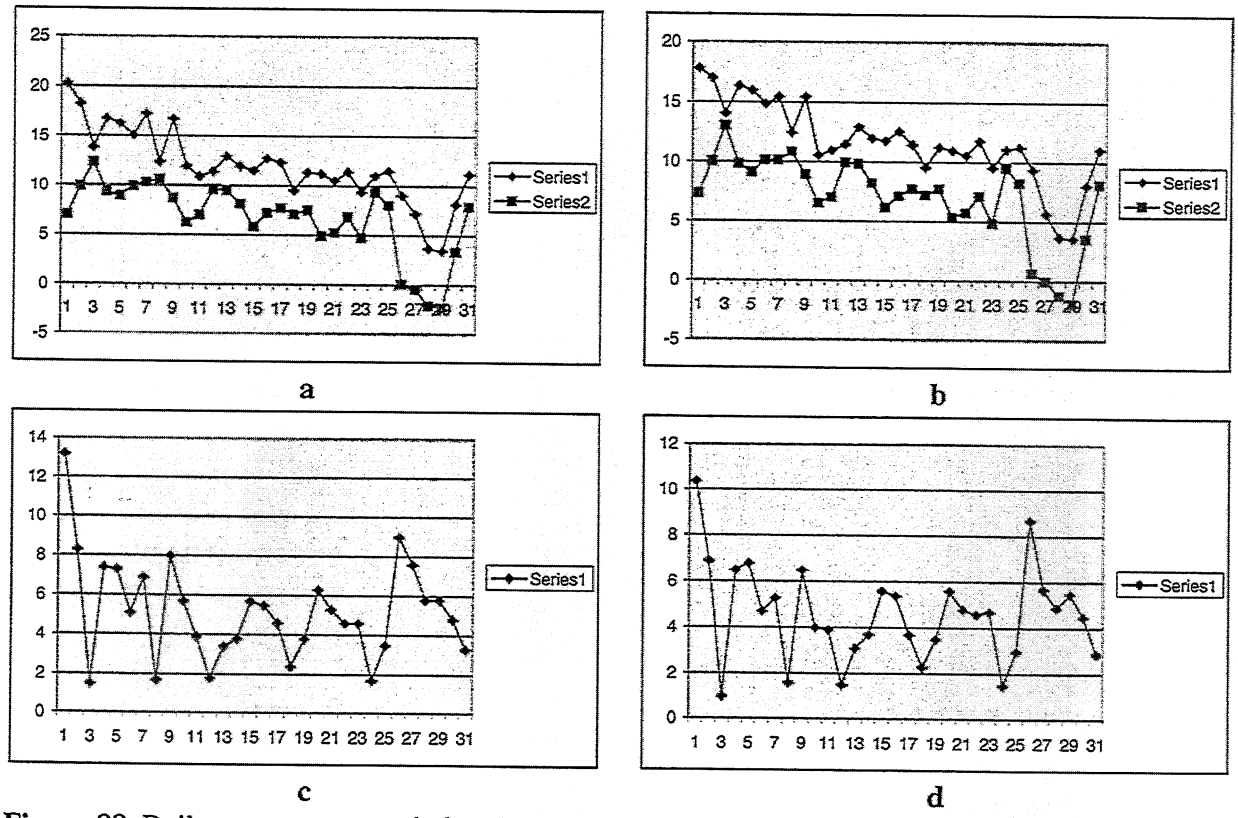

Figure 88. Daily temperature variation during measurement period 1.10.-31.10.2000.

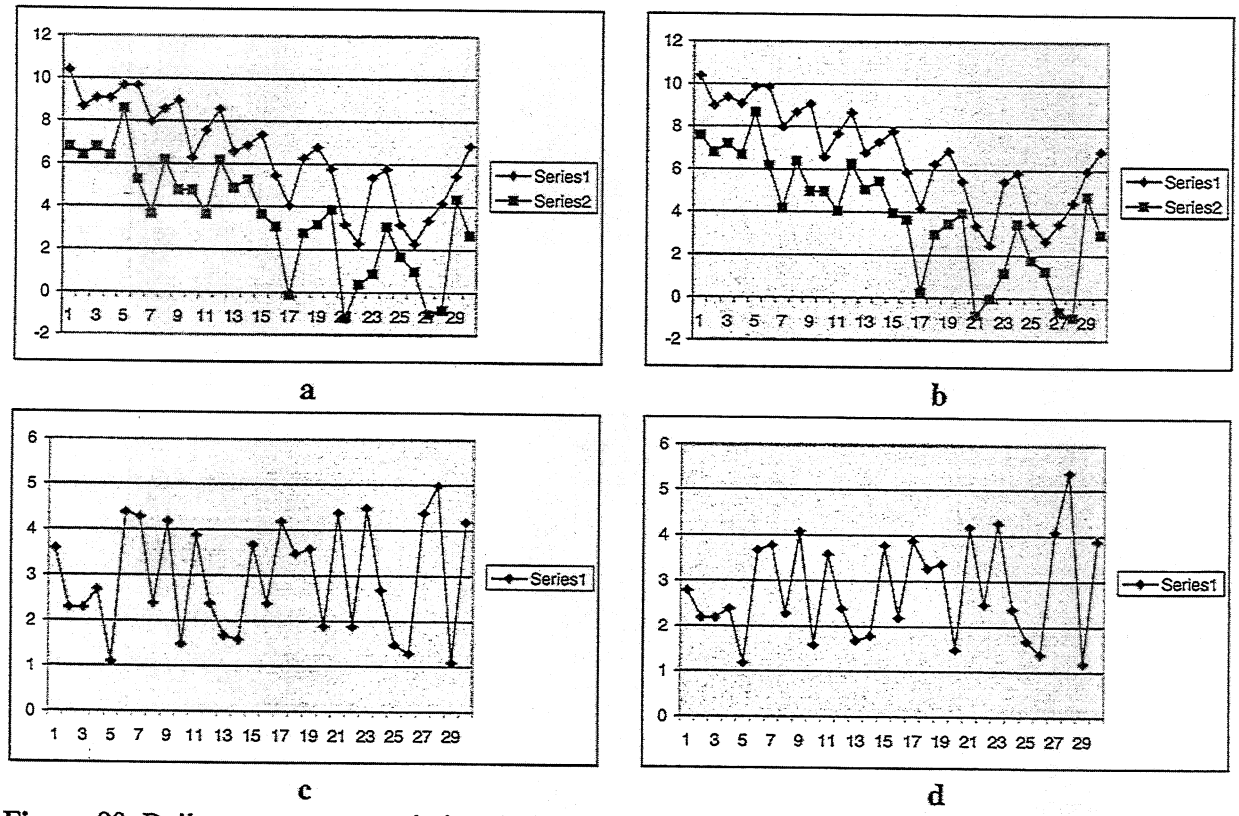

Figure 89. Daily temperature variation during measurement period 1.11.-30.11.2000.

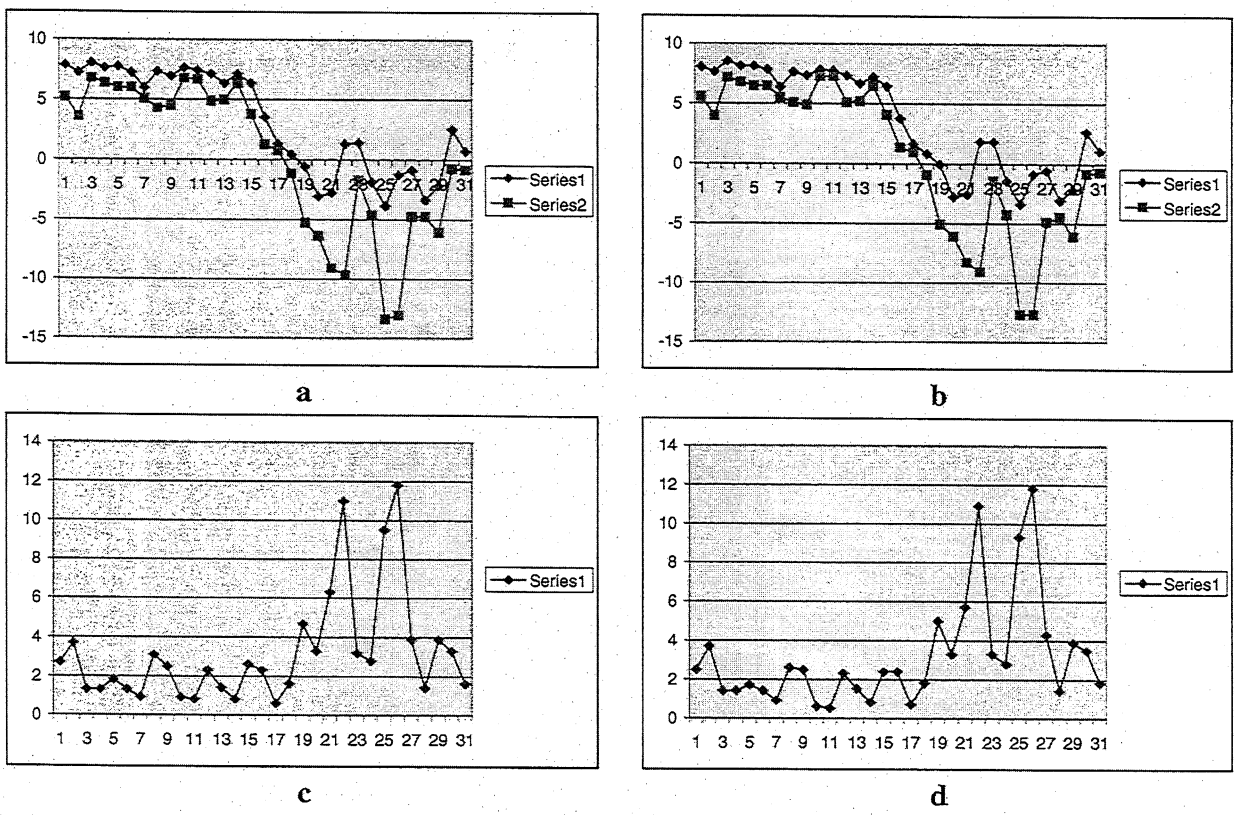

Figure 90. Daily temperature variation during measurement period 1.12.-31.12.2000.

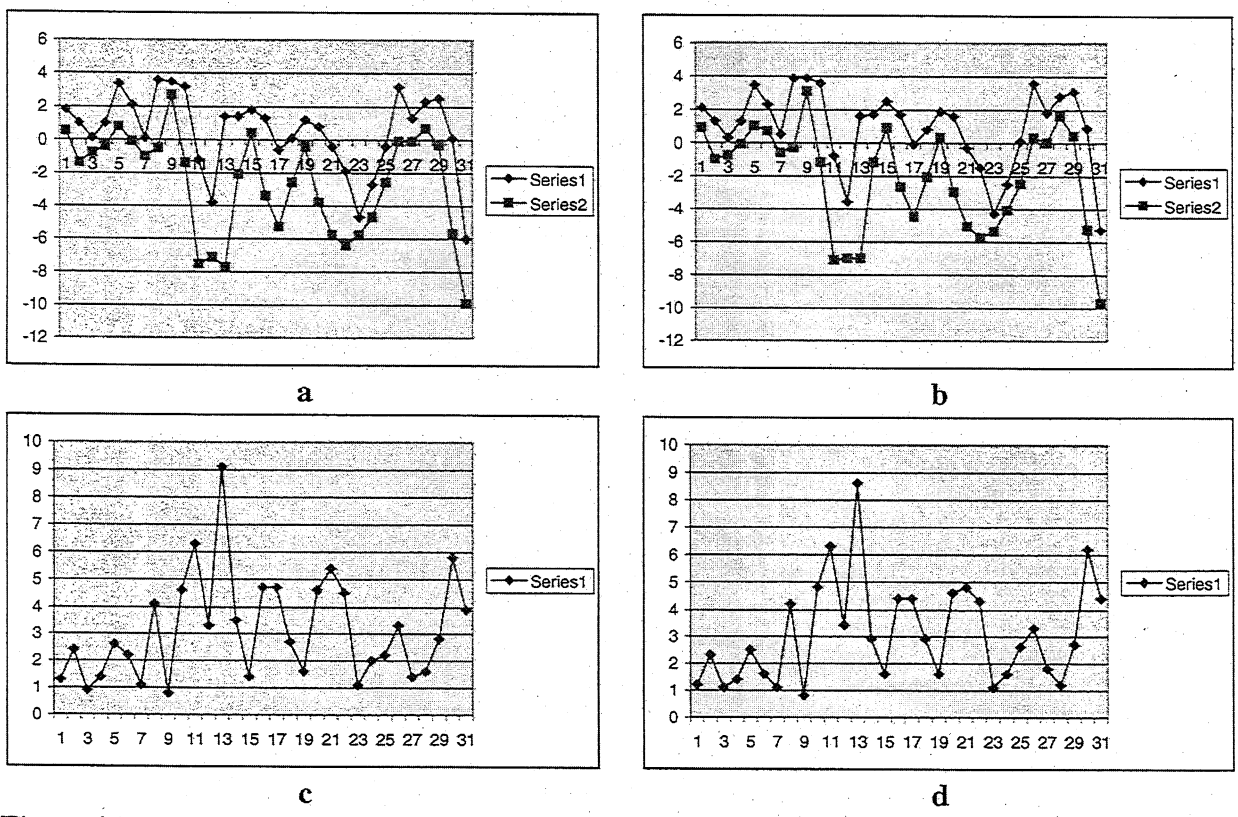

Figure 91. Daily temperature variation during measurement period 1.1.-31.1.2001.

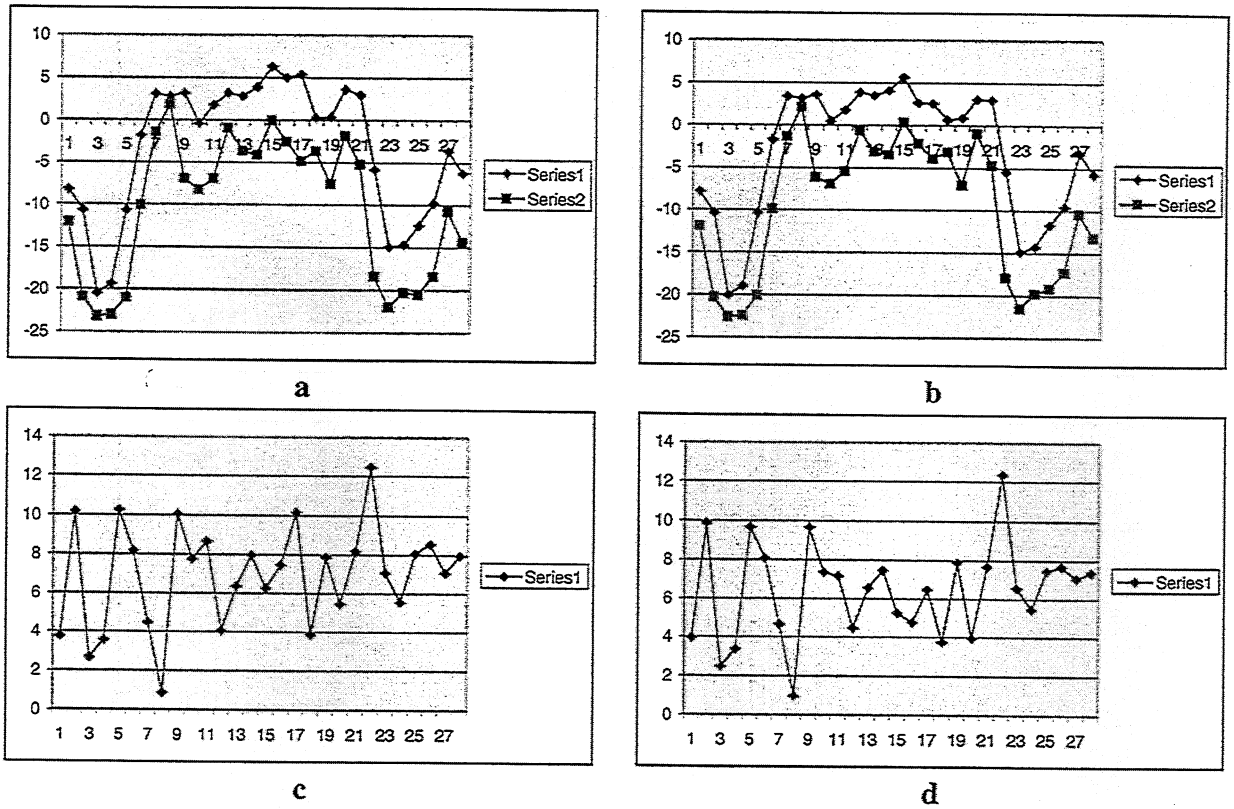

Figure 92. Daily temperature variation during measurement period 1.2.-28.2.2001.

4.4 Gradient of temperature variation in marble

The gradient of temperature variation over the marble slabs was examined as the difference between the range of temperature variation on outer and inner surfaces. The difference is calculated in such a way that the variation on inner surface is diminished from the variation on outer surface. Thus, a positive difference means that the variation has been greater on outer surface and a negative difference that the variation has been greater on inner surface. The results are shown in Figs. 93-179.

4.4.1 Measuring point A

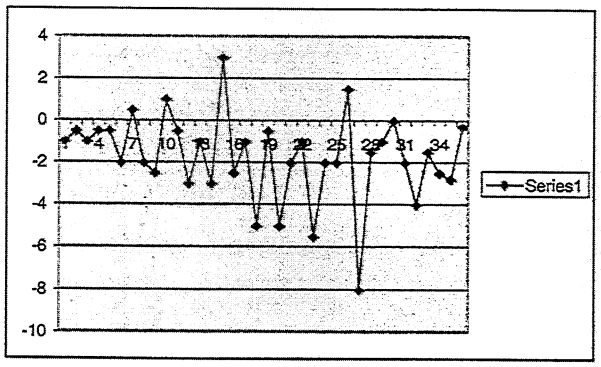

Figure 93. Gradient of temperature variation during measurement period 26.5.-30.6.1999.

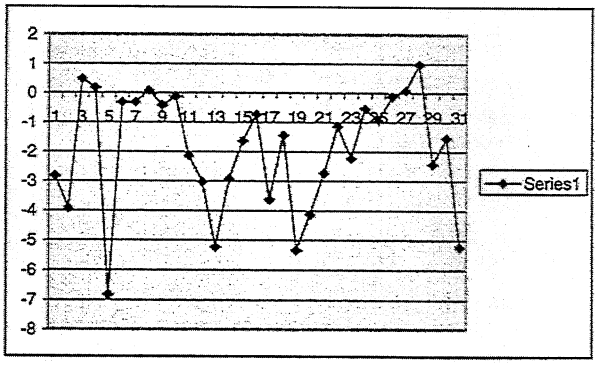

Figure 94. Gradient of temperature variation during measurement period 1.7.-31.7.1999.

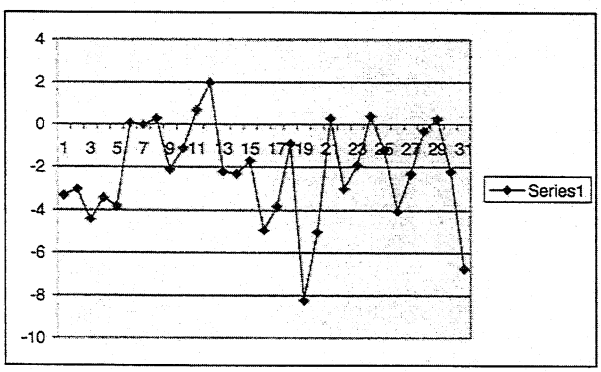

Figure 95. Gradient of temperature variation during measurement period 1.8.-31.8.1999.

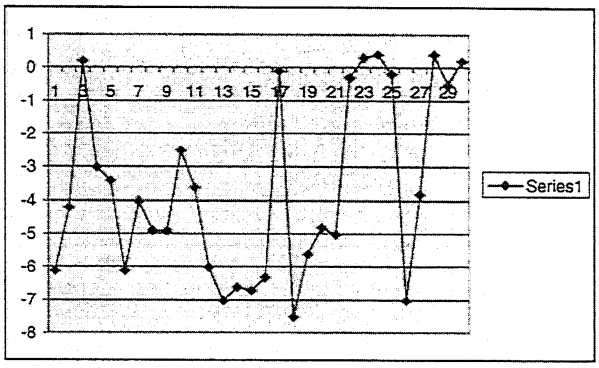

Figure 96. Gradient of temperature variation during measurement period 1.9.-30.9.1999.

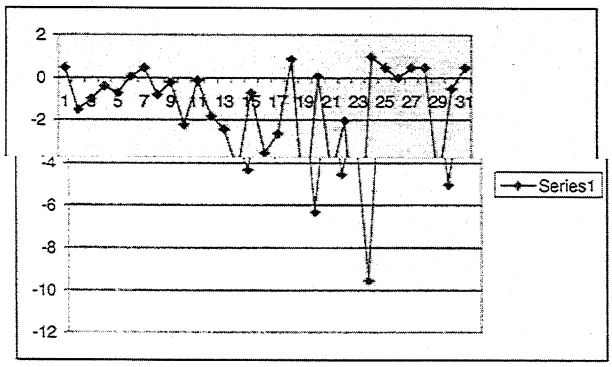

Figure 97. Gradient of temperature variation during measurement period 1.10.-31.10.1999.

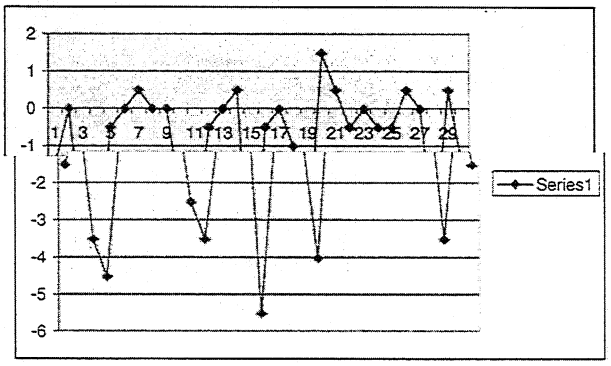

Figure 98. Gradient of temperature variation during measurement period 1.11.-30.11.1999.

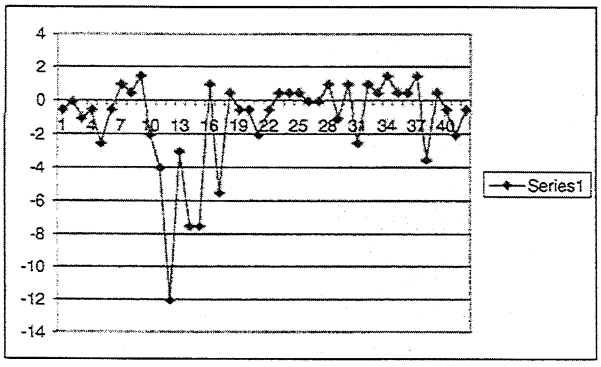

Figure 99. Gradient of temperature variation during measurement period 1.12.1999-11.1.2000.

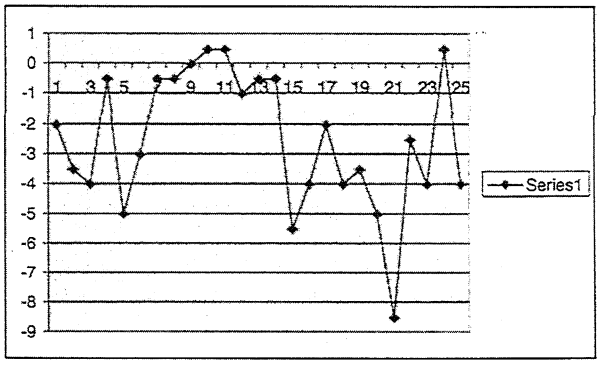

Figure 100. Gradient of temperature variation during measurement period 7.3.-31.3.2000.

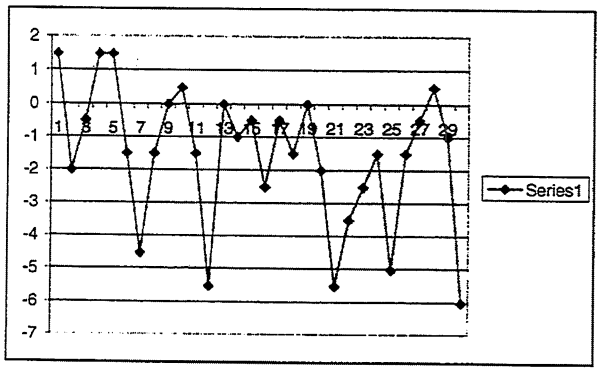

Figure 101. Gradient of temperature variation during measurement period 1.4.-30.4.2000.

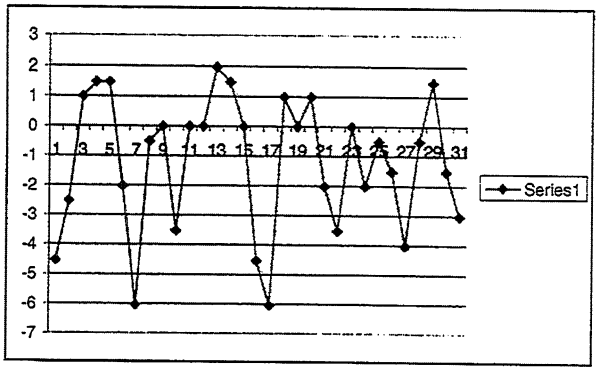

Figure 102. Gradient of temperature variation during measurement period 1.5.-31.5.2000.

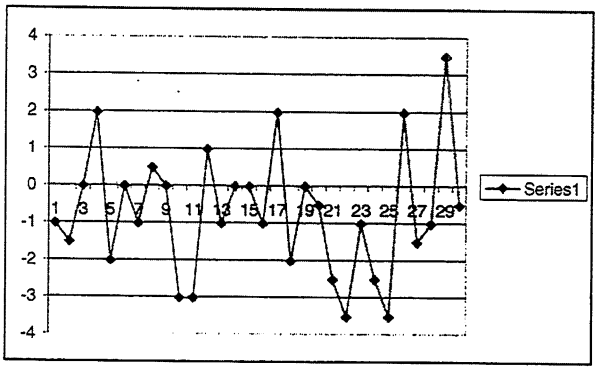

Figure 103. Gradient of temperature variation during measurement period 1.6.-30.6.2000.

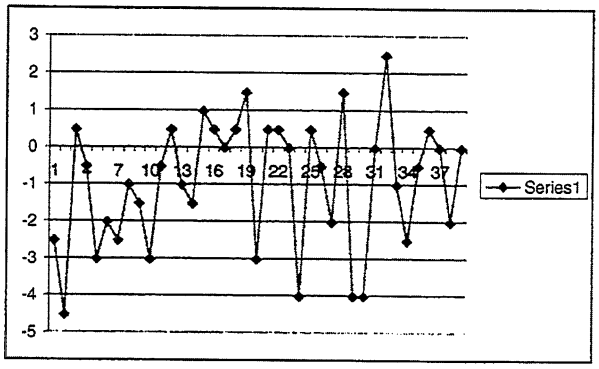

Figure 104. Gradient of temperature variation during measurement period 1.7.-8.8.2000.

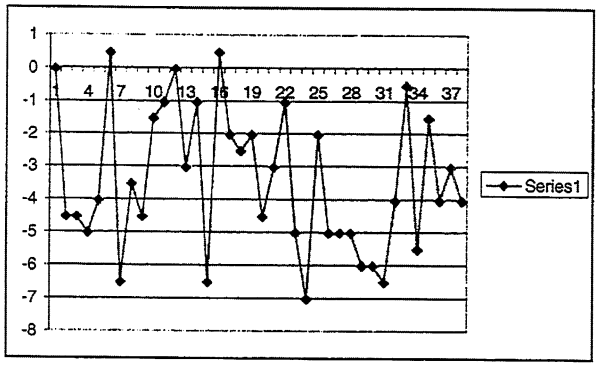

Figure 105. Gradient of temperature variation during measurement period 24.8.-30.9.2000.

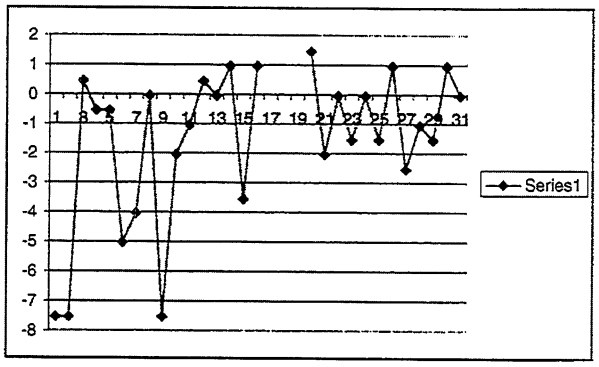

Figure 106. Gradient of temperature variation during measurement period 1.10.-31.10.2000.

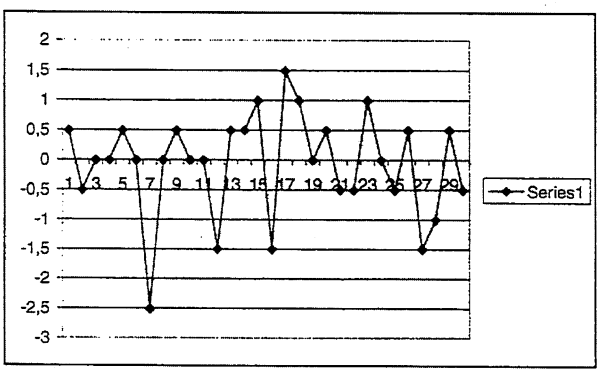

Figure 107. Gradient of temperature variation during measurement period 1.11.-30.11.2000.

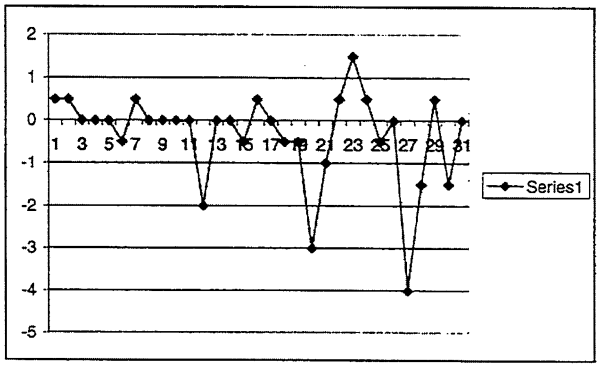

Figure 108. Gradient of temperature variation during measurement period 1.12.-31.12.2000.

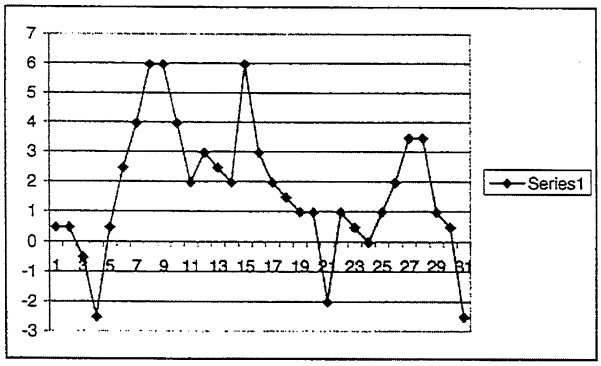

Figure 109. Gradient of temperature variation during measurement period 1.1.-31.1.2001.

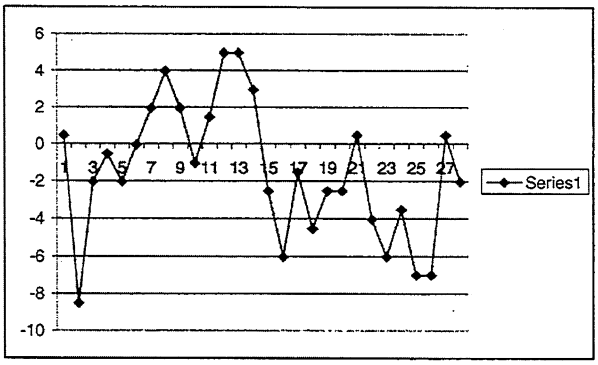

Figure 110. Gradient of temperature variation during measurement period 1.2.-28.2.2001.

4.4.2 Measuring point B

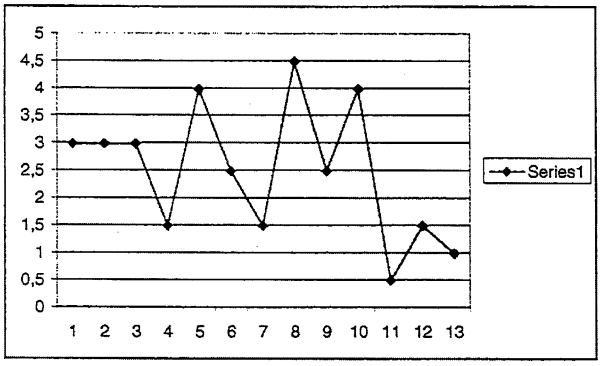

Figure 111. Gradient of temperature variation during measurement period 11.6.-23.6.1999.

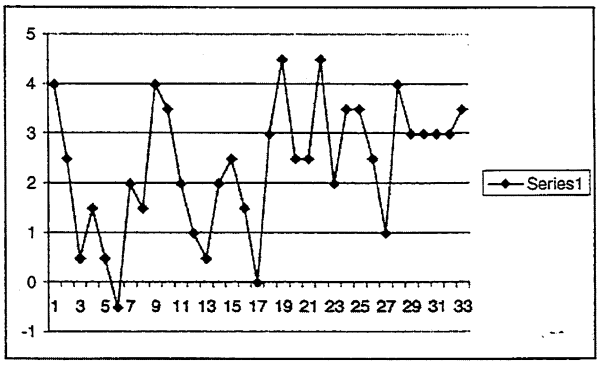

Figure 112. Gradient of temperature variation during measurement period 29.3.-30.4.2000.

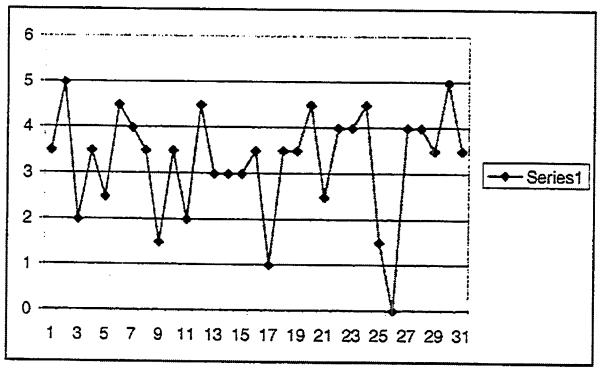

Figure 113. Gradient of temperature variation during measurement period 1.5.-31.5.2000.

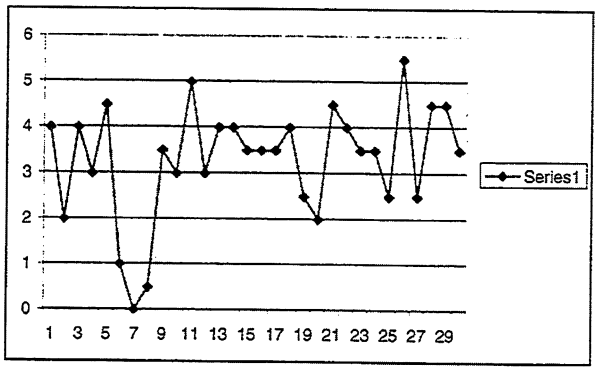

Figure 114. Gradient of temperature variation during measurement period 1.6.-30.6.2000.

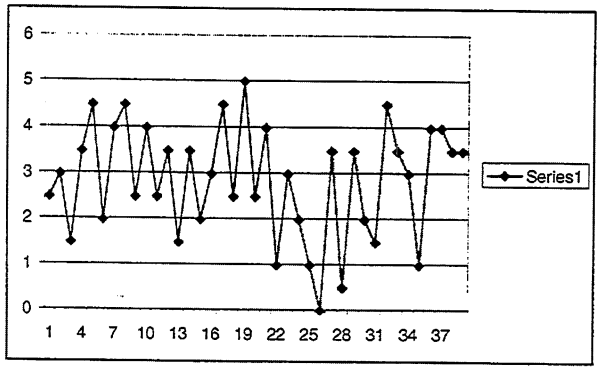

Figure 115. Gradient of temperature variation during measurement period 1.7.-8.8.2000.

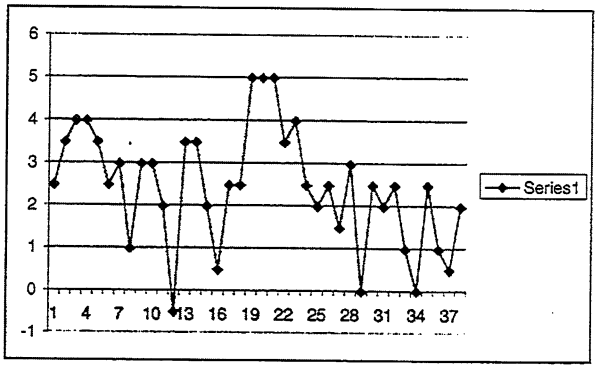

Figure 116. Gradient of temperature variation during measurement period 24.8.-30.9.2000.

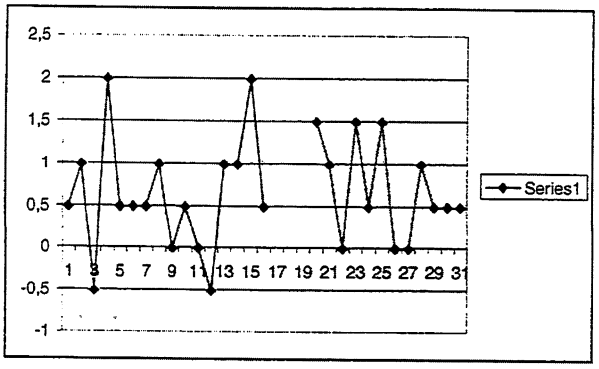

Figure 117. Gradient of temperature variation during measurement period 1.10.-31.10.2000.

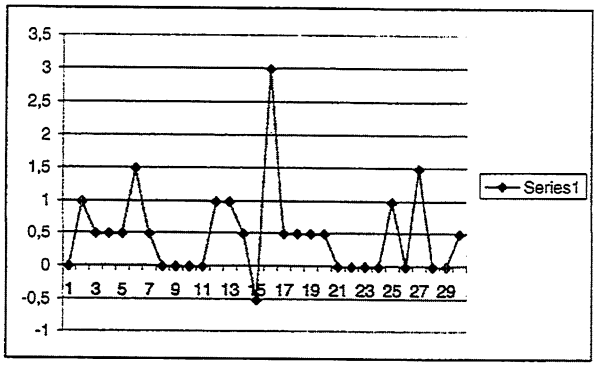

Figure 118. Gradient of temperature variation during measurement period 1.11.-30.11.2000.

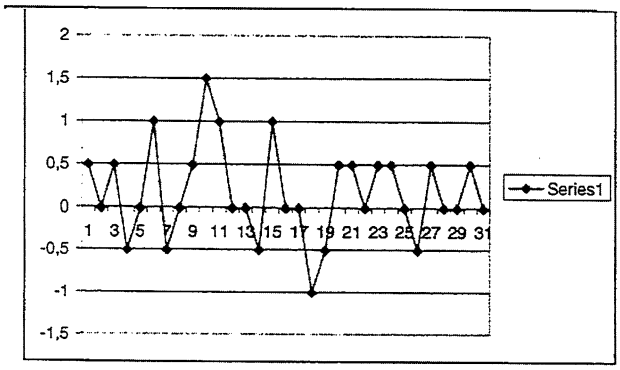

Figure 119. Gradient of temperature variation during measurement period 1.12.-31.12.2000.

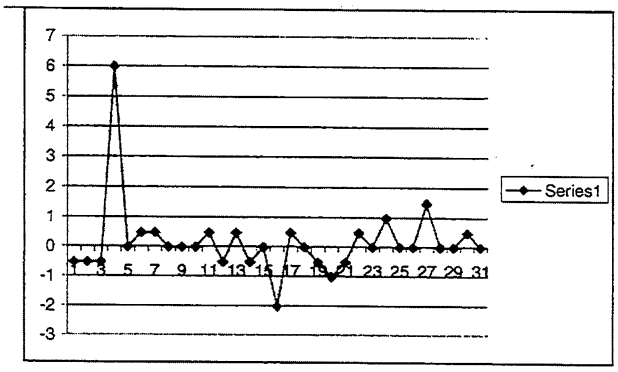

Figure 120. Gradient of temperature variation during measurement period 1.1.-31.1.2001.

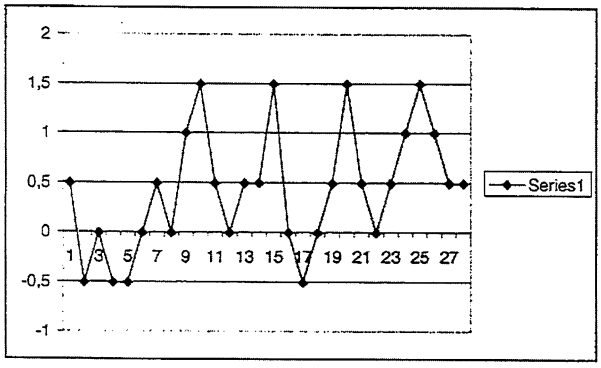

Figure 121. Gradient of temperature variation during measurement period 1.2.-28.2.2001.

4.4.3 Measuring point C

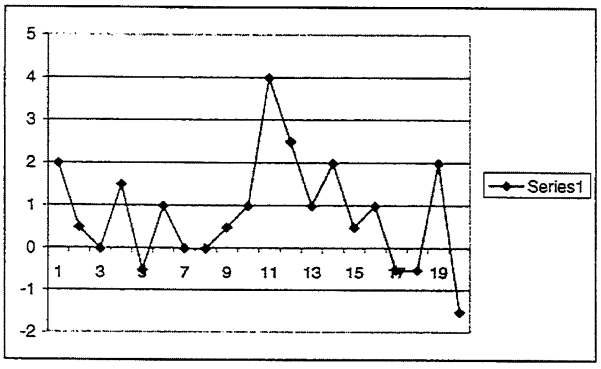

Figure 122. Gradient of temperature variation during measurement period 11.6.-30.6.1999.

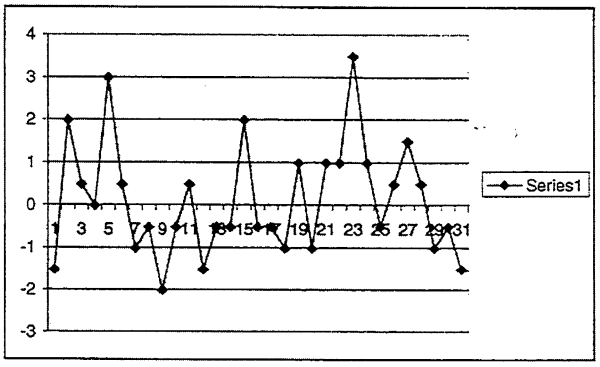

Figure 123. Gradient of temperature variation during measurement period 1.7.-31.7.1999.

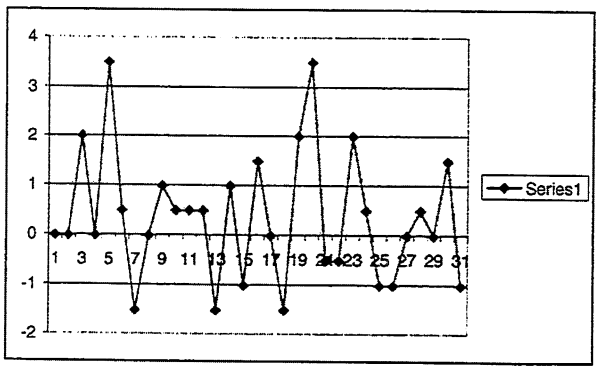

Figure 124. Gradient of temperature variation during measurement period 1.8.-31.8.1999.

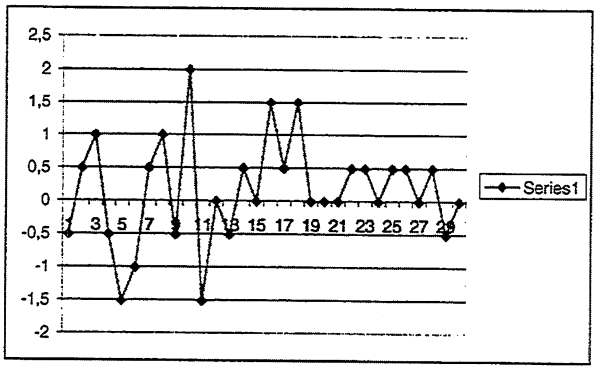

Figure 125. Gradient of temperature variation during measurement period 1.9.-30.9.1999.

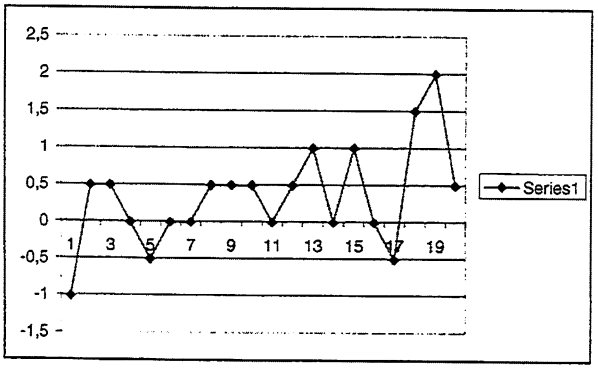

Figure 126. Gradient of temperature variation during measurement period 1.10.-20.10.1999.

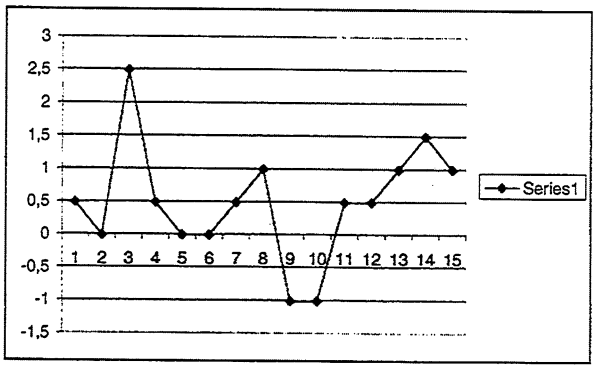

Figure 127. Gradient of temperature variation during measurement period 29.3.-12.4.2000.

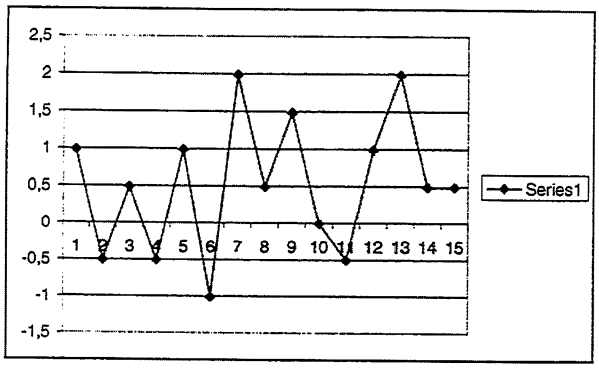

Figure 128. Gradient of temperature variation during measurement period 17.5.-31.5.2000.

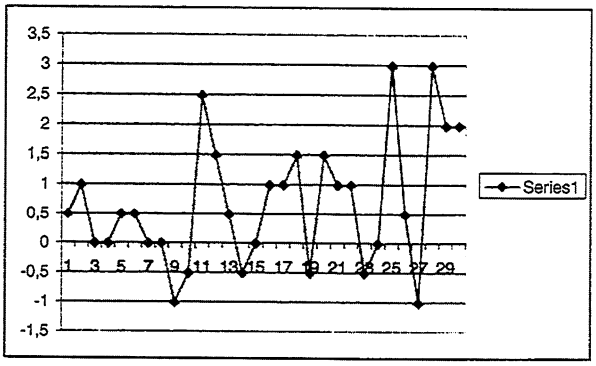

Figure 129. Gradient of temperature variation during measurement period 1.6.-30.6.2000.

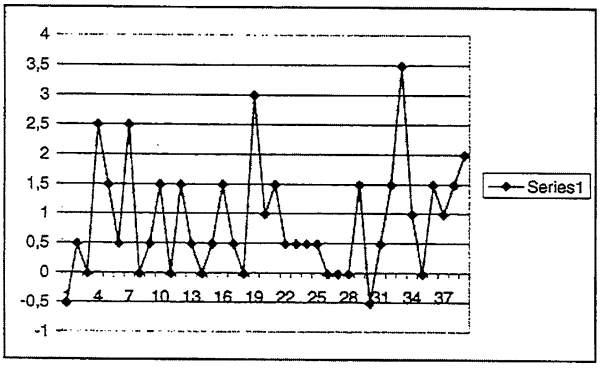

Figure 130. Gradient of temperature variation during measurement period 1.7.-8.8.2000.

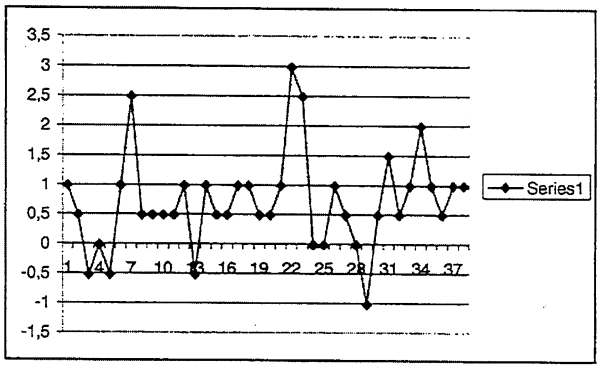

Figure 131. Gradient of temperature variation during measurement period 24.8.-30.9.2000.

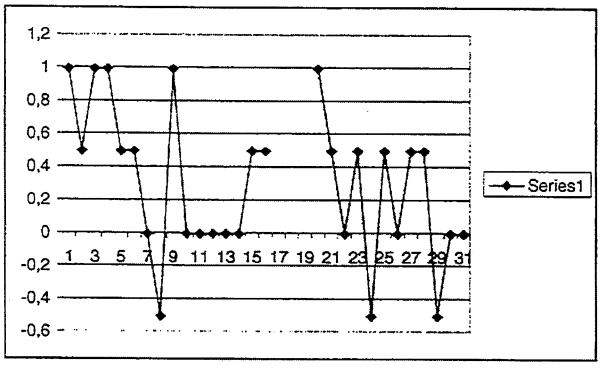

Figure 132. Gradient of temperature variation during measurement period 1.10.-31.10.2000.

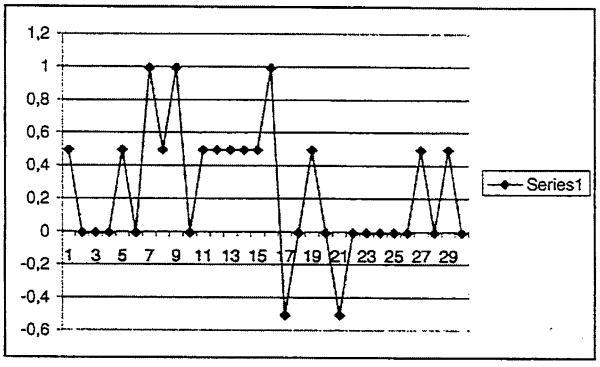

Figure 133. Gradient of temperature variation during measurement period 1.11.-30.11.2000.

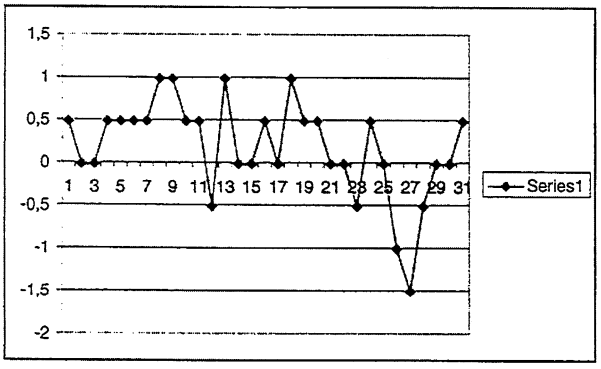

Figure 134. Gradient of temperature variation during measurement period 1.12.-31.12.2000.

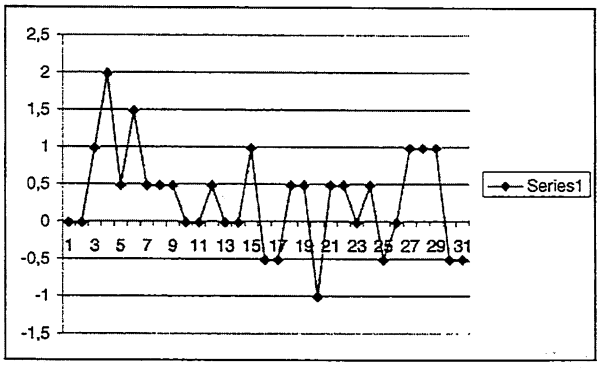

Figure 135. Gradient of temperature variation during measurement period 1.1.-31.1.2001.

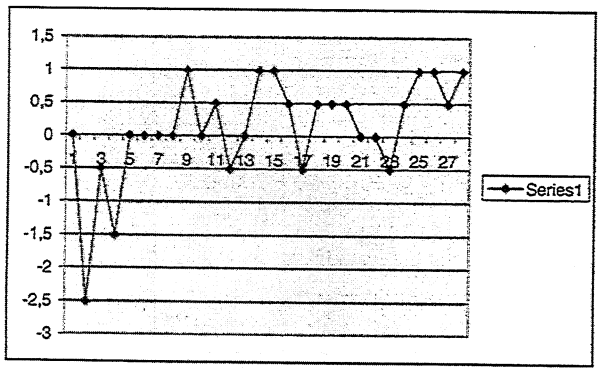

Figure 136. Gradient of temperature variation during measurement period 1.2.-28.2.2001.

4.4.4 Measuring point D

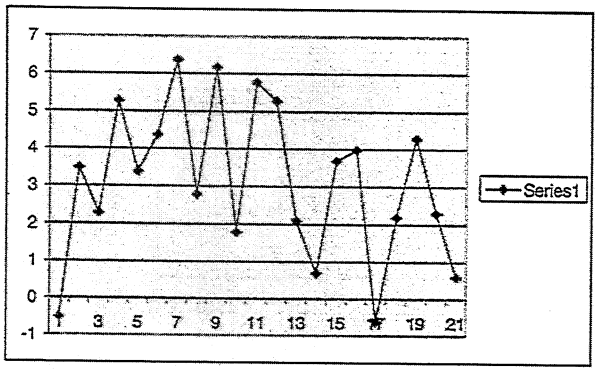

Figure 137. Gradient of temperature variation during measurement period 11.5.-31.5.1999.

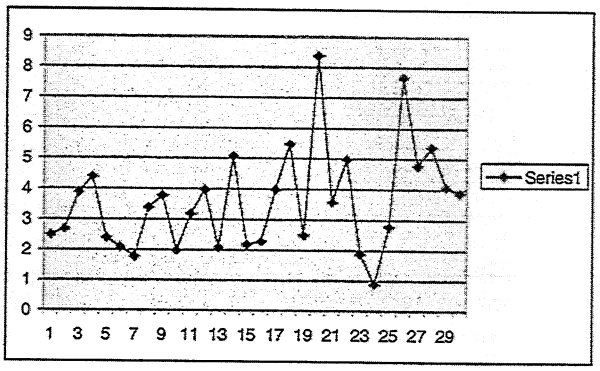

Figure 138. Gradient of temperature variation during measurement period 1.6.-30.6.1999.

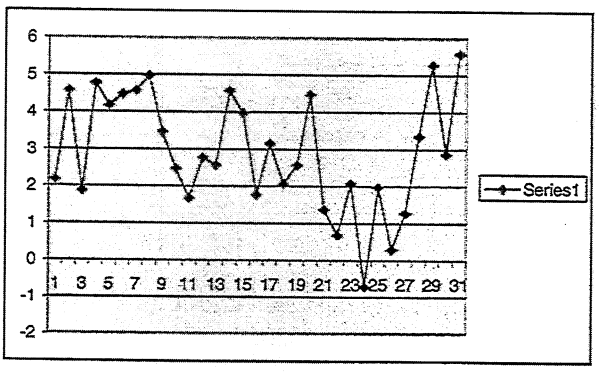

Figure 139. Gradient of temperature variation during measurement period 1.7.-31.7.1999.

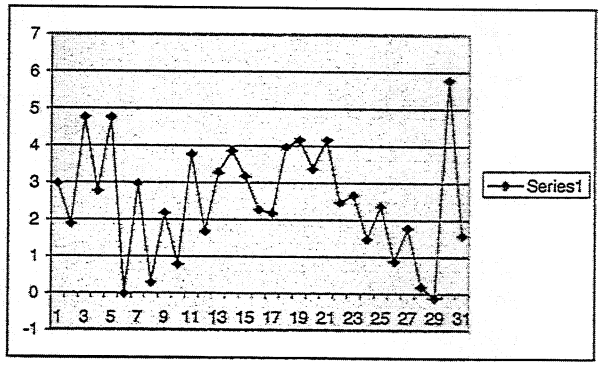

Figure 140. Gradient of temperature variation during measurement period 1.8.-31.8.1999.

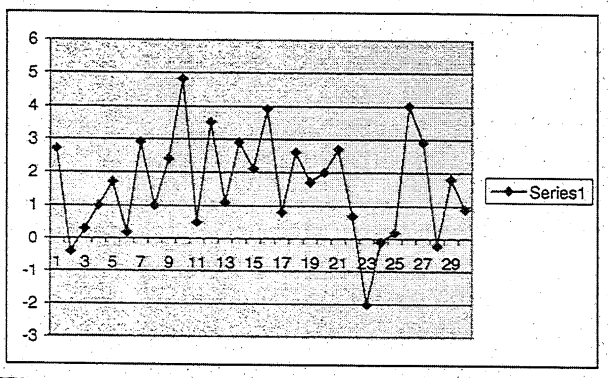

Figure 141. Gradient of temperature variation during measurement period 1.9.-30.9.1999.

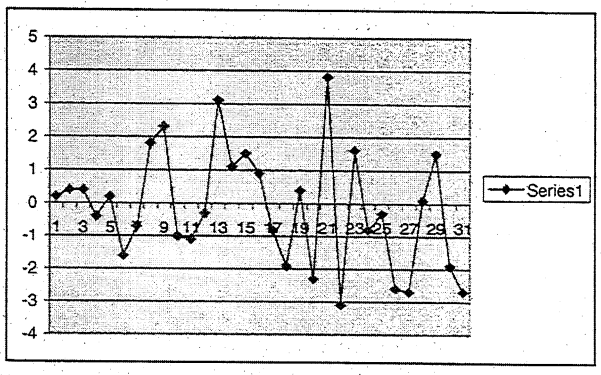

Figure 142. Gradient of temperature variation during measurement period 1.10.-31.10.1999.

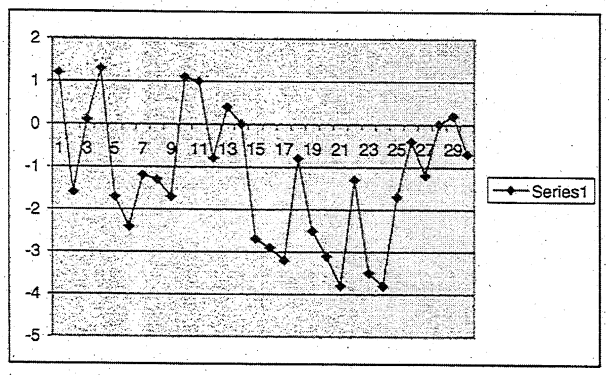

Figure 143. Gradient of temperature variation during measurement period 1.11.-30.11.1999.

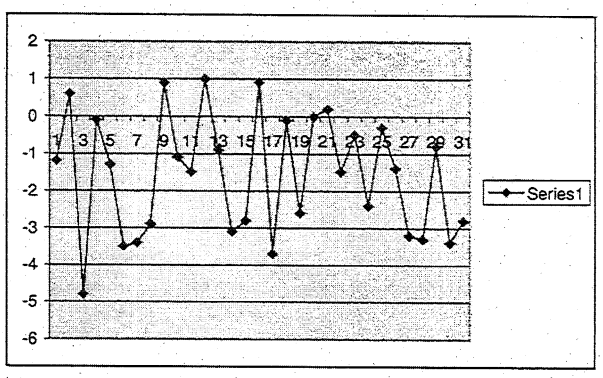

Figure 144. Gradient of temperature variation during measurement period 1.12.-31.12.1999.

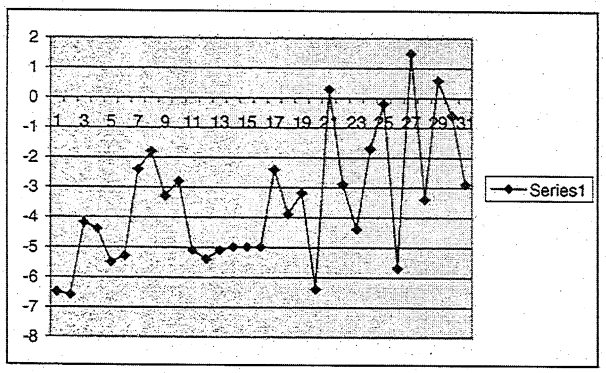

Figure 145. Gradient of temperature variation during measurement period 1.1.-31.1.2000.

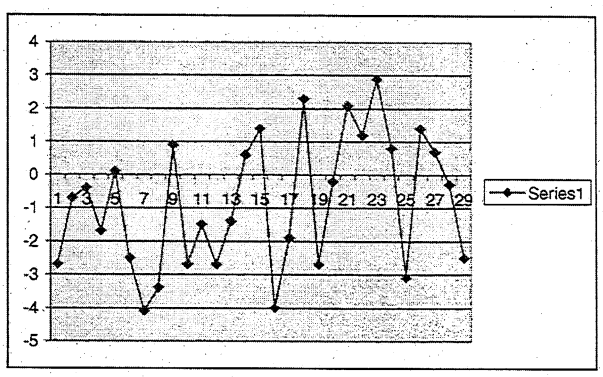

Figure 146. Gradient of temperature variation during measurement period 1.2.-29.2.2000.

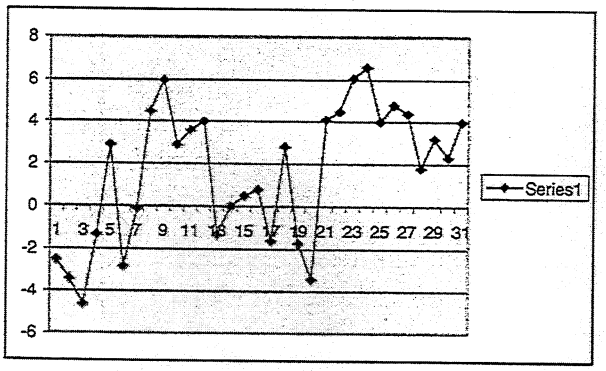

Figure 147. Gradient of temperature variation during measurement period 1.3.-31.3.2000.

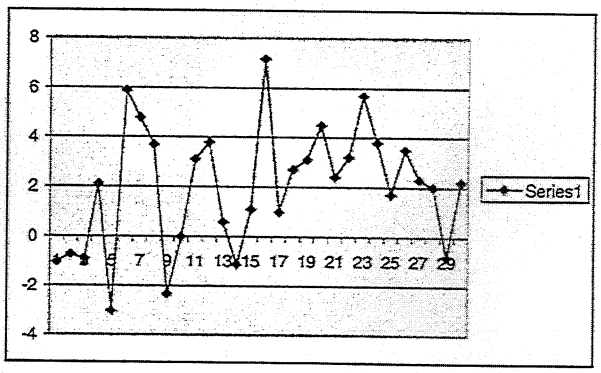

Figure 148. Gradient of temperature variation during measurement period 1.4.-30.4.2000.

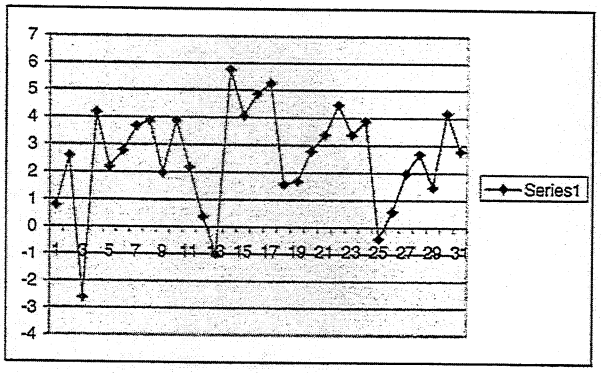

Figure 149. Gradient of temperature variation during measurement period 1.5.-31.5.2000.

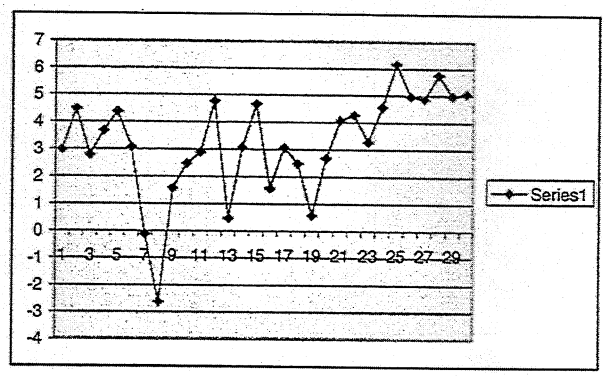

Figure 150. Gradient of temperature variation during measurement period 1.6.-30.6.2000.

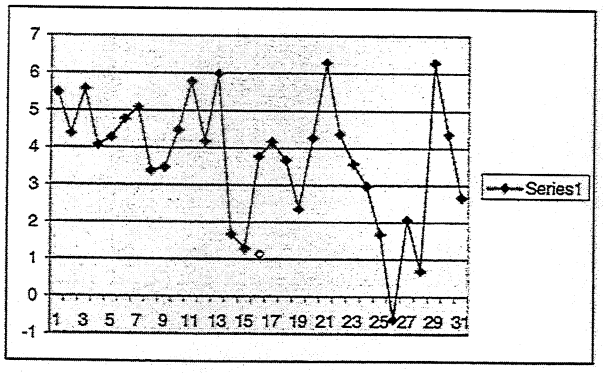

Figure 151. Gradient of temperature variation during measurement period 1.7.-31.7.2000.

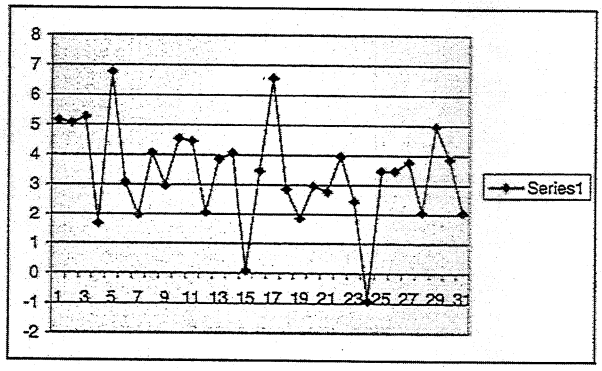

Figure 152. Gradient of temperature variation during measurement period 1.8.-31.8.2000.

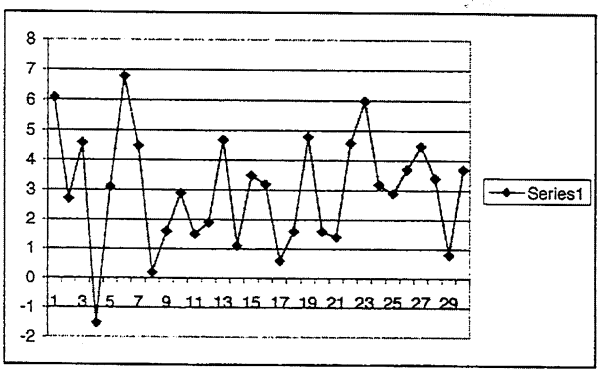

Figure 153. Gradient of temperature variation during measurement period 1.9.-30.9.2000.

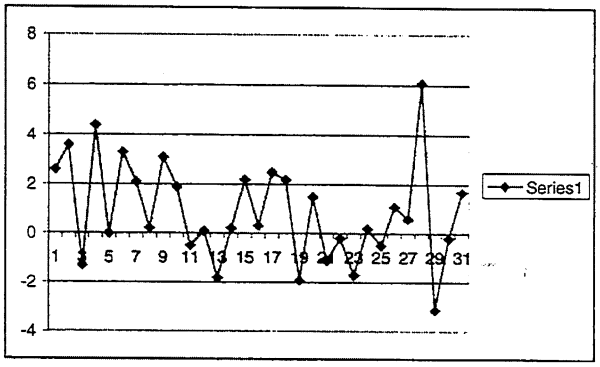

Figure 154. Gradient of temperature variation during measurement period 1.10.-31.10.2000.

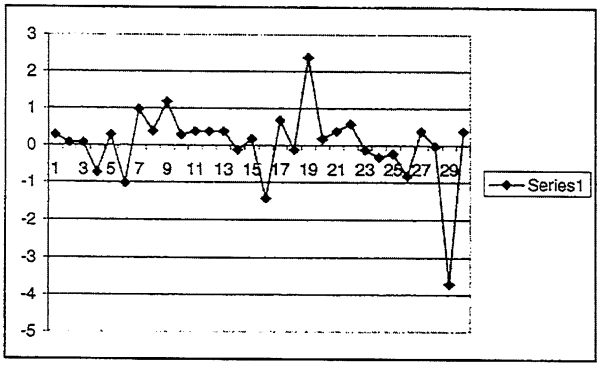

Figure 155. Gradient of temperature variation during measurement period 1.11.-30.11.2000.

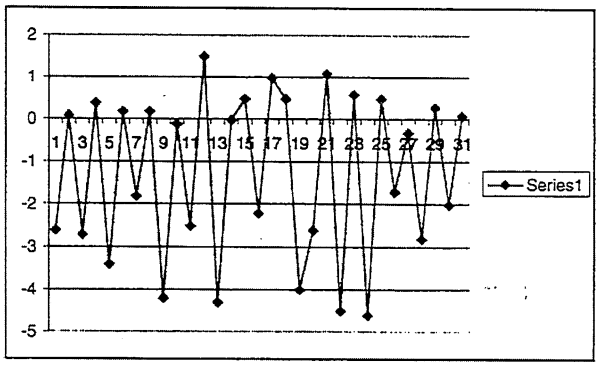

Figure 156. Gradient of temperature variation during measurement period 1.12.-31.12.2000.

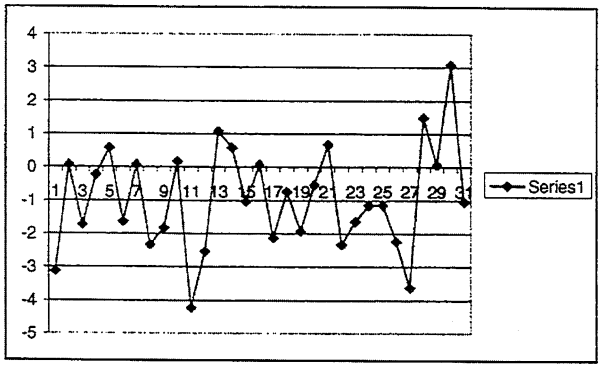

Figure 157. Gradient of temperature variation during measurement period 1.1.-31.1.2001.

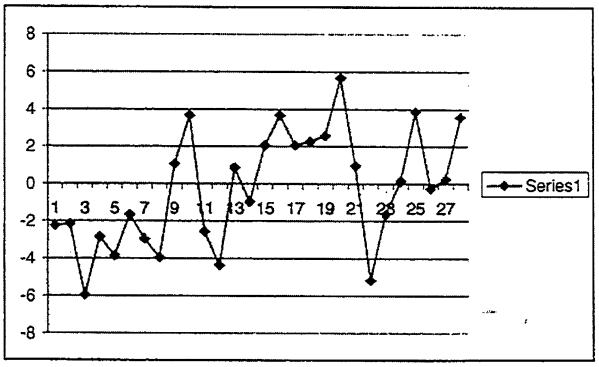

Figure 158. Gradient of temperature variation during measurement period 1.2.-28.2.2001.

4.4.5 Measuring point E

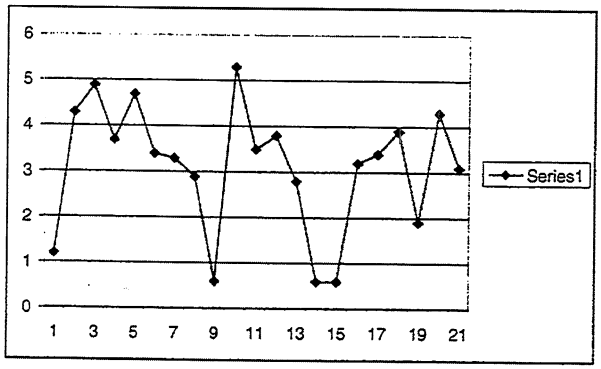

Figure 159. Gradient of temperature variation during measurement period 11.5.-31.5.1999.

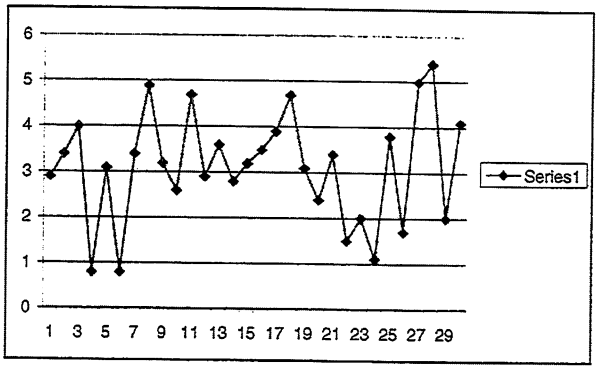

Figure 160. Gradient of temperature variation during measurement period 1.6.-30.6.1999.

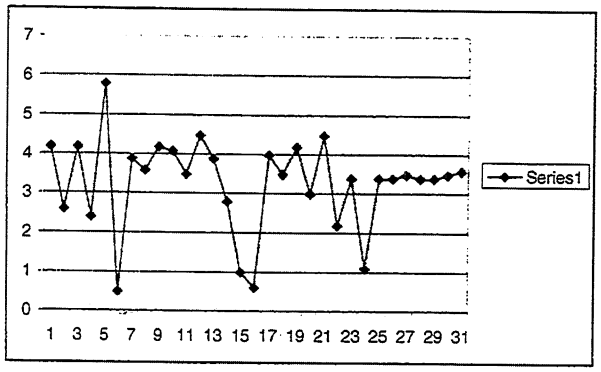

Figure 161. Gradient of temperature variation during measurement period 1.7.-31.7.1999.

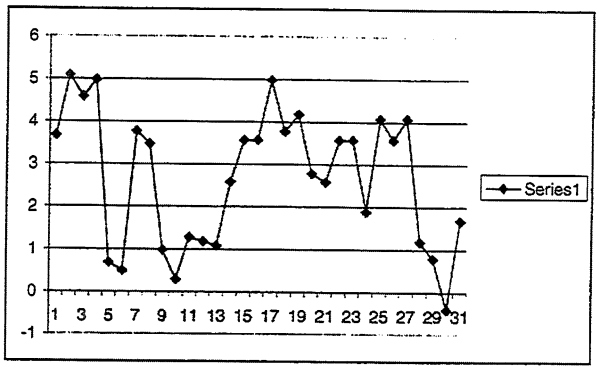

Figure 162. Gradient of temperature variation during measurement period 1.8.-31.8.1999.

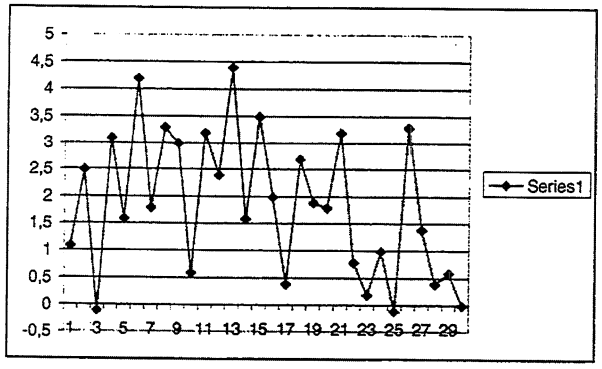

Figure 163. Gradient of temperature variation during measurement period 1.9.-30.9.1999.

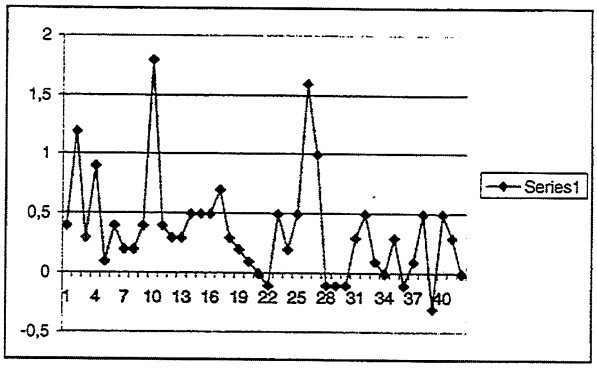

Figure 164. Gradient of temperature variation during measurement period 20.10.-30.11.1999.

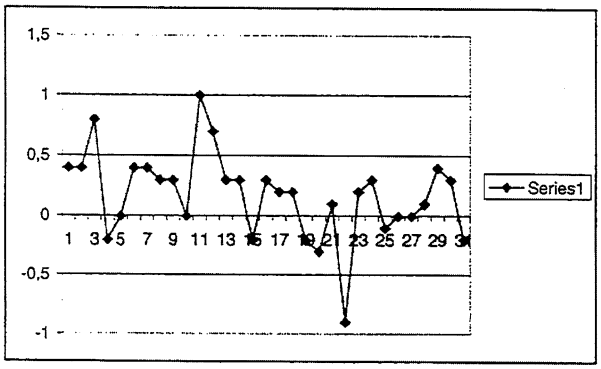

Figure 165. Gradient of temperature variation during measurement period 1.12.-31.12.1999.

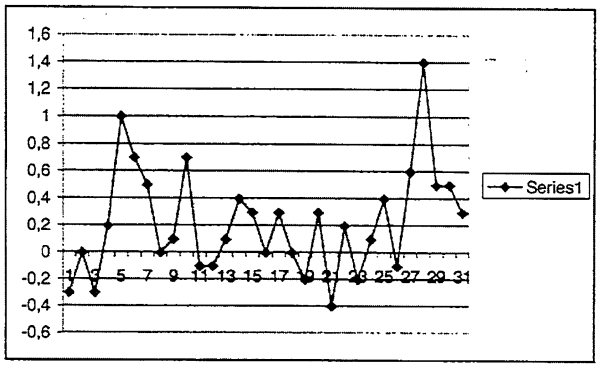

Figure 166. Gradient of temperature variation during measurement period 1.1.-31.1.2000.

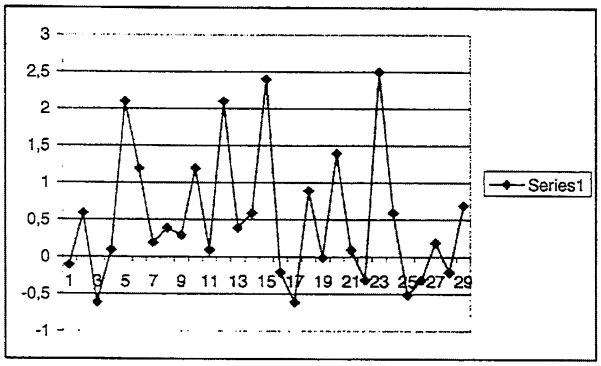

Figure 167. Gradient of temperature variation during measurement period 1.2.-29.2.2000.

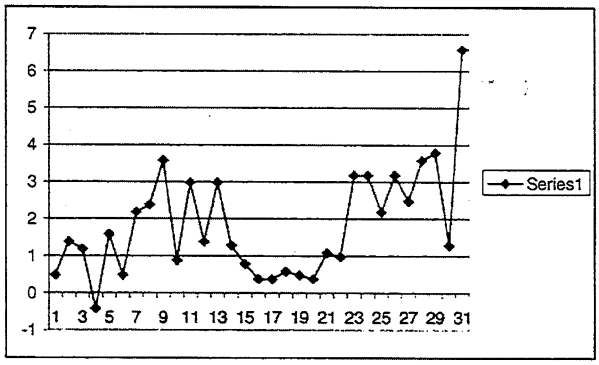

Figure 168. Gradient of temperature variation during measurement period 1.3.-31.3.2000.

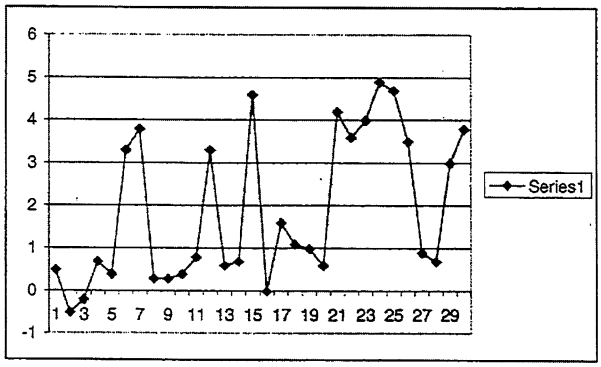

Figure 169. Gradient of temperature variation during measurement period 1.4.-30.4.2000.

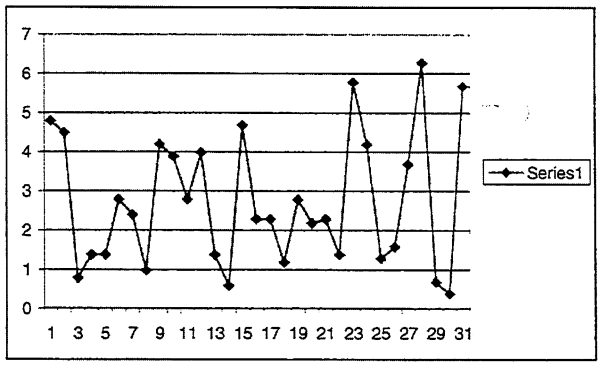

Figure 170. Gradient of temperature variation during measurement period 1.5.-31.5.2000.

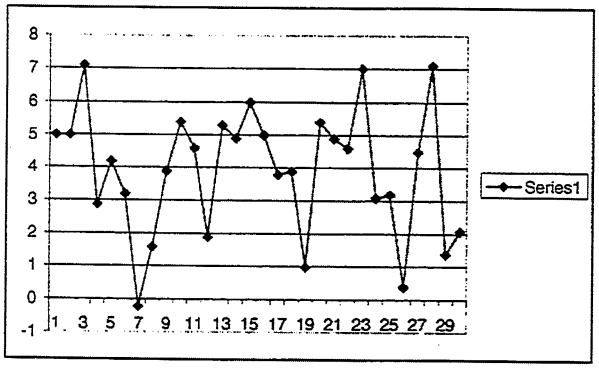

Figure 171. Gradient of temperature variation during measurement period 1.6.-30.6.2000.

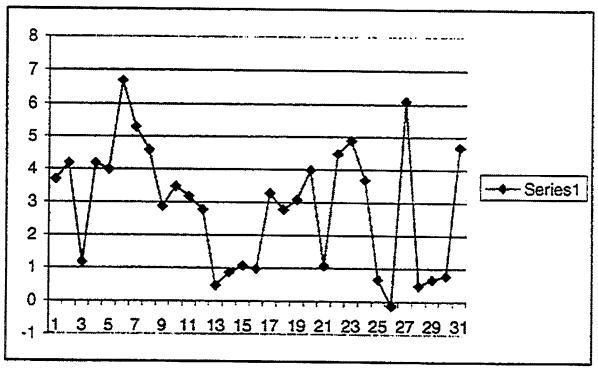

Figure 172. Gradient of temperature variation during measurement period 1.7.-31.7.2000.

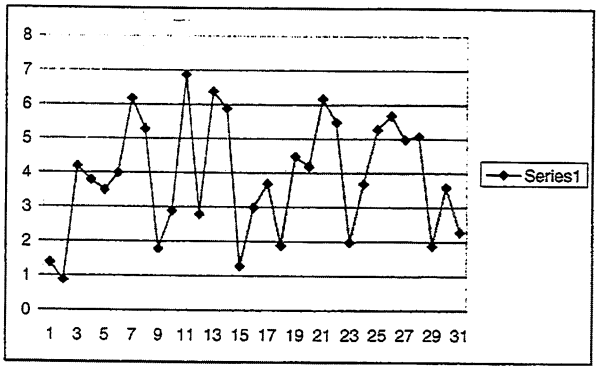

Figure 173. Gradient of temperature variation during measurement period 1.8.-31.8.2000.

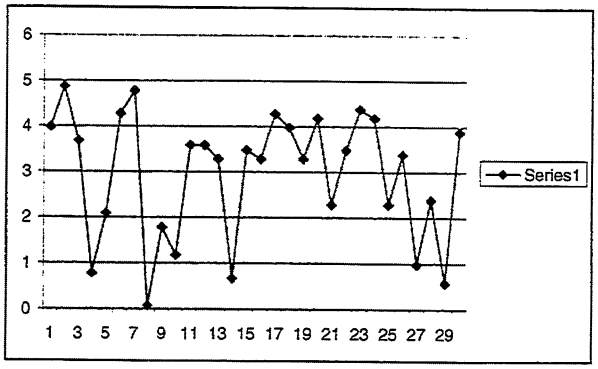

Figure 174. Gradient of temperature variation during measurement period 1.9.-30.9.2000.

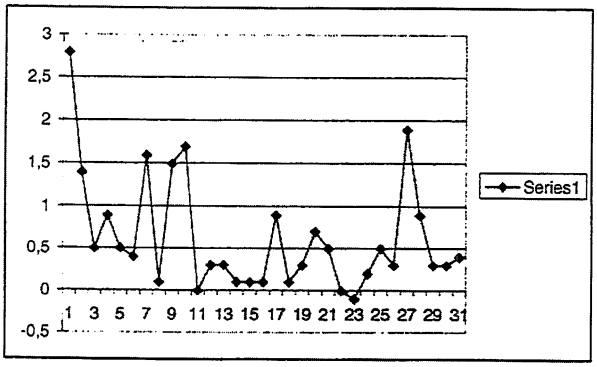

Figure 175. Gradient of temperature variation during measurement period 1.10.-31.10.2000.

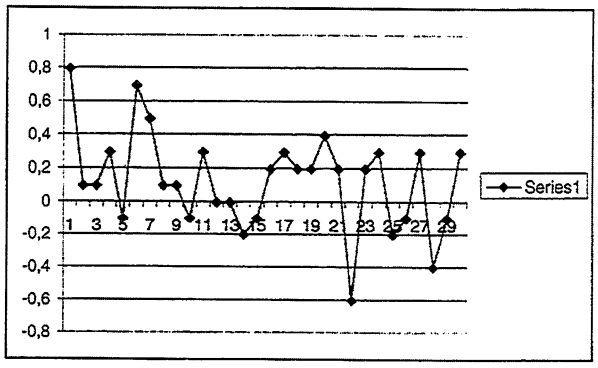

Figure 176. Gradient of temperature variation during measurement period 1.11.-30.11.2000.

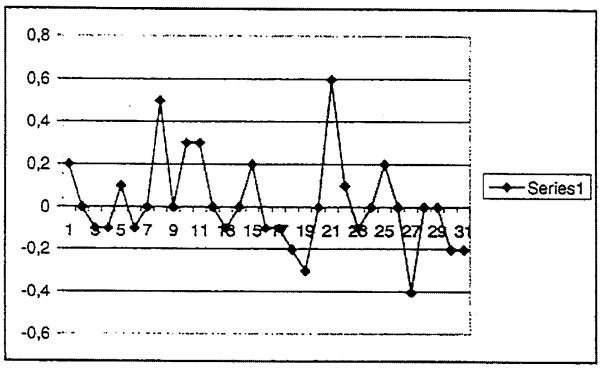

Figure 177. Gradient of temperature variation during measurement period 1.12.-31.12.2000.

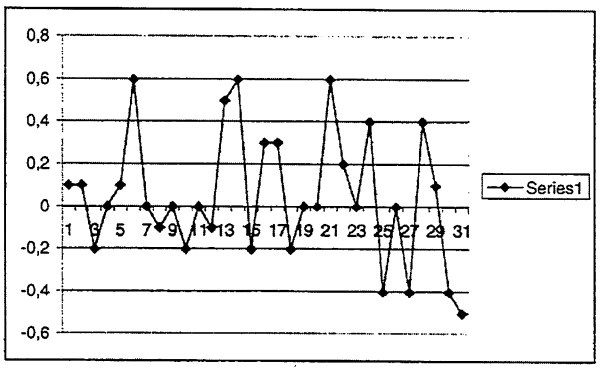

Figure 178. Gradient of temperature variation during measurement period 1.1.-31.1.2001.

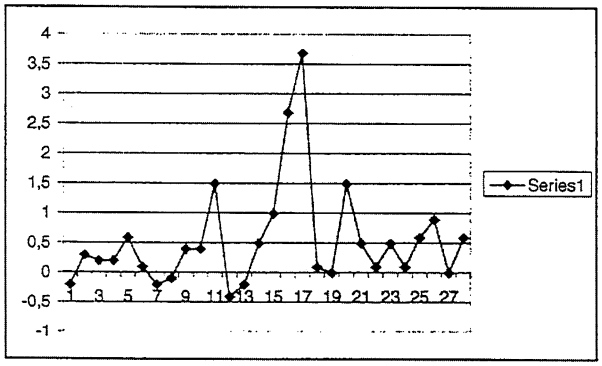

Figure 179. Gradient of temperature variation during measurement period 1.2.-28.2.2001.

4.5 Freeze/thaw -cycling of marble

The number of freeze/thaw -cycles occurred on marble surfaces was calculated from the data dealing with the daily variation of temperature presented in chapter 4.3. In this case freeze/thaw -cycle was defined as a day during which the maximum temperature was higher than +0.3°C and the minimum temperature lower than -0.3°C. The number of such days in every month, i.e. the number of freeze/thaw -cycles, on outer (OUT) and inner (IN) surfaces of each measuring slab is presented in Table 1.

Table 1. The number of freeze/thaw -cycles on marble surfaces.

month/year	slab A		slab B		slab C		slab D		slab E	
	OUT	IN	OUT	IN	OUT	IN	OUT	IN	OUT	IN
5/1999	x	x	x	x	x	x	1 [7]	1 [7]	4 [7]	2 [7]
6/1999	0	0	0	0	0	0	0	0	0	0
7/1999	0	0	x	x	0	0	0	0	0	0
8/1999	0	0	x	x	0	0	0	0	0	0
9/1999	0	0	x	x	0	0	0	0	0	0
10/1999	1	0	x	x	4 [4]	3 [4]	1	1	1 [8]	1 [8]
11/1999	7	5	x	x	x	x	10	9	7	5
12/1999	14	13	x	x	x	x	23	21	15	13
1/2000	4 [1]	4 [1]	x	x	x	x	16	15	13	14
2/2000	x	x	x	x	x	x	8	3	12	11
3/2000	16 [2]	14 [2]	x	x	x	x	1	0	25	23
4/2000	5	2	14 [3]	8 [3]	10 [5]	8 [5]	0	0	5	4
5/2000	0	0	4	3	0 [6]	0 [6]	1	1	1	0
6/2000	0	0	0	0	0	0	0	0	0	0
7/2000	0	0	0	0	0	0	0	0	0	0
8/2000	0	0	0	0	0	0	0	0	0	0
9/2000	0	0	1	0	1	0	0	0	0	0
10/2000	2	1	4	3	4	3	2	2	3	2
11/2000	2	0	7	5	6	4	1	1	3	3
12/2000	7	6	1	2	2	2	11	11	5	5
1/2001	21	20	0	0	5	7	9	8	10	11
2/2001	19	20	2	2	1	7	9	10	12	13

x = no results available

[1] → 11.1.2000 [2] 7.3.2000 → [3] 29.3.2000 → [4] → 20.10.1999

[5] 29.3.-12.4.2000 [6] 17.5.2000 → [7] 11.5.1999 → [8] 20.10.1999 →

4.6 Humidity gradient over the marble slab

The gradient of relative humidity over the marble slabs was studied by using the maximum and minimum relative humidities observed daily in outdoor air above the slab and inside the ventilation slot behind the slab. The results from measuring points D and E are shown as pictures presented below, Figs. 180-222. There are four curves in every picture. They are coded with numbers 1-4, and they have the following meaning:

Series 1 maximum relative humidity in outdoor air
Series 2 minimum relative humidity in outdoor air
Series 3 maximum relative humidity in ventilation slot
Series 4 minimum relative humidity in ventilation slot

4.6.1 Measuring point D

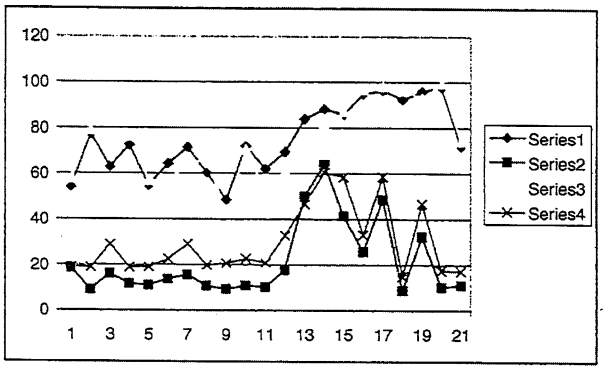

Figure 180. Daily variation of relative humidity during measuring period 11.5.-31.5.1999.

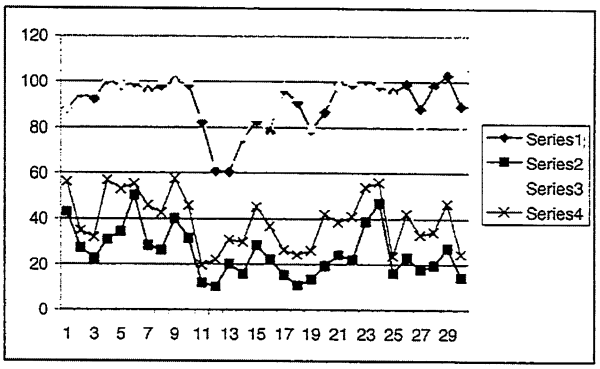

Figure 181. Daily variation of relative humidity during measuring period 1.6.-30.6.1999.

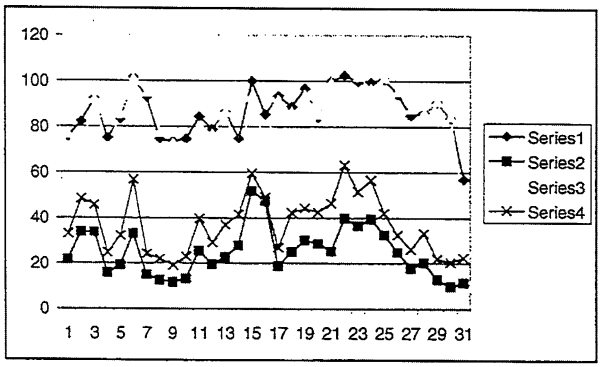

Figure 182. Daily variation of relative humidity during measuring period 1.7.-31.7.1999.

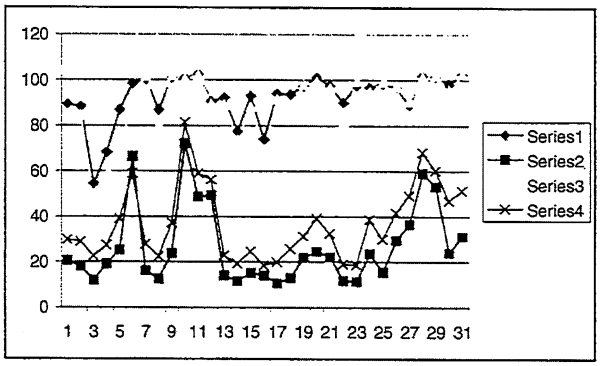

Figure 183. Daily variation of relative humidity during measuring period 1.8.-31.8.1999.

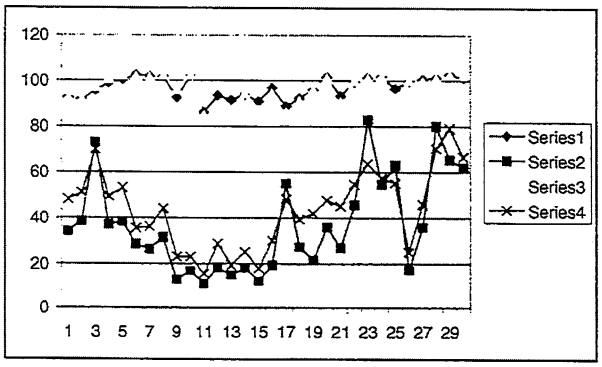

Figure 184. Daily variation of relative humidity during measuring period 1.9.-30.9.1999.

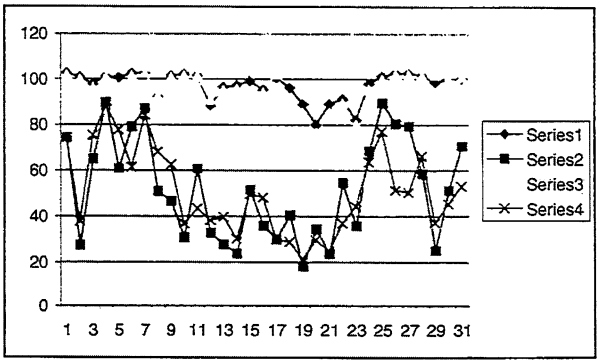

Figure 185. Daily variation of relative humidity during measuring period 1.10.-31.10.1999.

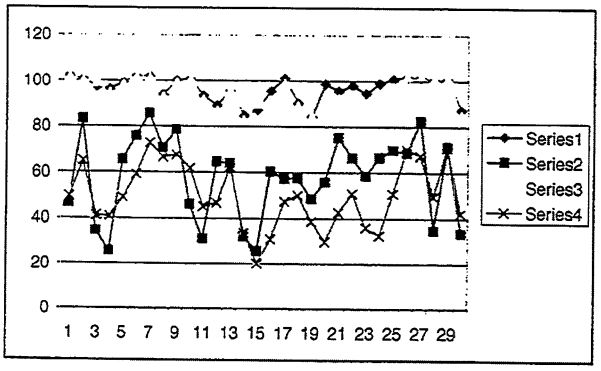

Figure 186. Daily variation of relative humidity during measuring period 1.11.-30.11.1999.

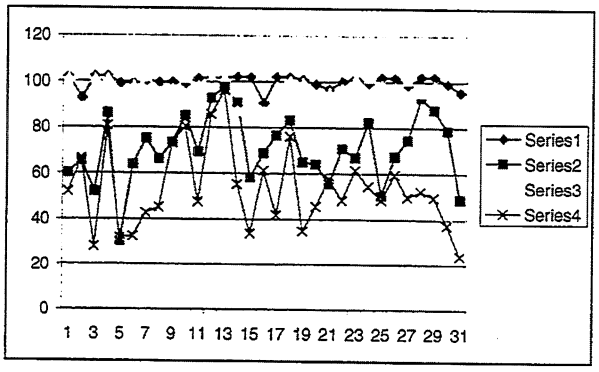

Figure 187. Daily variation of relative humidity during measuring period 1.12.-31.12.1999.

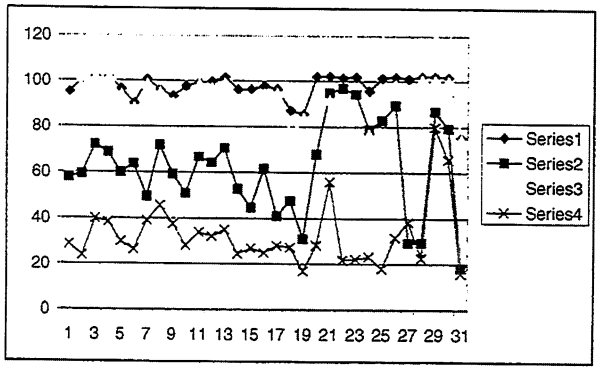

Figure 188. Daily variation of relative humidity during measuring period 1.1.-31.1.2000.

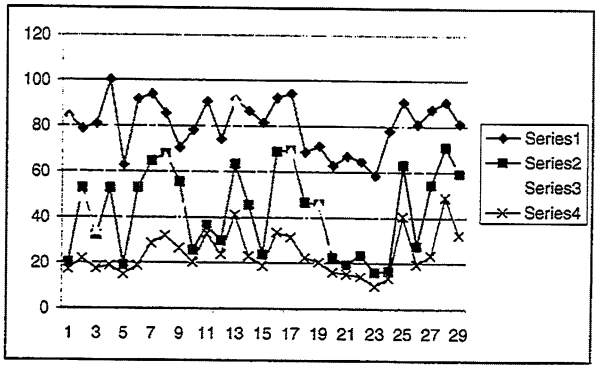

Figure 189. Daily variation of relative humidity during measuring period 1.2.-29.2.2000.

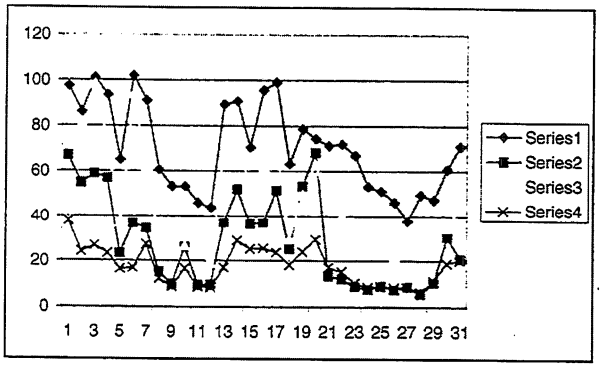

Figure 190. Daily variation of relative humidity during measuring period 1.3.-31.3.2000.

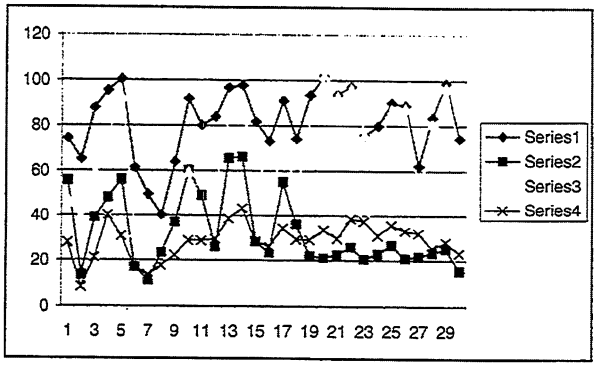

Figure 191. Daily variation of relative humidity during measuring period 1.4.-30.4.2000.

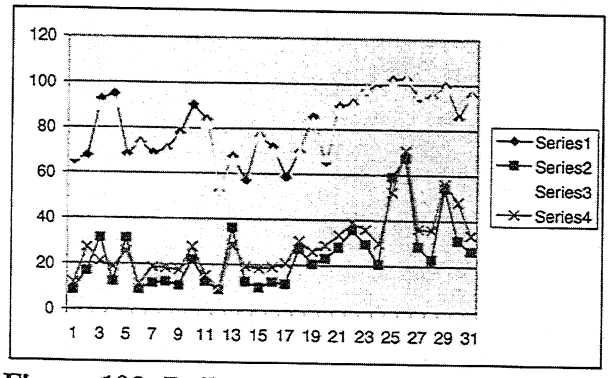

Figure 192. Daily variation of relative humidity during measuring period 1.5.-31.5.2000.

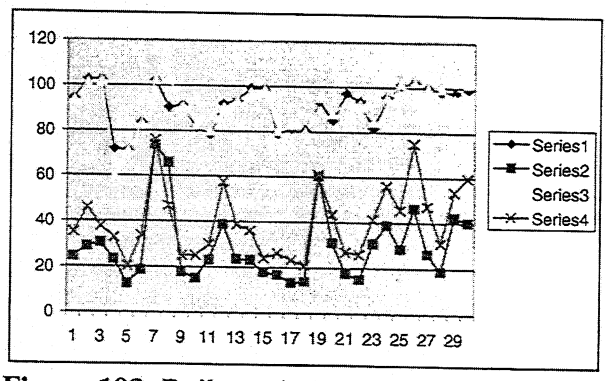

Figure 193. Daily variation of relative humidity during measuring period 1.6.-30.6.2000.

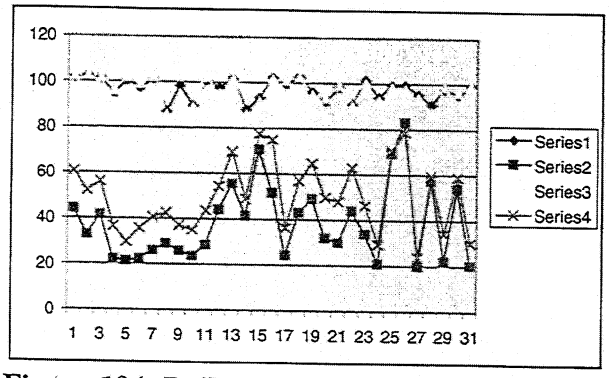

Figure 194. Daily variation of relative humidity during measuring period 1.7.-31.7.2000.

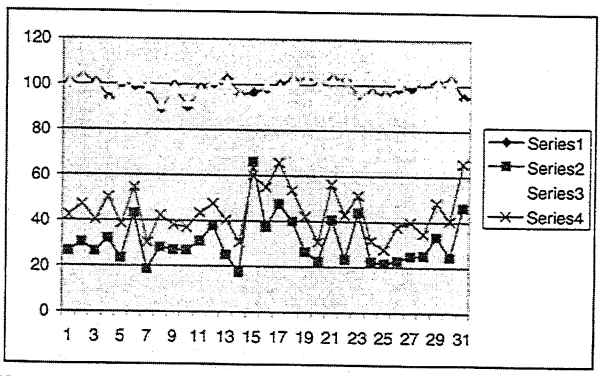

Figure 195. Daily variation of relative humidity during measuring period 1.8.-31.8.2000.

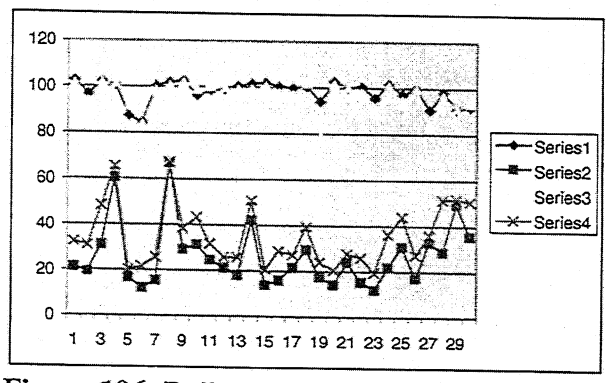

Figure 196. Daily variation of relative humidity during measuring period 1.9.-30.9.2000.

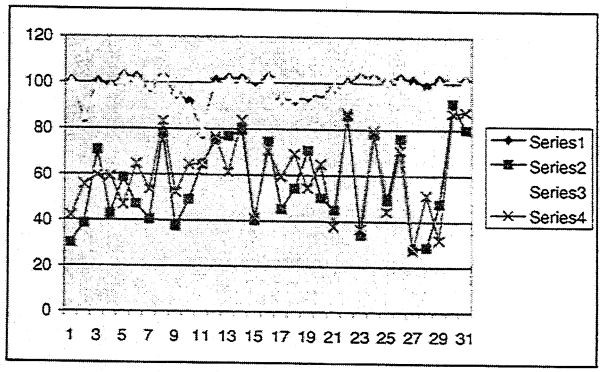

Figure 197. Daily variation of relative humidity during measuring period 1.10.-31.10.2000.

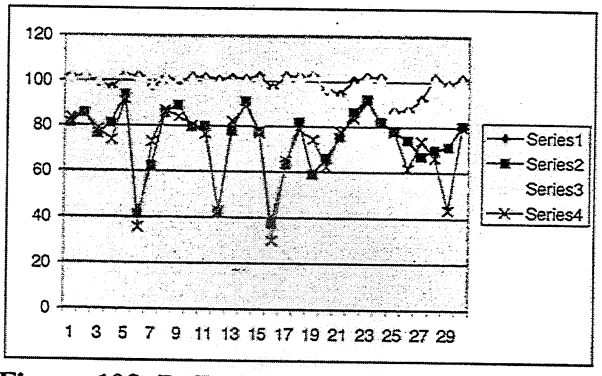

Figure 198. Daily variation of relative humidity during measuring period 1.11.-30.11.2000.

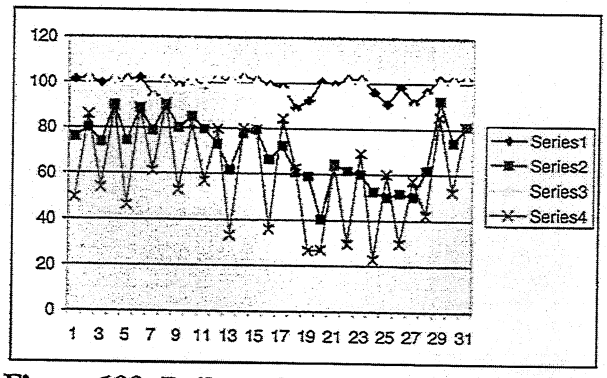

Figure 199. Daily variation of relative humidity during measuring period 1.12.-31.12.2000.

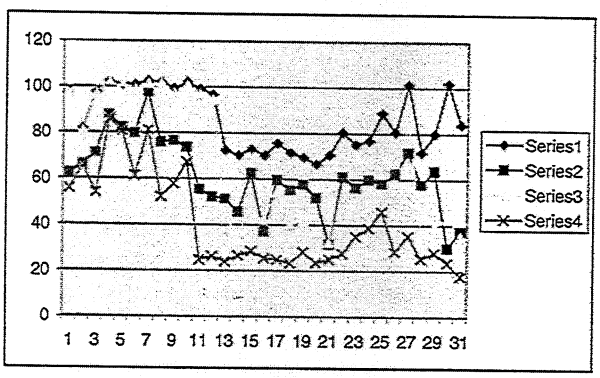

Figure 200. Daily variation of relative humidity during measuring period 1.1.-31.1.2001.

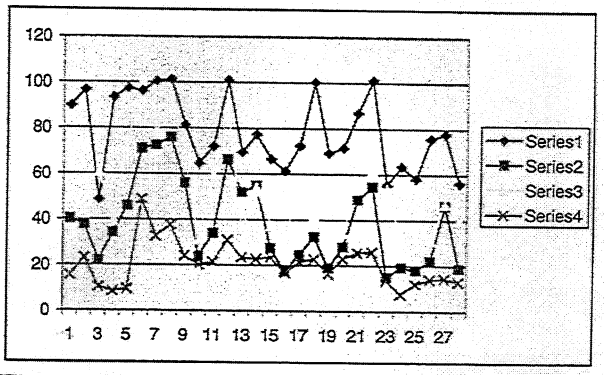

Figure 201. Daily variation of relative humidity during measuring period 1.2.-28.2.2001.

4.6.2 Measuring point E

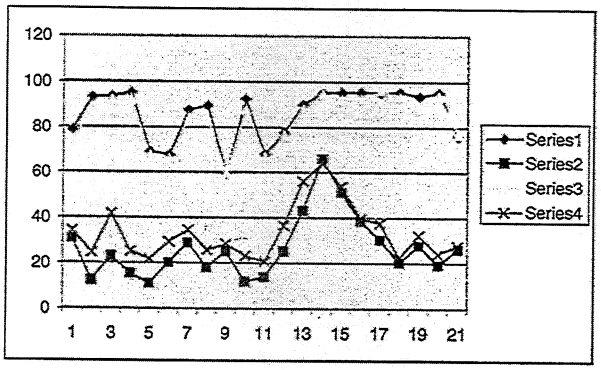

Figure 202. Daily variation of relative humidity during measuring period 11.5.-31.5.1999.

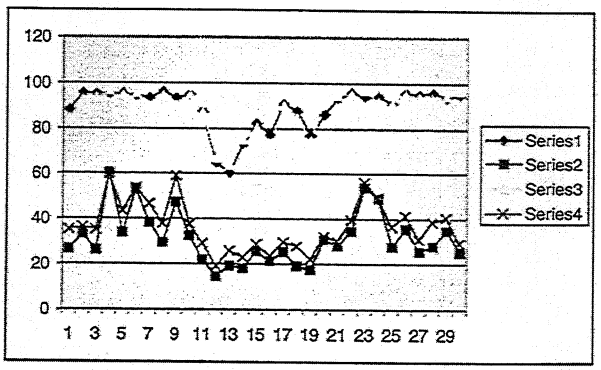

Figure 203. Daily variation of relative humidity during measuring period 1.6.-30.6.1999.

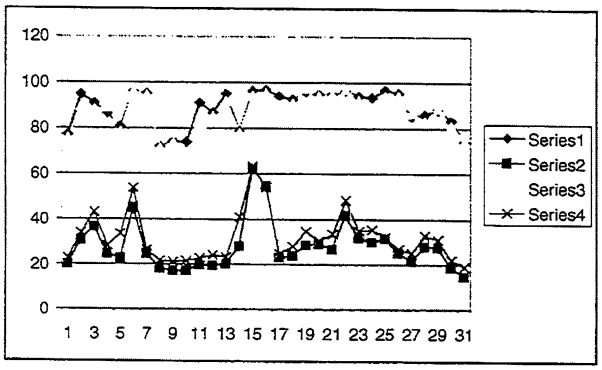

Figure 204. Daily variation of relative humidity during measuring period 1.7.-31.7.1999.

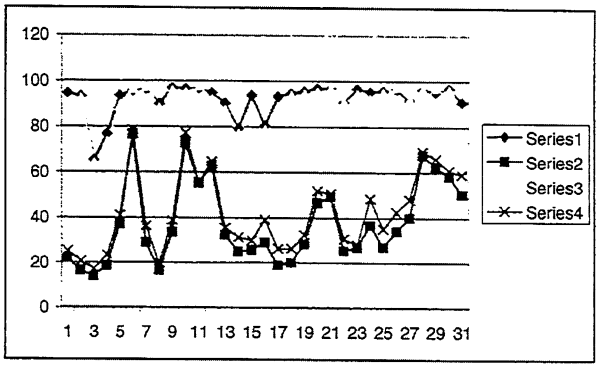

Figure 205. Daily variation of relative humidity during measuring period 1.8.-31.8.1999.

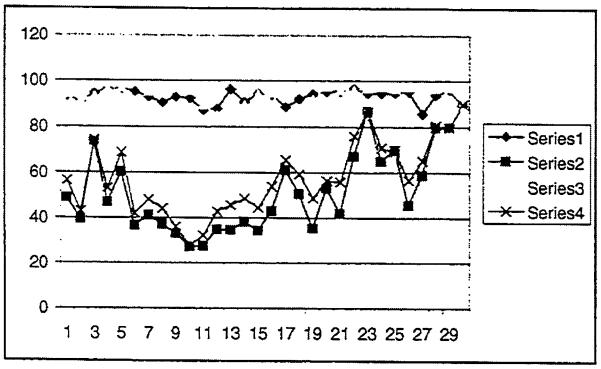

Figure 206. Daily variation of relative humidity during measuring period 1.9.-30.9.1999.

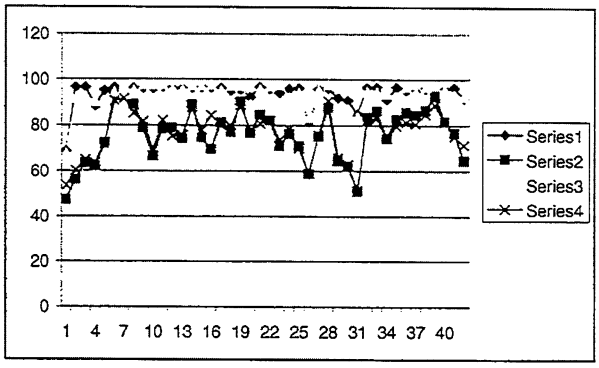

Figure 207. Daily variation of relative humidity during measuring period 20.10.-30.11.1999.

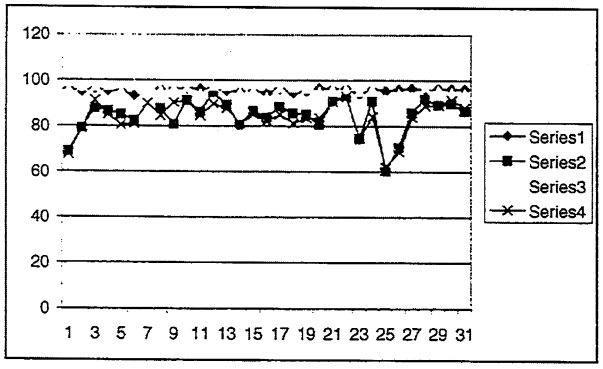

Figure 208. Daily variation of relative humidity during measuring period 1.12.-31.12.1999.

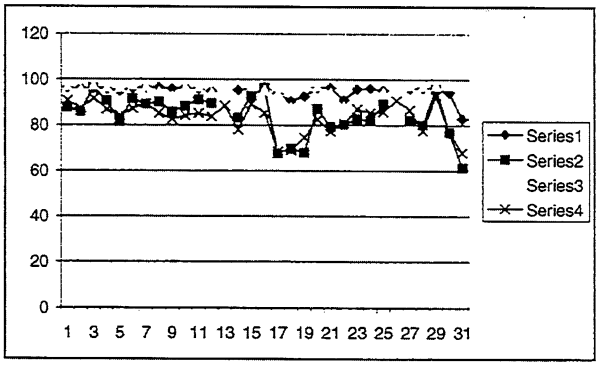

Figure 209. Daily variation of relative humidity during measuring period 1.1.-31.1.2000.

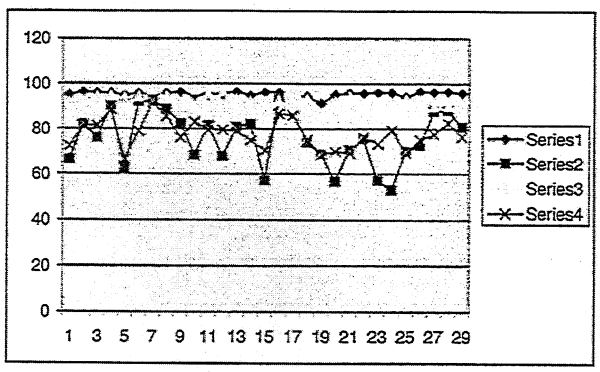

Figure 210. Daily variation of relative humidity during measuring period 1.2.-29.2.2000.

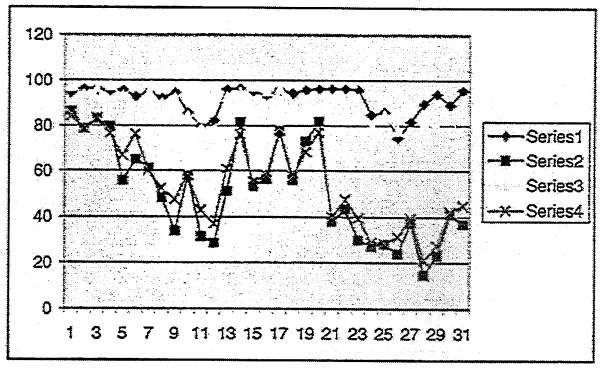

Figure 211. Daily variation of relative humidity during measuring period 1.3.-31.3.2000.

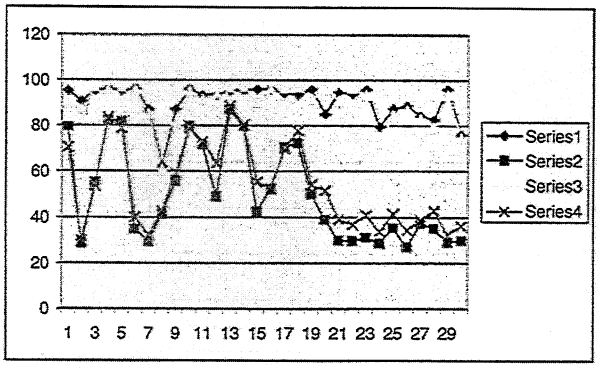

Figure 212. Daily variation of relative humidity during measuring period 1.4.-30.4.2000.

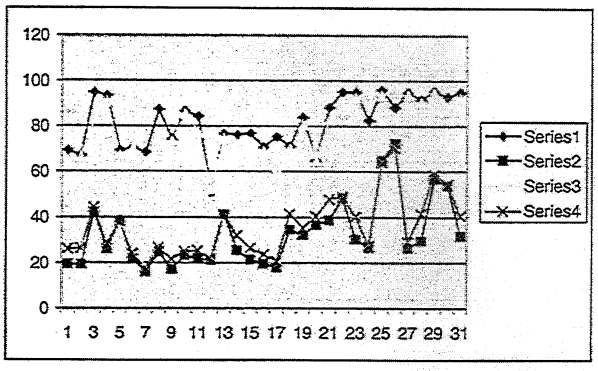

Figure 213. Daily variation of relative humidity during measuring period 1.5.-31.5.2000.

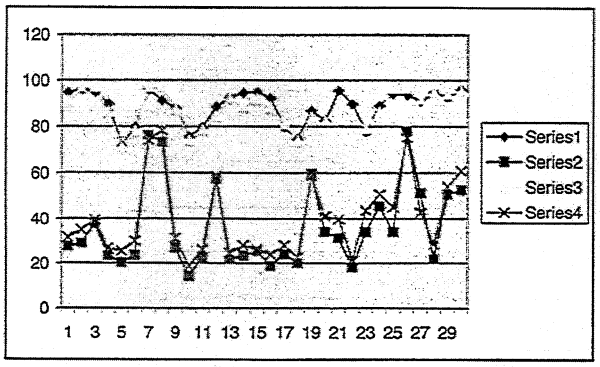

Figure 214. Daily variation of relative humidity during measuring period 1.6.-30.6.2000.

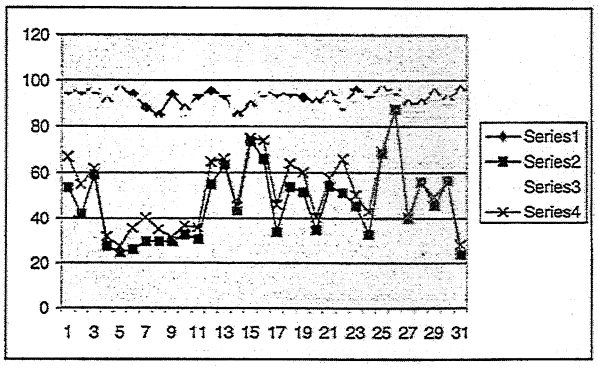

Figure 215. Daily variation of relative humidity during measuring period 1.7.-31.7.2000.

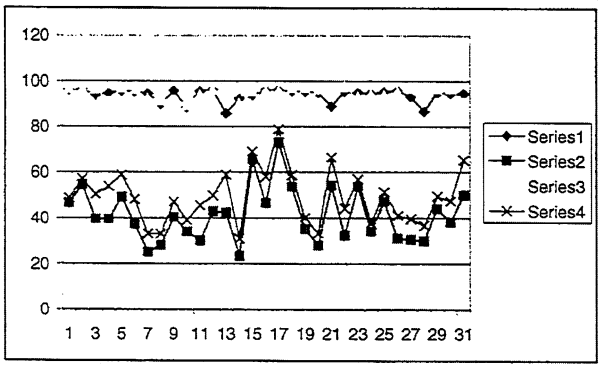

Figure 216. Daily variation of relative humidity during measuring period 1.8.-31.8.2000.

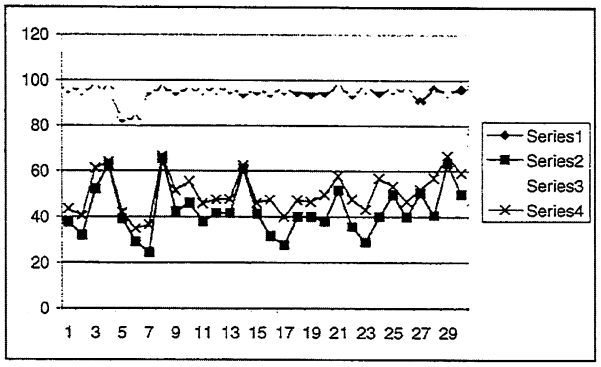

Figure 217. Daily variation of relative humidity during measuring period 1.9.-30.9.2000.

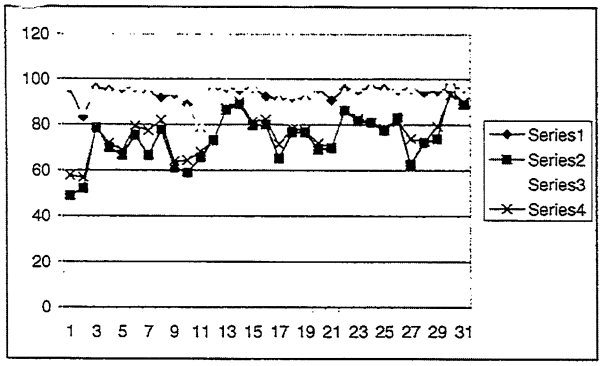

Figure 218. Daily variation of relative humidity during measuring period 1.10.-31.10.2000.

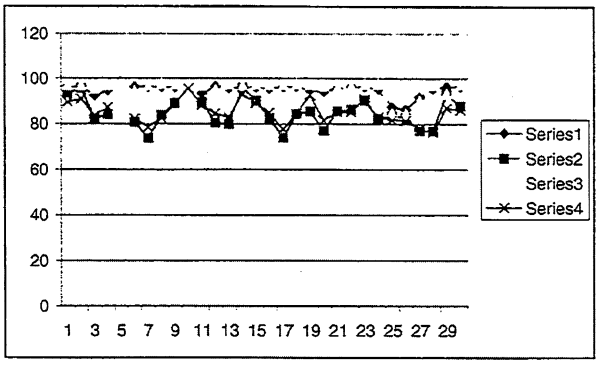

Figure 219. Daily variation of relative humidity during measuring period 1.11.-30.11.2000.

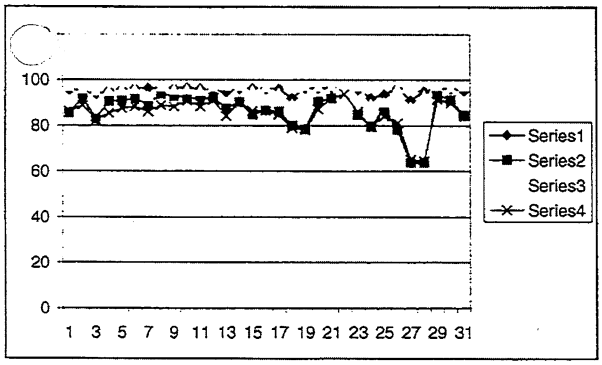

Figure 220. Daily variation of relative humidity during measuring period 1.12.-31.12.2000.

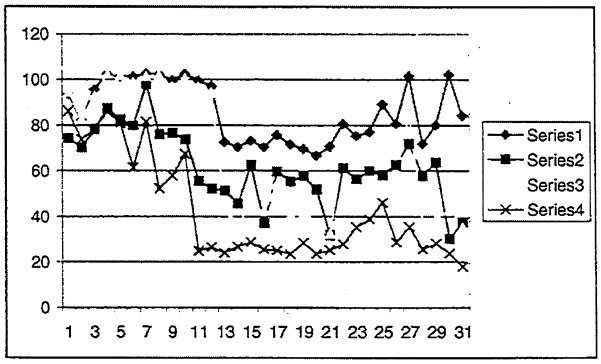

Figure 221. Daily variation of relative humidity during measuring period 1.1.-31.1.2001.

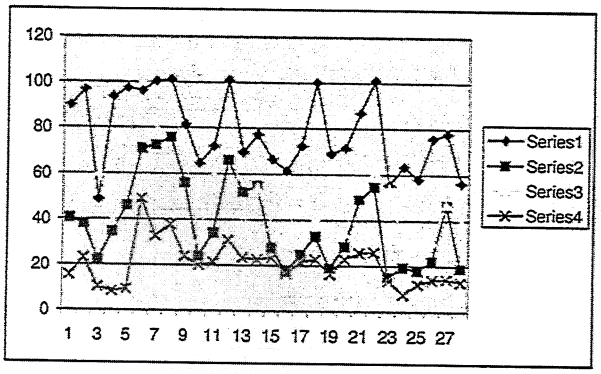

Figure 222. Daily variation of relative humidity during measuring period 1.2.-28.2.2001.

4.7 Acidity of rain water

Finnish Environment Institute has a measurement station at Nupuri, Espoo, about 20 km northwest from Finlandia Hall, where pH of rain water is continuously monitored. Monthly averages from the year 1999 are presented in Table 2.

Table 2. Acidity of rain water at Nupuri measurement station in 1999.

month	pH
January	4.30
February	4.80
March	4.89
April	5.32
May	*
June	*
July	5.34
August	*
September	4.93
October	5.06
November	4.98
December	4.63

* result abandoned due to contamination

The weighted pH-average of the year 1999 was 4.80. It was calculated from the monthly averages by weighting the values with the monthly depths of rainfall. The results from the year 2000 were not available by the time of reporting.

4.8 Weather conditions

4.8.1 Temperature and humidity

Daily maximum and minimum temperatures and corresponding relative humidities in Helsinki area are presented in Figs. 223-266 according to the data of Finnish Meteorological Institute. In the figures Series 1 represents the maximum values and Series 2 the minimum values.

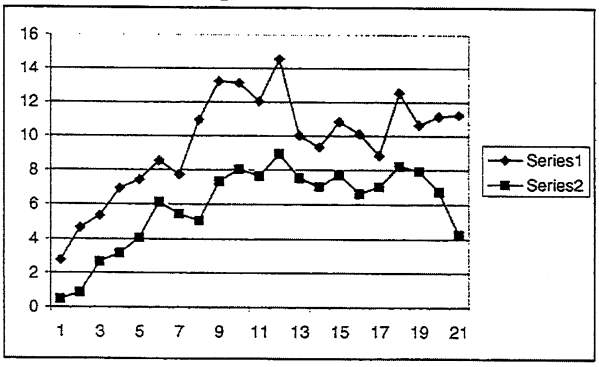

Figure 223. Daily variation of temperature (°C) in Helsinki during measurement period 11.5.-31.5.1999.

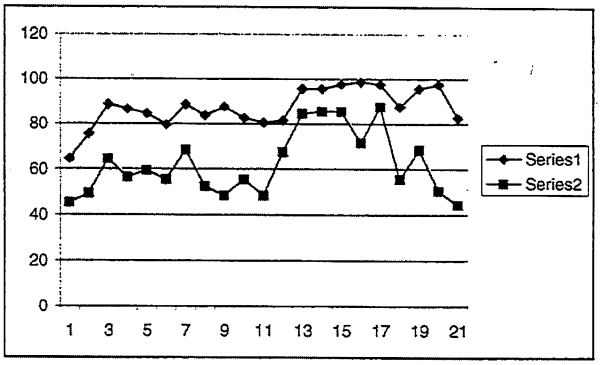

Figure 224. Daily variation of relative humidity (%) in Helsinki during measurement period 11.5.-31.5.1999.

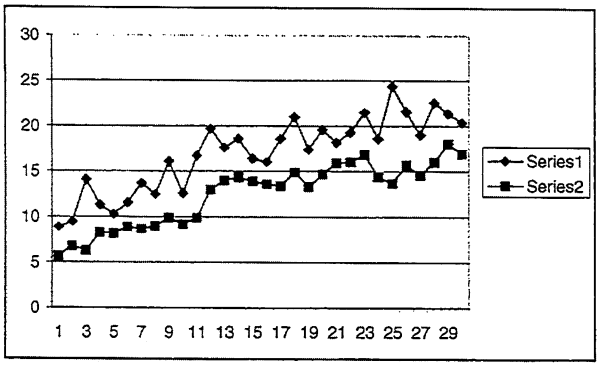

Figure 225. Daily variation of temperature (°C) in Helsinki during measurement period 1.6.-30.6.1999.

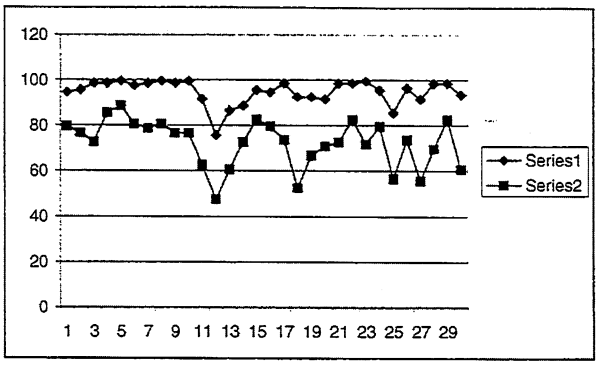

Figure 226. Daily variation of relative humidity (%) in Helsinki during measurement period 1.6.-30.6.1999.

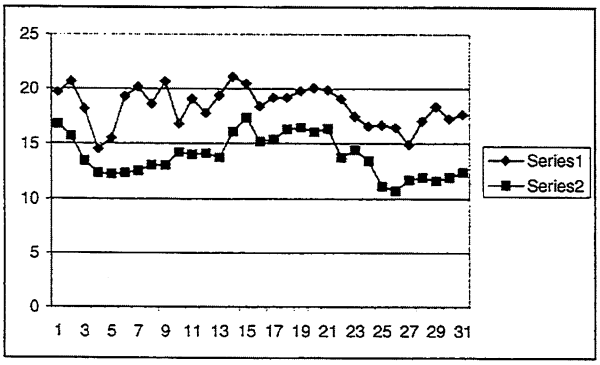

Figure 227. Daily variation of temperature (°C) in Helsinki during measurement period 1.7.-31.7.1999.

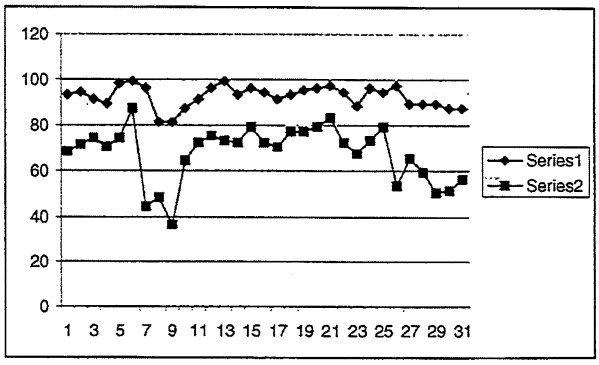

Figure 228. Daily variation of relative humidity (%) in Helsinki during measurement period 1.7.-31.7.1999.

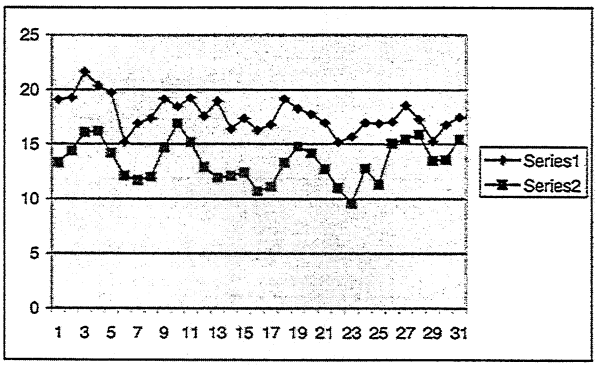

Figure 229. Daily variation of temperature (°C) in Helsinki during measurement period 1.8.-31.8.1999.

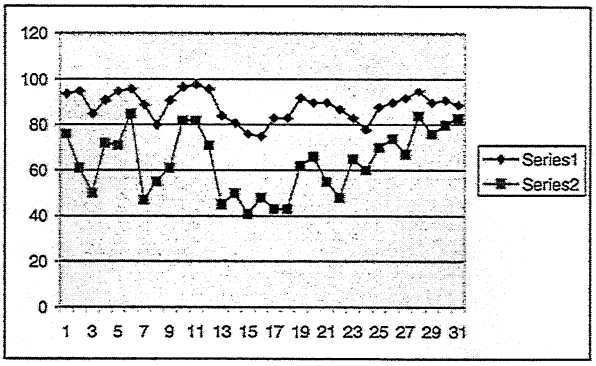

Figure 230. Daily variation of relative humidity (%) in Helsinki during measurement period 1.8.-31.8.1999.

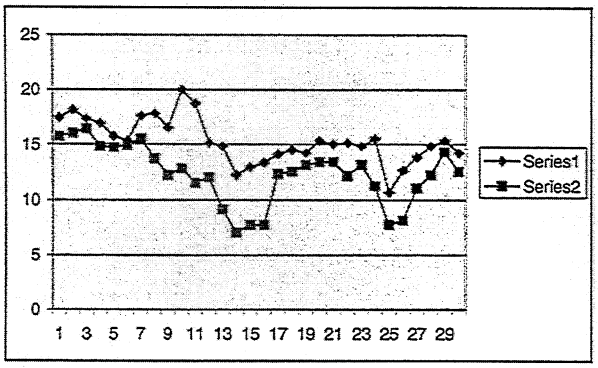

Figure 231. Daily variation of temperature (°C) in Helsinki during measurement period 1.9.-30.9.1999.

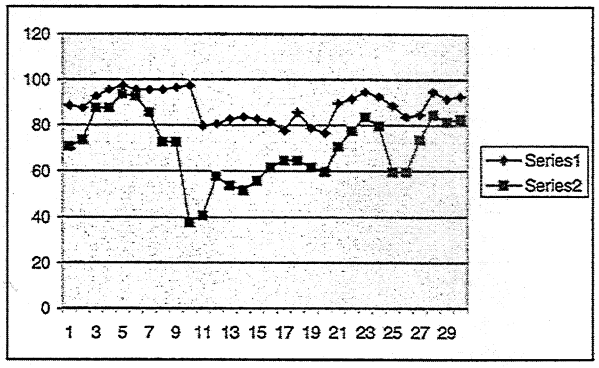

Figure 232. Daily variation of relative humidity (%) in Helsinki during measurement period 1.9.-30.9.1999.

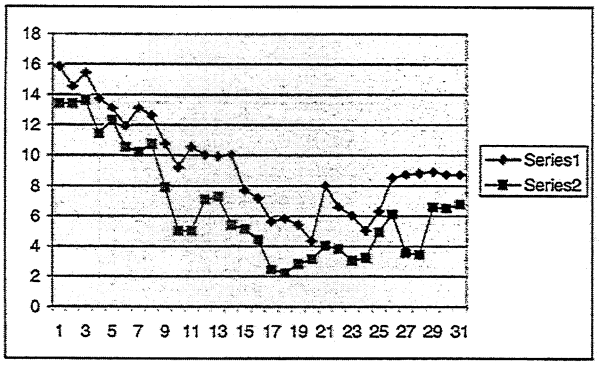

Figure 233. Daily variation of temperature (°C) in Helsinki during measurement period 1.10.-31.10.1999.

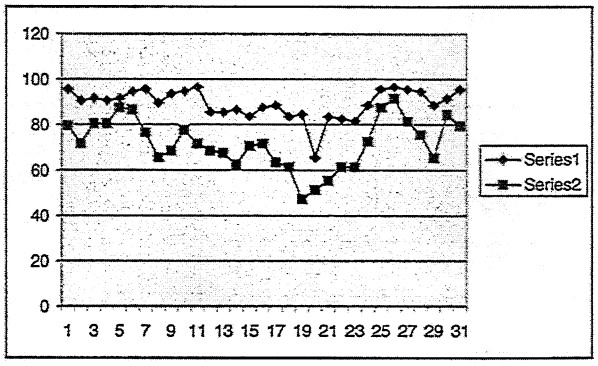

Figure 234. Daily variation of relative humidity (%) in Helsinki during measurement period 1.10.-31.10.1999.

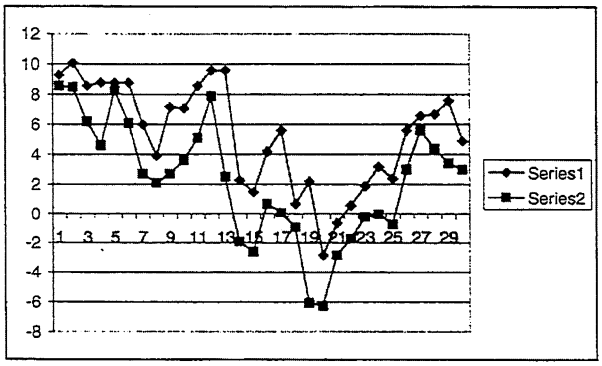

Figure 235. Daily variation of temperature (°C) in Helsinki during measurement period 1.11.-30.11.1999.

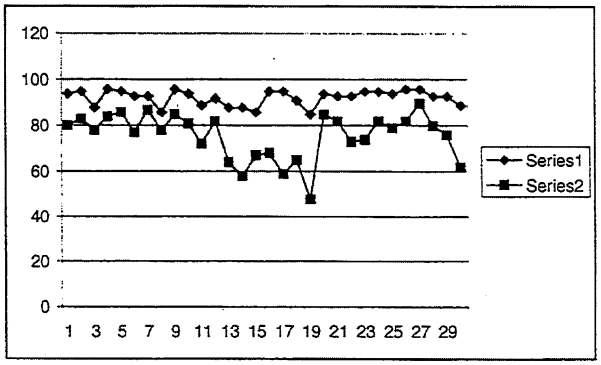

Figure 236. Daily variation of relative humidity (%) in Helsinki during measurement period 1.11.-30.11.1999.

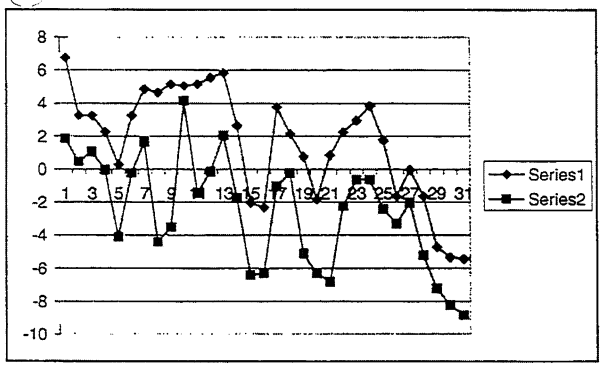

Figure 237. Daily variation of temperature (°C) in Helsinki during measurement period 1.12.-31.12.1999.

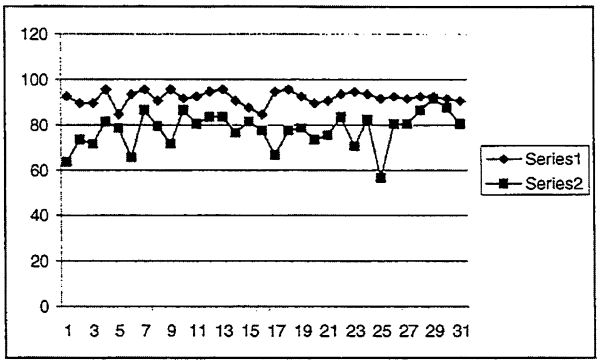

Figure 238. Daily variation of relative humidity (%) in Helsinki during measurement period 1.12.-31.12.1999.

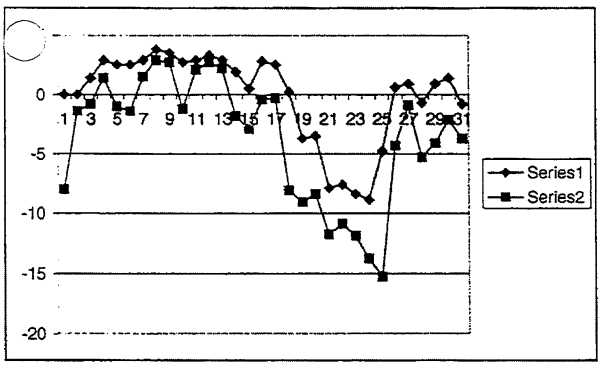

Figure 239. Daily variation of temperature (°C) in Helsinki during measurement period 1.1.-31.1.2000.

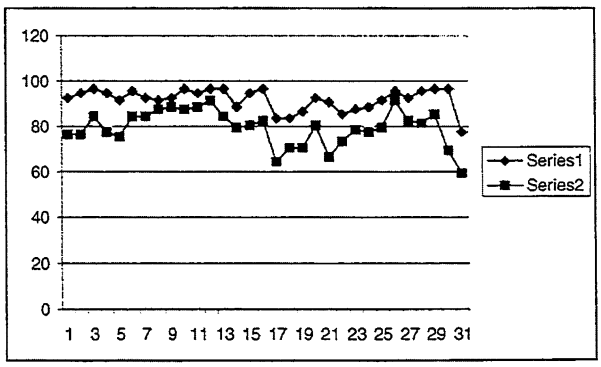

Figure 240. Daily variation of relative humidity (%) in Helsinki during measurement period 1.1.-31.1.2000.

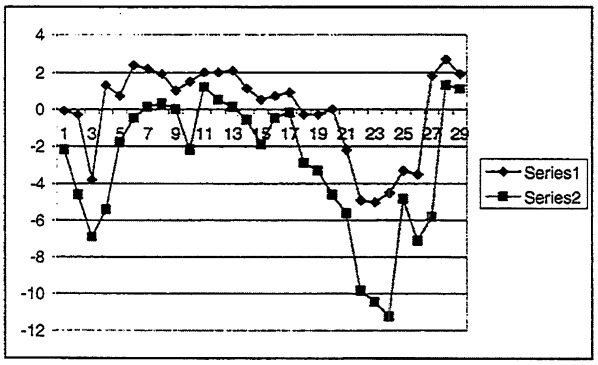

Figure 241. Daily variation of temperature (°C) in Helsinki during measurement period 1.2.-29.2.2000.

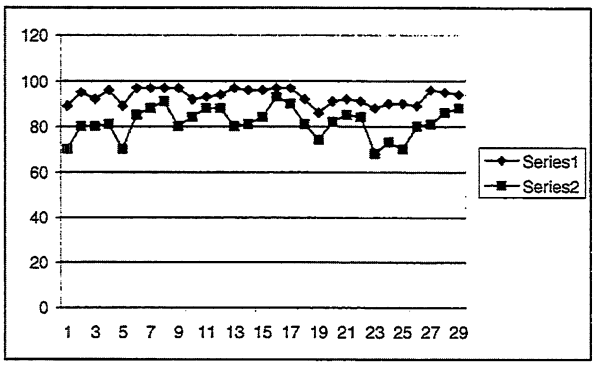

Figure 242. Daily variation of relative humidity (%) in Helsinki during measurement period 1.2.-29.2.2000.

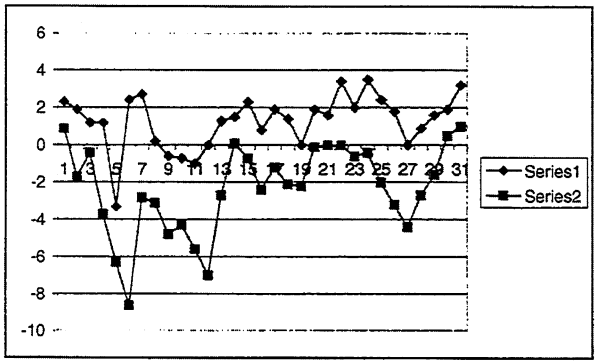

Figure 243. Daily variation of temperature (°C) in Helsinki during measurement period 1.3.-31.3.2000.

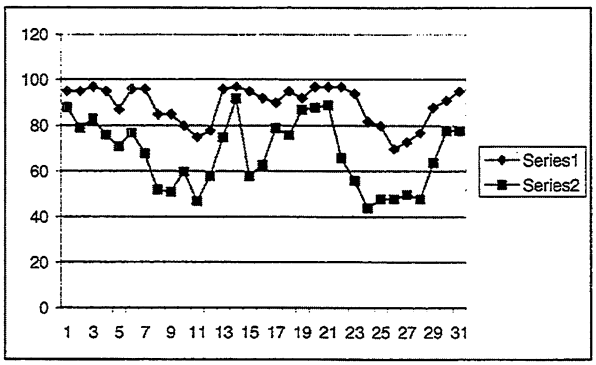

Figure 244. Daily variation of relative humidity (%) in Helsinki during measurement period 1.3.-31.3.2000.

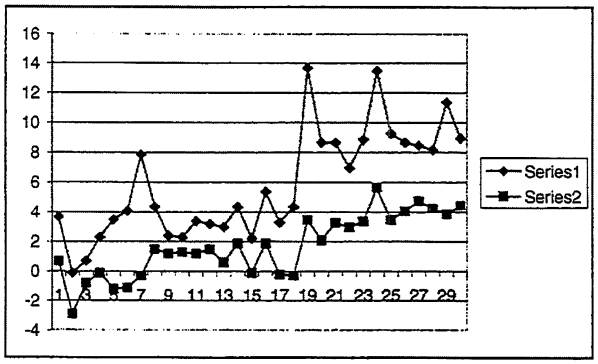

Figure 245. Daily variation of temperature (°C) in Helsinki during measurement period 1.4.-30.4.2000.

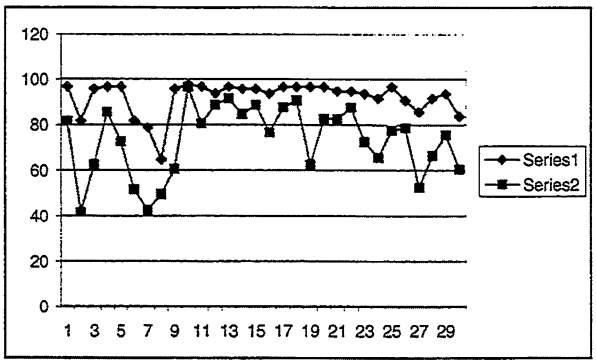

Figure 246. Daily variation of relative humidity (%) in Helsinki during measurement period 1.4.-30.4.2000.

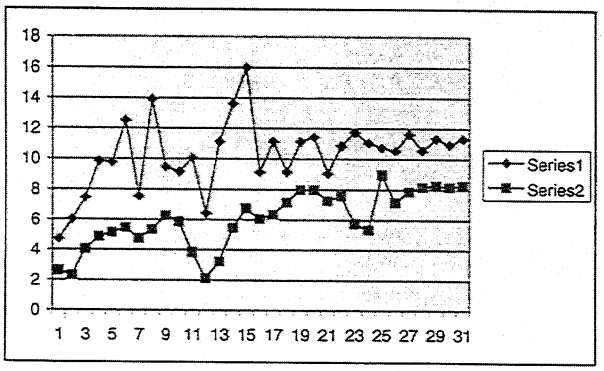

Figure 247. Daily variation of temperature (°C) in Helsinki during measurement period 1.5.-31.5.2000.

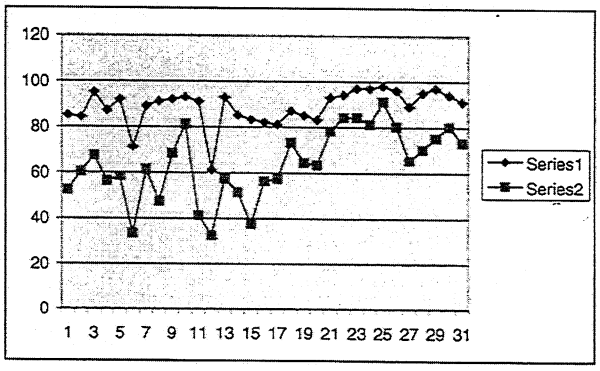

Figure 248. Daily variation of relative humidity (%) in Helsinki during measurement period 1.5.-31.5.2000.

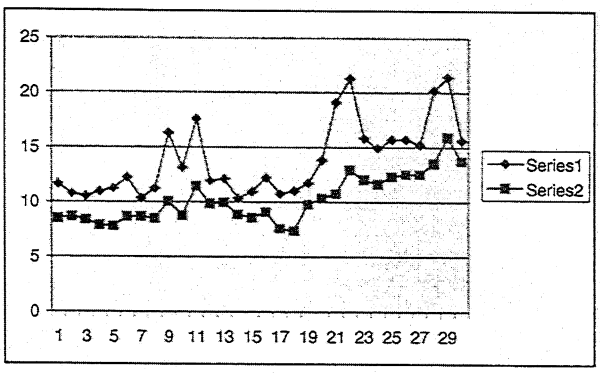

Figure 249. Daily variation of temperature (°C) in Helsinki during measurement period 1.6.-30.6.2000.

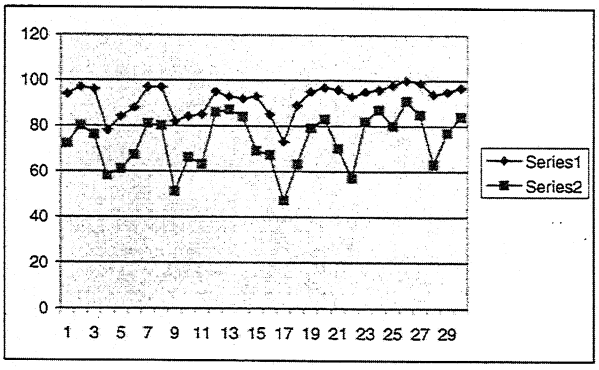

Figure 250. Daily variation of relative humidity (%) in Helsinki during measurement period 1.6.-30.6.2000.

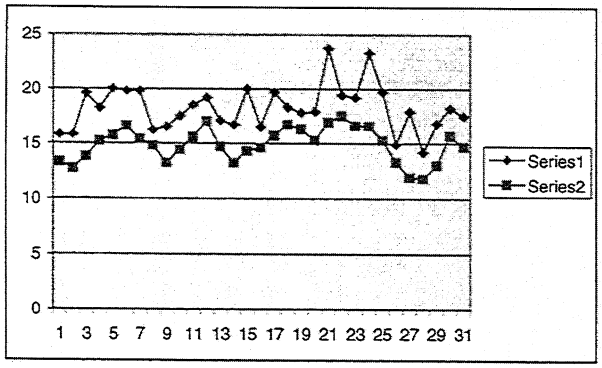

Figure 251. Daily variation of temperature (°C) in Helsinki during measurement period 1.7.-31.7.2000.

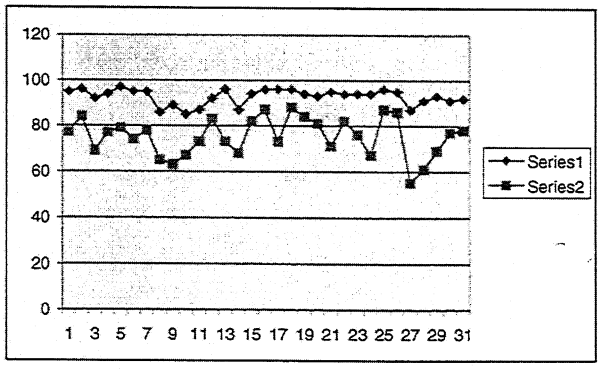

Figure 252. Daily variation of relative humidity (%) in Helsinki during measurement period 1.7.-31.7.2000.

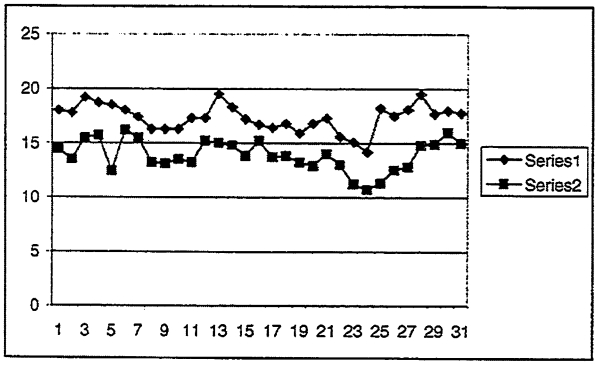

Figure 253. Daily variation of temperature (°C) in Helsinki during measurement period 1.8.-31.8.2000.

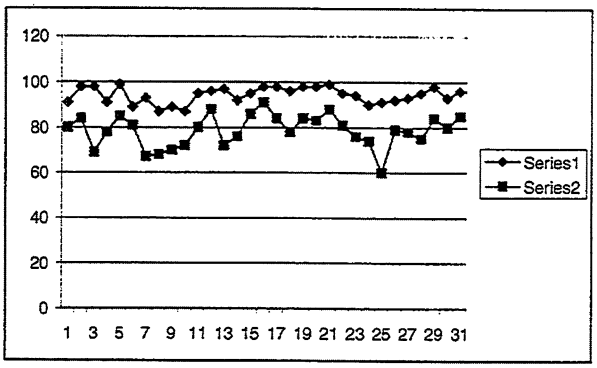

Figure 254. Daily variation of relative humidity (%) in Helsinki during measurement period 1.8.-31.8.2000.

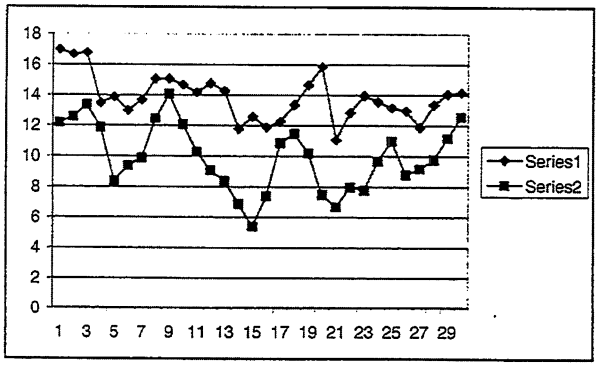

Figure 255. Daily variation of temperature (°C) in Helsinki during measurement period 1.9.-30.9.2000.

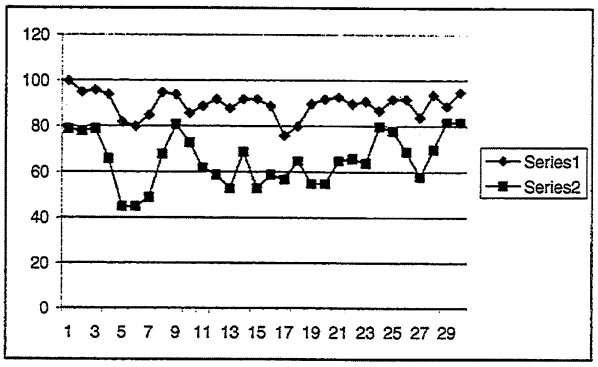

Figure 256. Daily variation of relative humidity (%) in Helsinki during measurement period 1.9.-30.9.2000.

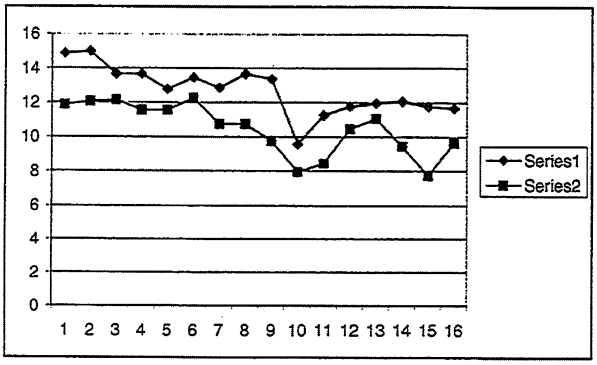

Figure 257. Daily variation of temperature (°C) in Helsinki during measurement period 1.10.-16.10.2000.

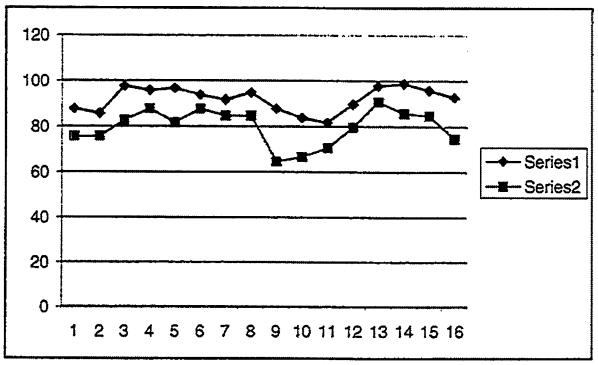

Figure 258. Daily variation of relative humidity (%) in Helsinki during measurement period 1.10.-16.10.2000.

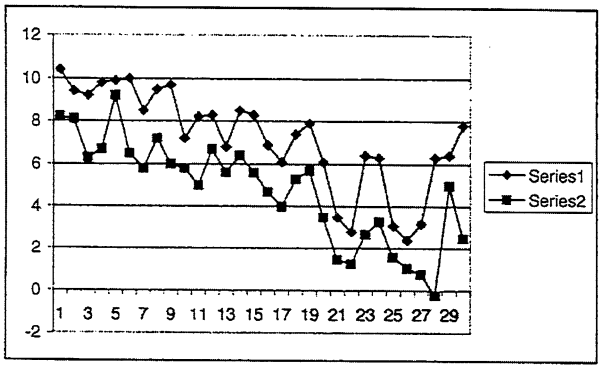

Figure 259. Daily variation of temperature (°C) in Helsinki during measurement period 1.11.-30.11.2000.

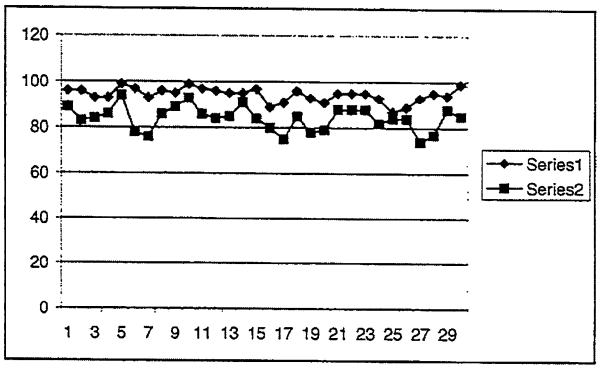

Figure 260. Daily variation of relative humidity (%) in Helsinki during measurement period 1.11.-30.11.2000.

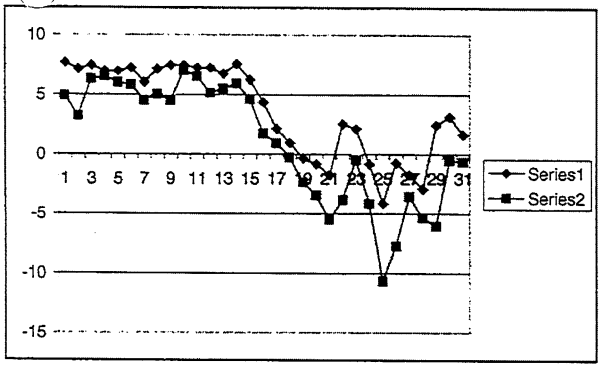

Figure 261. Daily variation of temperature (°C) in Helsinki during measurement period 1.12.-31.12.2000.

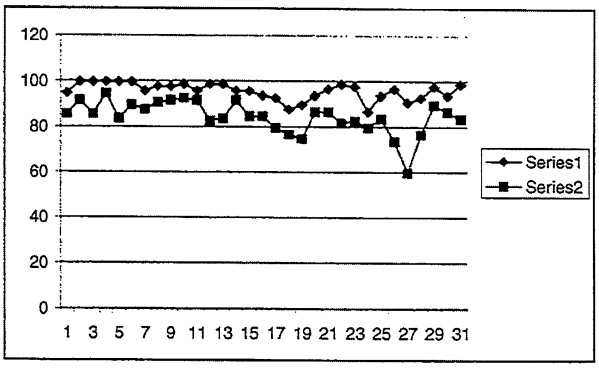

Figure 262. Daily variation of relative humidity (%) in Helsinki during measurement period 1.12.-31.12.2000.

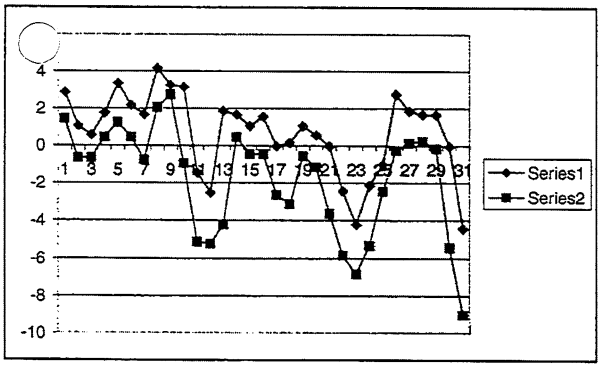

Figure 263. Daily variation of temperature (°C) in Helsinki during measurement period 1.1.-31.1.2001.

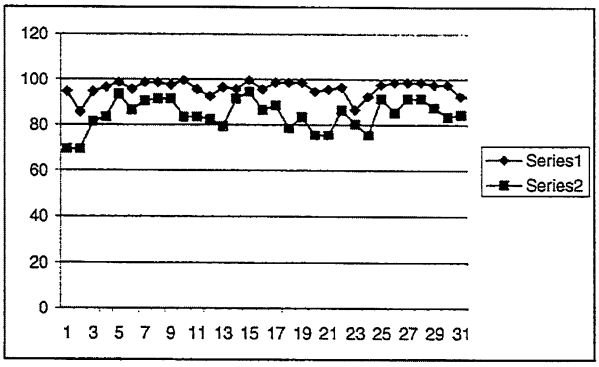

Figure 264. Daily variation of relative humidity (%) in Helsinki during measurement period 1.1.-31.1.2001.

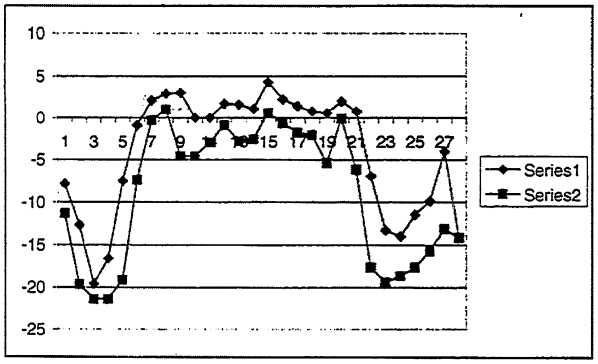

Figure 265. Daily variation of temperature (°C) in Helsinki during measurement period 1.2.-28.2.2001.

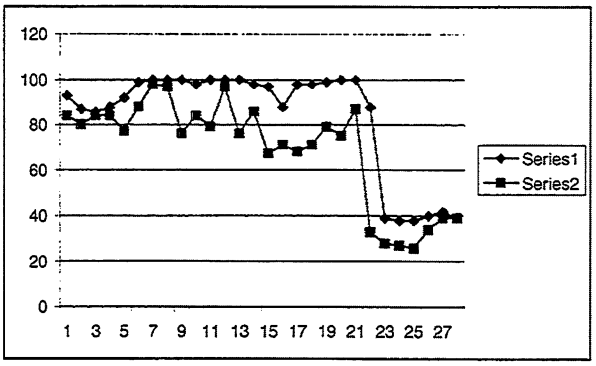

Figure 266. Daily variation of relative humidity (%) in Helsinki during measurement period 1.2.-28.2.2001.

4.8.2 Rainfall and sunshine

Daily rainfall and amount of sunshine in Helsinki area are presented in Figs. 267-310 according to the data of Finnish Meteorological Institute.

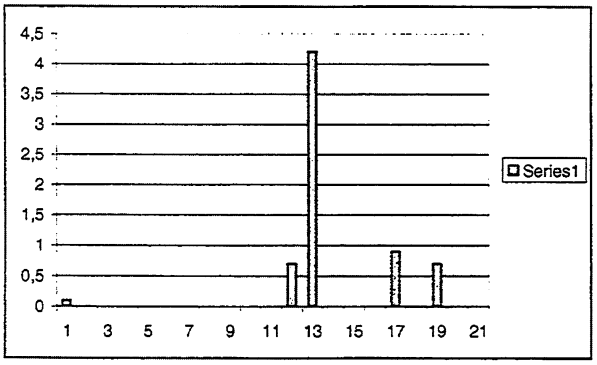

Figure 267. Daily rainfall (mm) in Helsinki during measurement period 11.5.-31.5.1999.

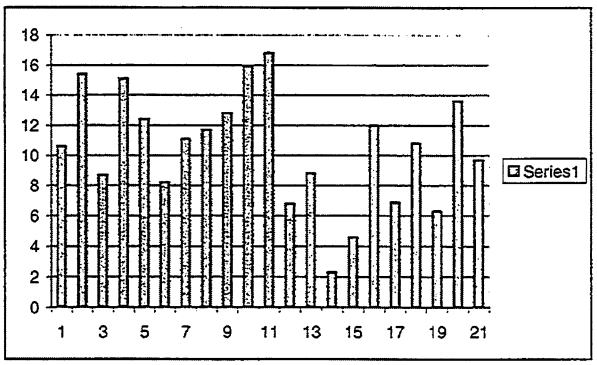

Figure 268. Daily amount of sunshine (h) in Helsinki during measurement period 11.5.-31.5.1999.

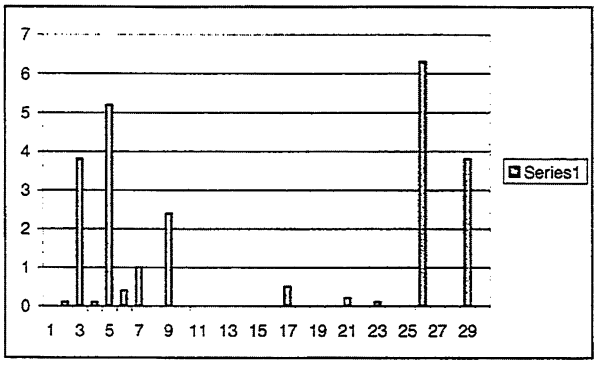

Figure 269. Daily rainfall (mm) in Helsinki during measurement period 1.6.-30.6.1999.

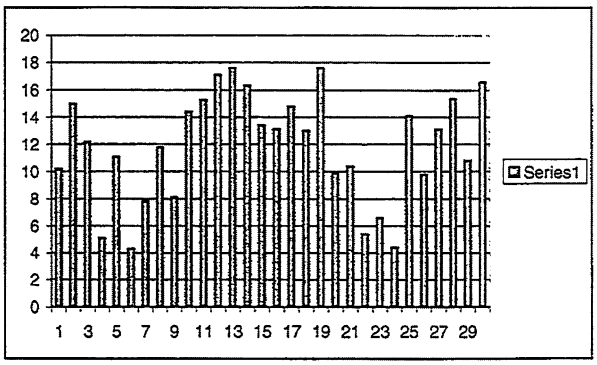

Figure 270. Daily amount of sunshine (h) in Helsinki during measurement period 1.6.-30.6.1999.

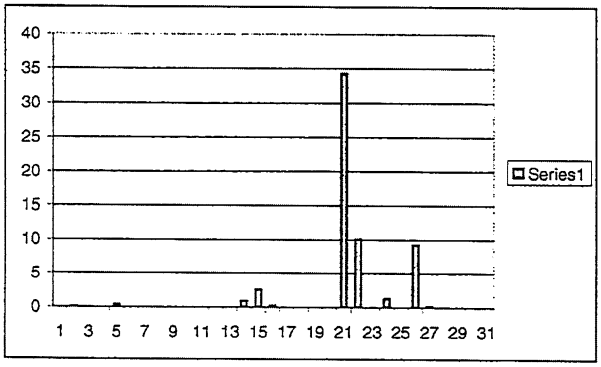

Figure 271. Daily rainfall (mm) in Helsinki during measurement period 1.7.-31.7.1999.

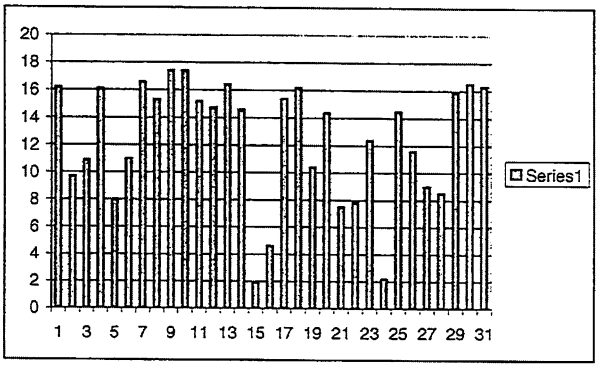

Figure 272. Daily amount of sunshine (h) in Helsinki during measurement period 1.7.-31.7.1999.

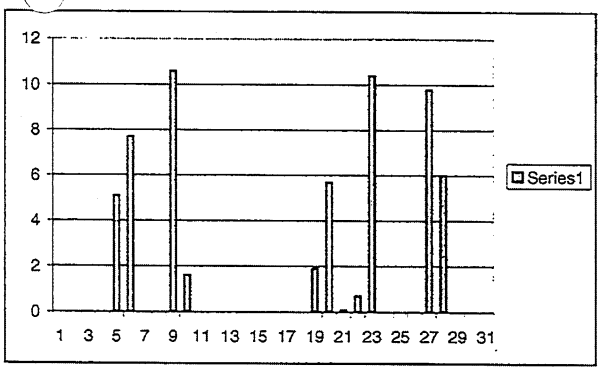

Figure 273. Daily rainfall (mm) in Helsinki during measurement period 1.8.-31.8.1999.

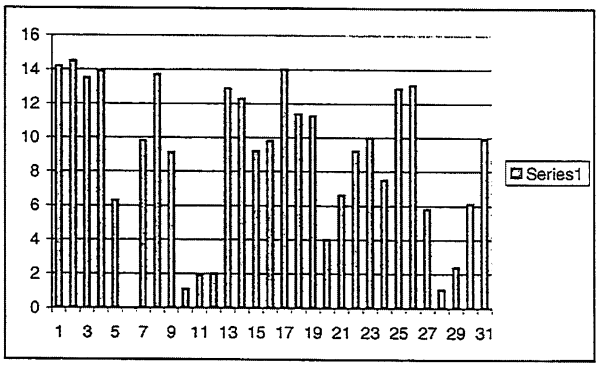

Figure 274. Daily amount of sunshine (h) in Helsinki during measurement period 1.8.-31.8.1999.

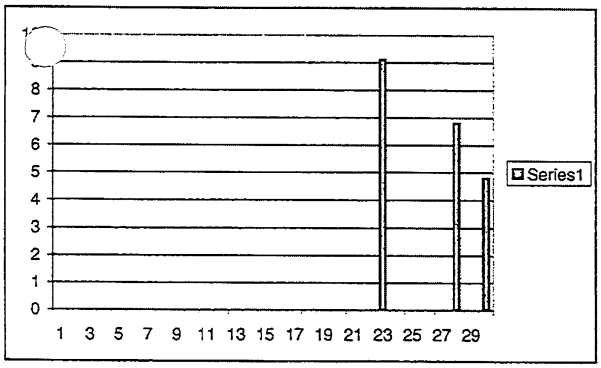

Figure 275. Daily rainfall (mm) in Helsinki during measurement period 1.9.-30.9.1999.

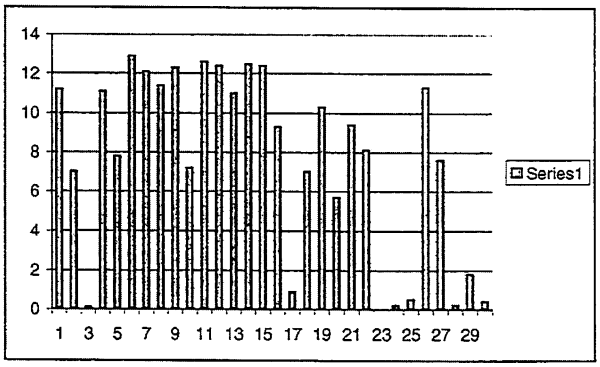

Figure 276. Daily amount of sunshine (h) in Helsinki during measurement period 1.9.-30.9.1999.

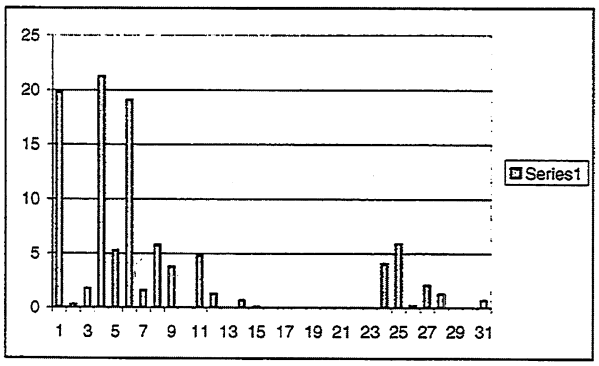

Figure 277. Daily rainfall (mm) in Helsinki during measurement period 1.10.-31.10.1999.

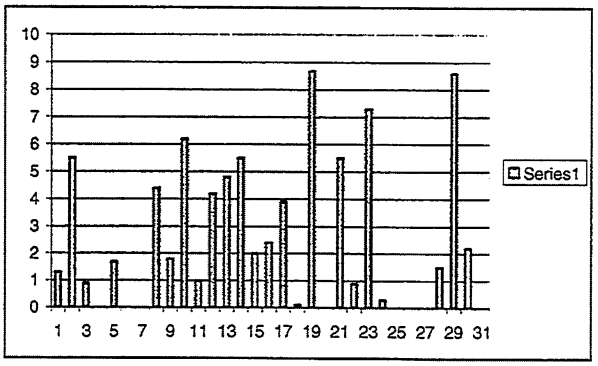

Figure 278. Daily amount of sunshine (h) in Helsinki during measurement period 1.10.-31.10.1999.

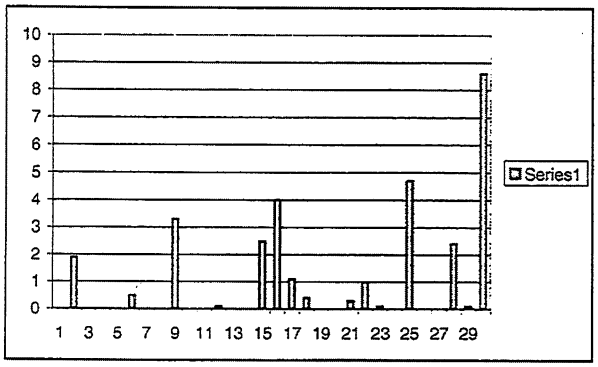

Figure 279. Daily rainfall (mm) in Helsinki during measurement period 1.11.-30.11.1999.

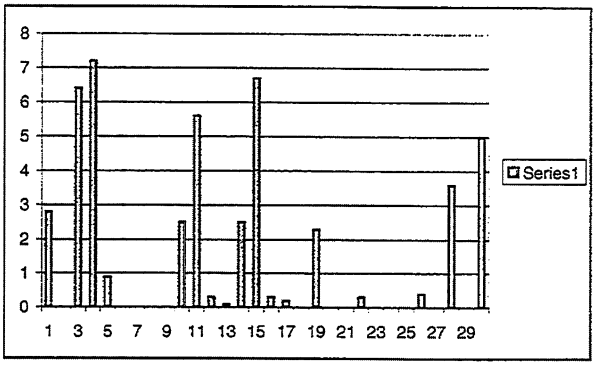

Figure 280. Daily amount of sunshine (h) in Helsinki during measurement period 1.11.-30.11.1999.

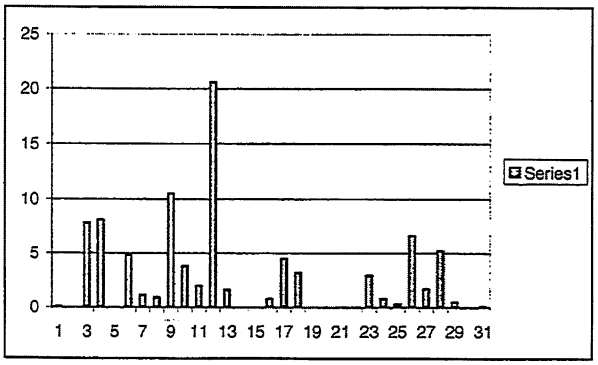

Figure 281. Daily rainfall (mm) in Helsinki during measurement period 1.12.-31.12.1999.

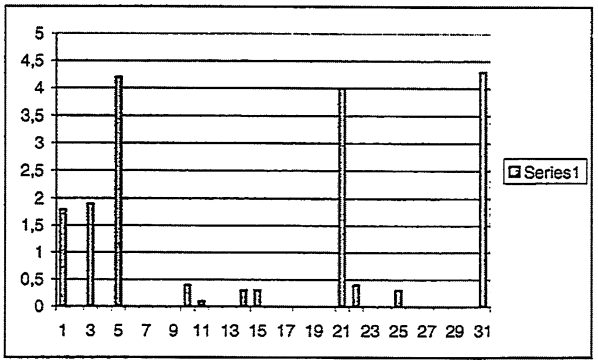

Figure 282. Daily amount of sunshine (h) in Helsinki during measurement period 1.12.-31.12.1999.

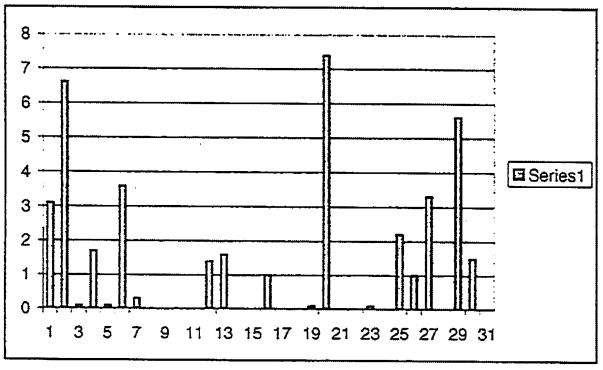

Figure 283. Daily rainfall (mm) in Helsinki during measurement period 1.1.-31.1.2000.

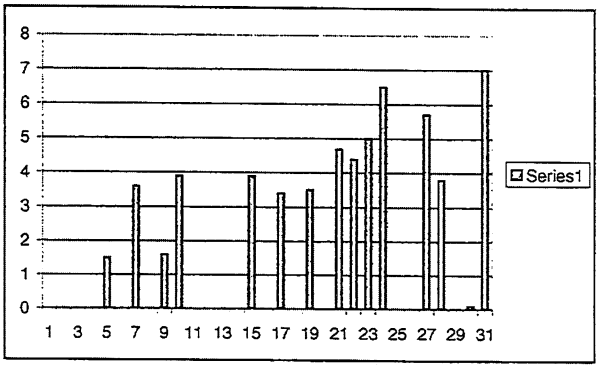

Figure 284. Daily amount of sunshine (h) in Helsinki during measurement period 1.1.-31.1.2000.

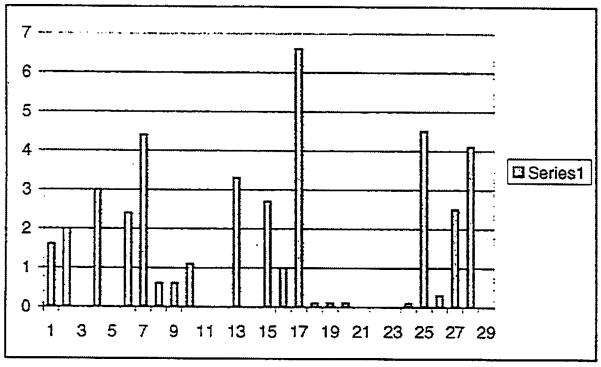

Figure 285. Daily rainfall (mm) in Helsinki during measurement period 1.2.-29.2.2000.

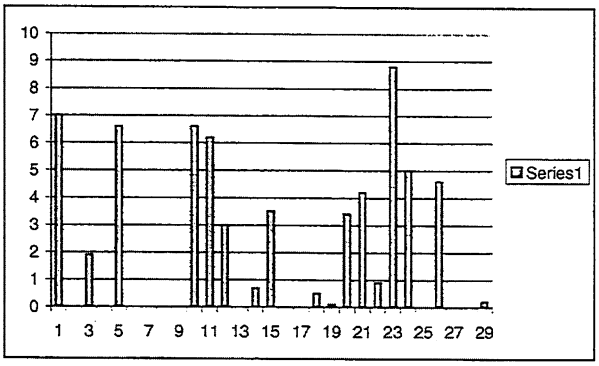

Figure 286. Daily amount of sunshine (h) in Helsinki during measurement period 1.2.-29.2.2000.

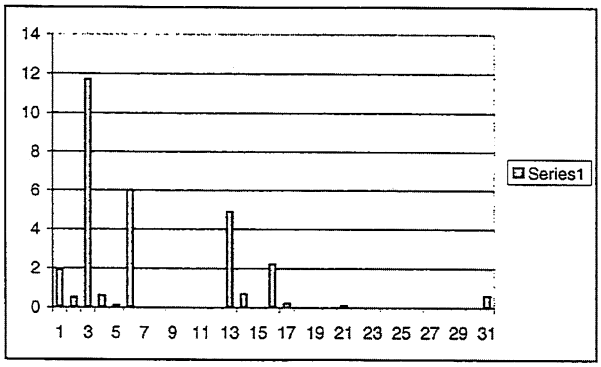

Figure 287. Daily rainfall (mm) in Helsinki during measurement period 1.3.-31.3.2000.

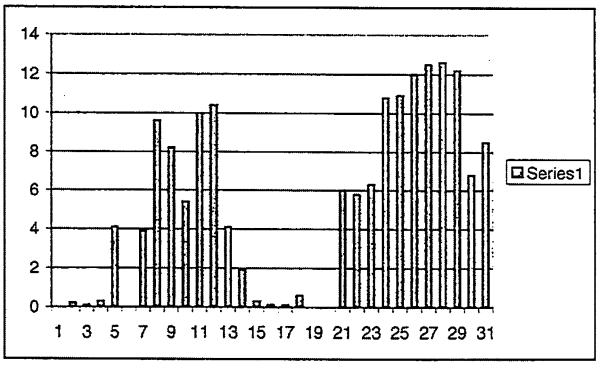

Figure 288. Daily amount of sunshine (h) in Helsinki during measurement period 1.3.-31.3.2000.

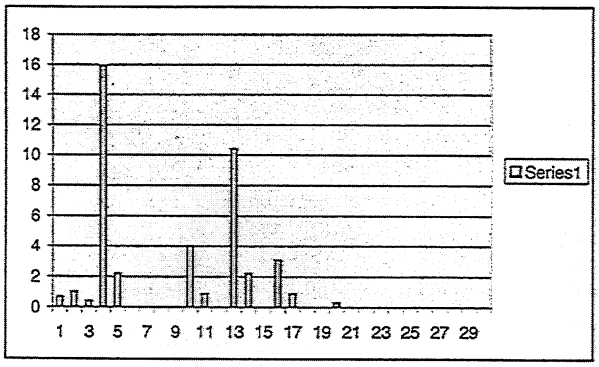

Figure 289. Daily rainfall (mm) in Helsinki during measurement period 1.4.-30.4.2000.

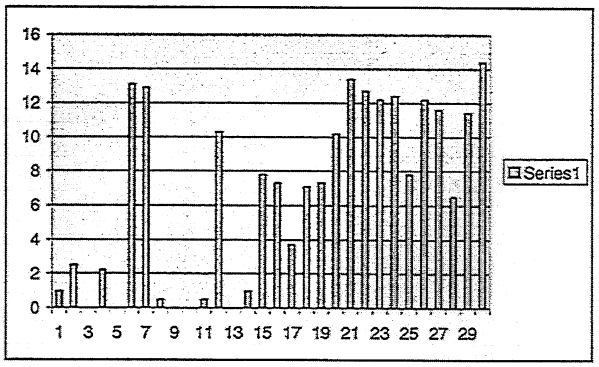

Figure 290. Daily amount of sunshine (h) in Helsinki during measurement period 1.4.-30.4.2000.

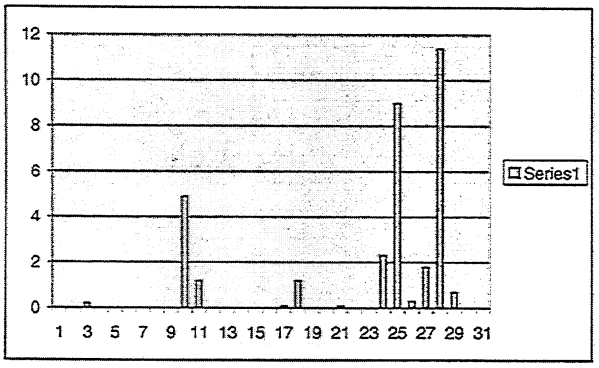

Figure 291. Daily rainfall (mm) in Helsinki during measurement period 1.5.-31.5.2000.

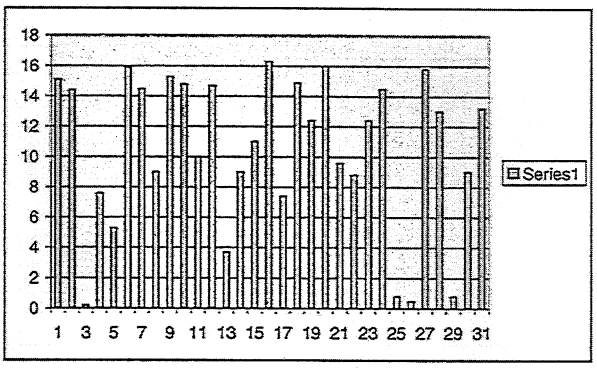

Figure 292. Daily amount of sunshine (h) in Helsinki during measurement period 1.5.-31.5.2000.

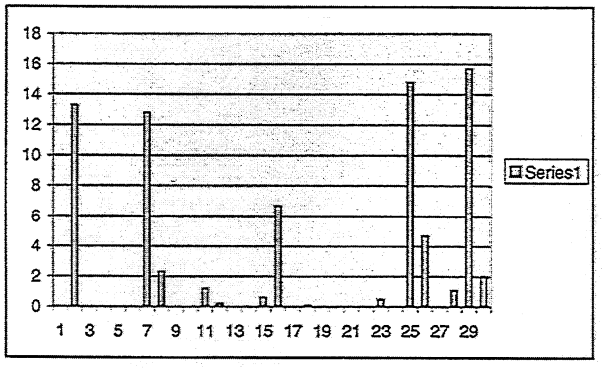

Figure 293. Daily rainfall (mm) in Helsinki during measurement period 1.6.-30.6.2000.

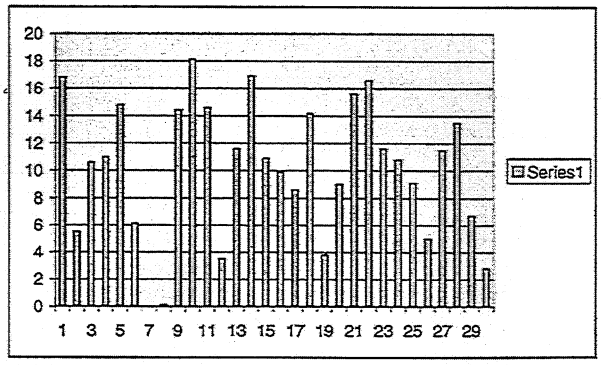

Figure 294. Daily amount of sunshine (h) in Helsinki during measurement period 1.6.-30.6.2000.

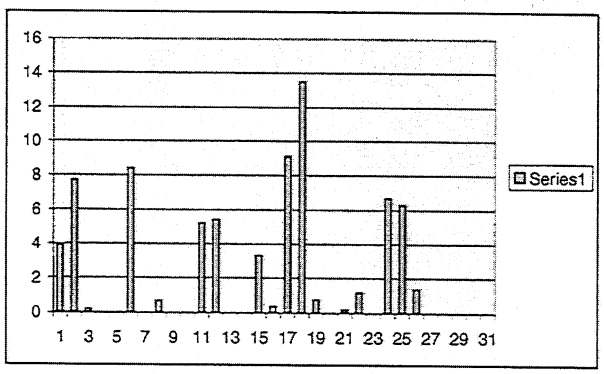

Figure 295. Daily rainfall (mm) in Helsinki during measurement period 1.7.-31.7.2000.

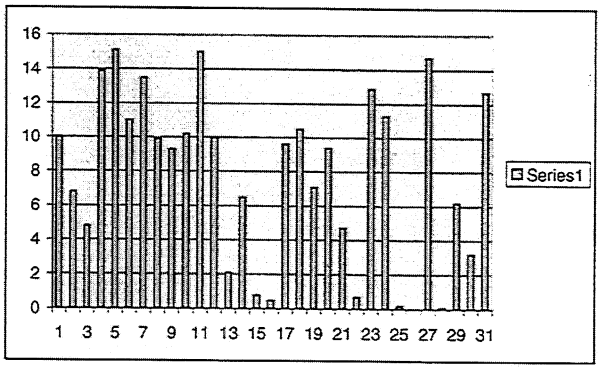

Figure 296. Daily amount of sunshine (h) in Helsinki during measurement period 1.7.-31.7.2000.

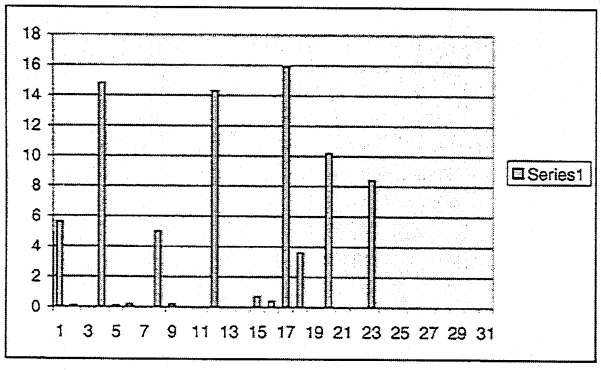

Figure 297. Daily rainfall (mm) in Helsinki during measurement period 1.8.-31.8.2000.

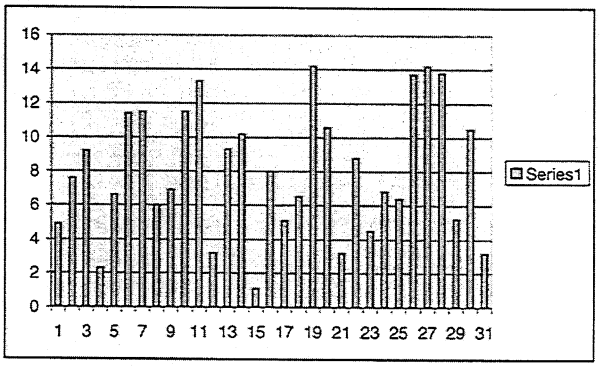

Figure 298. Daily amount of sunshine (h) in Helsinki during measurement period 1.8.-31.8.2000.

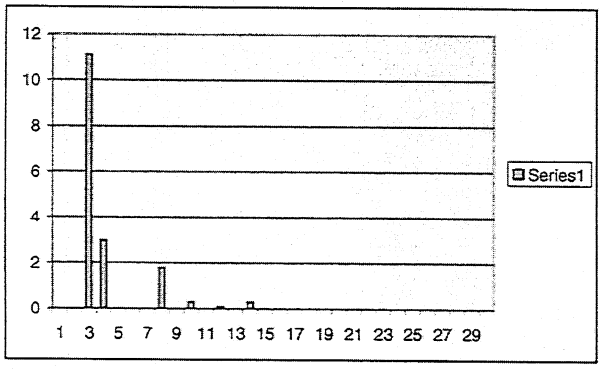

Figure 299. Daily rainfall (mm) in Helsinki during measurement period 1.9.-30.9.2000.

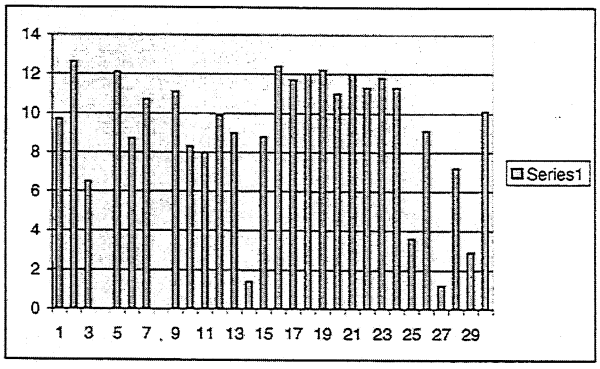

Figure 300. Daily amount of sunshine (h) in Helsinki during measurement period 1.9.-30.9.2000.

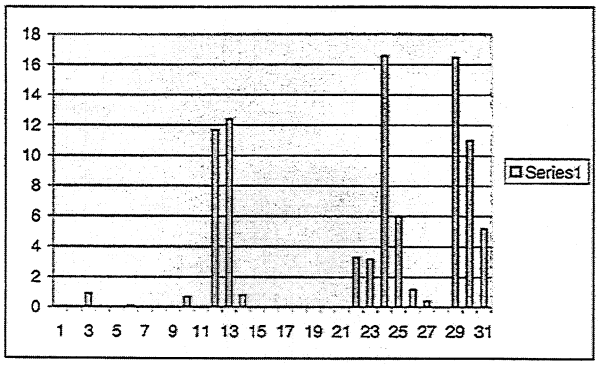

Figure 301. Daily rainfall (mm) in Helsinki during measurement period 1.10.-31.10.2000.

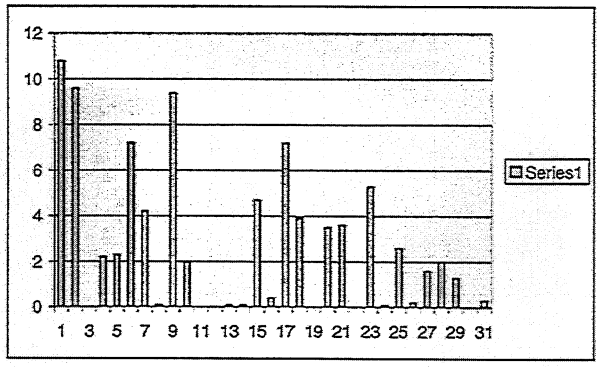

Figure 302. Daily amount of sunshine (h) in Helsinki during measurement period 1.10.-31.10.2000.

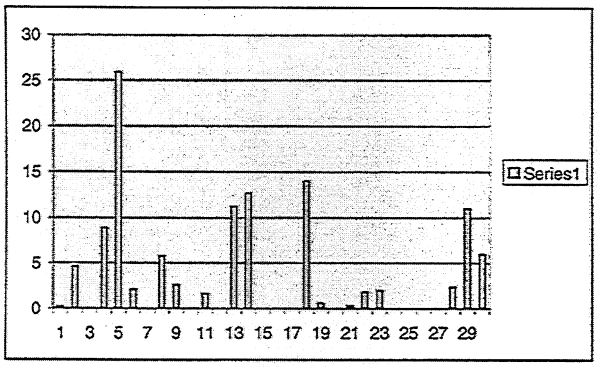

Figure 303. Daily rainfall (mm) in Helsinki during measurement period 1.11.-30.11.2000.

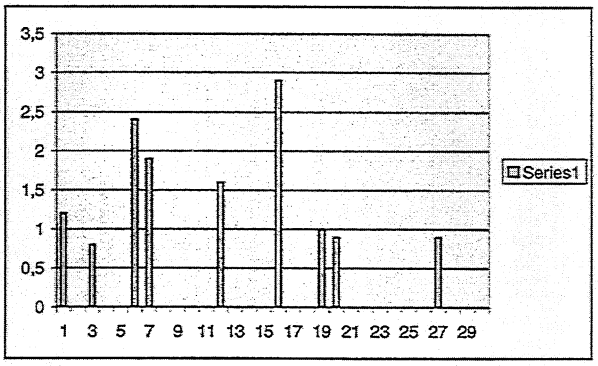

Figure 304. Daily amount of sunshine (h) in Helsinki during measurement period 1.11.-30.11.2000.

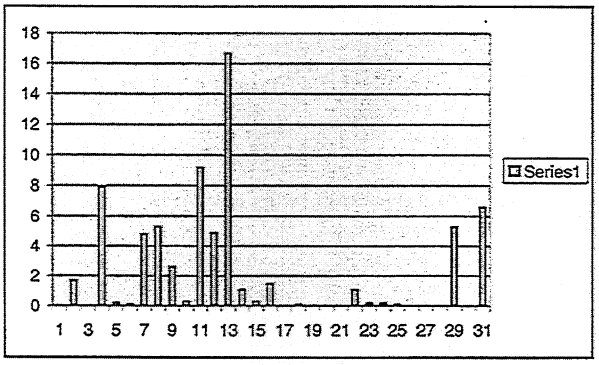

Figure 305. Daily rainfall (mm) in Helsinki during measurement period 1.12.-31.12.2000.

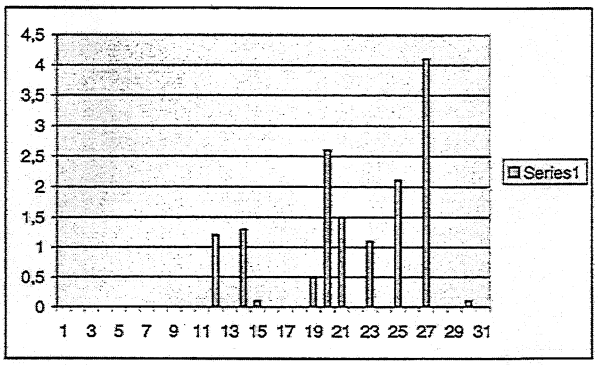

Figure 306. Daily amount of sunshine (h) in Helsinki during measurement period 1.12.-31.12.2000.

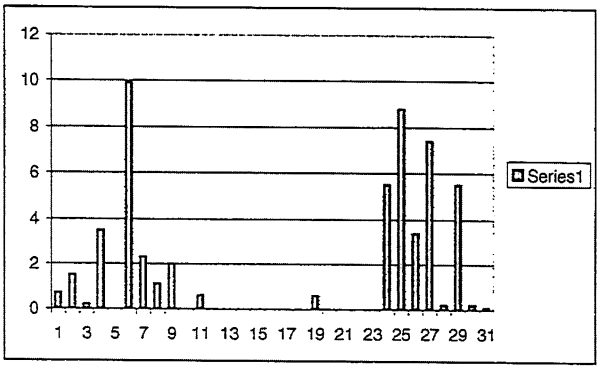

Figure 307. Daily rainfall (mm) in Helsinki during measurement period 1.1.-31.1.2001.

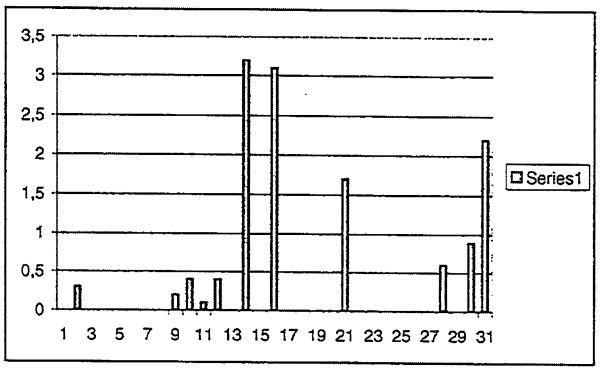

Figure 308. Daily amount of sunshine (h) in Helsinki during measurement period 1.1.-31.1.2001.

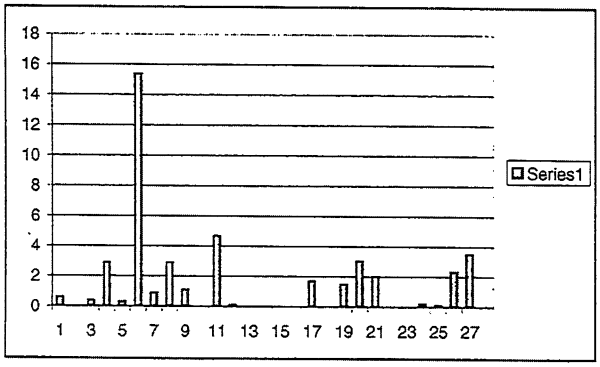

Figure 309. Daily rainfall (mm) in Helsinki during measurement period 1.2.-28.2.2001.

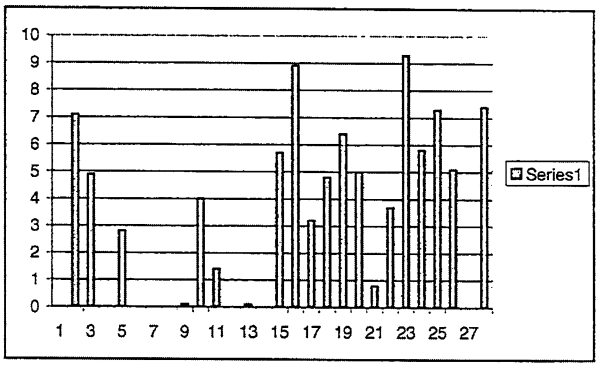

Figure 310. Daily amount of sunshine (h) in Helsinki during measurement period 1.2.-28.2.2001.

5 DISCUSSION

5.1 Temperature gradient

According to the temperature data recorded it seems that in general the temperature of the inner surface of marble slabs was higher than that of the outer surface. Especially this was the case on western and northern walls, where the inner surface temperature was 1-2°C higher than the corresponding outer surface temperature. Only during the warmest season of the year, June-August, the temperatures were almost the same on both sides of the slabs. The outer surface temperature was occasionally even higher.

On eastern walls the outer surface temperature was usually higher than the inner surface temperature during summer time. The temperature difference varied between 1-4°C. A similar trend was observed in the warmest days of autumn, but then the temperature difference was only about 1°C in favour of the outer surface. For the rest of the year the inner surface was a little warmer than the outer surface.

Measurement results from southern walls resembled those from eastern walls. During summer time and during the warmest days of autumn the outer surface was warmer, but otherwise the temperature was higher on the inner surface. The temperature differencies during summer and autumn were approximately as high as on eastern walls, but during winter the inner surface was about 1°C and during spring even 1-5°C warmer than the outer surface. However, the results from the measuring point A, which was also on southern wall, were different from those presented above. At that point the inner surface temperature was always 1-2°C, during summer time even 2-4°C, higher than the outer surface temperature. Because the measuring point A located on top of the wall of the tower part of the building, this could be due to "chimney effect". In that case high inner surface temperatures would be a consequence of the effect of warm air rising up from the roof through the ventilation slot.

5.2 Daily variation of temperature

The daily variation of temperature of the marble slabs was substantial. It was most prominent during the warm seasons reflecting the natural weather conditions. In addition to the season the amount of variation depended also on the location of the slab with respect to the cardinal points.

On northern walls the average daily variation of temperature was 10-15°C during summer (June-August), 5-10°C during spring (February-April) and only 2-3°C during winter (November-January). In May and in September it was around 10°C and in October around 5°C. The maximum temperature recorded varied accordingly from 30-35°C in summer to around zero in winter. The minimum temperature varied between 5-10°C in summer, but could be as low as -25°C in winter.

On western walls the average daily variation of temperature varied between 15-20°C during the time period from March to September. In winter, from November to January, the variation was only 1-5°C. Between these two periods, i.e. during February and October, the variation was 5-10°C. The maximum temperature varied from 35-40°C in summer to around zero in mid-winter. The minimum temperature was around 10°C in summer but as low as -25°C in winter.

On eastern walls the average daily variation of temperature varied between 15-20°C in summer (June-August), between 5-10°C in spring (March-April) and between 2-5°C in winter (November-January). During May and September it was 10-15°C and during February and October around 5°C. The maximum temperature varied from 35-40°C in summer to about 5°C in winter. The corresponding minimum temperatures were 10°C and -25°C.

On southern walls the average daily variation of temperature varied between 15-20°C in summer (May-September), between 10-15°C in spring (March-April) and between 5-10°C in winter (October-February). The maximum temperature varied from 35-40°C in summer to about 15°C in winter. The minimum temperature was about 10°C in summer and about -25°C in winter.

On top of the tower wall (measuring point A) the daily variation of temperature during summer and spring was roughly 5°C higher than on southern walls in general. Correspondingly, the maximum temperatures were even 10°C higher than on lower parts of the roof walls. Highest temperatures were measured on the outer surface of black granite slab beside the measuring point A. They were in general 5-10°C higher than the temperatures on the outer surface of the marble slab.

5.3 Gradient of temperature variation

The daily variation of temperature did not occur evenly in the marble slabs. This can be considered to be significant, because uneven stressing of marble could be one of the factors leading to bowing of the slabs.

On northern walls the differencies in the temperature variation between the surfaces were small, and the direction of the gradient changed frequently from one side to another. Most of the time, however, the variation was wider on the outer surface of the slab. Compared to the variation on the inner surface the difference was only 0-1°C.

On western walls the temperature variation was wider on the outer surface of the slab. The difference was noteworthy, 2-4°C, during warm season (April-September), but almost insignificant, 0-1°C, for the rest of the year. In mid-winter the difference between the surfaces in this respect was practically zero.

Also on eastern walls the temperature variation was wider on the outer surface of the slab. The difference was remarkable, 3-4°C, in summer (May-September). During spring (February-April) and late autumn (October) the difference was smaller but clear, 0-2°C. In winter (November-January) the variation was practically equal on both sides of the slab.

On southern walls the temperature variation was wider on the outer surface of the slab except during winter time when the situation was the other way around. In winter (November-February) the difference was 1-2°C, in January even 3-4°C, in favour of the inner surface, but during the rest of the year the difference was 2-3°C, in May-June even 3-4°C, higher on the outer surface. During the turning periods, in October-November on one hand and in March on the other, the direction of the gradient could be either way.

The results from the measuring point A deviated again from the general trend presented for southern walls. Excluding the mid-winter the variation at that point was wider on the inner surface of the slab. The difference was 2-3°C during February-September and 0-2°C during October-December. In March it was 3-4°C and in September even 5°C. In January the variation was 2-3°C wider on the outer surface. The observed behaviour could be a consequence of the "chimney effect" as discussed in chapter 5.1.

5.4 Freeze/thaw -cycling

The number of freeze/thaw -cycles during the whole monitoring period of 22 months was amazingly high. The most reliable results were those from the measuring points D and E as their data covered the time period almost completely. The number of freeze/thaw -cycles defined as presented in chapter 4.5 was around 90 in the point D and even 110 in the point E. In addition, it must be noted that for two whole years the data from two important months, March and April, was missing. These could have meant 20-30 cycles more, so that the total amount of cycles during two years would have been 120-140. Thus the annual amount of freeze/thaw -cycles seems to have been something like 60-70, while the earlier estimate has been about 20.

The definition of the freeze/thaw -cycle used in this study can be criticized for not being strict enough as the temperature limits were set to -0.3°C for freezing and +0.3°C for thawing. Water in marble probably requires lower temperatures in order to freeze, correspondingly higher temperatures in order to melt. Setting the temperature limits further from zero would diminish the amount of freeze/thaw -cycles, even considerably if the limits are set far enough. However, as the threshold values for temperatures are not known, the estimates presented here can be used as long as the limitations connected to the definition are remembered. On the other hand only one cycle per day was calculated in this study as maximum and minimum daily temperatures were used. In reality more than one cycle can occur even in the same day.

The worst directions from the frost resistance point of view seem to be south and east. Considerable amount of data was lacking from northern and western walls. The results would indicate that the amount of cycles has been lower in these directions, though it has been rather high especially on western walls.

The amount of freeze/thaw -cycles seemed to be a little lower on the inner surface of the marble slab than on the outer surface. The difference was about 10%. As this causes a higher stress to the outer surface than to the inner this could be one of the factors contributing to bowing of the slabs.

Only during the three summer months, June-August, no freeze/thaw -cycles were observed. The worst period of time in this respect was naturally that from November to March. It seemed that southern walls were especially stressed during November-January while the others suffered most during February-March. During October some cycles were detected on all walls. Excluding southern walls the situation was the same during April. During May and September some occasional freeze/thaw -cycles were observed on other walls except the southern ones.

5.5 Relative humidity

In general the values of relative humidity were fairly high. During autumn and winter the average relative humidity values were even higher than during spring and summer. This was due to the fact that the daily minimum rose from the value of about 20%, which was typical of summer, to 60-80%, or even higher.

On southern walls there seemed to be a difference between the relative humidity of outdoor air and that of the ventilation slot for the most of the year meaning a humidity gradient over the marble slab. The direction of the gradient was not the same all of the time, however. During summer (May-August) the average relative humidity was higher inside the ventilation slot, though the difference was rather small. It was due to the fact that the minimum value was higher than that of outdoor air and thus the variation of relative humidity was smaller inside. The situation was exactly the other way around during November-December, when the minimum relative humidity inside the ventilation slot was smaller than that of outdoor air meaning wider variation of humidity inside. However, the most remarkable difference was observed during January-April. During that time period both the maximum and the minimum relative humidities were higher in outdoor air than in the ventilation slot. Thus, the conditions were considerably more humid on the outer surface of marble than on the inner surface. Only during September-October the humidity conditions were similar on both sides of the marble slab.

On eastern walls the humidity conditions were much more even than on southern walls. There were no great differencies between the relative humidities of outdoor air and that of the ventilation slot. Only during winter time, from January to March, both the maximum and the minimum relative humidities were higher in outdoor air than in the ventilation slot. Thus, the conditions were considerably more humid on the outer surface of marble than on the inner surface.

The difference in relative humidity between outdoor air and the ventilation slot causes a higher stress on the outer surface of marble than on the inner. Thus, this could be one of the factors contributing to bowing of the slabs.

5.6 Acidity of rain water

The pH-value of rain water varied between 4.3 and 5.3 during 1999 the weighted average being 4.8. The values of the year 2000 were not available, but most probably the situation was very similar to that in 1999. Although the acidity of rain water has diminished, i.e. the pH-value increased, during the last decade it still acts like a weak acid. Thus, it forms a stressing factor to all materials subjected to rain water. Its effect must especially be taken into account when materials like marble which are very reactive in acidic surroundings are considered.

6 CONCLUSIONS

According to the temperature and humidity data recorded the prevailing environmental conditions include several factors that cause stress to the marble facades of Finlandia Hall. The intensity of these factors was not the same everywhere but depended on the cardinal point towards which the walls were directed. It seemed that in general the sum of the stressing factors was highest on southern walls and lowest on northern walls.

The annual variation of temperature is one of the stressing factors. The minimum temperature recorded during the monitoring period was about -25°C on all walls. The corresponding maximum temperature varied from about 35°C on the northern side to about 50°C on top of the southern side of the tower part of the building.

The daily variation of temperature was also considerable. The average variation was highest on southern walls, 15-20°C during summer and 5-10°C during winter time. On northern walls the average variation was lowest varying between 10-15°C during summer and 2-3°C during winter. Occasionally the daily variation could be even twice the average.

Freeze/thaw -cycling caused also stresses to marble and facade structures. According to the results the annual amount of cycles can be as high as 60-70. The freeze/thaw -effect was prominent at least on southern and eastern walls, probably also on western walls.

At least two other stressing factors were observed: variation of humidity and acidity of rain water. During summer and spring the relative humidities, especially the daily minimum values, were varying sharply depending on whether it was raining or not. During colder seasons the humidity conditions were much more even. The pH-value of rain water varied between 4 and 5 creating acidic conditions that can affect the highly reactive marble.

In addition, three factors causing a higher stress on the outer surface of marble than on the inner were observed: the average daily variation of temperature, the number of freeze/thaw -cycles and the relative humidity were higher on the outer surface. The differencies were small, but all of them had a parallel effect. Thus, these could be at least some of the factors contributing to bowing of the slabs.

APPENDIX 2

VTT BUILDING AND TRANSPORT

RESEARCH REPORT

Developing long term durability of marble facades

Subproject "Test wall"

Espoo, April 20, 2001

Juho Saarimaa
Research Director

Pertti Koskinen
Senior Research Scientist

Encl.: Final report (91 pages + 4 Appendices with 22 pages)

VTT

CONTENTS

	page
CONTENTS	2
1 BACKGROUND	4
2 OBJECTIVE	5
3 EXPERIMENTAL	5
3.1 General arrangements	5
3.2 Marbles	6
3.2.1 Flexural strength	6
3.2.2 Water absorption, apparent porosity, bulk density	6
3.2.3 Mineral composition	7
3.2.3.1 X-ray diffraction	7
3.2.3.2 Thermal analysis	8
3.2.4 Microstructure	8
3.2.4.1 Thin section study	8
3.2.4.2 Elementary composition, distribution of elements	8
3.2.4.3 SEM-study	8
3.3 Marble clad elements	9
3.3.1 Bond strength	9
3.3.2 Microstructure	9
3.4 Colour measurements at Finlandia Hall	9
3.5 Field samples	10
3.5.1 Mineral composition	10
3.5.2 Thin section study	10
3.5.3 SEM-study	11
4 RESULTS	11
4.1 Marbles	11
4.1.1 Flexural strength	11
4.1.2 Water absorption, apparent porosity, bulk density	16
4.1.3 Mineral composition	21
4.1.3.1 X-ray diffraction	21
4.1.3.2 Thermal analysis	24
4.1.4 Microstructure	26
4.1.4.1 Thin section study	26
4.1.4.2 Elementary composition, distribution of elements	33
4.1.4.3 SEM-study	35

page

4.2 Marble clad elements 55
4.2.1 Bond strength 55
4.2.2 Microstructure 57
4.3 Colour measurements at Finlandia Hall 63
4.4 Field samples 71
4.4.1 Mineral composition 72
4.4.2 Thin section study 76
4.4.3 SEM-study 80

5 DISCUSSION 85

5.1 Strength properties 85
5.2 Water absorption properties 86
5.3 Composition and microstructure 87
5.4 Marble clad elements 88
5.5 Colour measuments 89
5.6 Field samples 90

6 CONCLUSIONS 90

APPENDIX 1 Results from the flexural strength measurements of the marbles.

APPENDIX 2 Results from the water absorption measurements of the marbles.

APPENDIX 3 Bond strength of marble in marble clad elements.

APPENDIX 4 Results from the colour measurements of marble slabs.

1 BACKGROUND

The need for conserving, restoring and protecting stone buildings and monuments throughout the world is growing continuously. This is particularly actual in the historic cities of Europe where marble and other calcareous stones have been commonly used. The decay of old stone structures is becoming a remarkable technical and economic problem. Deteriorated stone facades may in some cases even represent a considerable safety risk. The durability problems have led to a strong decrease in the use of marble for outdoor applications.

One of the most important reasons for the deterioration and fouling of natural stones is the rising amount of acid compounds and other impurities coming mainly from industrial and traffic sources. Today stone structures are exposed to harsher environmental conditions than ever before. Thin stone veneers that are commonly used nowadays are even more sensitive for weathering than traditional massive stone structures.

Carrara marble was used as the original facade material for Finlandia Hall. In the early 1980's the marble plates began to warp. Warping was especially noticeable in larger plates because of lapping. It also became apparent that the plates' inner strength was rapidly weakening. Extensive studies were undertaken to determine the cause of the deterioration. The conclusion was that the phenomenon was mainly due to climatic factors and especially to acid rain, which gradually converts marble to gypsum.

The badly damaged marble facade of Finlandia Hall was renewed during the autumn of 1998 and the spring of 1999. In connection with the refurbishment, the City of Helsinki launched the research project "Developing long-term durability of marble facades" known as "MARA-project". The main aims of the project were to extend the service life of the new facade, to formulate an appropriate maintenance strategy and to create reliable technical criteria and methods to assess the suitability of marble for facade applications.

As already stated above the degradation of marble is a universal problem, which has been especially highlighted by recent cases of damage to old buildings and historic monuments. However, in Europe there are also a number of other architecturally significant new buildings that have fallen victim to the same kind of deterioration as Finlandia Hall. Because research results can therefore be widely exploited, the MARA-project received financial support from the EU's Raphael cultural heritage programme.

VTT Building and Transport was responsible for four subprojects of the main study. The primary goals of these subprojects were to determine the deterioration mechanism of marble, to set requirements for a durable marble facade structure and to develop a reliable method for testing marble quality. The subprojects also included studies of the environmental conditions at Finlandia Hall and of the stresses these cause to marble, of the durability of different types of marble, of the performance of alternative structural solutions and of the possibilities of using protective treatments. The studies were made in co-operation with Helsinki University of Technology, Parma University in Italy and Cevalor in Portugal.

2 OBJECTIVE

The aim of the subproject "Test wall" was to determine the durability of various marbles in the facades of Finlandia Hall and to study the connection between their real behaviour and that observed in laboratory conditions. In addition, the aim of the subproject was to examine the behaviour of various structural solutions.

In order to achieve the goals set for the subproject it was divided into four tasks:

- the effect of the environmental stresses prevailing at Finlandia Hall on the strength properties of marbles and marble clad elements
- the effect of the environmental stresses prevailing at Finlandia Hall on the microstructure and the composition of marbles
- the effect of the environmental stresses prevailing at Finlandia Hall on the colour and the appearance of marbles
- reporting of the results and conclusions made from them

3 EXPERIMENTAL

3.1 General arrangements

The marbles for the project were chosen by the representatives of the City of Helsinki. Four different types of marbles were used in the studies, and they were coded with letters A, D, E and K. All the marble types were white and originated from the area of Carrara in Italy (Carrara Bianco). One of the marble types (A) was the same that was used for the renewal of the facades of Finlandia Hall. According to a general assumption formed from practical experiences two of the marble types (E, K) should show a relatively good durability in outdoor applications. Correspondingly, one of the marble types (D) was thought to be not durable and thus unsuitable for facades.

The City of Helsinki delivered one unused slab of each marble type for the laboratory studies. The measures of the slabs were approximately 30x800x1200 mm^3. In order to study the effect of the prevailing environmental conditions on the properties of the marbles a test wall was constructed on the roof of Finlandia Hall. The test wall was a simple wooden frame that supported the test slabs from lower and upper edges of the slabs and prevented them from falling. Air could circulate freely around the slabs. The frame was placed on the roof in such a manner that the faces of the slabs were directing towards south.

One slab of each marble type was installed on the test wall in May 1999. In May 2000 the slabs were cut vertically in half. The other halves were taken to laboratory while the others were left on the test wall for another 6 months. These were taken for the laboratory studies in November 2000.

The City of Helsinki delivered also three marble clad elements, which were coded with letters F, H and L. The element F, measuring about 40x800x1200 mm^3, consisted of a thin (10 mm) marble plate and a thick (30 mm) concrete background. The element H, measuring about 25x800x1200

mm^3, consisted of a very thin (5 mm) marble plate glued on an aluminium honeycomb structure (20 mm). The honeycomb structure was covered with thin glass fiber sheets. The element L, measuring about 23x800x1200 mm^3, consisted of a thin (11 mm) marble plate glued on a steel honeycomb structure (22 mm). Marbles for the elements were chosen by the manufacturers, and their types or qualities have not not been made public.

One element of each type was installed on the test wall at the same time as the marble slabs. The sampling procedure was similar to that of the marble slabs described above.

3.2 MARBLES

3.2.1 Flexural strength

The flexural strength of the marbles was determined by using the slabs taken from Finlandia Hall after 1 and 1.5 years on the test wall. The reference values were measured from the unused slabs.

The flexural strength of the marbles was determined according to the standard EN 12372:1999. Test specimens were prisms with a height of 30 mm, width of 70 mm and length of 180 mm. The distance between the supporting rollers during the tests was 150 mm. The load was increased uniformly at a rate of 70 N/s. Deviating from the clauses of the standard the specimens were dried at (40 ± 2)°C instead of (70 ± 5)°C. The flexural strength, R_{tf}, of each specimen was calculated by using the formula (1):

$$R_{tf} = 3Fl / 2bh^2 \qquad (1),$$

where F = breaking force, N
l = distance between the supporting rollers, 150 mm
b = width of the specimen, mm
h = height of the specimen, mm

The specimens were sawn from the slabs in such a way that the length of the prisms was either parallel (direction A) or perpendicular (direction B) to the longer side (1200 mm) of the original slabs, Fig. 1. Ten specimens were prepared in both directions for each test.

3.2.2 Water absorption, apparent porosity, bulk density

The water absorption, apparent (open) porosity and bulk density of the marbles were determined by using the slabs taken from Finlandia Hall after 1 and 1.5 years on the test wall. The reference values were measured from the unused slabs.

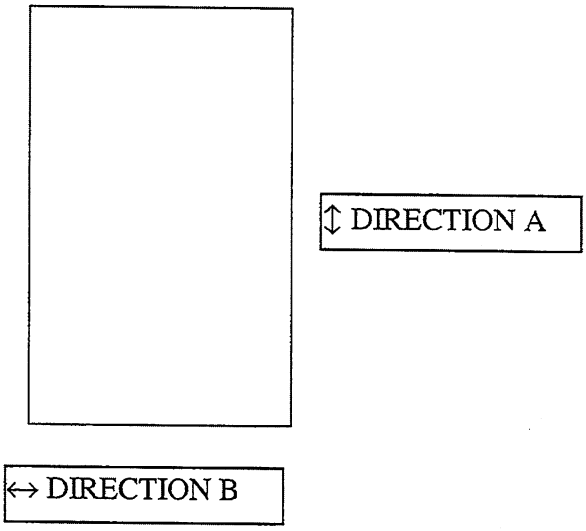

Figure 1. Flexural strength of marbles. Testing directions.

The water absorption properties of the marbles were determined according to the standard EN 1936:1999. Test specimens were prisms with a height of 30 mm, width of 70 mm and length of 180 mm. The surface area to volume ratio, A/V, of the specimens was 0.106. Deviating from the clauses of the standard the specimens were dried at (40 ± 2)°C instead of (70 ± 5)°C. Six specimens were prepared for each test. The water absorption, W, the apparent porosity, p_o, and the bulk density, ρ_b, of each specimen were calculated by using the formulae (2)-(4):

$$W = 100\% \times [(m_s - m_d) / m_d] \quad (2),$$

$$p_o = 100\% \times [(m_s - m_d) / (m_s - m_h)] \quad (3),$$

$$\rho_b = m_d / (m_s - m_h) \quad (4),$$

where

m_d = mass of the dry specimen, g
m_s = mass of the saturated specimen, g
m_h = mass of the specimen immersed in water, g

3.2.3 Mineral composition

3.2.3.1 X-ray diffraction

The mineral composition of the marbles was studied with a Philips PW 1710 X-ray diffractometer. The runs were made by using CuK_α -radiation, which was produced with a voltage of 50 kV and a current strength of 20 mA. Powder samples were used. Powders needed for the analyses were prepared by pulverizing pieces that were left over from the specimen prisms after their flexural strengths had been measured. In order to ascertain the homogeneity of the diffraction samples, the size of the batch that was pulverized was approximately 2 kg.

3.2.3.2 Thermal analysis

The mineral composition of the marbles was studied also with thermal analysis. The runs were made from the same powder samples that were prepared for X-ray diffraction by using a Netzsch STA 429 thermobalance. The run parameters were as follows:

atmosphere	flowing air, 6 cm^3/min	
heating rate	5°C/min	
end temperature	1000°C (sample)	
sample size	240-250 mg	
reference	Al_2O_3-powder, 195.2 mg	
crucibles	Al_2O_3	
thermocouples	Pt-Pt/Rh(10)	
scales	TG	125 mg
	DTG	500 µV
	DTA	200 µV

3.2.4 Microstructure

3.2.4.1 Thin section study

Thin sections of the marble specimens, 0.025x30x50 mm^3, were prepared at right angles to the surface of the slabs. Pieces were cut from the slabs with a diamond saw, impregnated with epoxy resin and ground first with a grinding machine and then by hand to final thickness (0.025 mm). The thin sections were studied with a Leica DM HC LP polarising light microscope and photographed with a Leica Q500IW image analysis equipment.

3.2.4.2 Elementary composition, distribution of elements

Similar pieces as for thin section studies were cut from the marble slabs. The surfaces of the sawn pieces were sequentially ground with a SiC paper of grit 320, 600, 800 and 1200. The ground surfaces were carbon coated and studied with a Jeol JSM 820 scanning electron microscope (SEM) in a backscattered electron mode (BSE). BSE-images were taken with an Imix image analysis system. Elementary analyses were made with an energy dispersive spectrometer (EDS) from areas that represented the materials just beneath the surfaces of the marble slabs. Elementary dot maps were collected over the same areas of elements Ca, Si, Al, Mg, Na, K, S, Cl, P, Fe and Mn. Ag-map was used to eliminate the effect of the background spectrum.

3.2.4.3 SEM-study

First part of the SEM-study was made by using polished marble sections. The surfaces of the sawn sections were sequentially ground with a SiC paper of grit 320, 600, 800 and 1200 and polished with diamond suspensions of grain sizes 6 and 0.25 µm. The sections were carbon coated and studied with a Jeol JSM 820 scanning electron microscope (SEM). The study was made in a backscattered electron mode (BSE) with a 50-fold magnification and in a secondary electron mode

(SE) with a 500-fold magnification. BSE and SE images were taken with an Imix image analysis equipment. BSE-images give information about the mean atomic weight of the compounds (the lighter the colour the higher the atomic weight of the compound). SE-images show the topography of the samples.

Second part of the SEM-study was made by using fractured surface samples of marbles. The samples were broken from the marble slabs, any loose material was wiped off and the fractured surfaces were carbon coated. The samples were studied with a Jeol JSM 820 scanning electron microscope (SEM) in a secondary electron mode (SE). SE-images were taken with an Imix image analysis equipment.

3.3 MARBLE CLAD ELEMENTS

3.3.1 Bond strength

The bond between the marble plate and the rest of the element structure was studied by measuring the force needed to loosen the marble from the base structure. In order to perform the measurement a cylinder-shaped drill core extending through the marble plate was first drilled on the surface of the slab. A metal plate with a drawhook was then glued on the marble inside the drill core. The plate was exactly the same size as the drilled core with a diameter of 50 mm. Finally, the drill core was pulled loose with a pulling machine which used the hook of the metal plate and which took its support from three points around the core. The tensile strength was calculated by dividing the required force with the area of the core. The place where the loosening had taken place was also recorded.

Six individual measurements were made from each slab. The measurement points formed a straight line which was parallel to the longer side of the element.

3.3.2 Microstructure

Microscopic study of the elements was made by using polished element sections. Pieces of the elements were cut at right angles to the surface of the slabs with a diamond saw and impregnated with epoxy resin containing fluorescent dye. Smaller samples (about 3x5 cm^2, thickness 3-5 mm) were sawn from the pieces, again perpendicular to the original slab surface, and glued on object glasses. The surfaces of the sawn samples were impregnated once again with epoxy and then sequentially ground with a SiC paper of grit 600, 800 and 1200. The sections were studied with a Leica DM HC LP polarising light microscope and photographed with a Leica Q500IW image analysis equipment. Both oblique illumination and fluorescent light from above were used.

3.4 COLOUR MEASUREMENTS AT FINLANDIA HALL

The behaviour of marble slabs on the walls of Finlandia Hall was studied also by measuring the colour of the slab surfaces at regular intervals. CIELAB system was used to define the colour. In

this system any colour can be defined with the help of Lab co-ordinates L, a and b. The co-ordinate L describes the degree of lightness in such a way that the value L = 0 corresponds to totally black and the value L = 100 to totally white. The co-ordinates a and b describe the colour saturation, a in the axis of green...red (-60...+60) and b in the axis of blue...yellow (-60...+60).

The colour difference, ΔE, between two samples or between two measurements from the same sample is defined by using the formula (5).

$$\Delta E = (\Delta L^2 + \Delta a^2 + \Delta b^2)^{1/2} \quad (5)$$

The colour difference is clear if $\Delta E > 3$, but cannot be observed if $\Delta E < 1$.

The colour measurements were made by using an automatic Minolta CM-525i reflectance spectrometer. The light source was D_{65} corresponding to CIE standard.

Altogether nine slabs were chosen for the colour measurements, three representing marble A and two representing each of marbles D, E and K. All the slabs were placed on the roof walls directing either towards south (walls 24 and 202) or towards east (wall 23). Two of the slabs of marble A were directing towards south and one towards east. With the other marbles one of the slabs was directing towards south and the other one towards east. The colour of the slabs was measured from eight points, each including three spots. Thus, the colour of the slabs was presented as an average of total 24 individual measurement values.

3.5 FIELD SAMPLES

In order to get a little wider view of the material behaviour in real environmental conditions a few field samples were collected and studied. By the permission of the owners samples were taken from buildings with marble facades. All except one of these facades showed clear bowing and considerable loss of strength. All facades were 20-30 years old.

3.5.1 Mineral composition

The mineral composition of the field samples was studied with a Philips PW 1710 X-ray diffractometer and a Netzsch STA 429 thermobalance. The runs were made as described earlier in chapters 3.2.3.1 and 3.2.3.2. Powder samples were used. Powders needed for the analyses were prepared by pulverizing some of the sample pieces.

3.5.2 Thin section study

Thin sections of about 0.025x30x50 mm^3 were prepared from the marble specimens taken at right angles to the surfaces of the original slabs. Specimens were impregnated with epoxy resin and ground first with a grinding machine and then by hand to final thickness (0.025 mm). The thin sections were studied with a Leica DM HC LP polarising light microscope and photographed with a Leica Q500IW image analysis equipment.

3.5.3 SEM-study

SEM-study of the field samples was made by using fractured surface specimens. The specimens were broken from the marble pieces available, any loose material was wiped off and the fractured surfaces were carbon coated. The specimens were studied with a Jeol JSM 820 scanning electron microscope (SEM) in a secondary electron mode (SE). SE-images were taken with an Imix image analysis equipment.

4 RESULTS

4.1 MARBLES

4.1.1 Flexural strength

The flexural strength of marble A in initial stage and after 1 and 1.5 years on the test wall at Finlandia Hall is presented in Table 1. The corresponding values of marbles D, E and K are presented in Tables 2-4, respectively. The presented results are average values (av.) and standard deviations (s.d.) calculated from the testing data of individual specimens. The measurement results are shown in detail in Appendix 1.

Table 1. Flexural strength of marble A.

	flexural strength		
	direction A MPa	direction B MPa	A/B
unused			
av.	12.5	16.9	0.74
s.d.	1.2	0.6	
s.d. (%)	9.6	3.4	
test wall / 1 year			
av.	10.5	14.0	0.75
s.d.	1.0	1.1	
s.d. (%)	9.2	8.1	
test wall / 1.5 years			
av.	10.1	14.1	0.72
s.d.	1.1	1.0	
s.d. (%)	10.6	7.4	

Table 2. Flexural strength of marble D.

	flexural strength direction A MPa	direction B MPa	A/B
unused			
av.	5.4	7.0	0.77
s.d.	0.7	0.7	
s.d. (%)	12.2	10.4	
test wall / 1 year			
av.	3.5	3.7	0.96
s.d.	0.2	0.6	
s.d. (%)	6.8	16.3	
test wall / 1.5 years			
av.	3.6	4.1	0.88
s.d.	0.4	0.4	
s.d. (%)	9.8	10.8	

Table 3. Flexural strength of marble E.

	flexural strength direction A MPa	direction B MPa	A/B
unused			
av.	20.4	19.9	1.02
s.d.	1.3	1.8	
s.d. (%)	6.4	8.8	
test wall / 1 year			
av.	17.0	24.0	0.71
s.d.	4.0	1.0	
s.d. (%)	23.4	4.1	
test wall / 1.5 years			
av.	22.5	24.1	0.94
s.d.	2.7	1.3	
s.d. (%)	12.1	5.4	

Table 4. Flexural strength of marble K.

	flexural strength direction A MPa	direction B MPa	A/B
unused			
av.	22.4	19.6	1.14
s.d.	0.9	1.4	
s.d. (%)	3.9	7.0	
test wall / 1 year			
av.	21.6	19.3	1.12
s.d.	0.7	1.4	
s.d. (%)	3.1	7.3	
test wall / 1.5 years			
av.	21.9	20.4	1.07
s.d.	1.6	0.9	
s.d. (%)	7.4	4.2	

For comparison the flexural strengths of the unused marbles are shown in Fig. 2.

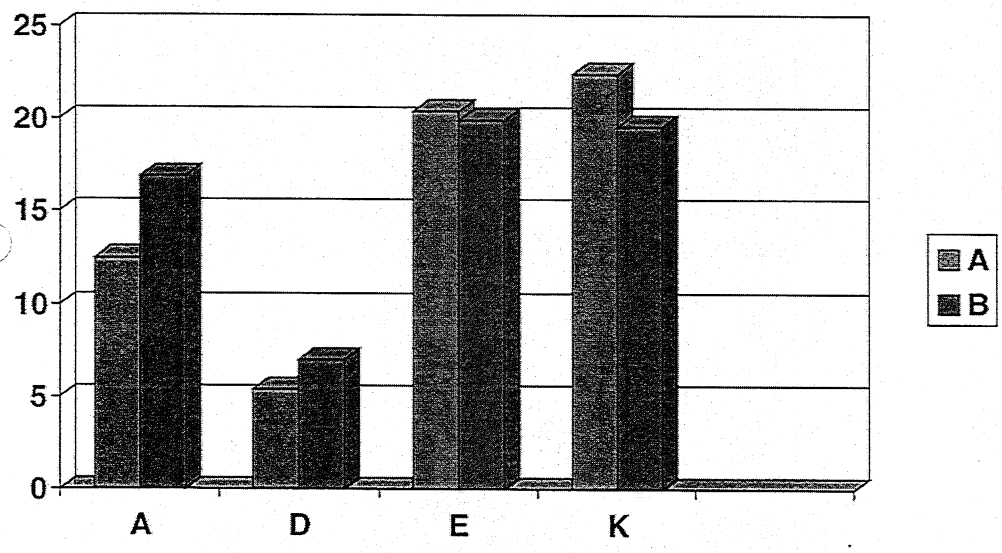

Figure 2. Flexural strengths of the unused marbles (MPa).

The relative changes of the flexural strengths, ΔR_{tf}, of the marbles that have taken place on the test wall are presented in Table 5. The basis of the comparison is in all cases the flexural strength of the unused marble.

Table 5. The relative changes of the flexural strengths of the marbles on the test wall.

marble	ΔR_{tf} 1 year %	1.5 years %
A		
direction A	-16	-20
direction B	-17	-17
D		
direction A	-35	-34
direction B	-48	-42
E		
direction A	-17	+11
direction B	+20	+21
K		
direction A	-3	-2
direction B	-2	+4

The loss of marble strength on the test wall is illustrated also in Figs. 3-6. In each case the flexural strength of unused marble has been given the value of 100.

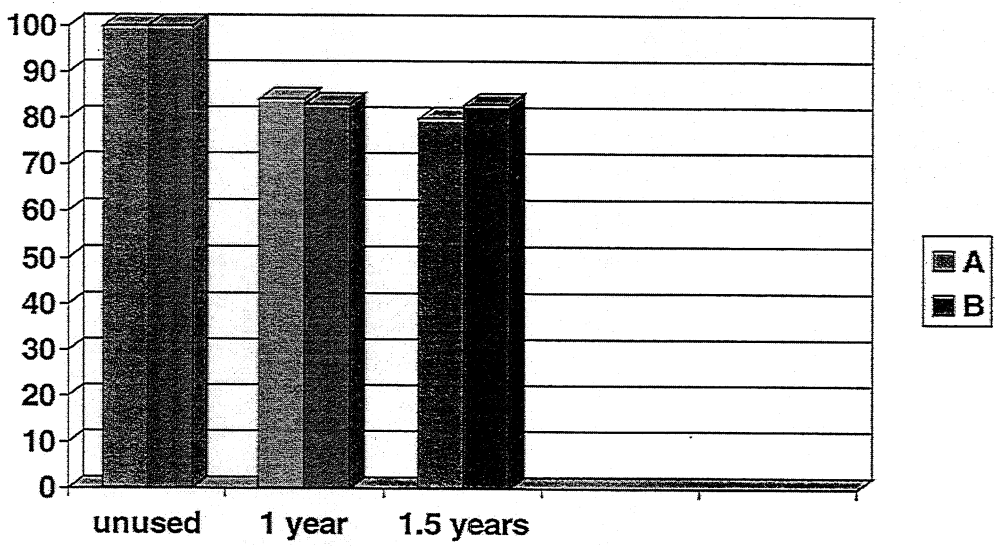

Figure 3. Flexural strength of marble A. A relative scale.

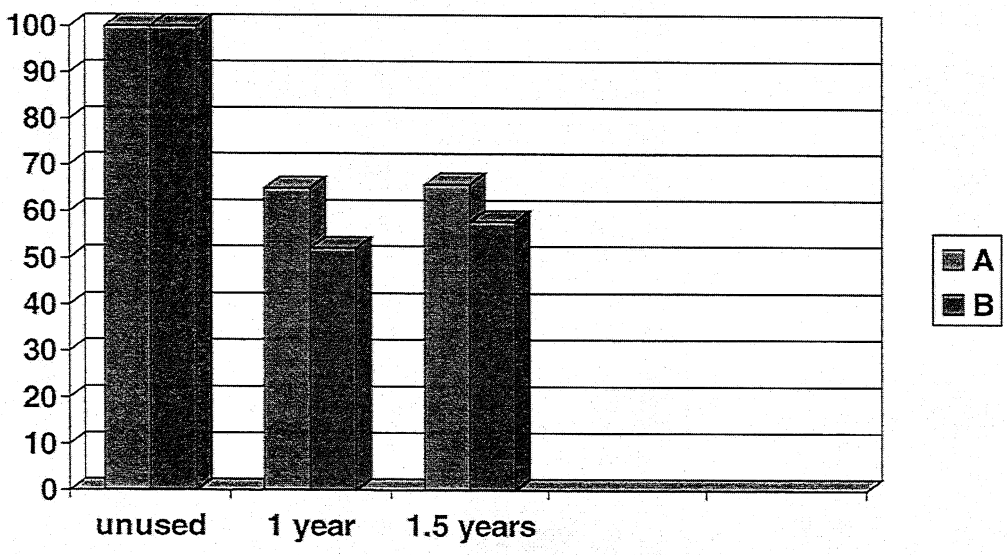

Figure 4. Flexural strength of marble D. A relative scale.

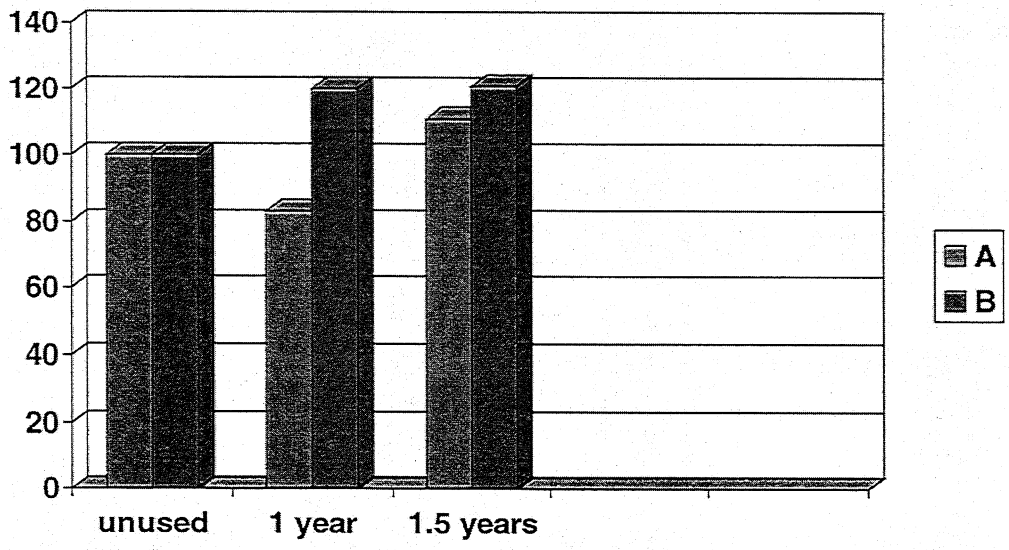

Figure 5. Flexural strength of marble E. A relative scale.

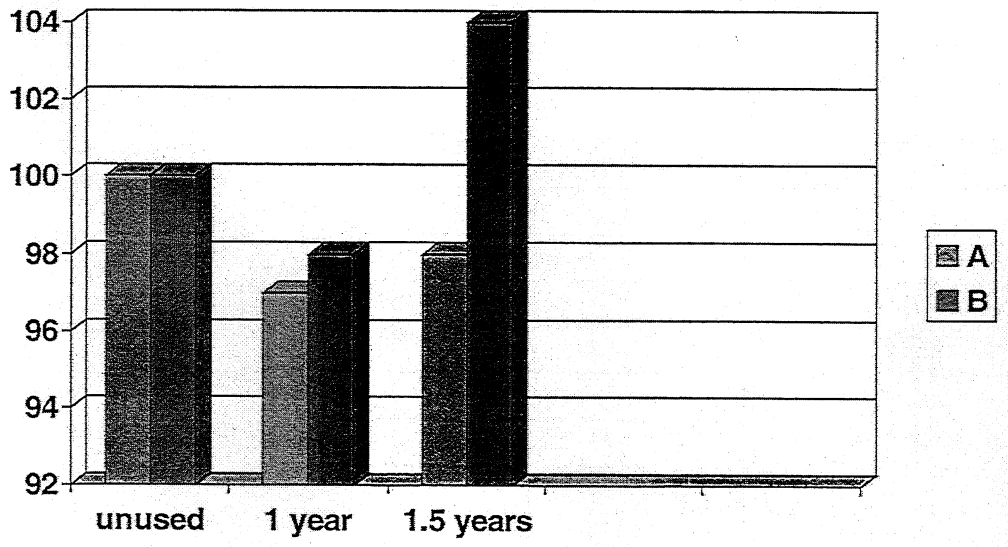

Figure 6. Flexural strength of marble K. A relative scale.

4.1.2 Water absorption, apparent porosity, bulk density

The water absorption, apparent porosity and bulk density of marble A in initial stage and after 1 and 1.5 years on the test wall at Finlandia Hall are presented in Table 6. The corresponding values of marbles D, E and K are presented in Tables 7-9, respectively. The presented results are average values (av.) and standard deviations (s.d.) calculated from the testing data of individual specimens. The measurement results are shown in detail in Appendix 2.

Table 6. Water absorption, apparent porosity and bulk density of marble A.

	water absorption w-%	apparent porosity vol-%	bulk density kg/m^3
unused			
av.	0.113	0.307	2713
s.d.	0.003	0.009	0
s.d. (%)	2.7	2.9	0
test wall / 1 year			
av.	0.202	0.546	2710
s.d.	0.010	0.027	2
s.d. (%)	5.0	5.0	0.07
test wall / 1.5 years			
av.	0.200	0.540	2706
s.d.	0.018	0.049	1
s.d. (%)	9.0	9.1	0.04

Table 7. Water absorption, apparent porosity and bulk density of marble D.

	water absorption w-%	apparent porosity vol-%	bulk density kg/m^3
unused			
av.	0.125	0.339	2718
s.d.	0.011	0.028	7
s.d. (%)	8.8	8.3	0.26
test wall / 1 year			
av.	0.240	0.650	2706
s.d.	0.009	0.023	1
s.d. (%)	3.8	3.5	0.04
test wall / 1.5 years			
av.	0.221	0.597	2705
s.d.	0.026	0.069	2
s.d. (%)	11.8	11.6	0.07

Table 8. Water absorption, apparent porosity and bulk density of marble E.

	water absorption w-%	apparent porosity vol-%	bulk density kg/m^3
unused			
av.	0.111	0.301	2715
s.d.	0.006	0.016	3
s.d. (%)	5.4	5.3	0.11
test wall / 1 year			
av.	0.124	0.339	2732
s.d.	0.006	0.018	23
s.d. (%)	4.8	5.3	0.84
test wall / 1.5 years			
av.	0.121	0.329	2713
s.d.	0.008	0.021	1
s.d. (%)	6.6	6.4	0.04

Table 9. Water absorption, apparent porosity and bulk density of marble K.

	water absorption w-%	apparent porosity vol-%	bulk density kg/m^3
unused			
av.	0.069	0.188	2716
s.d.	0.009	0.025	1
s.d. (%)	13.0	13.3	0.04
test wall / 1 year			
av.	0.108	0.294	2715
s.d.	0.013	0.036	1
s.d. (%)	12.0	12.2	0.04
test wall / 1.5 years			
av.	0.104	0.282	2713
s.d.	0.017	0.047	1
s.d. (%)	16.4	16.7	0.04

The water absorptions and apparent porosities of the marbles are shown in Figs. 7 and 8.

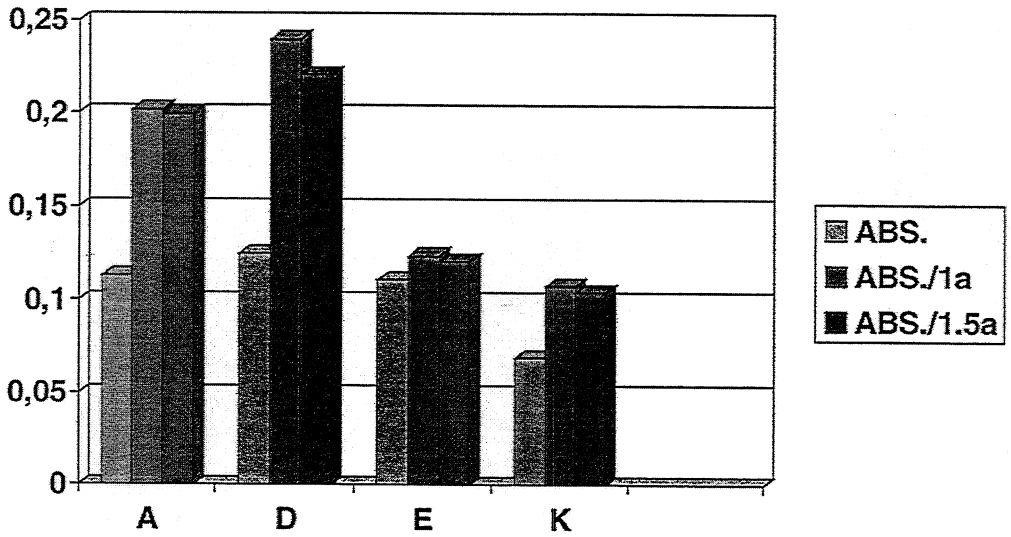

Figure 7. Water absorption of the marbles (w-%).

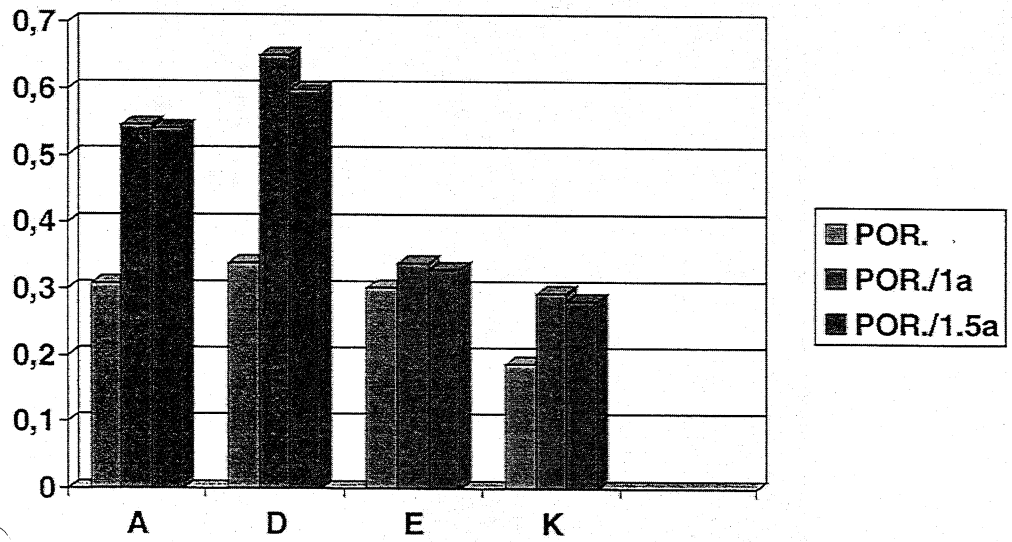

Figure 8. Apparent porosity of the marbles (vol-%).

The relative changes of the water absorption, ΔW, and apparent porosity, Δp_o, of the marbles that have taken place on the test wall are presented in Table 10. The basis of the comparison is in all cases the value of the unused marble.

Table 10. The relative changes of the water absorption and apparent porosity of the marbles on the test wall.

marble	ΔW		Δp_o	
	1 year %	1.5 years %	1 year %	1.5 years %
A	+79	+77	+78	+76
D	+92	+77	+92	+76
E	+12	+9	+13	+9
K	+57	+51	+56	+50

The increase of water absorption and porosity on the test wall is illustrated also in Figs. 9-12. In each case the water absorption (porosity) of unused marble has been given the value of 100.

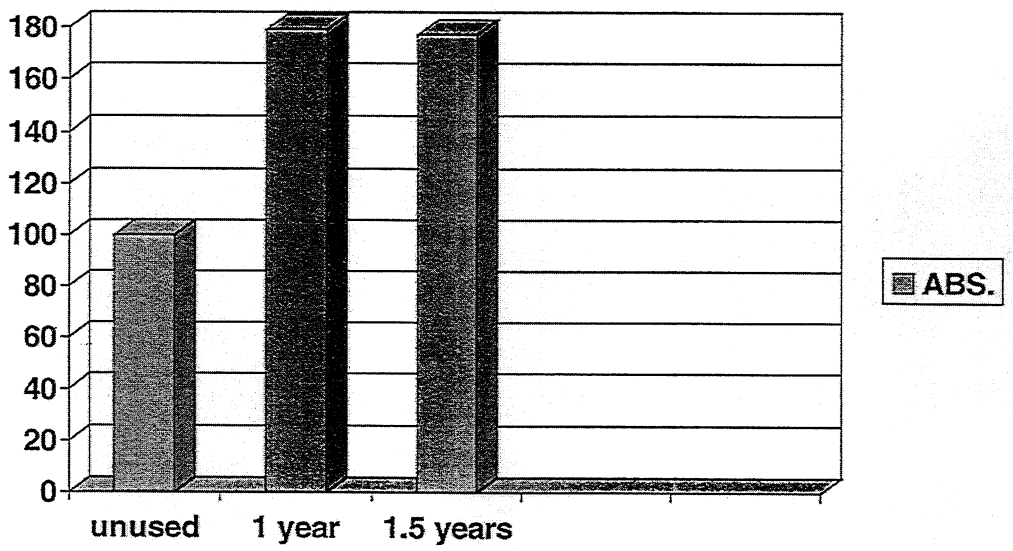

Figure 9. Water absorption (porosity) of marble A. A relative scale.

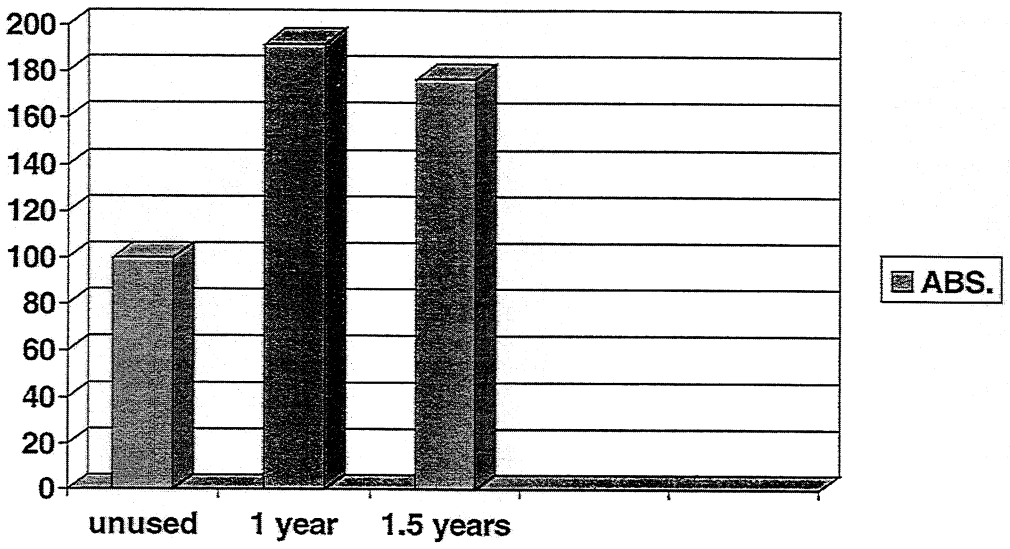

Figure 10. Water absorption (porosity) of marble D. A relative scale.

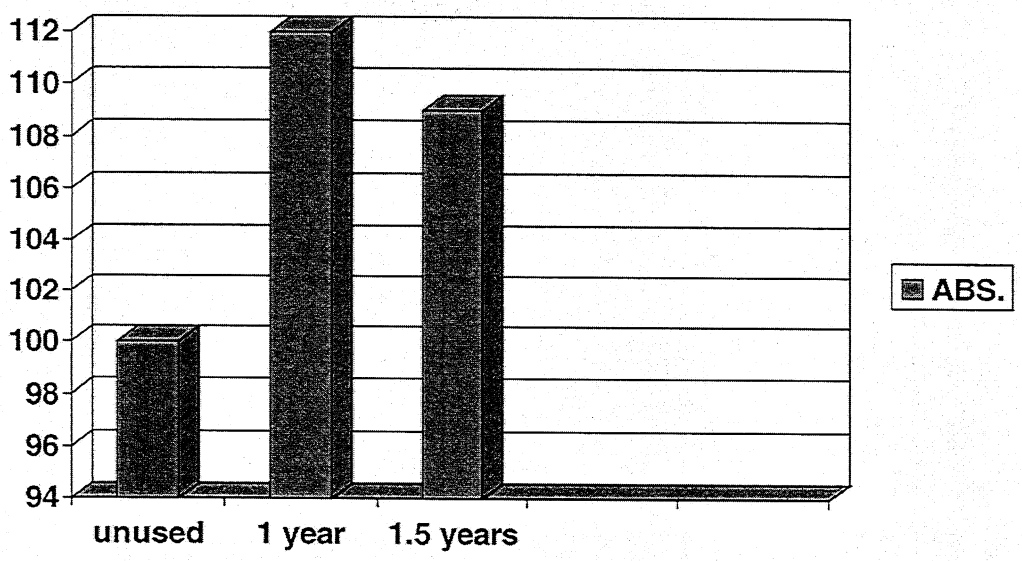

Figure 11. Water absorption (porosity) of marble E. A relative scale.

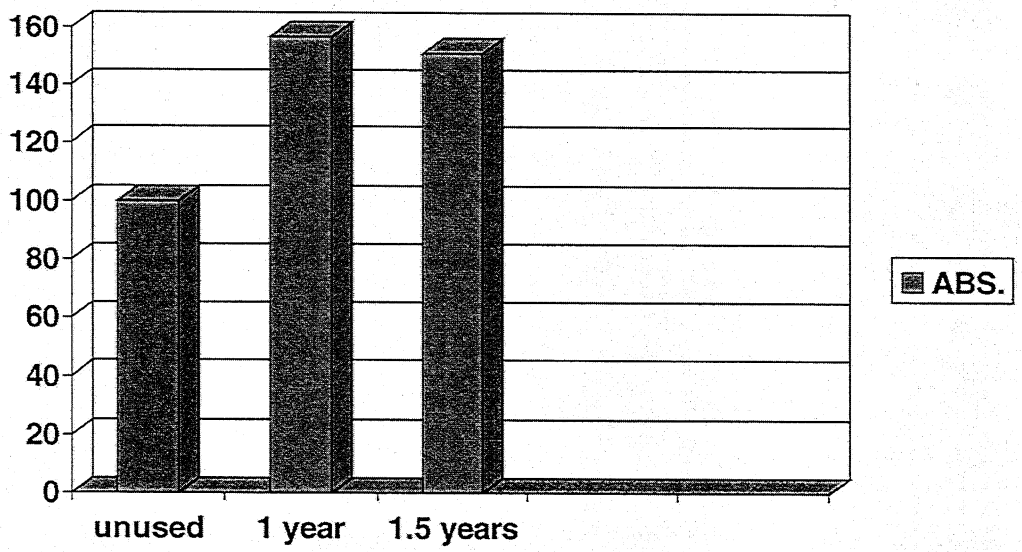

Figure 12. Water absorption (porosity) of marble K. A relative scale.

4.1.3 Mineral composition

4.1.3.1 X-ray diffraction

According to the X-ray diffraction diagram marble A consisted almost entirely of calcite, i.e. calcium carbonate, $CaCO_3$. Quartz, α-SiO_2, and feldspar, Na-K-Ca-aluminium silicate, were also observed. The contents of these accessory minerals were, however, low, at most only a couple of weight percents. The diffraction diagram of marble A is shown in Fig. 13.

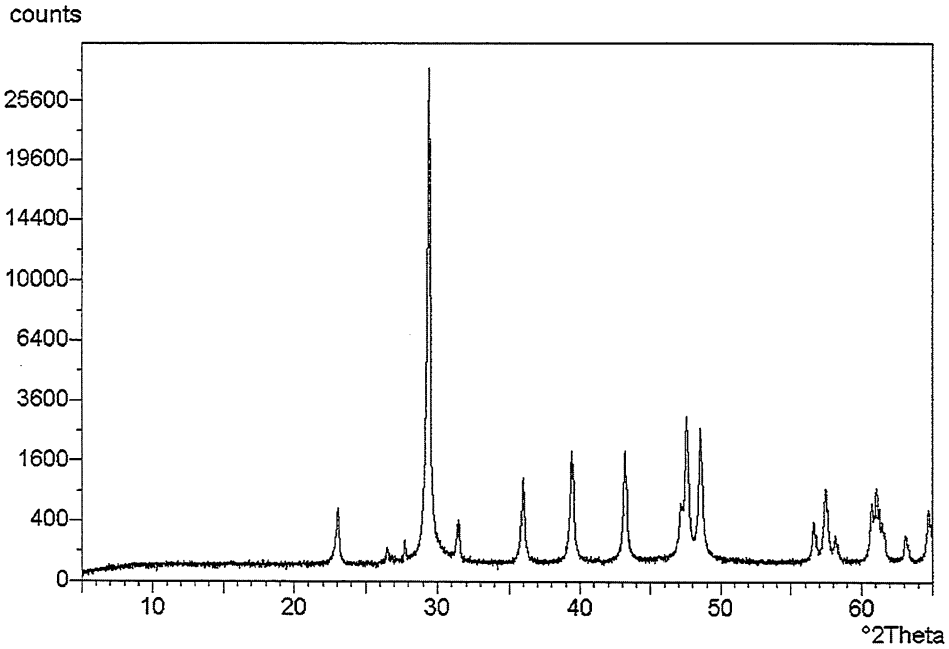

Figure 13. X-ray diffraction diagram of marble A.

According to the X-ray diffraction diagram marble D consisted almost entirely of calcite, i.e. calcium carbonate, $CaCO_3$. Quartz, α-SiO_2, and dolomite, $CaMg(CO_3)_2$, were also observed. The contents of these accessory minerals were, however, low, at most only a couple of weight percents. The diffraction diagram of marble D is shown in Fig. 14.

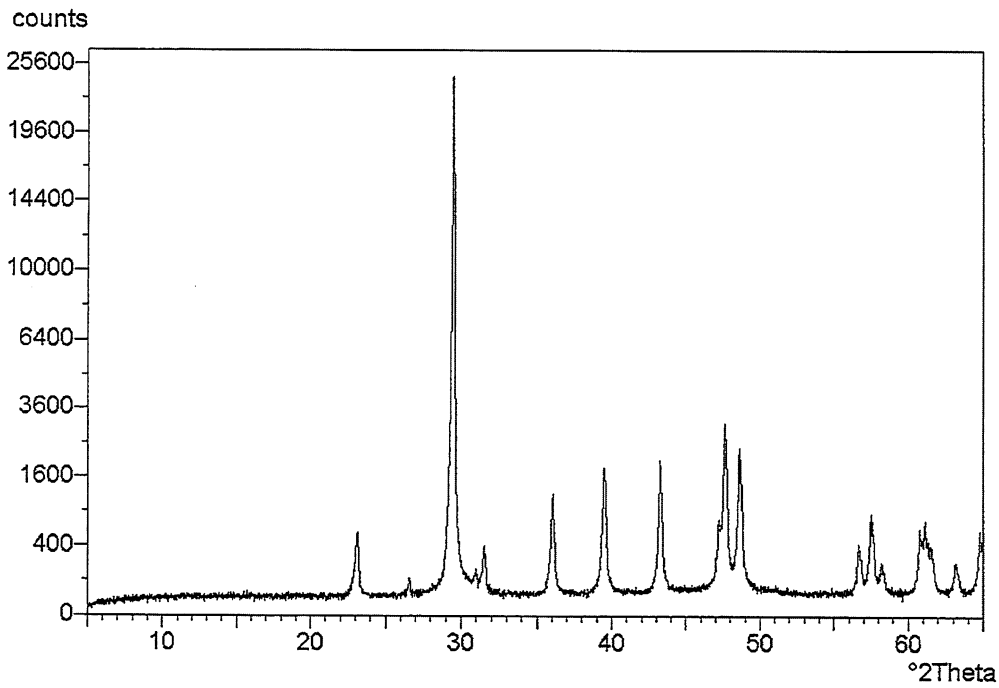

Figure 14. X-ray diffraction diagram of marble D.

According to the X-ray diffraction diagram marble E consisted almost entirely of calcite, i.e. calcium carbonate, $CaCO_3$. Marble contained also a substantial amount, probably 5-10 w-%, of dolomite, $CaMg(CO_3)_2$. Quartz, α-SiO_2, was also observed, but its content was low. The diffraction diagram of marble E is shown in Fig. 15.

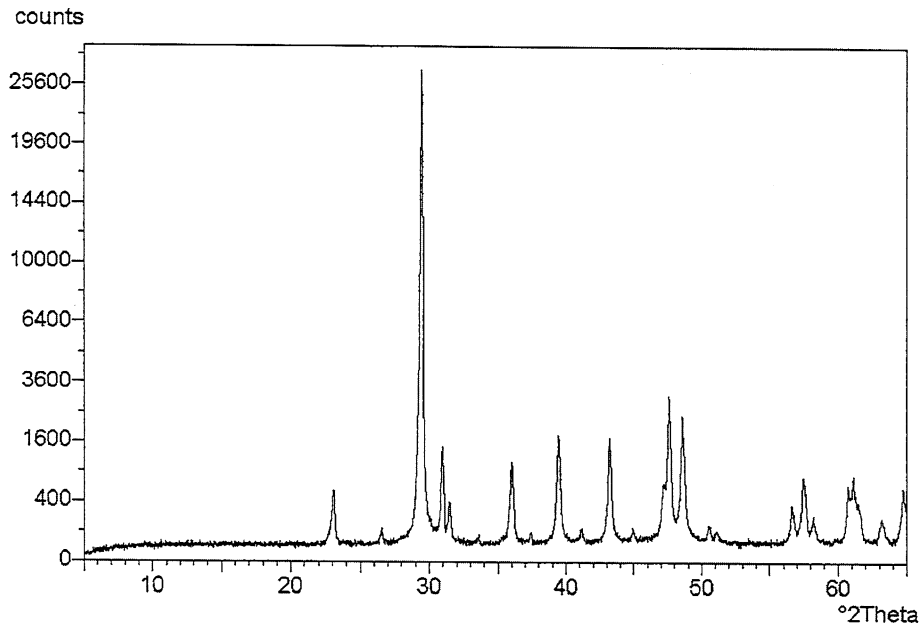

Figure 15. X-ray diffraction diagram of marble E.

According to the X-ray diffraction diagram marble K consisted almost entirely of calcite, i.e. calcium carbonate, $CaCO_3$. Quartz, α-SiO_2, and dolomite, $CaMg(CO_3)_2$, were also observed. The contents of these accessory minerals were, however, low, at most only a couple of weight percents. The diffraction diagram of marble K is shown in Fig. 16.

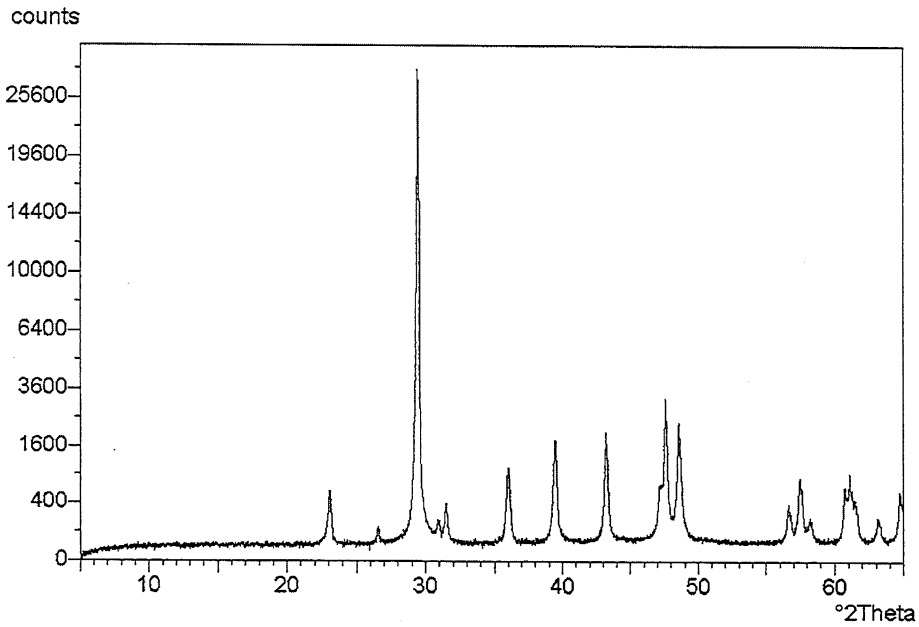

Figure 16. X-ray diffraction diagram of marble K.

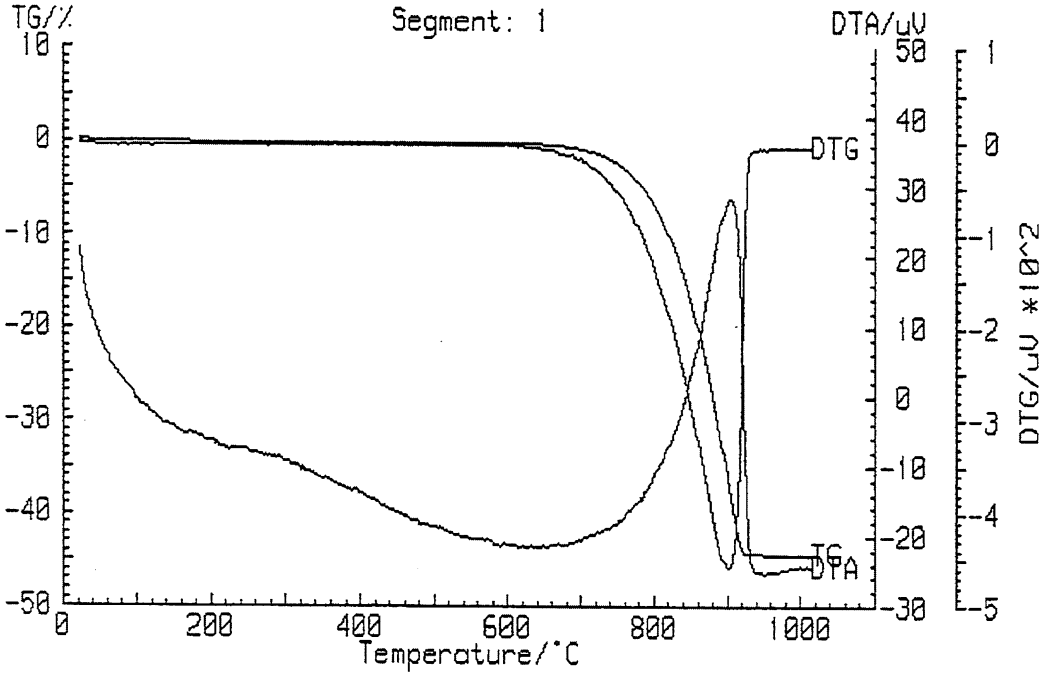

Figure 18. Thermal curves of marble D.

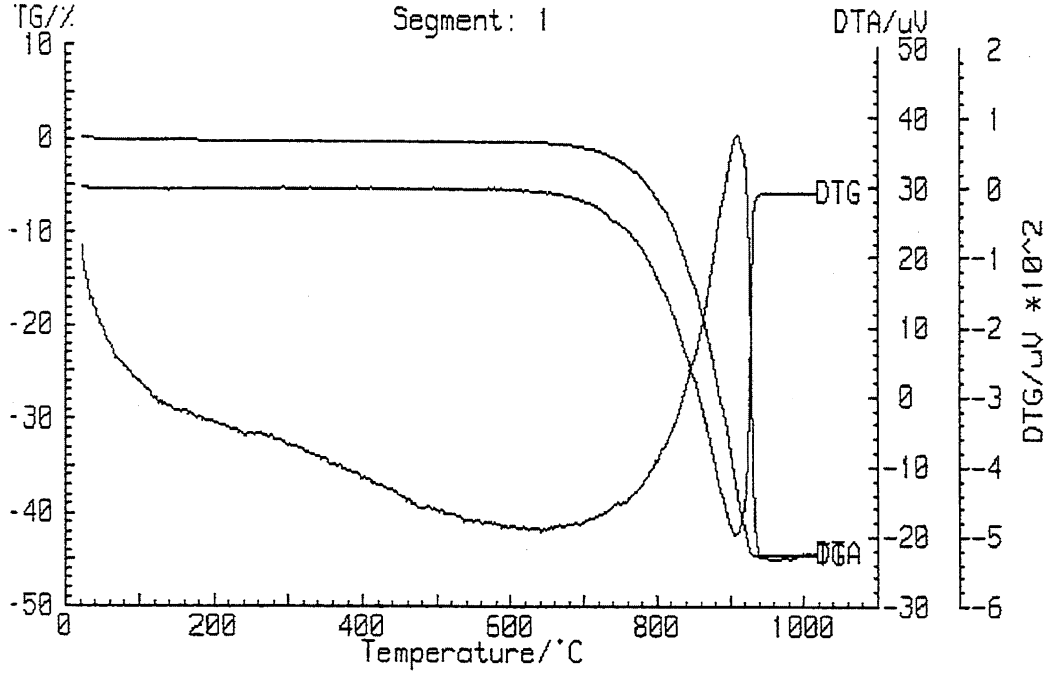

Figure 19. Thermal curves of marble E.

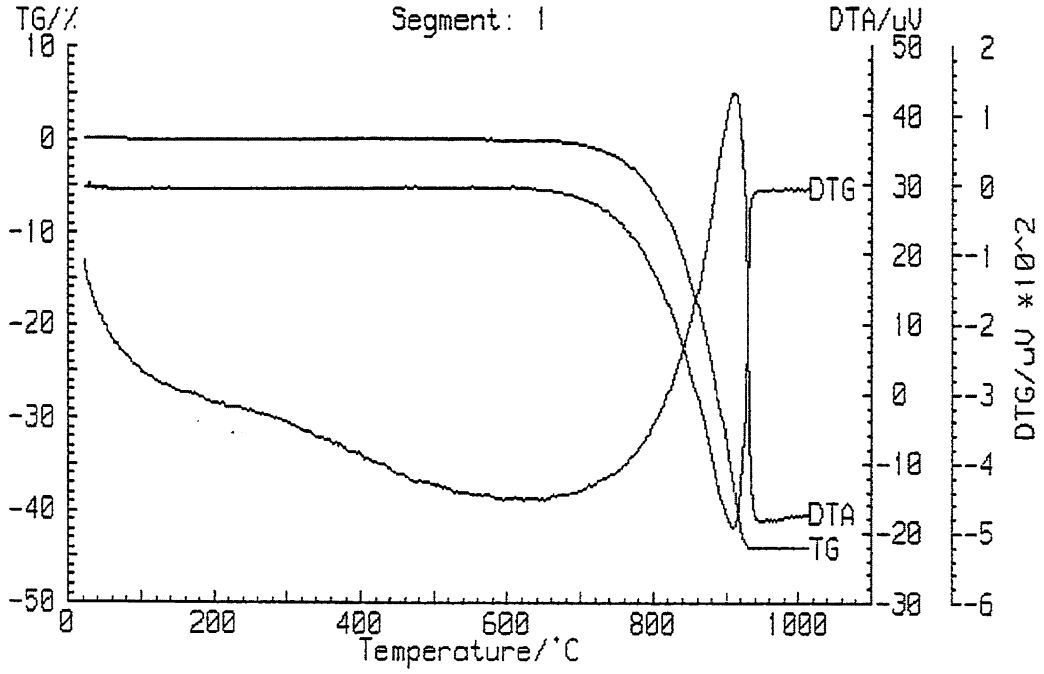

Figure 20. Thermal curves of marble K.

4.1.4 Microstructure

4.1.4.1 Thin section study

Photographs of the microstructure of marble A, unused and after 1 year on the test wall, are shown in Figs. 21-23. Following observations were made:

- groundmass fine-grained, fairly even-grained, not oriented, massive
- average grain size 200-300 µm
- slightly porphyroblastic, some larger porphyroblasts (max ∅ 6 mm) in the groundmass
- nearly pure carbonate rock, contains only very little opaque minerals
- alteration of the grains insignificant
- no changes observable after 1 year on the test wall

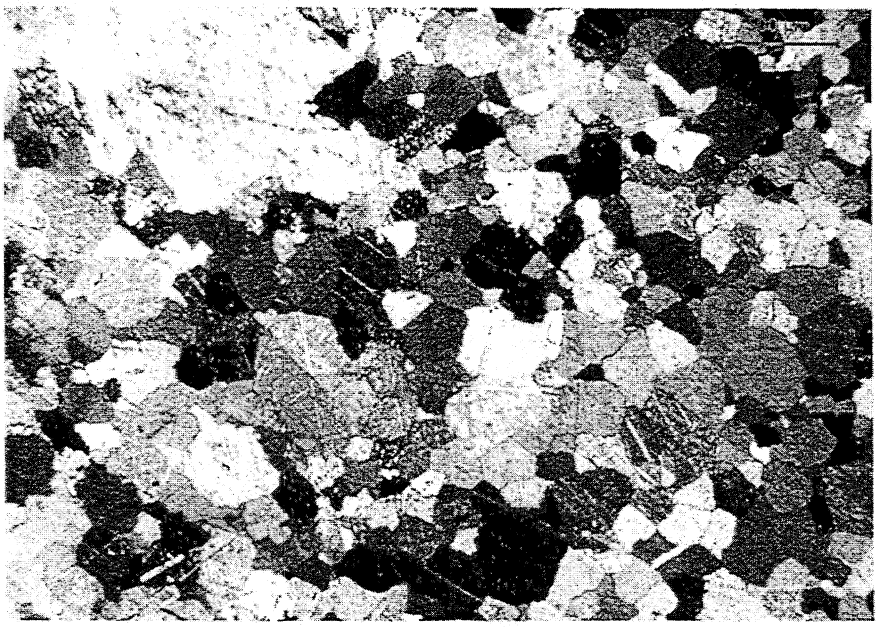

Figure 21. Microstructure of marble A. Unused. Cross-polarized light.

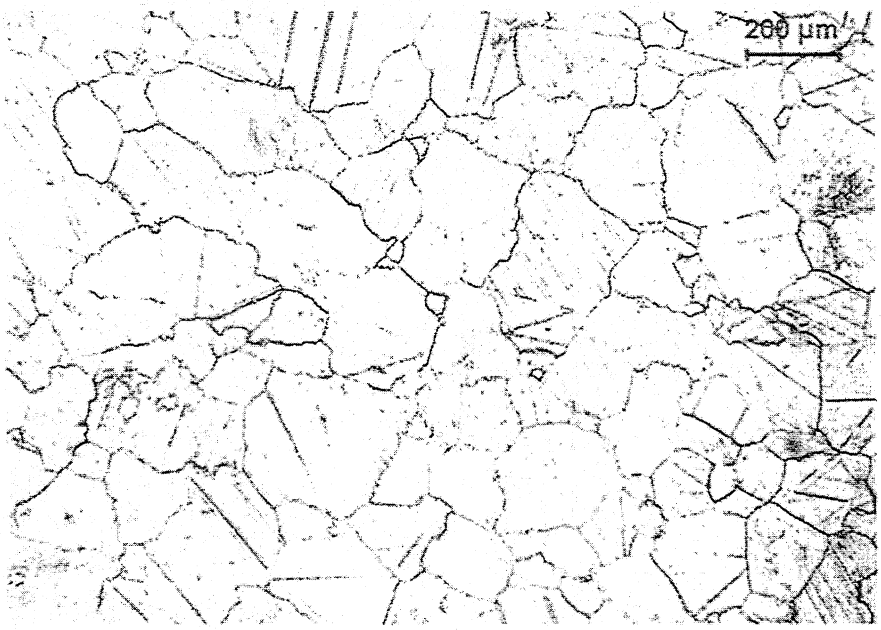

Figure 22. Microstructure of marble A. Unused. Plane-polarized light.

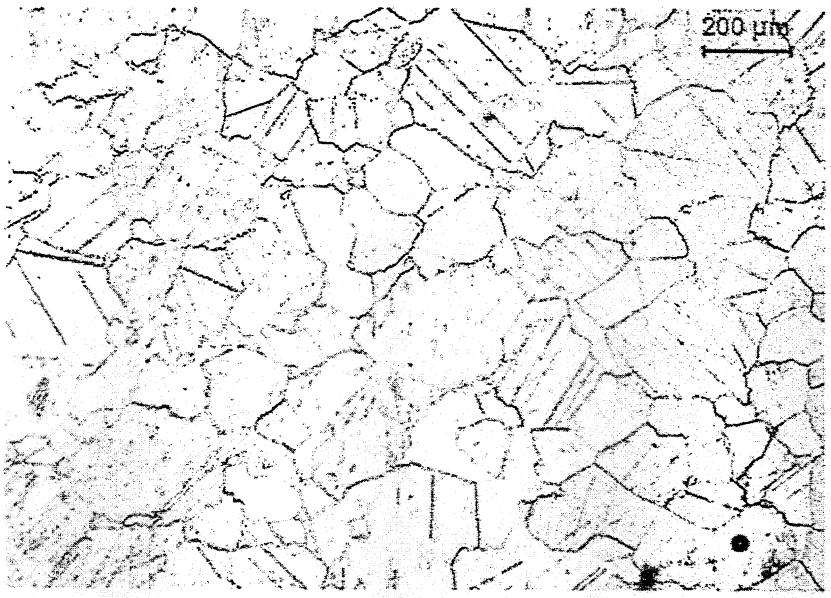

Figure 23. Microstructure of marble A. 1 year on the test wall. Plane-polarized light.

Photographs of the microstructure of marble D, unused and after 1 year on the test wall, are shown in Figs. 24-26. Following observations were made:

- fine-grained, fairly even-grained, not oriented, massive
- average grain size 200-300 µm
- nearly pure carbonate rock, contains very little mica type minerals
- some alteration of the grains
- no changes observable after 1 year on the test wall

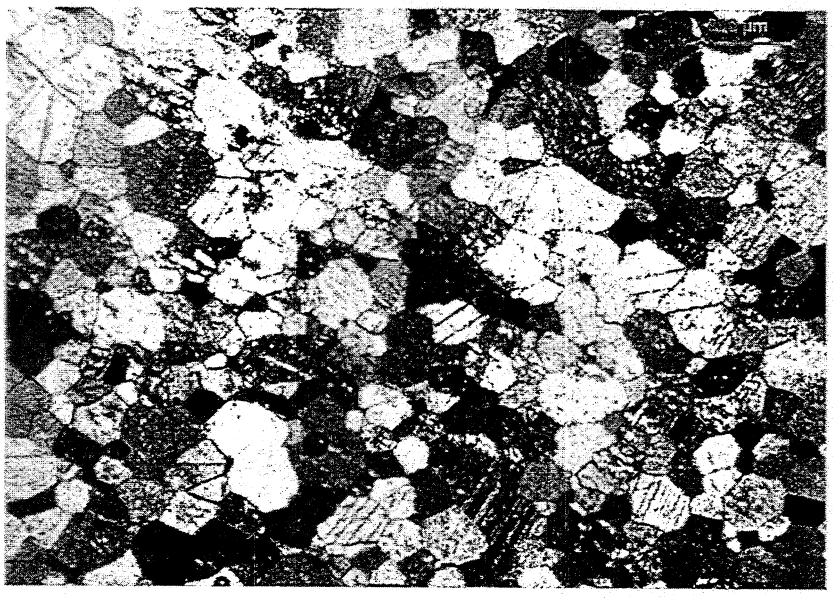

Figure 24. Microstructure of marble D. Unused. Cross-polarized light.

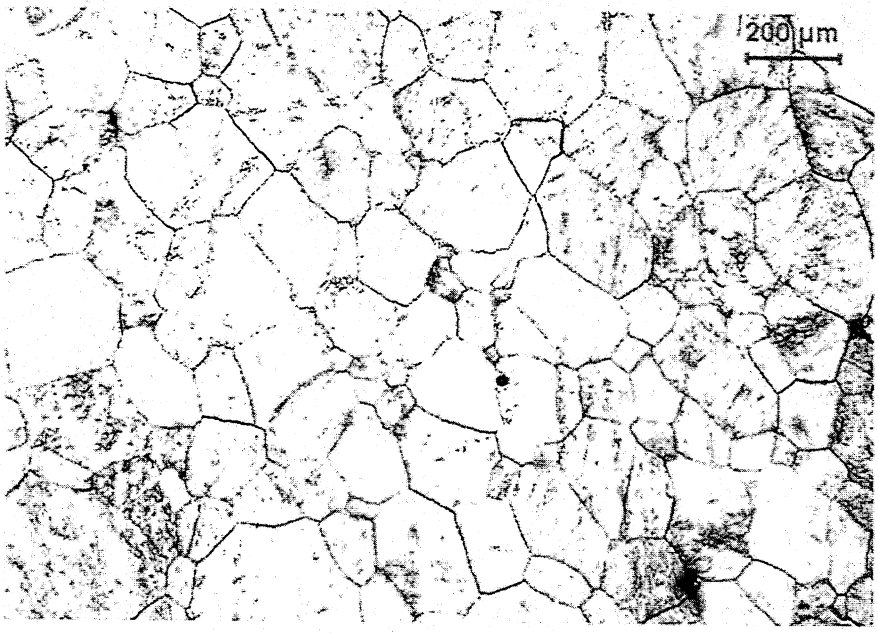

Figure 25. Microstructure of marble D. Unused. Plane-polarized light.

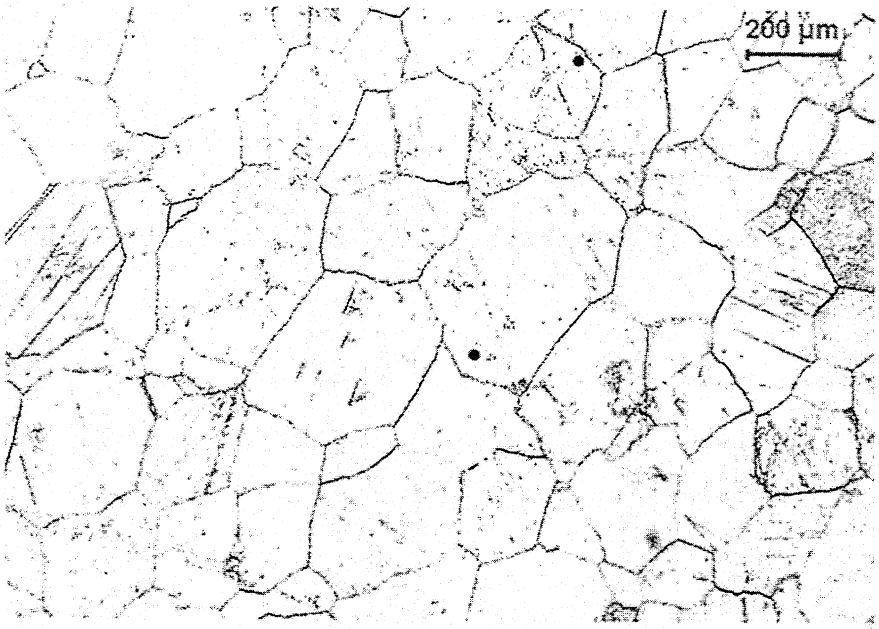

Figure 26. Microstructure of marble D. 1 year on the test wall. Plane-polarized light.

Photographs of the microstructure of marble E, unused and after 1 year on the test wall, are shown in Figs. 27-29. Following observations were made:

- fine-grained, not oriented
- grain size varies from microcrystalline up to 0.8 mm

- very fine-grained (cryptocrystalline) lenses among the groundmass, the lenses pass gradually into groundmass
- nearly pure carbonate rock, contains some opaque and mica type minerals
- some alteration of the grains
- no changes observable after 1 year on the test wall

Figure 27. Microstructure of marble E. Unused. Cross-polarized light.

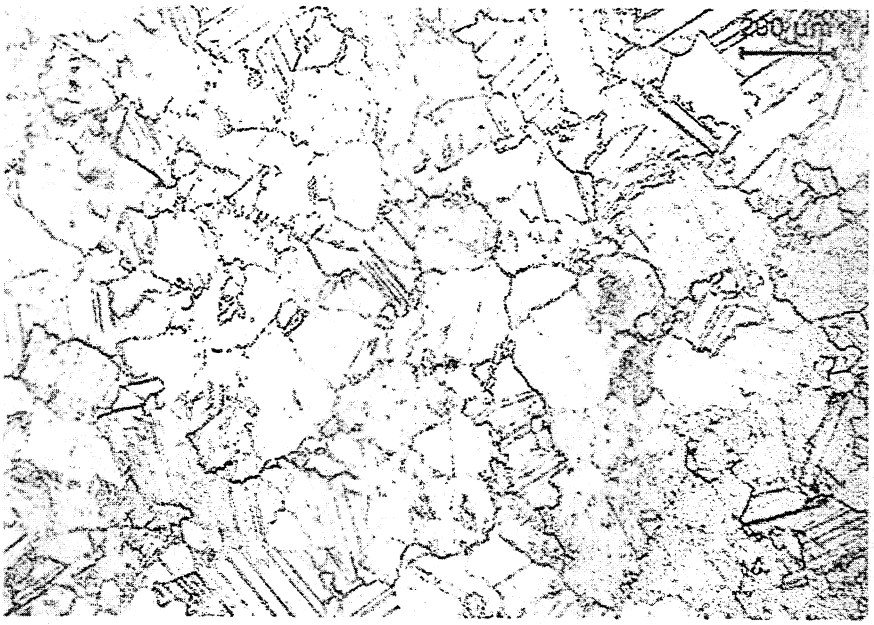

Figure 28. Microstructure of marble E. Unused. Plane-polarized light.

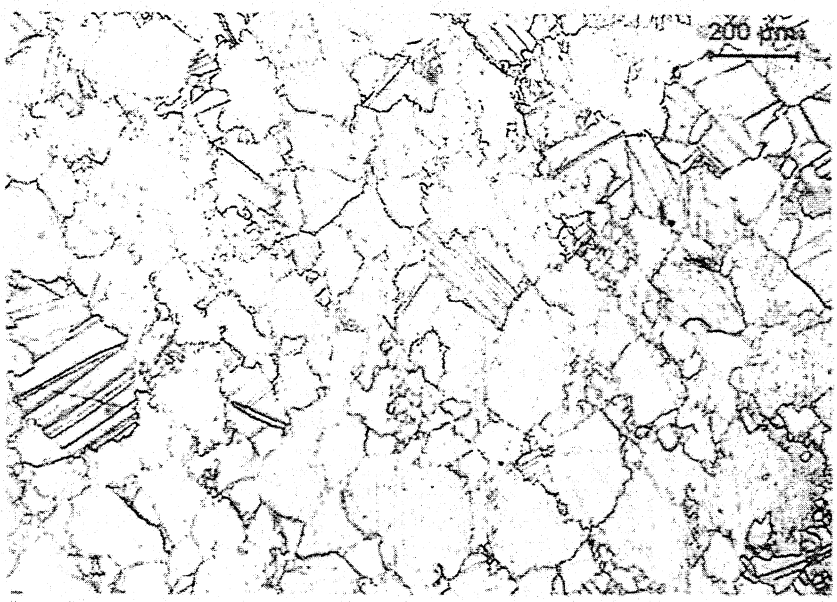

Figure 29. Microstructure of marble E. 1 year on the test wall. Plane-polarized light.

Photographs of the microstructure of marble K, unused and after 1 year on the test wall, are shown in Figs. 30-32. Following observations were made:

- fine-grained, not oriented
- average grain size about 200 µm
- very fine-grained (cryptocrystalline) lenses and veins among the groundmass, the lense boundaries are usually distinguished from the groundmass
- nearly pure carbonate rock, contains some opaque minerals
- little alteration of the grains
- no changes observable after 1 year on the test wall

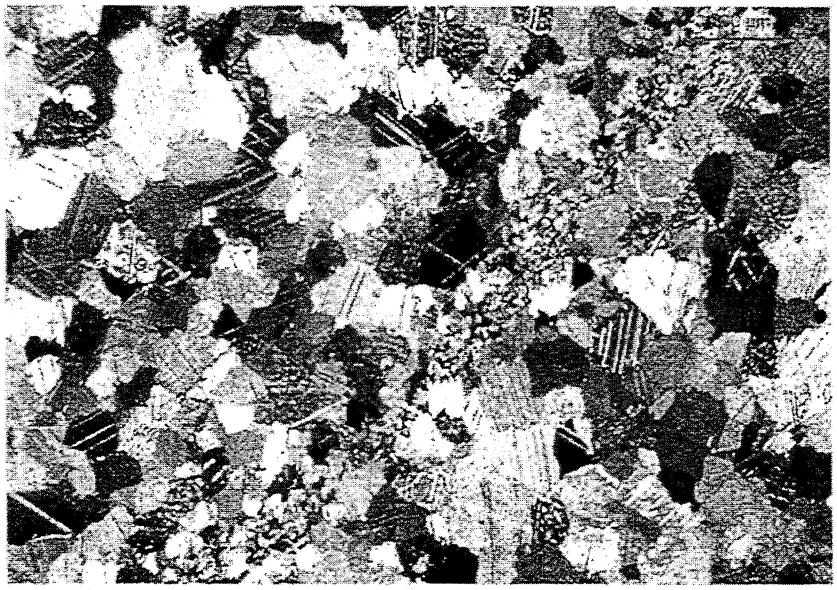

Figure 30. Microstructure of marble K. Unused. Cross-polarized light.

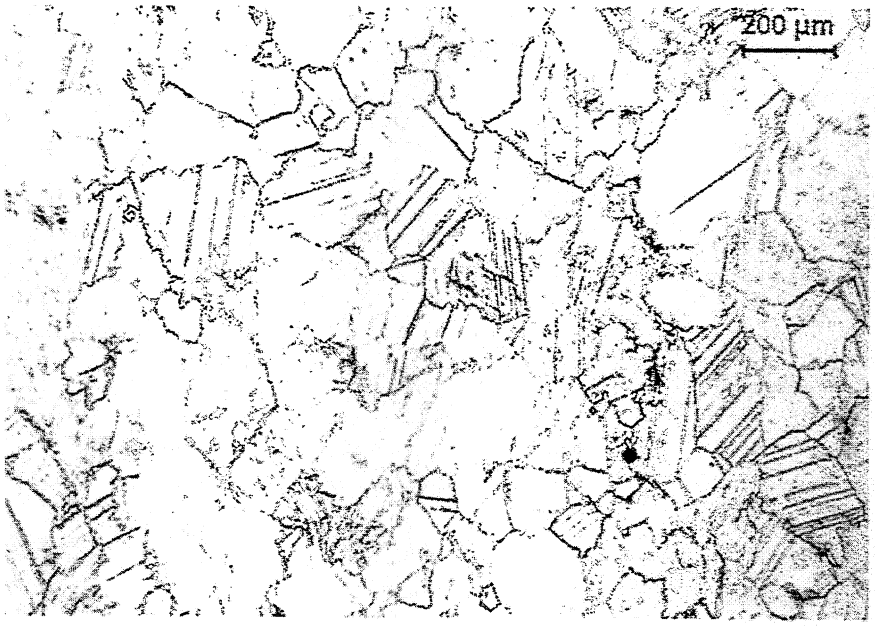

Figure 31. Microstructure of marble K. Unused. Plane-polarized light.

Figure 32. Microstructure of marble K. 1 year on the test wall. Plane-polarized light.

4.1.4.2 Elementary composition, distribution of elements

According to the EDS-analysis marble A consisted almost entirely of calcium, carbon and oxygen, i.e. calcium carbonate. Several small grains with high atomic weight were, however, observed. These grains contained iron and sulphur referring to iron sulphides. Elementary dot maps showed that there were also spots with a high content of silicon and spots with high contents of silicon, aluminium and potassium, Fig. 33. The former were probably due to quartz and the latter to feldspar. Other elements were very evenly distributed.

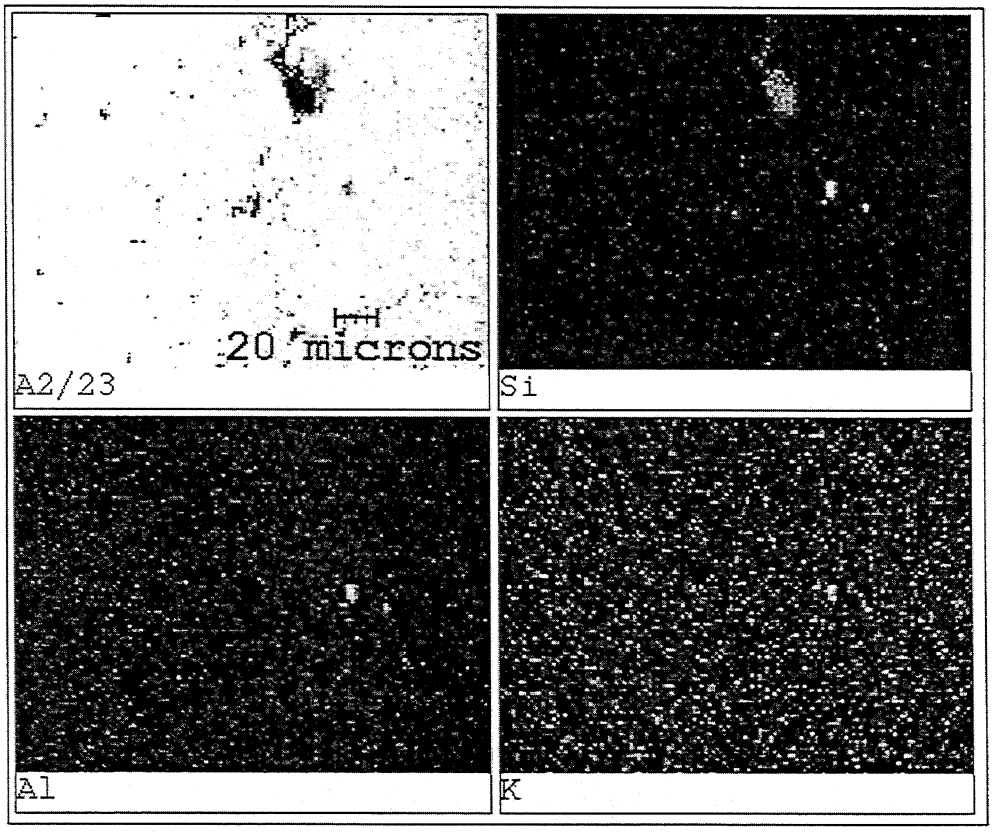

Figure 33. Marble A. Unused. BSE-image (500x, near the surface) and elementary dot maps of silicon (Si), aluminium (Al) and potassium (K).

According to the EDS-analysis marble D consisted almost entirely of calcium, carbon and oxygen, i.e. calcium carbonate. Some spots, a few mm in size, with low atomic weight were, however, observed. These grains contained magnesium and calcium. Thus, they were dolomite. Associated with these dolomitic spots some small grains with high atomic weight were also found. These contained iron, zinc and sulphur referring to sulphide minerals. Elementary dot maps showed that there were also spots with a high content of silicon, Fig. 34. These spots, which seemed to concentrate on the grain boundaries, were probably due to quartz. Other elements were very evenly distributed.

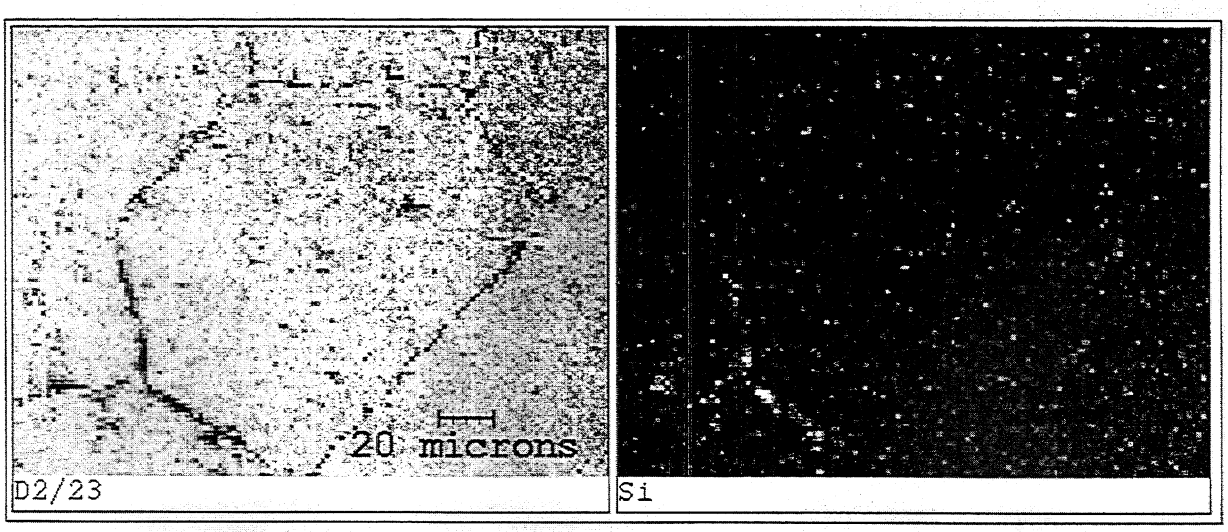

Figure 34. Marble D. Unused. BSE-image (500x, near the surface) and elementary dot map of silicon (Si).

According to the EDS-analysis marble E consisted almost entirely of calcium, carbon and oxygen, i.e. calcium carbonate. Some large spots, several mm in size, with low atomic weight were, however, observed. These grains contained magnesium and calcium. Thus, they were dolomite. Elementary dot maps showed that there were also spots with a high content of silicon, Fig. 35. These spots were probably due to quartz. Other elements were very evenly distributed.

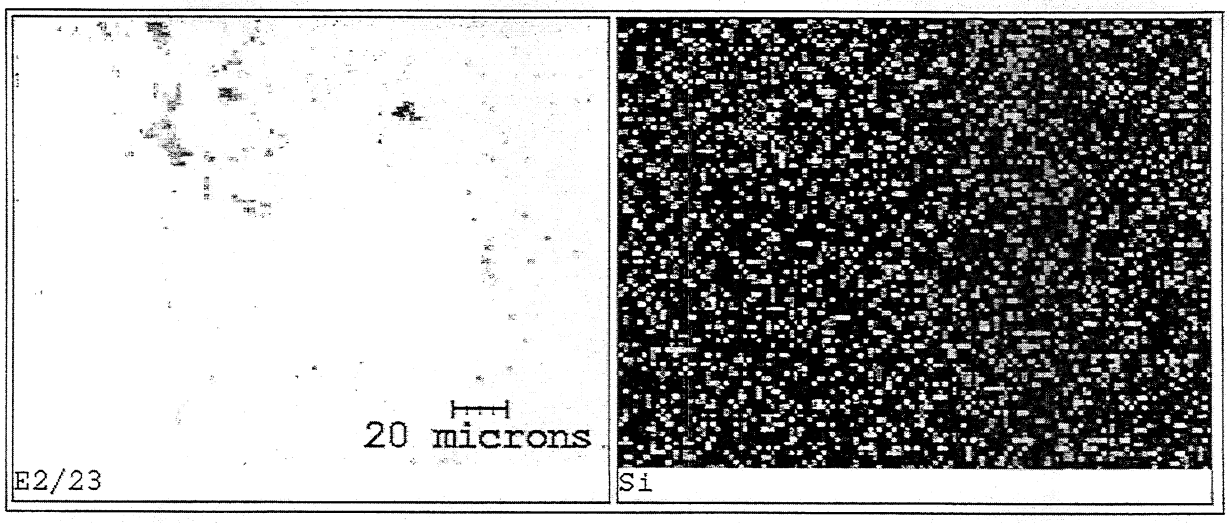

Figure 35. Marble E. Unused. BSE-image (500x, near the surface) and elementary dot map of silicon (Si).

According to the EDS-analysis marble K consisted almost entirely of calcium, carbon and oxygen, i.e. calcium carbonate. A couple of narrow veins with low atomic weight were, however, observed. These veins contained magnesium and calcium. Thus, they were dolomite. Elementary dot maps showed that there were also spots with a high content of silicon, Fig. 36. These spots, which seemed concentrate on the grain boundaries, were probably due to quartz. Other elements were very evenly distributed.

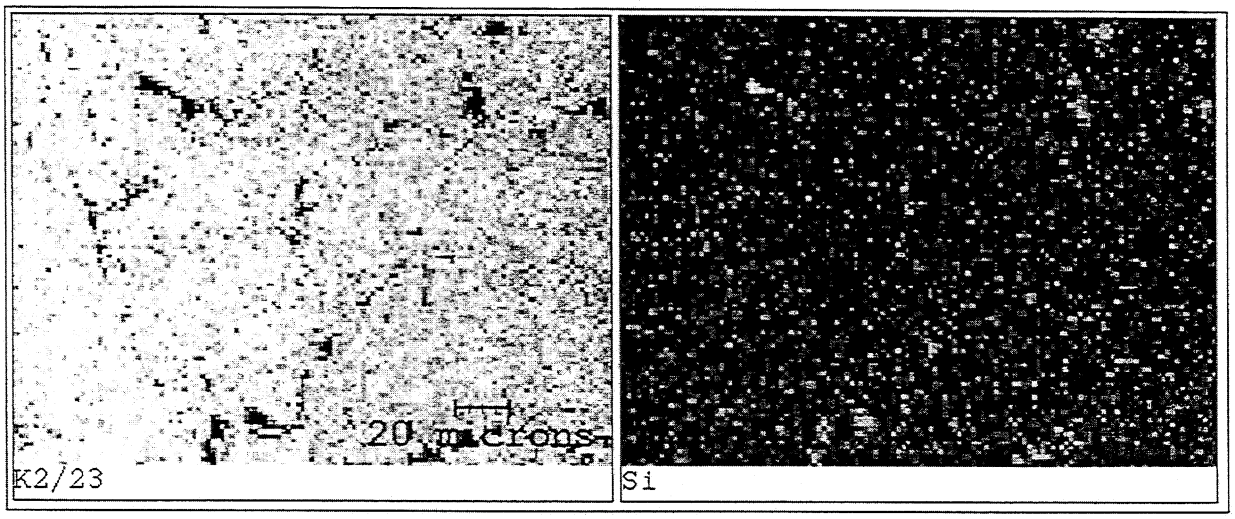

Figure 36. Marble K. Unused. BSE-image (500x, near the surface) and elementary dot map of silicon (Si).

No changes could be observed either in the general chemical composition or in the distribution of elements of any of the marbles after 1 and 1.5 years on the test wall.

4.1.4.3 SEM-study

BSE- and SE-images of marble A, both unused and after 1 year on the test wall, are shown in Figs. 37-40. Grain boundaries can partly be distinguished. No changes could be seen in the structure of the marble after 1 year on the test wall.

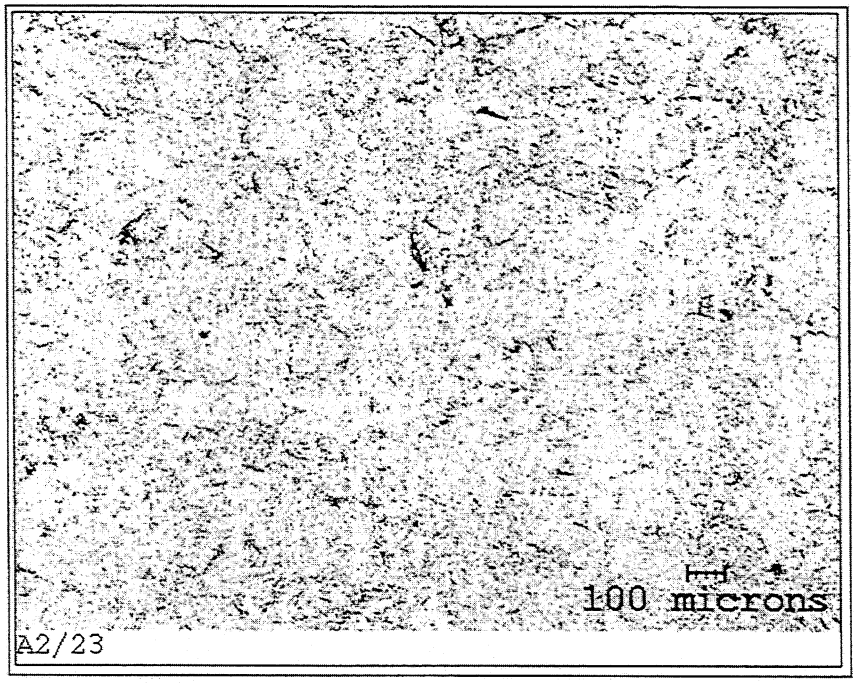

Figure 37. Marble A, unused. BSE-image, 50x.

Figure 38. Marble A, 1 year on the test wall. BSE-image, 50x.

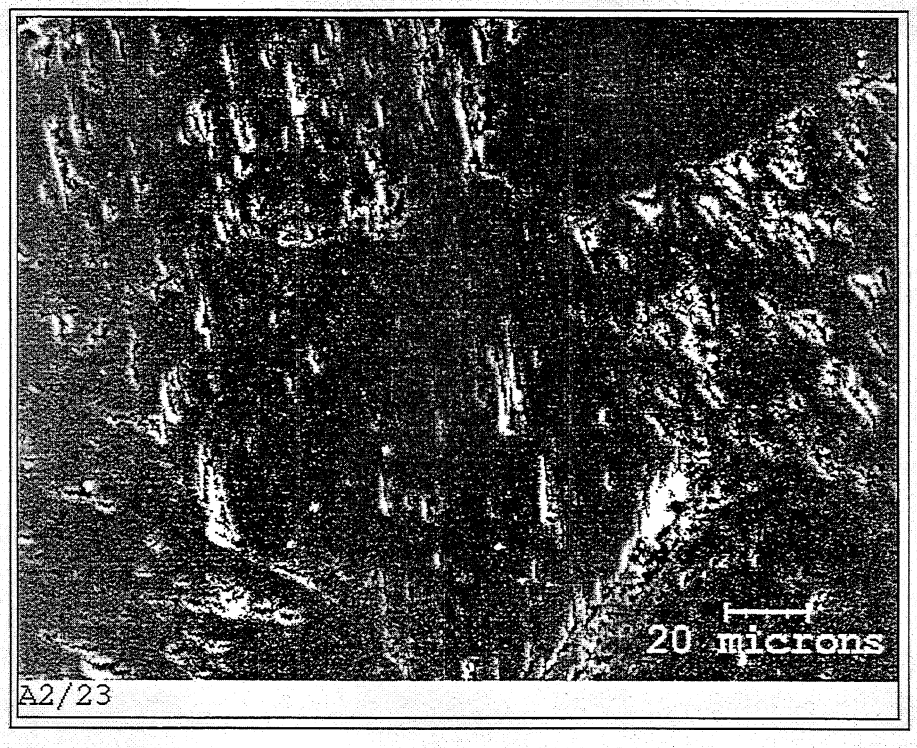

Figure 39. Marble A, unused. SE-image, 500x.

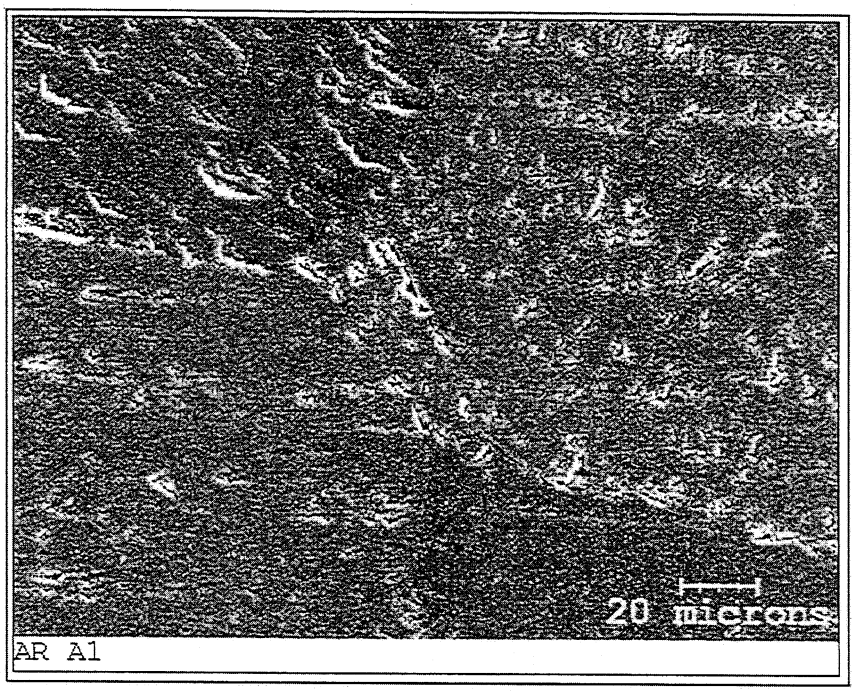

Figure 40. Marble A, 1 year on the test wall. SE-image, 500x.

BSE- and SE-images of marble D, both unused and after 1 year on the test wall, are shown in Figs. 41-44. Grain boundaries can clearly be distinguished. Stresses caused by 1 year on the test wall seemed to affect the structure of the marble in such a way that the grain boundaries could be distinguished even more easily.

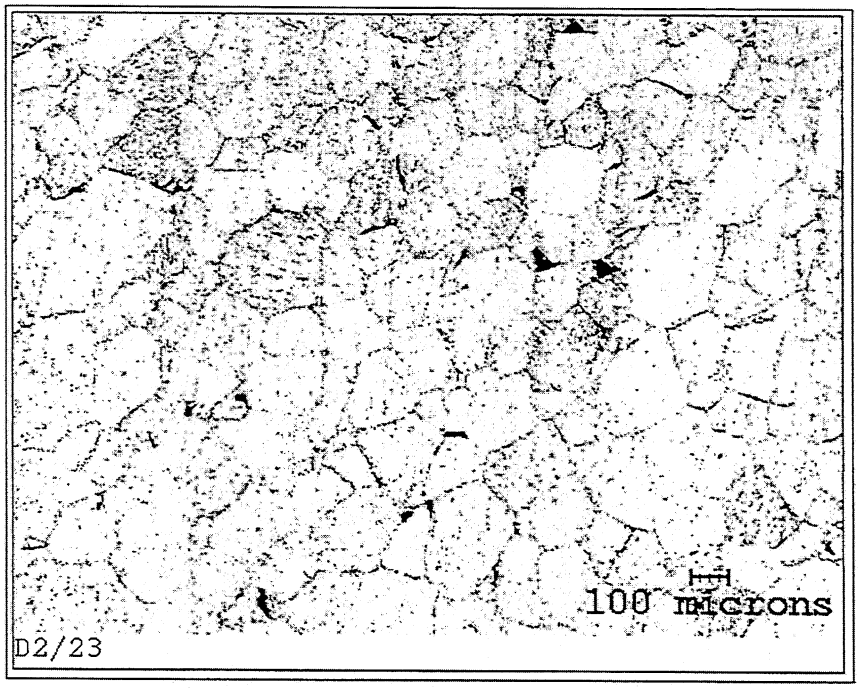

Figure 41. Marble D, unused. BSE-image, 50x.

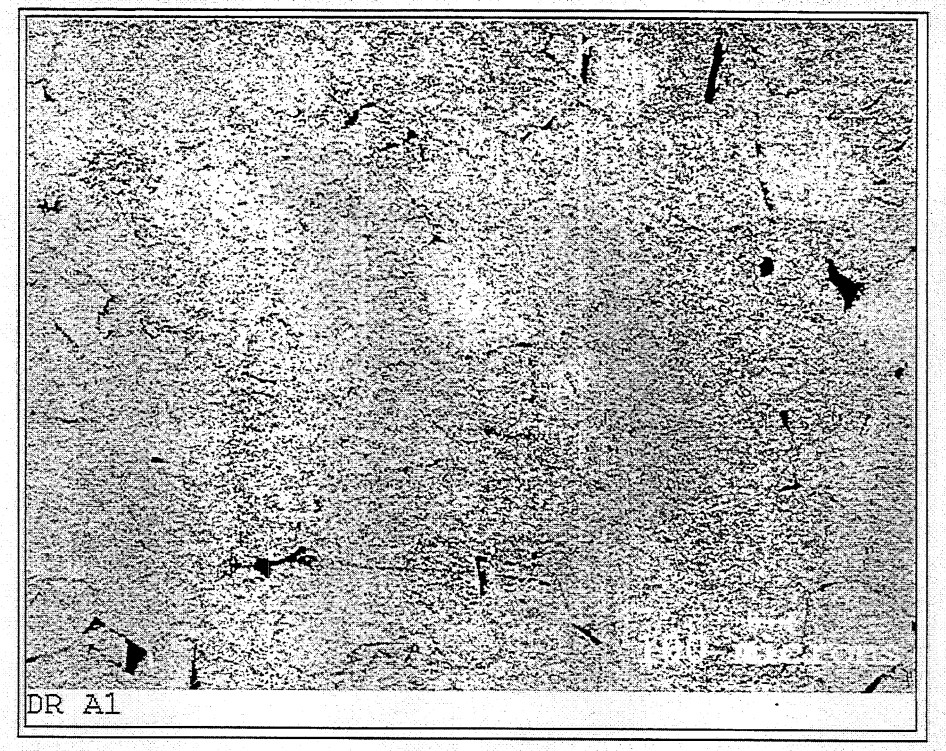

Figure 42. Marble D, 1 year on the test wall. BSE-image, 50x.

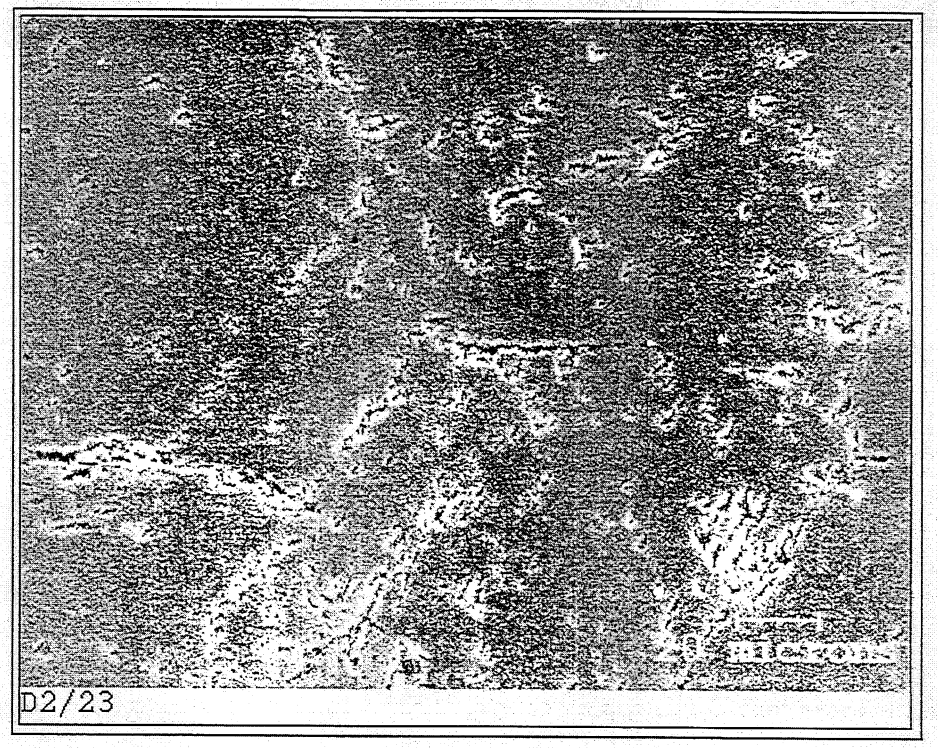

Figure 43. Marble D, unused. SE-image, 500x.

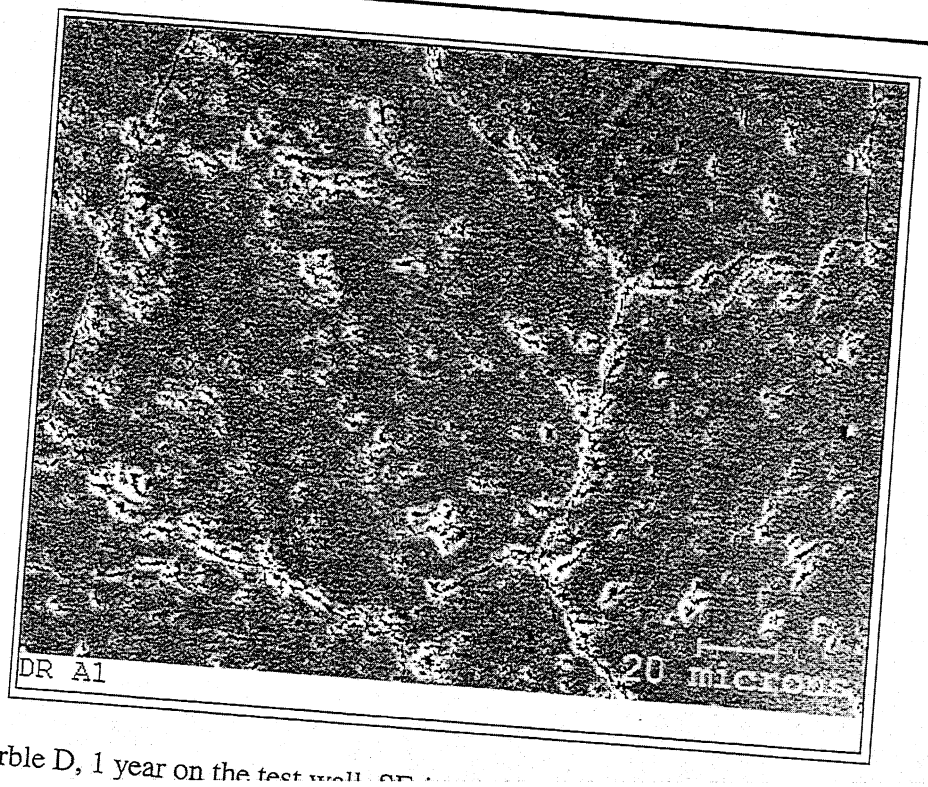

gure 44. Marble D, 1 year on the test wall, SE

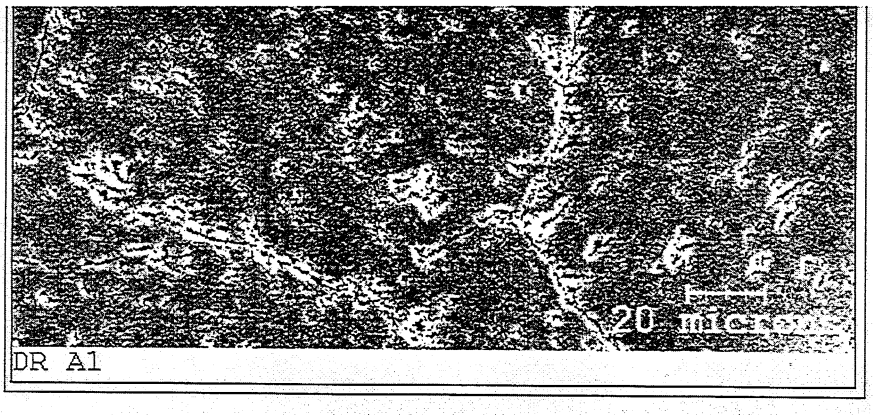

Figure 44. Marble D, 1 year on the test wall. SE-image, 500x.

BSE- and SE-images of marble E, both unused and after 1 year on the test wall, are shown in Figs. 45-48. Grain boundaries can only partly and even then very vaguely be distinguished. No changes could be seen in the structure of the marble after 1 year on the test wall.

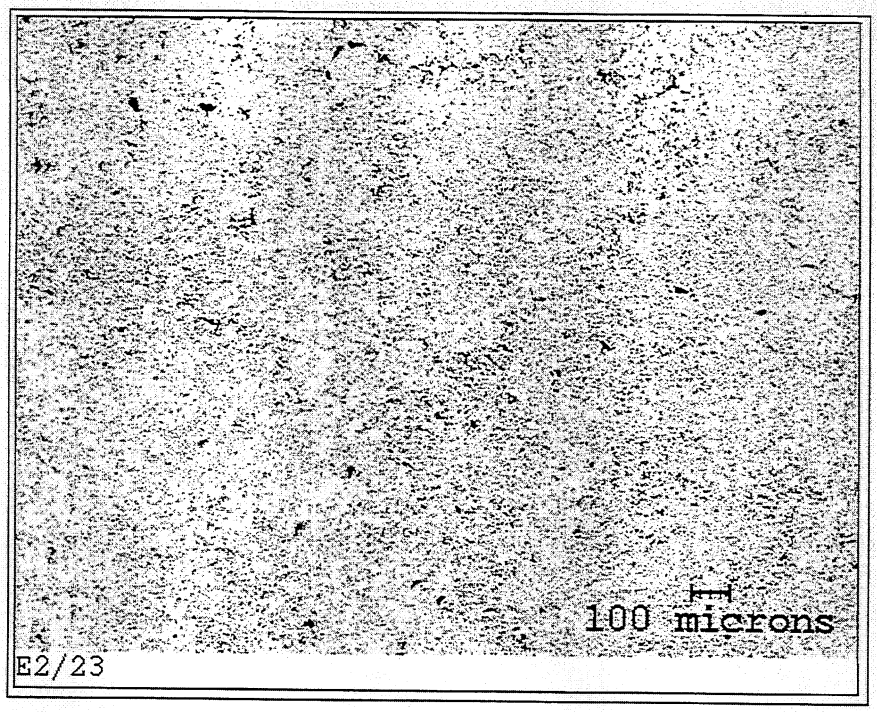

Figure 45. Marble E, unused. BSE-image, 50x.

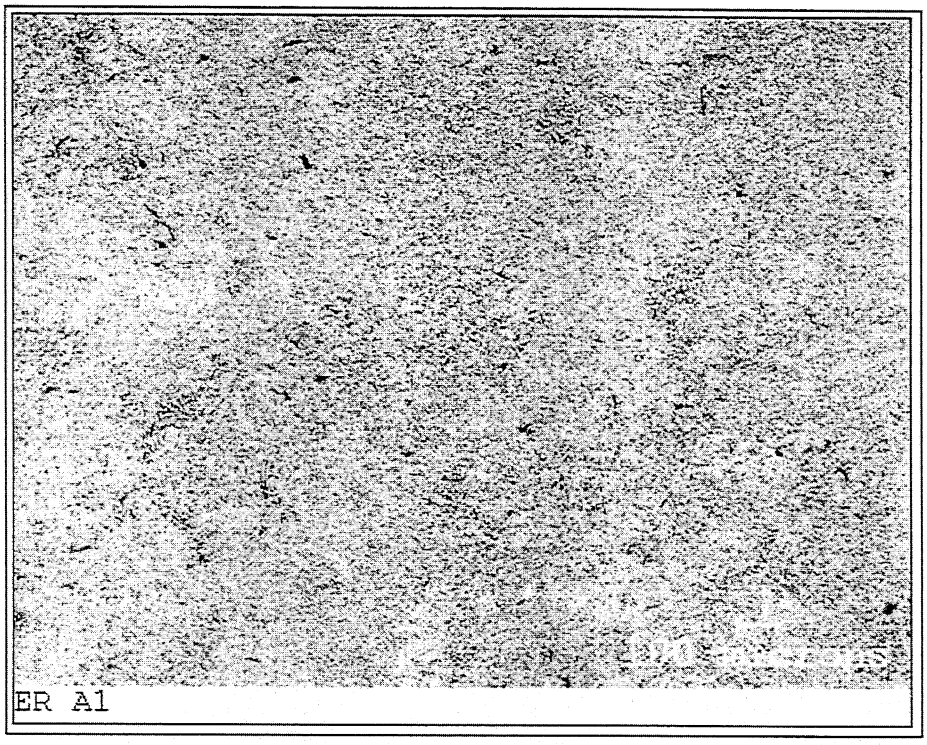

Figure 46. Marble E, 1 year on the test wall. BSE-image, 50x.

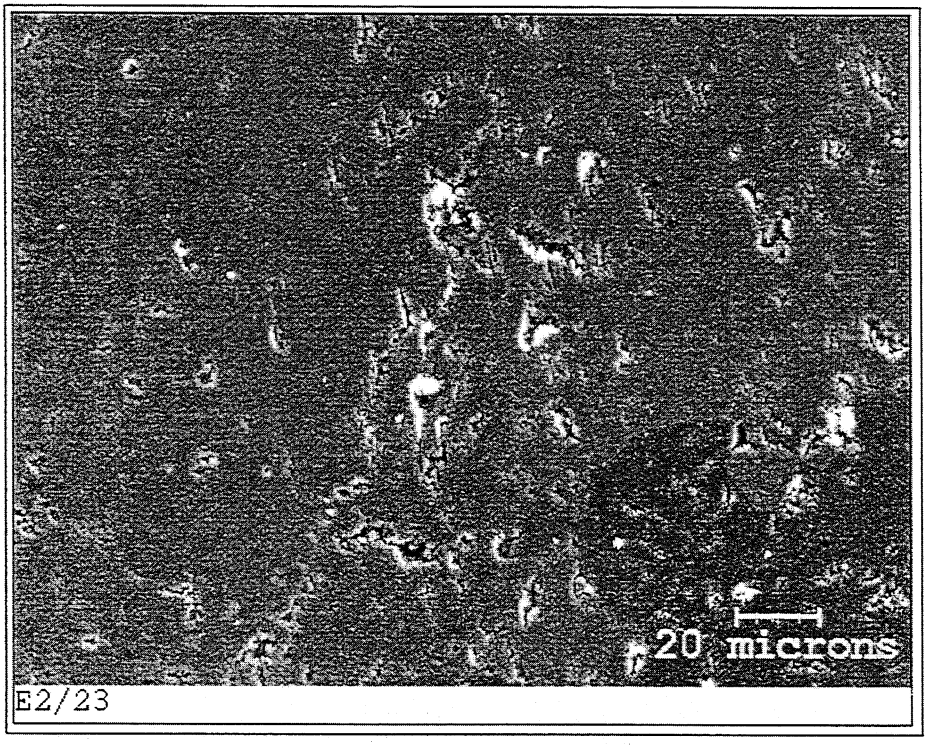

Figure 47. Marble E, unused. SE-image, 500x.

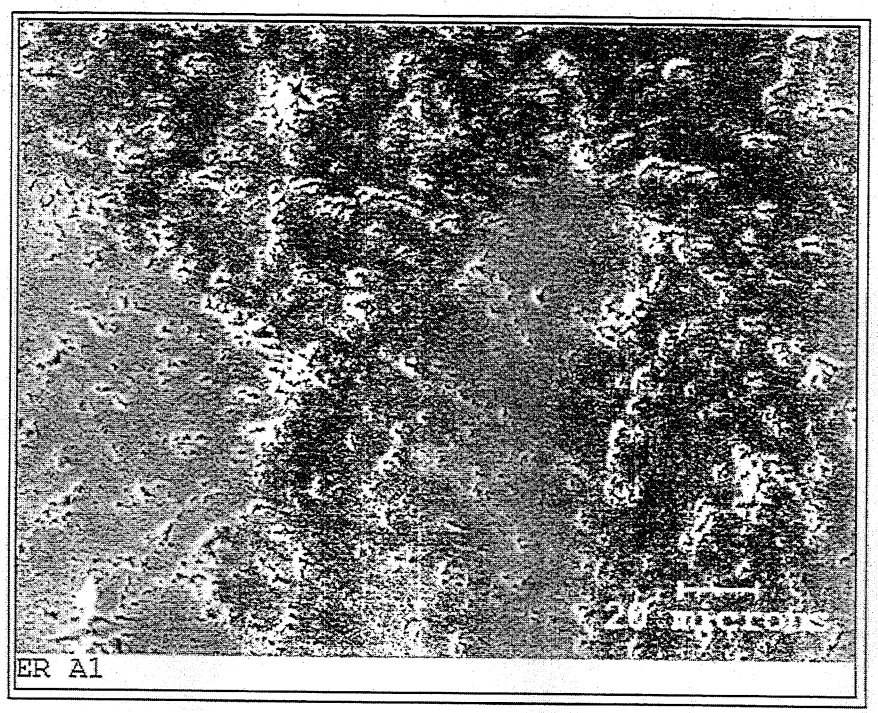

Figure 48. Marble E, 1 year on the test wall. SE-image, 500x.

BSE- and SE-images of marble K, both unused and after 1 year on the test wall, are shown in Figs. 49-52. Grain boundaries can only partly and even then very vaguely be distinguished. No changes could be seen in the structure of the marble after 1 year on the test wall.

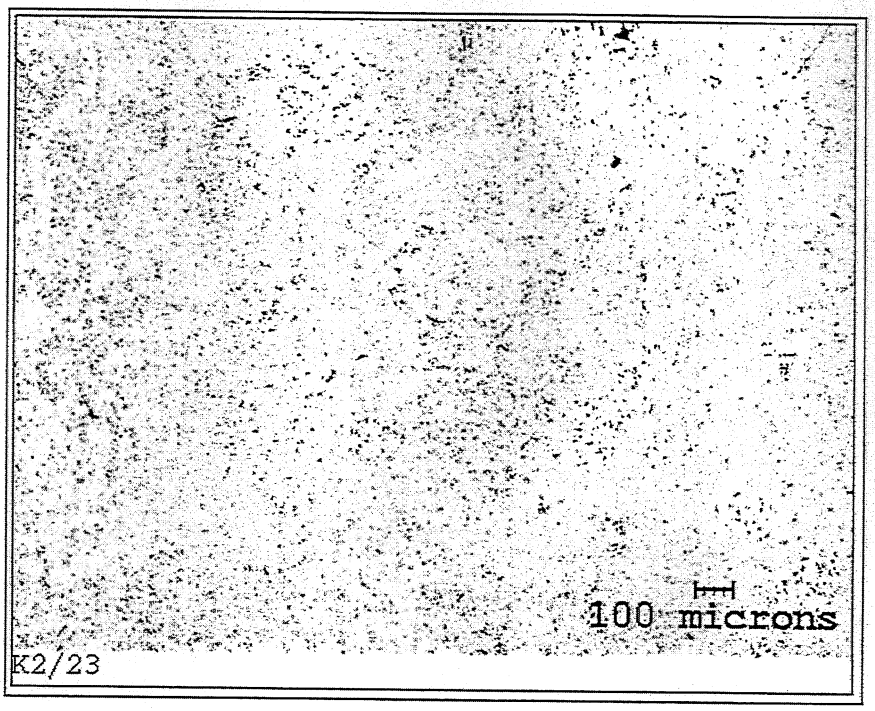

Figure 49. Marble K, unused. BSE-image, 50x.

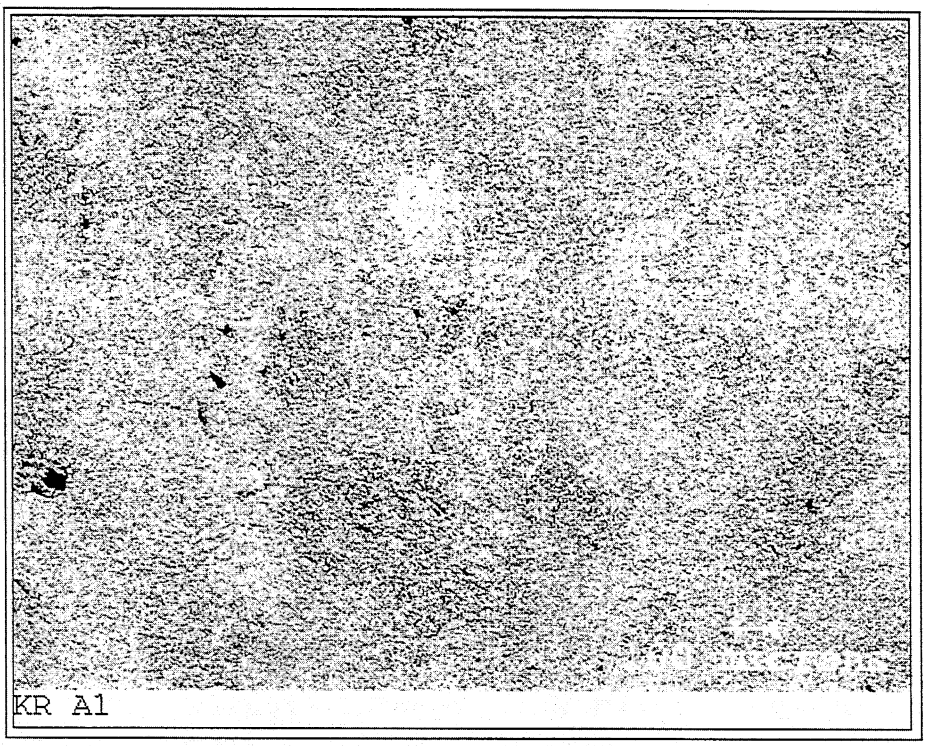

Figure 50. Marble K, 1 year on the test wall. BSE-image, 50x.

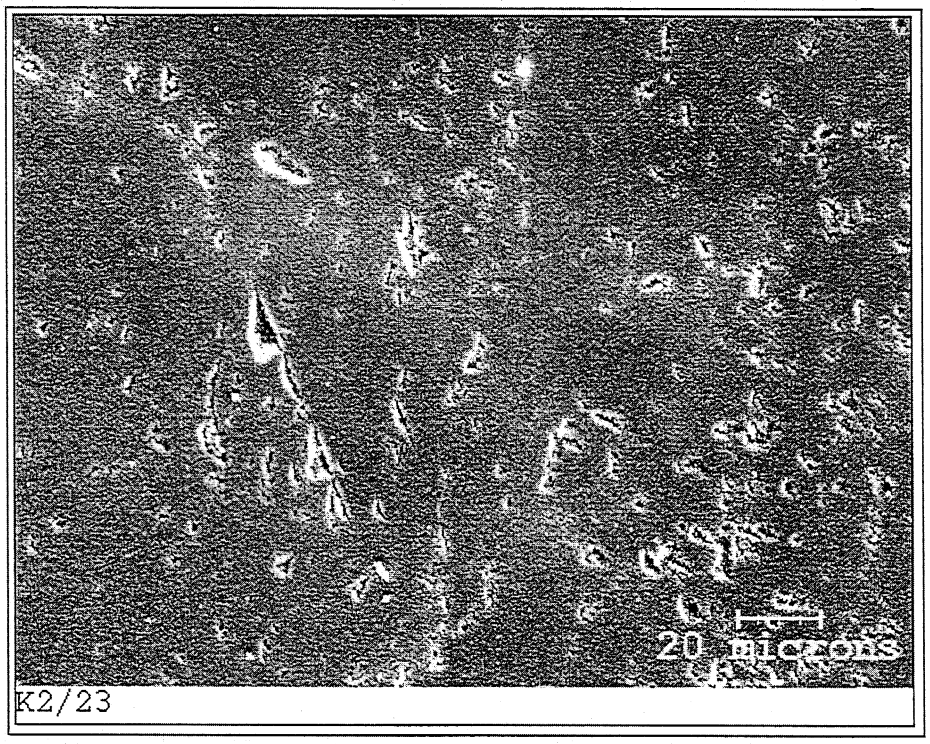

Figure 51. Marble K, unused. SE-image, 500x.

Figure 52. Marble K, 1 year on the test wall. SE-image, 500x.

SEM-pictures of fractured surfaces of marble A, both unused and after 1 and 1.5 years on the test wall, are shown in Figs. 53-58. The individual grains can at least partly be distinguished from each other. Narrow cracks can also be noticed between some of the grains. More and wider cracks were detected when the marble had been exposed to the environmental stresses on the test wall. The maximum crack width after 1.5 years on the test wall is around 0.6-0.7 µm.

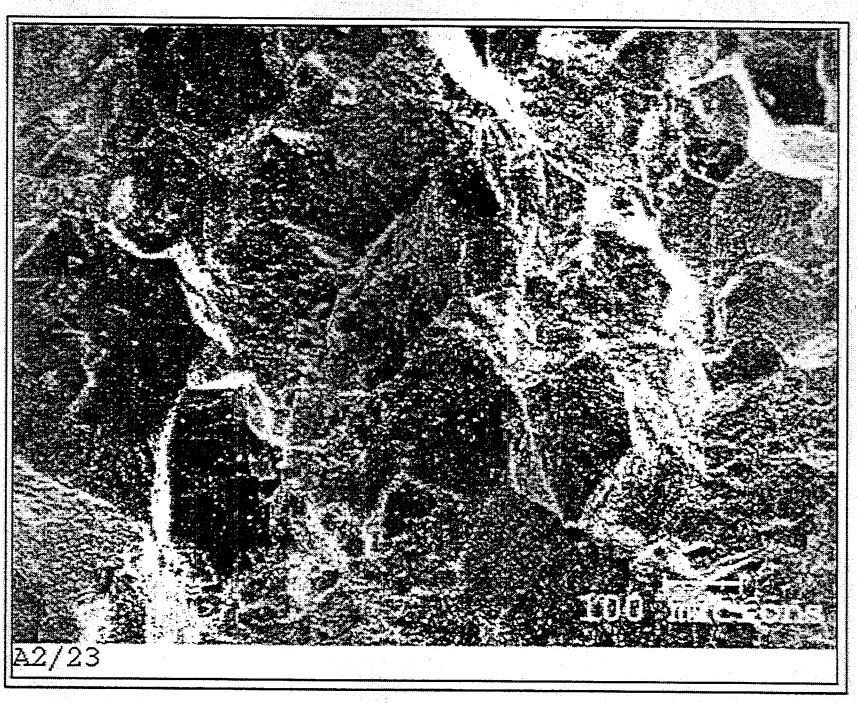

Figure 53. Marble A, unused. SE-image of fractured surface, 100x.

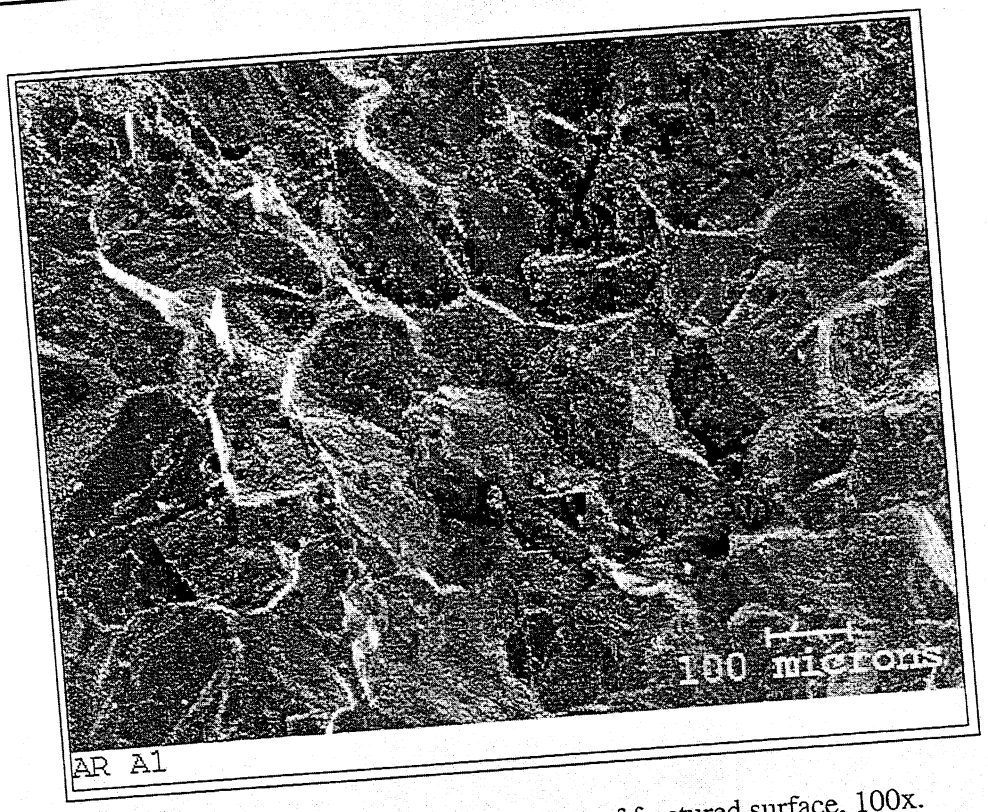

Figure 54. Marble A, 1 year on the test wall. SE-image of fractured surface, 100x.

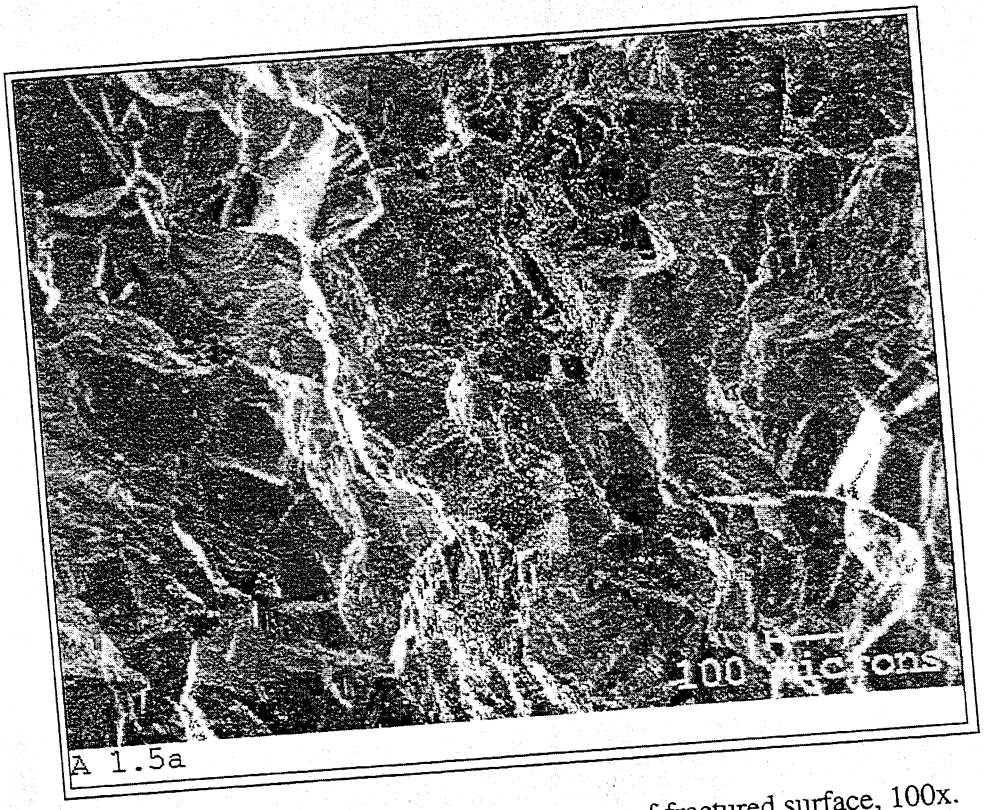

Figure 55. Marble A, 1.5 years on the test wall. SE-image of fractured surface, 100x.

A2/23

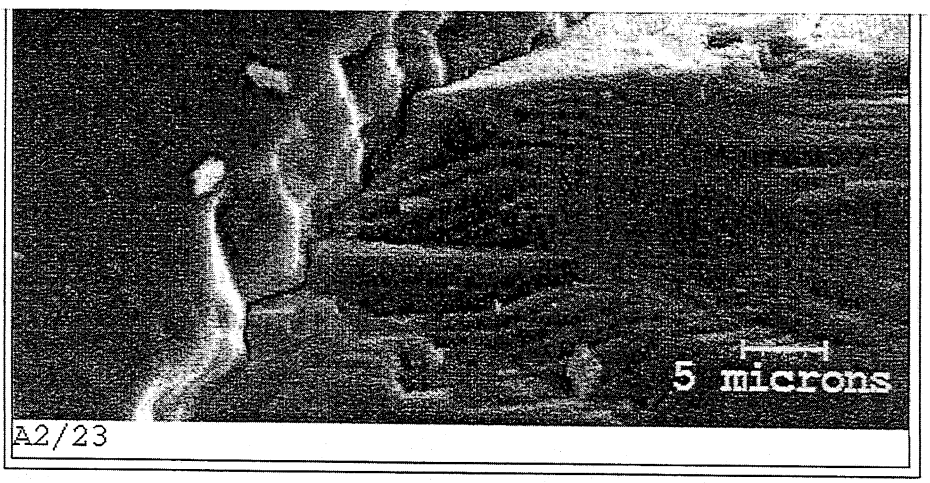

Figure 56. Marble A, unused. SE-image of fractured surface, 2500x.

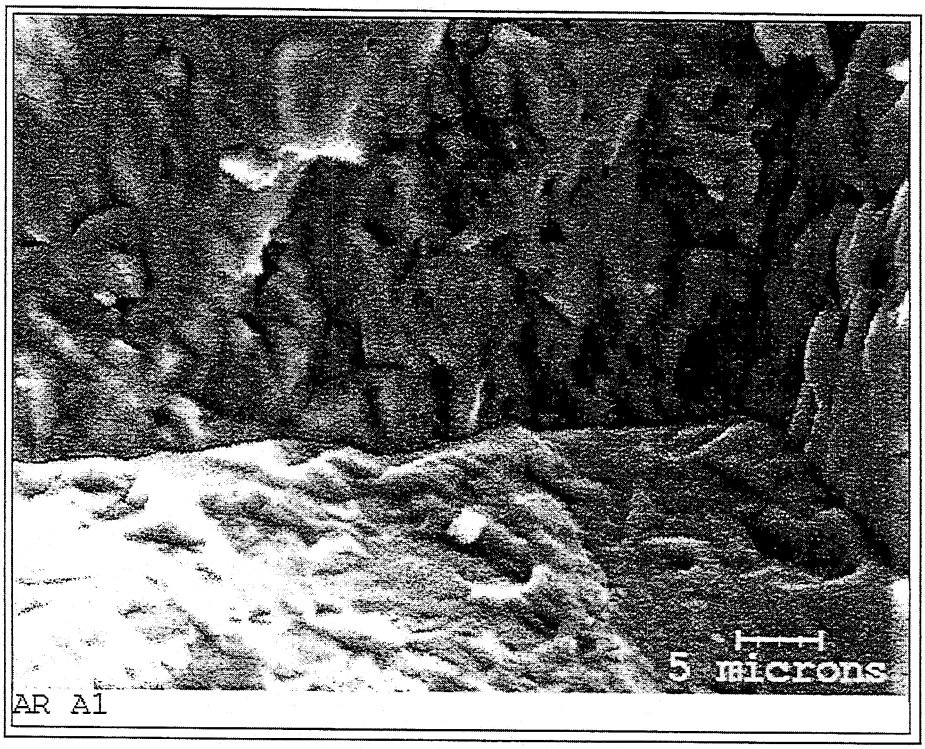

Figure 57. Marble A, 1 year on the test wall. SE-image of fractured surface, 2500x.

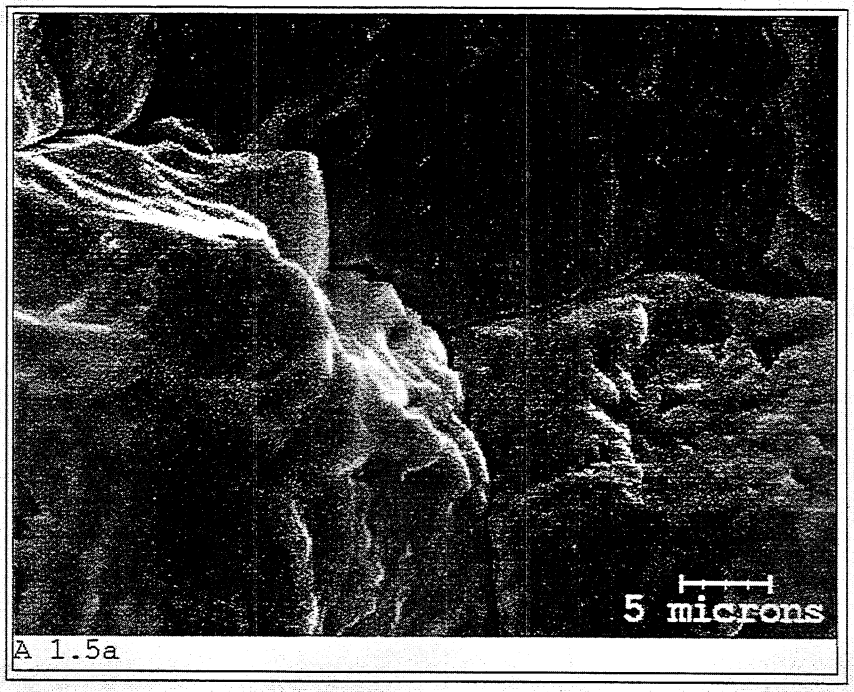

Figure 58. Marble A, 1.5 years on the test wall. SE-image of fractured surface, 2500x.

SEM-pictures of fractured surfaces of marble D, both unused and after 1 and 1.5 years on the test wall, are shown in Figs. 59-64. The individual grains can easily be distinguished from each other. Clear cracks can also be noticed between all the grains. These cracks were wider when the marble had been exposed to the environmental stresses on the test wall. The maximum crack width after 1.5 years on the test wall is around 1 µm.

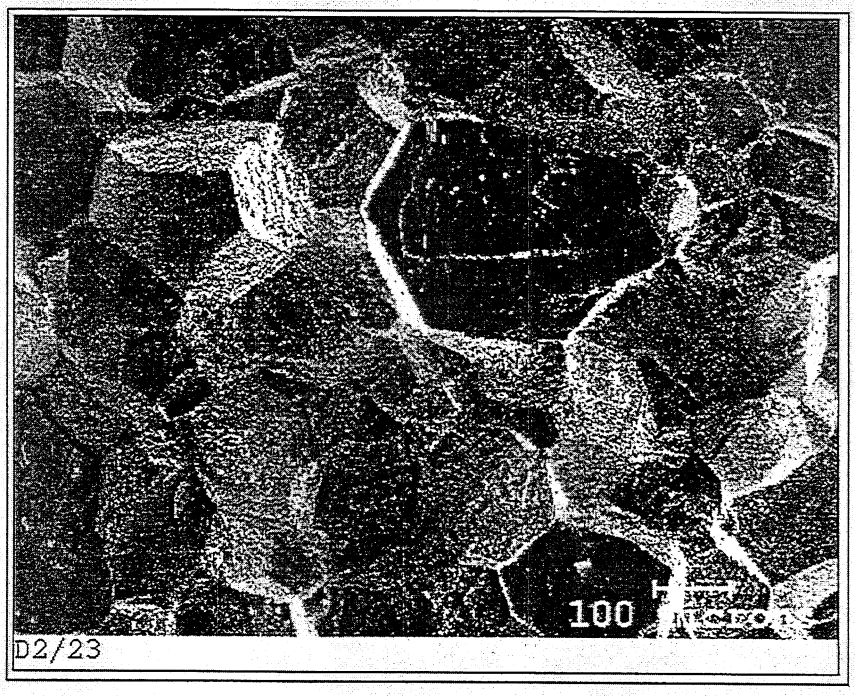

Figure 59. Marble D, unused. SE-image of fractured surface, 100x.

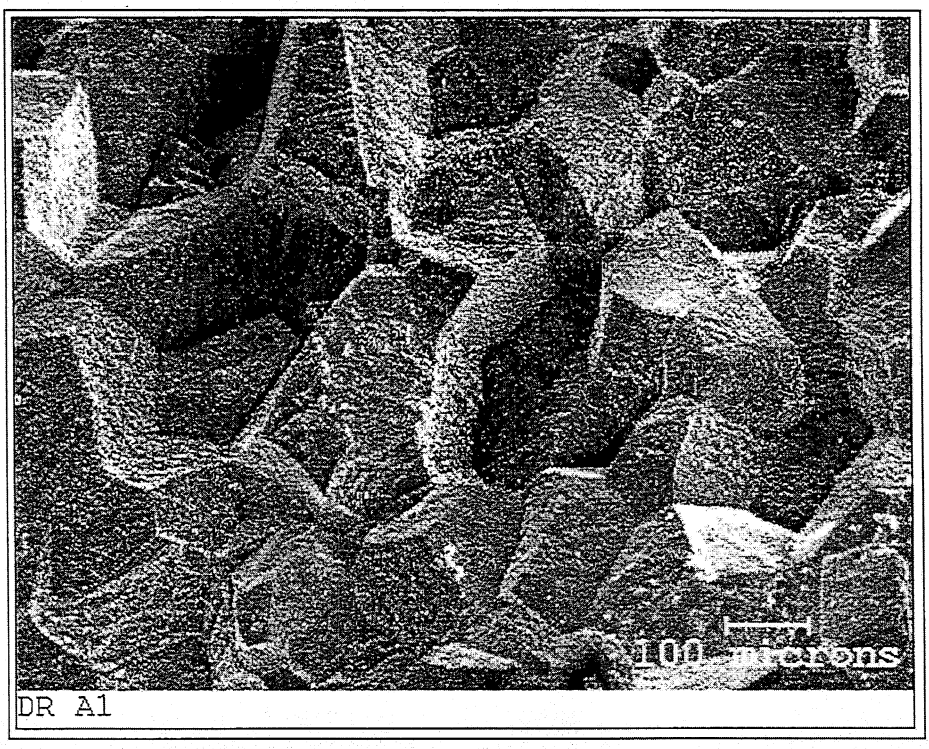

Figure 60. Marble D, 1 year on the test wall. SE-image of fractured surface, 100x.

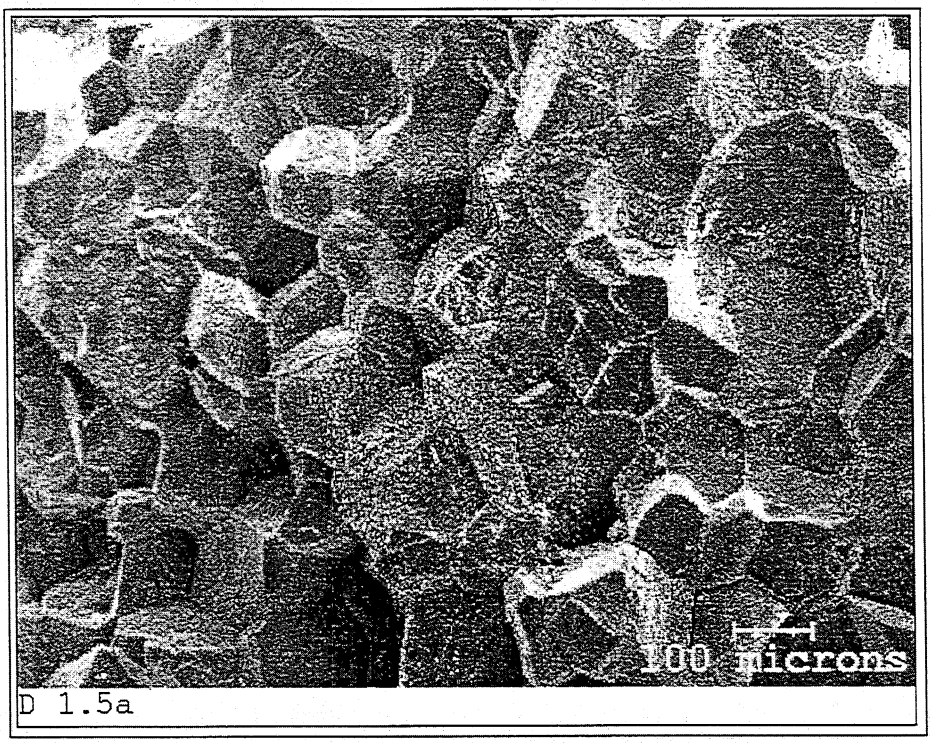

Figure 61. Marble D, 1.5 years on the test wall. SE-image of fractured surface, 100x.

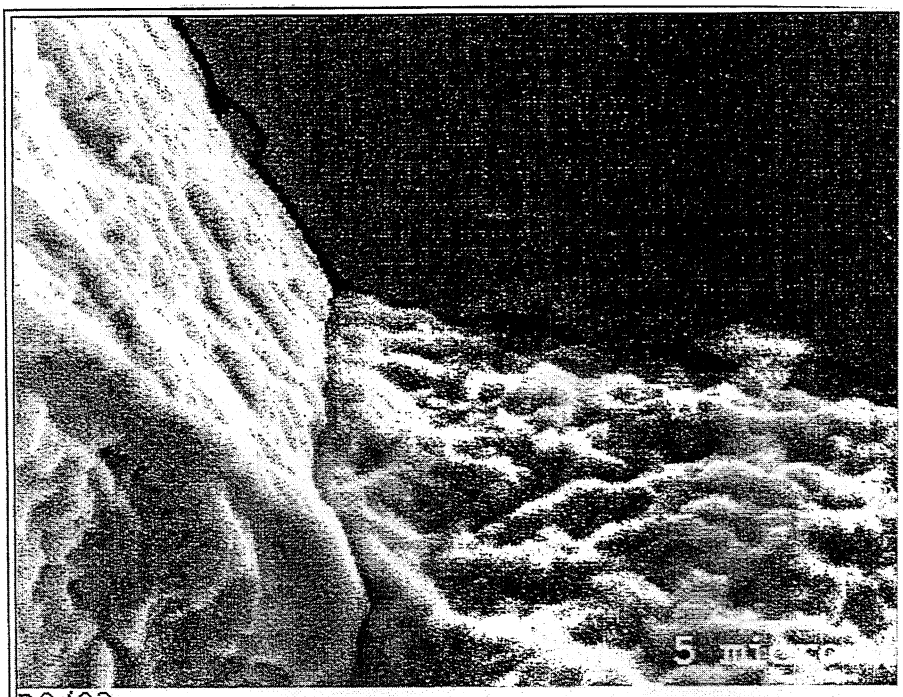

D2/23

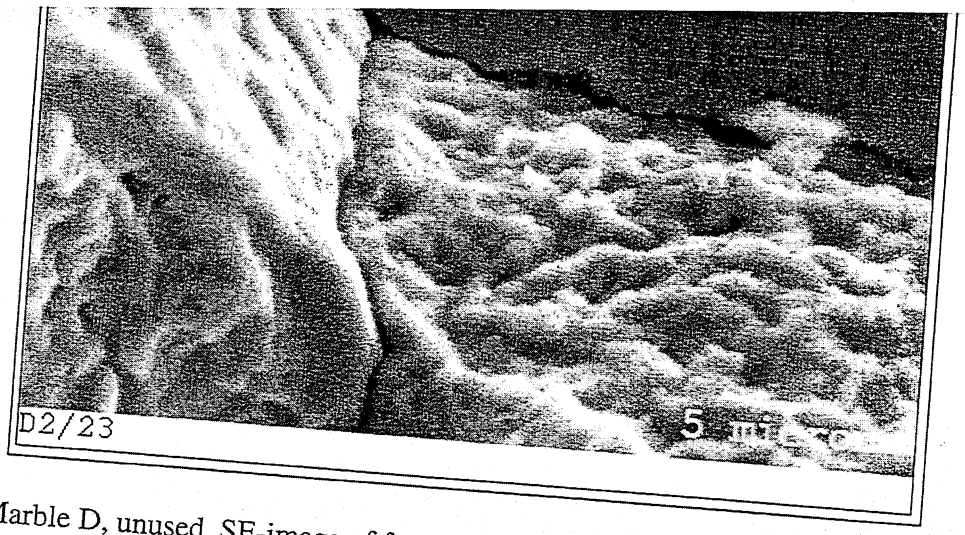

Figure 62. Marble D, unused. SE-image of fractured surface, 2500x.

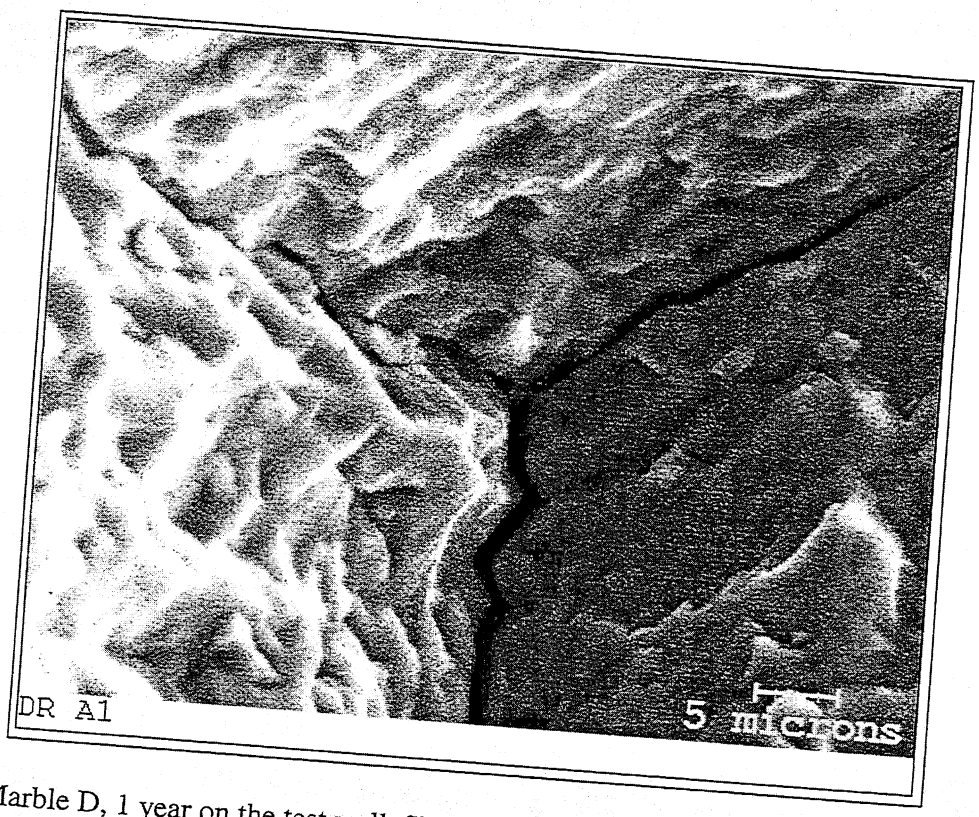

Figure 63. Marble D, 1 year on the test wall. SE-image of fractured surface, 2500x.

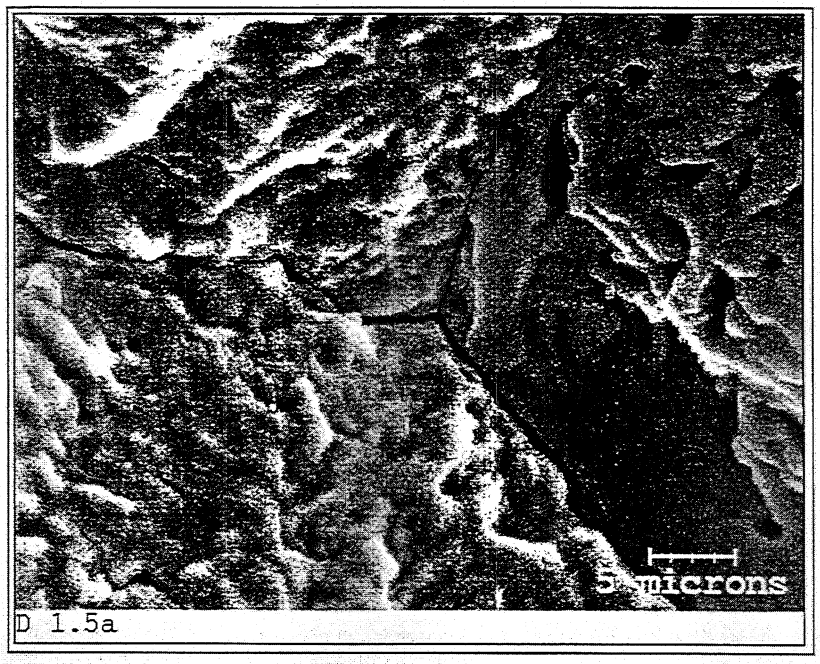

Figure 64. Marble D, 1.5 years on the test wall. SE-image of fractured surface, 2500x.

SEM-pictures of fractured surfaces of marble E, both unused and after 1 and 1.5 years on the test wall, are shown in Figs. 65-70. The grain boundaries can be seen only in some places. Thus, it is impossible to distinguish the grains from each other. Some very narrow cracks can be noticed between some of the grains. Some more and a little wider cracks were detected when the marble had been exposed to the environmental stresses on the test wall. The maximum crack width after 1.5 years on the test wall is around 0.3 µm.

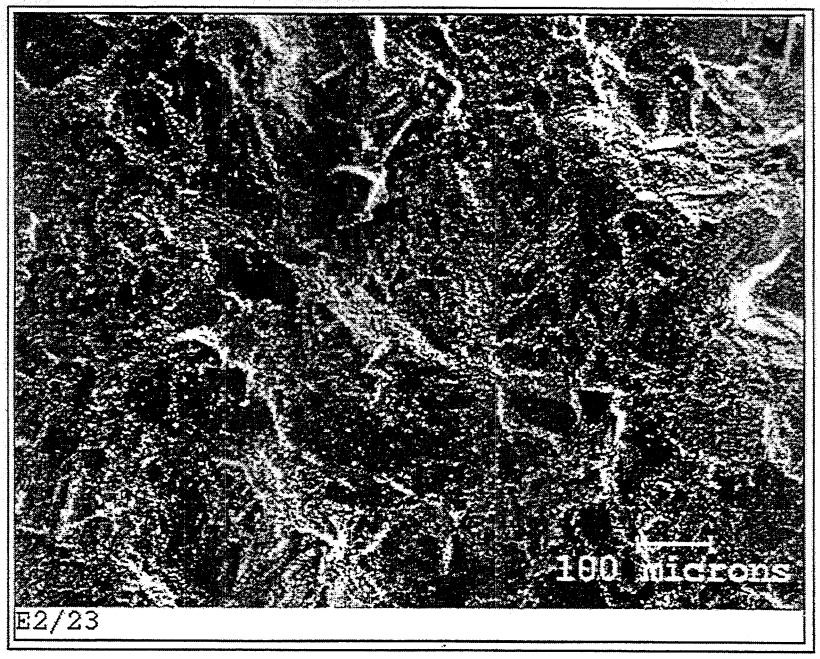

Figure 65. Marble E, unused. SE-image of fractured surface, 100x.

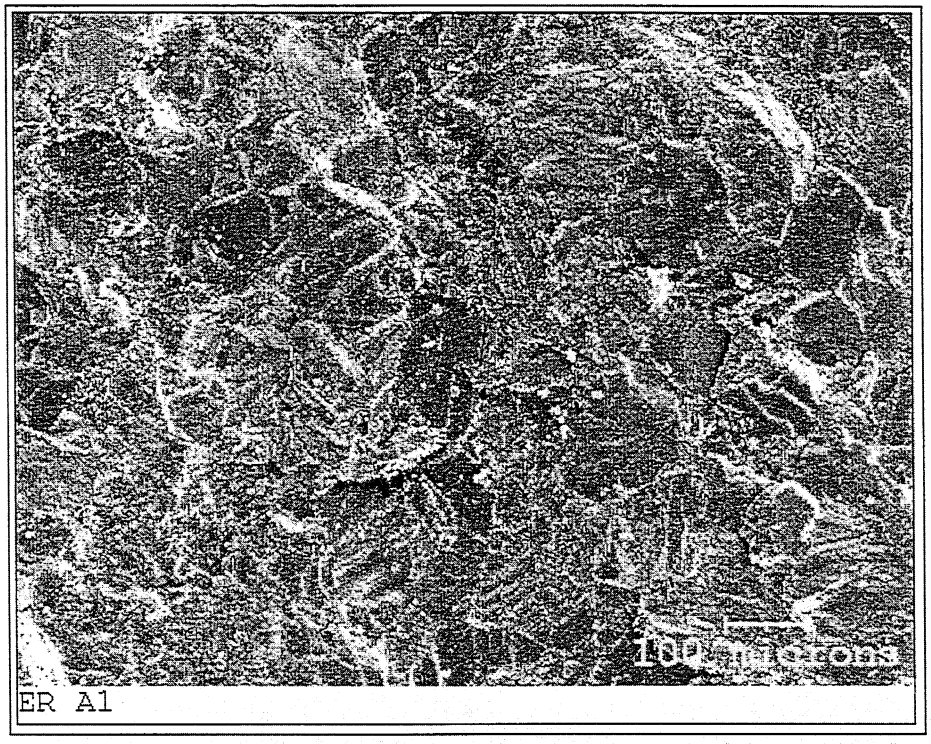

Figure 66. Marble E, 1 year on the test wall. SE-image of fractured surface, 100x.

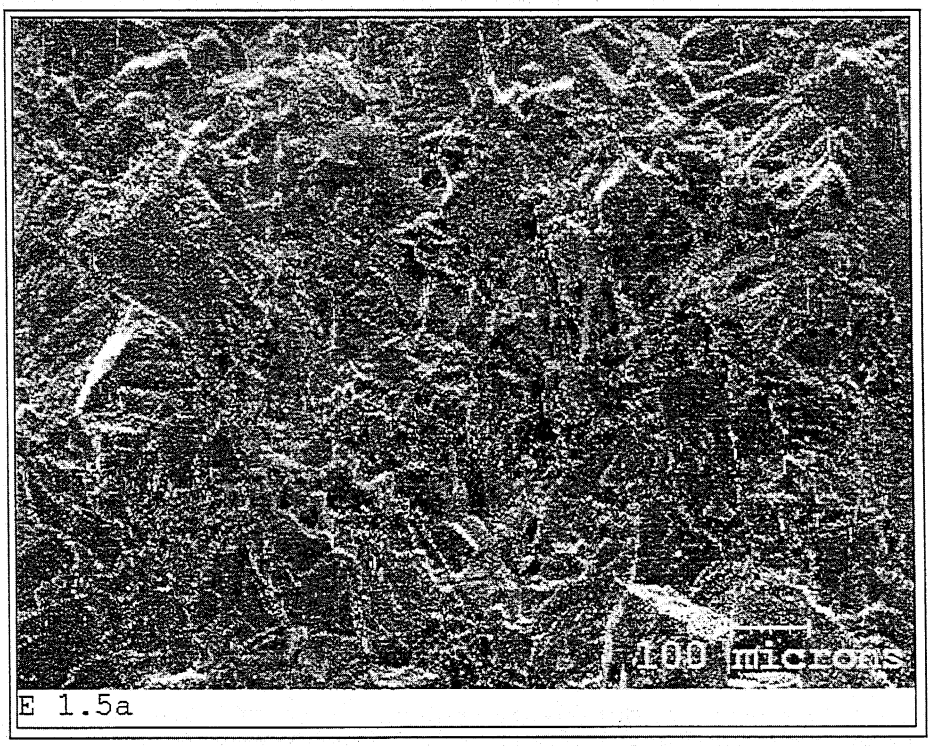

Figure 67. Marble E, 1.5 years on the test wall. SE-image of fractured surface, 100x.

E2/23

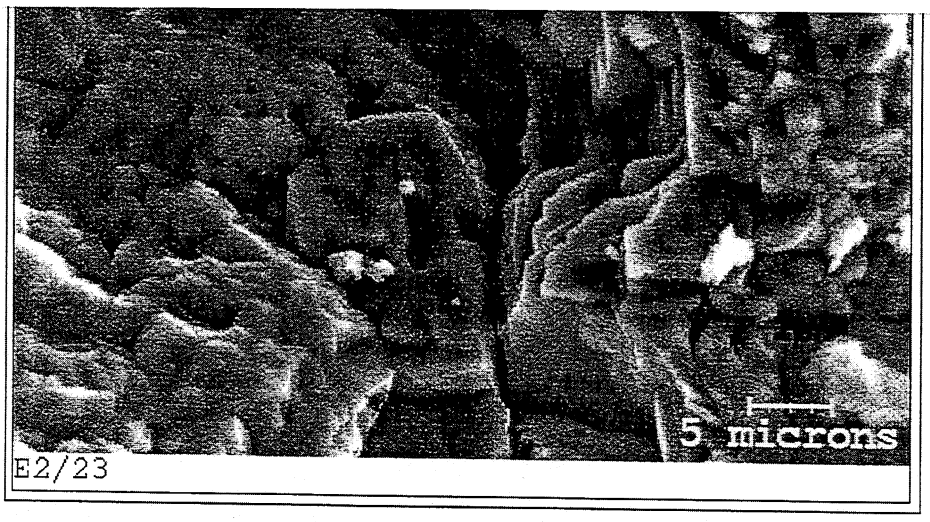

Figure 68. Marble E, unused. SE-image of fractured surface, 2500x.

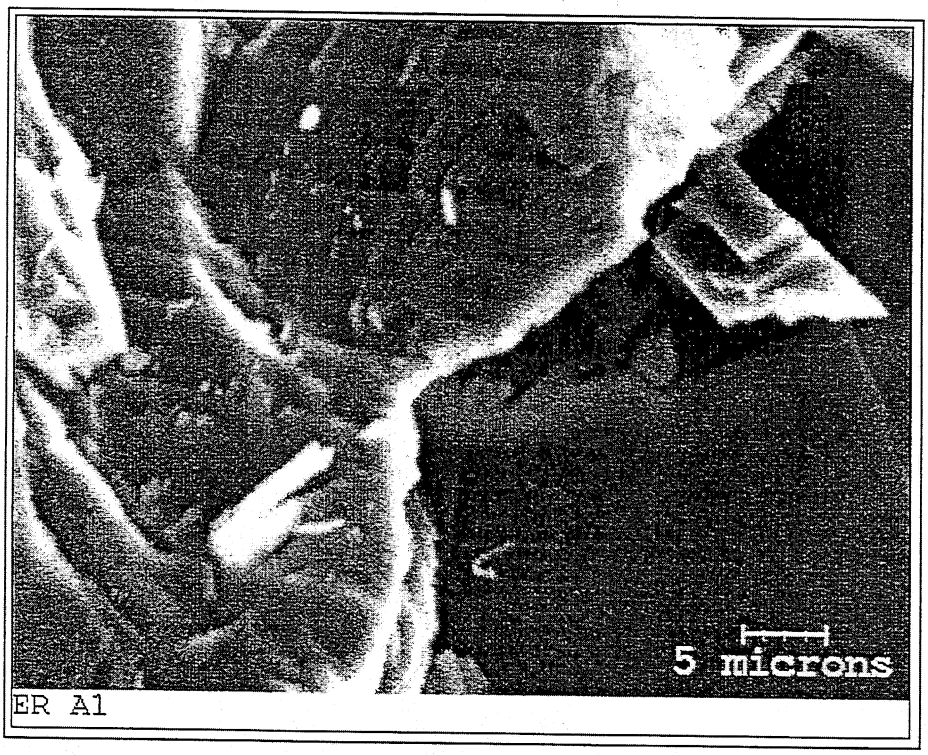

Figure 69. Marble E, 1 year on the test wall. SE-image of fractured surface, 2500x.

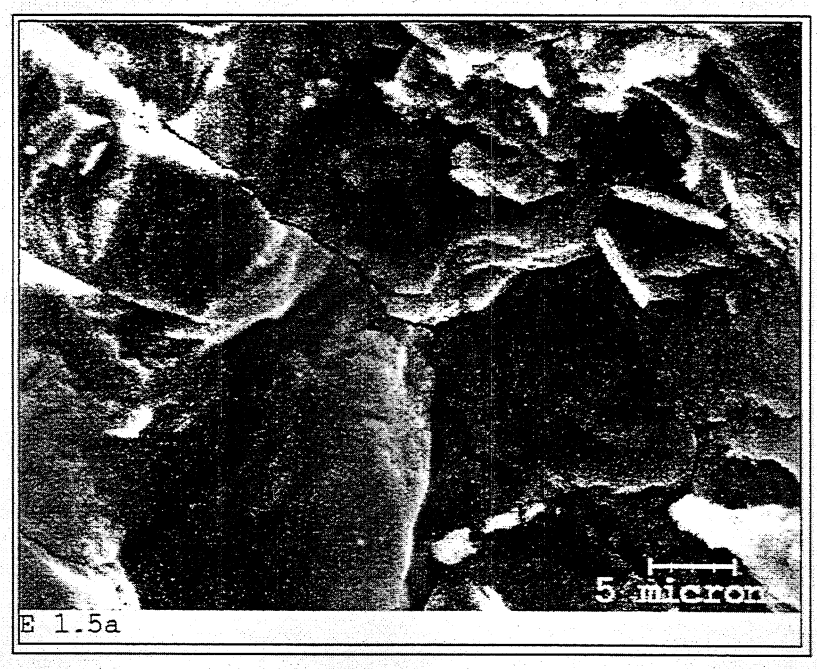

Figure 70. Marble E, 1.5 years on the test wall. SE-image of fractured surface, 2500x.

SEM-pictures of fractured surfaces of marble K, both unused and after 1 and 1.5 years on the test wall, are shown in Figs. 71-76. The grain boundaries can be seen only in some places. Thus, it is impossible to distinguish the grains from each other. Some very narrow cracks can be noticed between some of the grains. Some more and a little wider cracks were detected when the marble had been exposed to the environmental stresses on the test wall. The maximum crack width after 1.5 years on the test wall is around 0.3 µm.

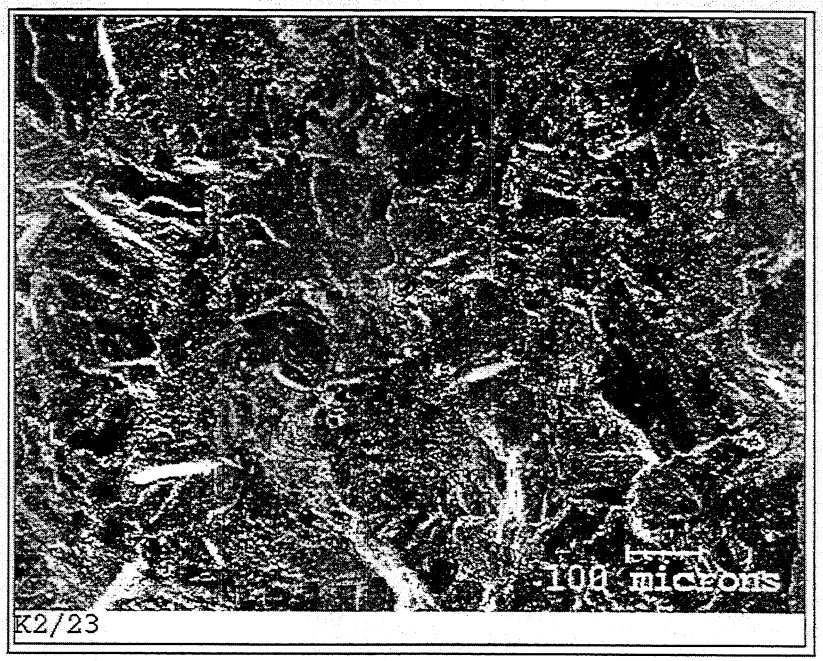

Figure 71. Marble K, unused. SE-image of fractured surface, 100x.

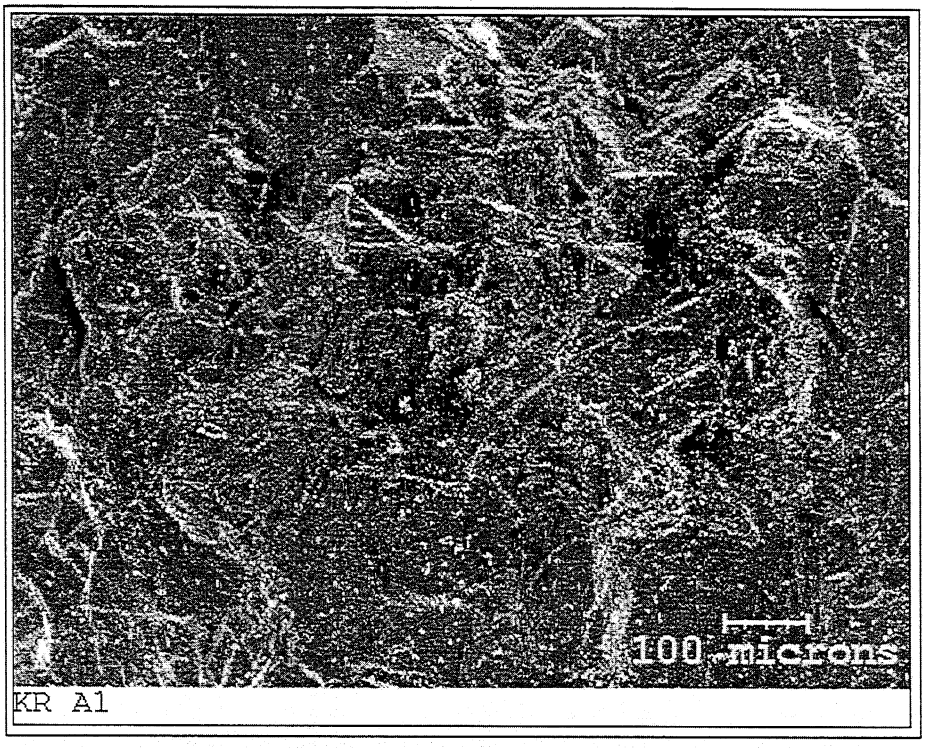

Figure 72. Marble K, 1 year on the test wall. SE-image of fractured surface, 100x.

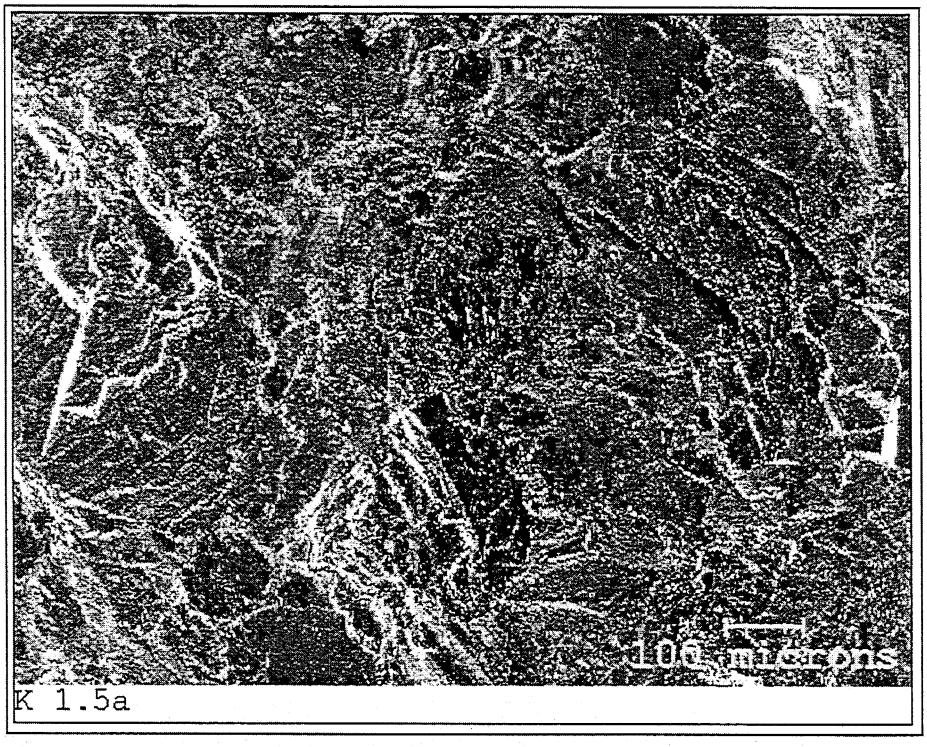

Figure 73. Marble K, 1.5 years on the test wall. SE-image of fractured surface, 100x.

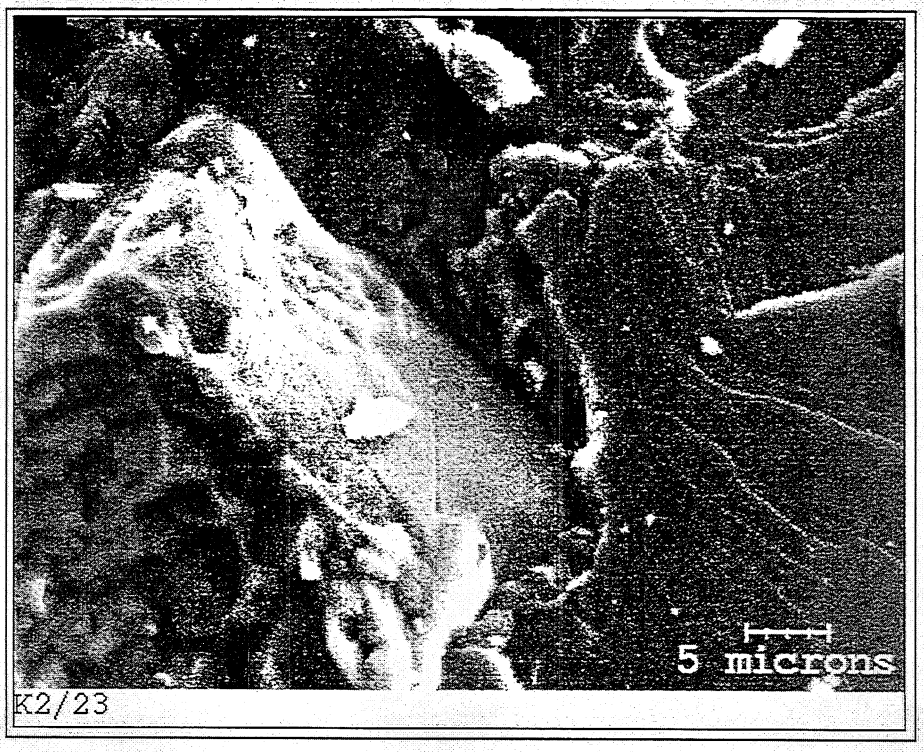

Figure 74. Marble K, unused. SE-image of fractured surface, 2500x.

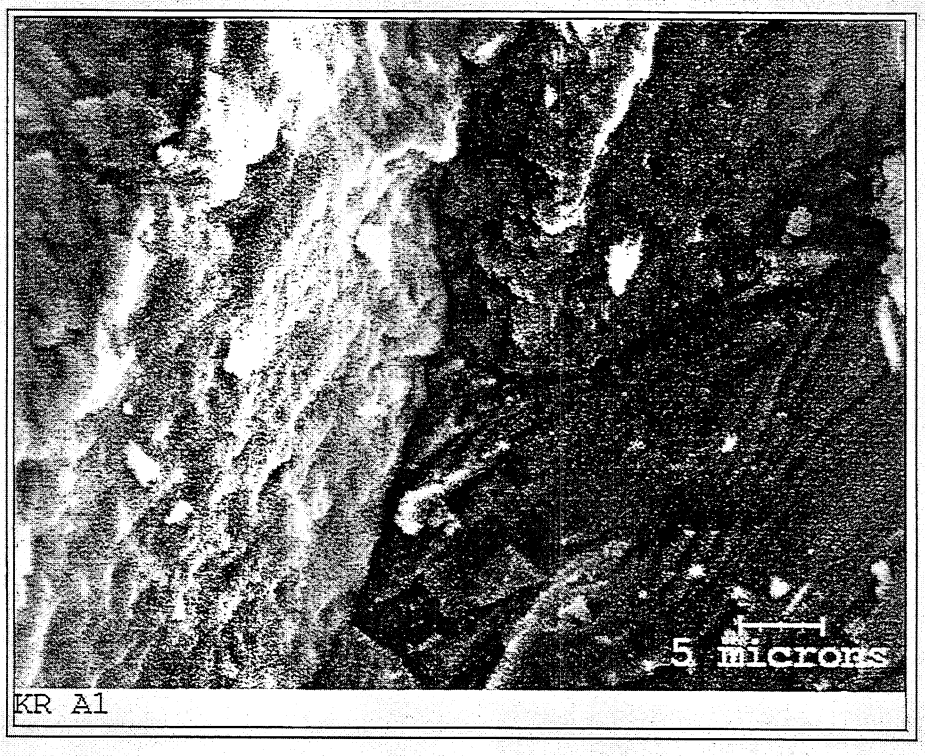

Figure 75. Marble K, 1 year on the test wall. SE-image of fractured surface, 2500x.

Figure 76. Marble K, 1.5 years on the test wall. SE-image of fractured surface, 2500x.

4.2 MARBLE CLAD ELEMENTS

4.2.1 Bond strength

The bond strengths of marbles of the marble clad elements in initial stage and after 1 and 1.5 years on the test wall at Finlandia Hall are presented in Table 12 and in Fig. 77. The presented results are average values (av.) and standard deviations (s.d.) calculated from the testing data of individual specimens. The measurement results are shown in detail in Appendix 3.

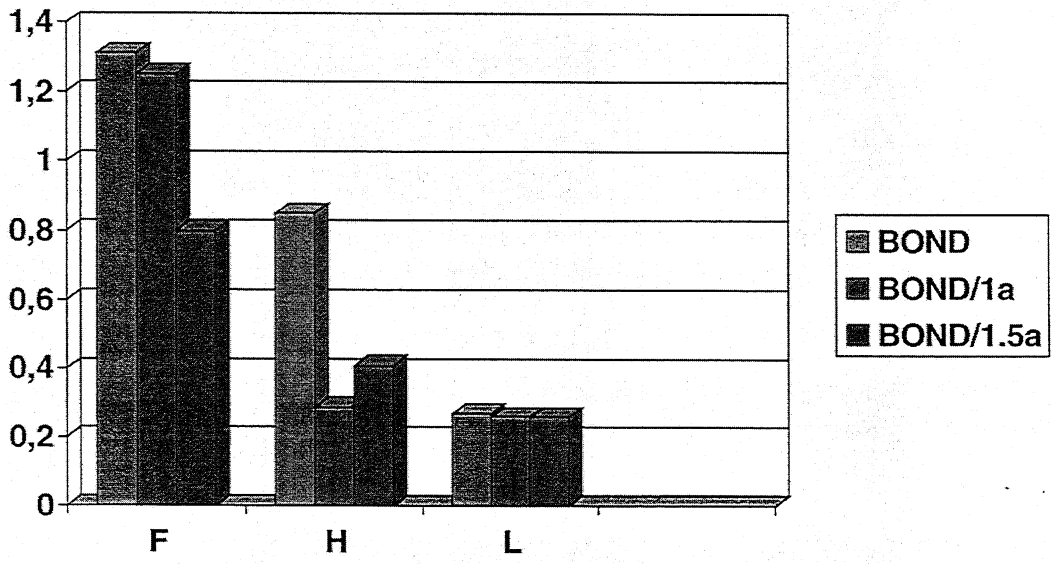

Figure 77. Bond strength of marble in marble clad elements (MPa).

Table 12. Bond strength of marble in marble clad elements.

	bond strength element F MPa	element H MPa	element L MPa
unused			
av.	1.31	0.85	0.27
s.d.	0.26	0.12	0.05
s.d. (%)	19.9	14.1	18.5
test wall / 1 year			
av.	1.25	0.29	0.26
s.d.	0.34	0.09	0.12
s.d. (%)	27.2	31.0	46.2
test wall / 1.5 years			
av.	0.80	0.41	0.26
s.d.	0.21	0.15	0.06
s.d. (%)	26.3	36.6	23.1

The relative changes of the bond strength that have taken place on the test wall are presented in Table 13. The basis of the comparison is in all cases the bond strength in the unused elements.

Table 13. The relative changes of the bond strengths of marble in the marble clad elements on the test wall.

element type	change of bond strength 1 year %	1.5 years %
F	-5	-39
H	-66	-52
L	-4	-4

In the element type F the breaking point was usually the interface between marble and concrete. Only in a couple of cases the loosening took place, at least partly, deeper inside concrete.

In the unused element of type H the breaking point was either the interface between marble and the rest of the structure (1/3) or the interface between the glass fiber sheet and the aluminium honey comb structure (2/3). In the elements of type H that had been on the test wall the breaking point was, however, always the interface between marble and the rest of the structure.

In the element type L the breaking point was always the interface between marble and the rest of the structure. Thus, the loosening of marble took place from the top of the glue layer.

4.2.2 Microstructure

Photographs of the microstructure of marble clad element F, unused and after 1.5 years on the test wall, are shown in Figs. 78-81. Following observations were made:

- contact between marble and concrete tight and cohesive
- a thin layer of third material, probably primer, between marble and concrete
- material (primer) layer rather continuous, though pores are common; thickness of the layer generally 20-30 µm, in places even 60 µm
- in the unused element only a few very tiny cracks along the marble/concrete contact zone
- in the element stressed for 1.5 years on the test wall some slight and narrow cracking at the marble/concrete contact zone

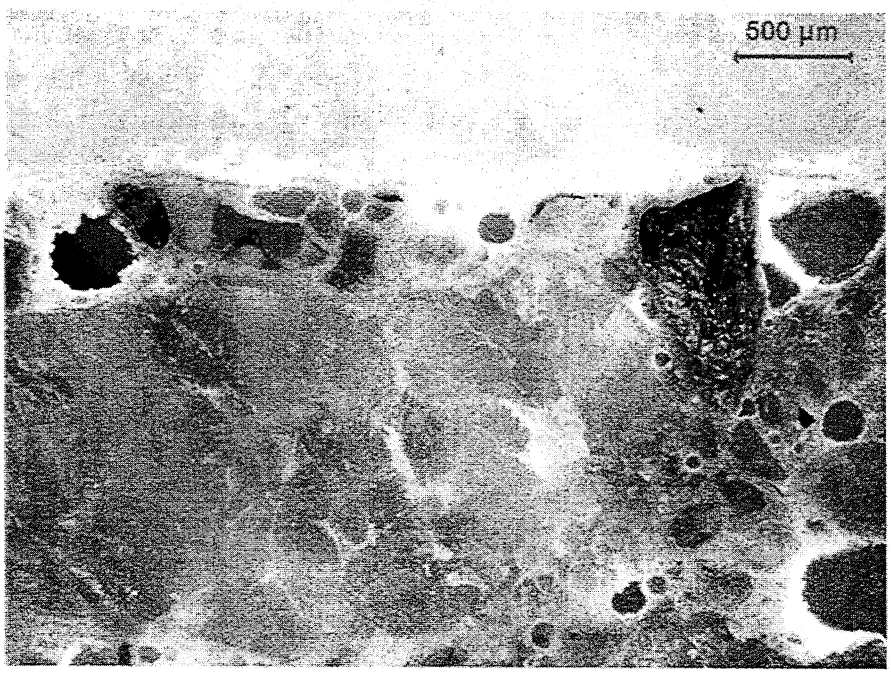

Figure 78. Microstructure of marble clad element F. Unused. Objective 2.5x, oblique illumination.

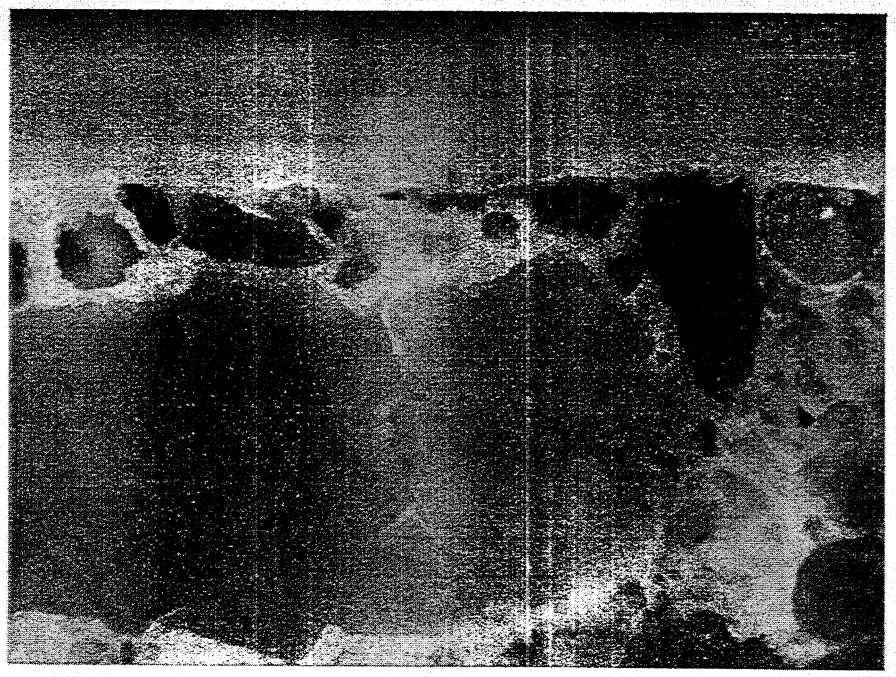

Figure 79. Microstructure of marble clad element F. Unused. Objective 2.5x, fluorescent light.

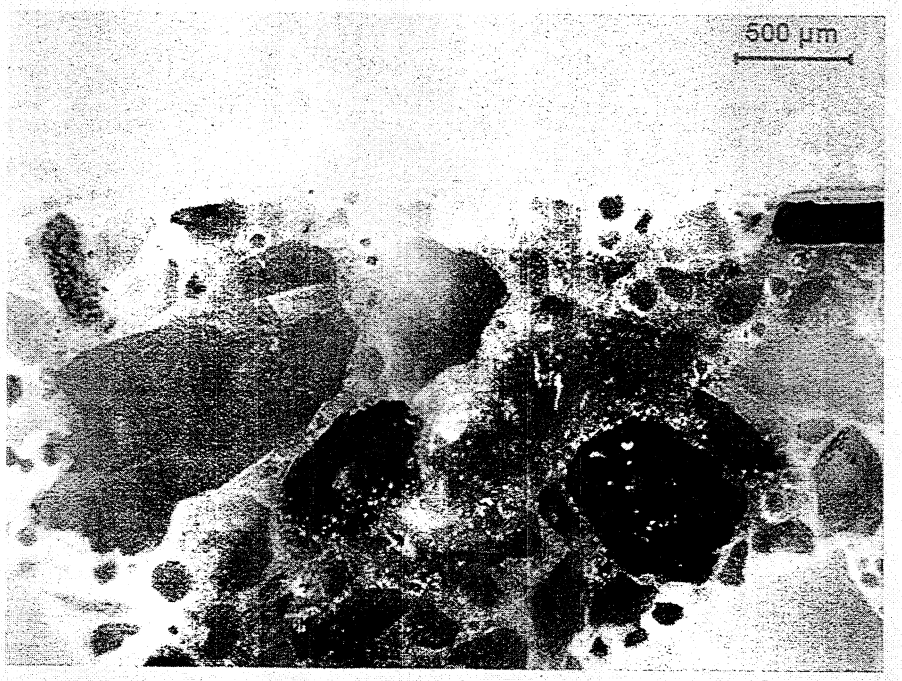

Figure 80. Microstructure of marble clad element F. 1.5 years on the test wall. Objective 2.5x, oblique illumination.

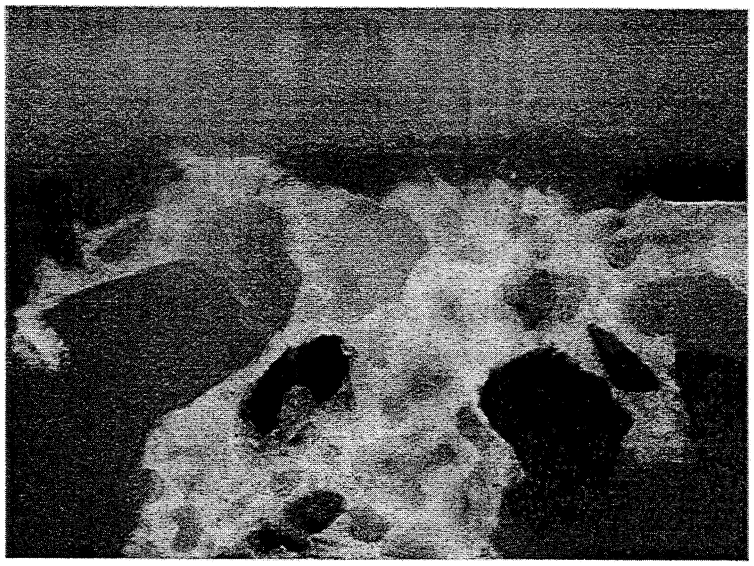

Figure 81. Microstructure of marble clad element F. 1.5 years on the test wall. Objective 2.5x, fluorescent light.

Photographs of the microstructure of marble clad element H, unused and after 1.5 years on the test wall, are shown in Figs. 82-85. Following observations were made:

- a layer of glue between marble and metal structure, thickness of the layer approximately 1 mm
- structure of the unused element partly cracked along the contact zone marble/glue
- in the unused element the upper half of the glue layer tinted yellowish
- in the element stressed for 1.5 years on the test wall the upper half of the glue layer tinted brownish
- in the element stressed for 1.5 years on the test wall open crack on about 60% of the contact zone marble/glue

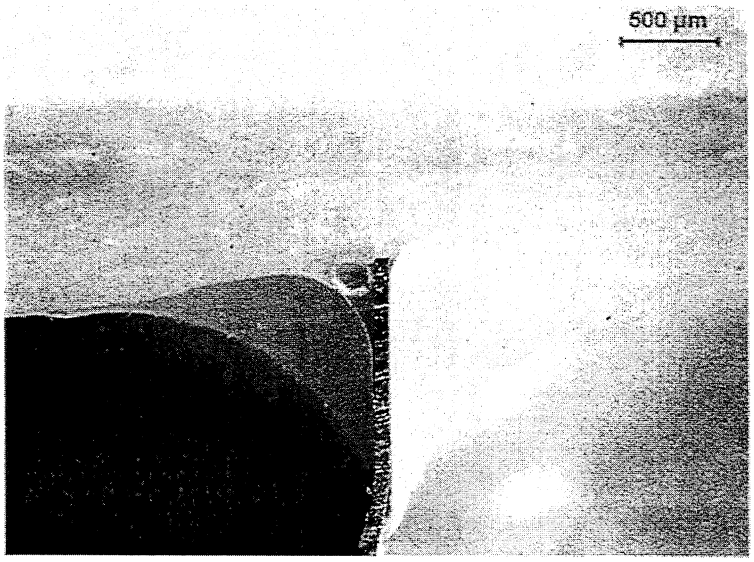

Figure 82. Microstructure of marble clad element H. Unused. Objective 2.5x, oblique illumination.

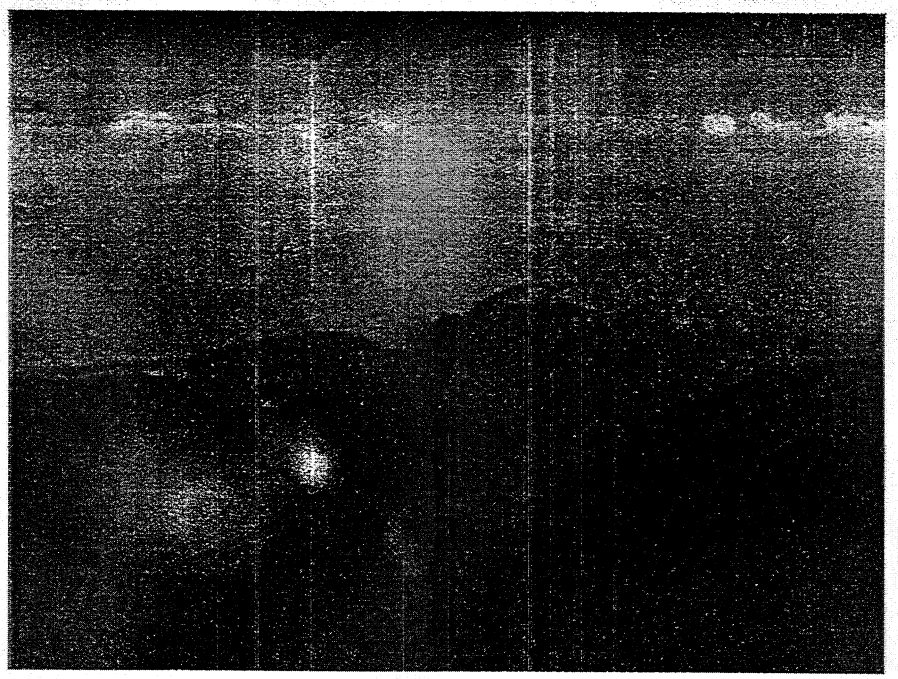

Figure 83. Microstructure of marble clad element H. Unused. Objective 2.5x, fluorescent light.

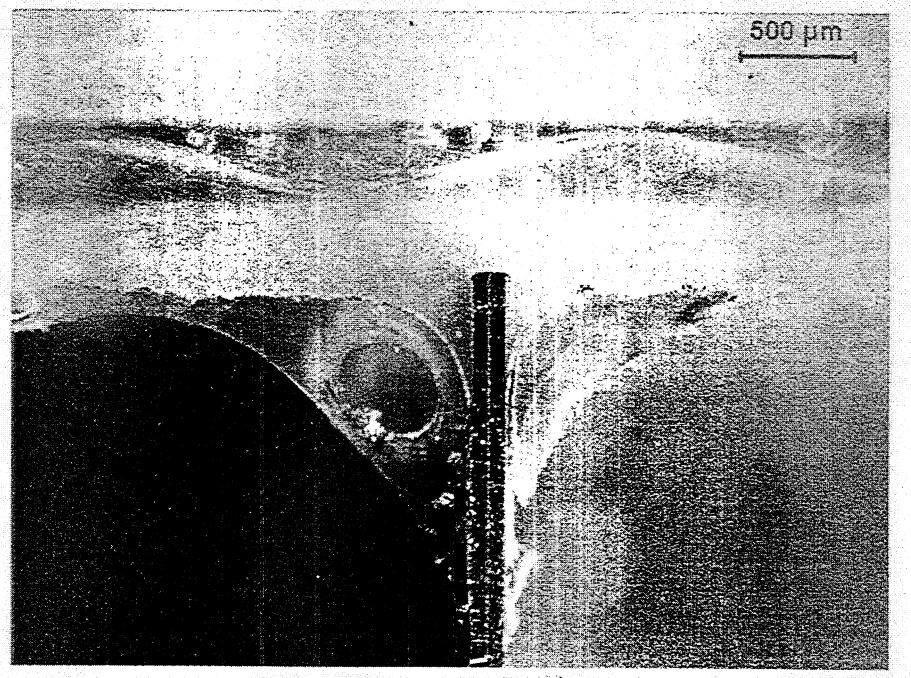

Figure 84. Microstructure of marble clad element H. 1.5 years on the test wall. Objective 2.5x, oblique illumination.

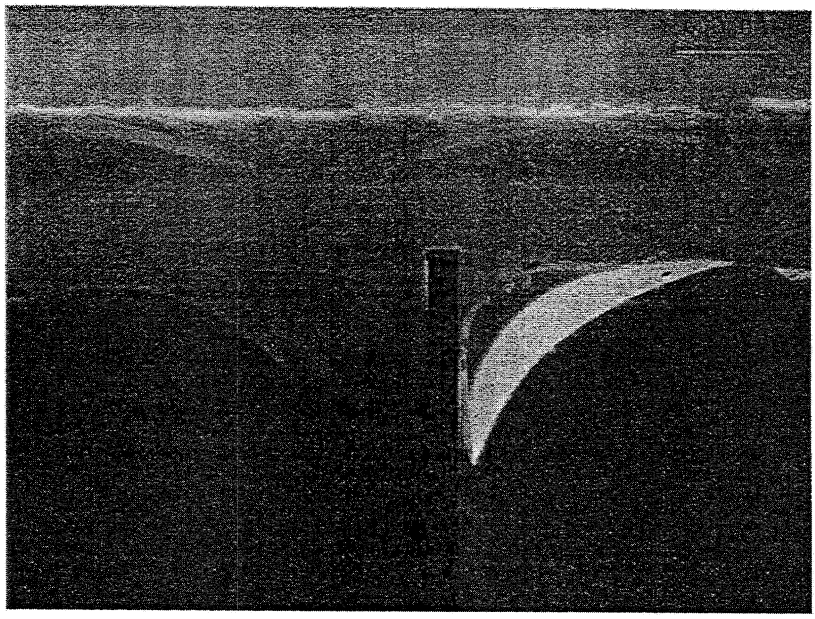

Figure 85. Microstructure of marble clad element H. 1.5 years on the test wall. Objective 2.5x, fluorescent light.

Photographs of the microstructure of marble clad element L, unused and after 1.5 years on the test wall, are shown in Figs. 86-89. Following observations were made:

- a layer of glue between marble and metal structure, thickness of the layer approximately 0.5 mm
- the glue contains a lot of porosity
- in the unused element the glue layer partly detached from marble
- in the element stressed for 1.5 years on the test wall the glue layer rather tightly attached to marble, only minor cracking in some parts of the contact zone

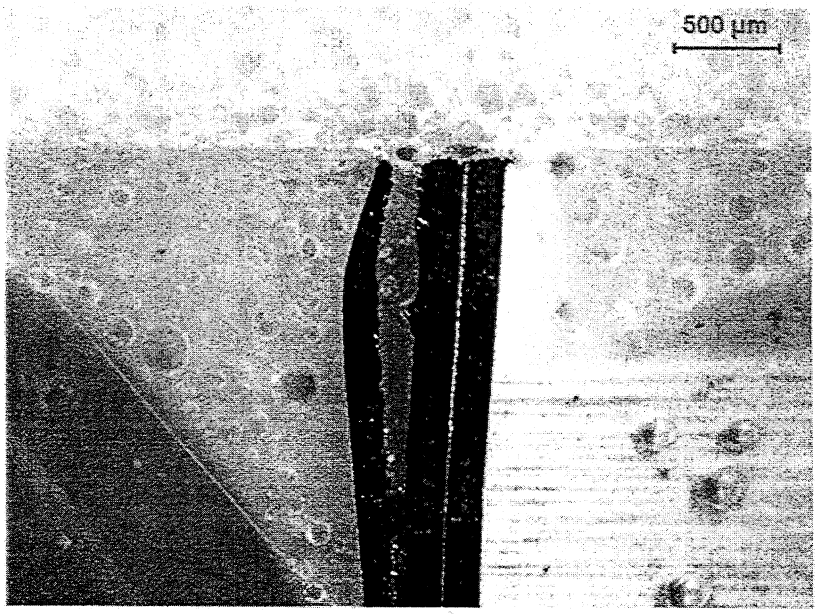

Figure 86. Microstructure of marble clad element L. Unused. Objective 2.5x, oblique illumination.

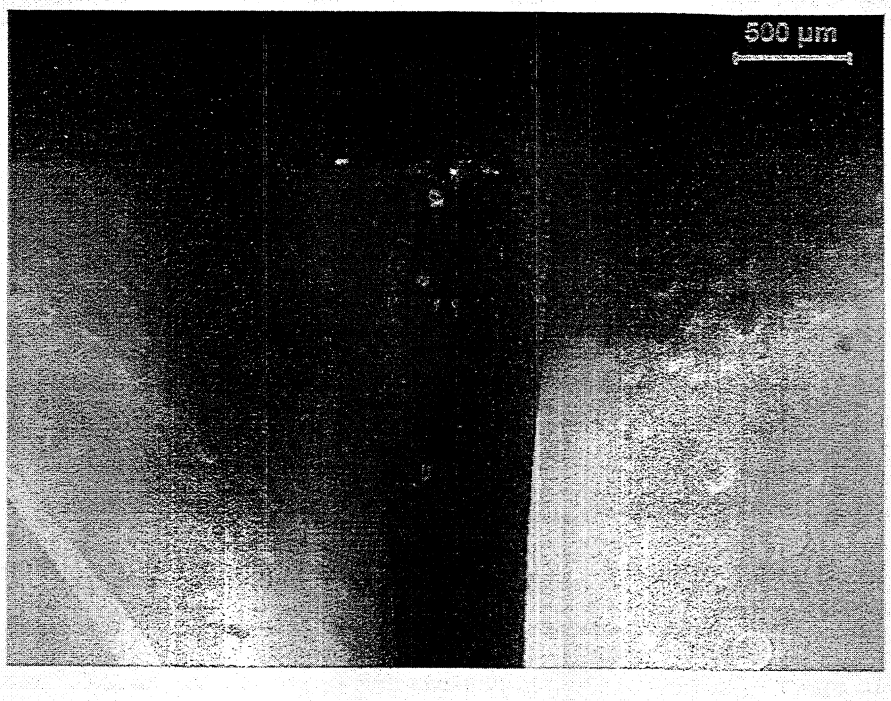

Figure 87. Microstructure of marble clad element L. Unused. Objective 2.5x, fluorescent light.

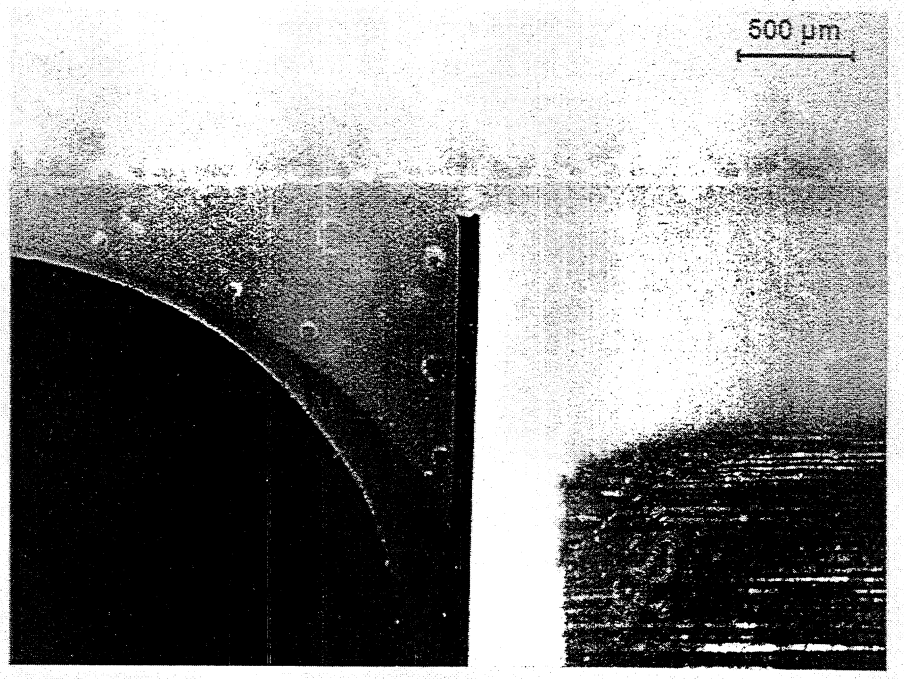

Figure 88. Microstructure of marble clad element L. 1.5 years on the test wall. Objective 2.5x, oblique illumination.

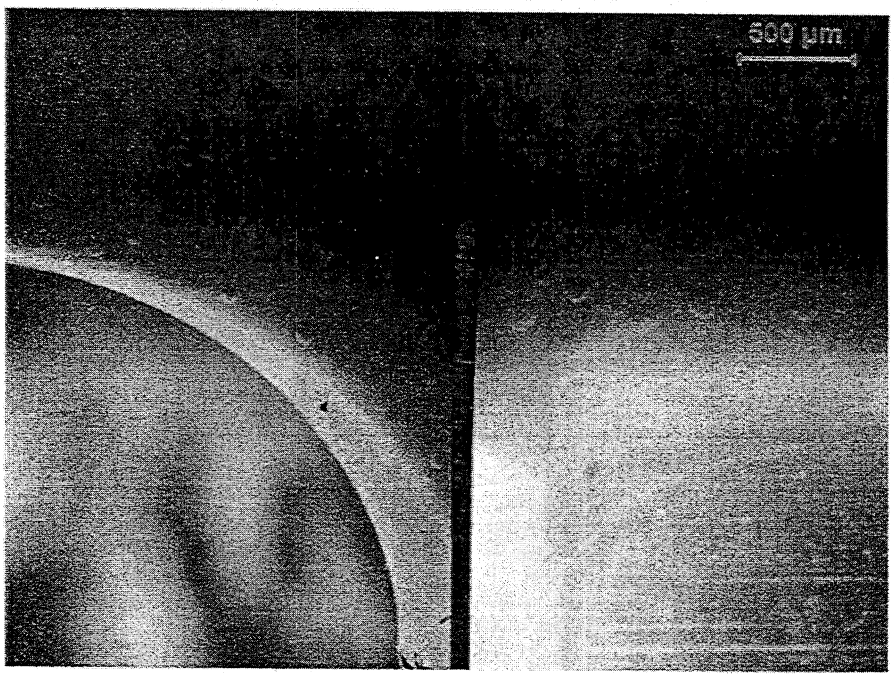

Figure 89. Microstructure of marble clad element L. 1.5 years on the test wall. Objective 2.5x, fluorescent light.

4.3 COLOUR MEASUREMENTS AT FINLANDIA HALL

The colour of the marble slabs chosen for this part of the study was measured 5 times during the project. The dates of the measurements were as follows:

code	date
1	23.06.1999
2	30.11.1999
3	17.05.2000
4	16.10.2000
5	08.03.2001

All the marble types were white, the L value of the unused slabs varying between 80 and 90. Marbles D and E had the highest L value and marble K the lowest. The values of the co-ordinates a and b were near zero, even though all the marble types had a slight greenish-blueish hue. The colour co-ordinates of the marble slabs placed on the eastern wall (23) in initial stage (measurement 1) are shown in Figs. 90-92.

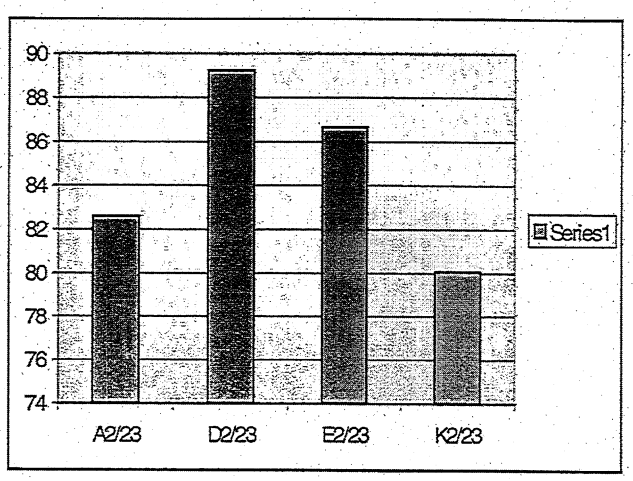

Figure 90. CIELAB colour co-ordinate L of the marbles. Eastern wall (23), first measurement 23.6.1999 (1).

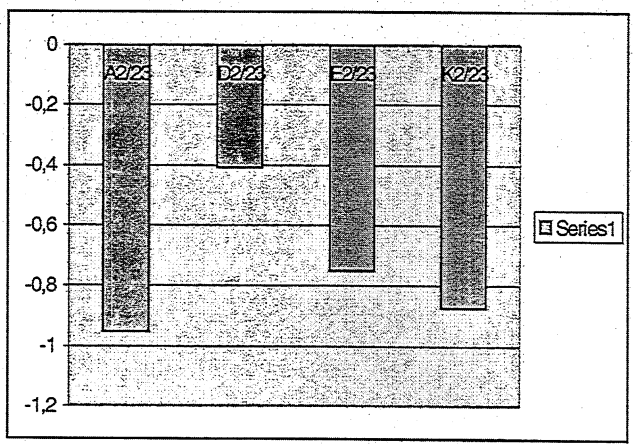

Figure 91. CIELAB colour co-ordinate a of the marbles. Eastern wall (23), first measurement 23.6.1999 (1).

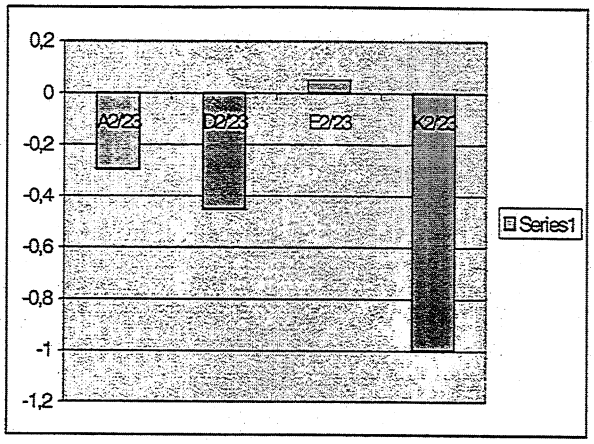

Figure 92. CIELAB colour co-ordinate b of the marbles. Eastern wall (23), first measurement 23.6.1999 (1).

According to the colour measurements the whiteness of the marbles increased. This was evident especially during the first year. After that the changes seem to have been slow, if not negligible. Also, there has been a slight tendency for the co-ordinates a and b to move towards more positive values. This means that the marbles are getting more red and more yellow, which could refer to fouling of the marble surfaces. So far the changes have, however, been small. The results from the colour measurements are shown in Figs. 93-104. The detailed results are presented in Appendix 4.

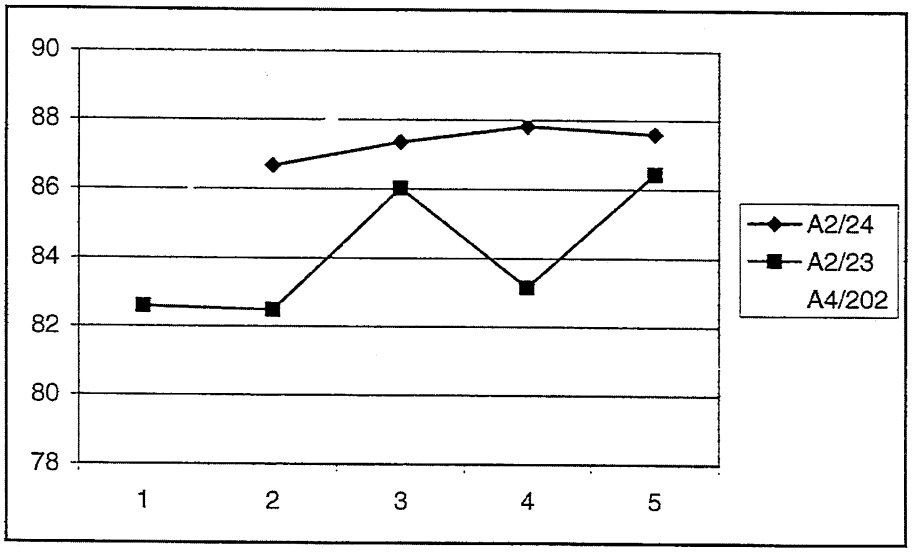

Figure 93. CIELAB colour co-ordinate L of marble A.

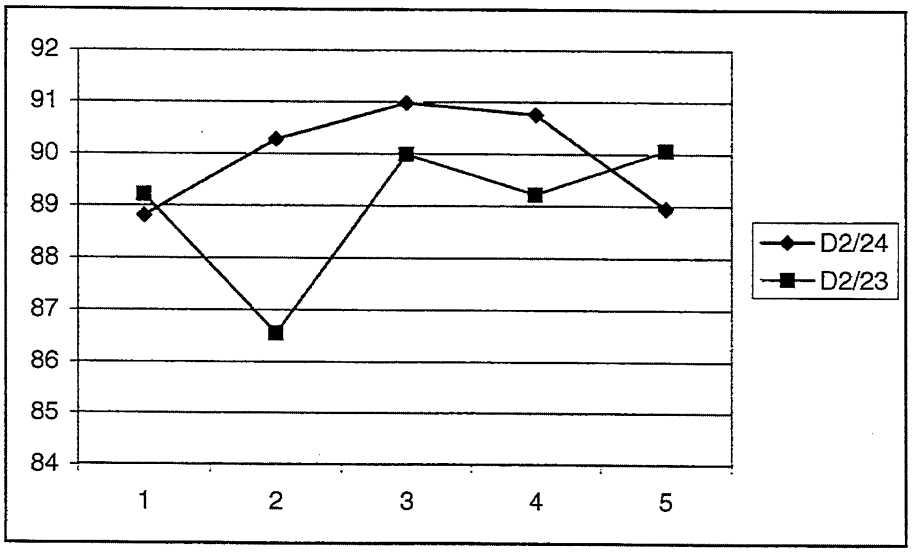

Figure 94. CIELAB colour co-ordinate L of marble D.

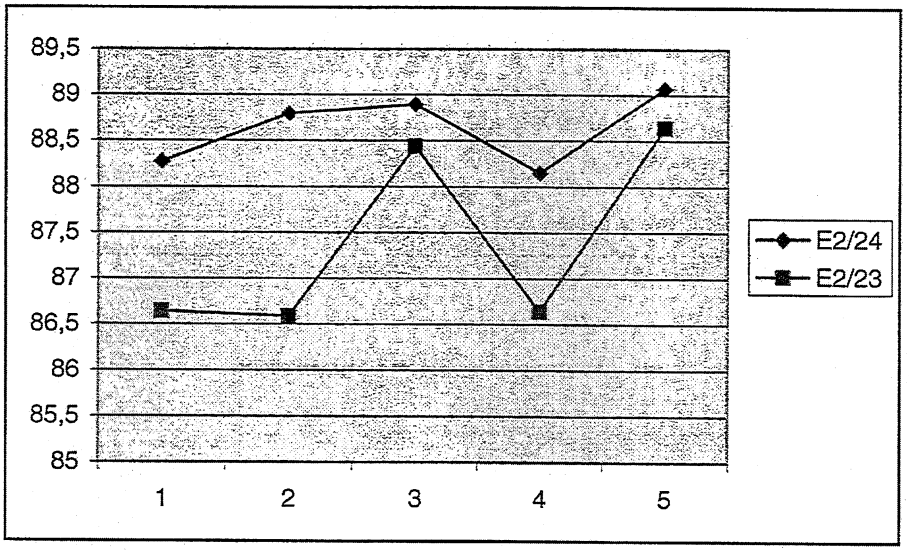

Figure 95. CIELAB colour co-ordinate L of marble E.

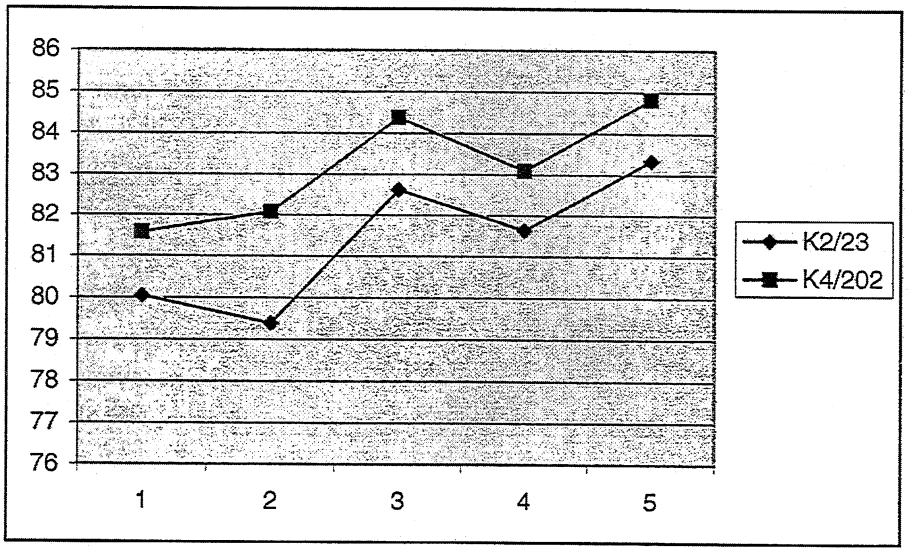

Figure 96. CIELAB colour co-ordinate L of marble K.

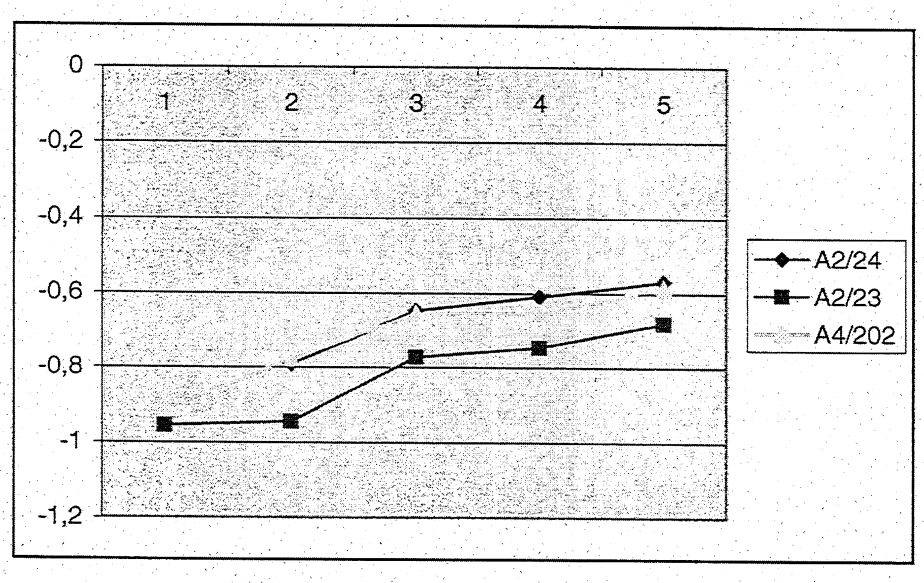

Figure 97. CIELAB colour co-ordinate a of marble A.

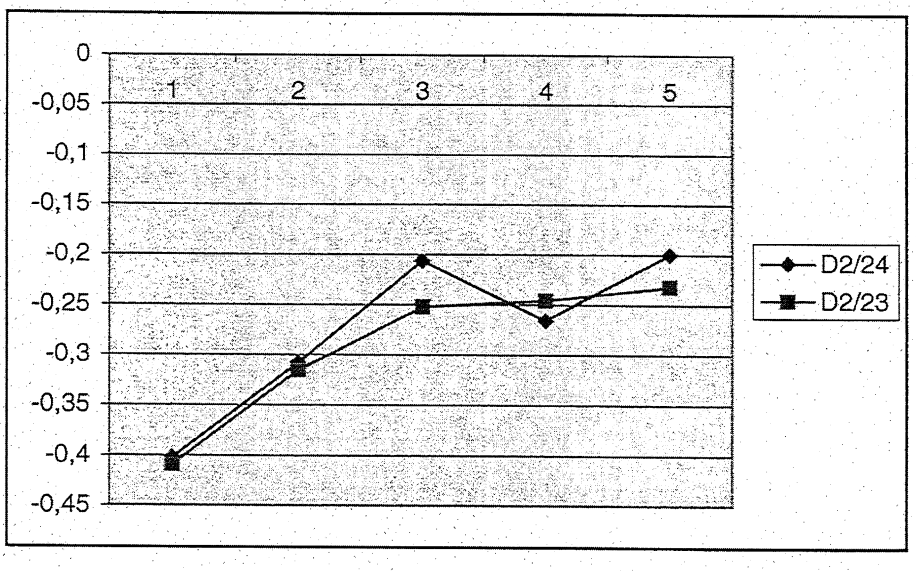

Figure 98. CIELAB colour co-ordinate a of marble D.

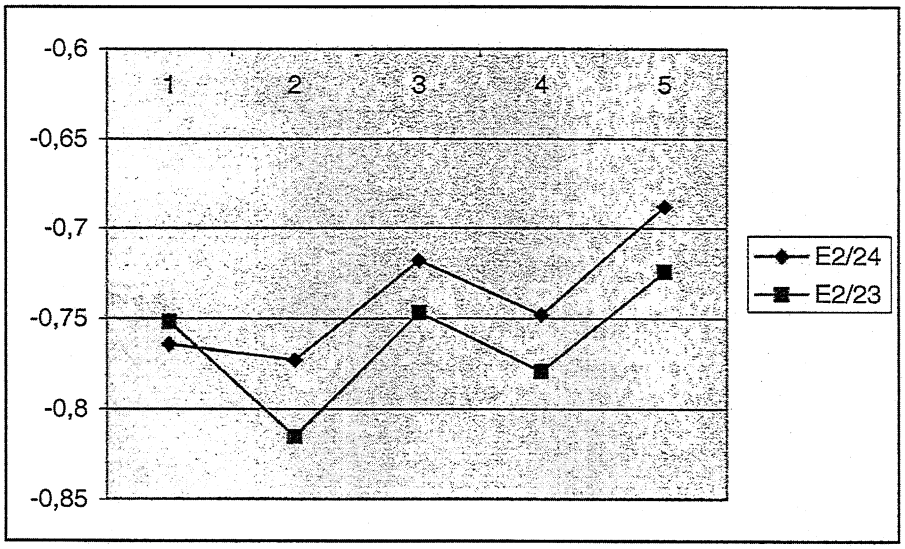

Figure 99. CIELAB colour co-ordinate a of marble E.

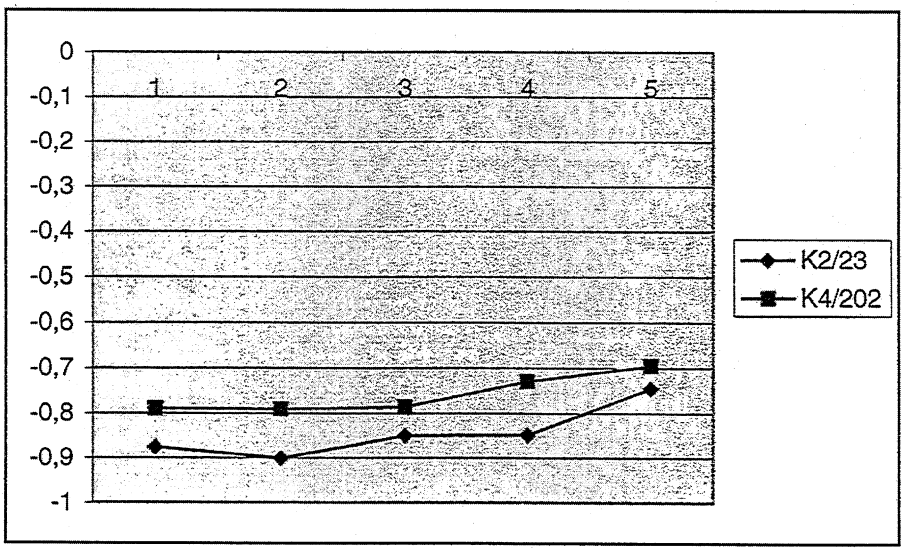

Figure 100. CIELAB colour co-ordinate a of marble K.

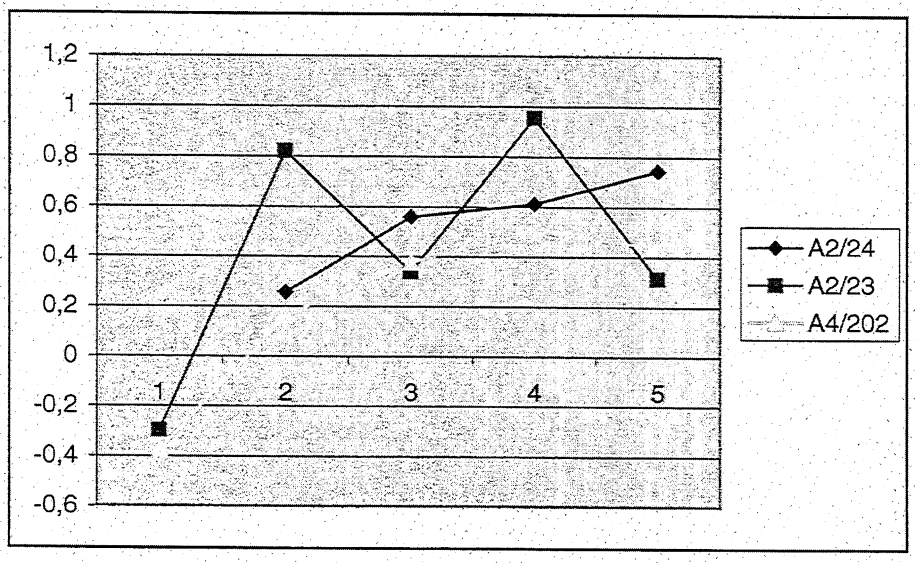

Figure 101. CIELAB colour co-ordinate b of marble A.

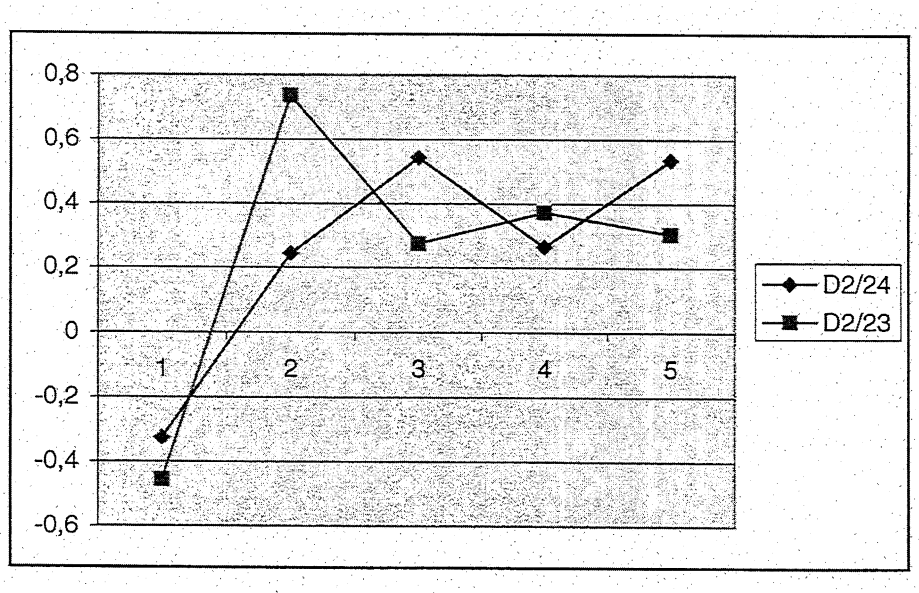

Figure 102. CIELAB colour co-ordinate b of marble D.

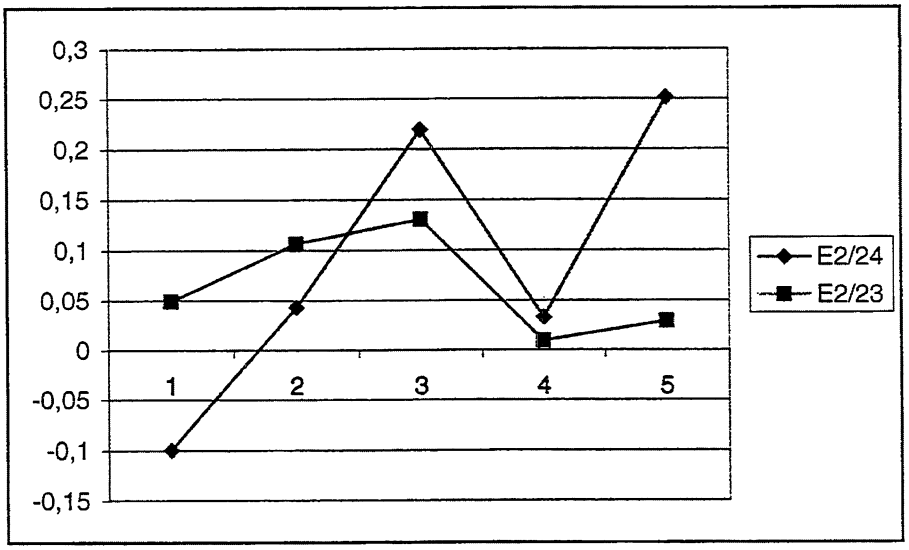

Figure 103. CIELAB colour co-ordinate b of marble E.

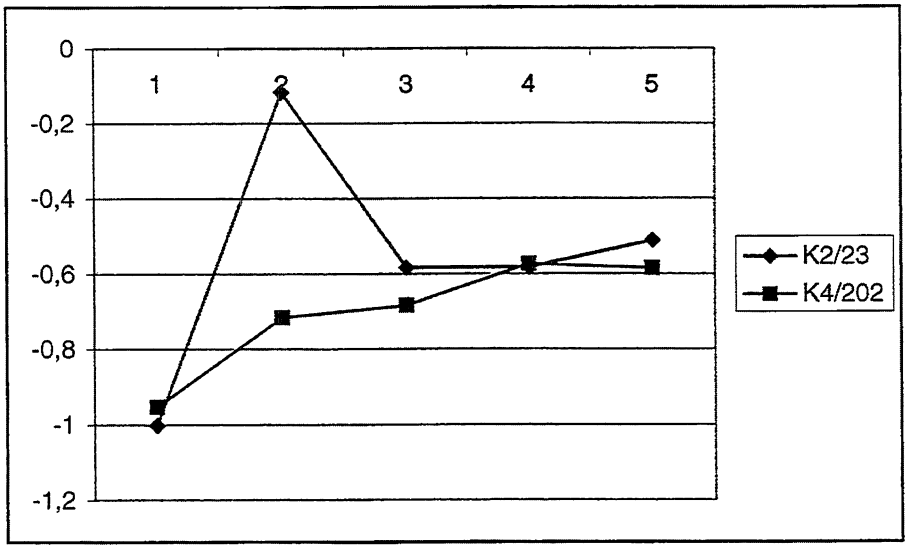

Figure 104. CIELAB colour co-ordinate b of marble K.

The colour differences, ΔE, of the marbles calculated from the values of the first (1) and the last (5) measurements are shown in Table 14. According to the results the colour change of marbles A and K, with the exception of slab A2/24, is evident. However, the colour change of marbles D and E is hardly noticeable so far.

Table 14. Colour change of the marbles during time period 6/99-3/01 (CIELAB).

marble	wall	ΔE
A	23	3.93
	24	1.08
	202	3.88
D	23	1.16
	24	0.90
E	23	1.99
	24	0.88
K	23	3.33
	202	3.24

4.4 FIELD SAMPLES

Marble samples from three different buildings were studied. Some background information dealing with the cases are presented as follows:

case 1

- private owned building situated in Helsinki
- part of the facades coated with marble, supporting structure from concrete elements, ventilation slot between marble and concrete, metal fixings
- built in 1965-1966
- severe deterioration: very notable warping and considerable loss of strength
- marble slabs taken off in 1999
- white marble from Carrara, exact type or origin unknown

case 2

- private owned building situated in Helsinki
- facades coated with marble, supporting structure from concrete elements, ventilation slot between marble and concrete, metal fixings
- built in two parts: older part is approximately 25 years and younger part approximately 15 years old
- severe deterioration: some warping and considerable loss of strength
- older part in much better condition
- white marble from Carrara, exact type or origin unknown

case 3

- public building situated in Oulu
- facades coated with marble, supporting structure from concrete elements, ventilation slot between marble and concrete, metal fixings
- built in 1979
- no warping, no loss of strength, breaking around the fixings
- slabs taken off in 2000
- white, heavily structured marble from finnish Lapland

In addition, the microstructure of a sample taken from the northern wall of the tower part of Finlandia Hall was studied. The cylindrical sample, ∅ 30 mm, was taken in November 2000 by drilling through a 30 mm thick slab. The slabs on that wall had been installed during summer-autumn 1998.

4.4.1 Mineral composition

Marble from the building representing the case 1 was practically pure calcite, i.e. calcium carbonate. It contained only a few percents of quartz, feldspar and possibly mica as impurities. The weight loss of the marble in thermal analysis was 44.0 w-%. The X-ray diffraction diagram of the marble is shown in Fig.105 and its thermal curves in Fig. 106.

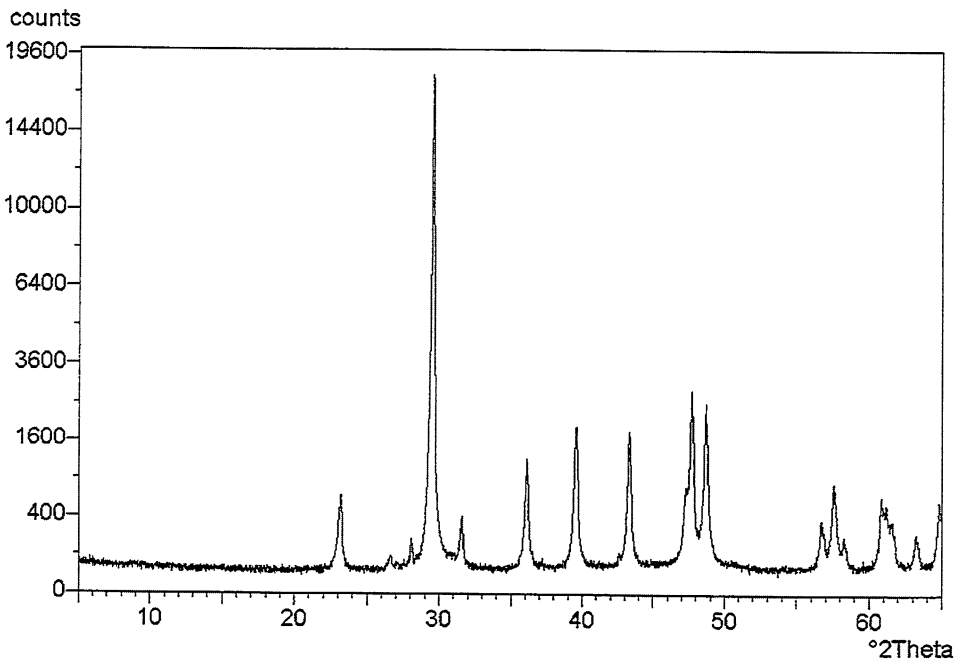

Figure 105. X-ray diffraction diagram of marble from case 1.

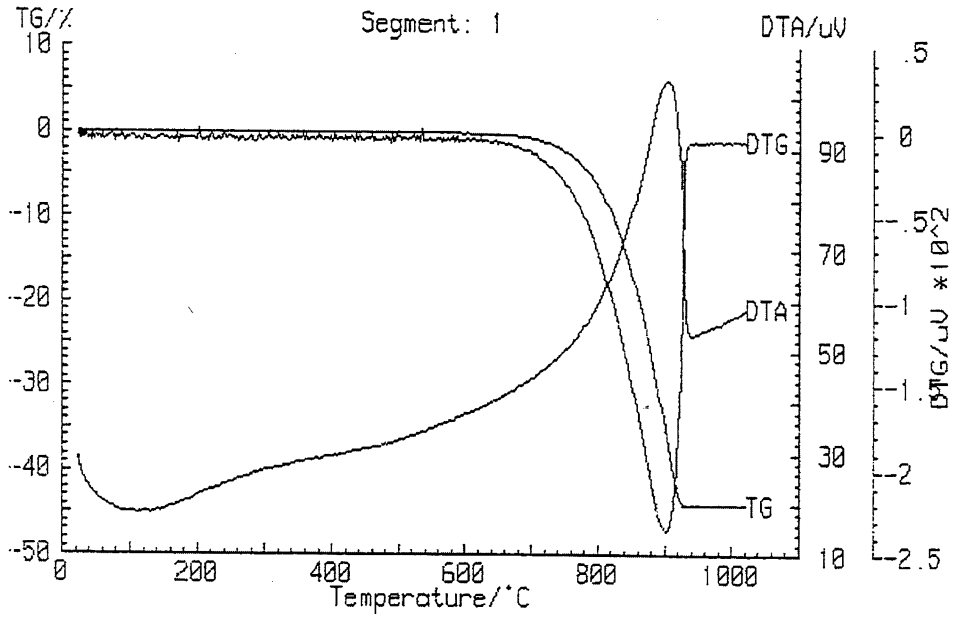

Figure 106. Thermal curves of marble from case 1.

Marbles from the building representing the case 2 were practically pure calcite, i.e. calcium carbonate. Marble from the older part contained only a few percents of quartz, marble from the younger part a few percents of quartz and feldspar as impurities. The weight loss of older marble in thermal analysis was 44.3 w-% and that of younger 44.2 w-%. The X-ray diffraction diagrams of marbles are shown in Figs. 107 and 108 and their thermal curves in Figs. 109 and 110.

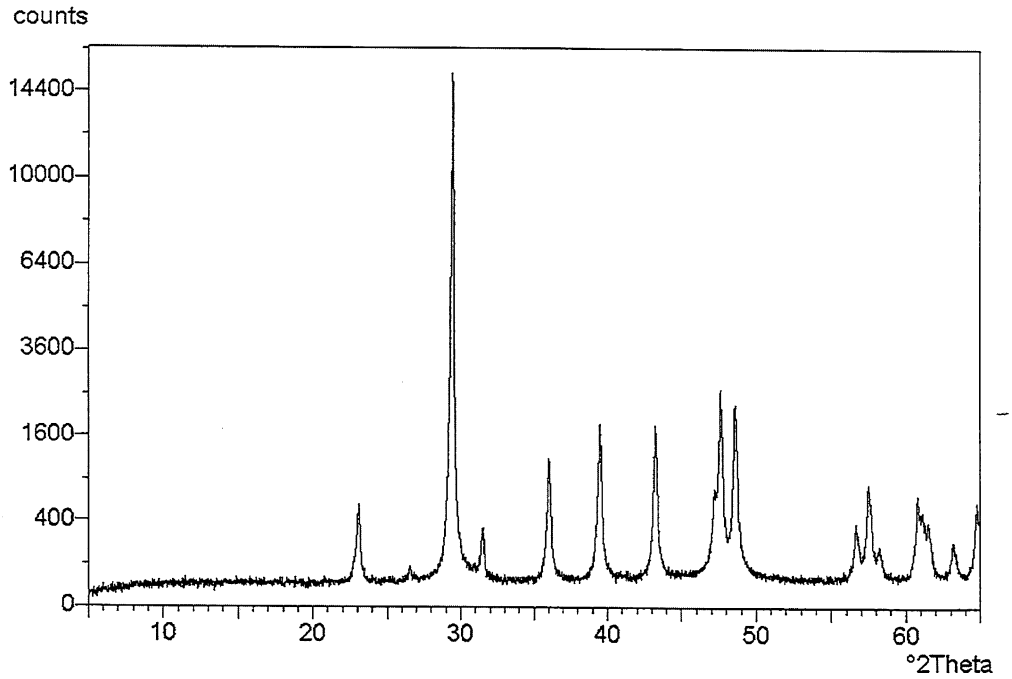

Figure 107. X-ray diffraction diagram of marble from case 2. Older part.

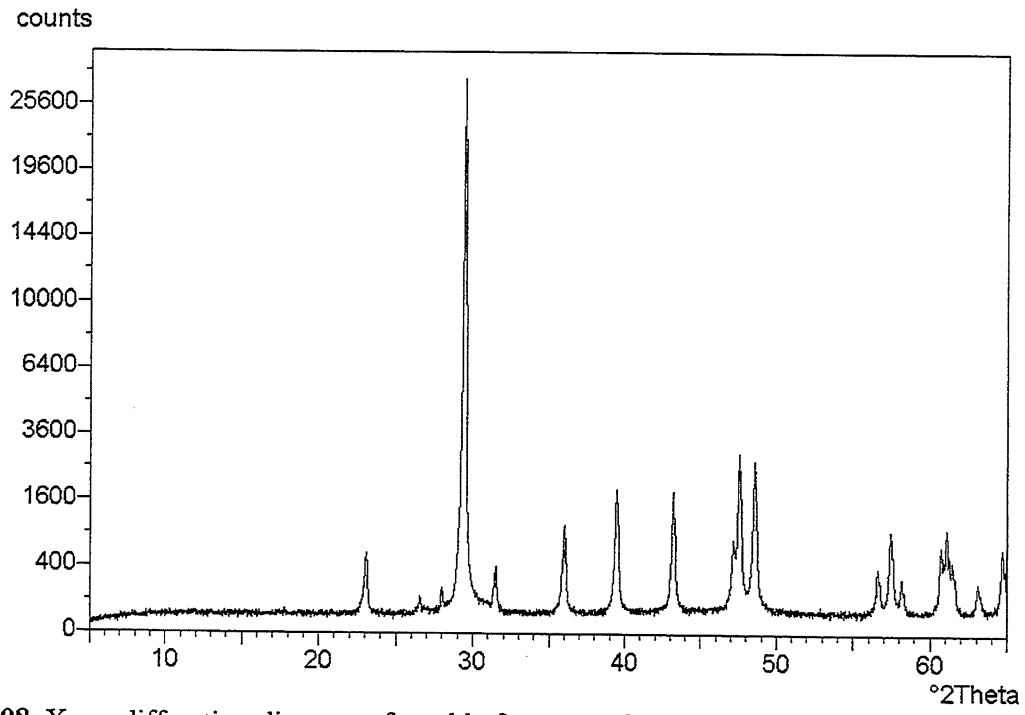

Figure 108. X-ray diffraction diagram of marble from case 2. Younger part.

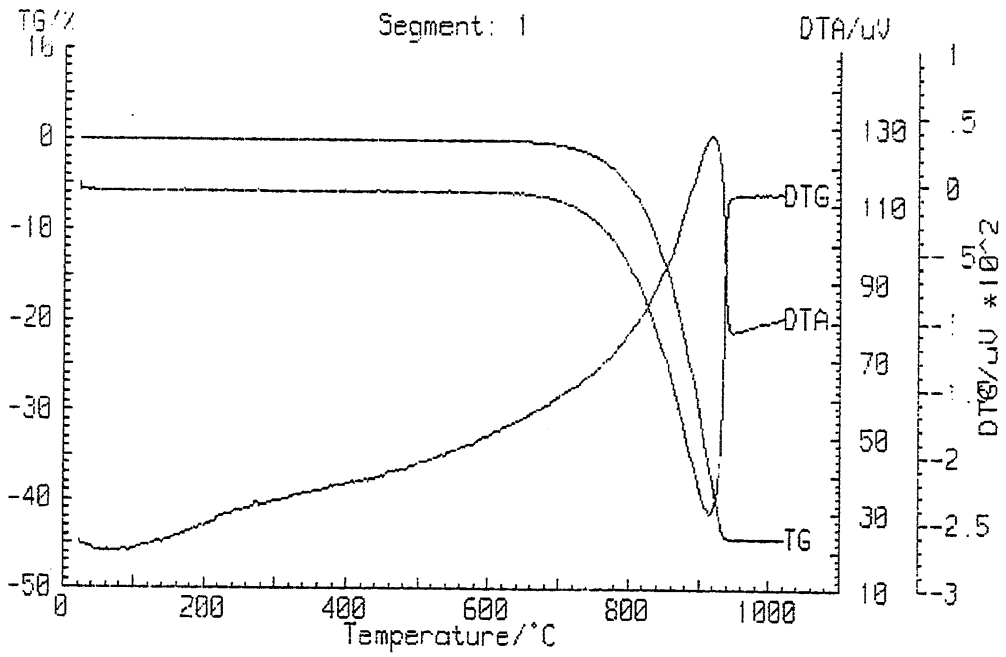

Figure 109. Thermal curves of marble from case 2. Older part.

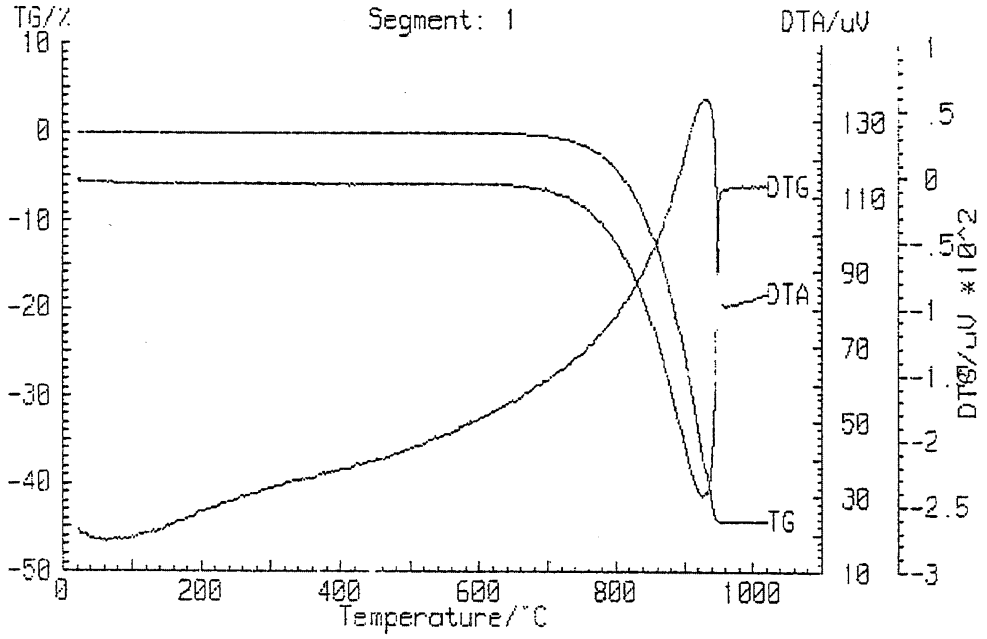

Figure 110. Thermal curves of marble from case 2. Younger part.

The main component of marble from the building representing the case 3 was dolomite, i.e. calcium magnesium carbonate. Thus, it was not question about marble. It contained also a notable amount of quartz and feldspar plus some mica and calcite as impurities. The weight loss of stone in thermal analysis was 43.3 w-%. The X-ray diffraction diagram of stone is shown in Fig.111 and its thermal curves in Fig. 112.

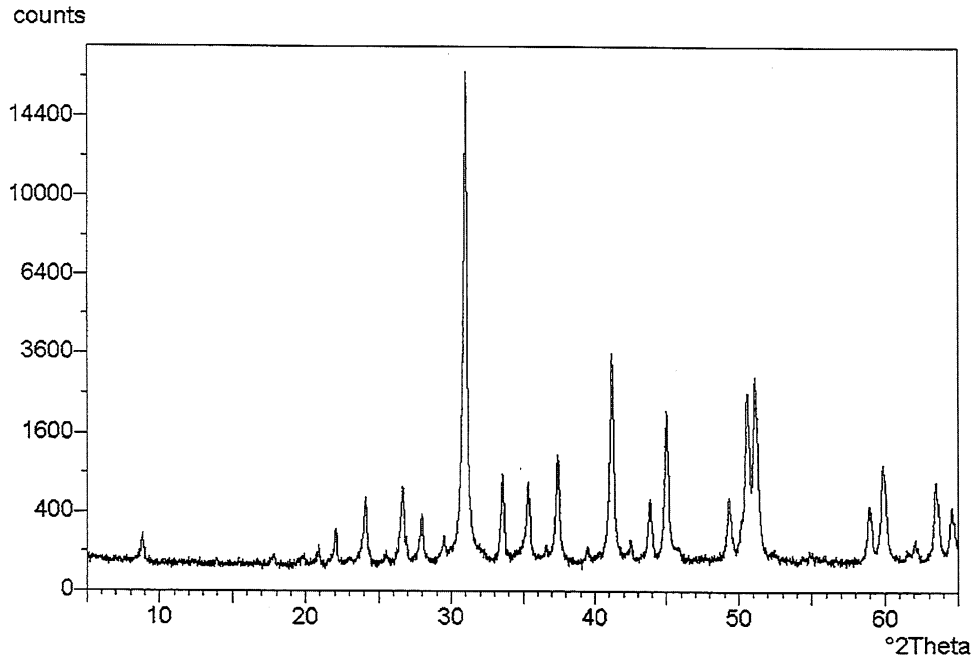

Figure 111. X-ray diffraction diagram of dolomite from case 3.

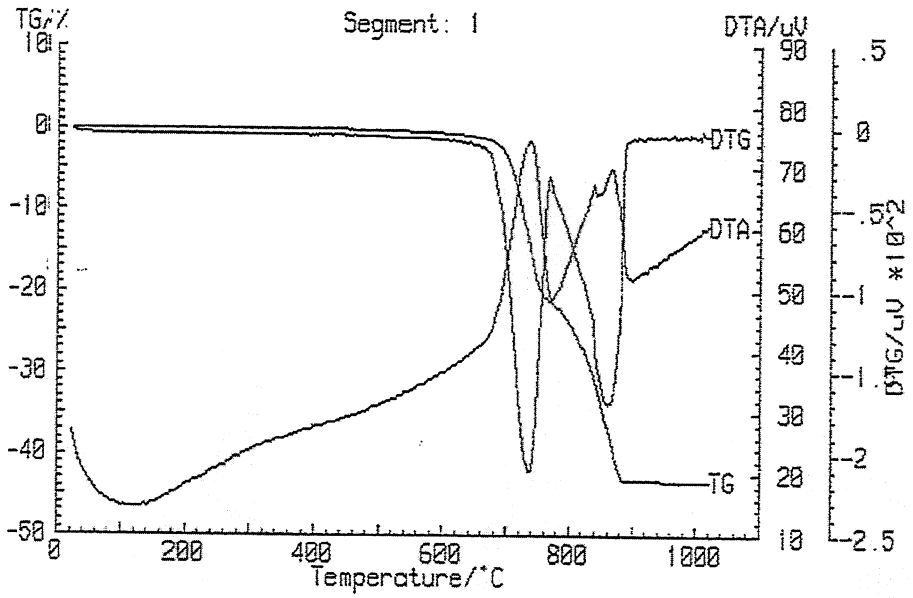

Figure 112. Thermal curves of dolomite from case 3.

4.4.2 Thin section study

A photograph of the microstructure of marble from the case 1 is shown in Fig. 113. Following observations were made:

- fine-grained ground mass, slightly oriented, average grain size 0.1-0.2 mm
- in places more coarse-grained veinlets with a thickness of about 1 mm, veinlets show the same orientation as the ground mass
- grain boundaries clear, often straight, grains easily distinguished
- nearly pure carbonate rock, only a little quartz and opaque minerals, possibly feldspar

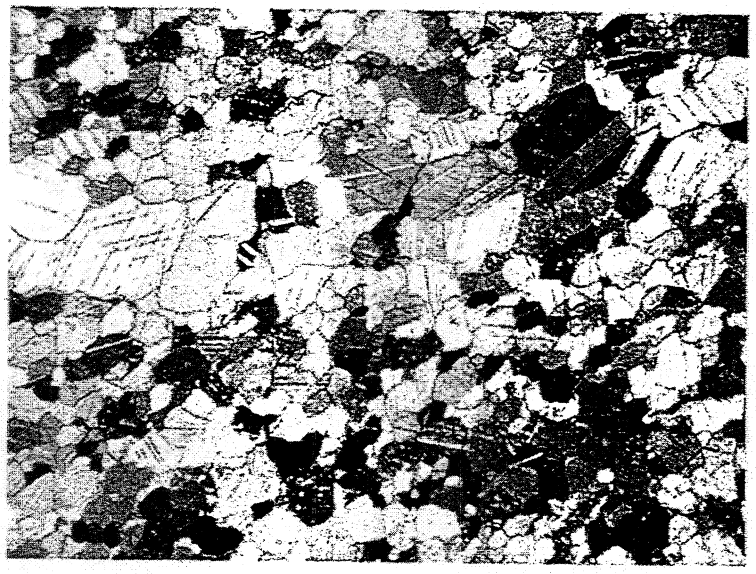

Figure 113. Microstructure of marble from case 1. Cross-polarized light.

Photographs of the microstructure of older marble from the case 2 are shown in Figs. 114 and 115. Following observations were made:

- ground mass fine-grained, even-grained, not oriented
- grain boundaries easily distinguished
- a few very fine-grained cryptocrystalline lenses, max. length about 10 mm, inside the ground mass
- no heavy cracking
- outer surface dirty and uneven

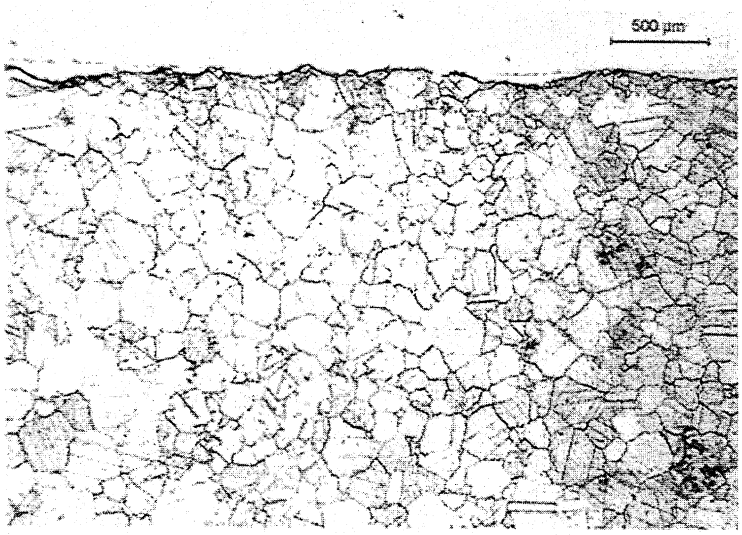

Figure 114. Microstructure of older marble from case 2. Plane-polarized light.

Figure 115. Microstructure of older marble from case 2. Fluorescent light.

Photographs of the microstructure of younger marble from the case 2 are shown in Figs. 116 and 117. Following observations were made:

- ground mass fine-grained, fairly even-grained, not oriented
- grain boundaries easily distinguished
- a few very fine-grained cryptocrystalline lenses, max. length about 2-3 mm, inside the ground mass
- cracks between the grains extending to a depth of about 2-3 mm from the outer surface and to a depth of about 1-2 mm from the inner surface, some cracks cut the surface
- outer surface dirty

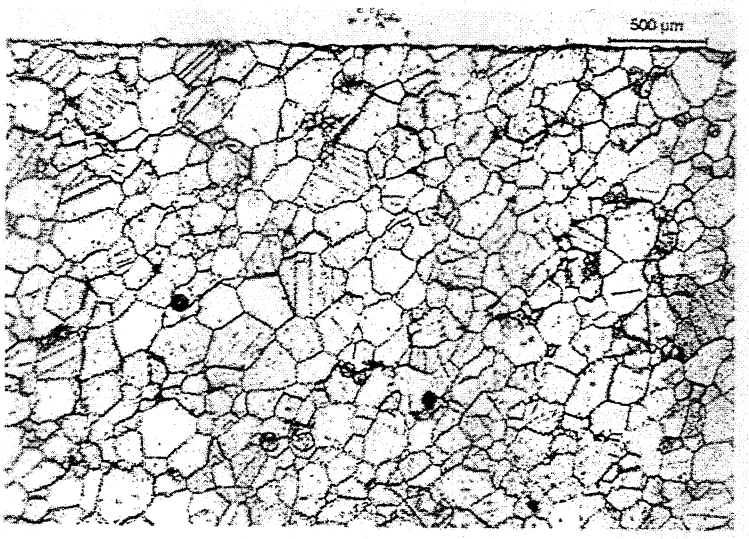

Figure 116. Microstructure of younger marble from case 2. Plane-polarized light.

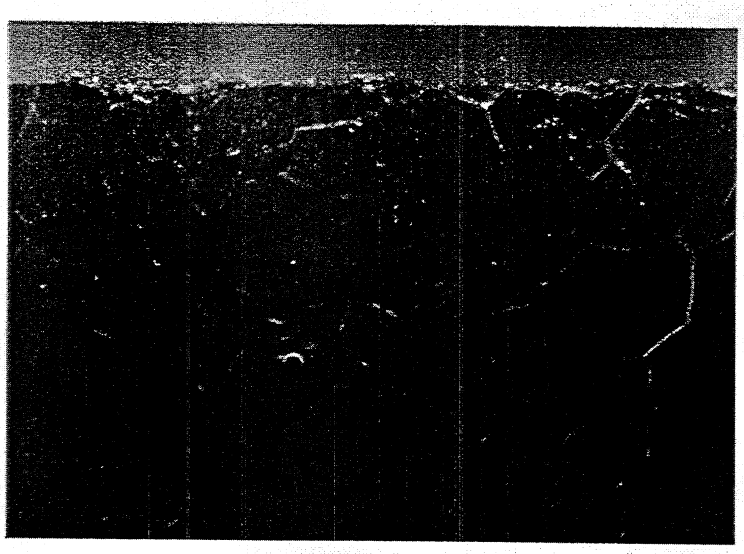

Figure 117. Microstructure of younger marble from case 2. Fluorescent light.

A photograph of the microstructure of dolomite from the case 3 is shown in Fig. 118. Following observations were made:

- ground mass very fine-grained, microcrystalline, dense
- clearly oriented, layered
- in places more coarse-grained veinlets with a thickness of about 1 mm, mostly oriented parallel to layering, a few also cross the layering
- some separate fine- to medium-grained quartz grains in rows, parallel to layering
- mainly carbonate rock, moderate content of quartz, other minerals include feldspar (probably plagioclase), mica (probably muscovite) and opaque minerals
- in places mica forms veinlets, partly with opaque minerals

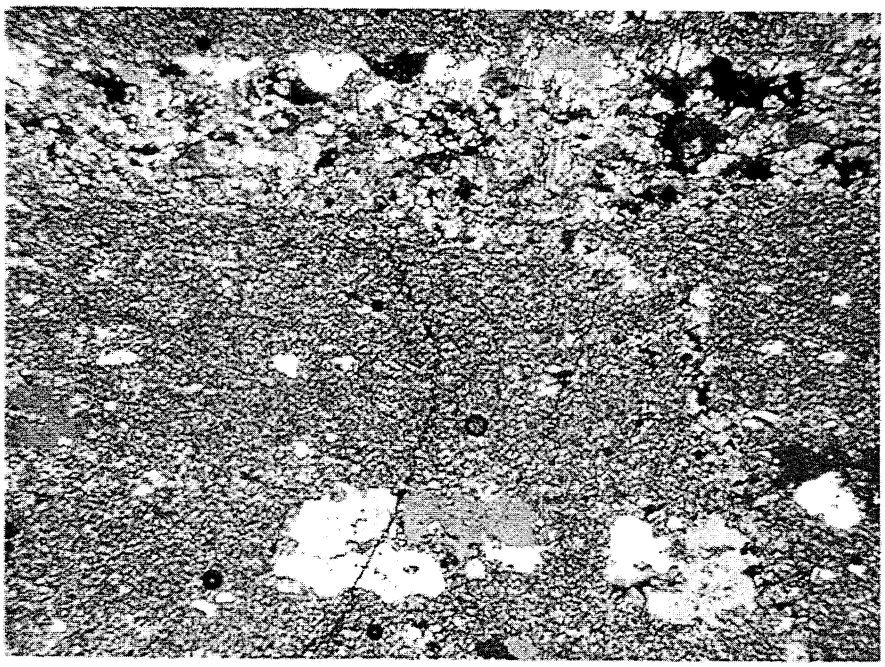

Figure 118. Microstructure of dolomite from case 3. Cross-polarized light.

A photograph of the microstructure of marble from Finlandia Hall is shown in Fig. 119. Following observations were made:

- fine-grained, fairly even-grained, slightly oriented
- average grain size 0.2-0.3 mm
- grain boundaries clear, straight, grains easily distinguished
- nearly pure carbonate rock, a little quartz and opaque minerals

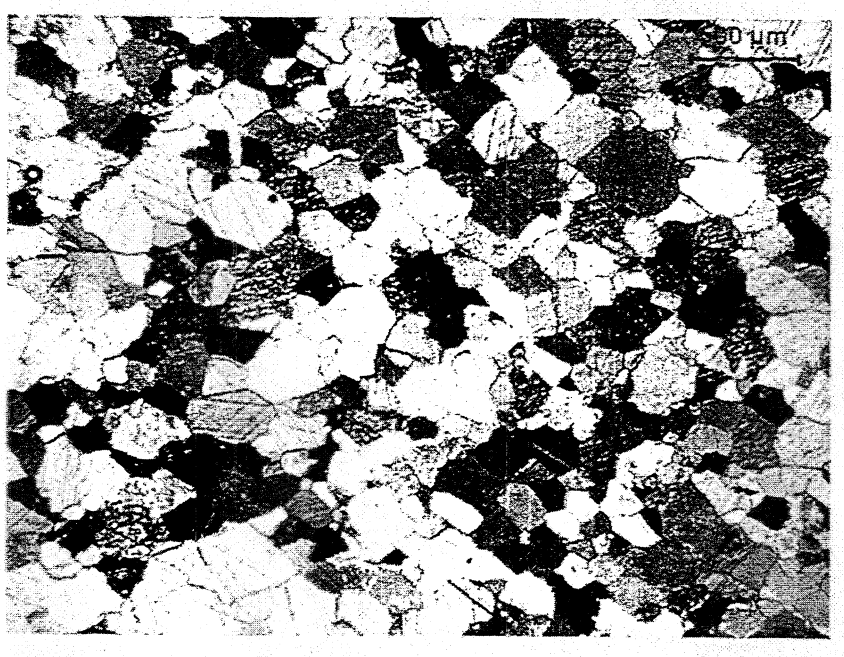

Figure 119. Microstructure of marble from Finlandia Hall. Cross-polarized light.

4.4.3 SEM-study

SEM-pictures of fractured surfaces of marble from the case 1 are shown in Figs. 120 and 121. The individual grains can at least for the most part be distinguished from each other. Cracks can be noticed practically between all the grains. The maximum crack width is around 2 µm. The average grain size of marble is about 200 µm.

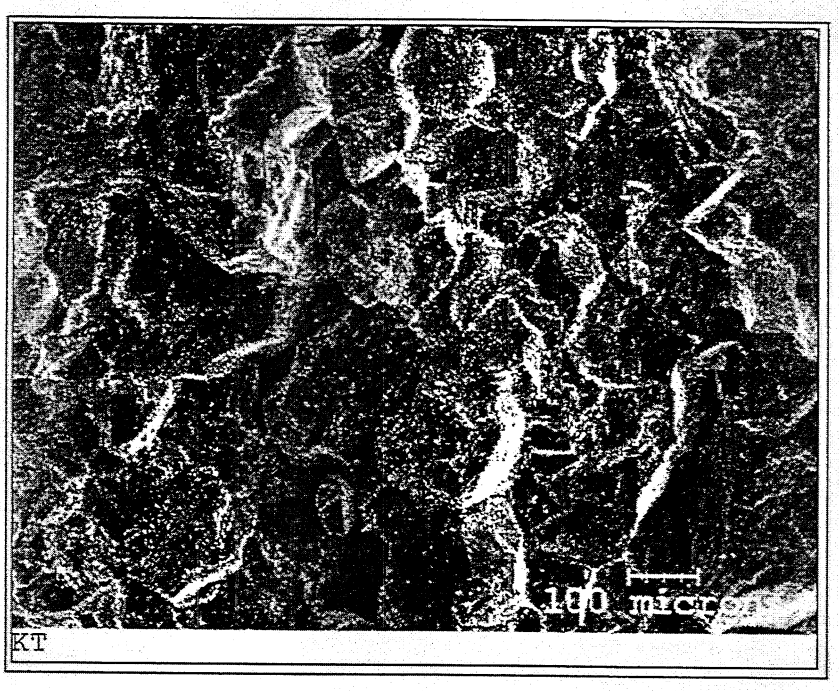

Figure 120. Marble from case 1. SE-image of fractured surface, 100x.

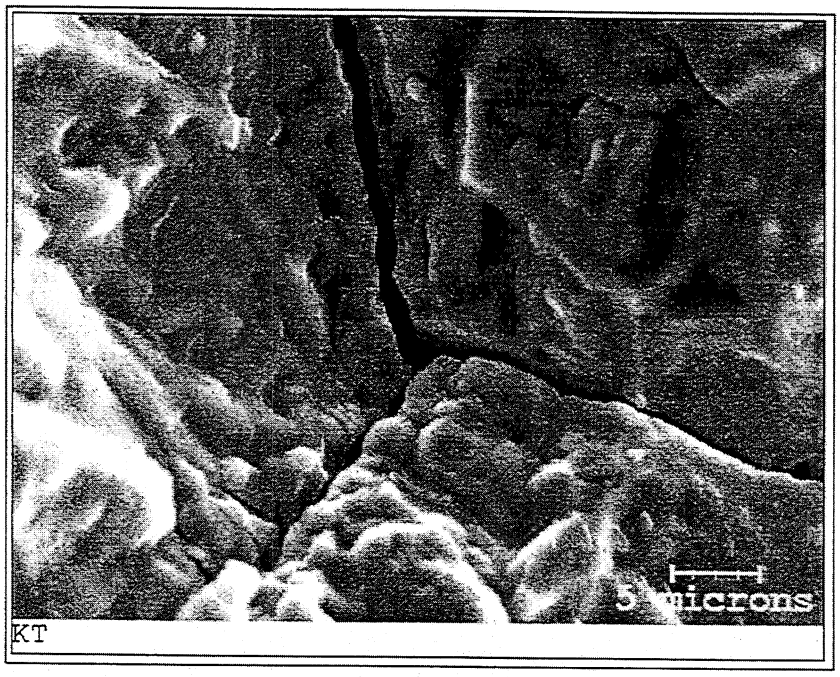

Figure 121. Marble from case 1. SE-image of fractured surface, 2500x.

SEM-pictures of fractured surfaces of marble from the case 2 are shown in Figs. 122 and 123. In marble of the older part the individual grains can at least for the most part be distinguished from each other. In marble of the younger part the grains are almost detached from each other. Wide cracks can be noticed between all the grains. The average grain size of older marble is about 200 µm, that of younger marble around 200-300 µm.

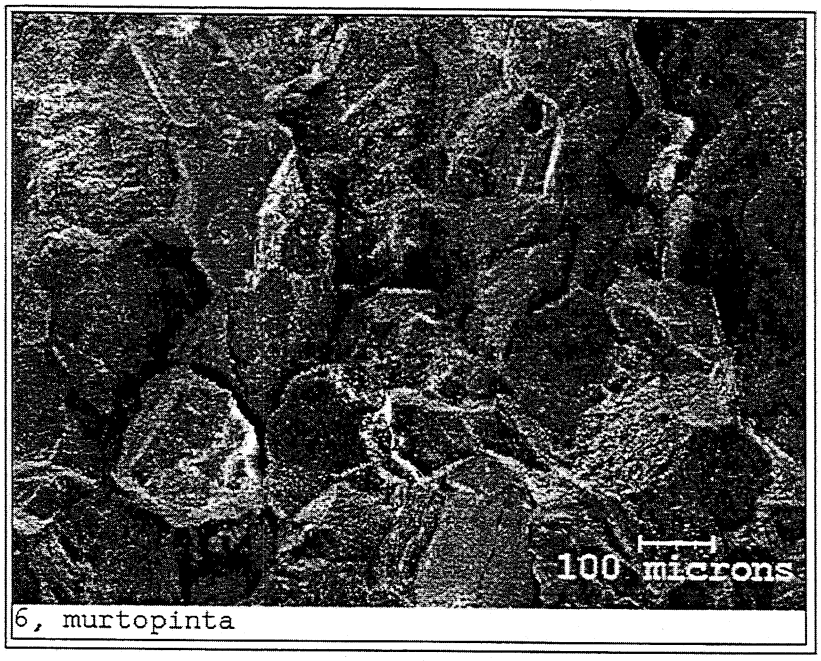

Figure 122. Marble from case 2, older part. SE-image of fractured surface, 100x.

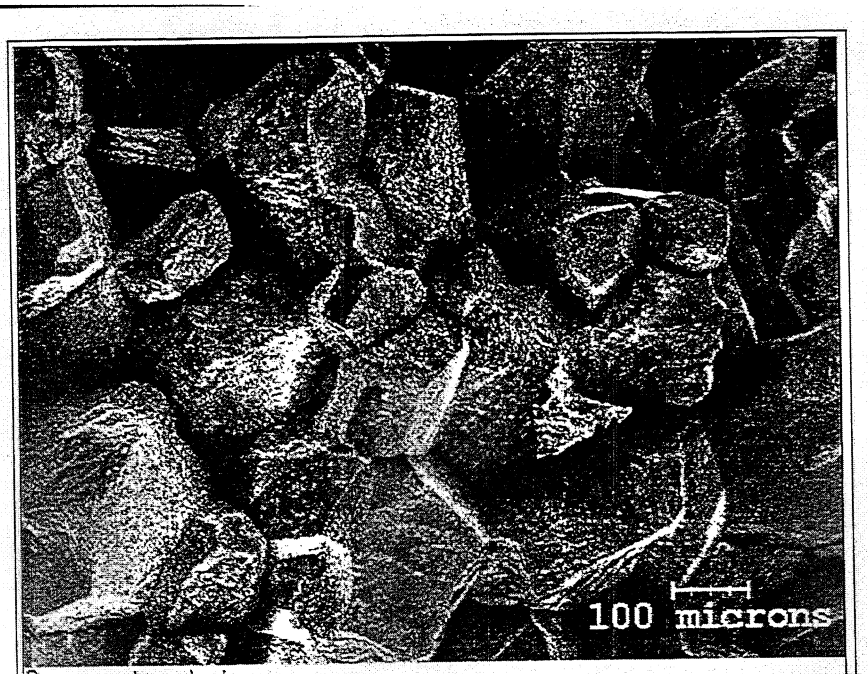

3, murtopinta

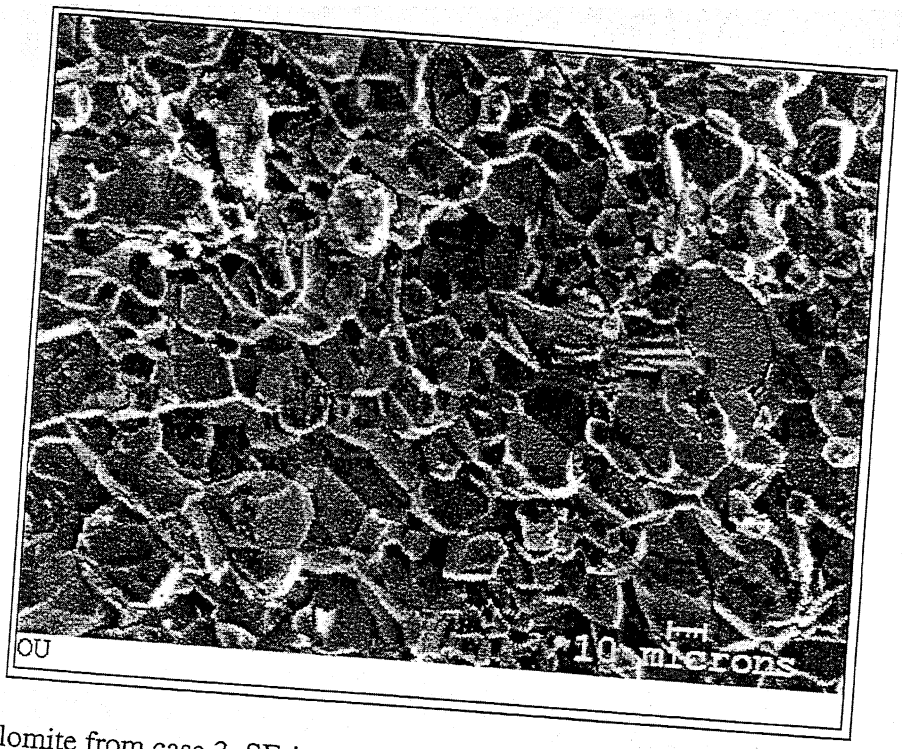

Figure 124. Dolomite from case 3. SE-image of fractured surface, 500x.

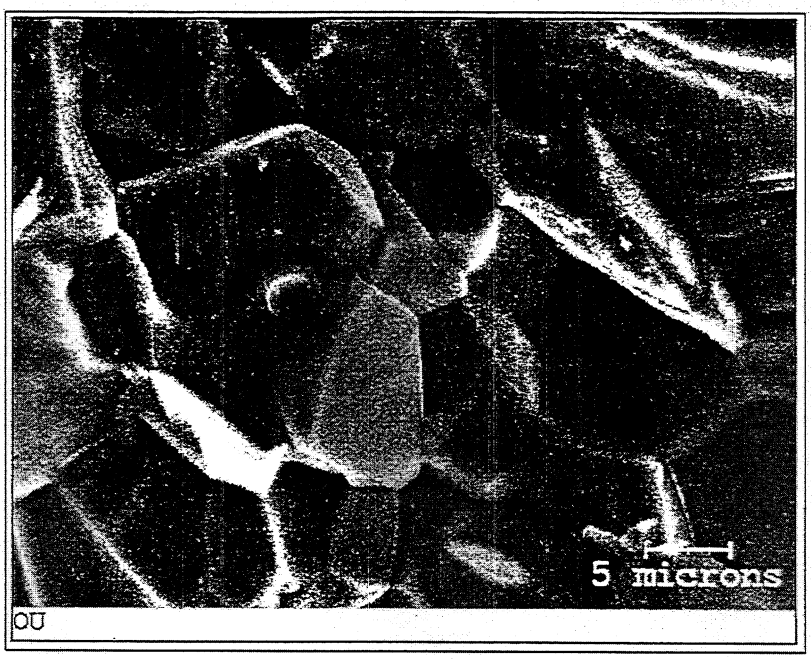

Figure 125. Dolomite from case 3. SE-image of fractured surface, 2500x.

SEM-pictures of fractured surfaces of marble from Finlandia Hall are shown in Figs. 126 and 127. The individual grains can at least partly be distinguished from each other. Cracks can be noticed between some of the grains. The maximum crack width is around 0.8-0.9 µm. The average grain size of marble is about 200 µm.

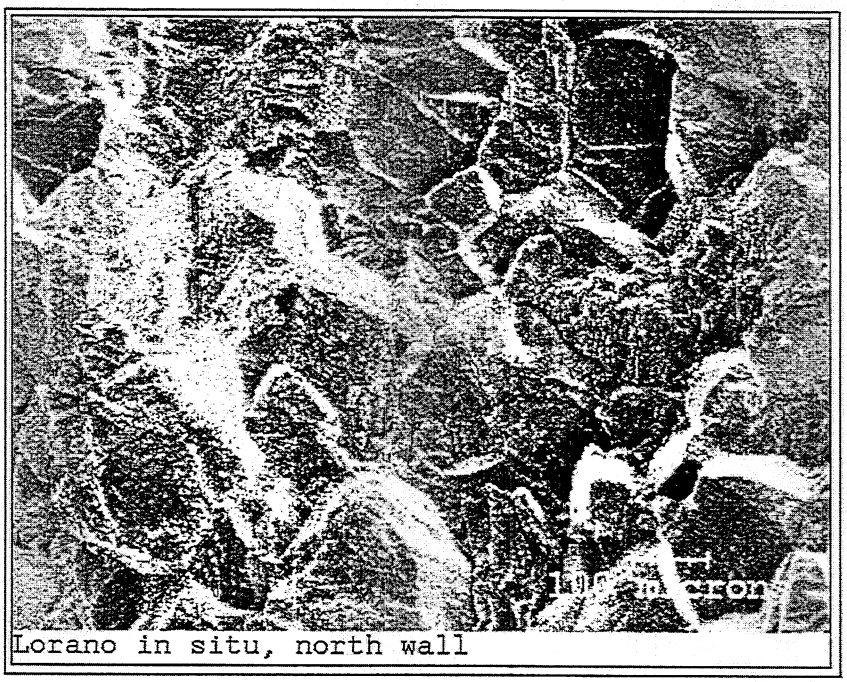

Figure 126. Marble from Finlandia Hall, north wall. SE-image of fractured surface, 100x.

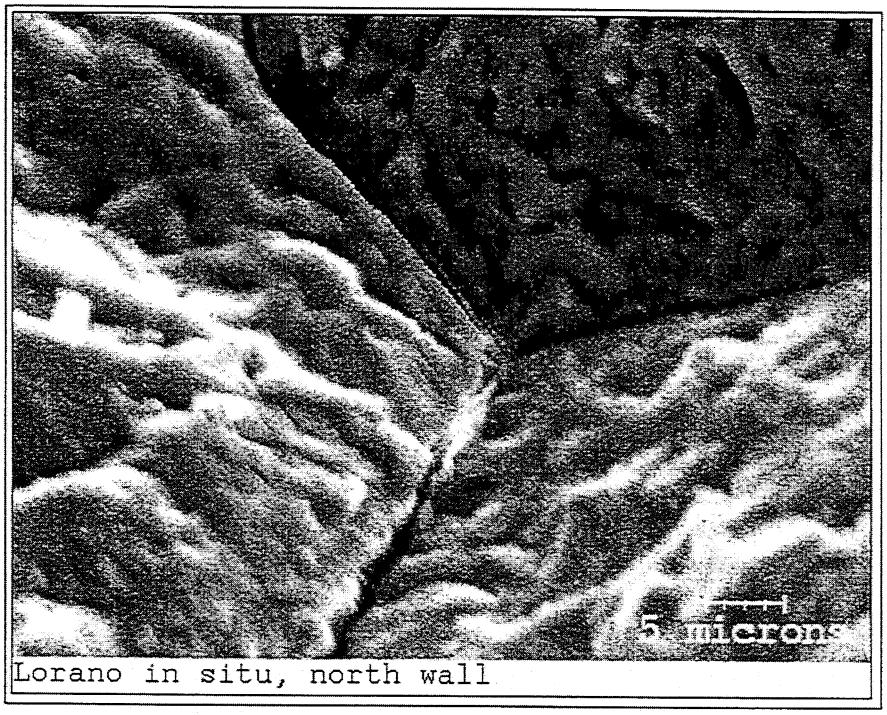

Figure 127. Marble from Finlandia Hall, north wall. SE-image of fractured surface, 2500x.

In connection with the SEM-study also the chemical composition of marble from the northern wall of Finlandia Hall was surveyed by using an energy dispersive PGT Imix spectrometer (EDS). The analysis was made from the fractured surface very close to the outer surface of the slab. The composition observed was practically that of the unused marble, only a little chlorine was detected. The EDS-spectra of marble are shown in Figs. 128 and 129.

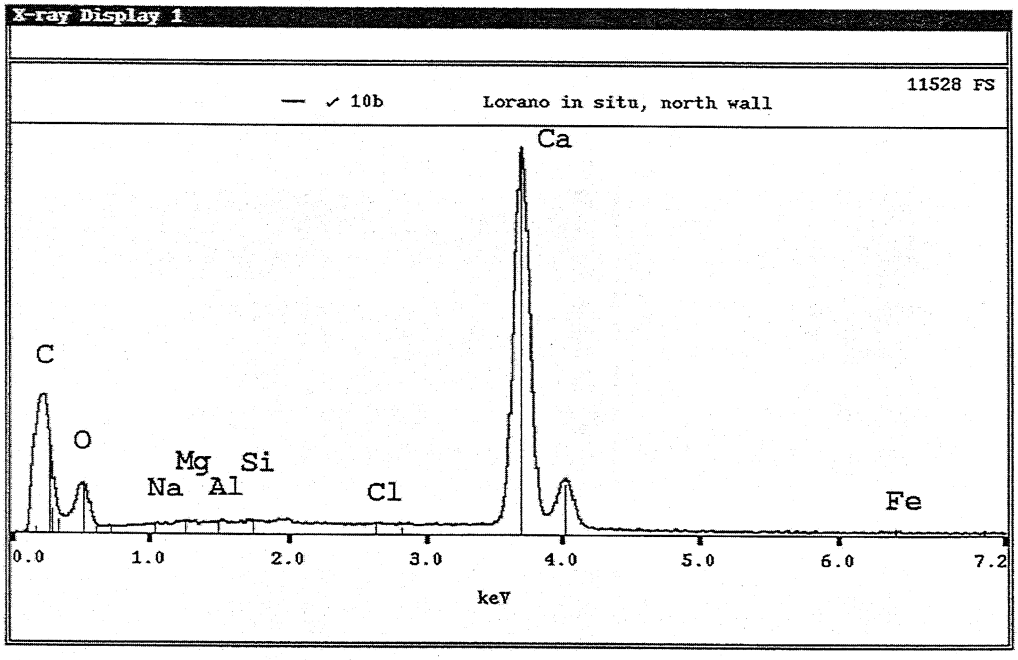

Figure 128. EDS-spectrum of marble from Finlandia Hall, north wall.

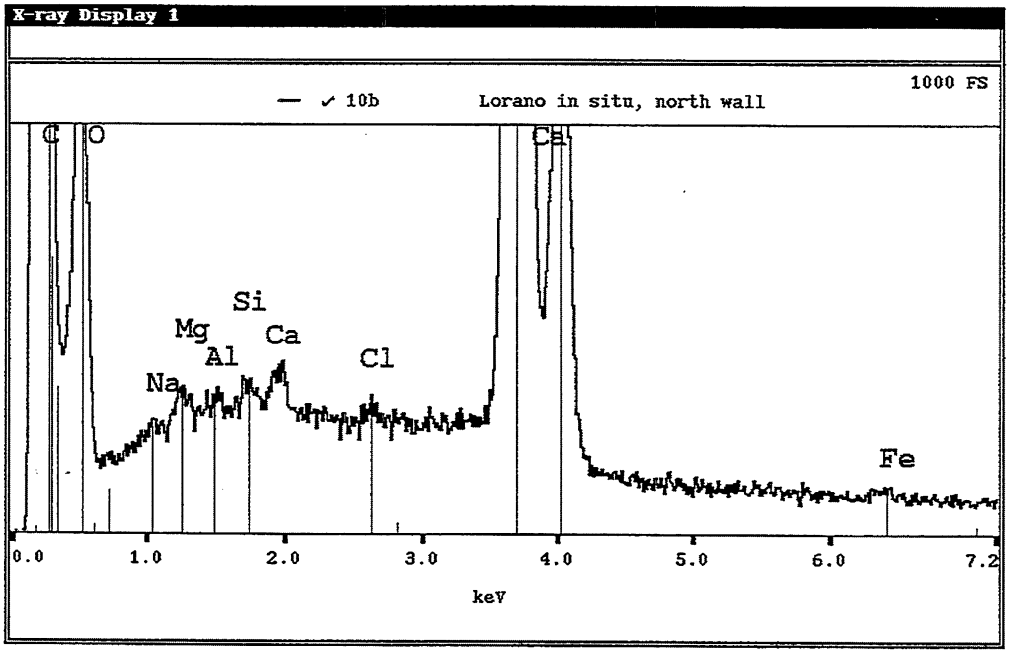

Figure 129. EDS-spectrum of marble from Finlandia Hall, north wall. Small peaks.

5 DISCUSSION

5.1 Strength properties

The flexural strengths of the marble types chosen for the study differed considerably from each other. Marbles E and K were very strong with an initial flexural strength of around 20 MPa or even higher. On the other hand marble D was weak with an initial flexural strength of 5-7 MPa. The initial flexural strength of marble A was between these two extremes varying in the area of 12-17 MPa. Marbles A and D seemed to be somewhat (20-30%) weaker in testing direction A than in direction B. This could refer to some kind of schistosity in stone structure. In this respect, the strength results of marbles E and K were more even.

The strengths of marbles A and D decreased noticeably on the test wall, which most probably is a sign of the effect of some sort of a deterioration process. The loss of strength of marble A was nearly 20%, and it was about the same in both directions. The loss of strength of marble D was even 35-40%, and it seemed to be more pronounced in the direction where the marble originally was stronger. The results for marble A in the subproject "Protective agent" were parallel to those discussed here. Correspondingly, the behaviour of marble D in the subproject "One-sided weather resistance test" was very similar to that observed on the test wall. Thus, the loss of strength can be considered to be a real phenomenon, and it can't be explained to be due to sampling or random variation of strength.

The fact that the strengths were of the same order of magnitude after 1 and 1.5 years on the test wall was also a very noteworthy feature in the results of marbles A and D. This would indicate that the loss of strength on the test wall happened very soon after the slabs were installed, and after that the deterioration of marbles proceeded slowly if at all.

Deviating from the results of marbles A and D no significant loss of strength could be observed in marbles E and K. The results of marble E were, however, somewhat inconsistent. First of all the general strength level of the slab that was installed on the test wall seemed to have been clearly higher than that of the unused reference slab. Otherwise, it would be impossible to explain the high strength values measured from the test wall specimens. This explanation is supported by the results achieved in the Subproject "One-sided weather resistance test", as the strength level measured for marble E in those tests was around 25 MPa. Secondly, a fairly remarkable loss of strength, 17%, was measured in marble E in testing direction A after 1 year on the test wall. The standard deviation in that measurement was exceptionally high, and it was due to three specimens with very low strength level. It seems probable that those three specimens had been taken from an area that had suffered from some extra mechanical damage which had caused cracks to marble structure. If the results of those three specimens are excluded the average flexural strength of marble E in direction A after 1 year on the test wall is 19.3 MPa meaning a decrease of about 5% compared to the initial strength. This value is more in line with the other values of this subproject and with the values achieved in the weather resistance tests (5-10%).

5.2 Water absorption properties

All the marble types were very dense. The water absorption of marbles A, D and E was 0.11-0.13 w-% (apparent porosity 0.30-0.34 vol-%) and that of marble K only 0.07 w-% (apparent porosity 0.19 vol-%). The bulk density of every type was between 2713-2718 kg/m^3.

The water absorption and apparent porosity of marbles A and D increased considerably, approximately 80%, on the test wall. Also in marble K the relative increase of the water absorption and apparent porosity was fairly high, about 50%, but as its initial values were very low, the absolute increase can be considered to have been modest. The relative (also absolute) increase of the water absorption and apparent porosity of marble E was the lowest, only around 10%. No further increase in the values of the water absorption properties could be observed between 1 and 1.5 years on the test wall. Thus, the results in this respect as well as in whole are in line with those from the strength determinations discussed above.

The fact that porosity of marbles increases when subjected to environmental stresses refers to a deterioration mechanism that causes cracks to marble structure. These cracks can go either straight through the individual grains or, more probably, along the grain boundaries. Emergence of cracks to marble structure would also explain the loss of strength observed. It seems, however, that at least a certain amount of cracks appears almost immediately when marble is subjected to stresses but then the process slows down and the degree of cracking stays more or less at the same level. Also, it is obvious that the various marble types show very different tendencies for cracking.